

03/29/2024

**STRUCTURAL AND ELECTRICAL ASSESSMENT OF
THE BENNINGTON BATTLE MONUMENT**

**PHASE II: COMPREHENSIVE STRUCTURAL &
MATERIAL TESTING AND EVALUATION AND
OUTLINE OF RESTORATION APPROACH**

15 MONUMENT CIRCLE
BENNINGTON, VT, 05201

PREPARED FOR:
VERMONT DEPARTMENT OF BUILDINGS & GENERAL SERVICES
BGS PROJECT ID #200016

TABLE OF CONTENTS

I. Executive Summary.....	1
II. Methodology.....	7
III. Project Approach.....	9
IV. Synthesis of Findings.....	14
V. Evaluation of Integrity and Significance.....	47
VI. Architecture & Preservation.....	51
VII. Recommendations & Next Steps.....	71
VIII. Appendix: Consultant Reports.....	81
TYLin Silman Structural Solutions.....	82
Atkinson-Noland Associates.....	124
Jablonski Building Conservation.....	198
Landmark Facilities Group.....	444
Steven Winter & Associates.....	463
Smokestack Lightning.....	512
Langan Engineering.....	524

THIS PAGE INTENTIONALLY LEFT BLANK



- | -
EXECUTIVE
SUMMARY

EXECUTIVE SUMMARY



Image 01. Battle monument, Bennington, Vt.. *Detroit Publishing Co.; 1905*

Executive Summary

The Bennington Battle Monument commemorates a site foundational to Vermont’s unique cultural identity and statehood. Our team acknowledges with deep respect the work performed to date and for the exceptional stewardship by the State of Vermont of this historic architectural structure. The Monument is integral to not just the history of Vermont and its statehood, but the founding of our Nation as well. Construction of The Bennington Battle Monument began in 1887 and was completed in 1891. Several architects and designs were considered, though ultimately Boston architect John Phillip Rinn won the commission. Although initially the Bennington Battle Monument was cared for by the “Bennington Battle Monument and Historical Association,” complete control of the monument (including the entirety of the property as well as the gift shop) was handed over to Vermont State in 1953 due to the monument falling into disrepair.

The Team of Stevens & Associates, Easton Architects, and Silman, are engaging with the State of Vermont Department of Building & General Services to lead the preservation, restoration, and conservation project

for the Bennington Battle Monument. Following the initial Phase 1 research, documentation and physical assessment of the Monument, this Phase 2 report provides the findings and recommendations of detailed investigation and analysis by experts in numerous fields related to historic masonry, environmental controls, structural analysis and building infrastructure. The project goal of Phase 2 was to assess, analyze and synthesize all data prepared by the consultant team addressing the performance of the monument and the cause and impact of the deterioration mechanisms at work; and to propose next steps and an outline to conserve and restore the structure based on the highest caliber of conservation science, preservation technology and restoration best practices to ensure the long-term preservation of this historic monument.

Historic Significance

The Bennington Battle Monument was constructed between 1887-1891 and opened in June of 1891. The cornerstone of the Bennington Battle Monument was laid on August 16, 1887. The Bennington Battle Monument capstone was placed, November 25, 1889.¹ The Bennington Battle Monument was dedicated August 19, 1891.² The monument weighs an estimated 19 million pounds. The 306-foot tall, unreinforced masonry obelisk is constructed of Sandy Hill Dolomite, a dolomitic limestone, and the monument is designated at the local, state, and national levels. In December 1969, it was nominated the U.S. National Register of Historic Places where it was entered in the National Register in March 1971.

Project Approach

The approach for the Bennington Battle Monument Conservation and Restoration project is centered on the development and implementation of a holistic restoration and conservation methodology for the original building materials, interior space and access, and character-defining features that will appropriately balance history, use and maintainability, which will lead us to accurately determine the most appropriate treatment recommendations. All treatment recommendations will comply with the Secretary of the Interior's Standards for the Treatment of Historic Properties (the Standards) and the guidelines set forth by the American Institute for Conservation (AIC). The implementation will be guided by scholarship and best practices for the treatment of heritage sites.

With the completion of Phase 2 presented here, the proposed work would likely be performed according to the following phases and sequence:

- Phase 1: Structural, Electrical and Elevator Assessment (Completed 12.16.2022)
- **Phase 2: Additional Recommended Scopes of Work (March 29, 2024)**
- Phase 3: Planning & Feasibility Study
- Phase 4: Schematic Design

¹ John Spargo, An illustrated descriptive sketch of Bennington Battle Monument, with an account of Bennington Battle, August 16, 1777 (Bennington, VT: PUBLISHER, 1947), 9.

² Spargo, The Bennington Battle Monument, 121.

- Phase 5: Conservation and Restoration Documents and Technical Specifications
- Phase 6: Construction Administration and Oversight

Phase 2 Objective

The intended result of this second phase of work was to:

- Further investigate the conditions of the stone masonry identified in phase 1 in order to identify the key issues of the Bennington Battle Monument that need to be considered in our process of determining the most appropriate treatment approach and methodology for the monument restoration. This includes stone stress test analysis, construction assembly and wall make up, stone material testing, moisture monitoring results, petrography, mortar analysis, humidity and hydrographic analysis, and structural finite analysis.

The condition of the masonry and the mortar types were mapped as it relates to past repair campaigns, identification and location of cores, tests, and samples have been recorded on the drawings.

Past Research

In reviewing the documentation and archival history, numerous repair campaigns have been performed dating back as early as 1907 to address persistent issues of humidity, water infiltration and moisture on the inside of the Monument. There has not been, until Phase 1 completed in 2022, a full assessment of the Monument to understand the mechanisms of deterioration of the masonry walls; and testing and analysis of materials in order to develop appropriate repair techniques and perform effective, full-scale repairs. The previous work was done without a comprehensive understanding of the behavior of the Monument and its materials and the complexity of the issues challenging the integrity and stability of the building fabric. The documentation of large-scale cracking and water infiltration warrants a holistic restoration and conservation strategy that is urgently needed to halt the aggressive deterioration of the historic masonry.

Findings

Mechanisms of Deterioration

Critical to the success of the project is the acknowledgement of the continuum of deterioration. Masonry deterioration has occurred since the start of the construction and has been evident throughout the history of the Monument. There is some natural stone degradation that contributes fissures and cracking. Stress on the stone due to eccentric loading is also a contributing factor to the cracking of the stone. The most damaging factor to the degradation of the stone is water, water vapor and excessive humidity on the interior of the monument. Additional stress cracks, and water ingress are the result of past repair campaigns that introduced inappropriate mortar, sealant, caulk, epoxy, and other repair techniques that have resulted in exacerbating the deterioration.

Materials with Compromised Performance

Select materials and building components including select masonry and pointing mortar on both exterior and interior wythes of stone, stair and stair components, structural elements including some headers, and elevator components, lightning protection equipment and the absence of functioning mechanical ventilation, are near or have exceeded their serviceable life due to age, exposure to the elements, and natural degradation over time.

Poor Technical Design Performance

The mechanical and building infrastructure systems are aging and ineffective. The lack of natural ventilation and no introduction of mechanical ventilation in the structures contributes to the high relative humidity inside the monument, creating water in liquid form (condensation) and vapor form, which has a deleterious effect for the activation of salts within the masonry wall assemblies, contributes to an abusive frost jacking effect, and is aiding in the accelerated rate of deterioration.

Restoration and Conservation Treatment Recommendations

Our approach to the restoration, conservation and preservation treatments for the Bennington Battle Monument focuses on three key elements= Prevention, Mitigation, Adaptation.

The recommendations from Phase 2 have been categorized into two groups with potential execution dates noted in parenthesis:

- Treatment Recommendations (2024-2025)
- Schematic Design Work & Preservation Work Plan (2025)

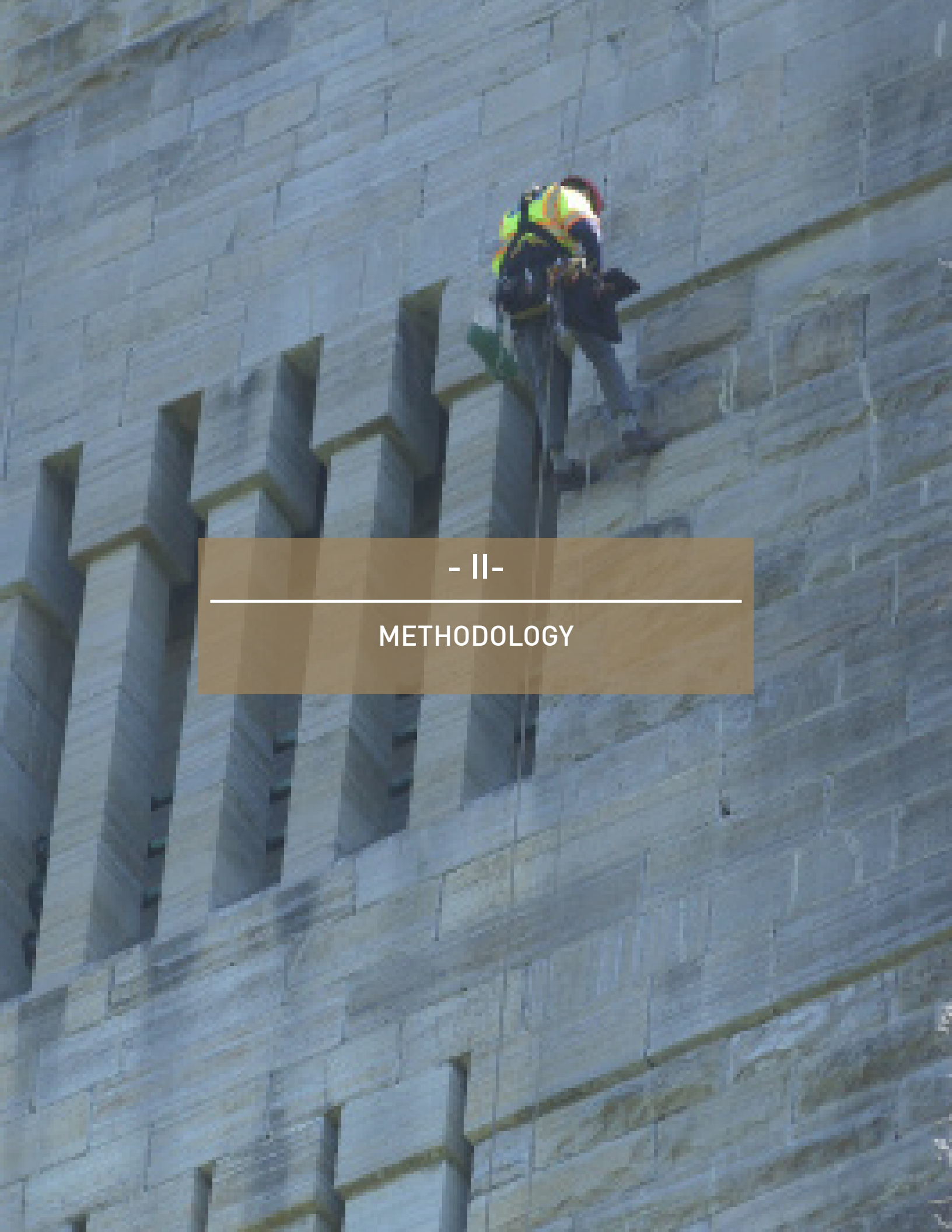
Project Success

In considering the project scope and financial commitment for a full preservation/restoration of the monument, it is easy to raise the question of what are the alternatives, especially a project with a large price tag. Of course, doing nothing, or the very minimal, is an option. But the State of Vermont has the gift of an important cultural heritage resource that was a major factor in the battle for the creation of our nation. Cultural heritage sites are more than physical landmarks and structures, it's what they represent that is intrinsic in its value to the site, an historic timeline, and its enduring legacy as a marker of time. As a steward to this monument, while the state is responsible for the maintenance of the monument, it also has the benefit of owning the history, the story, and the telling of this story.

This story is expressed as a unique obelisk that specifically represents the zenith of an important moment in our history, and create an emotional connection. There are the names and places associated with this emotional connection, from highways and roadways to state parks, hotels and motels, restaurants and bars. It is all based on memorializing and preserving the richness of our past so we can understand the reasons behind where we are today.

In this particular case, we embrace the legacy of Major General Stark (who also fought at Bunker Hill, and the Battles of Princeton and Trenton), Colonel Seth Warner (who also fought at Ticonderoga and at the Battle of Hubbardton) and the Green Mountain Boys, the Republic of Vermont, the negotiations with Quebec before British surrender, then the negotiations with the U.S. to enter the Union, with all of this representative of the Battle of Bennington as a key victory in our Revolutionary War, as much as it is of Vermont's battle for its own statehood, and the efforts of ultimately becoming the 14th state of the Union.

As the Vermont Historical Society professes "Every person and every moment create the story of Vermont. Through sharing these collective stories, Vermonters will increase their knowledge of our state's complex past, inform our present, and understand how our unique experiences impact and shape this ongoing narrative." The Bennington Battle Monument is part of this story, is a valuable link in Vermont's history, and a source of pride that can be continuously celebrated.



- || -

METHODOLOGY

METHODOLOGY

Methodology

Our team specializes in providing restoration and conservation strategies for the maintenance and preservation of historic properties, developed through research and forensic analysis of historic fabric to determine the mechanisms of deterioration at work. Our project approach begins with research—both archival and in the field—to understand the history and evolution of the site, climate, and environmental conditions. A thorough understanding of existing conditions and building materials provides an essential foundation for this project; this knowledge informs strategic decisions for determining the restoration and conservation treatment recommendations.

Best Practices for Treatment Recommendations

Our restoration and conservation treatment recommendations are based on conservation science, best practices, and applicable standards to ensure long-term solutions to preserve this culturally significant monument. Our methodology and restoration approach are developed using accepted and established preservation theory and practices as advocated by:

- The Secretary of the Interior's Standards for the Treatment of Historic Properties
- The National Trust for Historic Preservation
- American Institute for Conservation

PROJECT APPROACH

Project Approach

Following a thorough internal study and review of the assessment of existing conditions and reports completed in Phase 1, and the engagement of a full complement of consultants prior to the commencement of Phase 2, we have synthesized all data and analyses delivered from our consultant team and developed a clear approach with treatment recommendations and considerations for next steps for project planning for the holistic preservation, restoration, and rehabilitation of the Monument.

Our methodology is based philosophically on accepted and established preservation theory and practice as advocated by The Secretary of the Interior's Standards for the Treatment of Historic Properties, the National Trust for Historic Preservation, and the American Institute of Conservation. As much original material as possible shall be maintained, interventions shall be the minimum necessary to ensure the extended life of all building and landscape features, and all restoration procedures shall be proven reversible where feasible and accurately recorded.

Our team of architects, preservationists and conservators specializes in providing restoration and conservation strategies for the maintenance and preservation of historic properties, developed through research and forensic analysis of historic fabric to determine the mechanisms of deterioration at work. It is precisely this specialty that is required for the comprehensive restoration program for the Bennington Battle Monument. Our project approach began with research—both archival and hands-on—to understand the history and evolution of the Monument site, including existing conditions, climate, and its impact on materials and the structures, and surrounding environmental conditions. A comprehensive understanding of the existing conditions and an analysis of the building materials provided our team with an essential foundation for the development of our restoration program; and this knowledge will enable us and the State to make informed and strategic decisions. This understanding allows us to comprise our overall approach to organizing this information in the following order:

Project Assessment & Report Synthesis Components

1. Structural & Material Testing and Performance Analysis
2. Building Systems including Thermal Dynamics & Hygrographic Analysis
3. Architectural Preservation Review and Analysis
4. Project Planning and Implementation Considerations/Recommendations

Items 1 & 2 refer to the assessment process, 3&4 address conclusions from the Architectural Synthesis which highlight the highest priorities for preservation and the critical planning and implementation decisions for the team to address for the project's success.

Structural & Material Testing and Performance Analysis

- Structural Modeling & Analysis
- Onsite testing
- Laboratory Material Testing



- III -

PROJECT APPROACH

PROJECT APPROACH

- Petrography and Mortar Testing

Building Systems including Thermal Dynamics & Hygrographic Analysis

- Existing stair and viewing platform (as components of the structure's circulation system)
- Existing elevator and shaft and electrical service/operation
- Moisture/water penetration testing and analysis
- Intervention of passive ventilation and potential for new active ventilation
- Existing electrical services
- Misc. building systems integration (lightning protection, emergency generator services, etc)
- Methods of dehumidification and ventilation- what sort of arrangements are we looking at?
- What size equipment?
- How feasible is this to be performed on such a building as this?
- What sort of energy requirements may be required?
- Will upgrades of the electrical system be required?
- How do we evaluate the utility of passive vs. active ventilation?

Architectural Preservation Review and Analysis

Primary Factors for Consideration:

- Waterproofing of exterior and interior
- Stone repair/replacement
- Crack repair
- Mortar and repointing
- Stone makeup- understanding porosity, density and sourcing
- Sensitive integration of structural recommendations (grouting, pinning, etc)
- Moisture control on interior (prevent salt leeching)

Principal Focus for Next Steps in Project Planning and Implementation

- Completion of a Planning & Feasibility Study
- Mock ups/monitoring required-types, timing and sequence
- Development of strategies for work, and development of project scope(s) of work

PROJECT APPROACH

- Practical components (covering, scaffolding, power, timing, cost, drying, procurement)

Phase 2 Objectives and Considerations

The purpose of the Phase 1 Assessment Report was to identify the key findings and recommendations of a year-long investigation conducted by Stevens & Associates in partnership with Silman. The investigation assessed the conditions of the stone masonry, interior steel framing, stairs, elevator, and the existing electrical systems, with the goal of understanding the unique issues that have caused distress in each component, and to provide thoughtful recommendations that will address the root causes of the observed distress.

The primary objective of Phase 2 was to complete additional recommended scopes of work to further identify the architectural, material and engineering conditions of the Monument as it stands today. This included in-depth stone testing and mortar analysis, extraction of stone cores and samples, petrography, building enclosure and hygrothermal review, mechanical engineering preliminary assessment, water infiltration and IR testing, architectural preservation review and analysis, masonry strength testing, structural finite element analysis, lightning protection and grounding assessment, preliminary geotechnical investigation, additional electronic crack and moisture monitoring, and non-destructive evaluation included rope access for documentation. This information has been synthesized to create a restoration strategy that is based on these findings, and the application of best practices for restoration, rehabilitation, repair, and conservation.

Synthesis of Data: Synopsis of Individual Consultant Reports

The strength of our team lies in the relationships we have established within the preservation community specifically and the architectural and engineering industries in general. Onsite assessment work and documenting and reporting is a shared language. Understanding the strengths of each consultant, providing them with the means to perform their work, and knowing how to interpret the language, implement the data and capitalize on the investment in time and material to perform the conditions assessment are the key components to a successful project.

In looking at the specific challenges presented by the Bennington Battle Monument, the type of structure, material, construction period and location all play a critical role in understanding the project and how the structure is behaving.

The Team's understanding of the task at hand enabled us to determine the appropriate restoration approach. The resulting investigative work included performing highly specialized material and structural testing. The key aspects of the Monument that demanded the expertise brought to the project are:

- A. The Monument is the second tallest unreinforced masonry obelisk in the United States. The Team has detailed experience with this type of structure.
- B. Structural analysis and evaluation of this type of masonry construction requires specialized knowledge and experience in the performance and material properties of such construction.

PROJECT APPROACH

- C. National Historic Landmarks. Our team has decades of experience working on high profile buildings and monuments across the country that require a customized team of experts.
- D. Understanding the complex behavior and deterioration cycles that occur on such structures—especially including tall masonry structures. This informs our recommendations for restoration strategies for mass masonry buildings.
- E. Understanding—through practical experience—the parameters for designing and implementing successful restoration strategies including pinning, grouting, stone sourcing and replacement, waterproofing, and moisture control.
- F. Project planning and pre-schematic design leadership provides a thorough understanding of the complexities of the project.

CONSULTANT TEAM

STEVENS & ASSOCIATES

Civil Engineers and Architects, Project Manager

EASTON ARCHITECTS

Preservation Architects

SILMAN

Structural Engineers

ATKINSON-NOLAND & ASSOCIATES

Non-Destructive Evaluation and Testing

JABLONSKI BUILDING CONSERVATION

Stone petrography and mortar analysis

LANDMARK FACILITIES GROUP

Mechanical Engineers

STEVEN WINTER & ASSOCIATES

Exterior building envelope consultants

LANGAN ENGINEERING

Geotechnical Engineers/Civil and Laser Scanning (Phase 1)

SMOKESTACK LIGHTNING

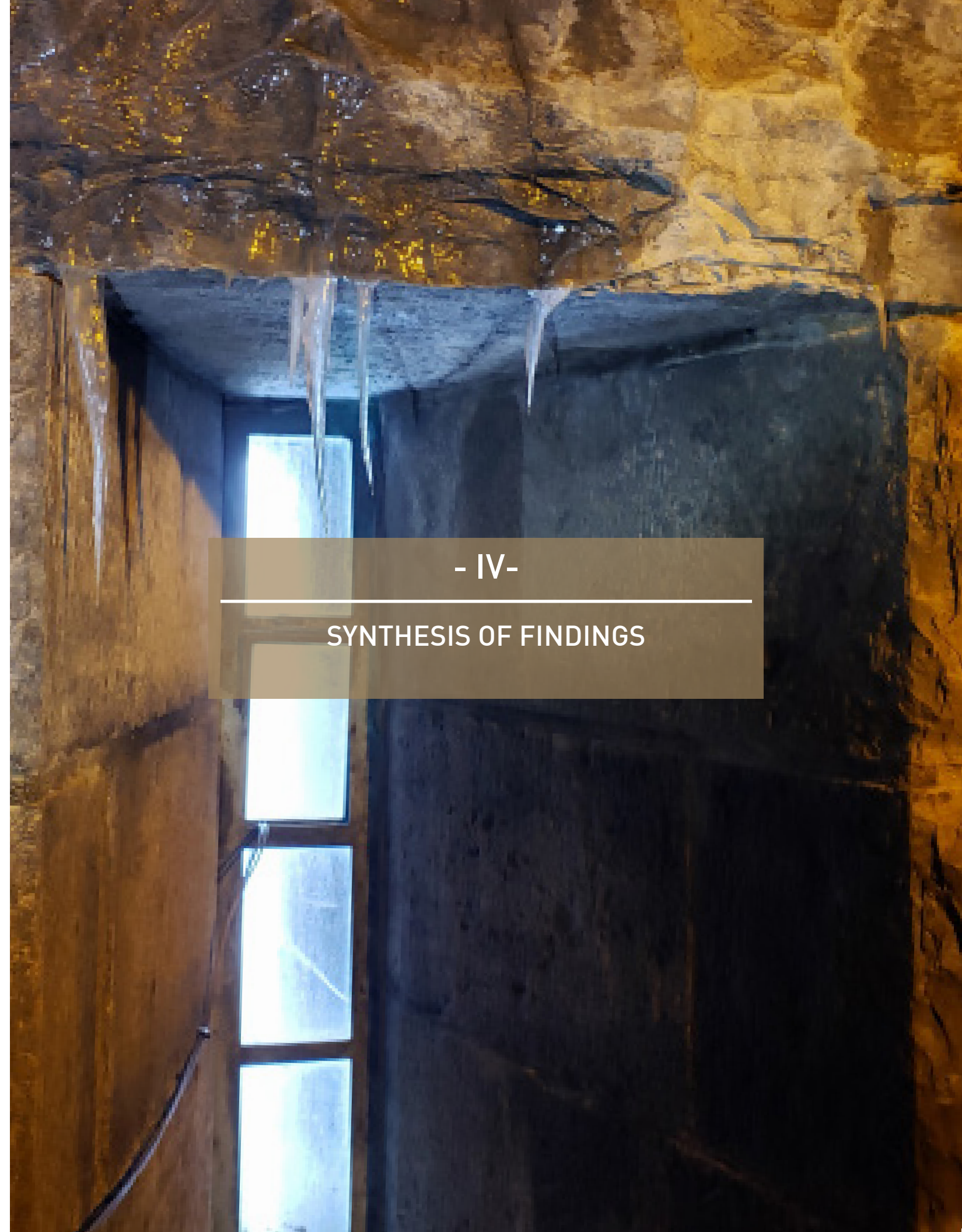
Lighting Protection Consultant

VERTICAL ACCESS (Phase 1)

Exterior Envelope Access and Assessment Consultant

LERCH BATES (Phase 1)

Elevator Consultant



- IV -

SYNTHESIS OF FINDINGS

Consultant Report Summaries**Silman: Structural Engineers (Full Report Appendix XX)**

Phase 1 work performed by Silman provided beneficial information about the stone masonry of the Monument, including the general cross section of the wall, the pattern of visible cracking, the structural performance of the building relative to plumbness, measurement of overall forms of movement, and the structural performance of the building relative to dead loads and lateral loads. The wide breadth of this phase of the investigation has allowed the design team to explore several potential causes of the widespread cracking observed throughout the stone masonry of the Monument. A singular cause for the cracking has not been identified, but rather a number of potential contributing factors have been established, including the following areas which will require further study and investigation:

1. **Stone Material:** The original stone used to construct the Monument may not have been the optimal choice for this type of structure. The stone was identified as dolomitic stone and is a harder and stronger stone than calciferous limestone, but it is nevertheless a sedimentary stone that is porous and permeable, and susceptible to moisture migration and freeze thaw damage. We recognize that this is not something that can be changed about the Monument. Preliminary analysis suggests that the strength properties of this stone may not be a primary concern, but rather the vulnerability of the stone to moisture related processes will need to be further understood to identify an effective restoration strategy.

2. **Mortar:** Original construction documents specified Rosendale and Portland cement-based mortars. Based on our limited sampling, the handful of previous masonry repairs appeared to utilize Portland cement-based mortars as well. Rosendale and Portland cement mortars tend to be harder and stronger than the expected strength of the dolomitic stone, though strength tests were not part of this phase of the investigation. Typically, in historic masonry construction, the desire is for the mortar to be the softer, sacrificial element in the wall assembly that will absorb and disperse localized stresses from the harder stones. These internal and external forces come from seasonal and even daily changes in volume and moisture expansion, thermal cycles caused by shifting of the stones, and freeze-thaw cycles. When the mortar is too hard, the stones become the softer, sacrificial component of the wall system.

Both the original mortar and repointing mortars on the monument do not appear to have the preferred qualities of a soft cement lime-based mortar. The compatibility of the Rosendale mortar is less clear as it had become obsolete for nearly a century as Portland cement became dominant in construction. The mortar is becoming relevant again as preservation projects have bolstered demand and more information is becoming available.

Further investigation is required for multiple reasons; firstly, to help establish if the original mortar selection was a leading cause of the frequent cracks and overall sub-optimal performance of the mortar, and secondly, to ensure that future repair mortars are compatible with the existing masonry and can be correctly specified to avoid perpetuating any incompatibility.

Silman's primary structural engineering scope of work in Phase 2 was to perform more detailed structural modeling of the Monument for global and local performance of the structure to investigate potential modes of failure and states of stress. Finite Element Modeling and hand calculations were further informed by incorporating the material condition, movement data, strength, stress, and stiffness provided by the additional testing performed in Phase 2.

During this phase, a structural analysis of the Monument was performed. Below is a synopsis of the methods used:

- Hand calculations (using spreadsheets developed by Silman for this project) were used to analyze building elements to verify whether they are sufficient to resist the global forces and stresses including seismic and wind forces.
- A three-dimensional analytical Finite Element (FE) shell model was created from the laser dimensional point cloud using the software SAP2000. This allowed for review of the stresses, forces, and deformed shape under different load conditions and combinations, including behavior under its own self-weight, wind forces, and a nonlinear pushover analysis.
- A three-dimensional analytical Finite Element (FE) solid model was created to achieve a more detailed understanding of the effects of cracks, specifically in situations with a reduction of cross section or a disconnected corner. By completing a linear gravity and lateral wind analysis, an evaluation of the potential increases of stress from such conditions was completed.
- The structural effect of reduced material cross sections was studied through hand calculations and the FE model. Specifically, we investigated the effects of having a structure in which the stresses were redistributed through a smaller area due to cracks in the Monument.
- Capacity of individual masonry units was determined (via lab and in situ) and compared against stress values from the hand calculations and FE models. This was done to understand if localized failures are occurring due to high localized bending and/ or shear stresses.
- Potential stress build-up due to thermal differentials in the masonry was calculated and compared against the structural capacity of the masonry.

During Silman's Phase 1 study, it was concluded that the Monument's walls were stable and that stresses were within allowable limits based on hand calculations using current codes and idealized assumptions about the wall construction. Based on the Phase 2 analysis, including updated wall calculations, Finite Element Models, capacity checks and thermal analysis, a synopsis of Silman's conclusions is summarized below:

- It was concluded in Phase 1 that loads in the wall exceed allowable tension and compression stresses under a full code-defined seismic event. However, based on updated material properties and assuming a uniformly built and loaded wall, this net stress exceedance scenario does not

SYNTHESIS OF FINDINGS

occur.

- Assuming a solely uniform distribution of loads across the wall section, no issues were seen under gravity loads or lateral wind loads in both the hand calculations and Finite Element Models, with both the tension and compressive stresses below the limit of the tested compressive stress value. It is important to realize that this is an idealized assumption, and real-world conditions may present higher than desirable stress concentrations.
- The hand calculations showed that a reduction in the cross section of the wall leads to an increase to the stresses at the base of the Monument. A reduced cross section with just the inner wall working showed the most significant increase in stress (with both tensile and compressive stresses exceeding allowable values under code-defined conditions). This is representative of the cracked behavior of the structure, as cracks can change the load paths of the Monument, and lead to significant stress concentrations, such as the ones seen here.
- The cracked shell and solid models showed no global issues when analyzed under gravity loads and wind loads under idealized conditions. No tension developed in the model during the application of wind loads.
- The nonlinear analysis showed that the forces needed before inelastic behavior (permanent deformation) occurred were well above any limits it would realistically see through code-defined wind and seismic forces. Nevertheless, this analysis highlighted the effect that such large-scale cracking has on the concentration of forces and stresses.
- Unsupported lengths of individual stone units allow beam action in the masonry. Once the masonry is cracked, stresses due to lateral loading such as seismic and wind are higher than the allowable bending and shear capacity of some geometries and spans of stone present on the Monument. Issues such as mortar deterioration or missing mortar can cause a loss of support resulting in bending type action that can increase stresses locally. The extent of mortar loss would have to be significant to crack the masonry, but if combined with other structural stresses such as thermal or gravity it could cause overstress.
- Thermal stresses due to temperature fluctuations experienced by the Monument can exceed the allowable tensile capacity of the masonry. This may be a cause of widespread cracking that must be considered when designing repairs.
- Although no single item was proven as the cause of the cracking, it is likely that multiple of these issues occurring at the same time, has led to a cumulative effect of forces and stresses.
- The cracks were reported very early on in the Monument's history, so a rare, large lateral loading event (wind or seismic) is unlikely to have caused initial cracking. Rather, it is most likely that the repetitive nature of climatic stresses experienced in the short-term, like freeze-thaw and temperature cycles, were the initial cause of cracking. However, loading and the localized re-distribution of loads that has happened over time or may happen in the future could worsen the cracking.

SYNTHESIS OF FINDINGS

A key observation in Silman's report notes from a structural perspective, while all the items in the list above are contributing factors to the deterioration of the masonry, it is the local stress concentrations that appear to be the initial cause of cracking. The cumulative effects of lateral loading, mortar loss altering the load path, progressive cracking changing the connectivity of the cross section, thermal and freeze-thaw effects could cause overstress in the masonry.

Any one of these mechanisms acting alone is not sufficient to cause the widespread cracking observed in the Monument, but the buildup of various stresses has the potential to exceed the allowable capacity of the masonry. Cracks and deterioration are due to local stresses rather than global behavior of the Monument under self-weight or lateral loads. The presence of cracks creates higher areas of localized, concentrated stresses, which in turn can cause more cracks.

From a structural perspective, while all the items in the list above are contributing factors to the deterioration of the masonry, it is the local stress concentrations that appear to be the initial cause of cracking. The cumulative effects of lateral loading, mortar loss altering the load path, progressive cracking changing the connectivity of the cross section, thermal and freeze-thaw effects could cause overstress in the masonry. Any one of these mechanisms acting alone is not sufficient to cause the widespread cracking observed in the Monument, but the buildup of various stresses has the potential to exceed the allowable capacity of the masonry. Cracks and deterioration are due to local stresses rather than global behavior of the Monument under self-weight or lateral loads. The presence of cracks creates higher areas of localized, concentrated stresses, which in turn can cause more cracks.

Atkinson-Noland & Associates: Consulting Engineers (full report see Appendix XX)

Atkinson-Noland & Associates (ANA) was on site to conduct supplemental nondestructive evaluation (NDE), facilitate the installation of additional structural health monitoring sensors, and to conduct material tests at the stone masonry walls.

This scope expands upon the 2022 Phase 1 ANA work that included NDE and one year of structural health monitoring, with the findings summarized in ANA's report titled, 'Final Report – Bennington Battle Monument 6-30-2022'. The main objectives of the work included confirming typical wall sections and the nature of internal wall construction with additional NDE via rope access, investigating stone unit and masonry wall assembly material properties and in-situ stresses (goodman jack and flat jack test), and to install additional sensors to expand and extend the duration of the structural health monitoring program.

ANA conducted the NDE and material testing from areas where walk-up access was available. Vertical Access (VA) assisted by conducting all other exterior NDE and sensor installation from higher portions of the monument via rope access. ANA personnel were on site May 22-25, 2023, for the NDE and expansion of the structural health monitoring program, and from July 17-20, 2023 for the material testing portions of the scope. Personnel from Silman, Stevens & Associates (S&A) and Easton Architects (EA) were on site during portions of ANA's field work to discuss findings and identify specific areas of importance through the monument. Contractor assistance by means of stone core removals and housekeeping support was

SYNTHESIS OF FINDINGS

provided by Alegrone during ANA's field work. The following bullets summarize the general wall construction of the Monument:

- Stone masonry walls are constructed of two- to three-wythes of stone masonry with dolostone and limestone.
- At the thicker base, the wall is three distinct wythes of stone masonry and further to the top it transitions to two distinct wythes. The uppermost approximately 20 courses are single wythe.
- The exterior face wythe appears to consist of only dolostone units with consistent coursing.
- The interior face wythe appears to consist of a combination of dolostone and limestone with more dolostone present lower on the monument, and more limestone present higher on the Monument.
- The interior face wythe is uncoursed and not dressed.
- Project contract and specifications from 1887 indicate the walls are to be built with one fifth headers. Generally, bond stones appear to bridge between two wythes of stones
- Mortar formulation was determined to match most closely that of a Type K mortar.
- Collar joint mortar appears different in composition and is more like a poured concrete. They contain large, crushed stone aggregates and appear to be 3" to 6" thick indicating that it would need to be poured in place rather than troweled by hand

ANA performed the following nondestructive evaluation tests to ascertain baseline information, including wall thickness and construction, and internal wythe construction. This information becomes valuable in understanding what exists in between the exterior and interior stone coursing, and its assembly, to help determine the cause of cracking, movement, voids, and solid surfaces and infill. The following investigative tests were performed:

Microwave Radar Scanning (page 4 of report)

Surface penetrating radar (SPR) was used to assess internal wall construction of the monument's stone masonry walls. The primary goal of the SPR scanning on this mobilization was to determine if stone thicknesses at the interior and exterior face wythes at higher portions of the monument were consistent with the findings from Phase I NDE work. Another main goal was to determine the consistency of internal wall conditions at varying heights up the monument, related to internal voiding and/or any presence of rubble construction. Previous findings from Phase I determined that the walls are primarily solid multi-wythe stone construction with coursed masonry throughout the thickness of the wall and not containing a rubble core.

- Approximately 125 SPR scans were collected and saved at four (4) interior and four (4) exterior locations higher up on the monument.

SYNTHESIS OF FINDINGS

- There is a clear shift in stone thicknesses at the interior face wythe higher up the monument to favor thinner stone units. This is expected as the overall wall thickness reduces up the height of the monument.
- At approximately 150-foot up the monument, full depth bond stones began to be visible in the SPR data
- Though the overall wall thickness reduces up the height of the monument, there are still a similar frequency of bond stones.

Videoscope Evaluation (page 11 of report)

A series of 3/8-inch diameter holes were drilled into mortar joints such that a fiberoptic videoscope could be used to make visual observations. The videoscope investigation intended to determine the size and frequency of internal voiding within the wall, if present, and to characterize the materiality and solidity of the masonry between interior and exterior face wythes. The Phase II videoscope probes were selected in locations higher up the monument at the interior and exterior to supplement previous videoscope findings from Phase I.

Goodman Jack Cores (page 11 of report)

A Goodman Jack core is an extraction method of in-situ stone to investigate the deformability of the stone along its thickness. The goodman jack test then uses a special probe in the core hole to investigate the deformability of the stone in-situ as-existing in the wall assembly. In the case of the Monument, ANA had two (2) 6'-0" x 3" diameter cores extracted for investigation. This provided an additional opportunity to observe internal wall conditions at greater depths than was previously possible with the videoscope evaluation.

General Observations at Goodman Jack Cores Holes

South Core

- Visible condensation at the top of the core hole unrelated to the material extraction.
- 1st interior collar joint was previously 100% solid but shows visible distress after testing. A ruptured membrane came from the test as it pressed into the soft mortar

North Core

- The stone was visibly intact before the testing, but loading the masonry resulted in a vertical fracture through the stone unit for the full depth of the unit
- Interior face wythe and exterior face wythe appeared to be intact solid stone units
- Center of the wall appeared mostly solid with stone to mortar interfaces generally solid with some slight delamination

SYNTHESIS OF FINDINGS

Spray Testing (page 17 of report)

Water spray testing was conducted to evaluate moisture intrusion through the stone masonry assembly of the Monument. Testing involved spraying pressurized water through a spray rack at the exterior of the north elevation.

The spray test was successful in producing leaks at the interior of the monument over the course of the testing. The first leaks were noted approximately 60 to 90 minutes into testing. These were small trickles of water flowing through visibly cracked stones at the interior approximately 40 feet below the spray frame. An example of such a leak is included in Figure 25. With more time (90 to 120-minutes), wet spots began to become observable at interior mortar joints. The first leaks noted (60 to 120-minutes) were those lower down on the monument starting above stair landing 22, approximately 40 feet below the spray frame. With time, leaks were noted higher up the monument closer to the elevation of water application.

Spray test results were generally consistent with the stone assembly being largely solid with a set of small, narrow gaps or cracks present between stones and mortar fill as well as cracked stones for moisture to migrate through.

Summary of Non-Destructive Investigations (page 21 of report)

Further nondestructive evaluation of the stone masonry walls at various heights up the monument on the interior and exterior determined that as-built conditions appear consistent across all four elevations and across all heights evaluated. The masonry walls typically appear to be coursed masonry through the entire wall thickness with some limited stone/mortar rubble fill at the center of the wall. Mortar/concrete and small pieces of stone or large pieces of aggregate were used to fill gaps between stone units.

Bond stones were located with Surface Penetrating Radar (SPR) throughout the monument at select elevations and heights up the Monument. Starting at heights of approximately 150-feet above grade, bond stone units that were full depth through the thickness of the wall were observed with SPR scans. Below 150 ft the bond stones were not full through-wall units.

In-Situ Materials Testing: (page 21 of report)

In-situ material testing was determined to be necessary to understand the compressibility behavior of the masonry. This test method for determining the deformation properties of existing unreinforced solid-unit masonry concerns the measurement of in-situ masonry deformability properties in existing masonry by use of thin, bladder-like flatjack devices that are installed in cut mortar joints in the masonry wall. This test method provides a relatively non-destructive means of determining masonry properties.

In-situ Deformability Testing

As the flatjacks are pressurized, the corresponding deformations of the masonry between the jacks are measured using a set of surface-mounted linear variable differential transformers (LVDTs). Two cycles of loading were conducted for each test. The initial cycle is used to seat the flatjacks and the second cycle provides a more accurate measure of the compression behavior of the masonry. The results are then

SYNTHESIS OF FINDINGS

directly applied as known variables in calculations for determining the masonry wall compressive strength and behavior, to assist in determining if the stone is failing under its own weight, or if it has yet to meet its compressive strength capabilities (refer to *Silman Report for additional analysis on compressive strength*)

- Investigated compression behavior of the existing masonry using the flatjack method of ASTM C1197, *In Situ Measurement of Masonry Deformability Properties Using the Flatjack Method*
- Involved removing bed joint mortar for insertion of two parallel flatjacks
- Maximum stress applied was 1550 psi, at which point the test was stopped

In-situ Goodman Jack Testing (page 31 of report)

The elastic modulus of the stone masonry assembly was measured at two locations using a borehole dilatometer inserted into the two (2) Goodman Jack core holes. The dilatometer uses a radially expandable membrane that is pressurized within a cylindrical hole drilled into the stone. During the test, the applied pressure and hydraulic volume pumped into the membrane are measured to generate a test curve. As the membrane tightens against the walls of the core and begins to push against the stone, a linear relationship is observed between the volume that can be pumped into the dilatometer (a corollary for the expansion of the core diameter) and the hydraulic pressure. From this linear elastic region, a relationship between the hydraulic volume and pressure is calculated to determine the modulus.

Laboratory Stone Material Testing (page 35 of report)

Six (6) locations throughout the Bennington Battle Monument were selected by ANA, Silman, S&A, and representatives from the State of Vermont for stone cores to be removed for laboratory testing. Core locations were marked on site and Alegrone subsequently used a core drill to extract the samples and turn them over to ANA. Four (4) stone cores were sourced from interior stones and two (2) cores were sourced from exterior stones. The two tests performed on these samples were *Compressive Strength Testing* and *Dynamic Modulus Testing*.

Compressive Strength Tests are used to determine a material's behavior under applied crushing loads and are typically conducted by applying compressive pressure to a test specimen (in this case, extracted stone cores) using platens or specialized fixtures on a universal testing machine. During the test, various properties of the material are calculated and plotted as a stress-strain diagram which is used to determine qualities such as elastic limit, proportional limit, yield point, yield strength, and, for some materials, compressive strength. In the case of these tests, compressive strength was provided for all the tests. ANA also got compressive *modulus* for a few specimens. The compressive modulus is a ratio (basically the same thing as elastic modulus or Young's ratio) that relates the compressive stress to how much compression happens, meaning how much a stone will actually compress under a given stress.

Both wet and dry samples were tested for compressive strength. The modulus of compression for dry stone was 40% higher than for the wet samples, and the maximum pressure sustainable for the dry stone

PETROGRAPHIC ANALYSIS - ANA

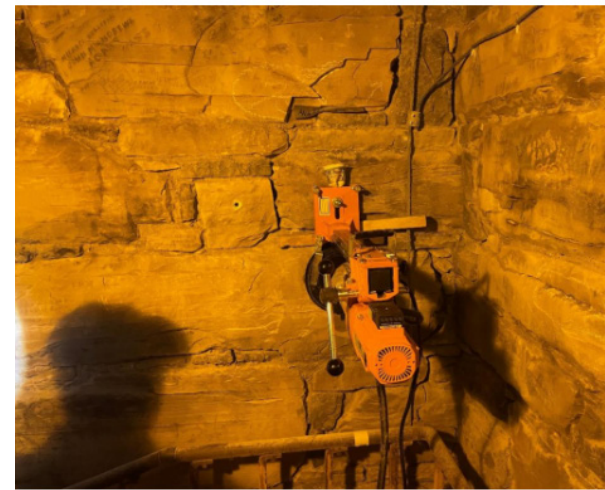
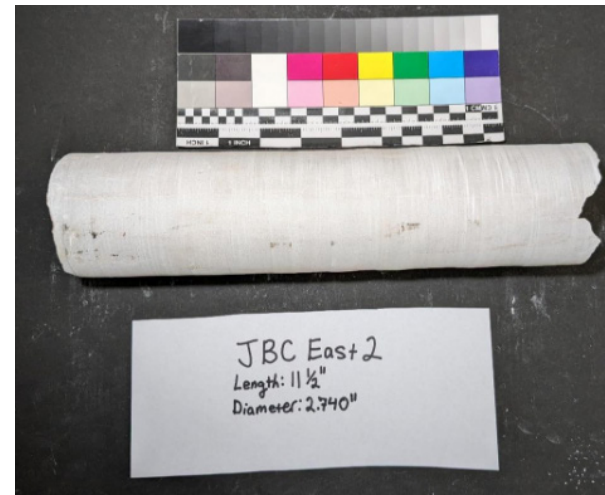
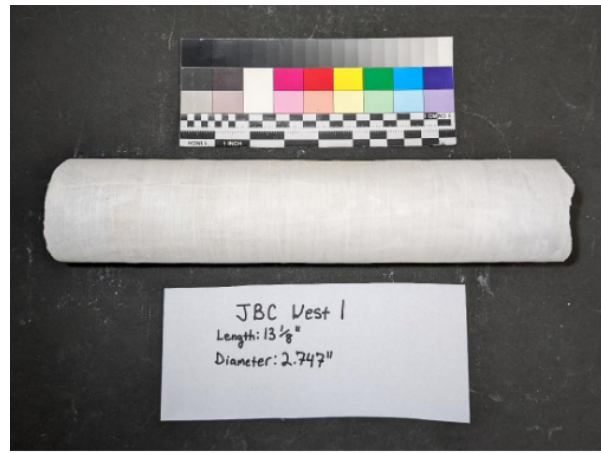


Image 03. Interior JBC-West-1

Image 02. Interior JBC-East-2



Image 04. Interior JBC-West-4

Image 05. Interior JBC-West-3 - 2 pieces

PETROGRAPHIC ANALYSIS - JBC



Image 07. Exterior JBC-North-5

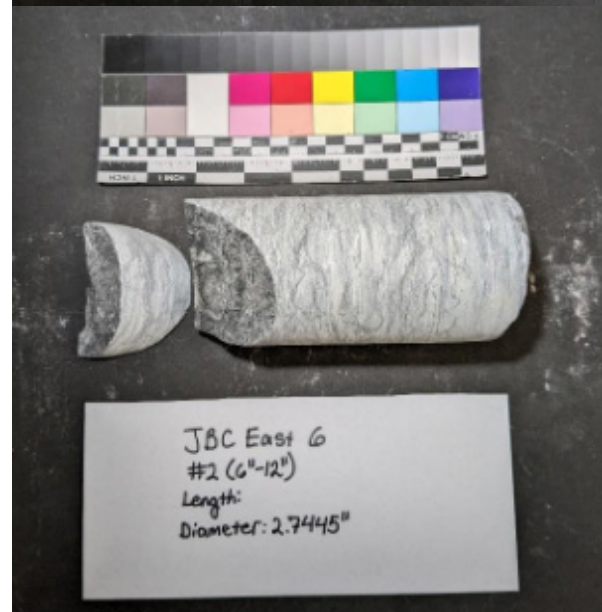
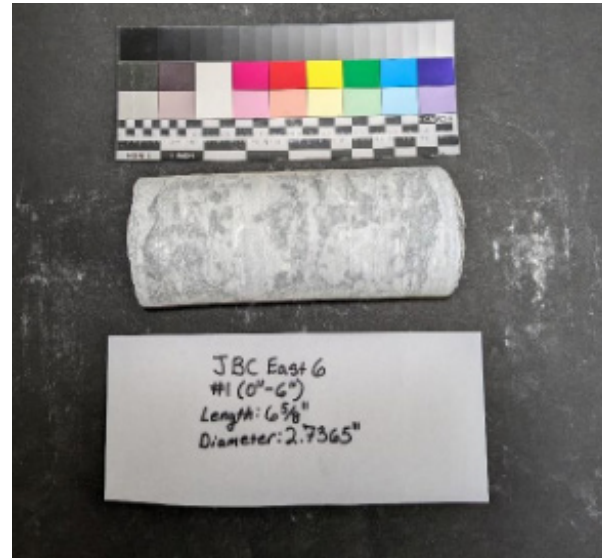


Image 06. Exterior JBC-East-6 - 2 pieces



Image 09. Exterior JBC-East-7



Image 08. Exterior JBC-North-5

HANDS-ON ARCHITECTURAL ASSESSMENT OF EXISTING CONDITIONS

GOODMAN JACK TEST



Image 15. Goodman Jack Test. Stevens & Associates 07.17.2023



Image 12. Flat Jack Test. Stevens & Associates 07.17.2023



Image 14. Goodman Jack Test. Stevens & Associates 07.17.2023

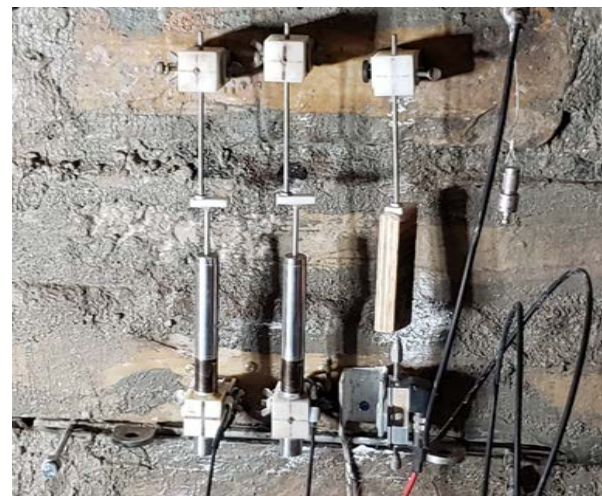


Image 11. Flat Jack Test. Stevens & Associates 07.17.2023



Image 13. Flat Jack Test. Stevens & Associates 07.17.2023



Image 10. Flat Jack Test. Stevens & Associates 07.17.2023

HANDS-ON ARCHITECTURAL ASSESSMENT OF EXISTING CONDITIONS

GOODMAN JACK TEST - Atkinson-Noland & Associates

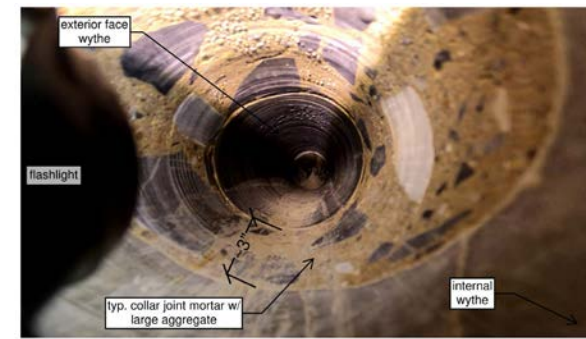


Image 17. CORE-SOUTH after Goodman Jack testing. Atkinson-Noland & Associates

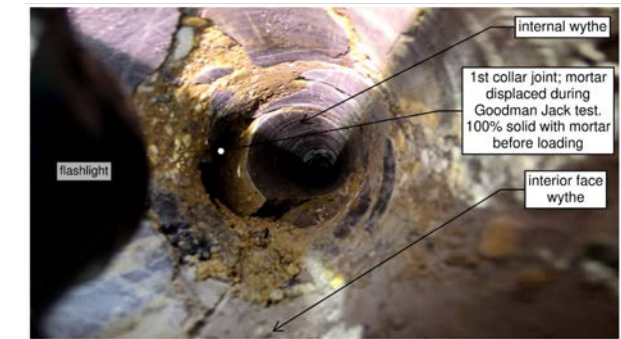


Image 23. CORE-SOUTH after Goodman Jack testing. Atkinson-Noland & Associates



Image 16. Internal wythe, CORE-SOUTH after Goodman Jack testing. Atkinson-Noland & Associates

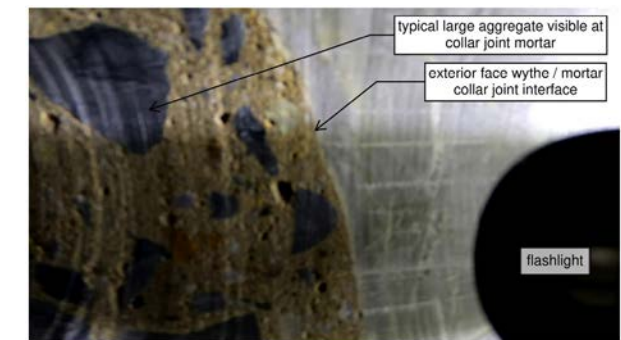


Image 20. Second collar joint, CORE-SOUTH after Goodman Jack testing. Atkinson-Noland & Associates



Image 18. Interior face wythe, CORE-NORTH after Goodman Jack testing. Atkinson-Noland & Associates



Image 21. Between interior and exterior face wythes, CORE-NORTH. Atkinson-Noland & Associates



Image 19. Between interior and exterior face wythes, CORE-NORTH. Atkinson-Noland & Associates



Image 22. Between interior and exterior face wythes, CORE-NORTH. Atkinson-Noland & Associates

HANDS-ON ARCHITECTURAL ASSESSMENT OF EXISTING CONDITIONS

SPRAY TEST - Atkinson-Noland & Associates



Image 26. North Elevation. Atkinson-Noland & Associates



Image 27. North wall following rainstorm with the prevailing wind coming directly from the north. The monument largely blocked wind driven rain from the leeward walls, with a small amount of moisture being blown and wrapping around the corners of the monument creating a clear line of moisture approximately half the length of a stone unit to the East and West elevations.. Atkinson-Noland & Associates

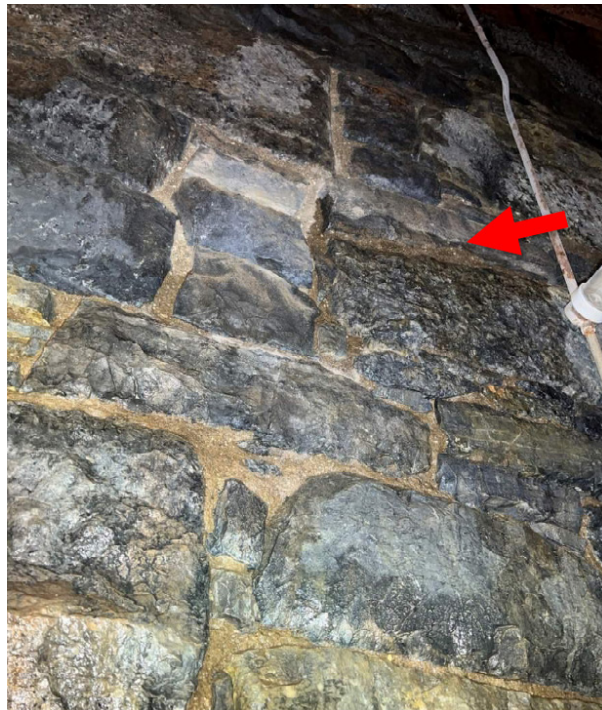


Image 25. Appearance of damp observed at mortar joint below interior stone work. Atkinson-Noland & Associates



Image 24. Leak observed as a result of spray testing below crack at interior stone. Atkinson-Noland & Associates

SYNTHESIS OF FINDINGS

samples was 18% higher than the wet samples. As an observation, the wet stone is clearly compromised in its compressive strength, further defending the argument that a critical first step is drying the Monument.

Dynamic Modulus Tests apply a repeated axial cyclic load of fixed magnitude and cycle duration to a test specimen (in our case, the extracted stone cores). Test specimens can be tested at different temperatures and three different loading frequencies (commonly 1, 4 and 16 Hz). The applied load varies and is usually applied in a haversine wave (inverted cosine offset by half its amplitude – a continuous haversine wave would look like a sine wave whose negative peak is at zero). Dynamic modulus tests differ from the repeated load tests in their loading cycles and frequencies. The dynamic modulus test measures a specimen's stress-strain relationship under a continuous sinusoidal loading.

Test results charts are part of ANA's full report, located on page 37-38.

Jablonski Building Conservation: Materials Conservator (full report see Appendix XX)

Jablonski Building Conservation, Inc. (JBC) was contracted to analyze masonry materials and investigate deteriorated conditions at the Monument. The analysis included an on-site assessment of existing conditions, field testing of moisture properties, and laboratory analyses of stone, mortar, and salt samples removed from the Monument. The analysis was performed to identify the masonry materials and understand their deterioration mechanisms to inform repair work. A summary of the stone masonry as observed is as follows:

Methodology

To perform their work, JBC was onsite for a visual assessment June 20-23, 2023, and during this period performed a visual assessment of areas accessible on both the interior and exterior of the Monument, performed moisture measurements, and located and oversaw the extraction of eight (8) stone core samples, four (4) on the exterior and four (4) on the interior for testing. Eight (8) mortar samples were removed from selected areas of the Monument for testing, and seven salt samples were extracted for analysis using x-ray diffraction. Additionally, samples of stone and the large stone chip aggregate concrete from the deep cores recovered during the Goodman Jack tests were visually analyzed and tested. The following is a summary of the analyses and findings.

Materials Identification and Analyses

Stone-Exterior (Dolomitic Limestone)

- Minor superficial weathering considering the bulk of the stone to be cohesive and sound.
- Potential durability issue as the presence of pyrite, minor geological microcracks, and stylolites are found
- No deterioration related to this issue in the sample sent for analysis, but these could explain the delamination on the upper portion of the monument
- Microcracks pose a threat to moisture infiltration and ingress of salts and are susceptible to swelling during wet/dry cycles and to frost wedging

SYNTHESIS OF FINDINGS

Interior (Calcitic Marble)

- Fine-grained calcitic marble; a locally quarried dolomitic limestone inferred to be from Southern Vermont
- As a calcitic marble, one great threat to the structural stability of the stone is granular disaggregation, or sugaring. These samples do not show evidence of sugaring and no potential durability issues were identified

Interior Dark Gray Stone (Dolomitic Breccia)

- Silicified dolomitic breccia described as clasts of uniform dolostone bound by recrystallized quartz. Locally quarried, though provenance could not be determined
- Sound and durable with no identified potential weaknesses within the bulk of the stone
- The veining is a potential weakness due to intrinsic properties iron oxide possess when exposed to wet/ dry cycles which may be the cause of the widespread cracking of the dark gray interior stone.

Mortar

- The natural cement mortars contain no lime as was typical of the time period.
- 1887 specifications indicated that the mortar joints were to be raked and repointed using Portland cement mortar after the stones had been laid in natural cement- a not uncommon practice of the time.
- The original natural cement mortars tend to have a moderate hardness and high permeability.
- Two later Portland cement-based mortars are also relatively permeable despite their cement-rich compositions.
- In one sample there is a minor incipient alkali-aggregate reaction (AAR) between the cement paste and the coarse limestone aggregate. Durability issues presented here are quite low.

Salt Identification-Potassium Salts

Carbonates

- Calcite is typically deposited from water that has passed through calcium hydroxide-bearing material including natural cement and Portland cement in mortars and concrete used to construct the masonry. When exposed to significant amounts of water, the free calcium hydroxide in these materials dissolves.
- Calcite deposits do not typically damage masonry. Rather, it is the underlying water infiltration causing the deposits that is likely to contribute to damage.
- Abundant calcite deposits also indicate depletion of the cementitious binder in mortar and concrete.

SYNTHESIS OF FINDINGS

Nitrates

- Nitrates in this context can derive from the decomposition of organic materials.
- Danger of supersaturated salt solutions filling masonry pores in cold weather and subsequent crystallization and damage during dry periods and higher temperatures.
- Nitrate contribution to the deterioration of the Monument is likely limited and confined to the base of the Monument.

Summary of Observed Conditions

Exterior

- Main concern on the exterior Sandy Hill dolomite is the severe level of scaling and spalling with small to moderately sized fragments of the stone falling from the monument. No large spalls noted near the base.
- The second typical condition is vertical hairline cracks. Efflorescence is found along these cracks adjacent to previous repairs
- Previous caulk repairs are likely trapping moisture, leading to efflorescence and/or carbonate crusts as a result of wet and dry cycles
- Mortar loss is another typical condition; the bedding mortar is completely disaggregated on the interior of the joints.
- Biological growth is typical. It appears to be concentrated on the stone units with heavier rustication, the top third of the monument, and the northwest and southwest corners.

Interior

- The interior is in fair to poor condition, with the stone being damp to fully saturated. This is concentrated at the corners
- Large cracks and separation at the joints were noted at the corners running the height of the obelisk
- Cracks are a typical condition for both limestones on the interior.
- This includes vertical and horizontal cracks running along the bedding planes of the stone and “alligatored” cracking. The combination of these two in certain stones creates a polygon pattern
- Several window lintels have hairline vertical cracks at the center of the stone running the full height of the unit
- Due to dampness in the bottom third, efflorescence and disaggregated mortar are found along the corners of the monument. This is in a thin and patchy condition.

SYNTHESIS OF FINDINGS

- In several locations the dark gray stone has eroded unevenly, leaving behind small, raised portions of unseated stone, likely due to the internal geology of the stone. This may have structural stress implications.

RILEM Surface Water Absorption Testing

RILEM Surface Water Absorption Tests were performed to analyze the rate at which water was absorbed by the exterior stone of the Monument. The goal was to gauge the absorptive capacity of the stone to understand how much water moving into the Monument is absorbed. This can help determine the rate of drying necessary of the stone, the interior of the Monument, and understand the variability of water that is absorbed versus water that is moving through the cracks and open joints.

Tests were performed only on the exterior of the Monument, as JBC attempted to perform RILEM surface water absorption tests on the interior masonry in order to understand and measure the porosity of the stone. However, all attempts failed because soiling, the friable surfaces of the stone and mortar, and the moisture already present in these materials prevented the adhesive putty required to hold the measuring tube in place from sticking to the surface. A general conclusion can be drawn that the interior stone is saturated to close to 100% capacity.

RILEM is an acronym for the International Union of Laboratories and Experts in Construction Materials, Systems and Structures (RILEM, from the name in French *Réunion Internationale des Laboratoires et Experts des Matériaux, systèmes de construction et ouvrages*) The organization was founded in June 1947, with the aim to promote scientific cooperation in the area of construction materials and structures. The mission of the association is to advance free-access scientific knowledge related to construction materials, systems, and structures and to encourage application of this knowledge world-wide.

Testing Methodology

A tube-like apparatus is used to measure the rate at which water is absorbed. This is affixed to the sample between the flat circular brim of the pipe and sample area. Water was added through the upper, open end of the pipe. The quantity absorbed was read from the tube every minute for five minutes, and the test was performed at four locations. All four locations were minimally absorbent; water is likely infiltrating at failed mortar joints.

Summary of Determinations:

- Based on BBM examination and nearby buildings constructed of similar materials, the conditions affecting the monument appear to be inherent to the properties of the Sandy Hill dolomite and locally quarried stone from Bennington, Vermont.
- The stone is in a petrographically sound condition
- The level of deterioration is consistent with the types of stone, age of the monument, and cycles of deferred maintenance.
- Moisture infiltration exacerbates many of the potential deterioration mechanisms

HANDS-ON ARCHITECTURAL ASSESSMENT OF EXISTING CONDITIONS

MATERIALS EXAMINATION - JBC



Image 33. Typical exterior condition. *Jablonski*



Image 30. Typical interior condition. *Jablonski*



Image 32. Typical interior condition. *Jablonski*



Image 29. Efflorescence and/or carbonate crusts below an earlier caulk repair. *Jablonski*



Image 31. Open joint near base of the monument. *Jablonski*



Image 28. Biological growth on surface of exterior stone. *Jablonski*



Image 39. Discoloration due to dampness in the corners of the observation platform. *Jablonski*



Image 36. Efflorescence and/or carbonate crusts along cracks and mortar joints. *Jablonski*



Image 38. Rust-colored crust on the surface of the dark gray stone. *Jablonski*



Image 35. Light efflorescence on the surface of the stone units and mortar joints. *Jablonski*



Image 37. Void between two stone units. *Jablonski*



Image 34. Uneven surface texture of dark gray stone unit. *Jablonski*



Image 45. Shallow spall. *Jablonski*

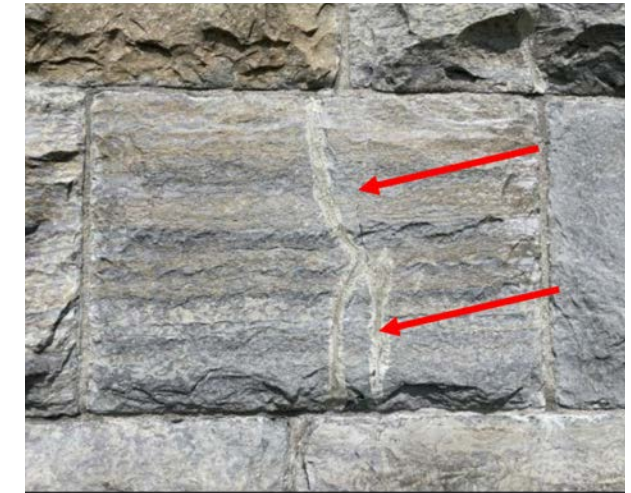


Image 42. Previously repaired crack and hairline crack extending from previous repair. *Jablonski*



Image 44. White growth along hairline crack. *Jablonski*



Image 41. Path of separation at the corner. *Jablonski*

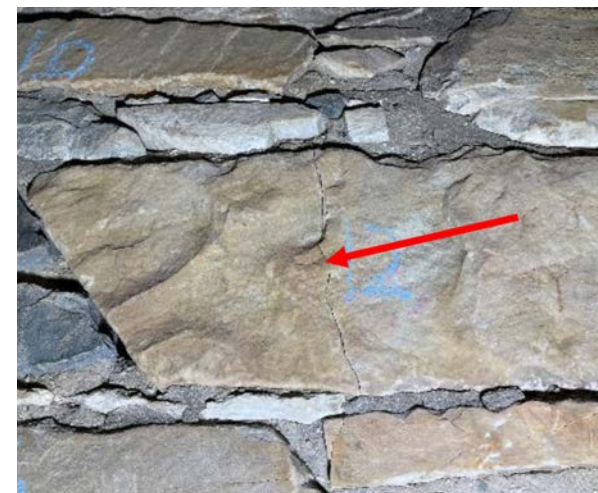


Image 43. Vertical crack. *Jablonski*



Image 40. Vertical crack running the full height of a window lintel. *Jablonski*

HANDS-ON ARCHITECTURAL ASSESSMENT OF EXISTING CONDITIONS

MATERIALS EXAMINATION - JBC



Image 51. Shallow spall. Jablonski

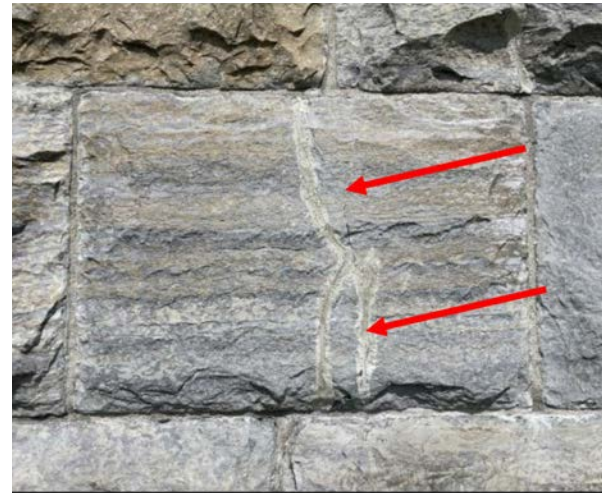


Image 48. Previously repaired crack and hairline crack extending from previous repair. Jablonski



Image 50. White growth along hairline crack. Jablonski



Image 47. Path of separation at the corner. Jablonski

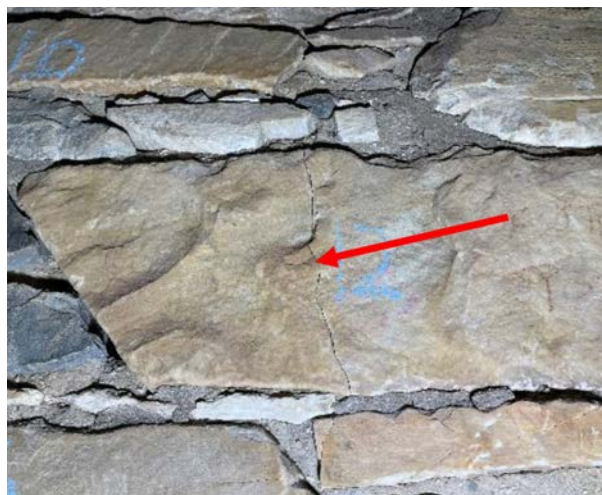


Image 49. Vertical crack. Jablonski



Image 46. Vertical crack running the full height of a window lintel. Jablonski

SYNTHESIS OF FINDINGS

- The top of the monument has seen the most repointing campaigns, and probably exhibits more of these deteriorations than the base of the monument which was studied.
- High cement content mortar is too hard compared to the stone, which could exert pressure on the stone to create microcracks and entrapment of moisture that can lead to cracking.
- The majority of the exterior mortar joints on the upper portion of the monument do not appear to be intact. Sandy Hill dolomite has a low water surface absorption rate (RILEM testing) which may cause infiltration openings in the exterior. These openings mean the interior stone and mortar have a high moisture content with the mortar particularly inundated.

A significant note is the observation that JBC states the stone cracking is not material, its structural. It was noted that a high percentage of the observed cracks are vertical through the stones and not along the natural bedding layers, suggesting that the forces cracking the stones are tensile likely caused by localized stresses. A differential moisture profile within the wall may also be contributing to the cracks due to the consistently wet interior stones being of a smaller face, marble, and as much as a third more open joints based on stone coursing. Flexural tension stresses may also be occurring locally near openings or where stones bridge missing or weakened mortar areas.

Landmark Facilities Group: (full report see Appendix XX)

Landmark Facilities Group (LFG) assessed the interior environmental conditions of the Monument, with both onsite work in May and June of 2023, and through intensive analysis of the data supplied from ANA. Understanding the interior environment of the Monument, the primary objective was to develop a method to reduce the saturation on the stone, and to reduce the overall relative humidity in the interior. The second objective was to provide an overview into the solution for managing the interior temperature and relative humidity, and the impact this solution would have on aiding the design team in developing the solution and duration for drying out the Monument.

Sources of Moisture within the Monument

There are two likely sources for the moisture found within the interior of the monument.

1. The first source is from water passing through the stone from the rain penetrating the exterior.
2. The second source is from condensation on the stone interior during certain periods of the year.

Since the stone has a large thermal mass, it likely stays cold enough to be below the outside air dew point well into the spring and summer. Since moisture in the air behaves like a gas, the moisture content of the air inside the monument will respond quickly to changes outside. As the higher dew point air hits the cold stone, it condenses. The ideal time for performing the intervention to dry the Monument is likely April to September.

Analysis of Monitoring Data

The data provided by Atkinson-Noland Associates shows the stone temperature within 9" of the interior surface of the stone and the interior space temperatures are very closely correlated. It reaches a high tem-

SYNTHESIS OF FINDINGS

perature of about 75°F in August and a low temperature of about 10°F for a short period in February. The cyclical range of temperature over the seasons also correlates closely with the range of temperature of the outside air. This is not surprising considering saturated stone offers very little insulating value (even when 84" thick!).

The monitoring data for the interior air in the monument shows the relative humidity experiences wide swings from lows of 30% to highs of 100%. These swings are occurring very rapidly, most likely in response to changes in weather. Starting in Late May through September, the RH swings are less dramatic and have lower peaks and higher troughs. The highs are down around 85% and the lows stay above 40%. The RH reduction starts roughly when the stone reaches about 70°F in late May and continues until the stone temperature drops below 60° in the fall. The fact that the RH peak values drop as the space warms seems to indicate that the moisture content of the air inside the monument is somewhat stable and that the saturated stone is not an unlimited source of moisture that causes continuous saturated air inside the monument.

Requirements for Moisture Removal

The first calculation is based on a formula for estimating the rate of evaporation from poured concrete. The formula was developed by Paul J. Uno based on the Menzel formula and uses the air temperature, material temperature and the air RH to predict the pounds of moisture per square foot of surface area. As expected, the evaporation rate is very near zero when the stone is cold (at or below the dewpoint of the air in the monument) and increases rapidly as the stone is warmed.

Based on this formula, and using the data collected by ANA, we arrived at 2 estimates:

- Average evaporation rate: 14 gallons per hour
- Peak summer evaporation rate: 61 gallons per hour

The second approach was based on analysis of the temperature and relative humidity data collected by ANA and converting the readings into the humidity ratio. The humidity ratio is defined as the ratio of the mass of water vapor in humid air over the mass of dry air in a body of air. The result is the pounds of water in the air per pound of dry air.

The approximate volume of air in the monument is roughly 96,000 cubic feet

Density of dry air equals 0.078 pounds/cubic ft-mass of dry air in the monument is roughly 7,500 pounds.

Since the humidity ratio (W) is known from the T & RH data, the pounds of moisture in the air can be calculated by multiplying the pounds of dry air by the humidity ratio. Judging from the T & RH data, the desired humidity ratio for drying out the stone is approximately 0.0038 pounds of water in the air per pound of dry air. On a peak day this is roughly 109 lbs of water or about 13 gallons of water. Assuming the monument has an air exchange rate of about once an hour when the entry door is open, the moisture removal rate to dry the stone calculates to a removal rate of about roughly 13 gallons per hour.

SYNTHESIS OF FINDINGS

Potential Volume of Water in the Monument

The testing to date has determined that the stone walls of the monument are saturated with water. The team has estimated the volume of stone comprising the monument roughly 150,000 cubic feet with roughly 5% of the volume being void spaces. If the stone is saturated as is believed, the water volume could be as high as 55,000 gallons.

Humidity Control

There are two primary means of removing moisture from the interior of the monument:

Natural Ventilation. Ventilation would involve introducing air at lower elevation of the monument and exhausting it at high elevation of the monument. Ideally this would be accomplished using the stack effect. Stack effect is the movement of air into and out of buildings and chimneys and is driven by air buoyancy.

Buoyancy occurs due to a difference in indoor-to outdoor air density resulting from temperature and moisture differences. The result is either a positive or negative buoyancy force. The greater the thermal difference and the height of the structure, the greater the buoyancy force, and thus the stack effect. If the air in the building is warmer than outside, this warmer air will float out the top opening, being replaced with cooler air from outside. If the air inside is cooler than that outside, the cooler air will drain out the low opening, being replaced with warmer air from outside. To develop a predictable ventilation rate in the winter, it may be necessary to introduce some heat within the monument to create a buoyant force.

Mechanical ventilation. Mechanical ventilation would require the use of a fan to exhaust the air from the structure. The most practical method would be to have a fan above the observation level drawing air from below the observation level and pressurizing the space above the observation level, so air was pushed out of the vents to the exterior. The challenges related to introducing ventilation are:

The observation level creates an obstruction to free ventilation between the bottom 200' of the monument and the roughly 100' above the observation level.

The ventilation would need to be controlled by monitoring inside air conditions and outside air conditions and only ventilating when the outside air had a lower moisture content than the inside air.

Dehumidification

Dehumidification would require a mechanical system to reduce the moisture content of the air and drain the moisture away from the interior. It may be possible to locate numerous dehumidifiers on the various stair landings below the observation level.

Sources of Heat

If it is determined that adding heat to the air in the monument to create a more predicable buoyant force for natural ventilation, the potential heat sources include Fuel Fired Boiler and Geothermal Heat Pumps.

SYNTHESIS OF FINDINGS

Fuel Fired Boiler

A fuel-fired boiler would have to be located remotely and steam or hot water piped underground to the monument-similar to what was done in the past.

Geothermal Heat Pumps

It may be feasible to locate water-to-water heat pumps in the basement of the monument tied to a geothermal loop field in the ground surrounding the monument. Geothermal heat pumps are an efficient way to produce heat.

Steven Winter Associates: *(full report see Appendix XX)*

Steven Winter Associates (SWA) was engaged to analyze the hygrothermal properties- heat and moisture as it relates to movement through a building or structure- of the masonry walls of the monument, which are currently saturated. SWA performed an analysis of the masonry wall to study options to promote drying of the masonry. The basis for this evaluation was the utilization of WUFI Pro 6.7 software to simulate the existing masonry wall assembly and options to promote drying.

WUFI software simulates one-dimensional dynamic models; as described by its developer, it “allows realistic calculation of the transient coupled one- and two-dimensional heat and moisture transport in walls and other multi-layer building components exposed to natural weather”. WUFI is a German acronym that stands for “*Wärme-und Feuchtetransport instationär*”. This translates in English to “Transient Heat and Moisture Transport”. This software is typically used to analyze and optimize hygrothermal properties of proposed exterior wall assemblies and is used here to evaluate how climate may be manipulated to optimize drying of the currently saturated masonry.

The simulation parameters were established from the petrography results, mortar tests, RILEM tests and Goodman Jack tests, to establish the input for the dynamic modeling. The reports reviewed include:

- Structural Engineering Evaluation, prepared by Silman and dated December 15, 2022
- Materials Examination Report prepared by Jablonski Building Conservation, Inc., (JBC) dated October 2023
- Stone Masonry Evaluation prepared by Atkinson-Noland & Associates, Inc. (ANA), dated September 20, 2023
- Monitoring Data Summary, prepared by ANA, dated March 4, 2023.

For additional material selection parameters, and calibration data, please refer to page 3 of the SWA report. Of all the variables that were manipulated, reduction of interior climate relative humidity was most effective for reducing masonry total water content (refer to Appendix A - WUFI Analysis, South Masonry Wall - No Added Moisture + Reduced Interior RH models, Pages 9-14 of SWA Report).

This model includes a combination of both the elimination of additional moisture source and reduction of interior relative humidity from the existing 72% RH with a 50% amplitude to 60% RH with a 20% amplitude. The elimination of additional moisture source represents repair of exterior masonry wall

SYNTHESIS OF FINDINGS

surfaces: repointing existing open mortar joints and repairing cracks that facilitate water infiltration. As water infiltration through the masonry wall is a primary contributor to elevated interior humidity, eliminating the additional moisture source is necessary to reduce interior relative humidity.

The most significant observation from the WUFI Model Analysis is to reduce interior elevated humidity by optimizing ventilation. This is in direct correlation with Landmark Facilities Group assessment, this may be achieved by passive or mechanical methods during optimal weather conditions, such as when exterior relative humidity is lower than interior relative humidity (generally during spring, winter and autumn). Consider strategies to improve ventilation and reduce humidity for a temporary period before repair campaign commences, temporarily during construction and by more permanent methods after completion of construction.

Langan Engineering: *(full report see Appendix XX)*

Langan Engineering was retained to provide a geotechnical engineering assessment on the grounds of the Monument to obtain necessary information on subsurface conditions and provide geotechnical related recommendations for a scaffolding system and covered walkway as well as verifying the depth to bedrock and the adequacy of the bedrock to support the loads imposed by the Monument that would be required for the proposed restoration work.

SUBSURFACE EXPLORATION AND FINDINGS

The subsurface exploration program consisted of drilling three geotechnical borings identified as B-1 through B-3 and installing a groundwater observation well in completed boring B-3. The borings were located at about 30 feet away from the monument. The borings were drilled by Cascade Remediation Services, LLC on 17 and 18 January 2024, under the full-time observation of a Langan engineer.

A groundwater observation well was installed in completed boring B-3. The well consisted of 10 feet of 2-inch-diameter Schedule-40 PVC slotted-pipe (screen) and a solid riser PVC-pipe extending to ground surface. The annulus around the pipes were backfilled with filter sand to about 2 feet above the screen and sealed with a 2-foot-thick layer of bentonite pellets. A protective flush-mounted steel well cap was installed at the ground surface.

SUBSURFACE CONDITIONS

The subsurface stratigraphy at the site consists of a layer of topsoil underlain by sandy clay, and then competent bedrock. A description of each stratum is given below in order of increasing depth.

Topsoil

A layer of topsoil was encountered immediately below the ground surface. The topsoil generally consists of brown fine to medium sand, with varying amounts of silt, and gravel and extends up to about two feet below grade.

SYNTHESIS OF FINDINGS

Sand and Sandy Clay

Below the layer of topsoil, a layer of brown, fine sand, with varying amounts of clay, silt and gravel was encountered in B-3(OW) and extended to a depth of about 5 feet, corresponding to about el. 862. The sand is classified generally as SC (clayey sand) in accordance with USCS.

Bedrock

Bedrock was encountered beneath the sand/clay layer in all three borings and depth to bedrock was observed to be vary from about 7 to 12 feet below the existing ground surface.

Groundwater

Groundwater level was monitored in the observation well installed in boring B-3(OW). The ground water level was measured at the end of the second day of our subsurface exploration. The measured static groundwater was about 10 feet below grade corresponding to about el 857. In general, the groundwater level was recorded within about two feet of the top of bedrock surface, indicative of potential “perched” water conditions.

Laboratory Testing

Laboratory tests were performed on selected rock and soil samples to define physical and mechanical properties. The laboratory tests consisted of:

- Two Sieve Analyses (ASTM D 6913)
- Two Atterberg limit Tests (ASTM D 4318)
- Two Rock Unconfined Compressive Strength (ASTM D 7012)

Existing Monument

In review of the Elevation Plan prepared by Langan in Phase 1 (Drawing No. EL-01 to EL-04), dated 11 May 2022, it is understood that the basement level is at about El. 860. The subsurface profile observed during the subsurface investigation encountered bedrock at varying elevations from El. 856 to El. 861. When comparing the elevation of the below grade level now with the depth to rock within the borings, it is believed that the existing monument is bearing on bedrock. Based on the borings performed at the site and discussions with Silman, it is believed that the foundations of the monument were likely proportioned for an allowable bearing capacity of about 10 tons per square foot (tsf).

When structures are bearing on bedrock and load is applied, there is not a traditional settlement of the structure, but more of a compression of the rock surface. We note that since the monument is believed to be bearing on bedrock, we anticipate that when the monument was constructed it likely exhibited compression of the rock surface on the order of ½ inch or less. If additional loading is planned to be applied to the existing monument structure or foundations, we recommend that a test pit excavation be performed to identify the size, character and bearing material of the existing foundation.

The data provided, and the appendices in Langan’s report support the structural approach that would be undertaken when the design of a scaffolding and covered walkway system is commenced. The considerations of ground water, uplift, seismic, bearing capacity on bedrock and additional loading on the

HANDS-ON ARCHITECTURAL ASSESSMENT OF EXISTING CONDITIONS

GEOTECH DRILLING



Image 52. Geotech Drilling. Stevens & Associates 01.17.2024



Image 55. Geotech Drilling. Stevens & Associates 01.17.2024



Image 53. Geotech Drilling. Stevens & Associates 01.17.2024



Image 56. Geotech Drilling. Stevens & Associates 01.17.2024



Image 54. Geotech Drilling. Stevens & Associates 01.17.2024



Image 57. Geotech Drilling. Stevens & Associates 01.17.2024

SYNTHESIS OF FINDINGS

Monument (external anchoring, covering, stabilization, etc.) raise key issues for consideration, with the data providing the basis for the engineering design work required. This is addressed in our Project Planning Phase.

Smokestack Lightning: Lightning Protection Design (full report see Appendix XX)

On Wednesday September 13th, 2023, a representative from Smokestack Lightning Inc. completed a visual inspection of the lightning protection system at the Monument. The results of the inspection are based on compliance with NFPA (National Fire Protection Association) 780, UL (Underwriters Laboratories) 96a and LPI (Lightning Protection Institute) 175 standards for lightning protection system installations. NFPA 780 and Ula 96 work in tandem as standards, and essentially provide guidelines for lightning protection systems. The major point is that lightning protection is not a code requirement, but an option and the National Fire Protection Association and the Lightning Protection Institute provide guidelines for best practices for design, installation, and inspection.

There are five (5) major components that make up the lightning protection system. These are:

- Air Terminal
- Conductor
- Grounding
- Common Bond
- Surge Protection

The existing system consists of 1 class II copper air terminal/lightning rod and 2 class II copper conductors that extend through the interior of the monument and leave the structure below grade. Class II conductors interconnect and carry current between strike termination devices and grounding electrodes on structures higher than 75' in height. The bulk of the system components that are installed are in place and in good condition, but there are deviations from the standard and issues of corrosion and deterioration that need to be rectified for full compliance. The largest issue is the design of the system with a single air terminal at the peak rather than additional air terminals at lower levels.

Overall, the lightning protection system components are in good condition, but there are maintenance issues and deviations from UL, NFPA and LPI standard that need to be addressed for full compliance. The original design of a single air terminal does not comply with NFPA 780 requirements and could potentially allow for lightning strikes to the lower sections of the tower. This report recommends further investigation of the condition of the grounding components of the lightning protection system and repairs and upgrades for full compliance with NFPA 780, UL 96 and LPI 175 standards.

The primary question becomes to what level of standards does the state want to meet with the protection system, and to what degree do they want to upgrade/repair or replace the entire system. With the overall budget we are looking at, a newly designed and installed system would be advisable to provide the highest degree of structural safety for the Monument and provide the highest level of protection (or insurance if you will) for the investment in restoring the Monument.

HANDS-ON ARCHITECTURAL ASSESSMENT OF EXISTING CONDITIONS LIGHTNING PROTECTION



Image 58. 1/2" diameter class II copper air terminal mounted with bolted copper strapping to star finial. *Smokestack Lightning.*



Image 60. Bolted connection from air terminal to class II copper lightning conductor. *Smokestack Lightning.*

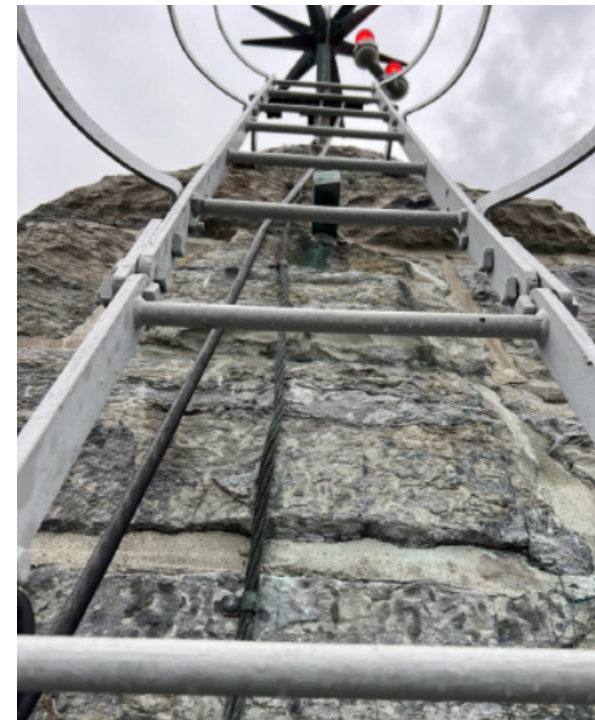


Image 59. Access ladder is directly over the main lightning conductor, bonded to the lightning protection system at the base of the ladder through a thru bolt into the tower. *Smokestack Lightning.*

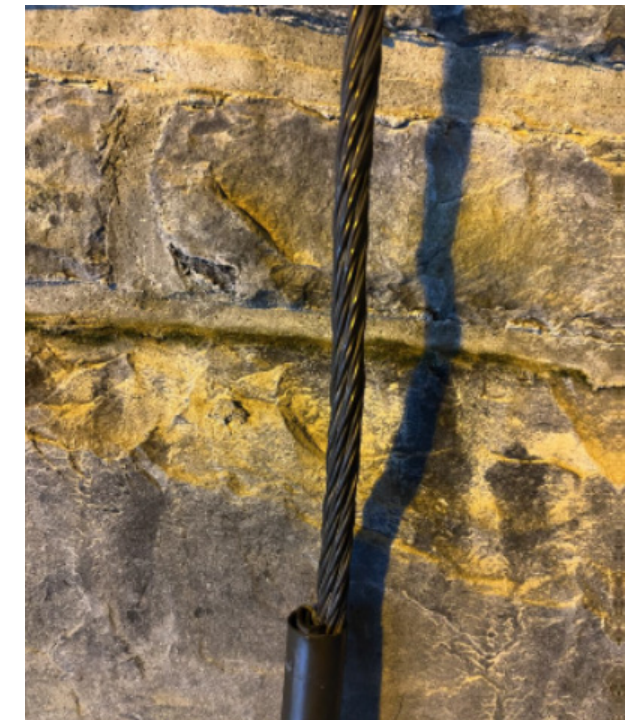
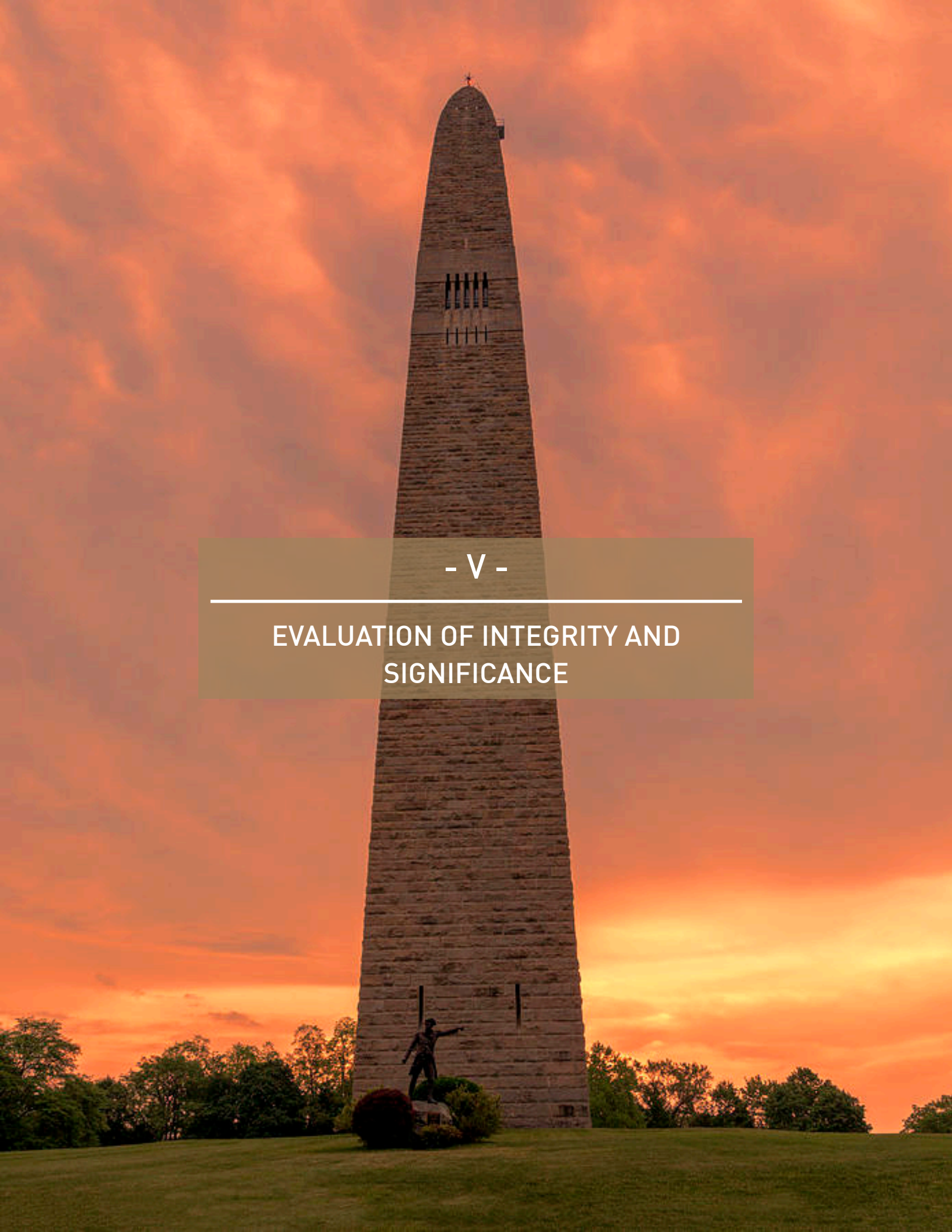


Image 62. Conductors are protected by a copper conduit. *Smokestack Lightning.*



- V -

EVALUATION OF INTEGRITY AND SIGNIFICANCE

EVALUATION OF INTEGRITY AND SIGNIFICANCE

Evaluation of Integrity and Significance

Introduction

The Bennington Battle Monument is an undeniably significant architectural structure with deep historical and cultural legacies, expressed in tangible and intangible ways. The design of all conservation and preservation work shall therefore be grounded in established preservation philosophy and concepts of significance, historic integrity, and precedents set by the site's unique development.

Significance – National Park Service

The Bennington Battle Monument is listed on the National Register of Historic Places, and it commemorates a significant battle during the Revolutionary War that ultimately led to our nation's independence. The monument possesses multiple levels of significance through its long, rich and varied histories from a pivotal battle ground for the American revolution, and as one of only very few unreinforced masonry obelisks in the country.

Integrity – National Park Service

The National Park Service's definition of Integrity is the ability of a property to convey its significance. Historic properties either retain integrity (that is, convey their significance) or they do not. To retain historic integrity a property will always possess several, and usually most, of the Seven Aspects of Integrity. Determining which of these aspects are most important to a particular property requires knowing why, where, and when the property is significant.

- **How does the National Park Service assess Integrity?**
- Integrity is the ability of a property to convey its significance. Historic properties either retain integrity (that is, convey their significance) or they do not.
- To retain historic integrity a property will always possess several, and usually most, of the seven aspects.
- Determining which of these aspects are most important to a particular property requires knowing why, where, and when the property is significant.

Integrity is evaluated according to seven aspects:

The Seven Aspects of Integrity

- *Location:* Location is the place where the historic property was constructed or the place where the historic event occurred.
- *Setting:* Setting is the physical environment of a historic property. It refers to the historic character of the place in which the property played its historical role. It involves how, not just where, the property is situated and its historical relationship to surrounding features and open space.

EVALUATION OF INTEGRITY AND SIGNIFICANCE

- **Design:** Design is the combination of elements that create the historic form, plan, space, structure, and style of a property. This includes such elements as organization of space, proportion, scale, technology, ornamentation, and materials.
- **Materials:** Materials are the physical elements that were combined or deposited during a particular period and in a particular pattern or configuration to form a historic property.
- **Workmanship:** Workmanship is the physical evidence of the crafts of a particular culture or people during any given period in history. It is the evidence of artisans' labor and skill in constructing or altering a building, structure, object, or site.
- **Feeling:** Feeling is a property's expression of the aesthetic or historic sense of a particular period of time. It results from the presence of physical features that, taken together, convey the property's historic character.
- **Association:** Association is the direct link between an important historic event or person and a historic property. Property retains association if it is the place where the event or activity occurred and is sufficiently intact to convey that relationship to an observer.

EVALUATION OF INTEGRITY AND SIGNIFICANCE



Image 64. Early stage of construction. Cranes on the ground are used to lift masonry units during the early stages of construction.

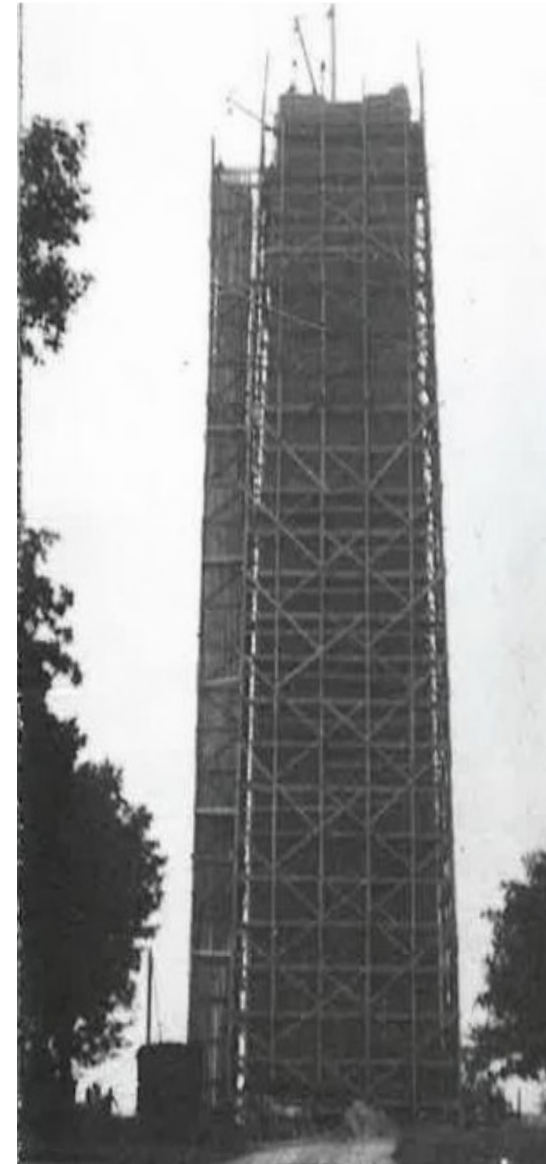


Image 67. Photograph of the Monument. Cranes are added at higher elevations, placed within the BBM's footprint. *Bennington's Battle Monument: Massive and Lofty*

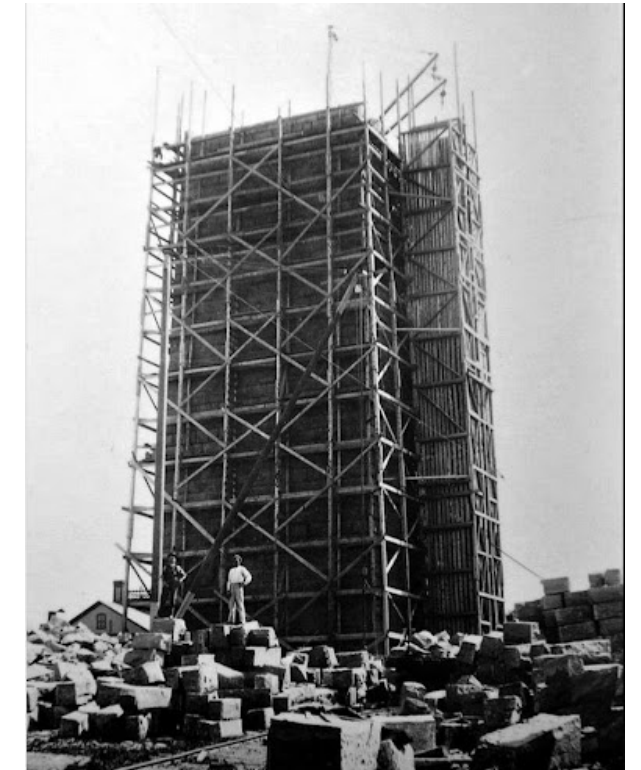


Image 66. Scaffolding surrounds the monument when its height clears the limits of cranes.



Image 65. The Monument in a later construction stage. Scaffolding continues to rise.

ARCHITECTURE & PRESERVATION

Architectural Restoration and Preservation

The development of Primary Factors of Consideration is important in understanding the key components that are contributing to the deterioration of the Monument, we can apply the information gleaned from the tests and analyses and draw conclusions on what is the best course of action for the restoration, rehabilitation and repair and maintenance of the Bennington Battle Monument.

Based on the observations, analyses and results of the consultant team, it is now possible to organize a preservation methodology for the preparation of a Restoration Project Approach with directives on developing a prioritized scope of work that provides a comparative analysis of the physical with the archival information to be used to synthesize these elements into a clear preservation philosophy and methodology that will balance aesthetic concerns with technical.

Our own charting of the previous repair campaigns and the current assessment of the deterioration of the Monument enables us to be particularly attentive to patterns of behavior or failure as a method of determining large-scale or persistent building conditions. Based on information gathered in these reports, we can now identify opportunities and constraints and evaluate their relevance to the project objectives and budget. Recommendations will be prioritized by *Immediate Life Safety Hazards, Stabilization, Full Scale Restoration, and Ongoing Maintenance*. The analysis shall address and clearly present the key issues identified including:

- Life safety hazards and required stabilization
- Deferred maintenance - major renovation/restoration
- Preventive maintenance/minor repair or replacement
- Restoration and preservation issues
- Physical constraints imposed by the original fabric
- Appearance
- Regulatory requirements such as the State Building Code (IBC), State Historic Preservation Office (SHPO) and the National Park Service (NPS)
- Time and schedule constraints
- The facility's ongoing operational requirements

The primary factors for consideration are categorized as follows: *Masonry; Moisture & Humidity; and Building Systems/Vertical Access*.

PRIMARY FACTORS OF CONSIDERATION: MASONRY

Phase 1 provided charting of the exterior and interior damage to the Monument, including cracks, spalls, and previous repair campaigns that are contributing to the deterioration, and this work was completed

- VI -

ARCHITECTURE & PRESERVATION

by Vertical Access in the beginning stage of Phase 2. In general, a singular cause of cracking has not been identified, but rather several potential contributing factors have been established, including the following:

Stone

- The dolomitic stone is harder and stronger than calciferous limestone but is nonetheless sedimentary stone that is porous and permeable. Cracks and fissures natural to the stone have occurred over time, and also as a result of quarrying, which is not atypical. These cracks are non-structural, but a potential outlet for water transmission.
- Some stones laid with their bedding plane, others laid against, or vertical, allowing for stresses to “slice” through the bedding plane, instead of being “stacked.”
- Cracking on the exterior stones and deterioration of the mortar joints is widespread on all four sides of the Monument. South and West faces of the monument have the most cracked stones and prevalent surface loss (exfoliation). Possibly because of exposure to prevailing winds and harsh weather, as well as solar energy.
- Cracks through single stones are common on all elevations at all heights.
- Crack systems were commonly observed below the observation deck level, and typically extended through five to ten horizontal courses.

Mortar

- While the original specification for the Monument specified a hard Portland cement mortar, none of the tested samples or visual observations found evidence of this original mortar still being present. Testing revealed all the mortar samples to be a soft Rosendale natural cement mortar. The material conservator confirmed that the type of mortar used during construction was appropriate for the Monument. However, significant mortar loss is present on the Monument due to freeze-thaw cycles, thermal action, and deferred maintenance. Improper prior mortar repairs with caulking and hard mortars may have contributed to damage of the masonry. Additionally, a moderate alkali-aggregate reaction (AAR) was observed in mortar removed from the interior of the wall.
- While AAR is often deleterious to masonry, if the scale of the reaction observed in the select sample is representative of the overall Monument condition it is not a cause for concern. While it is not believed that issues with mortar type or open joints were the cause of initial cracking, they do allow for significant moisture ingress that can contribute to a variety of deterioration methods over time. Continual appropriate maintenance and regular repointing campaigns will be necessary to keep water out of the Monument.
- Both the original mortar and repointing mortars on the monument do not appear to have the preferred qualities of a soft cement lime-based mortar. This doesn’t allow the mortar to be the “sacrificial” material and instead binds the stone to the mortar, transferring stress to the stone.

Freeze-Thaw Cycles

- Visual observation of the exterior found that a high percentage of the previously repaired cracks are no longer protected from bulk moisture migration because the sealants used 30 years ago are failing. Thus, water ingress into and through the stone wall remain trapped, and subject to the cycling of freezing and thawing resulting in masonry deterioration and frost jacking.

Moisture and Humidity

- Damp interior; continuous water infiltration; freeze/thaw cycle and frost jacking

Local Stresses

- High percentage of the observed cracks are vertical through the stones and not along the natural bedding layers, suggesting that the forces cracking the stones are tensile likely caused by localized stresses.
- A differential moisture profile within the wall may also be contributing to the cracks due to the consistently wet interior stones being of a smaller face, marble, and as much as a third more open joints based on stone coursing.
- Flexural tension stresses may also be occurring locally near openings or where stones bridge missing or weakened mortar areas.

Headers & Wall Construction

- At the lowest level of the monument, data suggests the header stone (40” to 60” thick does not extend all the way through the wider wall. The general stiffness of the wall is different where there are full through-wall header stones as opposed to “Cross-headers.”
- Interior bonding was done with a cement aggregate, essentially tying the wythes together and prohibiting natural expansion and contraction. This unreleased force can contribute to cracking.
- More crack systems were observed in the lower portion of the Monument- this is further addressed in our graphic charting of the cracks and where previous repair campaigns occurred. (and referenced in our section *Impact of Previous Repair Campaigns*)

Loading

- Silman’s analysis indicates that a current code level extreme seismic event would cause tension and compression stresses beyond the assumed allowable stresses of the masonry. By code it is not required to seismically upgrade the structure, but any repair options should consider performance-based design for future earthquake loads.

PRIMARY FACTORS OF CONSIDERATION: MOISTURE & HUMIDITY

- Temperature and humidity monitors with over one-year in data have monitored the conditions of the monument.

- Two of these monitors exist in the interior side of the masonry walls, and one exists to measure interior climate conditions.
- The two installed in the walls have rested at 100% RH for their monitoring period, with the one mounted on the wall inside averaging 72% with fluctuations between 15% and 100% RH.
- To reduce interior humidity, the first step will be to reduce water infiltration which is the primary source for interior atmospheric humidity.
- To reduce water infiltration through the masonry walls, design repairs are required to minimize infiltration liquid water while maximizing water vapor transmission to enhance outward drying of the masonry walls.
- In general, the upper half of the Monument typically has more signs of moisture than the lower elevations. An exception is that the below grade basement walls were observed to be damp in all visits, especially in the fall and spring. In the winter, a large area of ice was observed along the middle of the south wall below the sub-observation level and extending multiple landing heights down.
- Readings of moisture meters report a 100% relative humidity for extended periods of time and have rarely decreased. This held true over the summer months when Bennington was experiencing moderate drought conditions.
- ANA's tests in May, 2022 show that the relative humidity sensors, TH02 and TH03, that are sealed within the stone masonry walls, are showing values greater than expected.
- After one week they normalize at a 100% relative humidity and show the wall to be waterlogged after a few weeks of measuring.

PRIMARY FACTORS OF CONSIDERATION: BUILDING SYSTEMS:

HEATING/ELECTRICAL/ACCESS

Elevator:

- The original Otis machine from 1956 is leaking oil and makes a noticeable ticking noise that is believed to be bearing chatter. These may forecast a seized bearing, which could be a major and costly service event.
- Various sensors in the shaft consist of magnetic tape and copper contacts that usually need to be serviced or replaced every few years. These sensors malfunction multiple times a year despite being replaced and/or cleaned annually. The elevator shuts down when these sensors malfunction.
- Many parts are replaced semi-annually or annually due to high moisture conditions even when components should last much longer.

- Moisture intrusion from foundation walls in the basement disturbs the equipment.

Stairs:

- Seven metal framed floor levels, thirty-three staircases and landings, and steel framed elevator shaft.
- The main stairs were constructed in 1891 with selected repairs in 1987 and are best characterized as emergency stairs/ a fire escape as they do not meet dimensional requirements for standard egress stairs for public use.
- Coatings have failed and steel members show corrosion especially in embedded locations and bolt holes.
- Cast iron elements have brittle cracks where loading has compromised the base metal. Floor plate cracks, tread cracks, missing bolts, broken treads and deteriorated flanges, gaps in framing connections, unsupported beams, broken floor panels, differing riser slopes have been observed.
- Steel channels are not detailed to restrict corrosion and significant metal loss and failure.
- Bearing conditions of steel members have been compromised as the mortar decayed and has allowed the stone bearing shims to become unrestrained and, in many cases, dislodged.
- Stair landings supported by varying bearing conditions. Corrosion noted on all conditions, and loss of support was occasionally noted, primarily at stone ledger supports.
- Spiral staircase has a few brittle cracks and lateral ties to horizontal walls are heavily corroded.

PRIMARY FACTORS OF CONSIDERATION: BUILDING SYSTEMS:

HEATING/ELECTRICAL/ACCESS

- Rolled steel, such as supporting beams, is more prone to lamellar corrosion that causes expanding and flaking leading to rust jacking between the rolled steel beams and cast steel plates.
- Corroding beams induce stresses on the cast steel plates occasionally leading to fracture.
- UT Testing showed stair stringer beams near embedded corroded beam were nearly 12% less thick than original material.

Electrical:

- The current terminal, as originally designed, is in good condition but has flaws at connections across the monuments. The lack of fail-safe further puts the monument at risk for sever damage in a lightning strike that would overwhelm the system as currently in place.
- There is no backup electricity system in case of global failure.
- There is no surge protection on the main electrical service panel in the monument

- Several generations of abandoned and failed light fixtures throughout the monument.
- Not all emergency light fixtures work, creating unsafe conditions.
- Stairwell is not adequately illuminated to NFPA 101 performance requirements.
- Unclear if the newer emergency lighting battery unit equipment is suitable for cold weather operation.
- Several different wiring and conduit systems.
- Conditions of existing systems vary from serviceable and good, to rusted, deteriorating, and abandoned.

HVAC/Heating:

- There are no HVAC systems in the Monument today, though the abandoned remains of a former steam fed heating system still exists. These were fed via a boiler in the visitor center, which was removed, the pipes capped and extant between the two buildings.

Impact of Previous Repair Campaigns

The next factor to consider is the adverse effect previous repair campaigns have had on the performance, and deterioration, of the Monument. Our team is respectful of the stewardship the State of Vermont has shown to the Monument since its completion, and hindsight is not necessary, and no criticism of the maintenance is intended, insinuated, or directed. We are currently the benefactors of tremendous gains in material science investigation, conservation analysis, structural and building integrity modeling, and the continuous development of advanced restoration strategies, techniques, material and building technology, and workmanship. While the past cannot be undone, we can ensure that best practices will be applied now and in the future. We have charted the previous repair work performed on the building on elevation drawings in an to advance the theory of deterioration caused by this repair work. This can assist us in evaluating the result of natural degradation versus the impediments of the repair techniques that has exacerbated and accelerated the degradation.

- Previous repointing/mortar repair campaigns focused on the exterior and interior of the upper third of the monument. These replacement mortars, as well as other campaigns on the Monument, were too hard for the masonry, leading to cracking.
- Previous repair campaigns of the monument are not recommended by contemporary conservation standards, particularly caulk repairs and hard cementitious repairs.
- These campaigns removed traces of the original mortar, though forensic samples reveal that a black-colored mortar was found in joints as well as along the windows of the main shaft.
- Many cracks have been previously repaired by infilling the cracks with a bead of sealant. Other crack repairs include cementitious mortar repairs in wider or routed out cracks, and epoxy injection repairs in narrower cracks.

- Hazardous conditions involving sizable pieces of stone and loose material from failed patch repairs that are loose and have fallen.
- Sealant used for repairing a high percentage of cracks is failing, cracking, and separating from the stone surfaces. The failed sealant traps moisture within the wall and slows down the natural drying process.
- Wider cracks repaired with mortar are failing.
- Biological growth is noted in a percentage of mortar joints.
- Bronze U-shaped straps, or “staples,” are visible on the surface of cracked stone units. Oriented horizontally and generally covered with a urethane sealant, though some are encased in mortar.

Drawings

The chart on page 63 and subsequent drawings through page 69 represent a chronology of the past repair campaigns, with a graphic overlay to the existing conditions that were noted in Phase 1 by Vertical Access. The purpose of this analysis was to visually note any correlation between documented damage and the location as it relates to repair work. As of this DRAFT we can tentatively confirm that spalling, salt leeching, eroded/missing mortar, exfoliation, and surface deterioration is related to the earlier repair campaigns.



Image 72. Typical exterior rock-faced, coursed Sandy Hill dolomitic limestone ashlar. *Jablonski*

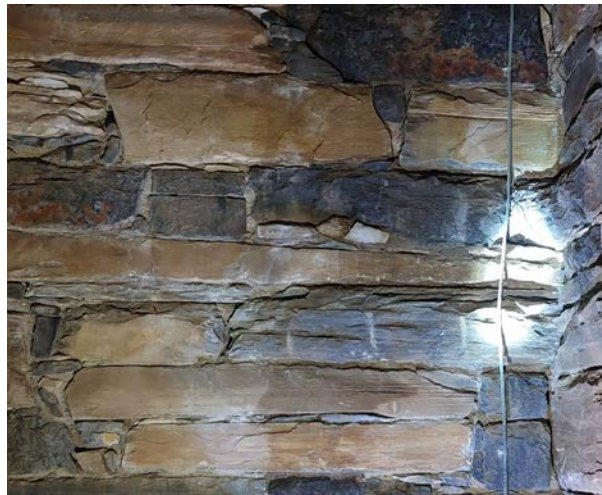


Image 73. Typical interior marble



Image 74. Caulk repair and current core hole



Image 75. Bronze staple condition through crack. *Easton Architects*



Image 79. Spall removed from the exterior stone masonry. *Vertical Access*



Image 78. Spall removed from the exterior stone masonry. *Vertical Access*



Image 76. Delamination in a stone at the upper portion of the monument. *Vertical Access*



Image 77. Exterior of monument with cracks highlighted in red. Note that most cracks fall below a vertical mortar joint. *JBC.*



Image 84. Cracked and failed parge coat applied over the face of a stone. *Vertical Access*



Image 85. Failed mortar joint at upper portion of monument. *Vertical Access*



Image 82. Cracked and spalled cementitious patch repair. *Vertical Access*



Image 83. Carbonate deposit (White material) below an epoxy crack repair. *Jablonski*



Image 80. Scaling in a stone at the upper portion of the monument. *Vertical Access*



Image 81. Heavy accumulation of carbonate material leached from a cracked and deteriorated mortar joint. *Jablonski*



Image 86. Original heating system and piping. *Stevens & Associates*



Image 90. Cracks creating an "alligatored" pattern, with white efflorescence along the cracks. *Jablonski*



Image 87. Corner condition at top of monument. *Stevens & Associates*

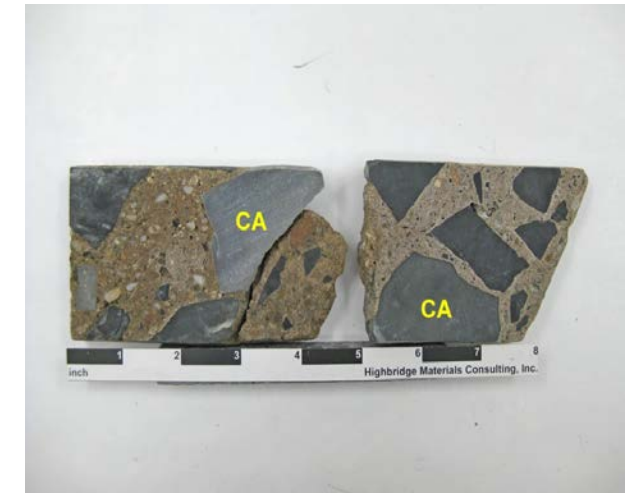


Image 91. Section through sample ANA-South-4 showing large, crushed limestone aggregate in paste of cement. *Jablonski*



Image 88. Ladder to Level A, above elevator mechanical room. *Stevens & Associates*

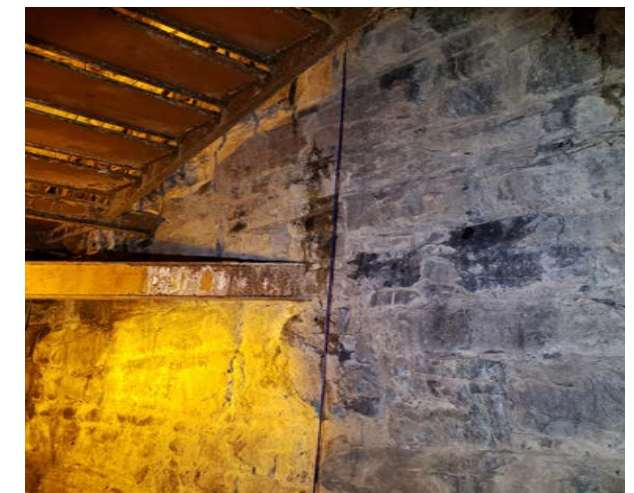


Image 89. Typical condition of stair support meeting masonry. *Stevens & Associates*

DATE	ITEM	ACTION	LOCATIONS	SOURCE
18-Aug-31	Bennington Evening Banner reports that August Lukeman, a famous sculptor living in Stockbridge, Massachusetts, said "within 25 years BBM will crumble on its own weight" while visiting the monument and accompanied by Joseph Franz, engineer, also from Stockbridge, Massachusetts.	OBSERVATION		SILMAN
1953-1954	The monument was considered badly deteriorated. A stone the size of a man's hand fell off the top and on July 1.	STONE FELL OFF		
1954-1955	Masonry repairs by Hayes & Coffey Company, Charlestown MA were performed on the top 100 feet. The monument was repointed. Bronze pins were driven into cracked stone.	REPOINT; BRONZE PINS IN BOTTOM	TOP 100' BOTTOM OF MONUMENT	SILMAN NPS National Register Filing
1955	Elevator added.	ADD ELEVATOR		
1959	The top 30 feet of the monument were repointed and the stone waterproofed with a silicone coating.	REPOINT; SILICONE COATING ON STONE	TOP 30' OBSERVATION LEVEL	SILMAN STEVENS & ASSOCIATES
1964	Windows installed in the observation level.	WINDOWS INSTALLED		
1965-1979	Thomas B. Oakes, an engineering consultant from the Vermont State Department of Administration prepared a report entitled "A Restoration Program for the Bennington Battle Monument." Within the report he indicated the signs of deterioration, including stone cracking near the corners, localized vertical cracking of stone between mortar joints, efflorescence on the inside walls, and disintegration of mortar of the interior masonry. He recommended the restoration begin as soon as possible with the following items: -Repoint all interior mortar joints; reset loose stones -Inspect all points where steel construction is embedded in masonry -Install metal liners and louvers at all exterior vent openings -Grout the walls to fill all stone voids -Repoint exterior mortar joints with expanding type mortar with the final 1/2" inch being a silicone flexibles ealant -Waterproof the exterior side Based on documents provided by the State, non of this was confirmed to have been carried out.	NONE		SILMAN
Fall 1980	The South wall was repointed from "upper horizontal joint of the lower of the two smooth stone belt courses running around at the approximate level of observation deck" approximately the top 90 feet of structure.	REPOINT	TOP 90'	SILMAN
21-Jul-81	Contract with Raymond E. Kelly Inc. of Bowmansville, New York for repairs to the monument. This included repair mortar joints and stone cracks in three walls (north, east, and west) of the upper third of the monument and apply two coats of water repellent. All exterior masonry surfaces, including joints to be treated with Flood coats of waterproofing equal to Cabot's Clear Cement Waterproofing (without silicone - for limestone) and at a coverage not greater than 75 square feet per gallon. Weeps were also placed in the relief joints even though there was no indication of them in the project specifications. Emergency repairs to stairs and landings completed.	REPAIR MORTAR AND CRACKS IN NORTH, EAST, AND WEST WALLS; APPLY TWO COATS OF WATER REPELLANT; ADDITION OF WEEPS IN RELIEF JOINTS	UPPER THIRD	SILMAN
1987	Monument restoration study initiated by Ryan-Biggs Associates (RBA), over time includes masonry, metal, and stair restoration reports. A small steel balcony was attached to the monument's upper-most portal (to capstone) (p29). In the early 1990s the monument was again scaffolded while another expensive round of repointing was completed on the exterior masonry, and a small steel balcony was placed beneath a new ladder that leads from the uppermost door to the very summit. (p37).	EMERGENCY REPAIRS BALCONY ADDED	UPPERMOST PORTAL	SILMAN <i>Bennington's Battle Monument: Massive and Lofy</i>
Late 1980s	The exterior of the Bennington Battle Monument was fully repointed in the late 1980s, with multiple later limited repointing campaigns on the top portion of the monument. The interior of the monument has been repointed at the observation deck and inside the top 100-feet. The corners of the interior appear to have had numerous repointing and repair campaigns. At the base of the monument, large bronze staples were used to stabilize large racks int he stone units at every corner. Caulk repairs for cracks are typical. They are found the entire height of the monument on all four elevations The monument underwent a deep repointing campaign, wich removed all traces of the original pointing mortar. There is also evidence that prior to the repointing campaign, caulk was used in the joints of the lower portion of the monument.	FULL REPOINT EXTERIOR; INTERIOR REPOINTED; STAPLES IN CORNERS AT BASE; CAULK REPAIRS ALONG FACE; CAULK IN LOWER JOINTS	OBSERVATION DECK AND INSIDE TOP 100'; INSIDE CORNERS REPOINTED AND REPAIRED VARIOUSLY; LOWER JOINTS	Jablonski; Bennington Monument_Materia Is Examination Report JBC
1987-1988 1988-1989	Stair restoration completed. Work inside was stopped short to address major repointing of exterior before going further on the stairs. Repointing work initiated but only partially completed.	STAIR RESTORATION COMPLETED PARTIAL REPOINTING		SILMAN SILMAN STEVENS & ASSOCIATES
1990-1991	Joseph Gnazzo Company (JGC) was the successful bidder for the masonry restoration work.	BID		
2000s	Department of Labor and Industry cites emergency repairs. Joseph Gnazzo Company (JGC) was the successful bidder. New beams were added directly below the original steel beams of the observation deck. Coatings are failing today. Level D cleaned and repaired. Coatings failing and cracked floor plates today. Newer steel psts installed near the end of floor beams under the lobby to add redundant support to beam ends embedded in stone walls.	EMERGENCY REPAIRS NEW BEAMS; NEW COLUMNS; CLEANINGS; STAIR REPAIRS	BEAMS UNDER OBSERVATION DECK C; COLUMNS UNDER LOBBY FLOOR; LEVEL D CLEANED.	STEVENS & ASSOCIATES
2005	Some emergency repairs to floors and stairs. RBA issues bid package for BBM Restoration. Misc. repairs included mortar repointing, reinforce floor framing, replace metal floor plates, and clean and paint stairs. Apr-05 It is not known if this repair work was performed.	BID PACKAGE ISSUED		SILMAN
2016	Elevator modernization due to motor failure. Includes a new MCE 4000 elevator controller with variable voltage variable frequency (VWVF) lift drive, a new 12.5 HP Imperial AC motor and coupling, a new Hillister Whitney governor, new ADA compliant car station, hall fixtures, position indicators, direction lanterns, and braille labels. Sheave and drive shaft retained. Motor today leaks oil and requires constant maintenance.	ELEVATOR MODERNIZATION		

Image 92. Chart documenting repair campaigns

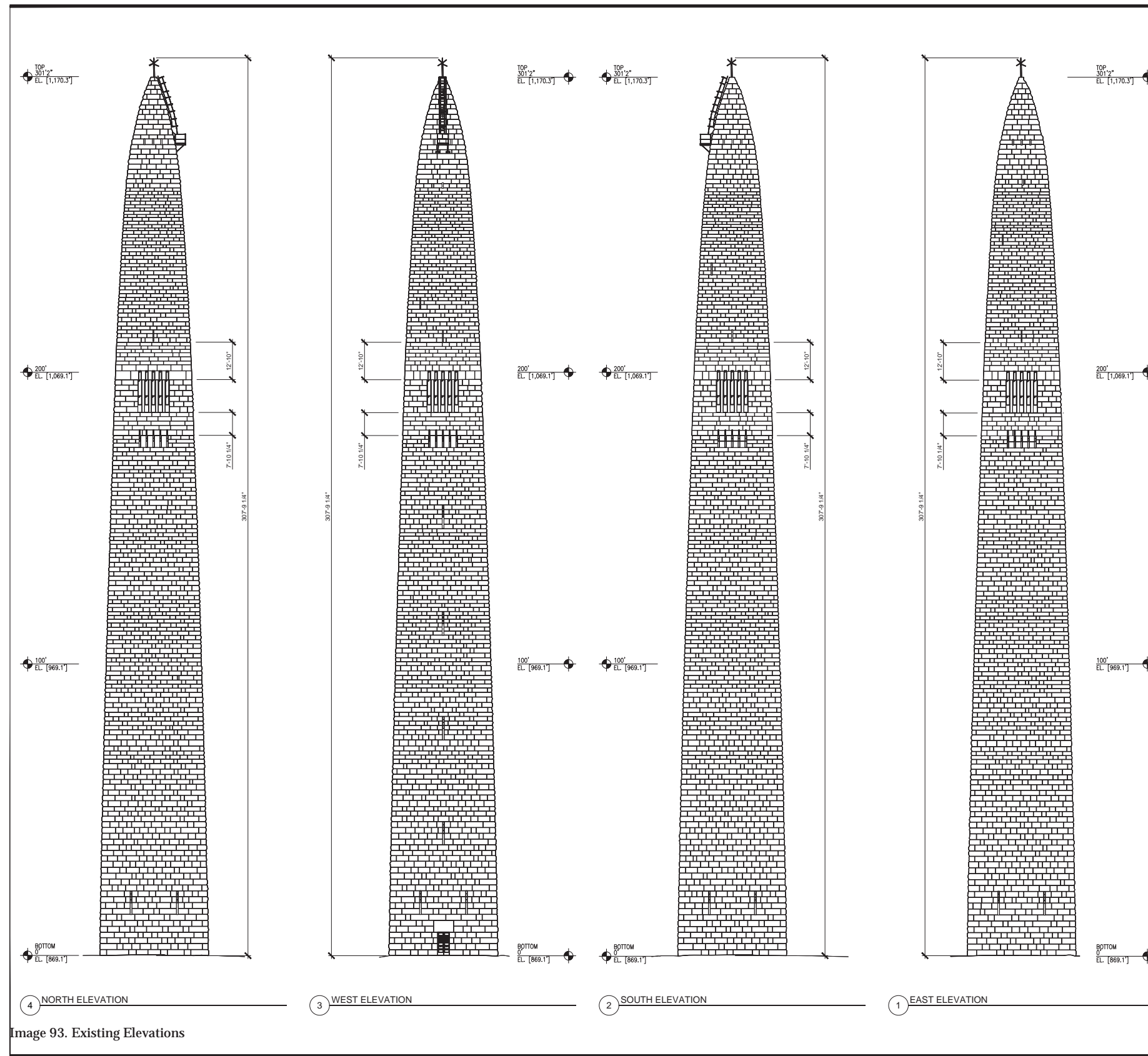


Image 93. Existing Elevations

CONDITIONS LEGEND	
GRAPHIC	LOCATION DESCRIPTION
04. DIVISION 04 - MASONRY	
04.1. STONE MASONRY (STONE)	
	BIOLOGICAL GROWTH
	CRACK -
	CRACK NETWORK
	COATING (SILICONE), INAPPROPRIATE
	CORROSION
	DELAMINATION
	DETACHMENT
	EFFLORESCENCE
	EXFOLIATION
	MATERIAL LOSS
	MECHANICAL DAMAGE
	OPEN JOINT
	PREVIOUS REPAIR
	SPALLING
	SPALL - REMOVAL
	SOILING / STAINING
	WEATHERING
	WEEPS, INAPPROPRIATE
04.2. STONE MASONRY (STONE) REPOINTING	
	NOT MAPPED
	POINTING FAILURES - INCLUDES, FOR EXAMPLE, INCORRECT IMPLEMENTATION, OPEN JOINTS, AND INAPPROPRIATE AESTHETIC AND PHYSICAL PROPERTIES.
	POINTING FAILURES - SEVERE (INCLUDES SEVERE OCCURRENCES OBSERVED OF THE ABOVE)
05. DIVISION 05 - METALS	
05.1. ARCHITECTURAL METALS	
	CORROSION
	EMBEDMENT

MEMBERSHIP AND USE OF DOCUMENTS		
DRAWINGS AND SPECIFICATIONS AS INSTRUMENTS OF PROFESSIONAL SERVICE ARE AND SHALL REMAIN THE PROPERTY OF THE ARCHITECT. THESE DOCUMENTS, PARTS, OR IN ANY OTHER PARTS, SHALL BE KEPT PROPERLY AUTHORIZED BY CONTRACT, WITHOUT THE SPECIFIC WRITTEN AUTHORIZATION OF EASTON ARCHITECTS, LLP.		
NO.	REVISIONS / SUBMISSIONS	DATE
01	-	-
PROJECT		
BENNINGTON BATTLE MONUMENT		
EXISTING CONDITIONS ASSESSMENT		
15 MONUMENT CIRCLE, BENNINGTON, VT 05201		
EXTERIOR ELEVATIONS		
SEAL & SIGNATURE	DATE:	2024-03-07
	PROJECT No:	2307.00
	DRAWN BY:	MP / DF
	CHECKED BY:	PE / LE
	DWG No:	A-201
	PAGE:	01 OF 01

A1	CONDITIONS LEGEND
NTS	

EASTON ARCHITECTS
30 WEST 44TH STREET 7, SUITE 604
NEW YORK, NY 10036
212.779.9070 TELEPHONE

STRUCTURAL ENGINEER
TYLIN SILMAN Structural Solutions
32 OLD SLIP, 10TH FLOOR
NEW YORK, NY 10002
212.620.7970

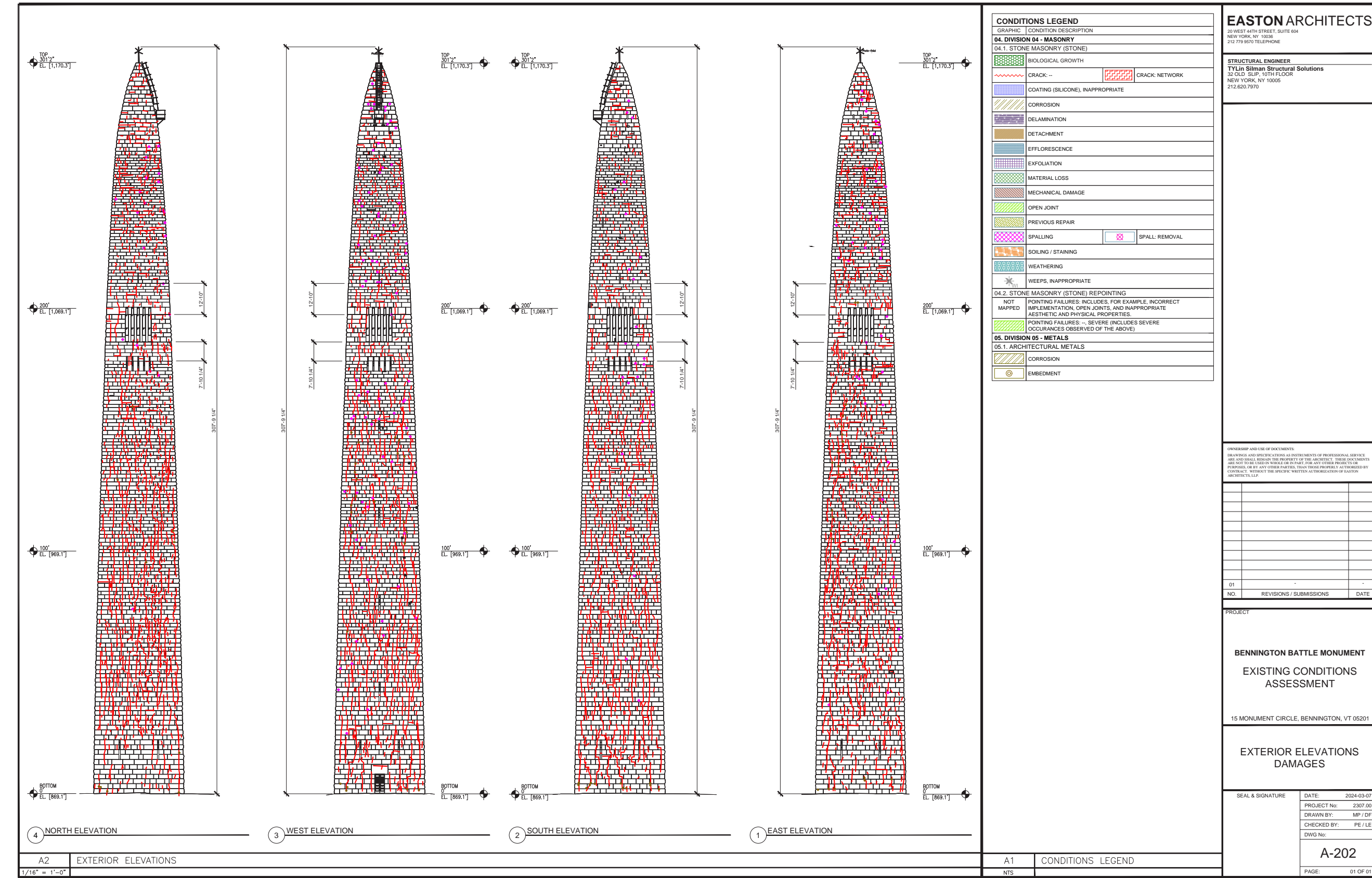


Image 94. Existing Conditions

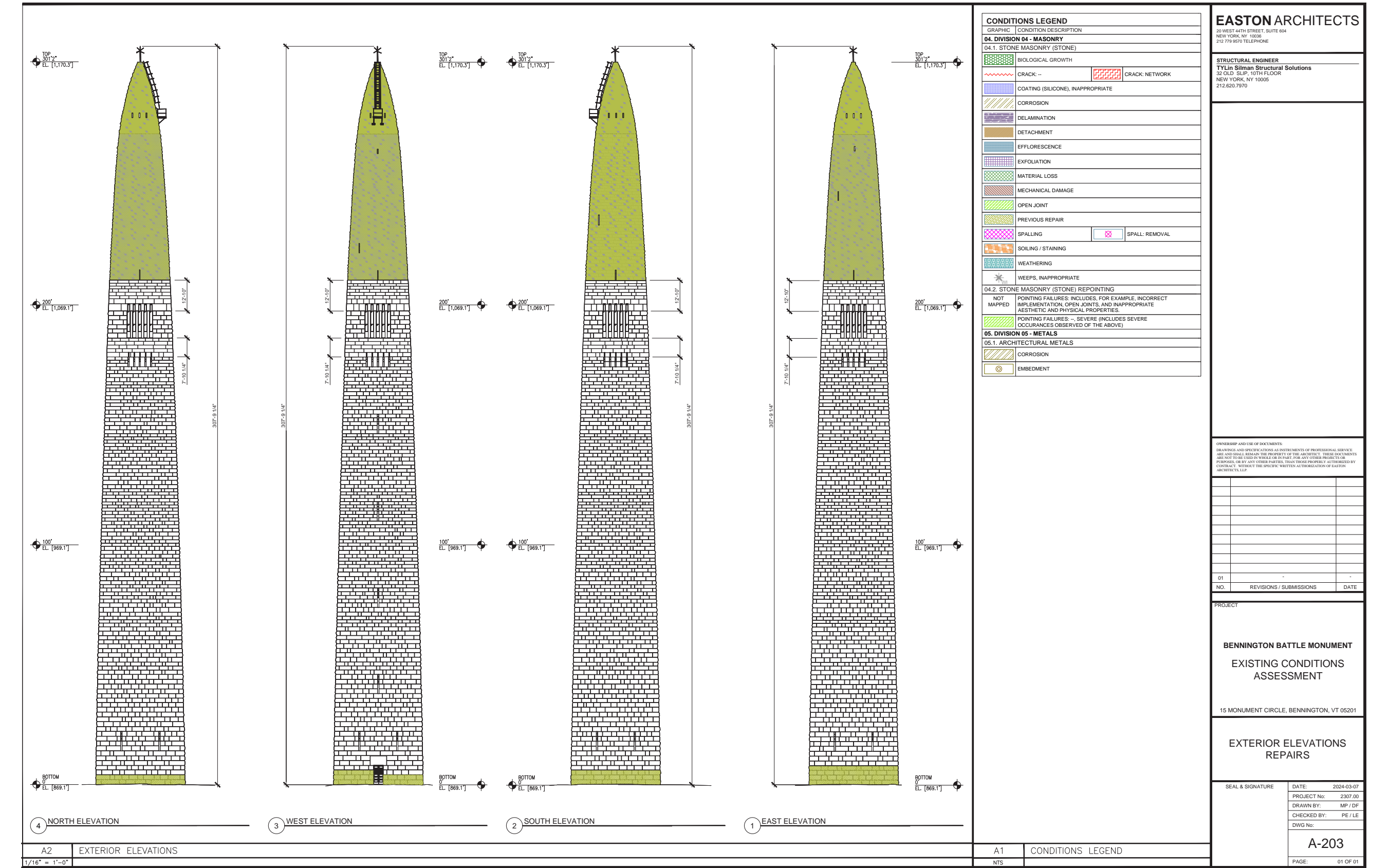


Image 95. Location of Repair Campaigns

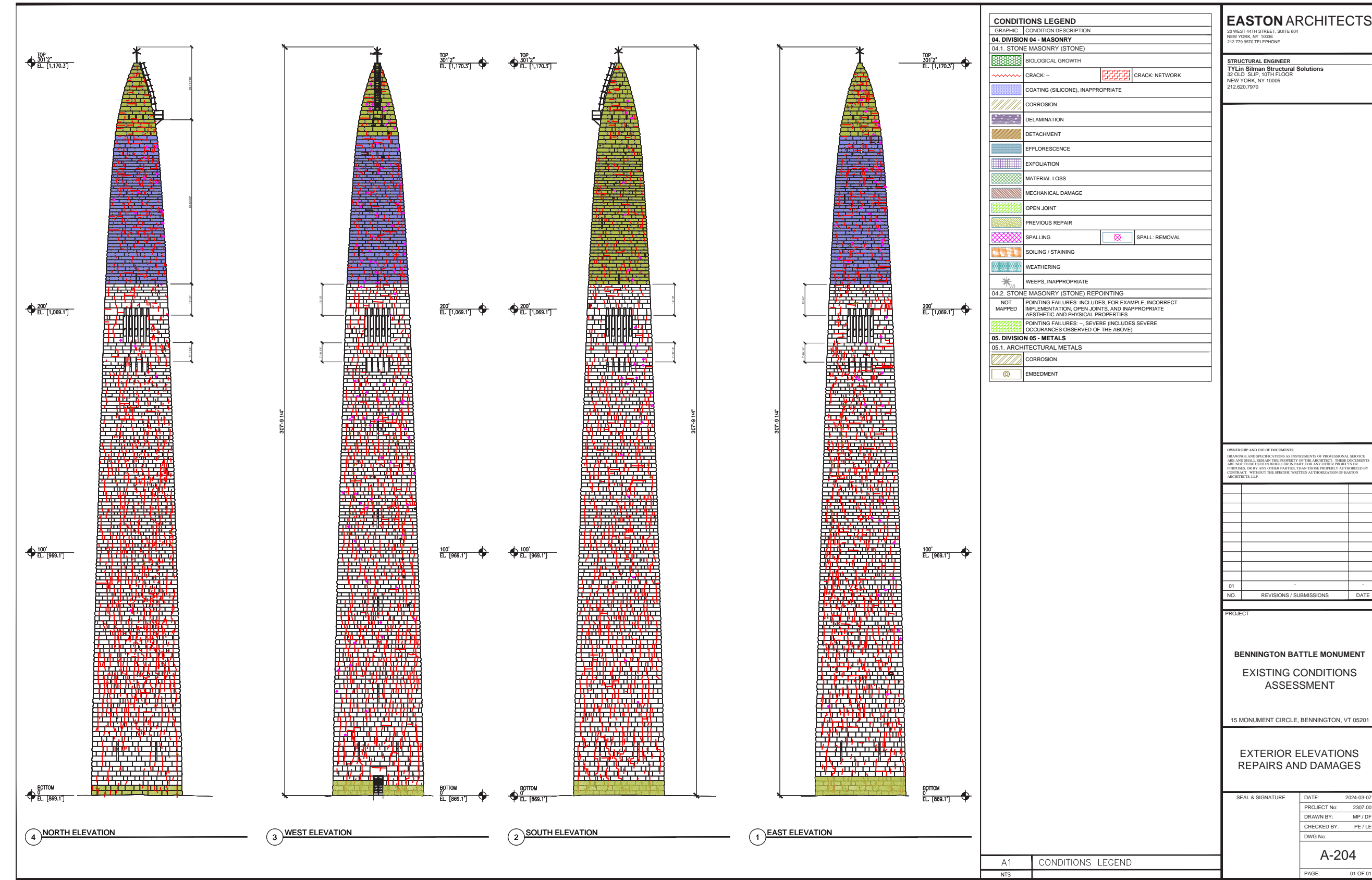


Image 96. Location of Repair Campaigns Overlaid on Conditions

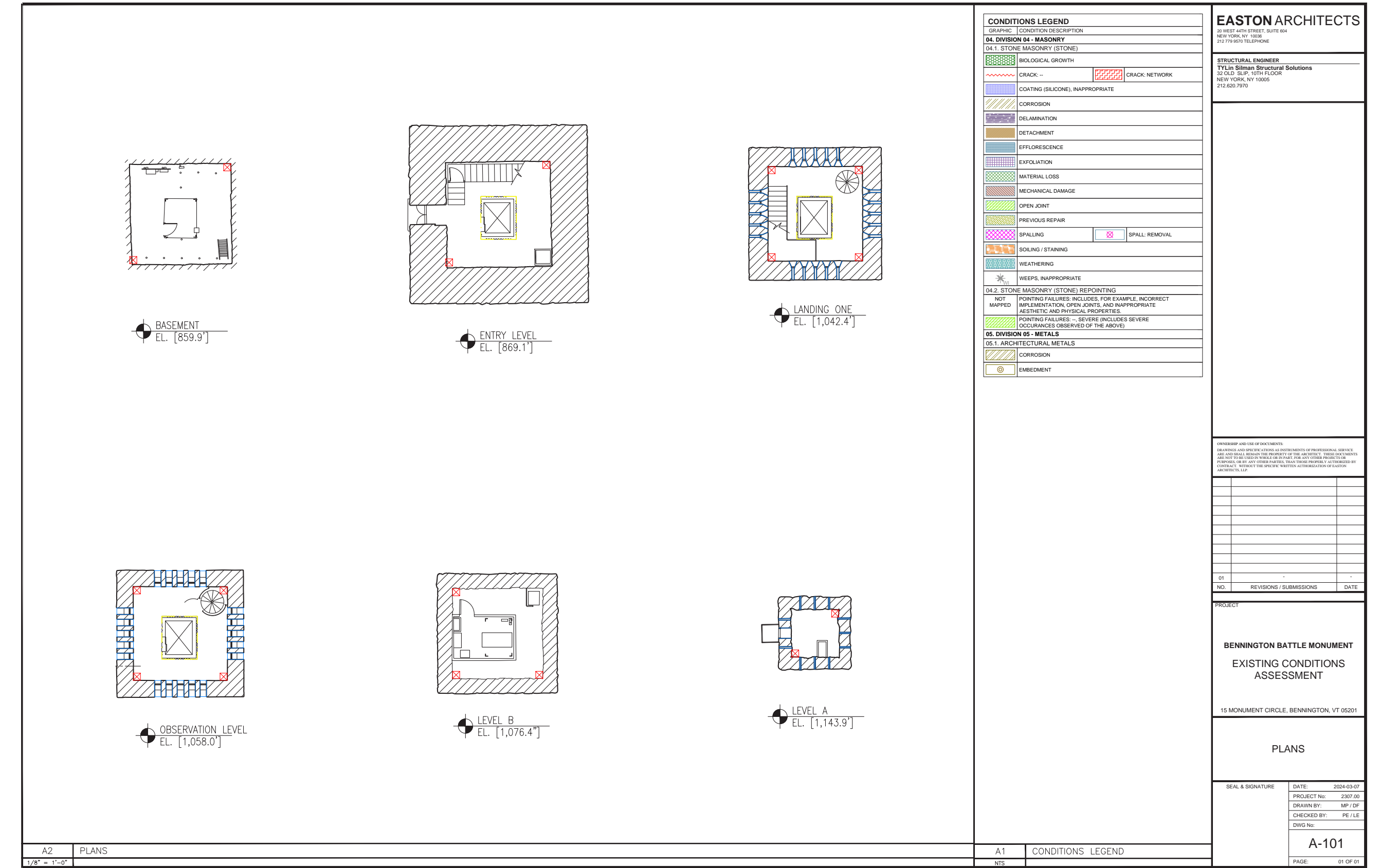


Image 97. Sketch of mechanical intervention location

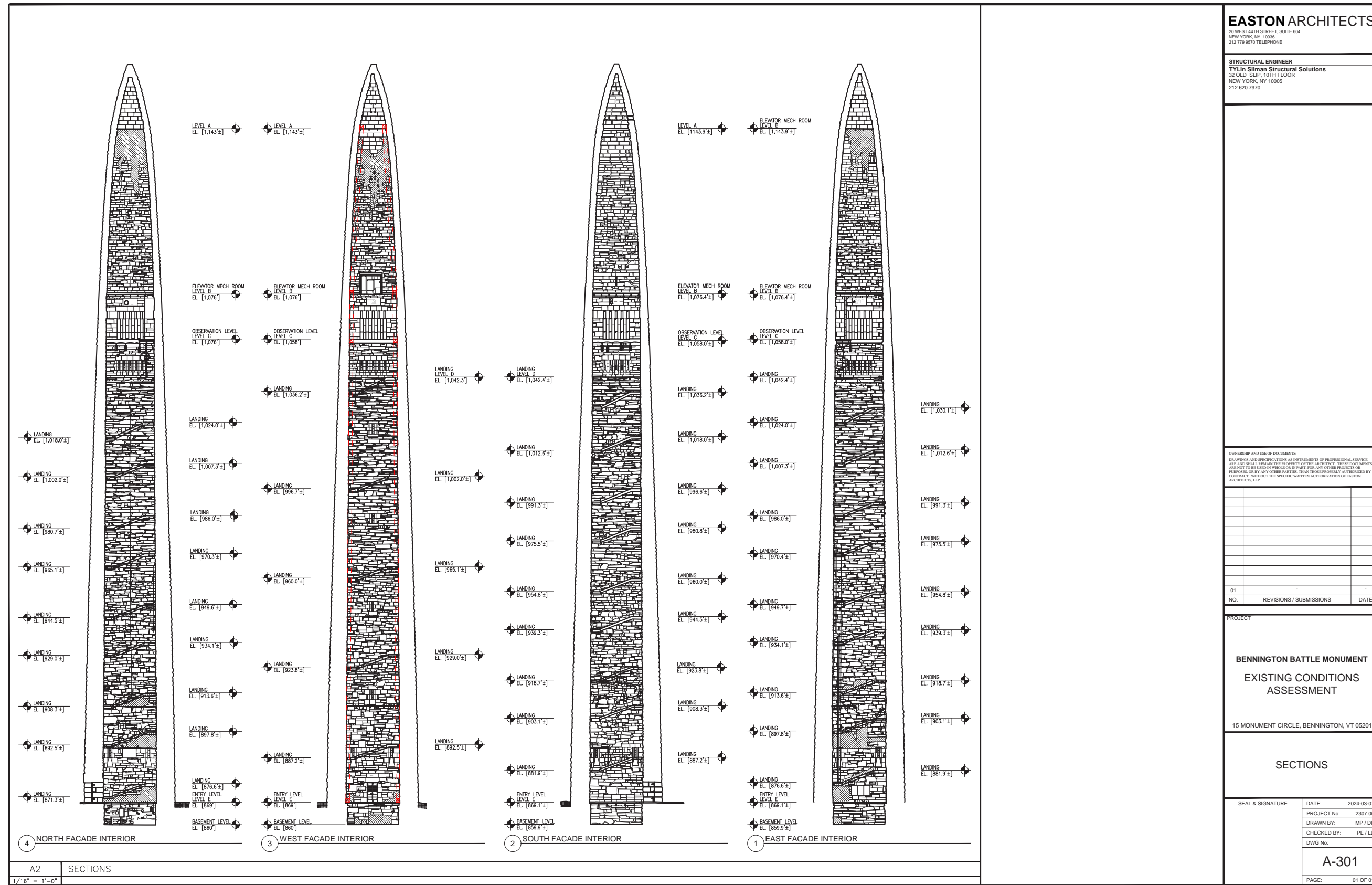


Image 98. Section for ventilation shafts

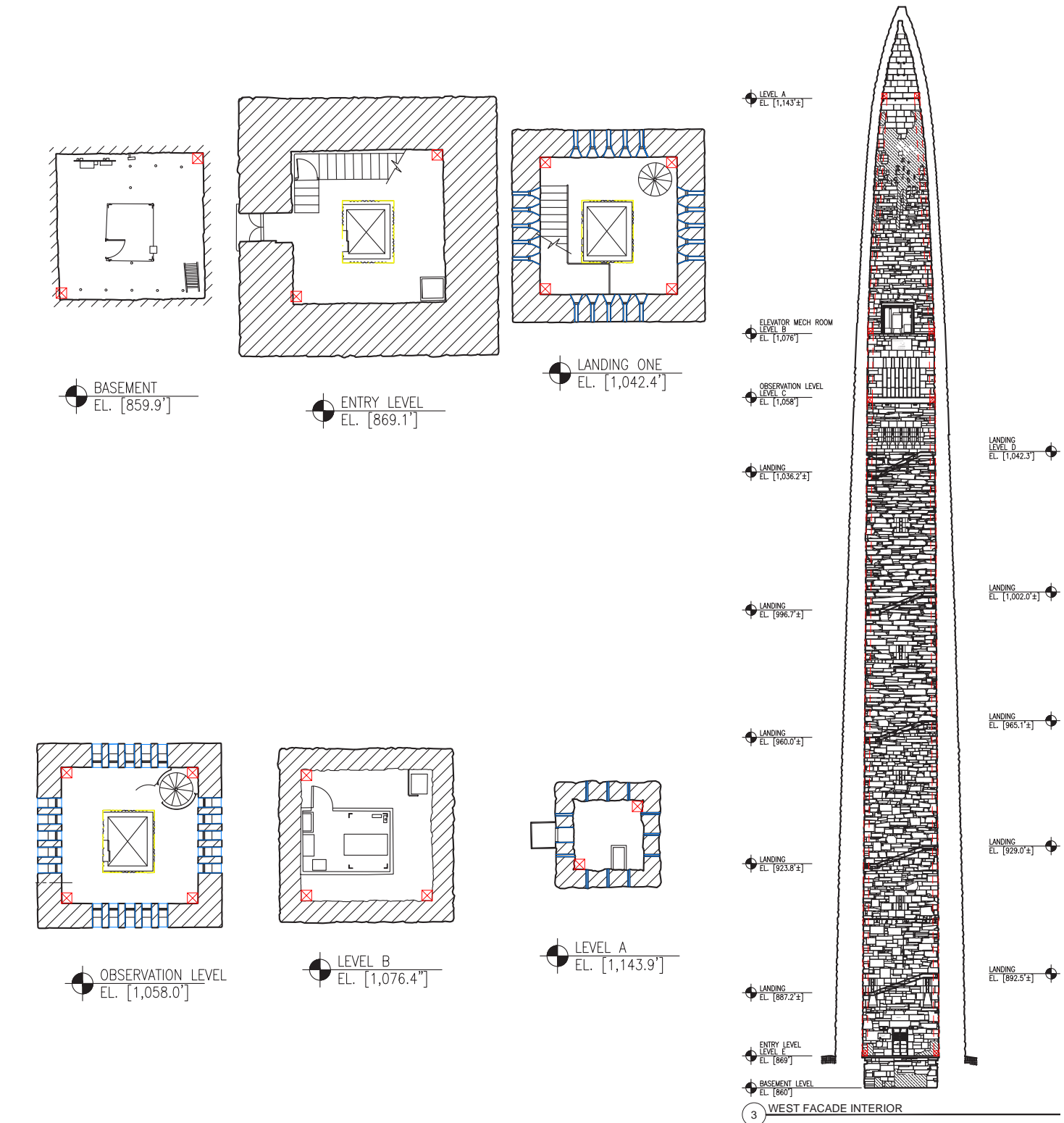


Image 99. Sketch of mechanical intervention location

RECOMMENDATIONS AND NEXT STEPS

Recommendations

In consideration of the appropriate restoration approach and a development of a Scope of Work for a Schematic Design Phase, the following categories present the key elements to be addressed in a holistic restoration campaign. These factors address the primary issues as they relate to environmental systems, ventilation, water infiltration, and the restoration, repair and preservation of the stone. In developing these recommendations, we have attempted to categorize and prioritize based on sequencing importance and prioritization. There are some elements that logically must be addressed first, and we've looked at varying factors that can have an impact, and where variables may still exist.

Scope of Work Items for Schematic Design Phase

Environmental Controls & Ventilation

The majority of test results, and perhaps the biggest adversary to the health of the Monument is water, in liquid and vapor form, and the continuous level of saturation in the stone and the relative humidity levels on the interior. Ideally, a sequence will occur where the interior relative humidity is lowered, the dryer air begins to draw moisture and water vapor from the stones to the interior, and as the temperature on the interior is regulated, a natural stack effect is in place, the water and water vapor will migrate to the interior of the monument, further increasing the drying rate of the stone. Making the exterior of the monument watertight, repointing with the appropriate mortar, tooling open joints, spalls, and cracks, and monitoring the monument's movement, will allow the structure to exist more passively, and experience significantly less damage. Addressing these issues is a key component to the success of all other work on the Monument. And while there is the potential to debate the chicken and egg theory, it is clear mitigation is a priority. The following interventions are recommended:

- Install dehumidifiers on multiple stair landings at designed intervals throughout the monument to begin drying the stone walls, and to install additional Temperature & Relative Humidity monitoring for the monument at key levels to gauge rate of drying and reduction of RH. This can be done as a "test chamber" to validate calculations and establish a baseline for energy output required and rate of drying, with an added variable of continued saturation and water infiltration.
- Consider designing an actively monitored mechanical system for installation to operate a ventilation system and active heating system based on temperature conditions throughout the year. Mechanically operate louvers can be utilized as dampers and controls when temperatures and humidity levels are less than ideal, and a passive system can be relied on during ideal temperatures and following the drying/dehumidification period.
- To reduce water infiltration through the masonry walls, design repairs are required to minimize liquid water and water vapor infiltration and transmission while maximizing water vapor transmission to the interior to enhance outward drying of the masonry walls. This will be impacted by the reduction of the RH on the interior which will in turn reverse the transmission of water and moisture vapor to move through to the interior of the monument instead of

- VII -

RECOMMENDATIONS & NEXT STEPS

RECOMMENDATIONS AND NEXT STEPS

trying to exit at the exterior (and effectively becoming trapped)

- Design and implementation of natural and mechanical ventilation systems. This will include design intervention to penetrate the observation deck floor in order to induce the proper vertical air flow (positive stack effect)

Stone Masonry

The deterioration of the stone masonry is an ongoing and continuous process. The related analyses of the masonry enables us to understand the characteristics of the differing wythes of stones, so we can further comprehend the behavior of the stone, in its natural stone, and the stone(s) as a component of the overall structure. The Schematic Design Phase would incorporate the technical data provided in the reports to develop the appropriate restoration, repair and preservation details. And while there are still variables to consider regarding the structural behavior of the monument as it relates to cracking, including the direction of the stone bedding- it is also proven that there is at a minimum necessary work to the exterior that will help mitigate the deterioration. These are primarily the following:

- Address watertight integrity of masonry walls by performing the following work:
 - a. Reverse inappropriate repair campaigns including removal of existing mortar, epoxies, sealants, and caulk.
 - b. 100% repointing of interior and exterior masonry with appropriate mortar.
 - c. Perform select area masonry repairs including tooling, patching, pinning, Dutchman repairs and full stone unit replacement when repairs are not possible.
 - d. Perform masonry crack repairs in coordination with structural engineering recommendations.
- Clean masonry surfaces to remove biological growth, atmospheric staining, and corrosion. This will remove ecosystems that feed on the stone.
- Perform select area repairs in areas of embedded steel for the stair and elevator support systems. This can happen in conjunction with stair repair, with appropriate anchoring details into stone, including flashing and weep details that allow for continuous transmission of water and moisture vapor.
- In theory, the bedding orientation should be as it was formed in the earth, so as to keep the stone in its natural state of compression. Vertical oriented bedding planes can force the stones to perform in tension (as strain is put onto the top of the stone, the bedding planes are stressed to the left and right “stretching” their natural position, thus creating a tensile effect.) Differential bedding could explain vertical cracks in discrete locations but, it is difficult to see how this could explain the global problem. There are just too many cracks for this explanation. However, once the cracks open, it creates space for water to wash out mortar as well as

RECOMMENDATIONS AND NEXT STEPS

freeze, exacerbating cracks that originated from something else.

- Local stresses are a contributing cause to the cracking and any repair we undertake cannot cause additional stress concentrations. The future repairs should not be implemented in low for the development of significant new stress concentrations.
- Any mechanical repairs, such as pinning, must consider the location of cracks with respect to header stones and the connectivity between wythes in the masonry. Any reinforcements to lintels, such as at windows or doorways, should be carefully detailed to address concerns about potential new stress concentrations. Continuing cyclical maintenance and repair of the Monument is required. This is discussed in detail in the Phase 1 Report. We cannot reverse the cracking that has occurred or any initial cracking that has been exacerbated by freeze-thaw and moisture ingress. The State of Vermont will need to plan for regular repair campaigns to prevent moisture ingress.
- Areas of future study should include an analysis of thermal stresses within the stone masonry at a molecular scale using techniques such as a Monte Carlo simulation, WUFI Thermal Analysis, and detailed Finite Element Analysis with THERM Software.
- Continued electronic thermal and movement monitoring of the Monument should be performed until repairs are made to ensure that any significant change to the state of the masonry is detected in a timely manner.

Vertical Circulation Systems (Elevator & Stair)

As part of the Phase 1 assessment work, Lerch Bates first audited the elevator at the Bennington Monument on November 12th, 2021 and then again on September 22nd, 2022 due to elevator reliability issues and lack of maintenance. Their recommendation would be to retain the current controller, fixtures, and entrance assemblies since they are all still maintainable and will be for another 10-13 years. We would then replace the machine assembly, the associated steel ropes, the tape reader, the travelling cable, add microswitches to each of the blind hoistway access doors, install a new NEMA rated door operator, replace the current door operator with a NEMA rated enclosed operator and replace corroded pit equipment including the governor relating cam.

- Design and implement holistic upgrades to the elevator system and controls based on Lerch Bates report and desired usability preferred by state. This would include, but not be limited to replacing the machine assembly, the associated steel ropes, the tape reader, the travelling cable, add microswitches to each of the blind hoistway access doors, install a new NEMA rated door operator, replace the current door operator with a NEMA rated enclosed operator and replace corroded pit equipment including the governor relating cam.

RECOMMENDATIONS AND NEXT STEPS

Also as part of the Phase 1 assessment work, Hodgman Engineering & Permitting Plc (HEP) observed and assessed the staircase from the ground floor to the floor directly below the observation deck, as well as the spiral stair up to the observation deck On May 11th and 12th, 2022. It was concluded the stair system, including the spiral staircase from sub-observation deck to the observation deck, is best characterized as emergency stairs, or a fire escape. This is due to its inability to meet dimensional requirements for standard egress stairs for public use. The final repairs are recommended:

- Provide additional bearing for all stringer channel supports at landings
- Provide additional bearing for major floor landings support beams
- Replacement of cracked treads and cracked landings.
- Removal and replacement of structural bolts in framing and tread locations that show
 - greatest levels of corrosion of bolts and/or surrounding base metal
 - New coatings for all handrail assemblies
 - Spiral staircase between sub-observation deck and the observation deck is due
- for in-place refurbishment.

Building Systems (Electrical, Lightning Protection)

The existing electrical system was assessed during Phase 1 by DuBois & King, and the existing lightning protection system was assessed by Smokestack Lightning for this phase (report attached). Both are integral elements in an overall Preservation Work Plan, and it is understandable that each can be considered for its own level of priority, based on scope, need and budget. Our recommendation is to design and implement a holistic electrical system upgrades based on demands of the mechanical ventilation system, interior and exterior lighting, emergency lighting, backup power, and elevator. This is an important consideration, and can be developed during the Schematic Design Phase with the State's input. There are multiple factors to consider, including intended future/expanded use (i.e. stairs as circulation, exterior lighting improvements, mechanical ventilation system, code requirements, etc)

The following items are a minimum recommended to be addressed:

- Provide backup electricity system in case of global failure.
- Provide surge protection on the main electrical service panel in the monument.
- Remove abandoned and failed light fixtures
- Upgrade emergency lighting
- Provide adequate lighting for stairwell
- Provide emergency lighting battery unit equipment suitable for cold weather operation.
- Conduct electrical tracing and combine/eliminate wiring and conduit systems.

RECOMMENDATIONS AND NEXT STEPS

- Design and install new lightning protection system. As outlined, there are no code requirements for a lightning protection system, only standards to follow that result in an effective system for the relevant structure. Based on Smokestack Lightning's report, the prudent approach is to have a new system installed. The current system can be addressed for upgrades, offering this section of work as a lower priority based on phasing and budget considerations.

Next Steps: Phase 3: Schematic Design Phase and Preservation Work Plan

The next phase of work includes developing the schematic design for the multi-disciplined restoration approach for the monument. The primary goal of the schematic design phase is to develop a Preservation Work Plan that defines the technical approach, develops and implements mock-ups and onsite technical engineering tests of the design that addresses key architectural and engineering concerns arising from the interpretation and synthesis of the data from Phase 2. The design, mock-ups and engineering tests will provide a clear path to addressing the mechanisms of deterioration at work, resolve the deficiencies that exist and can be presented to the State Historic Preservation Office. This phase will also develop a detailed approach for phasing possibilities, project sequencing, accurate cost estimates and timelines, budgeting forecasting for the State, and for construction management scheduling.

The logistics of the proposed project will be a significant component of the overall project cost and schedule. It is recommended to engage a shoring/ bracing/ scaffolding engineer as part of the Schematic Design Phase to address the challenges that will be faced in preparing the Monument for restoration, while protecting the Monument and keeping it open and safe for visitors.

Based on our assessment of conditions and verification of research performed in Phase 1, and the engagement of a full complement of consultants during Phase 2, we propose preparing a Preservation Work Plan that addresses the scope of work items presented here for the holistic preservation, restoration, and rehabilitation of the Monument. Our methodology is based philosophically on accepted and established preservation theory and practice as advocated by The Secretary of the Interior's Standards for the Treatment of Historic Properties, the National Trust for Historic Preservation, and the American Institute of Conservation.

The design of restoration, repair, rehabilitation, and preservation details and specifications will rely heavily on the development of mock ups to test the performance of the design, and develop the implementation process for the restoration techniques, dehumidification tests, and passive ventilation approach. These mock ups and tests will enable us to better understand the major factors involved in arriving at the most appropriate design solution. These mock ups and onsite tests will identify conflicts and challenges with potential treatment interventions that will inform our design solutions earlier in the design process. These options will be developed and coordinated with the State to ensure appropriate standards are followed. The following is a short list of recommended actions and items to be considered during the Schematic Design Phase that will inform the methodology:

- Masonry Cleaning test to remove sealants, epoxies, and biological growth
- Develop appropriate mortar mix and perform onsite testing

RECOMMENDATIONS AND NEXT STEPS

- Prepare a pointing mock up on interior and exterior
- Prepare mock up for tooling techniques at area of stone requiring repair
- Prepare mock up for area of patching of stone
- Perform test for mortar extraction- methodology, depth, sequence
- Source samples for stone replacement and perform mock up to match existing
- Mock up for stone pinning
- Mock up/technique for vertical crack repair
- Dehumidification chamber test
- Localized masonry drying test

Following the successful implementation of the mock ups and tests, the next step would be to test the validity of the work, primarily for the prevention of water intervention and for the maintaining of appropriate humidity levels and stone saturation and moisture levels. The tests performed on the repaired areas would include:

- Spray-bar water testing
- RILEM testing of the mockup areas to test for watertight integrity and success of dehumidification and reduction of water and water vapor in the masonry.

Project Sequencing

The final key component to the Schematic Design Phase is the design of an integrated scaffolding system to enclose the monument for drying and performing the conservation and restoration work for the project. This component addresses a number of key issues in the sequencing of the project and is closely related to the geotechnical report submitted by Langan Engineering. This scaffolding has numerous moving parts, timelines, and parameters to consider, but one approach can look as follows:

- Design and construction of walkway bridge over Monument entrance
- Scaffolding design for enclosing the entire Monument, with skrim, but constructed in sections
- Section 1 completed to allow for isolated testing and mock ups, i.e. creating a “work chamber”
- Following the successful implementation of mock ups and tests, scaffolding over entire Monument is constructed to begin the drying out and dehumidification process. Calculations for length of time can be performed based on chamber test.
- During this process, design and implementation of passive and mechanical ventilation system is developed and installation can begin independently of exterior work.
- Design Development and Construction Documents phases developed during the period of masonry drying and Monument dehumidification, along with other monitoring and testing procedures.

RECOMMENDATIONS AND NEXT STEPS

Prioritized Action Items: *Immediate Life Safety Hazards, Stabilization, Full Scale Restoration, and Ongoing Maintenance.*

- *Immediate Life Safety Hazards and Stabilization*
Scaffolding- provide walkway and scaffolding at perimeter base for safety and protection for visitors
- *Full Scale Restoration-Primary*
Stone masonry restoration design and mock ups
Passive and mechanical ventilation system design
Electrical upgrades
- *Full Scale Restoration-Secondary*
Elevator
Stair rehabilitation design
Lightning Protection System
- *Ongoing Maintenance*
Design of Monitoring systems (cracks, humidity, temperature control)
Proposed sequence for exterior/interior upkeep based on monitoring data. Design and process/schedule of work will be developed in coordination with a cyclical maintenance plan that is suitable for the state.

Summary:

The analyses provided from the work performed in Phase 2 has provided our team with a tremendous amount of relevant information, and we believe we have succeeded in narrowing our focus to not only what we believe are the mechanisms of deterioration at work, but most importantly, a clear path of how to approach the full restoration and develop a Preservation Work Plan. The major factors that need to be addressed include:

- Saturated stone
- Water infiltration
- Vertical cracking, spalling and stone damage
- High humidity
- Inverse stack effect for ventilation
- Outdated electrical and lightning protection systems
- General deterioration due to moisture and moisture vapor on stairs and elevator mechanisms
- Exacerbated deterioration due to ineffective and inappropriate repair campaigns
- Generalized material deterioration due to petrographic make up of stone

RECOMMENDATIONS AND NEXT STEPS

Our team believes, and we have stated in our documents, that as an objective, preservation enables us to gain a sense of ourselves, and the historic places we cherish tell us who we are, where we have come from and help direct us into a more consistent and meaningful path into the future. While the preservation of historic places is related to the significance of a physical landmark and its importance, there is more to it than the tangible, and/or practical side of a physical building, or in our case, an extraordinary monument. Preservation provides us with tangible objects that provide identity, memory and continuity to our communities and our own personal history. It helps root us in our heritage, it develops unity and provides a spirit that defines a neighborhood, a community, a city, and a nation. There is an emotional connection with these important places that provides a connection to the past that helps link the present.

There are the names and places associated with this emotional connection, from highways and roadways to state parks, hotels and motels, restaurants and bars. It is all based on memorializing and preserving the richness of our past so we can understand the reasons behind where we are today. In this particular case, we embrace the legacy of John Stark, Seth Warner, Ethan Allen, the Green Mountain Boys, the Republic of Vermont, the negotiations with Quebec before British surrender, then the negotiations with the U.S. to enter the Union, and all of this is representative of the Battle of Bennington as a key victory in our Revolutionary War, as much as it is of Vermont's battle for its own statehood, and the efforts of ultimately becoming the 14th state of the Union.

As the Vermont Historical Society professes "Every person and every moment create the story of Vermont. Through sharing these collective stories, Vermonters will increase their knowledge of our state's complex past, inform our present, and understand how our unique experiences impact and shape this ongoing narrative." The Bennington Battle Monument is part of this story, is a valuable link in Vermont's history, and a source of pride that can be continuously celebrated.

From a preservationist's perspective, it is important to understand a site's historic context, and this in return helps one understand a site's significance alongside the physical representation of this context. Historic context provides the political, social, cultural, and economic background for a particular idea, event, movement, or individual. Historians place historic events within a "historic context" to understand the meaning of an event or a property within a specific culture and/or period. Placing an event in its context enables historians to better understand if an event was unique or typical of the period, and/or how it may have impacted a culture or period. With a National Historic Landmark, the historic context enables us to understand the role the property played in American history overall.

From the practical perspective, Preservation is defined as the act or process of applying measures necessary to sustain the existing form, integrity, and materials of an historic property. Work, including preliminary measures to protect and stabilize the property, generally focuses on the ongoing maintenance and repair of historic materials and features rather than extensive replacement. The limited and sensitive upgrading of mechanical, electrical, and plumbing systems and other code-required work to make properties functional is appropriate within a preservation project. The Standards for Preservation require retention of the greatest amount of historic fabric along with the building's historic form. This is an important distinction when it comes to the development of the project scope of work and timeline.

THIS PAGE INTENTIONALLY LEFT BLANK

03/29/2024

**STRUCTURAL AND ELECTRICAL ASSESSMENT OF
THE BENNINGTON BATTLE MONUMENT**

**PHASE II: COMPREHENSIVE STRUCTURAL &
MATERIAL TESTING AND EVALUATION AND
OUTLINE OF RESTORATION APPROACH
APPENDIX: CONSULTANT REPORTS**

15 MONUMENT CIRCLE
BENNINGTON, VT, 05201

PREPARED FOR:
VERMONT DEPARTMENT OF BUILDINGS & GENERAL SERVICES
BGS PROJECT ID #200016

Bennington Battle Monument

Structural Engineering Evaluation Phase 2



March 29, 2024

Prepared for

Stevens & Associates, P.C.
91 Main Street, Brattleboro, VT 05301

Prepared by

Silman
32 Old Slip, 10th Floor
New York, NY 10005

Silman Project #20570

TABLE OF CONTENTS	
I. Executive Summary	2
I. Introduction	4
II. Literature Review	5
III. Structural Analysis	8
Basis of Design Material Properties and Loads	8
Wall Hand Calculations	12
Finite Element Shell Model – Modal and Linear Analysis	14
Finite Element Shell Model - Nonlinear Analysis	24
Finite Element Solid Model – Observation Level	27
Masonry Unit Capacity Checks	30
Thermal Analysis	32
Structural Analysis Conclusions	33
IV. Discussion	36
V. Recommendations	39
VI. References	40

I. EXECUTIVE SUMMARY

The Bennington Battle Monument has exhibited deterioration throughout its history, including stone cracking, efflorescence, disintegration of mortar, and corrosion of the interior metal staircase. As part of a larger team, Silman completed a prior structural engineering investigation of the existing cracking on the Bennington Monument. The summary of these results is included in our Phase 1 structural report, dated December 15, 2022. This investigation identified several potential contributing factors to the cracking of the Monument and recommended additional specialized testing and analysis, which was authorized by the State of Vermont as this Phase 2 scope of work.

Silman's Phase 2 scope of work included more detailed structural modeling of the Monument to evaluate potential causes of the existing cracking and to understand global and local performance of the structure. As discussed in previous reports, local stresses such as freeze-thaw, temperature and expansion, and concentrated loading were suspected to be a key contributing factor to cracks but this had never been proven analytically. It was important to take into account the existing cracks and non-uniform cross-section in the analysis of the monument. We studied this using multiple different methods of analysis including three-dimensional finite element (FE) shell and solid models, supplemented by hand calculations. The properties used in the modeling were taken from the in-situ materials testing and seismic properties were updated from the geotechnical evaluations done on the site.

The analysis showed that there are several forces acting on the structure that have the potential to lead to highly concentrated local stresses. The cumulative actions of thermal stress, improper previous repairs, moisture ingress, and missing mortar joints all create conditions where high concentrated forces or internal stresses can cause tension and cracking of the stone masonry. After the initial cracking of the structure, the Finite Element Analysis shows how the load path redistributes to stiffer, less cracked areas of the masonry, which causes new load concentrations and further cracking. The cracks were reported very early on in the Monument's history, so a rare, large lateral loading event (wind or seismic) is unlikely to have caused initial cracking. Rather, it is most likely that the repetitive nature of climatic stresses experienced in the short-term, like freeze-thaw and temperature cycles, were the initial cause of cracking. However, loading and the localized re-distribution of loads that have happened over time or may happen in the future could worsen the cracking. As has already been observed and documented by other team members, this cracking exacerbates the infiltration of water and the localized failure of masonry (stone and mortar).

Further global analysis of the uncracked structure using updated geometry and material properties from Phase 2 testing showed that under code prescribed wind and seismic loading, the Monument does not exceed allowable tension or compression limits and is globally stable. To

date, the Monument has not experienced any significant seismic event at code level loading but could in the future. However, the Monument does go into tension locally with a reduced (cracked) cross section. Thus, wind and seismic loading are not the cause of initial cracking in the Monument but may be contributing to ongoing cracking now that the initial damage has occurred, and there is a general vulnerability of the monument for a future code-defined seismic event.

Based on this analysis, our Phase 1 Recommendations have been updated to include the following additional considerations:

- Drying out the Monument is going to be critical, as the temperature differentials were found to be a potential contributing cause to the masonry deterioration. Given the need to address the water saturation deterioration of the masonry, please refer to the reports by others for additional discussion on options for this scope of work.
- Local stresses are a contributing cause to the cracking and any repair we undertake cannot cause additional stress concentrations. The future repairs should not be implemented in such a way that efforts to pin, repoint, grout, or otherwise repair the masonry allow for the development of significant new stress concentrations.
- Any mechanical repairs, such as pinning, must consider the location of cracks with respect to header stones and the connectivity between wythes in the masonry. Any reinforcements to lintels, such as at windows or doorways, should be carefully detailed to address concerns about potential new stress concentrations.
- Continuing cyclical maintenance and repair of the Monument is required. This is discussed in detail in the Phase 1 Report. We cannot reverse the cracking that has occurred or any initial cracking that has been exacerbated by freeze-thaw and moisture ingress. The State of Vermont will need to plan for regular repair campaigns to prevent moisture ingress.
- Areas of future study should include an analysis of thermal stresses within the stone masonry at a molecular scale using techniques such as a Monte Carlo simulation, WUFI Thermal Analysis, and detailed Finite Element Analysis with THERM Software. This level of modeling is beyond the scope of the Phase 2 investigation.
- Continued electronic thermal and movement monitoring of the Monument should be performed until repairs are made to ensure that any significant change to the state of the masonry is detected in a timely manner.

This study was focused on causes of the existing cracking in the Monument. The Schematic Design phase of work should investigate the effects of potential future loading on the Monument's stability including seismic loading.

I. INTRODUCTION

As part of a larger team, Silman completed a prior structural engineering investigation of the existing cracking on the Bennington Monument. This first phase of work prioritized initial field testing and investigation, including a conditions assessment, laser scan, initial non-destructive evaluation of the stone, and preliminary electronic monitoring. The summary of these results is included in our Phase 1 structural report, dated December 15, 2022. Upon the completion of our work in Phase 1, additional specialized testing and analysis was recommended. This included engaging a masonry conservator, additional materials testing, a building envelope and hygrothermal review, a mechanical engineering review, water infiltration (spray) testing and infrared testing, masonry strength testing, geotechnical survey, and architectural preservation review, as well as a more detailed structural Finite Element Analysis. The State of Vermont retained our project team for this Phase 2 scope of work.

For Silman, the primary structural engineering scope of work in Phase 2 was more detailed structural modeling of the Monument for global and local performance of the structure to investigate existing stress and distress on the monument. Finite Element Modeling and hand calculations were performed incorporating the geotechnical information, material condition, movement data, strength, stress, and stiffness provided by the additional testing performed in Phase 2. We have updated our initial recommendations and discussion points from this report based on the additional results obtained in Phase 2.

Included herein are Silman's additional structural engineering observations, analysis results, and recommendations for future work developed during Phase 2. These incorporate the Phase 2 information provided by the subconsultants, Atkison-Nolan & Associates (ANA), Jablonski Building Conservation (JBC), and Langan, as it applies to the scope of our structural engineering analysis, including our Finite Element Modeling (FEM).

The purpose of this investigation was to identify causes for the observed cracking. This scope of work does not constitute a full structural analysis for designing repairs for the Bennington Monument. Any potential repairs, identification of all vulnerabilities, designing for specific details in the Monument, etc. will be part of a separate, future phase when authorized by the State of Vermont.

II. LITERATURE REVIEW

A literature review was performed on potentially similar unreinforced masonry (URM) structures such as masonry towers, lighthouses, and obelisks to understand the causes of distress and prior collapses and to review repair precedents. Furthermore, this information was used as an opportunity to review recommended approaches and structural analysis precedents for Finite Element Modeling of tall unreinforced masonry to apply these techniques to our development of the FE model of the Bennington Monument.

Two main case studies investigated the collapse of the Pavia Civic Tower and the bell tower of Monza Cathedral, two tall URM towers located in Italy. The sudden collapse of the Pavia Civic Tower sparked intense investigations and theories, as no obvious causes could be blamed for the catastrophic event. Among performed investigations were geotechnical investigations, physical, chemical and mechanical tests, compression tests and fatigue tests [1]. These investigations highlighted the effect of long-term damage due high concentrated stresses, which led to the eventual collapse of the tower.



Figure 1 Pavia Tower Collapse [2]

The bell tower of the Cathedral of Monza was showing large vertical cracks across the walls which had been developing over the years. These included both large cracks and smaller thinner cracks. Testing and FE modelling was performed on this tower, and it was determined that damage was evolving over time due to the concentration of stresses near the openings at the base of the structure.

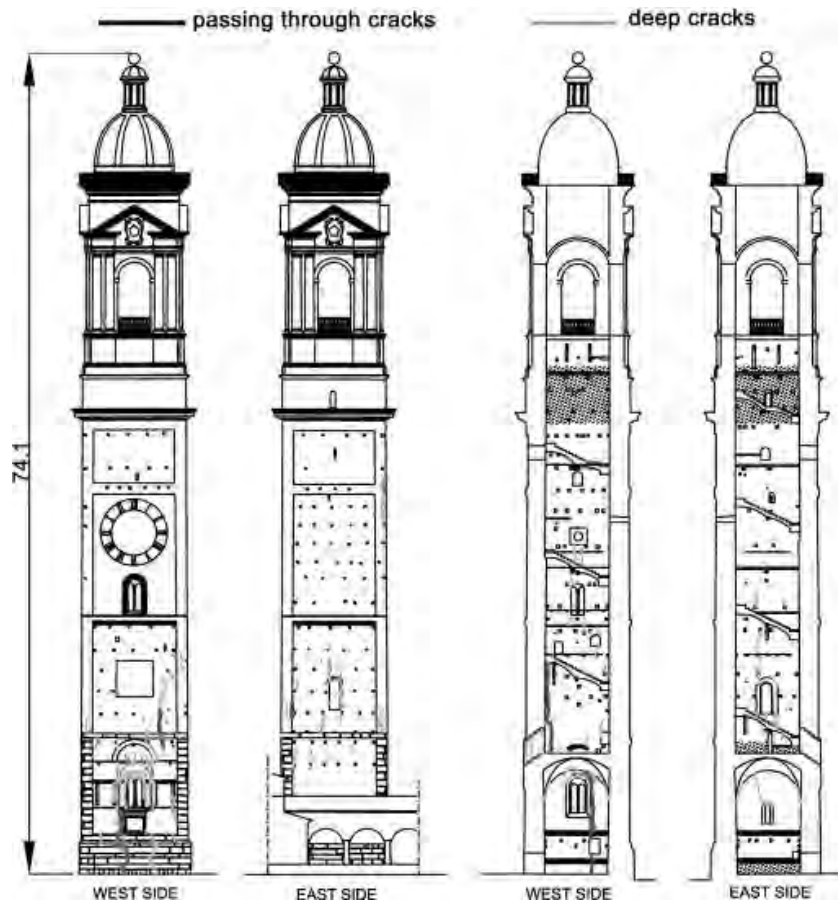


Figure 2 Survey of Cracks in the Bell Tower of the Cathedral of Monza [3]

The paper, *Failures due to long-term behavior of heavy structures: the Pavia Civic Rower and the Noto Cathedral* [4] emphasizes how creep deformations plays a significant role in the damage of towers and pillars, due to their geometry, the heavy persistent stress they endure, and potential changes in the state of stress or concentrations of stress. Furthermore, this reference notes how the load-bearing area of elements such as these often have a non-homogeneous cross section, due to their multiple wythe composition. We investigated whether this was a problem that Bennington Monument would face and whether there would be resultant areas of localized stresses.

This paper is also stated that the effects that temperature variation, wind and earthquake action may have on accelerating the fatigue effect of these materials. That is to say, multiple cycles of loading and unloading combined with inherent weaknesses of materials could lead to failure of these unreinforced masonry structures. This finding is also emphasized on the paper *Tall and Massive Ancient Masonry Buildings: Long Term Effects of Loading* [5], where such loadings are listed as a cause in the shortened lifespan of buildings. If Bennington has any areas of severe localized stress due to uneven cross-sections, its materials might be at higher risk of fatigue due its exposure to wind loads or extreme temperature variation due to environmental exposure.

When focusing on precedent studies for the analysis of unreinforced masonry structures, specifically on the implementation of a nonlinear analysis, it was seen that applications of different load patterns could influence the shape and behavior of the corresponding pushover curve. With regular linear analyses, such as gravity or wind loads, the structure can theoretically withstand an infinite number of loads without the FE model showing the deterioration of the material. With a pushover analysis, however, the yield point, the maximum bearing capacity, and the maximum allowable displacements that a structure can experience before the material is damaged (that is, it experiences plastic deformation), can be identified [6].

Through the review of different references, it was confirmed that a force displacement method was the recommended implementation of load patterns to the structure [7]. This method involves the application of a displacement at the top of a structure, with the structural analysis determining how much force needs to be applied as the structure gets pushed to that applied displacement. An important aspect of this method is that it captures the softening portion of the pushover curve. Seen in **Figure 3** [6], pushover line P3 shows the point (labeled as point C on the graph) where the material starts failing, with the downwards trend of the curve after that point indicating the possible collapse of the structure. As the pushover curve is needed to understand the limits of the material before plastic deformation (permanent deformation) is reached, the approach of a displacement-controlled analysis was pursued as part of our analysis.

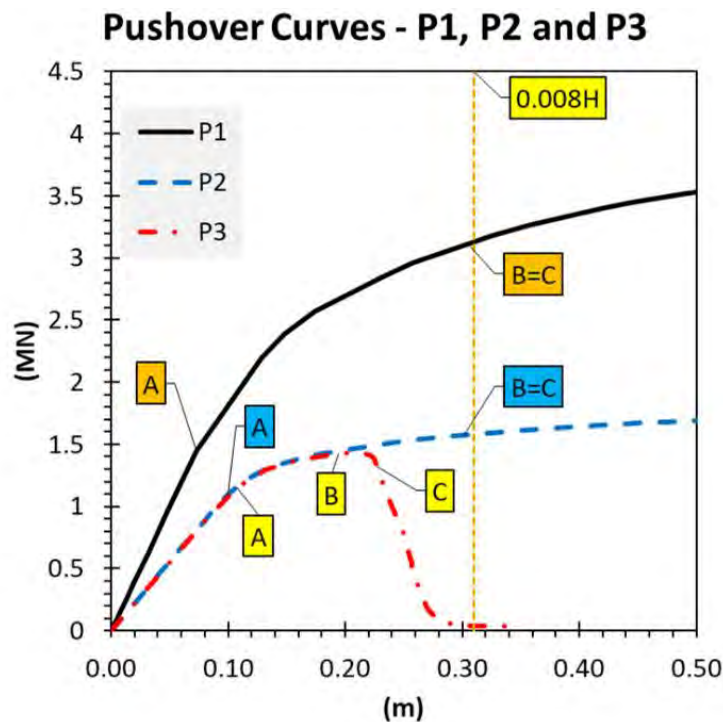


Figure 3 Example of Typical Pushover Curves as a Result of (P1) Inverse Triangular Shape Body Forces, (P2) Concentrated Lateral Load, (P3) Lateral Displacement at Top of a Miscellaneous Tower [6]

III. STRUCTURAL ANALYSIS

During this phase of our work, a structural analysis of the Bennington Battle Monument was performed using the following methods to evaluate potential causes of the existing cracking:

- Hand calculations (using spreadsheets developed by Silman for this project) were used to analyze building elements to verify whether they are sufficient to resist the global forces and stresses including seismic and wind forces.
- A three-dimensional analytical Finite Element (FE) *shell* model was created from the laser dimensional point cloud using the software SAP2000. This allowed for review of the stresses, forces, and deformed shape under different load conditions and combinations, including behavior under its own self-weight, wind forces, and a nonlinear pushover analysis.
- A three-dimensional analytical Finite Element (FE) *solid* model was created to achieve a more detailed understanding of the effects of cracks, specifically in situations with a reduction of cross section or a disconnected corner. By completing a linear gravity and lateral wind analysis, an evaluation of the potential increases of stress from such conditions was completed.
- The structural effect of reduced material cross sections was studied through hand calculations and the FE model. Specifically, we investigated the effects of having a structure in which the stresses were redistributed through a smaller area due to cracks in the Monument.
- Capacity of individual masonry units was determined (via lab and in situ material testing) and compared against stress values from the hand calculations and FE models. This was done to understand if localized failures are occurring due to high localized bending and/or shear stresses.
- Potential stress build-up due to thermal differentials in the masonry was calculated and compared against the structural capacity of the masonry.

Basis of Design Material Properties and Loads

The material properties used in the Finite Element Model were taken from the results of the material testing done by ANA during the Phase 2 Investigations [8]. The density of the masonry units was obtained from ANA's laboratory testing of the stone material. The Young's Modulus and the compressive strength were obtained from in-situ deformability tests, which provide the actual strength of the masonry matrix.

It is worth noting that the in-situ compressive strength obtained by deformability testing is an approximation of the ultimate strength and must be divided by a safety factor to obtain the allowable compressive strength. Historic resources define an allowable (ASD) compressive strength of 400 psi is appropriate for limestone with natural cement mortar, which results in a Safety Factor of approximately 4 compared to the measured compressive stress (Figure 4).

MASONRY				
	Portland cement mortar	Natural cement mortar	Cement lime mortar	Lime mortar
Dressed ashlar granite.	800	640	640	400
Dressed ashlar limestone.	500	400	400	250
Dressed ashlar marble.	500	400	400	250
Dressed ashlar sandstone.	400	320	320	160
Rubble stone.	140	100	100
Hollow clay or cinder block.	80	70	70
Solid clay or cinder block.	125	100	100
Neat cement grout, under bases.	1 000			

Figure 4 Allowable Stresses for Load-Bearing Masonry Wall [9]

The ultimate tensile strength of the masonry used for FEM was defined from the literature review. According to the book *Finite Element Analysis for Building Assessment* [10], the ultimate tensile strength of masonry may be taken as 10% of the ultimate compressive strength for masonry modeling. For the allowable tensile capacity, a reduction is taken. The allowable tensile strength of well bedded and consolidated historic masonry can be taken as 20 psi. These values are summarized in **Table 1** below.

Table 1 Masonry Material Properties

Masonry		
Density	165	pcf
Modulus of Elasticity, E	863500	psi
Measured Compressive Strength	1520	psi
Ultimate Tensile Strength	152	psi
Allowable Compressive Strength	400	psi
Allowable Tensile Strength	20	psi

For the nonlinear analysis, the stress-strain curves of the material under compression and tension were defined using the ultimate compressive and tensile strengths (**Figure 5**). The compression curve was defined using data from ANA's in situ deformability test (**Figure 6**). At the highest applied compression force, the masonry showed signs of reaching its plastic region, where it reaches a deformation level from which it does not go back to its original undeformed state once unloaded. This indicates that the highest measured compressive strength is close to the ultimate strength of the material.

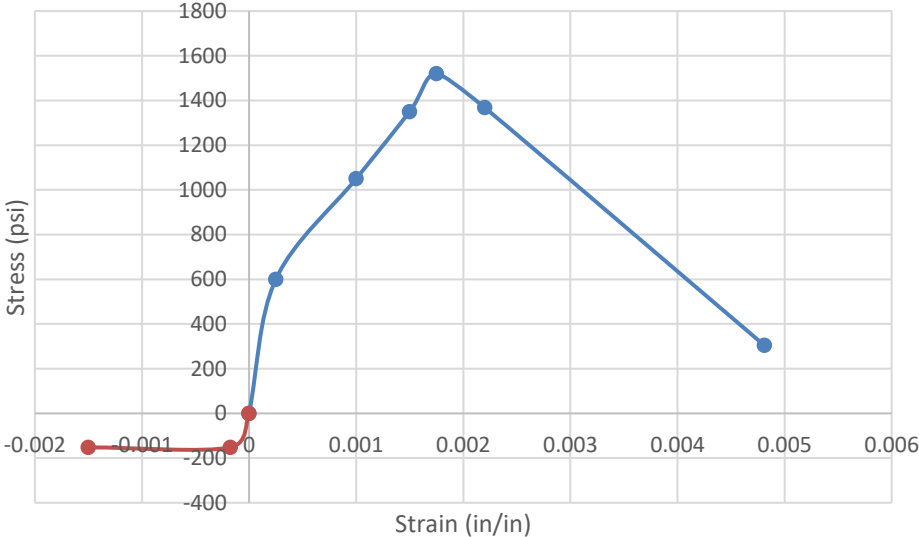


Figure 5 Definition of Masonry Stress-Strain Curve Under Tension and Compression for Finite Element Analysis

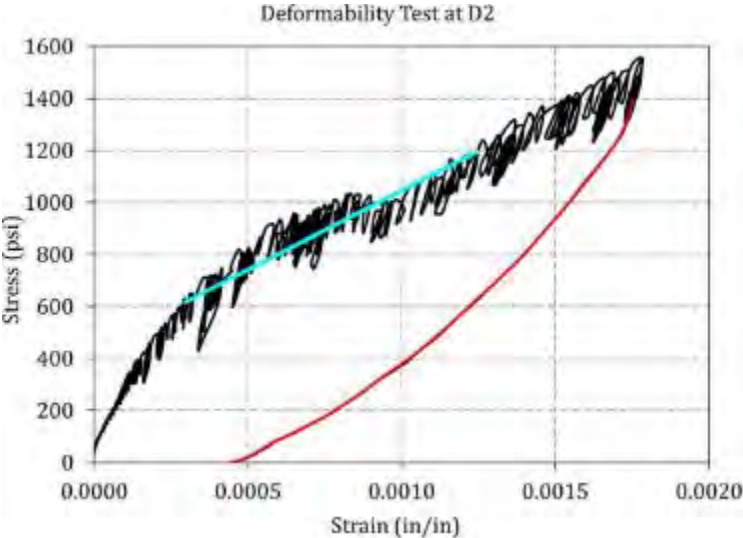


Figure 6 Stress-Strain Curve from Deformability Test at D2 (Source: Atkinson-Noland & Associates Phase 2 Report)

Code Review: The State of Vermont is governed by the following Building Codes and standards:

- 2015 International Building Code (IBC)
- 2015 International Existing Building Code (IEBC)
- ASCE 7-10 Minimum Design Loads (and Associated Criteria) for Buildings and Other Structures
- ASCE 41-13 Seismic Evaluation and Retrofit of Existing Buildings

The restoration and repair of the monument would not trigger a full seismic retrofit or compliance with modern code. The Monument is in Seismic Design Category "A" and is defined by code as a Historic Structure, which is exempt from seismic upgrade for Repairs based on the requirements in the IEBC. However, it was useful to verify the existing structure's performance under modern loads to understand level of performance and vulnerability to seismic risk. Furthermore, even if a seismic evaluation is not required by the IEBC, an owner may decide to initiate improvements to the structure without necessitating full compliance.

As discussed in the Phase 1 Report, the stability of the structure under gravity loading and modern code-required lateral loads (wind and seismic) was reviewed to investigate potential causes of the existing cracks in the masonry.

Code required lateral forces were determined using ASCE 7, with Risk Category III assumed. Based on the Geotechnical Report by Langan [11], the assumed seismic design parameters assumed during Phase 1 were updated to reflect the information gathered during the geotechnical investigation. These changes are summarized in **Table 2**. Note that the Seismic Design Category reduced from SDC B to SDC A, which results in a significant reduction to the seismic forces.

Table 2 Seismic Design Parameters

Seismic Design Parameter	Phase 1 Assumed Value	Phase 2 Langan Report Value
Short Period Spectral Acceleration (S_s)	0.2	0.184
1 Second Spectral Acceleration (S_1)	0.053	0.072
Soil Site Class	D	B
Long Period Site Coefficient (F_v)	2.4	1
Design S_s (S_{ds})	0.213	0.123
Design S_1 (S_{d1})	0.085	0.048
Seismic Design Category	B	A

The design wind pressure was calculated using ASCE and the code-required 120 miles per hour basic wind speed. The resulting average wind pressure was applied to the Finite Element Model.

Wall Hand Calculations

The structural analysis from Phase 1 was updated and further developed with the new material properties obtained from ANA's Phase 2 testing and from Langan's Phase 2 Geotechnical Report. Our Phase 2 analysis focused on investigating concentrated stresses and the potential distribution of such concentrations because of the observed widespread cracks in the Monument.

The crack patterns observed in the Monument indicate that the masonry may no longer act as a uniform cross section. Cracks at the corner header stones in the interior of the Monument indicate that perpendicular walls lack their original continuity. Large vertical cracks that propagate through stones and mortar head joints may reduce each wall's local stiffness. A lack of alignment between the interior and exterior masonry coursing indicates that in some locations, the wythes may be acting independently.

This is supported by the results of ANA's in situ existing compressive stress testing [8]. Their results show that at varying heights inside the monument, stresses vary significantly from what would be expected with an idealized, uniform cross section. For instance, we would expect that compressive forces would always increase under gravity loads towards the base of the monument, but their results show that this isn't always the case.

To investigate the effect of potential discontinuities in the masonry compared to the idealized cross section, we analyzed four reduced cross sections representing disconnected inner and outer wythes (**Figure 7a** and **b**) and disconnected corners (**Figure 7c** and **d**). The effective cross-sectional area over which the stress is distributed is represented in dark gray as a portion of the full area.

The uniform cross section analysis resulted in compressive stress under gravity of 180 pounds per square inch (psi), 216 psi under wind loading, and 240 psi under seismic loading (all based on modern code loads). While the wall was determined to be in tension in the case of a seismic event in Phase 1, the updated hand calculations determined this is no longer the case. This is driven by the reduction to the Seismic Design Category, increase in assumed masonry density based on materials testing, and refinement of calculations (see **Table 2**). However, if the masonry is not acting uniformly, stresses could get higher and closer to the allowable strength of the masonry under a code prescribed seismic event.

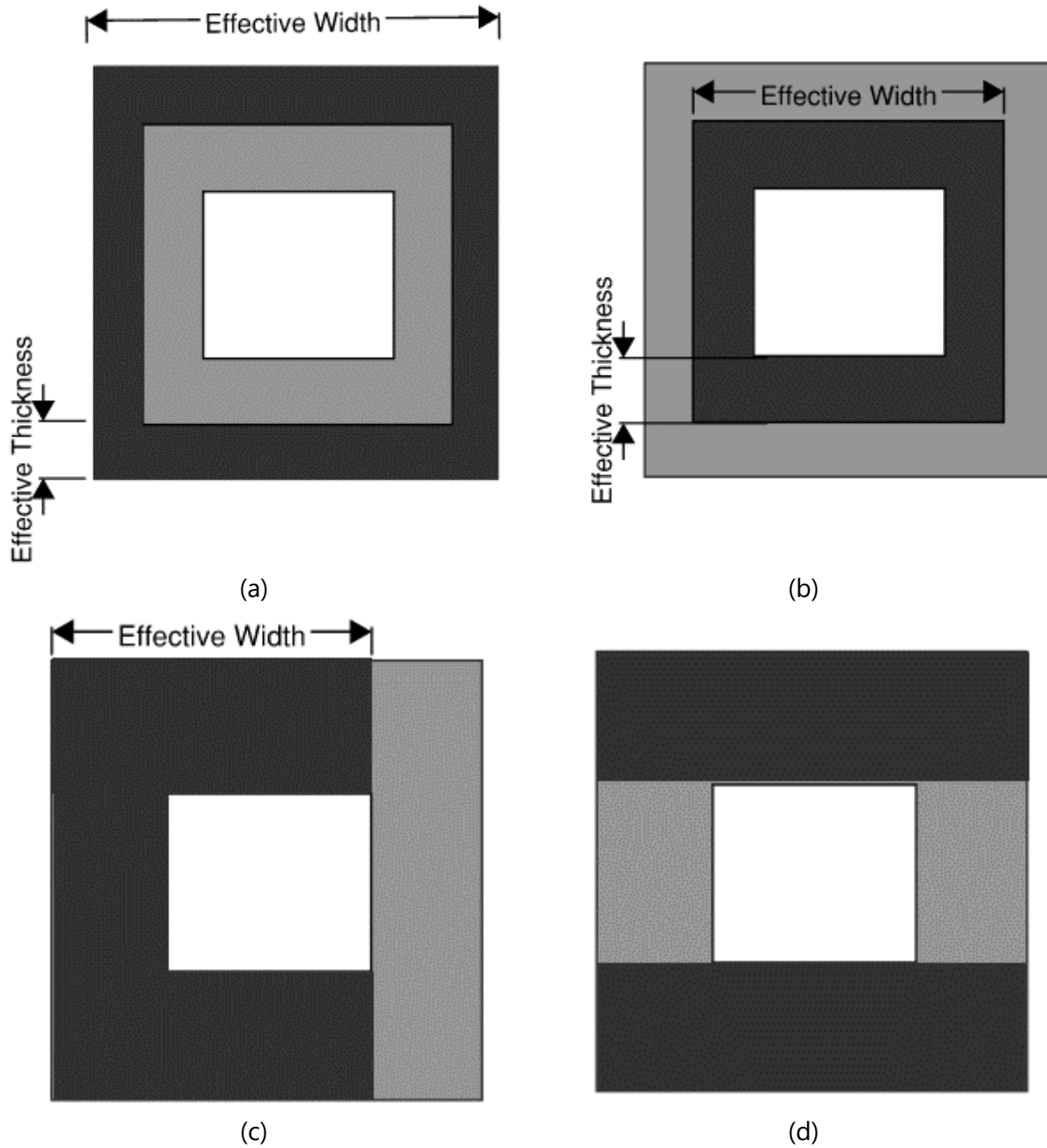


Figure 7 Modified Wall Cross Sections: (a) Outer Wall, (b) Inner Wall, (c) C-Section, (d) Parallel Walls

To study the effects of stress concentrations acting on a reduced or discontinuous section of the wall, different effective cross sections of the Monument were studied. These four scenarios included an assumption that the stress was distributed over the outer wall only, the inner wall only, over a C-shape section, and over two parallel walls. A summary of the impact of these cross-section changes is given in **Table 3**. Note that for the C-shape and parallel walls, the change of the stress at the base under gravity was not reviewed because these two analyses represent a

discontinuation of the cross section at the corners rather than a reduced cross section. Thus, the effects of the cross section are only seen in the lateral analysis.

For the lateral analysis under wind, the walls do not reach tension for any of the modified cross sections. The maximum compressive stress reached is 966 psi at the base of the Monument under the inner wall condition (case b). If a seismic event were to occur in accordance with modern codes under these modified cross sections, tension would be seen in the inner wall condition, with a maximum tensile stress of 76 psi. The outer wall condition (case a) was also determined to have a significantly higher compressive stress at the base, with a value of 619 psi. Although these values are not higher than the measured (ultimate) compressive strength, they are well above the allowable stresses and could cause distress due to local stress concentrations.

Table 3 Stress at Base and Percent Difference from Effective Cross Section Analysis

STRESS AT BASE (psi)					
	Gravity	Wind Compression Under Uplift	Wind Compression	Seismic Compression Under Uplift (+) or Tension (-)	Seismic Compression
Full Wall	183.8	151.8	215.7	123.6	243.9
Outer Wall	494.5	117.8	560.4	59.7	618.5
Inner Wall	707.0	45.9	844.9	-75.5	966.3
C-Shape	183.8	141.6	226.0	104.4	263.2
Parallel Walls	183.8	148.4	219.1	117.3	263.2

PERCENT DIFFERENCE (%)*					
	Gravity	Wind Compression Under Uplift	Wind Compression	Seismic Compression Under Uplift (+) or Tension (-)	Seismic Compression
Full Wall	-	-	-	-	-
Outer Wall	169%	22%	160%	52%	154%
Inner Wall	285%	70%	292%	161%	296%
C-Shape	-	7%	5%	16%	8%
Parallel Walls	-	2%	2%	5%	8%

Finite Element Shell Model – Modal and Linear Analysis

A three-dimensional Finite Element Model (FEM) was developed using the model presented in the Phase 1 analysis. This model was created in SAP2000 using scanned point cloud data provided by Langan. A modal analysis was performed to check the dynamic response of the Monument under different frequencies to validate the model against expected cantilever behavior. Then a linear elastic analysis was run to determine a baseline of how the Monument behaves under gravity, wind loads, and seismic loads as an idealized structure with no cracks, reduced cross sections, or

other discontinuities. This served to calibrate the model to the idealized hand calculations and ensure that results from both analyses agreed.

The results from the modal analysis were compared to those of a cantilever beam, as in its simplest form the Monument is a cantilever beam rotated by 90 degrees. **Figure 8** shows the expected *modal shapes* of a cantilever beam under its first, second and third natural frequencies. **Figure 9** shows the *deflected shapes* of the Monument under its first, second and third natural frequencies. The modal analysis response of the Monument model agreed with expected theoretical modal shapes of a cantilever beam. Note that the deflected shapes shown in these figures of the FE model have been amplified by a factor of 100 to clearly show the deformed shape.

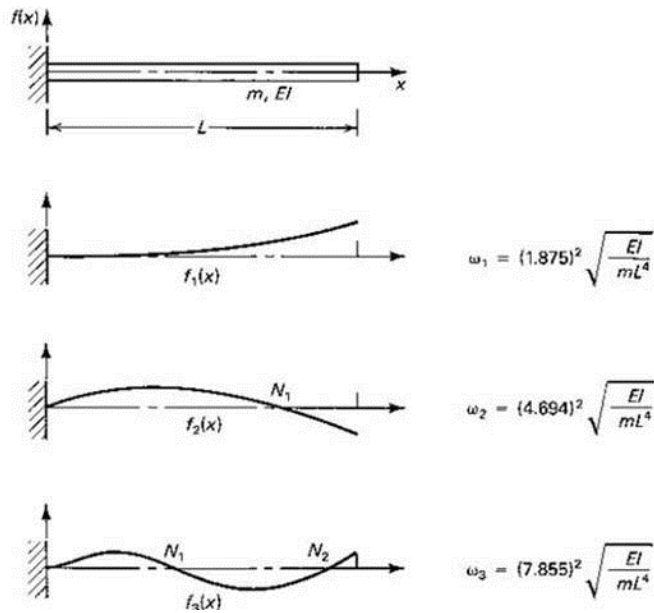


Figure 8 First Three Modal Shapes of Cantilever Beam [12]

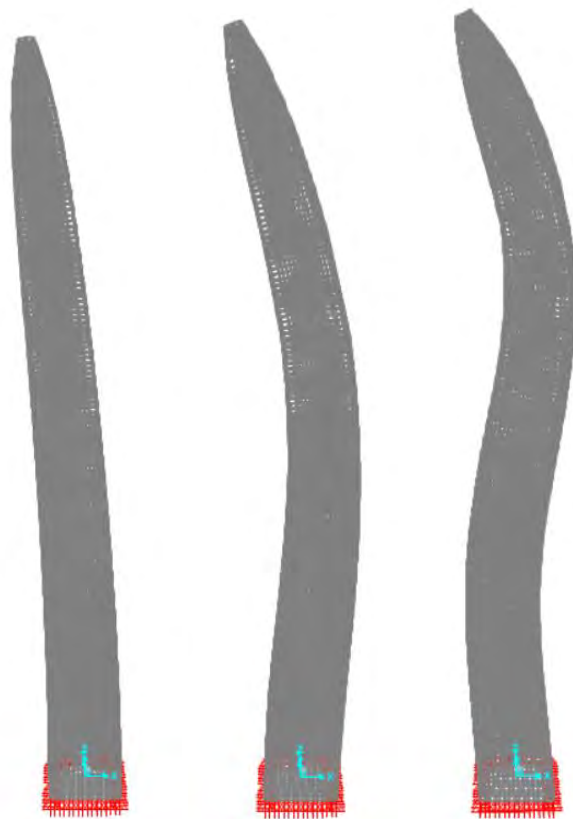


Figure 9 Modal Shapes of Monument Under its First Natural Frequency (Left), Second Natural Frequency (Middle), and Third Natural Frequency (Right) [amplified by a factor of 100]

For the linear seismic analysis, the stress values at the base of the structure generally agreed with the results of the hand calculations. The masonry does not see higher than allowable tensile stresses, and the compressive stresses at the base of the Monument are low. While it is believed that a seismic event was not the cause of the initial cracks observed in the Monument, any future code-level seismic events may amplify the effects of the cracks on the Monument.

Both Von Mises Stresses and the principal stresses are shown below. The Von Mises Stress gives the distortional stress in the material and is useful in determining if the materials are approaching their yielding capacity. The contour plot of these Von Mises Stresses were investigated (**Figure 10**) to identify of stress concentrations and changes to the load path under dead, wind, and seismic loads.

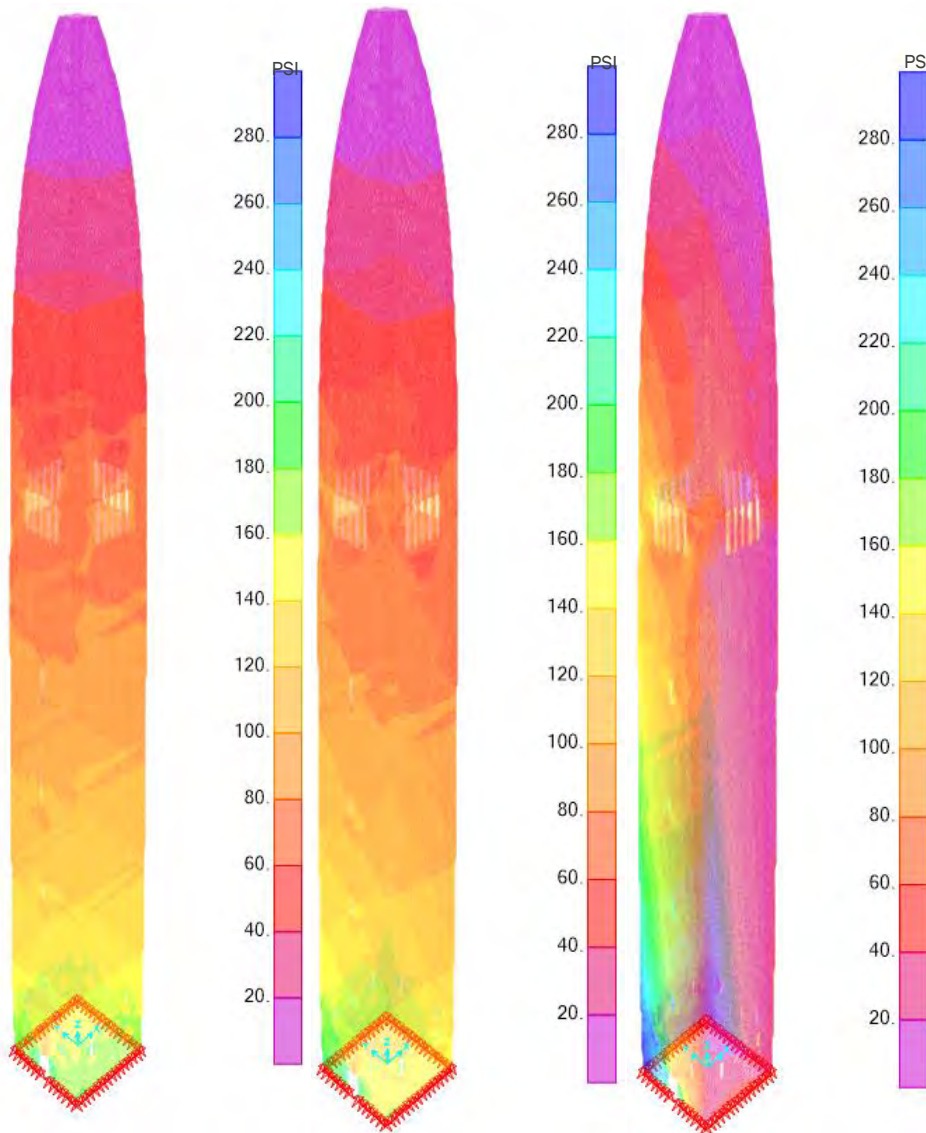


Figure 10 Von Mises Stresses Under Linear Analysis: Self-Weight (Left), Lateral Wind Loads (Middle) and Seismic (Right).

The contours of the principal stresses are presented in the figure below. These stresses identify the areas of tension and compression along the Monument, in which the compressive stresses are shown as negative values, and the tensile stresses are shown as positive values. For the wind and seismic loads, shown in **Figure 11**, the loads were applied in the positive y direction. Thus, for the wall section shown, the area of compression is on the left and the area of uplift is on the right. Areas around openings developed low values of compressive stresses and can start broaching low values of tensile stresses when lateral loads are applied. However, for a uniform cross section with no modeled cracks, these areas of stresses did not show forces getting close to the allowable limits in tension or compression. The most vulnerable areas are at reentrant corners and openings in the masonry, as expected.

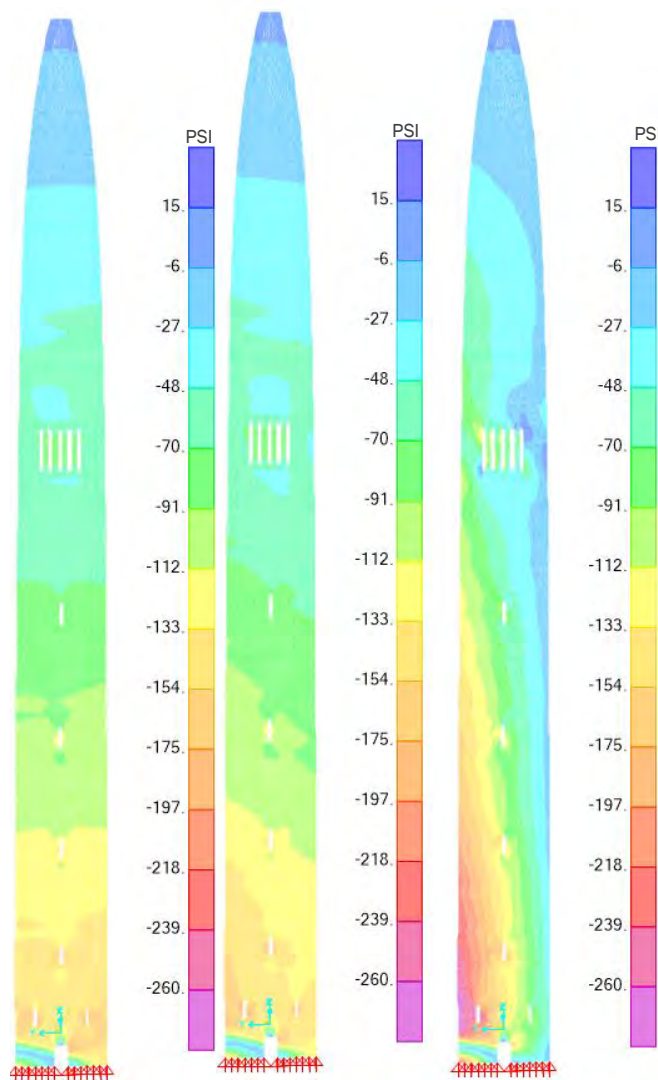


Figure 11 Principal Stresses Under Linear Analysis: Self-Weight (Left), Lateral Wind Loads (Middle) and Seismic (Right)

Once the model was calibrated and analyzed in its idealized state, we manipulated the model to experiment with its global response under different cracked conditions. The first condition studied was the reduction of the stiffness by the application of stiffness modifiers. These modifiers allow for the reduction of stiffness through altering the material properties.

The modifier was defined as 0.5 for axial and bending per Eurocode 8 recommendations for masonry modeling. The reduced stiffness led to non-homogenous stress redistribution in the model. Reentrant corners and around openings attracted more load and accumulated higher stresses compared to the uncracked model. Under the cracked condition, the maximum compressive stress was 200 psi, which is within allowable limits. The masonry did not experience tension due to the application of lateral wind forces or seismic forces. This is likely because the induced cracking relieved the tensile stresses that developed in the uncracked model. However, the concentration of stresses may indicate that wind and seismic forces may worsen the current cracked state of the Monument.

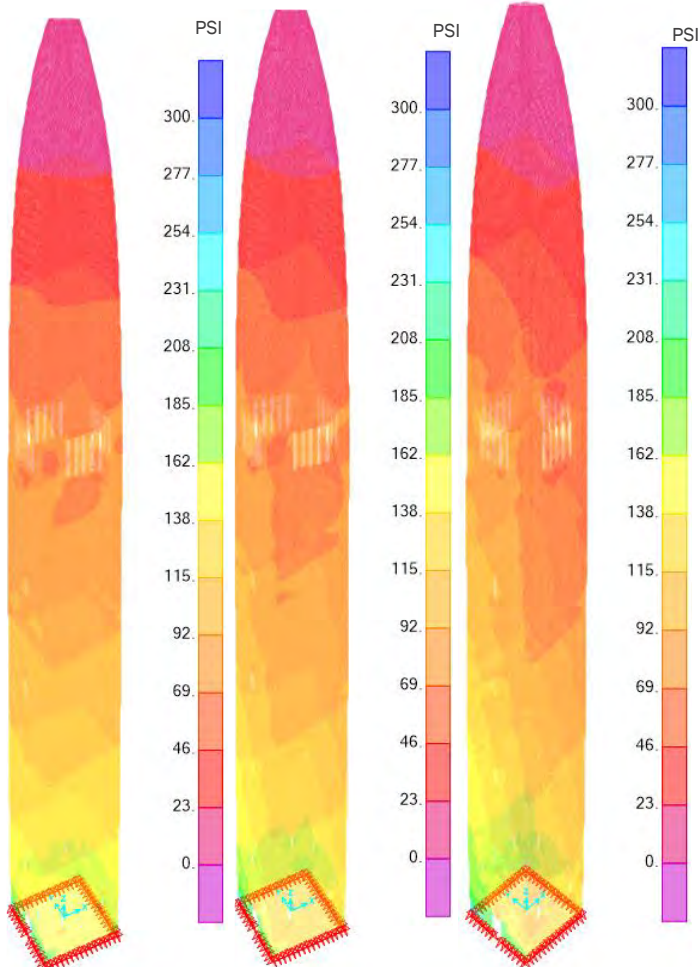


Figure 12 Von Mises Stresses (psi) of Cracked Model with 0.5 Stiffness Modifier Under Dead Loads Only (Left), Dead Loads + Wind Loads (Middle) and Dead Loads +Seismic Loads (Right)

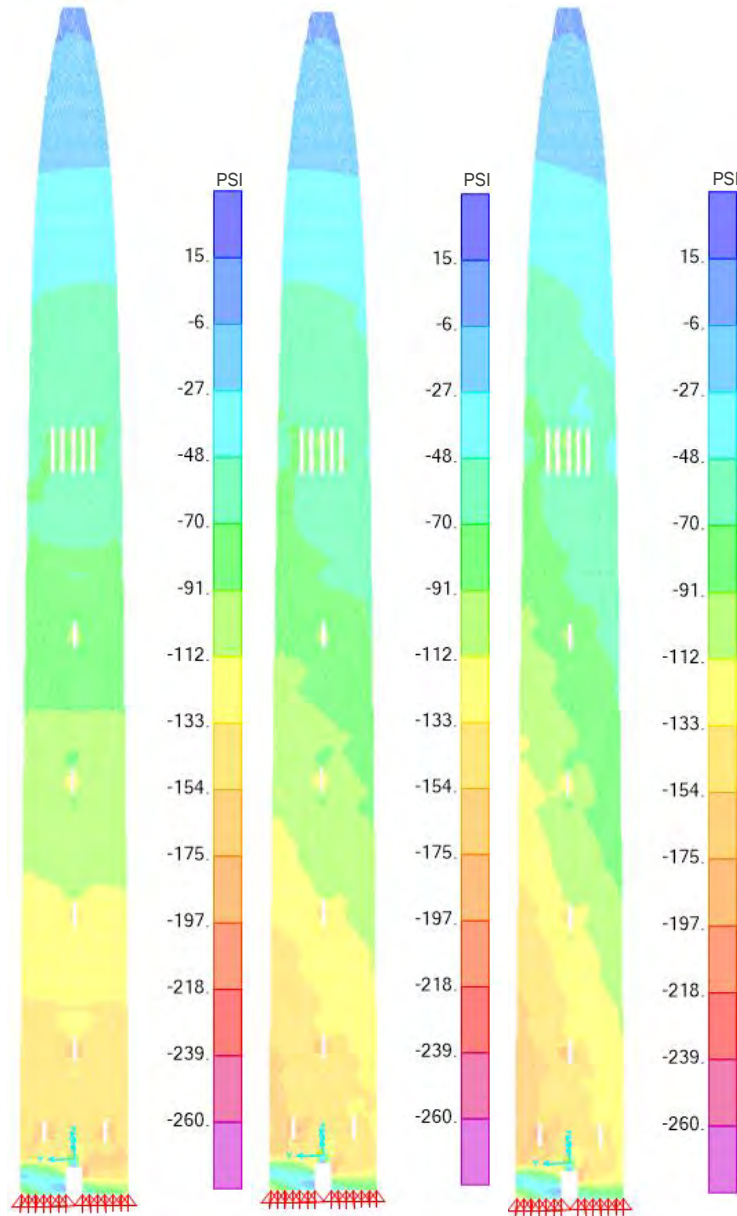


Figure 13 Principal Stress (psi) of Cracked Model with 0.5 Stiffness Modifier Under Dead Loads Only (Left), Dead Loads + Wind Loads (Middle) and Dead Loads + Seismic Loads (Right)

Table 4 Stresses at Midpoint and Corners Under Self Weight and Lateral Wind Forces

Self Weight (psi)		
	Stress at Midpoint of Wall	Stress at West Elevation Corner
Uncracked Model	175	194
Cracked Model (0.5 Modifier)	145	244
% Difference	-17%	26%

1.0D + 0.6W (psi)		
	Compressive Stress at Midpoint of Wall	Compression Under Uplift at Corner
Uncracked Model	221	175
Cracked Model (0.5 Modifier)	275	198
% Difference	24%	13%

Physical cracks were introduced to the linear FE model to experiment with cracks of multiple sizes and locations to examine the impact on the Monument's response.

Cracks were applied to the front and back of the model, with three different crack heights analyzed: 15 feet, 30 feet, and 50 feet cracks. It was observed that as the height of the cracks increased, the stress tended to concentrate around openings and corners like the behavior seen in the 0.5 crack modifier model. In none of these cases did the compressive stress exceed the allowable compressive stress. Tensile stress did develop at the corners of the introduced cracks, with the highest seen tensile stress measured at 40psi on seismic load of the 50 feet cracked model. This is slightly higher than the allowable tensile strength and indicates locations where additional cracking would occur.

Although the physical cracks are not an exact reflection of the conditions seen on the Monument, the analysis allows for the investigation of the effects of the stress concentrations and the effect of the reduced stiffness due to cracks. Once cracking has reached a certain level, represented by height in this case, it can cause progressive cracking in the masonry.

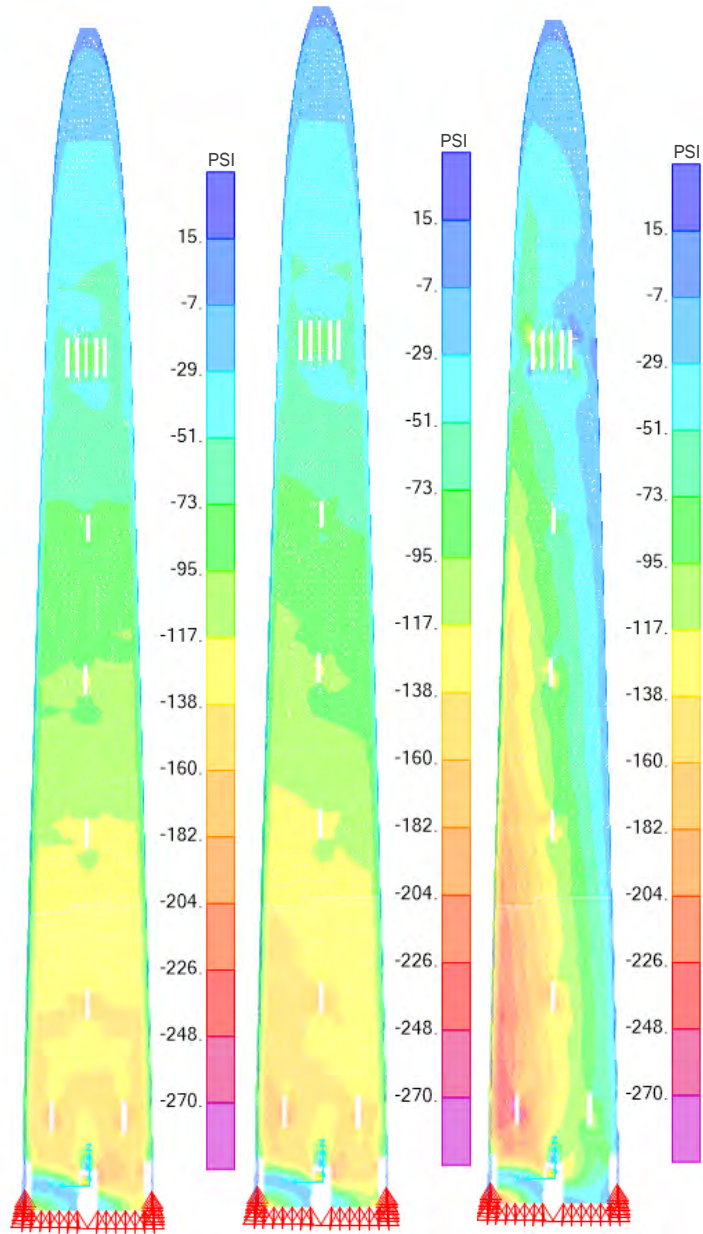


Figure 14 Principal Stress (psi) of Cracked Model with 15 Foot Cracks Under Dead Loads Only (Left), Dead Loads + Wind Loads (Middle) and Dead + Seismic Loads (Right)

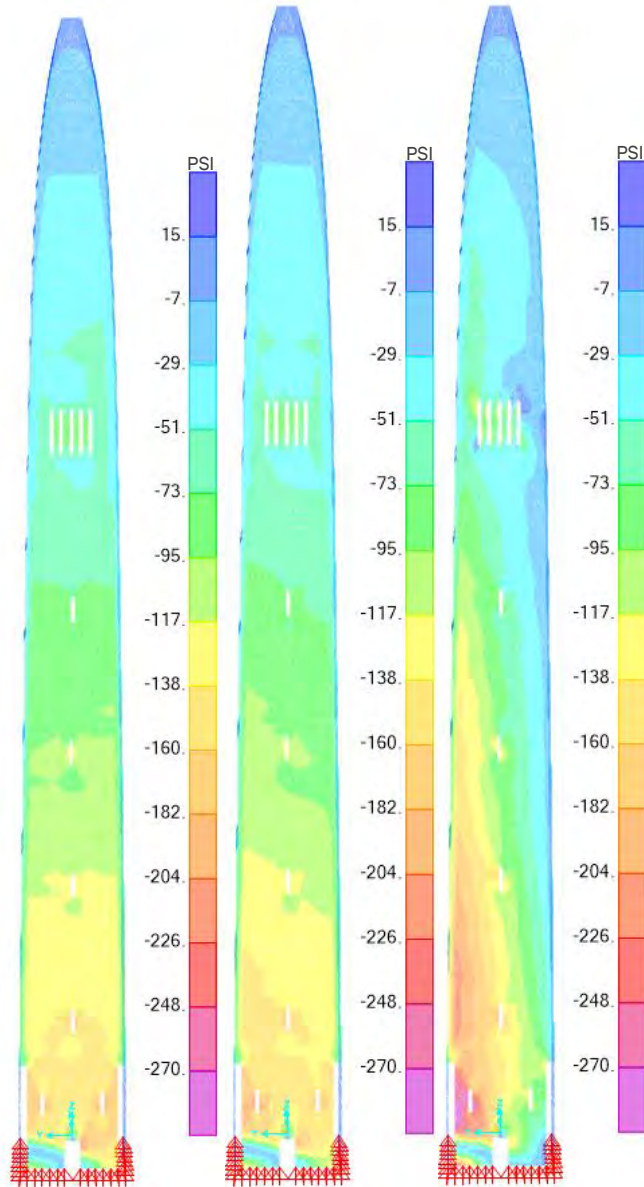


Figure 15 Principal Stress (psi) of Cracked Model with 30 Foot Cracks Under Dead Loads Only (Left), Dead Loads + Wind Loads (Middle) and Dead + Seismic Loads (Right)

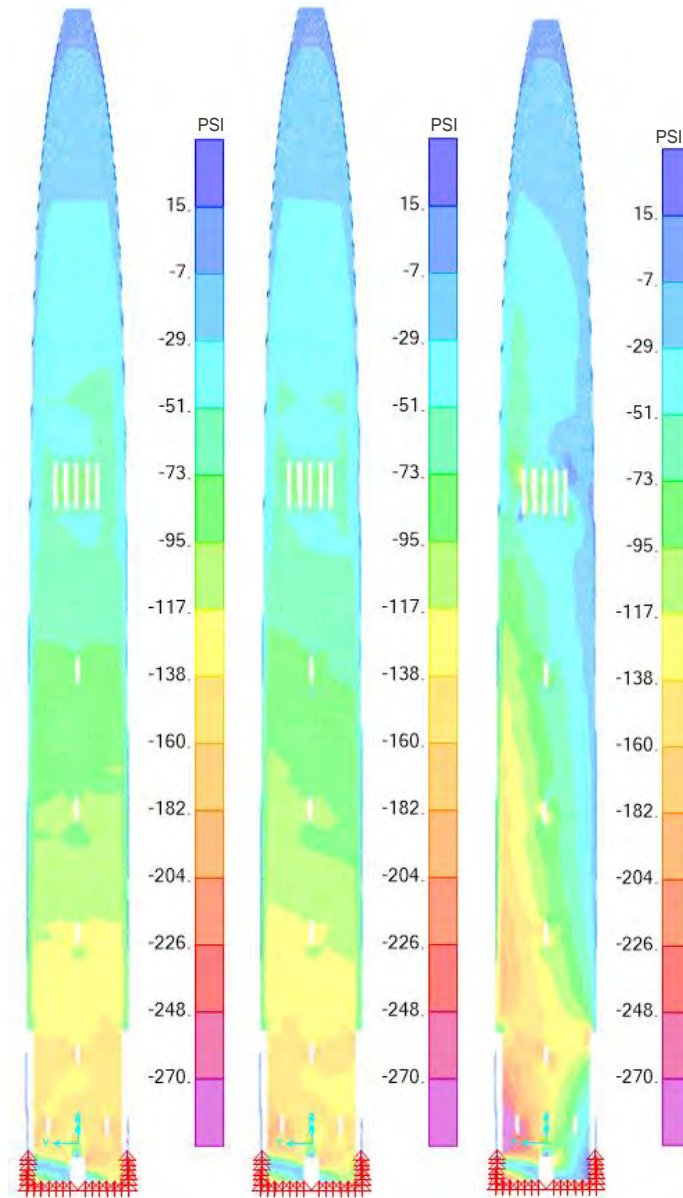


Figure 16 Principal Stress (psi) of Cracked Model with 30 Foot Cracks Under Dead Loads Only (Left), Dead Loads + Wind Loads (Middle) and Dead + Seismic Loads (Right)

Finite Element Shell Model - Nonlinear Analysis

Following the linear analyses, a study was conducted to examine the behavior of the Monument under nonlinear conditions through the performance of a pushover analysis. This analysis can give insight into the limits of the material, identifying how far the structure can be pushed before the material reaches plastic behavior. This behavior is of particular interest as it is the load under which a material can no longer rebound to its original shape when the load is removed and is an indication of the start of permanent damage to a structure. The first model of the nonlinear analysis that we completed was a *shell* model.

To conduct the pushover (nonlinear) analysis, a displacement-based approach was used based on literature review recommendations, with the model pushed to a limit of eighty-four inches to capture the full pushover curve. An uncracked model and models with 15 feet, 30 feet and 50 feet long physical cracks were used for these analyses. It was observed that in models with smaller cracks, the stresses looked more uniform and evenly distributed than when looking at models with larger cracks. The longer crack models showed significant stress concentrations due to redistribution of stresses to accommodate the cracking. This behavior was in accordance with the hand calculations of reduced cross-sectional areas, where it was also seen that a reduction in area led to increased concentrated stresses, particularly around the base.

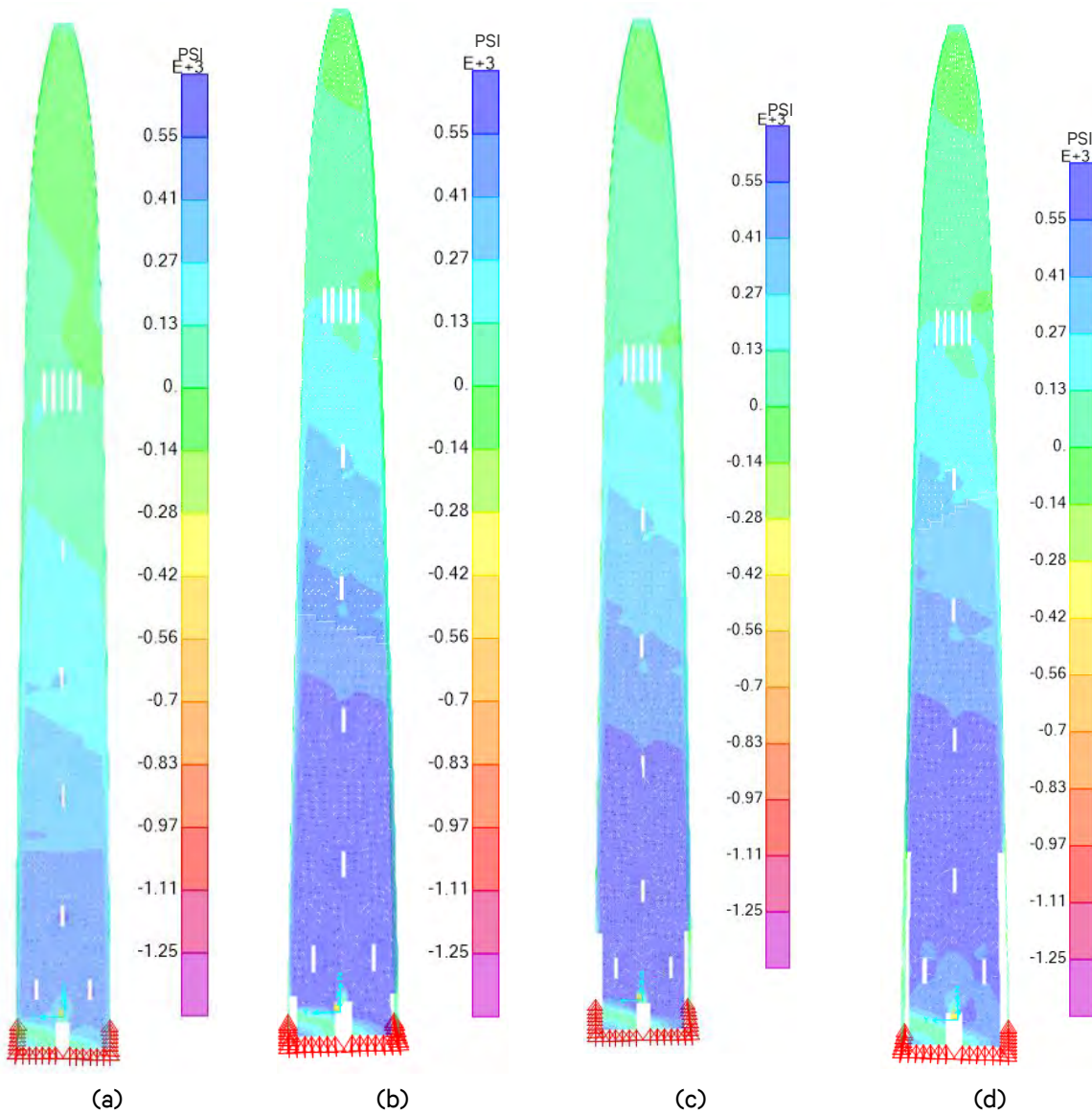


Figure 17 Resultant Pushover Analysis Principal Uplift Stress (psi) at Allowable Displacement: (a) Uncracked Shell Model, (b) 15' Cracks Model, (c) 30' Cracks Model, (d) 50' Cracks Model

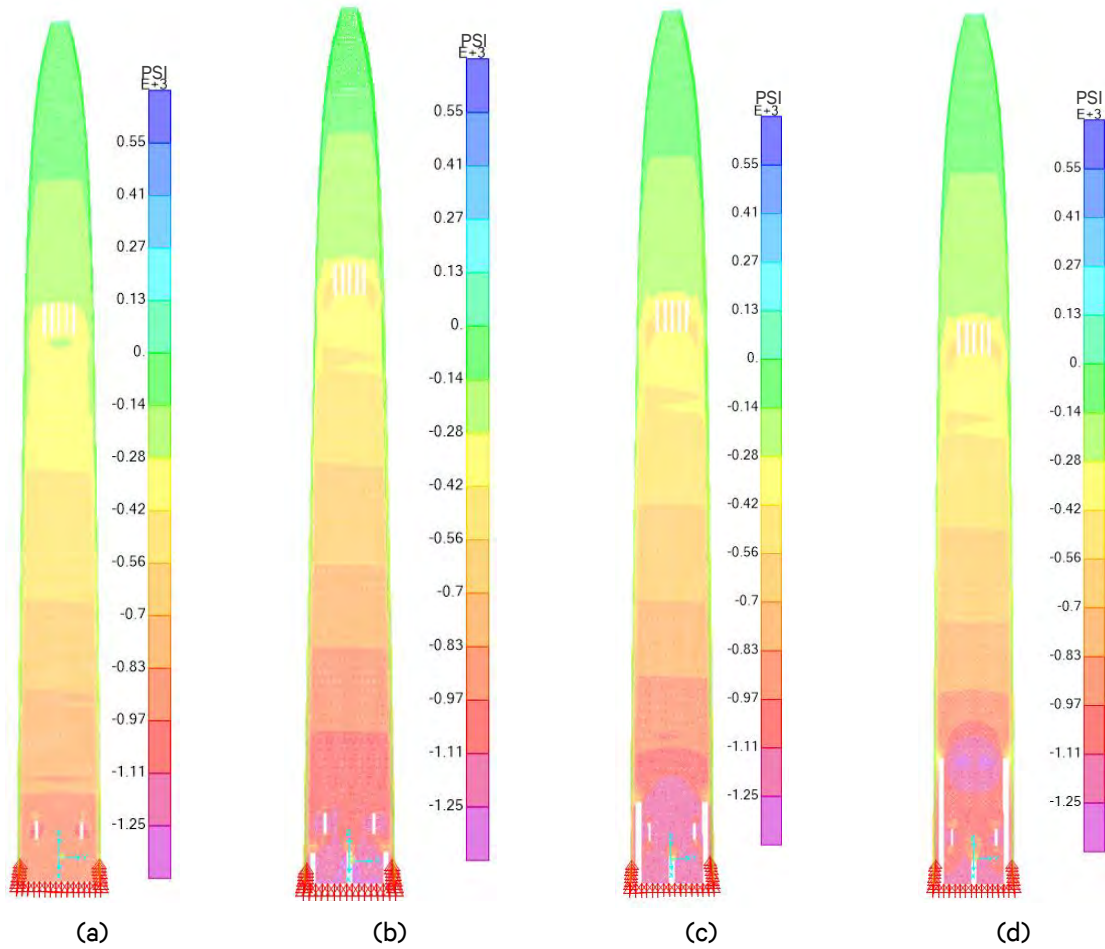


Figure 18 Resultant Pushover Analysis Principal Compressive Stress at Allowable Displacement: (a) Uncracked Shell Model, (b) 15' Cracks Model, (c) 30' Cracks Model, (d) 50' Cracks Model

The resultant pushover curves encompass the point at which softening of the material starts to occur. This happens at the inflection point in the curve and is an indication of failure of the material. These results were compared to the base shear values obtained from previously presented hand calculations (**Figure 19**). The seismic and wind base shear are far below the yield point of the material under all the tested conditions. The force required to reach the code allowable displacement of 11.8" (2H/600) far exceeds the code prescribed seismic and wind loading. Thus, it is unlikely that the Monument will experience global plastic deformation under a future code-prescribed event.

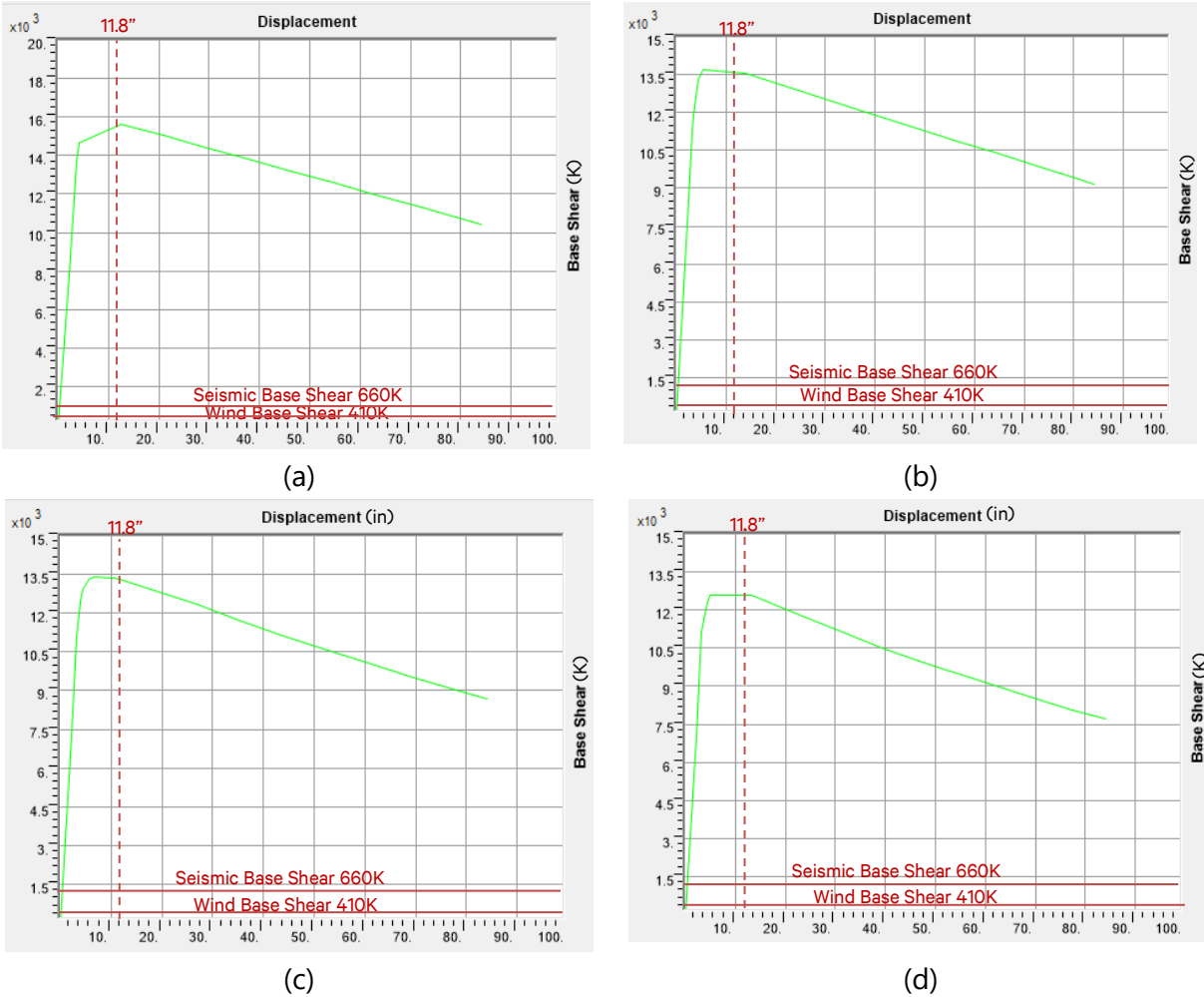


Figure 19 Pushover Curve of: (a) Uncracked Shell Model, (b) 15' Cracked Model, (c) 30' Cracked Model, (d) 50' Cracked Model

Finite Element Solid Model – Observation Level

A more detailed understanding of the effect the cracks have on the Monument was achieved by creating a 3D *solid* model, which represented the full thickness of the cross section of the wall. As this type of model requires more computational and analytical power, it was restricted to the observation level of the Monument where some of the greatest concentration of stresses and cracks were observed. In particular, this location was chosen as cracked lintels have been observed at this level; these warranted a closer analysis.

Two different scenarios were investigated, one in which a corner was completely disconnected from the Monument and another in which the stiffness of all 4 corners was reduced, similar to the approach taken for the full structure shell model.

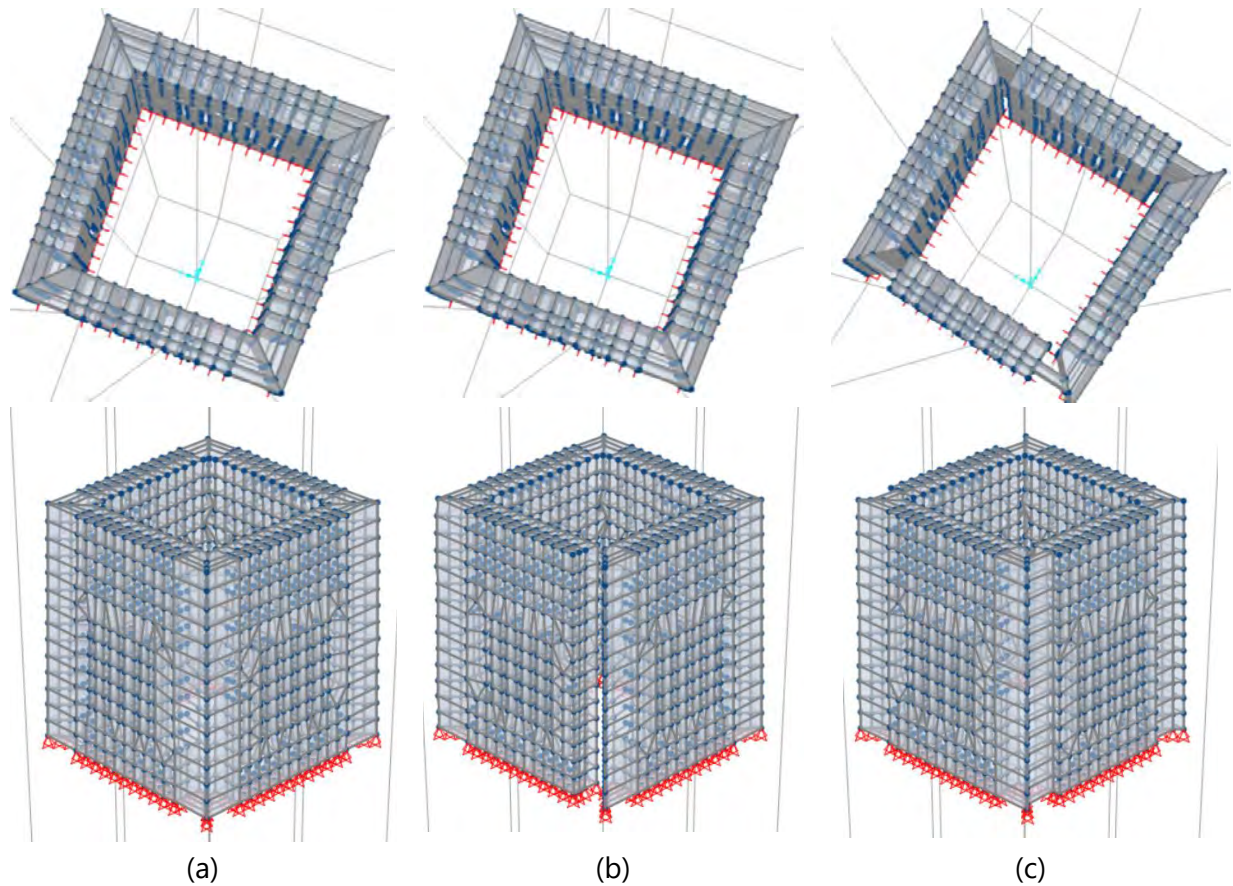


Figure 20 3D Solid Model: (a) Uncracked, (b) Fully Disconnected Corner, (c) Partially Disconnected Corners

Both a linear dead load and wind lateral load analysis were performed on the 3D models. Although no tension formed due to wind lateral forces, there was a significant reduction of compressive stress at the bottom of the windows. This means that although this area still sees compression, its reduction in stiffness increases the risk of failure from tensile forces. Furthermore, changes in the stress contour were observed, which are an indication of uneven stress distributions leading to a potential for localized failures.

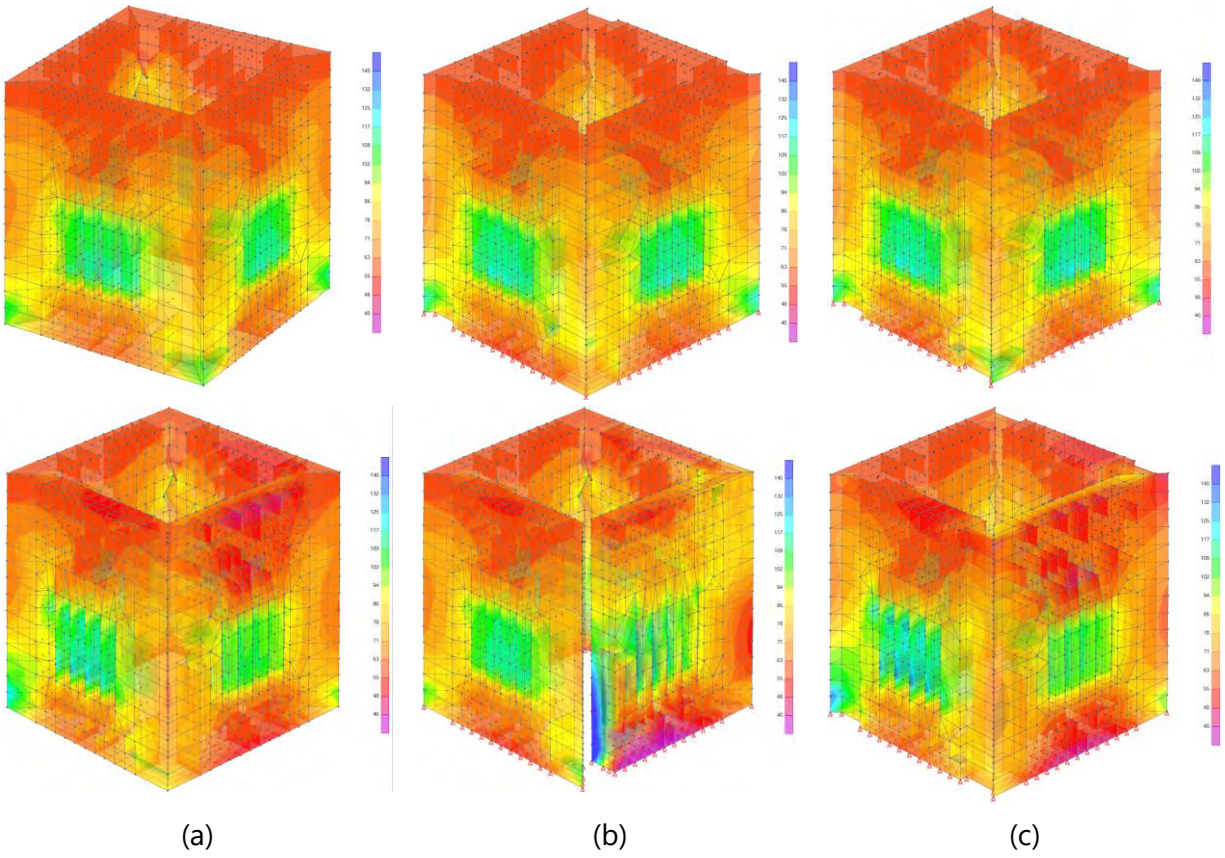


Figure 21 Von Mises Stress from Dead Loads (Top) and Dead Plus Wind Loads (Bottom) in the 3D Solid Model: (a) Uncracked, (b) Fully Disconnected Corner, (c) Partially Disconnected Corners

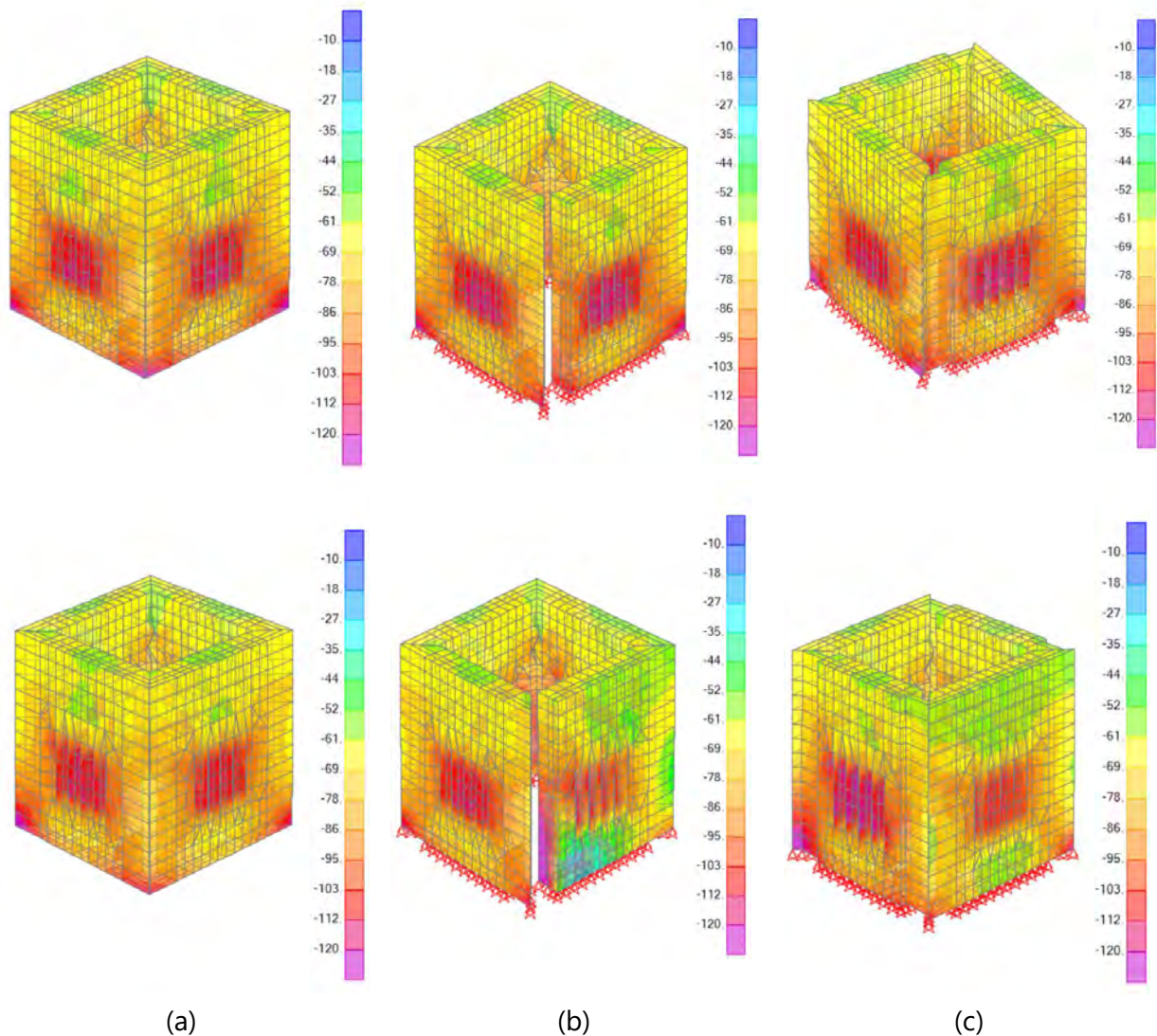


Figure 22 Principal Stress from Dead Loads (Top) and Dead Plus Wind Loads (Bottom) in the 3D Solid Model: (a) Uncracked, (b) Fully Disconnected Corner, (c) Partially Disconnected Corners

Masonry Unit Capacity Checks

To evaluate the potential for cracking due to the local stress concentrations seen in the Finite Element analysis, Silman also studied the bending and shear capacity of individual masonry units within the Monument (acting as beams with variable spans or distances between points of support). The studies assumed an unsupported length of masonry unit that could be caused by mortar deterioration or washout that has left open bed joints in the masonry. It is important to note that only short lengths (less than 12”) of unsupported stone were observed on the exterior and interior of the Monument and that **no** large voids were identified through Surface Penetrating Radar scanning or borescopes in the middle masonry wythe. However, the compressibility and relative softness of mortar compared to the masonry units could allow the units to experience

beam action similar to a true unsupported condition. This is significant because though no large open joints were observed on the Monument, bending action could still be happening without any observable distress until cracking occurs.

To capture the behavior of the varying stone geometries and possible support conditions, a spreadsheet analysis was completed to modify a single variable (unsupported length, height, or depth of stone highlighted in the tables below) while holding the other two variables constant. This was done to determine at what magnitude of distributed load or point load a stone with the given dimensions would experience failure due to bending and shear.

Based on the global FEM analysis, local compressive stress concentrations in the cracked masonry can be as high as 244 psi due to gravity alone and as high as 275 psi under wind loading. The allowable distributed loads in red in the table below are below the threshold of local stresses observed in the model, thus indicating masonry units that would crack due to code prescribed loading on the already cracked Monument. Generally, the compressive loads in the Monument are higher at the bottom of the structure and lower moving up its elevation.

Table 5 Allowable distributed and point load calculation for varying unsupported lengths of stone.

Unsupported length (in)	6	12	18	24	30	36	42	48
Height (in)	20	20	20	20	20	20	20	20
Depth (in)	24	24	24	24	24	24	24	24
S (in ³)	1600	1600	1600	1600	1600	1600	1600	1600
Allowable Moment (k-in)	267	267	267	267	267	267	267	267
Allowable Point Load (k)	178	89	59	44	36	30	25	22
Allowable Distributed Load (k/in)	59	15	7	4	2	2	1	1
Allowable Distributed Load (psi)	2469	617	274	154	99	69	50	39

Table 6 Allowable distributed and point load calculation for varying heights of stone. Note that the typical exterior stone is 20 inches tall.

Unsupported length (in)	12	12	12	12	12	12	12	12
Height (in)	8	10	12	14	16	18	20	22
Depth (in)	24	24	24	24	24	24	24	24
S (in ³)	256	400	576	784	1024	1296	1600	1936
Allowable Moment (k-in)	43	67	96	131	171	216	267	323
Allowable Point Load (k)	14	22	32	44	57	72	89	108
Allowable Distributed Load (k/in)	2	4	5	7	9	12	15	18
Allowable Distributed Load (psi)	99	154	222	302	395	500	617	747

Table 7 Allowable distributed and point load calculation for varying depths of stone. Note that the section modulus and area of applied loading are both linear with depth resulting in a constant allowable distributed load and varying allowable point load.

Unsupported length (in)	12	12	12	12	12	12	12	12
Height (in)	20	20	20	20	20	20	20	20
Depth (in)	12	16	20	24	28	32	36	40
S (in ³)	800	1067	1333	1600	1867	2133	2400	2667
Allowable Moment (k-in)	133	178	222	267	311	356	400	444
Allowable Point Load (k)	44	59	74	89	104	119	133	148
Allowable Distributed Load (k/in)	7	10	12	15	17	20	22	25
Allowable Distributed Load (psi)	617	617	617	617	617	617	617	617

Thermal Analysis

As discussed in the Phase 1 Report and confirmed by additional modeling in Phase 2, the global stresses of the Monument for loading on a uniform cross section are within allowable limits. Because of this, we hypothesize that the widespread cracking of masonry in the Monument is likely caused by local stress build ups due to temperature fluctuations. Thermal stress occurs when boundary conditions prohibit the natural expansion and contraction of a material due to changes in temperature. Seasonally, the Monument experiences large temperature swings; the record high temperature in Bennington is 101°F and record low temperature is -30°F, which demonstrates the potential maximum temperature range experienced by the Monument.

Our analysis assumes the baseline thermal state of the Monument is the average of the two extremes. With this potential for a 65° temperature change (from average to extreme), we calculated a maximum potential thermal stress of 275 psi. When acting expansively, this is higher than the allowable tensile capacity of the masonry and could result in cracking to relieve thermal stresses if the Monument is restrained at each corner by its perpendicular walls. It is also possible that the walls are thermally restrained internally within the thickness of the walls, as the wall reaches a maximum thickness of 7'-6" at the base of the Monument. However, boundary conditions have a significant effect on thermal stress calculations and should be further reviewed during the design phase.

Since electronic monitoring has begun on the Monument, the highest and lowest temperatures recorded inside the Monument have been 80.5°F and 25.8°F, respectively [8]. On those days, the exterior temperature was approximately 95°F and -13°F [13]. The thermal mass of the structure leads to a significant temperature gradient between the exterior masonry wythe and interior masonry wythe. The interior masonry will expand and contract slower than the exterior masonry that is directly exposed to the climate. For example, on a sunny day, the interior masonry will

remain cold while the exterior masonry expands as it is heated in the sun. Cracks on the exterior could form to release the buildup of thermal tensile stresses between the exterior and the interior.

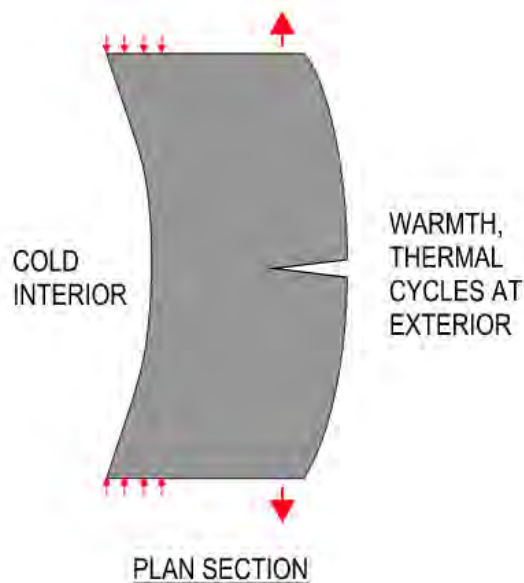


Figure 23. Schematic depiction of the boundary conditions through the masonry in the Monument. The relatively slow changing interior temperatures make the interior masonry act as a restrictive boundary condition to the exterior that experiences greater and faster temperature fluctuations.

It is well documented [14] that the rate of temperature change in the stone will have a large effect on its internal stresses. Small changes in temperature can cause large stresses due to differential strains that are beyond the scope of a structural analysis. This is a potential area of further study that is discussed in the Recommendations section of this report.

Structural Analysis Conclusions

During Phase 1 of our study, it was concluded that the wall was globally stable and that stresses were within allowable limits based on hand calculations using current codes. Based on the Phase 2 analysis, including updated wall calculations, Finite Element Models, capacity checks, and thermal analysis, the following conclusions can be made:

- It was concluded in Phase 1 that loads in the wall exceed allowable tension and compression stresses under a full code-defined seismic event. However, based on updated material properties and the revised Seismic Design Category from Phase 2, and assuming a uniformly built and loaded wall, this stress exceedance scenario does not occur. Under such strict conditions, which may not represent the actual in-service condition of the Monument, the masonry does not exceed allowable tension and compressive stresses. However, the loads have the potential to be high in an extreme seismic or wind scenario

and could cause local stress concentrations above allowable capacities when combined with other sources of stress or non-uniform load application.

- Assuming a solely uniform distribution of loads over the wall section, allowable stresses were not exceeded under gravity loads, lateral wind loads and seismic loads in both the hand calculations and Finite Element Mode. Both the tension and compressive stresses were below the limit of the allowable stress values. It is important to highlight that this is an idealized assumption and real-world conditions may present higher than desirable stress concentrations.
- The hand calculations showed that reductions and discontinuities in the cross section led to increased local stresses in the Monument. The inner wall effective cross section scenario showed the most significant increase in stress, with both tensile and compressive stresses exceeding allowable values. This represents how the cracked behavior of the structure can change the load path in the Monument and lead to significant stress concentrations.
- The shell and solid models did not exceed allowable stresses when analyzed under gravity, wind, and seismic loads. Only small amounts of tension (below 20 psi) developed in the model during the application of lateral wind and seismic forces. Allowable compressive stresses were not exceeded. However, significant changes to the stress contours indicate uneven distribution of stresses and potential for localized failures.
- The nonlinear analysis showed that the magnitude of loading needed to cause inelastic behavior is well above any limits the Monument would realistically see based on code-defined wind and seismic forces. This analysis highlighted the effect that large-scale cracking has on the concentration of forces and stresses.
- Unsupported lengths of individual stone units allow beam action in the masonry. Once the masonry is cracked, stresses due to lateral loading such as seismic and wind are higher than the allowable bending and shear capacity of some geometries and spans of stone present on the Monument. Issues such as mortar deterioration or missing mortar can cause bending type action that can increase stresses locally. The extent of mortar loss would have to be significant to crack the masonry, but if combined with other structural stresses such as thermal or gravity it could cause overstress.
- Thermal stresses due to temperature fluctuations experienced by the Monument may exceed the allowable tensile capacity of the masonry. This could be a cause of widespread cracking that must be considered when designing repairs. Further analysis is required to understand the effects of thermal stresses.

- Although no single item was proven as the cause of the cracking, it is likely that a combination of these issues occurring at the same time has led to a cumulative effect of stresses above the allowable capacity of the masonry.

IV. DISCUSSION

The information gathered and analysis performed in our Phase 2 effort has allowed the investigation team to further refine the potential causes for cracking in the Monument identified in Phase 1. The following items were discussed in the Phase 1 portion of this report as contributing factors and in need of further study. The following serves to update our initial findings based on the information learned in this Phase 2 investigation:

1. **Stone Material:** Materials testing performed by JBC and Highbridge revealed that the dolomitic limestone and calcitic marble that make up the Monument appear to be appropriate building stones for the scale of structure and local climate conditions. While the stone is completely saturated, the stones sampled had relatively low porosity. No evidence of internal freeze thaw damage was observed in petrographic analysis. Based on material testing, the stone material on its own is not obviously contributing to the cracking.
2. **Mortar:** While the original specification for the Monument specified a hard Portland cement mortar, none of the tested samples or visual observations found evidence of this original mortar still being present. Testing revealed all the mortar samples to be a soft Rosendale natural cement mortar. The material conservator confirmed that the type of mortar used during construction was appropriate for the Monument. However, significant mortar loss is present on the Monument due to freeze-thaw cycles, thermal action, and deferred maintenance. Improper prior mortar repairs with caulking and hard mortars may have contributed to damage of the masonry. Additionally, a moderate alkali-aggregate reaction (AAR) was observed in mortar removed from the interior of the wall. While AAR is often deleterious to masonry, if the scale of the reaction observed in the select sample is representative of the overall Monument condition it is not a cause for concern. While it is not believed that issues with mortar type or open joints were the cause of initial cracking, they do allow for significant moisture ingress that can contribute to a variety of deterioration methods over time. Continual appropriate maintenance and regular repointing campaigns will be necessary to keep water out of the Monument.
3. **Freeze-thaw cycles:** Refer to the Phase 1 Report for information on the deleterious effects of freeze-thaw cycles. Based on the petrographic analysis performed by Highbridge, we understand that freeze-thaw action is worsening the cracks on the Monument but was not the initial cause of the cracking.
4. **Moisture and Humidity:** Refer to the Phase 1 Report for the moisture and humidity conditions at the Monument. Refer to reports by Steven Winter Associates and Landmark Facilities Group for updates on the moisture and humidity studies performed during this phase. Generally, moisture and humidity exacerbate potential masonry deterioration

mechanisms. Preventing moisture ingress and drying out the Monument will be important to limiting future deterioration.

5. **Local Stresses:** There are several forces acting on the structure that have the potential to lead to highly concentrated local stresses. The cumulative actions of thermal stress, improper previous repairs, moisture ingress, and missing mortar joints all create conditions where high concentrated forces or internal stresses can cause tension and cracking of the stone masonry. After the initial cracking of the structure, the Finite Element Analysis shows how the load path redistributes to stiffer, less cracked areas of the masonry, which causes new load concentrations and further cracking. The cracks were reported very early on in the Monument's history, so a rare, large lateral loading event (wind or seismic) is unlikely to have caused initial cracking. Rather, it is most likely that the repetitive nature of climatic stresses experienced in the short-term, like freeze-thaw and temperature cycles, were the initial cause of cracking. However, loading and the localized re-distribution of loads that have happened over time or may happen in the future could worsen the cracking. As has already been observed and documented by other team members, this cracking exacerbates the infiltration of water and the localized failure of masonry (stone and mortar).
6. **Headers:** Refer to the Phase 1 Report for a description of the headers documented by ANA in Phase 1. The lack of connectivity through the wall section below the elevation of the observation deck should be considered when designing repairs for the Monument. Comparison of crack locations to the depth of individual stone units should be used to inform where mechanical repairs such as pinning may be necessary.
7. **Loading:** Further global analysis of the uncracked structure using updated geometry and material properties from Phase 2 testing showed that under code prescribed wind and seismic loading, the Monument does not exceed allowable tension or compression limits and is globally stable. To date, the Monument has not experienced any significant seismic event at code level loading but could in the future. However, the Monument does go into tension locally with a reduced (cracked) cross section. Thus, wind and seismic loading are not the cause of initial cracking in the Monument but may be contributing to ongoing cracking now that the initial damage has occurred, and there is a general vulnerability of the monument for a future code-defined seismic event.
8. **Geotechnical:** The geotechnical report confirmed that the calculated bearing stresses are within allowable limits. The Monument is located on rock with a bearing capacity of approximately 10 tons per square foot (tsf). The types of cracks observed as part of typical building settlement do not match what was observed at the Bennington Battle Monument. Settlement or inadequate foundations do not appear to be contributing to the cracking.

From a structural perspective, while all the items in the list above are contributing factors to the deterioration of the masonry, it is the local stress concentrations that appear to be the initial cause of cracking. The cumulative effects of lateral loading, mortar loss altering the load path, progressive cracking changing the connectivity of the cross section, thermal and freeze-thaw effects could cause overstress in the masonry. Any one of these mechanisms acting alone is not sufficient to cause the widespread cracking observed in the Monument, but the buildup of various stresses has the potential to exceed the allowable capacity of the masonry. Cracks and deterioration are due to local stresses rather than global behavior of the Monument under self-weight or lateral loads. The presence of cracks creates higher areas of localized, concentrated stresses, which in turn can cause more cracks.

V. RECOMMENDATIONS

Refer to the Phase 1 Report for full repair recommendations. Additional considerations for subsequent phases of design based on what we learned in Phase 2 include:

- Drying out the Monument is going to be critical, as the temperature differentials were found to be a potential contributing cause to the masonry deterioration. Given the need to address the water saturation deterioration of the masonry, please refer to the reports by others for additional discussion on options for this scope of work.
- Local stresses are a contributing cause to the cracking and any repair we undertake cannot cause additional stress concentrations. The future repairs should not be implemented in such a way that efforts to pin, repoint, grout, or otherwise repair the masonry allow for the development of significant new stress concentrations.
- Any mechanical repairs, such as pinning, must consider the location of cracks with respect to header stones and the connectivity between wythes in the masonry. Any reinforcements to lintels, such as at windows or doorways, should be carefully detailed to address concerns about potential new stress concentrations.
- Continuing cyclical maintenance and repair of the Monument is required. This is discussed in detail in the Phase 1 Report. We cannot reverse the cracking that has occurred or any initial cracking that has been exacerbated by freeze-thaw and moisture ingress. The State of Vermont will need to plan for regular repair campaigns to prevent moisture ingress.
- Areas of future study should include an analysis of thermal stresses within the stone masonry at a molecular scale using techniques such as a Monte Carlo simulation, WUFI Thermal Analysis, and detailed Finite Element Analysis with THERM Software. This level of modeling is beyond the scope of the Phase 2 investigation.
- Continued electronic thermal and movement monitoring of the Monument should be performed until repairs are made to ensure that any significant change to the state of the masonry is detected in a timely manner.
- This study focused on causes of the existing cracking in the Monument. The next phase of work should investigate the effects of potential future loading on the Monument's stability. We recommend a nonlinear time history analysis to analyze future seismic performance.
- Given the scale of the Monument and widespread cracking, we recommend that the State of Vermont engage an academic researcher who specializes in tall masonry towers, such as the towers discussed in the Literature Review section of this report, to peer review any proposed repair work on the Bennington Battle Monument.

VI. REFERENCES

- [1] L. Binda, *Learning from Failure: Long-Term Behavior of Heavy Masonry Structures*, Milano: WIT Press, 2008.
- [2] Milan, "Pavia, 30 anni fa il crollo della Torre Civica: "Teniamo viva la memoria collettiva di quella tragedia", *la Repubblica*, 17 March 2019.
- [3] C. Gentile and A. Saisi, "Ambient vibration testing of historic masonry towers for structural identification and damage assessment," *Construction and Building Materials*, vol. 21, no. 6, pp. 1311-1321, 2007.
- [4] L. Binda, A. Anzani and A. Saisi, "Failures due to long-term behavior of heavy structures: the Pavia Civi Tower and the Noto Cathedral," *Transaction on the Built Environment*, vol. 66, pp. 99-108, 2003.
- [5] L. A. Binda, A. Anzani and G. M. Roberti, "Tall and Massive Ancient Masonry Buildings: Long Term Effects of Loading," 2000.
- [6] R. Shehu, "Implementation of Pushover Analysis for Seismic Assessment of Masonry Towers: Issues and Practical Recommendations," *Buildings*, vol. 11, no. 71, 2021.
- [7] M. Bocciarelli and G. Barbieri, "A numerical procedure for the pushover analysis of masonry towers," *Soil Dynamics and Engineering*, vol. 93, pp. 162-171, 2017.
- [8] Atkinson-Noland & Associates, "Stone Masonry Evaluation," New York, 2023.
- [9] K. Parker, *The Architect's and Builder's Pocket-Book*, New York: John Wiley & Sons, 1886.
- [10] P. B. Lourenco and A. Gaetani, *Finite Element Analysis for Building Assessment*, Abigdon: Routledge, 2022.
- [11] LANGAN, "Geotechnical Engineering Memorandum," NYC, 2024.
- [12] N. Veerabhadraiah and E. Madhu, *Effect of Elastic Modulus and Density Ratio on Vibration Characteristics of Rotating Turbine Blade*, 2014.
- [13] TWC Product and Technology, "Latham, NY Weather History," Weather Underground, [Online]. Available: <https://www.wunderground.com/history/daily/us/vt/bennington/KALB/date/2022-8-8>. [Accessed March 2024].
- [14] W. H. Ito, T. Scussiato, F. Vagnon, A. M. Ferrero, M. R. Migliazza, J. Ramis and P. I. Braga de Queiroz, "On Thermal Stresses Due to Weathering in Natural Stones," *Applied Sciences*, vol. 11, no. 3, 2021.



REPORT

STONE MASONRY EVALUATION

Bennington Battle Monument
Bennington, VT

PREPARED FOR:

Stevens & Associates
95 Main Street
Battleboro, VT 05301

PREPARED BY:

Atkinson-Noland & Associates, Inc.
32 Old Slip, 10th Floor
New York, NY 10005
303.444.3620

Stone Masonry Evaluation
Bennington Battle Monument
ANA Job No. 23-031
September 20, 2023

1. INTRODUCTION

Atkinson-Noland & Associates (ANA) was on site to conduct supplemental nondestructive evaluation (NDE), facilitate the installation of additional structural health monitoring sensors, and to conduct material tests at the stone masonry walls of the Bennington Battle Monument in Bennington, Vermont. This scope expands upon the 2022 Phase 1 ANA scope that included NDE and one year of structural health monitoring, with the findings summarized in an ANA report titled, 'Final Report – Bennington Battle Monument 6-30-2022'. The main objectives of the work included confirming typical wall sections and the nature of internal wall construction with additional NDE via rope access, investigating stone unit and masonry wall assembly material properties, and to install additional sensors to expand and extend the duration of the structural health monitoring program.

ANA conducted the NDE and material testing from areas where walk-up access was available. Vertical Access (VA) assisted by conducting all other exterior NDE and sensor installation from higher portions of the monument via rope access. ANA personnel were on site from May 22nd to 25th for the NDE and expansion of the structural health monitoring program, and from July 17th to 20th for the material testing portions of the scope. Personnel from Silman and Stevens & Associates (S&A) were on site during portions of ANA's field work to discuss findings and identify specific areas of importance through the monument. Contractor assistance by means of stone core removals and housekeeping support was provided by Alegrone during ANA's field work.

1.1. General Wall Construction

The stone masonry walls at the Bennington Battle Monument are constructed of two- to three-wythes of stone masonry with dolostone and marble units. Where the wall is thicker towards the base of the monument, the wall appears to be three distinct wythes of stone masonry and further towards the top of the monument, the wall transitions to be two distinct wythes of stone masonry. The exterior face wythe appears to consist of only dolostone units with consistent coursing. The interior face wythe appears to consist of a combination of dolostone and marble with more dolostone present lower on the monument and more marble present higher on the monument. The interior face wythe appears to be uncoursed and not dressed.

Bond stones appear consistently present at the interior and exterior face wythes. The project contract and specifications from 1887 indicate that the walls are to be built with one fifth headers as highlighted in Figure 1. This specification appears to have generally been followed during the construction of the monument. Generally, bond stones appear to bridge between two wythes of stone. Therefore, the three-wythe portion of the monument likely has bond stones bridging the exterior face wythe and the internal wythe, as well as bridging the interior face wythe and the internal wythe. At the two-wythe portion of the monument, it appears the bond stones are through the full thickness of the wall.



Face stone. All face stone ~~shall be not less in depth than rise.~~
be not less in depth than rise.

Headers. **The walls are to be built with one fifth headers.** Headers are to extend through the walls.

Beds, builds and joints. All face stone are to have not less than 12 in, beds, builds and vertical joints, to be dressed to plane surface,

Figure 1. Excerpt from 1887 project contract and specifications indicating quantity of headers required.

Bed joint mortar has been evaluated in previous investigations using petrographic techniques and the mortar formulation was determined to match most closely that of a Type K mortar. Findings during the current phase of work determined that the collar joint mortar appears different in composition and is more similar to a poured concrete. That is, the collar joints were observed to contain large, crushed stone aggregates up to 2" to 3" wide as observed at the Goodman Jack core holes. The collar joints also appear to be 3" to 6" thick, as observed at core holes, indicating that the concrete mix would need to be poured in place rather than troweled by hand as typical collar joint mortar is placed. The material observed at the collar joints is more consistent with the description of concrete to be used in possible crevices at the foundation as identified in the 1887 specification, which is highlighted in Figure 2 and Figure 3.

The concrete to be used in possible crevices in the bed for foundation is to be of Portland cement. Clean gravel or sound and acceptable broken stones shall be used in forming the concrete; these materials shall be of varying sizes, none to be more than 2 in., and but very few to be less than one-fourth of an inch in their greatest diameters; they shall be free from clayey or other objectionable material, and shall be mixed with sand and cement of the qualities before specified, in the proportion of five parts, by measure, of gravel or broken stone to two parts of sand and one part of cement.

Figure 2. Excerpt from 1887 project contract and specifications indicating a concrete mix to be used in possible crevices at the foundation.



joints, the vertical joint to be from 1 in. to 10 in. Joints exceeding 3 in. to be filled in with concrete well rammed in place; other joints and the bedding of stone are to be done with cement mortar.

Figure 3. Excerpt from the 1887 project contract and specifications indicating how large joints at the foundation are to be filled with concrete rammed in place.

2. INVESTIGATIVE TESTING

2.1. Microwave Radar Scanning

Surface penetrating radar (SPR) was used to assess internal wall construction of the monument's stone masonry walls. The SPR method involves the transmission of high frequency electromagnetic radio (radar) pulses into the object of interest and measuring the time elapsed between transmission, reflection off a buried discontinuity, and reception back at the surface radar antenna. A pulse of radar energy is generated on a dipole-transmitting antenna that is placed on the surface of the wall. The resulting wave of electromagnetic energy propagates into the material and portions of it are reflected to the antenna especially at discontinuities. The discontinuities where reflections occur are created by changes in dielectric properties of the underlying material. Void spaces, metal presence, and any distinct change in material will generate significant radar reflections due to a change in radar wave velocity at the interface.

The scanning was conducted with multiple radar systems including a GSSI SIR 3000 and SIR 4000 using both 400 MHz and 1600 MHz antennas, and a Proceq GP8000 broadband radar system with stepped frequencies from 200 to 4000 MHz. The primary goal of the SPR scanning on this mobilization was to determine if stone thicknesses at the interior and exterior face wythes at higher portions of the monument were consistent with the findings from Phase I NDE work. Another main goal was to determine the consistency of internal wall conditions at varying heights up the monument, related to internal voiding and/or any presence of rubble construction. Previous findings from Phase I determined that the walls are primarily solid multi-wythe stone construction with coursed masonry throughout the thickness of the wall and not containing a rubble core.





Figure 4. VA technician collecting an SPR scan across a stone course at the exterior of the monument.

Approximately one-hundred and twenty-five (125) SPR scans were collected and saved at four (4) interior and four (4) exterior locations higher up on the monument compared to scans collected primarily at grade and interior during the Phase I NDE work. All interior scans were collected by ANA and all exterior scans were collected by VA via rope access under ANA's guidance with radio communication during the scanning process. Appendix A shows all SPR scan locations superimposed on elevation views of the monument. Previous SPR scan locations from Phase I are also included in Appendix A to give a complete picture of what portions of the monument have been scanned to date by ANA and VA.

A representative horizontal scan using the GSSI 4000 system is shown in Figure 5 with the scan showing the full thickness to the opposite surface of the wall, the collar joint between interior and exterior face wythes, and with markers at mortar head joints. The scan is collected from the elevator machine room approximately two-thirds up the height of the monument. This scan was typical and shows representative conditions of the wall at this height of the monument. There are two distinct wythes of stone with a bright radar reflection behind the face wythes indicating stone thicknesses clearly on the radar scans. Stone thicknesses vary and provide significant overlap between interior and exterior face wythes, consistent with NDE results elsewhere. This specific scan does not show a bond stone, which would have been full depth of the wall at this height of the monument.



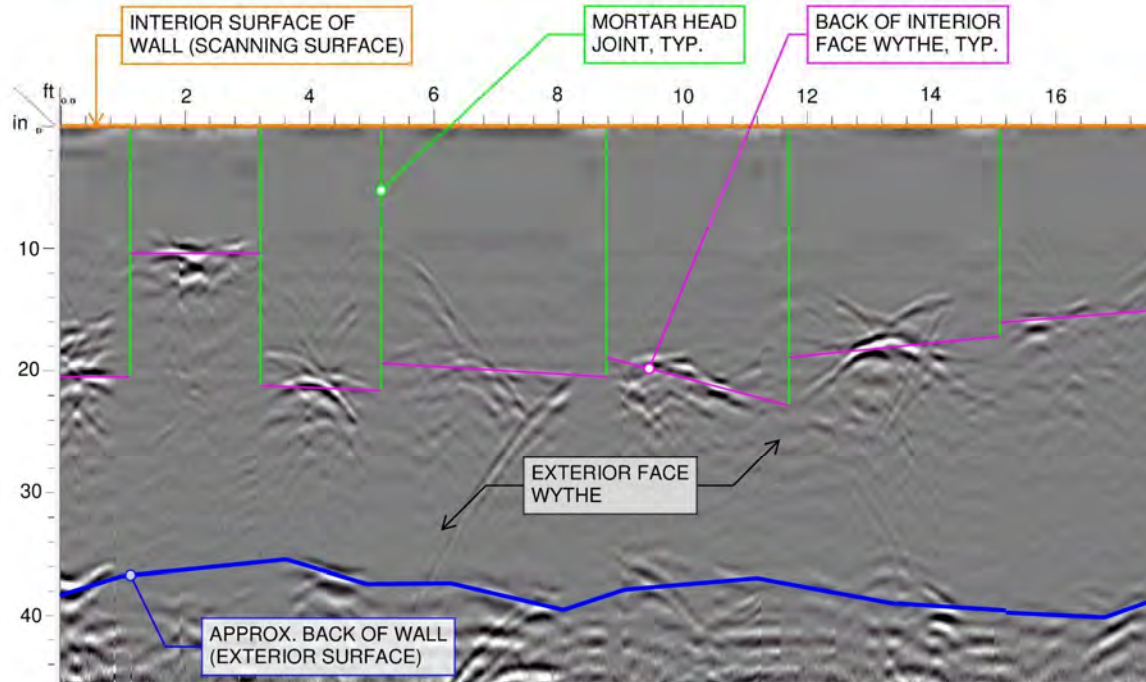


Figure 5. Typical SPR scan collected horizontally at the elevator machine room. Annotations describe elements of the scan.

ANA's interior scans were conducted at four different areas at heights up the monument ranging from 150-feet to 215-feet. Approximately one hundred and ten (110) stone units were scanned to determine their unit thickness. The back of the wall was only visible at the upper most scan area at the 215-foot elevation where the wall was thinnest. The higher frequency radar antenna was required to accurately determine stone thicknesses, and that antenna cannot send signal as deep through the wall as a result of the shorter signal wavelength. Had the lower frequency antenna been used, the back of the wall would be visible at all scan areas, but the stone thicknesses would be less accurate and likely not possible to determine in the field. Figure 6 and Figure 7 show partial elevation views with individual stone units colorized to represent their stone thickness as determined by the SPR scanning. Each color in the figures correlates to the colored stone thickness ranges in the histogram in Figure 8.



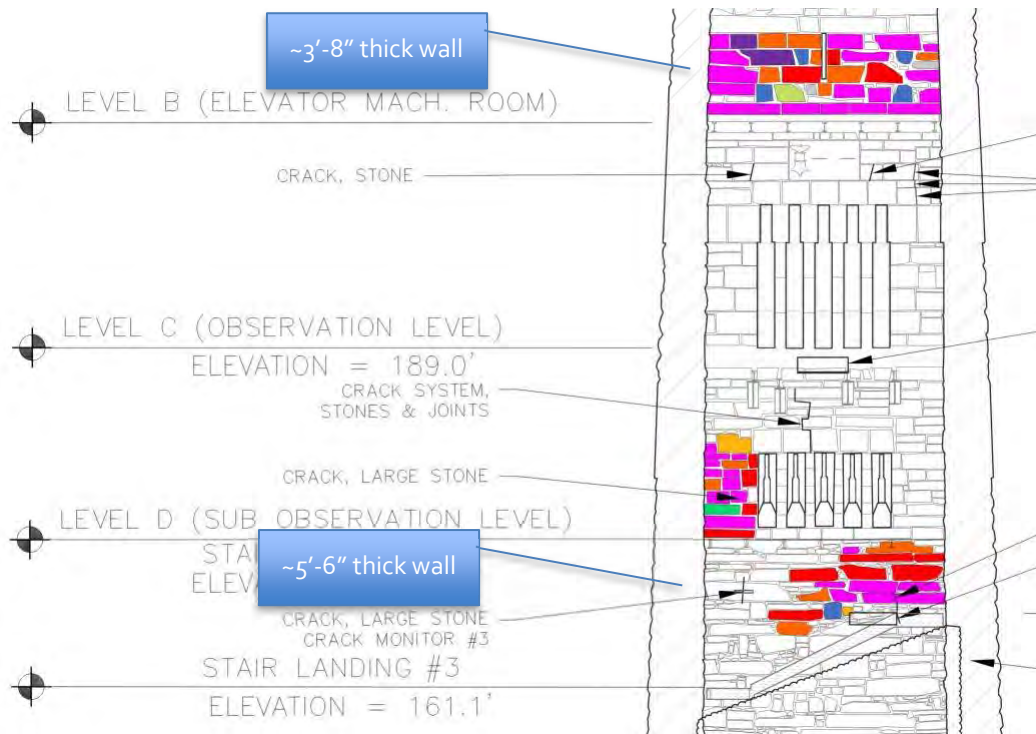


Figure 6. Annotated figure indicating interior face wythe stone thicknesses as determined by SPR at the **South Elevation**. The color of the shading correlates to the color of stone thickness on the histogram in Figure 8.



Figure 7. Annotated figure indicating interior face wythe stone thicknesses as determined by SPR at the **West Elevation**. The color of the shading correlates to the color of stone thickness on the histogram in Figure 8.

Summarizing interior face wythe stone thickness data into a histogram, Figure 8 shows the distribution of measured stone thicknesses. For reference, Figure 9 shows the same analysis conducted at the bottom half of the monument during ANA’s Phase I work. There is a clear shift in stone thicknesses at the interior face wythe higher up the monument to favor thinner stone units. This is expected as the overall wall thickness reduces up the height of the monument. At approximately 150-foot up the monument, full depth bond stones began to be visible in the SPR data. There may be some more full-depth bond stones lower down the monument that were not scanned by ANA, however. The lowest scan area for this phase of work was approximately 150-feet above grade.



TWO-WYTHE CONSTRUCTION
ELEVATION ≈ 150' TO 215' (PHASE II NDE)
 Histogram of Interior Stone Thicknesses

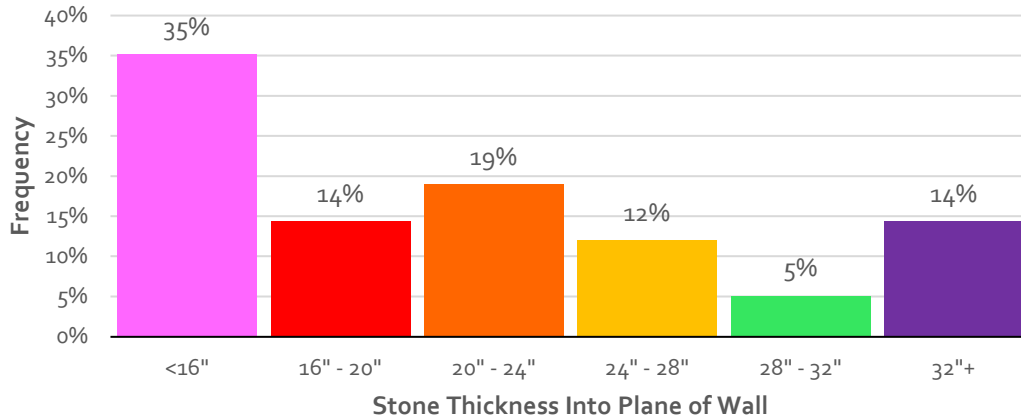


Figure 8. Histogram of interior stone face wythe stone thicknesses. These results are SPR scans collected at monument elevations between ~150' and ~215'. These are Phase II findings intended to represent masonry conditions higher up the monument.

THREE-WYTHE CONSTRUCTION
ELEVATION ≈ 0' TO 140' (PHASE I NDE):
 Histogram of Interior Stone Thicknesses

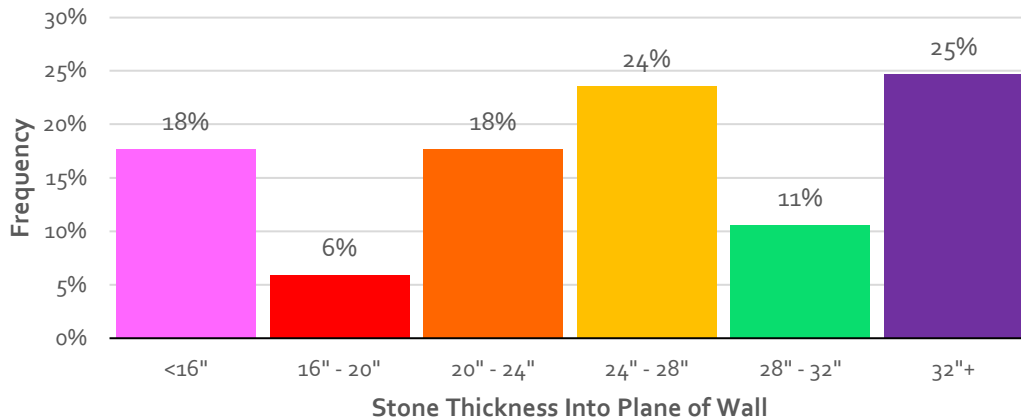


Figure 9. Histogram of interior stone face wythe stone thicknesses. THESE RESULTS ARE FOR THE BOTTOM HALF OF THE MONUMENT AND WERE COLLECTED DURING THE PHASE I NDE WORK.

VA's exterior scans were conducted at four different areas at heights up the monument averaging 65-feet, 80-feet, 150-feet, and 175-feet – as highlighted in Appendix A. Two of the scan areas were used to focus on individual stone units at the exterior wythe to determine their thicknesses – totaling approximately seventy (70) stone units. Similar to the interior scans, the high frequency radar was used



to determine the stone thicknesses. Figure 10 and Figure 11 show the field findings for exterior unit thicknesses with some additions and revisions shown by blue text from post-processing the scans.

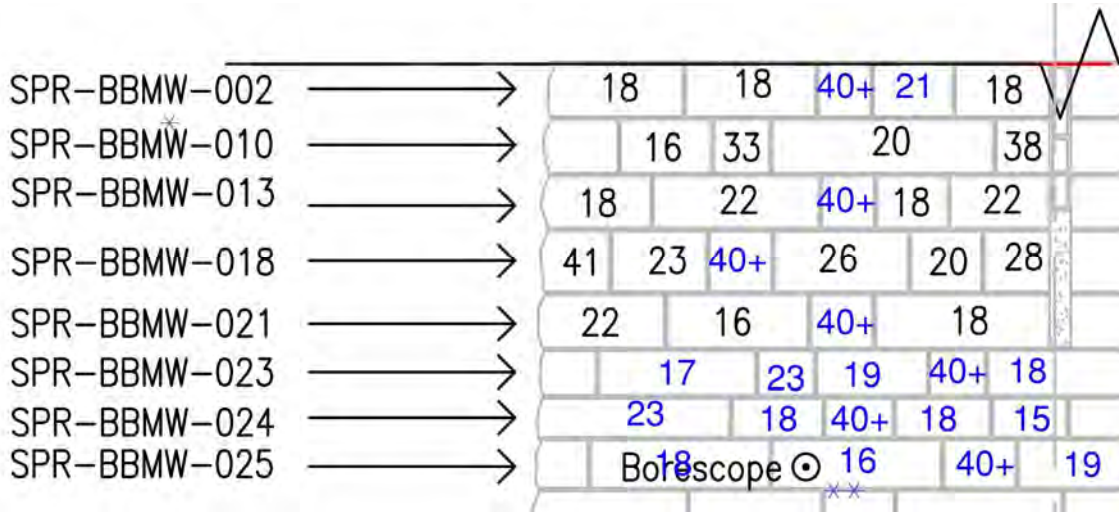


Figure 10. Annotated figure indicating exterior face wythe stone thicknesses as determined by SPR at approximately 150-feet high on the **West Elevation**. The number on the stone unit indicates the thickness into the wall in inches. The arrow and ID on the left indicate the SPR scan ID that was saved in the field.

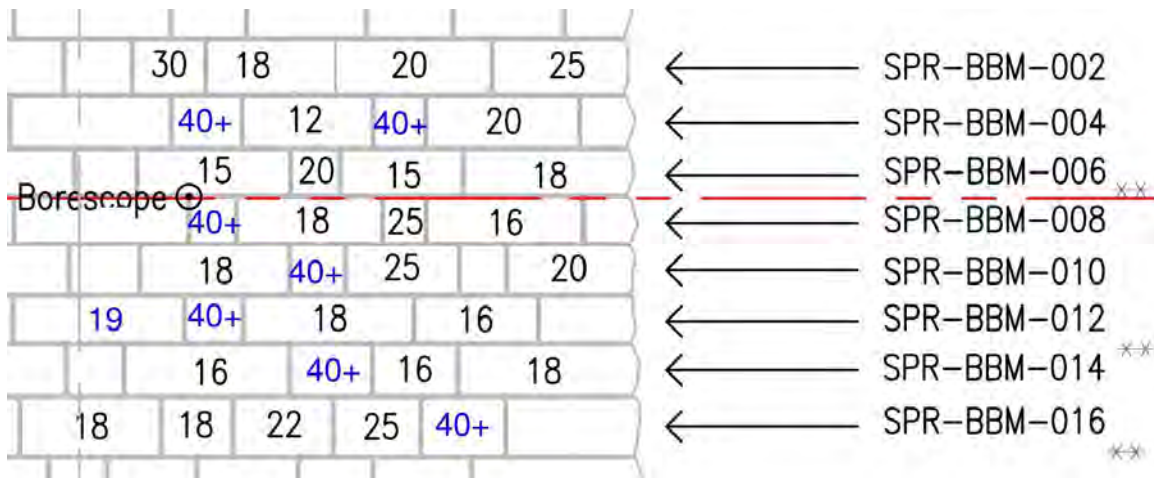


Figure 11. Annotated figure indicating exterior face wythe stone thicknesses as determined by SPR at approximately 80-feet high on the **South Elevation**. The number on the stone unit indicates the thickness into the wall in inches. The arrow and ID on the right indicate the SPR scan ID that was saved in the field.

Summarizing exterior face wythe stone thickness data into a histogram, Figure 12 shows the distribution of stone thicknesses. For reference, Figure 13 shows the same analysis conducted at the bottom four courses (approximately 8-feet) of the monument during ANA’s Phase I work. There is a clear shift in stone thicknesses at the exterior face wythe higher up the monument to favor thinner stone units. This is expected as the overall wall thickness reduces up the height of the monument. There are, however, still a similar frequency of bond stones.



**TWO-WYTHE CONSTRUCTION
ELEVATION ≈ 80' TO 150' (PHASE I NDE):
Histogram of Exterior Stone Thicknesses**

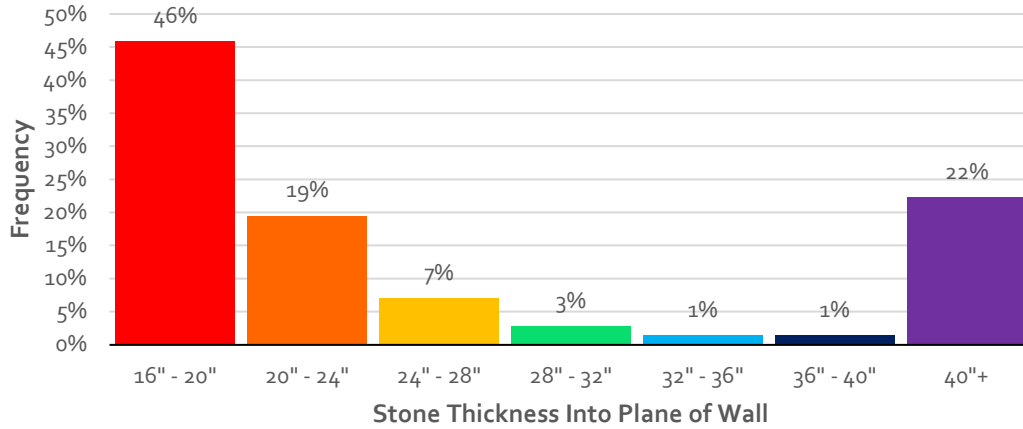


Figure 12. Histogram of exterior stone face wythe stone thicknesses. These results are SPR scans collected at monument elevations of 80-feet and 150-feet. These are Phase II findings intended to represent masonry conditions higher up the monument.

**THREE-WYTHE CONSTRUCTION
ELEVATION ≈ 0' TO 8' (PHASE I NDE):
Histogram of Exterior Stone Thicknesses**

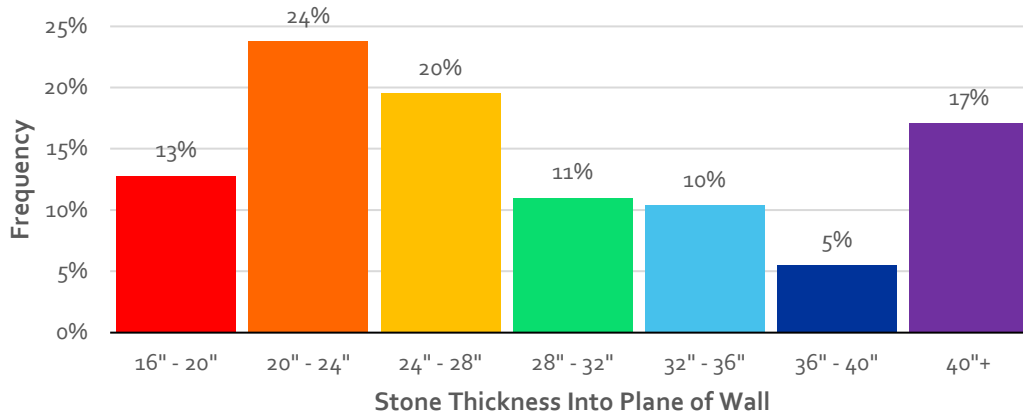


Figure 13. Histogram of exterior stone face wythe stone thicknesses. THESE RESULTS ARE FOR THE BOTTOM FOUR COURSES (APPROX. 8- FEET) OF THE MONUMENT AND WERE COLLECTED DURING THE PHASE I NDE WORK.



2.2. Videoscope Evaluation

A series of 3/8-inch diameter holes were drilled into mortar joints such that a fiberoptic videoscope could be used to make visual observations. The videoscope investigation intended to determine the size and frequency of internal voiding within the wall, if present, and to characterize the materiality and solidity of the masonry between interior and exterior face wythes. The Phase II videoscope probes were selected in locations higher up the monument at the interior and exterior to supplement previous videoscope findings from Phase I.

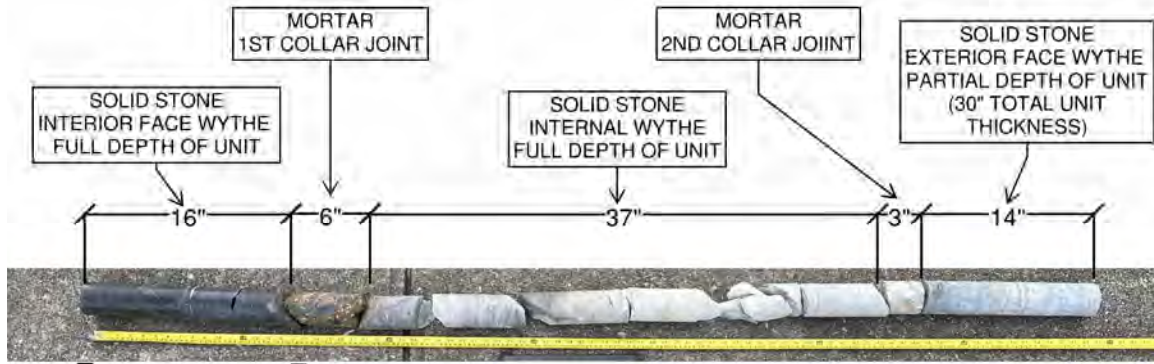
Seven (7) videoscope holes were drilled with three (3) from the interior and four (4) from the exterior. All holes were drilled at the most significant anomalies that were located with SPR scanning. All seven holes were observed to consist of primarily solid stone masonry with only one hole containing a small (1/16" thick) separation observed between the back of a face stone unit and the collar joint mortar. All other observations showed solid masonry and mortar fill. These results are consistent with Phase I videoscope results and core observations at stone material test locations.

2.2.1. Additional Observations at Goodman Jack Cores Holes

For the material testing portion of ANA's scope, Alegrone cored two (2) core holes at Goodman Jack test locations each specified to be 6'-0" long x 3" diameter core holes. The specific diameter and length of the core holes were strict requirements for the Goodman Jack test, but this provided an additional opportunity to observe internal wall conditions at greater depths than was previously possible with the videoscope evaluation. For the highest resolution images of the internal wall conditions a GoPro Hero8 camera was connected to a handheld pole and inserted into each of the core holes to document conditions. Additionally, Alegrone kept track of the portions of masonry that were extracted from the wall, such that a majority of the core hole extractions could be reassembled for visual observation. It is important to note that the core drilling procedure often fractures portions of stone that are not fractured in their in-situ condition within the wall. Additionally, portions of masonry within the wall that may have internal defects or cracks in their in-situ state can crumble in the core barrel. Thus, it is most representative of the in-situ conditions of the wall to observe the masonry at the outer perimeter of the core hole as it remains in the wall.

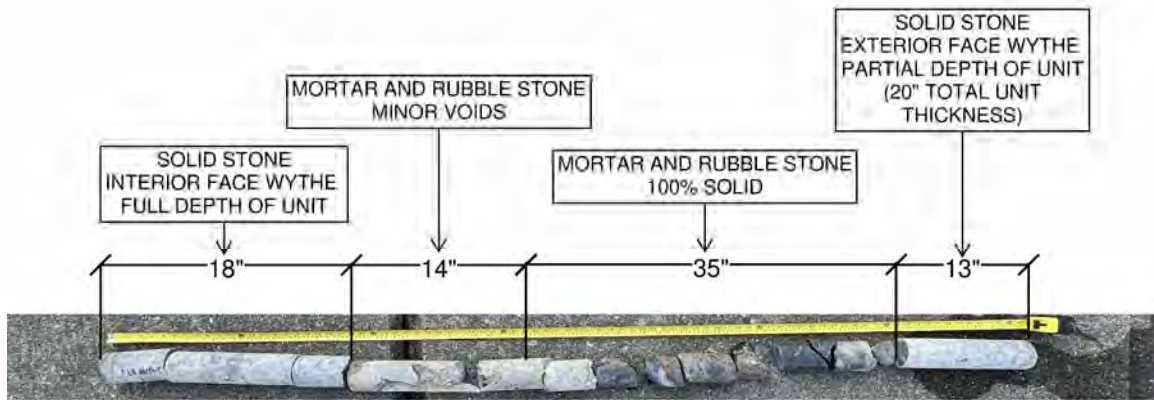
Figure 14 and Figure 15 show the core hole extractions for Goodman Jack test 'Ground Floor South Interior' and 'Landing 26 North Interior' respectively as they were laid out in the order they were removed from the wall. Dimensions for segments of masonry were measured in the field directly from within the vacant core holes using a videoscope to accurately represent in-situ conditions within the wall. The scale of the stone segments as laid out in the annotated photos can appear misleading because of small missing portions of masonry segments lost in the coring process and because the segments don't fit together tightly laid out on the ground, as they are in the wall. The portions of the interior face wythes were retained by ANA for laboratory testing. Other portions of the core extractions were retained by Alegrone to use for Dutchmen repairs to other core holes.





RETAINED FOR LABORATORY TESTING - CORE ID = ANA-SOUTH-4

Figure 14. Masonry core segments laid in order as they were removed from the wall from the core hole made for ANA Goodman Jack test 'Ground Floor South Interior'.



RETAINED FOR LABORATORY TESTING - CORE ID = ANA-NORTH-3

Figure 15. Masonry core segments laid in order as they were removed from the wall from the core hole made for ANA Goodman Jack test 'Landing 26 North Interior'.

Using the videoscope and GoPro camera, internal wall conditions were evaluated for the core hole at test location 'Ground Floor South Interior' herein referred to as SOUTH-CORE, and test location 'Landing 26 North Interior' herein referred to as NORTH-CORE. Core locations are indicated on elevation views in Appendix B.

Generally, the internal conditions at the SOUTH-CORE, prior to Goodman Jack testing, appeared to be 100% solid with no visible voiding, no internal delaminations, and no other gaps between masonry components. Figure 16 through Figure 19 show typical photos of the internal conditions observed at SOUTH-CORE. Annotated photos that have a forward-looking camera angle are all taken after Goodman Jack testing. As such, much of the damage to mortar joints and some stone fractures are caused by the material testing and were not present prior to loading the masonry.



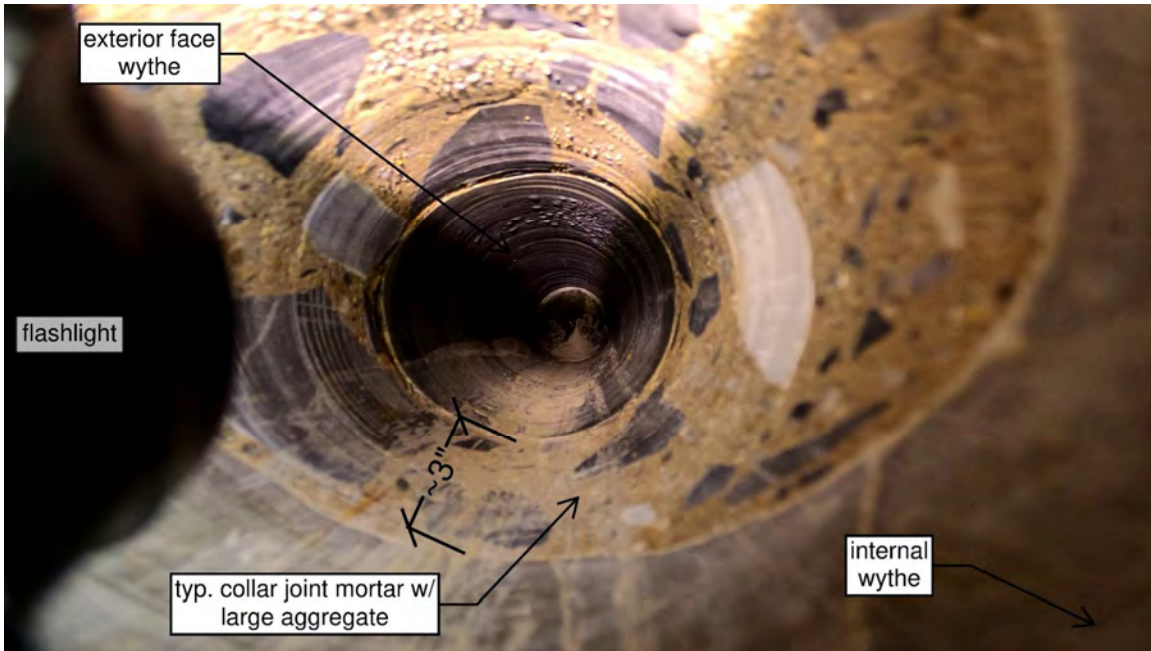


Figure 16. GoPro photo of the 2nd (exterior) collar joint at CORE-SOUTH after the Goodman Jack testing. The collar joint mortar is fully intact and the interface between the two stone wythes and the mortar is solid.

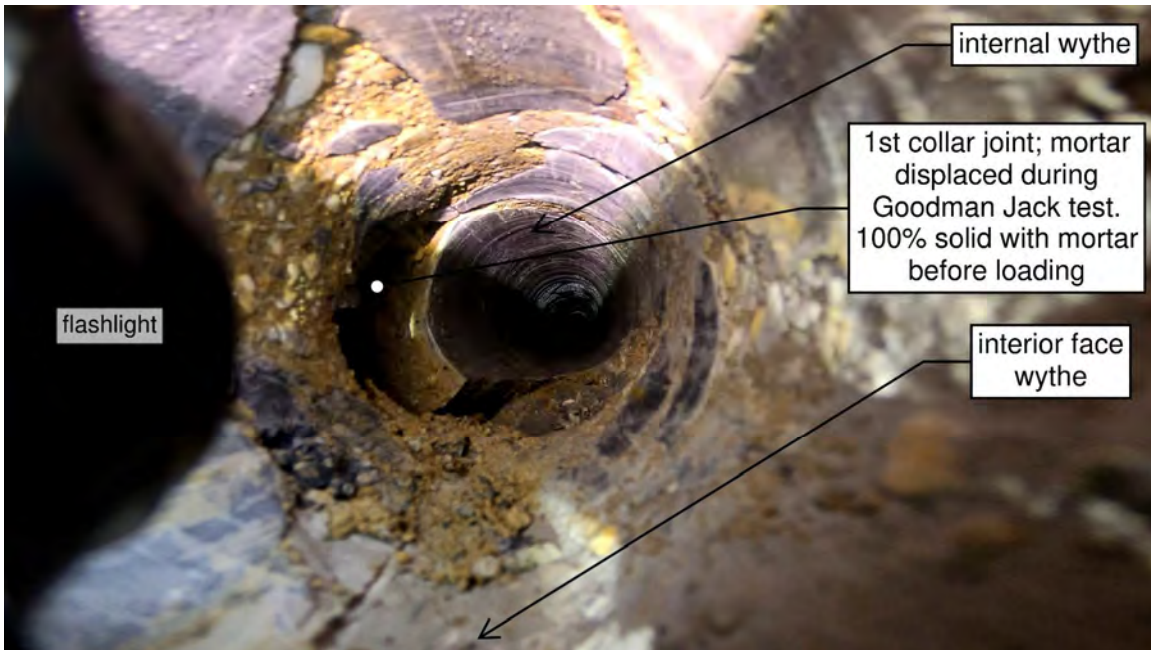


Figure 17. GoPro photo of the 1st (interior) collar joint at CORE-SOUTH after the Goodman Jack testing. The collar joint was previously 100% solid but after testing shows visible distress. This is the location of the Goodman Jack test that resulted in a ruptured membrane as it pressed into the soft mortar and was cut on the stone edge (Goodman Jack test ID: GS17-35).





Figure 18. GoPro photo of the internal wythe at CORE-SOUTH after the Goodman Jack testing. The stone is visibly intact. There is visible condensation at the top of the core hole for much of the depth of CORE-SOUTH unrelated to the material testing.

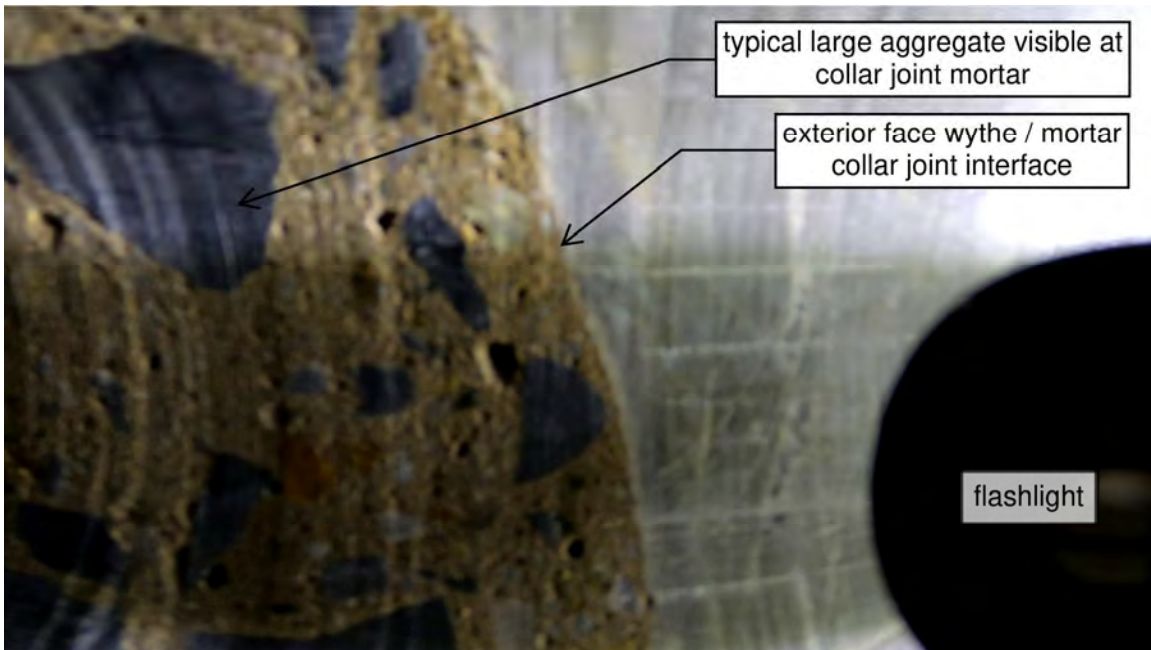


Figure 19. GoPro photo of the 2nd collar joint at CORE-SOUTH before the Goodman Jack testing. The interface between stone and mortar is solid. The large aggregate typically observed at the collar joint mortar is also visible.



Generally, the internal conditions at the NORTH-CORE, prior to Goodman Jack testing, appeared to be mostly solid with some minor voiding at the top of the core hole at depths ranging from 18- to 32-inches into the wall. The interior face wythe and exterior face wythe appeared to be intact solid stone units, and the portion of the wall between face wythes appeared to be a combination of stone and mortar rubble. Although not a discrete internal wythe, the center of the wall appeared mostly solid with stone to mortar interfaces generally solid with some showing slight delaminations. The voids observed were small in size and typically isolated voids, not part of an interconnected void system within the wall. Figure 20 through Figure 23 show typical photos of the internal conditions observed at NORTH CORE.

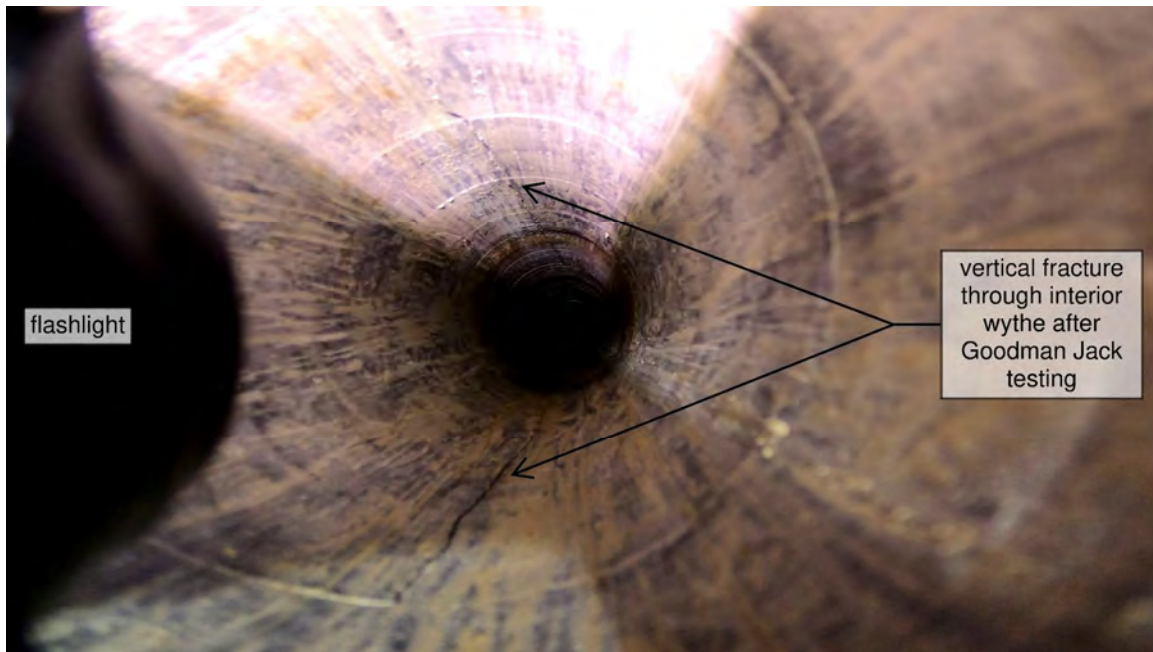


Figure 20. GoPro photo of the interior face wythe at CORE-NORTH after the Goodman Jack testing. The stone was visibly intact before the testing, but loading the masonry resulted in a vertical fracture through the stone unit for the full depth of the unit (16-inches). The fracture is visible at the top and bottom of the core hole in this photo.





Figure 21. GoPro photo of the masonry between the interior and exterior face wythes (approx. depth of photo = 22" into wall) at CORE-NORTH after the Goodman Jack testing. This portion of the wall was not loaded with the Goodman Jack due to the already present voiding. Figure 22 shows a closer view of the void called out by the annotation in this photo.



Figure 22. GoPro photo of the masonry between the interior and exterior face wythes (approx. depth of photo = 26" into wall) at CORE-NORTH after the Goodman Jack testing. This portion of the wall was not loaded with the Goodman Jack due to the already present voiding and exposed sharp stone edges.





Figure 23. GoPro photo masonry between the interior and exterior face wythes (approx. depth of photo = 40" into wall) at CORE-NORTH after the Goodman Jack testing. Some stone to mortar interfaces appear solid and others show slight separations between stone and mortar.

2.3. Spray Testing

Water spray testing was conducted to evaluate moisture intrusion through the stone masonry assembly of the monument. Testing involved spraying pressurized water through a spray rack at the exterior of the north elevation. Testing took place at the level of the interior stair landing number 12. Water was applied to the exterior through the frame approximately 1-foot from the surface of the stone at a pressure of 8-psi for a duration of 3 hours and 45 minutes. No simulated wind air pressure was applied. During the testing regular observations were made at the interior using visual observation and infrared thermographic imaging to identify the location and progression of leaks at the interior. A full documentation of identified leaks and the progression of the spray testing is summarized in Appendix C to this report.

The spray test was successful in producing leaks at the interior of the monument over the course of the testing. The first leaks were noted approximately 60 to 90-minutes into testing. These were small trickles of water flowing through visibly cracked stones at the interior approximately 40 feet below the spray frame. An example of such a leak is included in Figure 25. With more time (90 to 120-minutes), wet spots began to become observable at interior mortar joints. The first leaks noted (60 to 120-minutes) were those lower down on the monument starting above stair landing 22, approximately 40 feet below the spray frame. With time, leaks were noted higher up the monument closer to the elevation of water application.

In the afternoon approximately 140-minutes into the test, a rain shower occurred primarily wetting the north elevation for approximately an hour. Direct spray of the wall was maintained through the rain.



Figure 27 provides a photo showing the resulting moisture pattern of the afternoon rain. The test was stopped after just under four hours of spraying when moisture rundown from interior leaks began overlapping and new leaks could not be distinguished from ongoing.

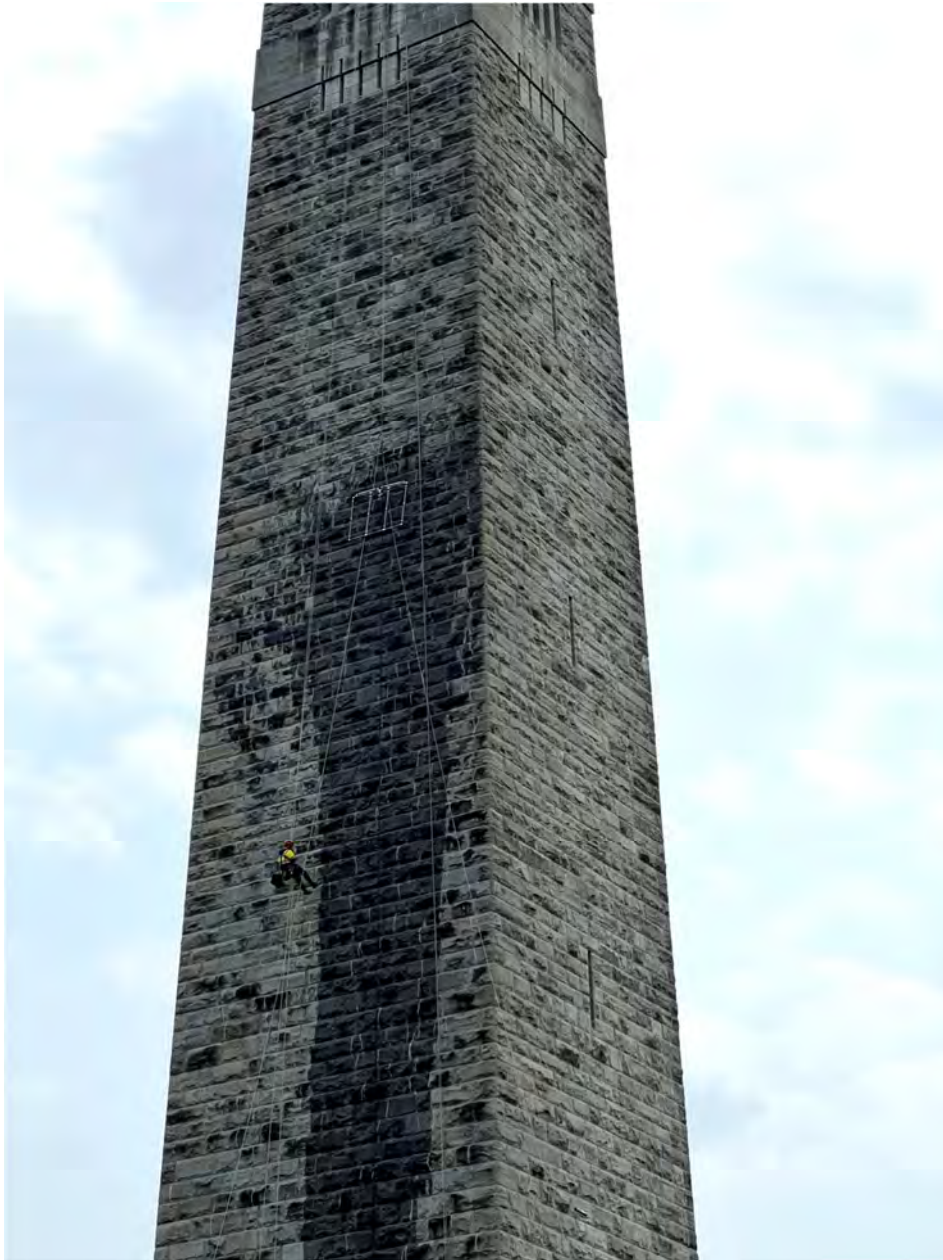


Figure 24. Photo of spray test from exterior – North Elevation.





Figure 25. Leak observed as a result of spray testing below crack at interior stone.

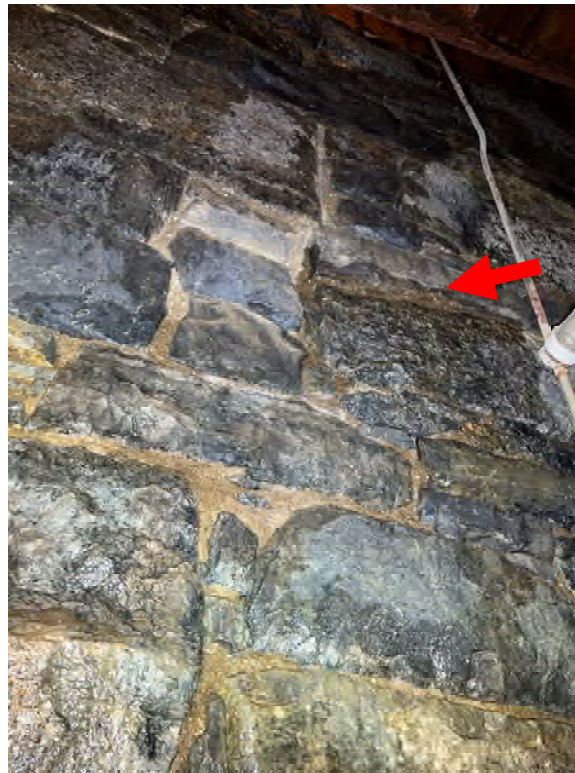


Figure 26. Appearance of damp observed at mortar joint below interior stone work.





Figure 27. Photo of north wall following rainstorm with the prevailing wind coming directly from the north. The monument largely blocked wind driven rain from the leeward walls, with a small amount of moisture being blown and wrapping around the corners of the monument creating a clear line of moisture approximately half the length of a stone unit to the east and west elevations.



SUMMARY OF NONDESTRUCTIVE INVESTIGATIONS

Further nondestructive evaluation of the stone masonry walls at various heights up the monument on the interior and exterior determined that as-built conditions appear consistent across all four elevations and across all heights evaluated. The masonry walls typically appear to be coursed masonry through the entire wall thickness with some limited stone/mortar rubble fill at the center of the wall. Mortar/concrete and small pieces of stone or large pieces of aggregate were used to fill gaps between stone units. Between the videoscope and core observations, one area of minor voiding was observed during the Phase II NDE work. This represented a small space within the mortar/concrete fill between stone wythes and did not appear to be connected to a larger network of voids within the wall. In general, the stone masonry of the monument appears to be laid in fully solid bed joints with solid fill between wythes (collar joints) based on the nondestructive test data to date.

Bond stones were located with SPR throughout the monument at all elevations and heights up the monument. Starting at heights of approximately 150-feet above grade, bond stone units that were full-depth through the thickness of the wall were observed with SPR scans. This observation, as well as the general wall thickness having reduced to approximately 4'-6", indicates that this is generally the transition from three-wythe construction below to two-wythe construction above. Generally, bond stones appear to bridge between two wythes of stone. Therefore, the three-wythe portion of the monument likely has bond stones bridging the exterior face wythe and the internal wythe, as well as bridging the interior face wythe and the internal wythe; not through the full wall thickness. At the two-wythe portion of the monument, it appears the bond stones are through the full thickness of the wall. Overall, conditions observed during the Phase II NDE were consistent with conditions observed during the Phase I NDE work.

Spray test results were generally consistent with the stone assembly being largely solid with a set of small, narrow gaps or cracks present between stones and mortar fill as well as cracked stones for moisture to migrate through. The first leaks were noted lower down on the monument. Leaks were first noted at direct paths through stone units such as cracks with leaks at mortar joints being noted later on. An indication that water was not building up in void spaced within the mortar fill but traveling through narrow gaps between stone and mortar interfaces.

3. IN-SITU STONE MATERIAL TESTING

3.1. In-situ Deformability Testing

Compression behavior of the existing masonry has been investigated using the flatjack method of ASTM C1197, *In Situ Measurement of Masonry Deformability Properties Using the Flatjack Method*. The deformability test method involves removing bed joint mortar for insertion of two parallel flatjacks, one located above the other and separated by approximately 16-inches and two horizontal bed joints. As the flatjacks are pressurized, the corresponding deformations of the masonry between the jacks are measured using a set of surface-mounted linear variable differential transformers (LVDTs). Two cycles of loading were conducted for each test. The initial cycle is used to seat the flatjacks and the second cycle provides a more accurate measure of the compression behavior of the masonry. For this project, an applied pressure of approximately 200 psi was used for the first cycle.



Two (2) deformability tests were conducted at the Bennington Battle Monument with the first, D1, located at stair landing #1 on the west elevation and the second, D2, at stair landing #24 on the south elevation. Specific deformability test locations are shown in Appendix B. The conditions observed at the two test locations appear representative of the stone masonry walls throughout the interior of the monument. Figure 28 shows the typical test setup for a deformability test.

Compressive modulus (E_m) is calculated as the slope of the stress-strain curve for the linear elastic portion of each test. The initial portion of the stress-strain curve can be nonlinear or skewed due to flatjack deformation at low pressures and closing of small cracks within the wall assembly; this behavior is neglected when calculating stiffness. The stress-strain curve and test setup of each deformability test are shown in Figure 29 and Figure 30. Stress-strain curve (left) and test setup (right) from deformability test D2. The maximum applied stress was 1550 psi, at which point the test was stopped, while still in the linear elastic region of the stress-strain relationship, due to the maximum working pressure of the equipment. The portion of the curve highlighted in red represents the unloading cycle of the test when pressure was released from the pump., and test results are summarized in Table 1.



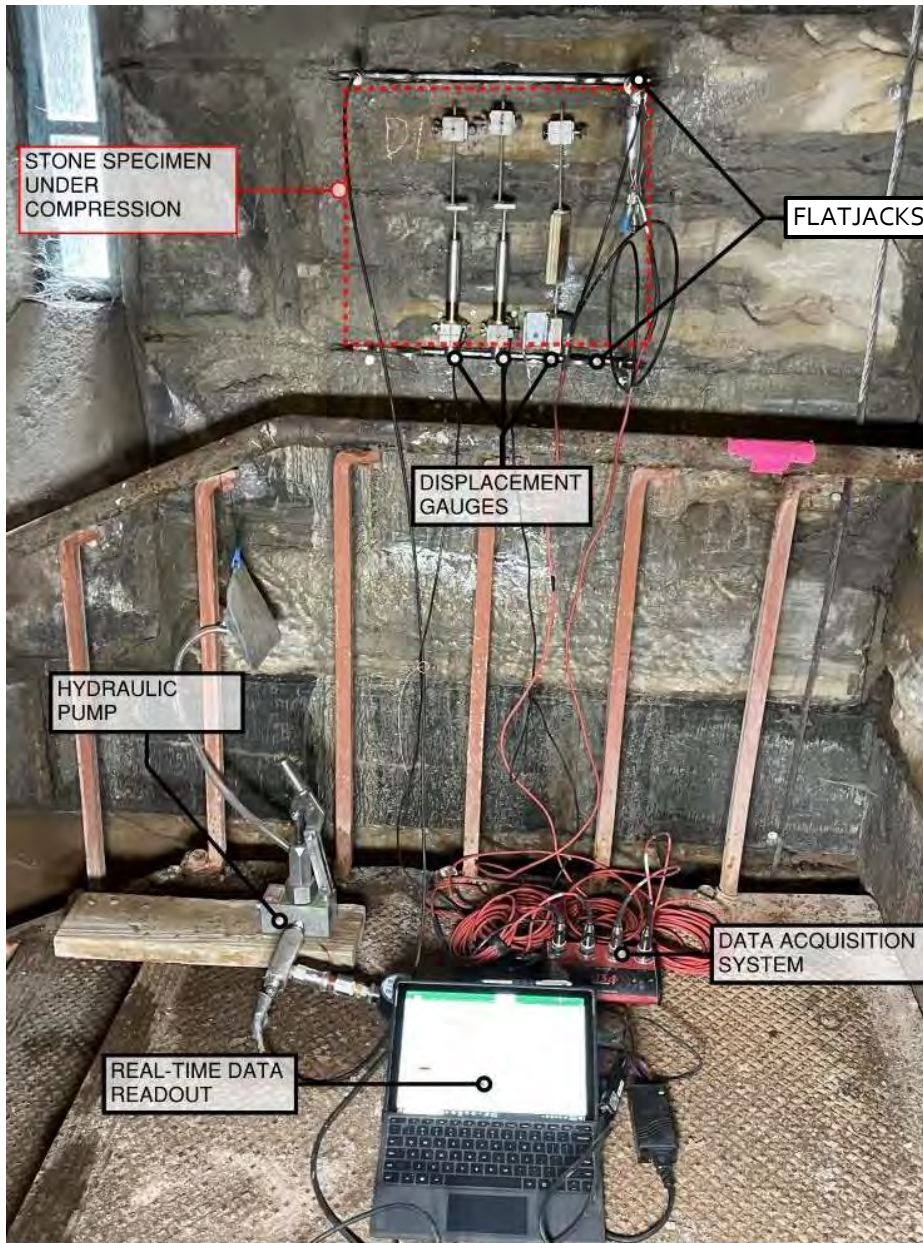


Figure 28. Typical test setup for in-situ deformability tests.



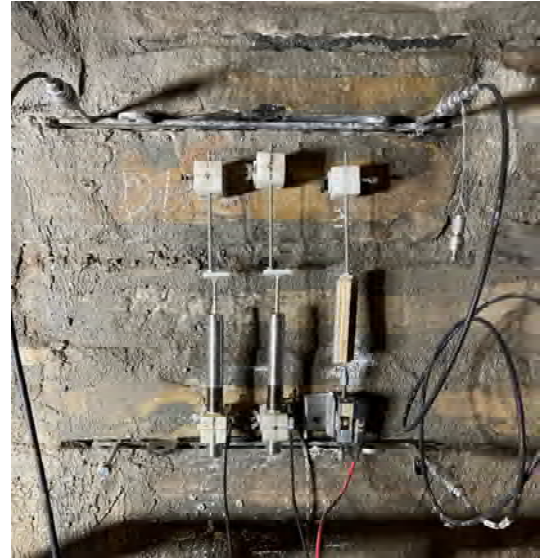
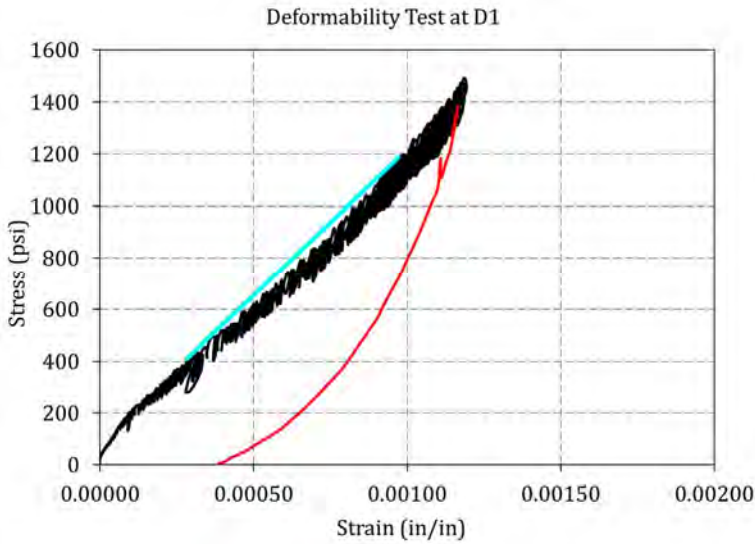


Figure 29. Stress-strain curve (left) and test setup (right) from deformability test D1. The maximum applied stress was approximately 1490 psi, at which point the test was stopped, while still in the linear elastic region of the stress-strain relationship, due to the maximum working pressure of the equipment. The portion of the curve highlighted in red represents the unloading cycle of the test when pressure was released from the pump. The cyan line indicates the portion of the curve where the tangent modulus was calculated for the Compression Modulus, E_m value reported in Table 1. For test D1, both slots were cut at mortar bed joints and two in-tact mortar bed joints were present between the two flatjacks during the test.

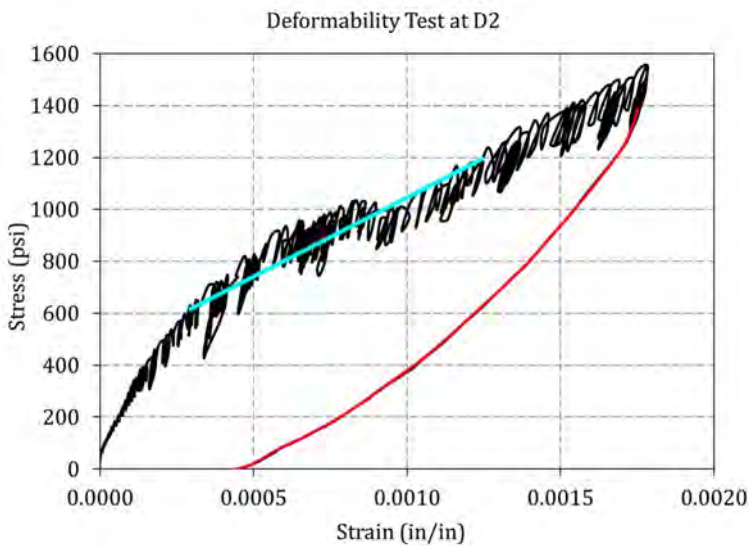


Figure 30. Stress-strain curve (left) and test setup (right) from deformability test D2. The maximum applied stress was 1550 psi, at which point the test was stopped, while still in the linear elastic region of the stress-strain relationship, due to the maximum working pressure of the equipment. The portion of the curve highlighted in red represents the unloading cycle of the test when pressure was released from the pump. The cyan line indicates the portion of the curve where the tangent modulus was calculated for the Compression Modulus, E_m value reported in Table 1. For test D2, both slots were cut through the face of stone units and two in-tact mortar bed joints were present between the two flatjacks during the test.



Table 1. In-situ deformability test results.

Test ID	Location	Calculated Compression Modulus E_m (psi)	Maximum Test Pressure (psi)
D1	Stair Landing #1- West	1,130,000	1,490
D2	Stair Landing #24- South	597,000	1,550
Average (psi):		863,500	1,520

Deformability tests D1 and D2 were brought to the maximum working pressure of the flatjack equipment. To prevent damaging equipment, both tests were stopped at an average of 1,520 psi. Test data shows that both test specimens still appeared to be within the linear elastic region of their stress-strain relationship at the time tests were stopped. As such, the estimated compressive strength, f'_m , is likely higher than the maximum test pressures reached.

Looking at the unloading portions of the two stress-strain curves, both did not return to zero strain when zero stress was reached at the end of the test. This indicates that some permanent (plastic) deformation was observed; behavior typically more significantly when material failure is close. As such, the maximum test pressure in Table 1 could be used as a conservative approximation of f'_m of the masonry.

3.2. In-situ Stress Testing

The compressive state of stress of the existing masonry was investigated using the flatjack method described in ASTM C1196, *Standard Test Method for In Situ Compressive Stress Within Solid Unit Masonry Estimated Using Flatjack Measurement*. A typical test setup is shown in Figure 31. This test method is a stress relief test using a single flatjack. Gage points above and below the selected test location are installed and the initial distance between them is measured. A slot in the selected stone or mortar joint is then cut out and the distances between gage points are measured again. When the masonry is in compression, removal of the material will relieve stress causing the gage points to move slightly closer towards each other. A flatjack is inserted in the empty bed joint and pressurized until the gage points are displaced back to their original position. The pressure in the flatjack at this state approximates the stress that was in the masonry prior to bed joint removal.

An average of readings between 4 gage points was used to estimate the restoring stress from the flatjacks as shown in Figure 32 through Figure 39. Results of the in-situ stress tests are summarized in Table 2.





Figure 31. Typical Stress Test Setup





Figure 32. Test setup at location S1. Slot was cut at a mortar bed joint.

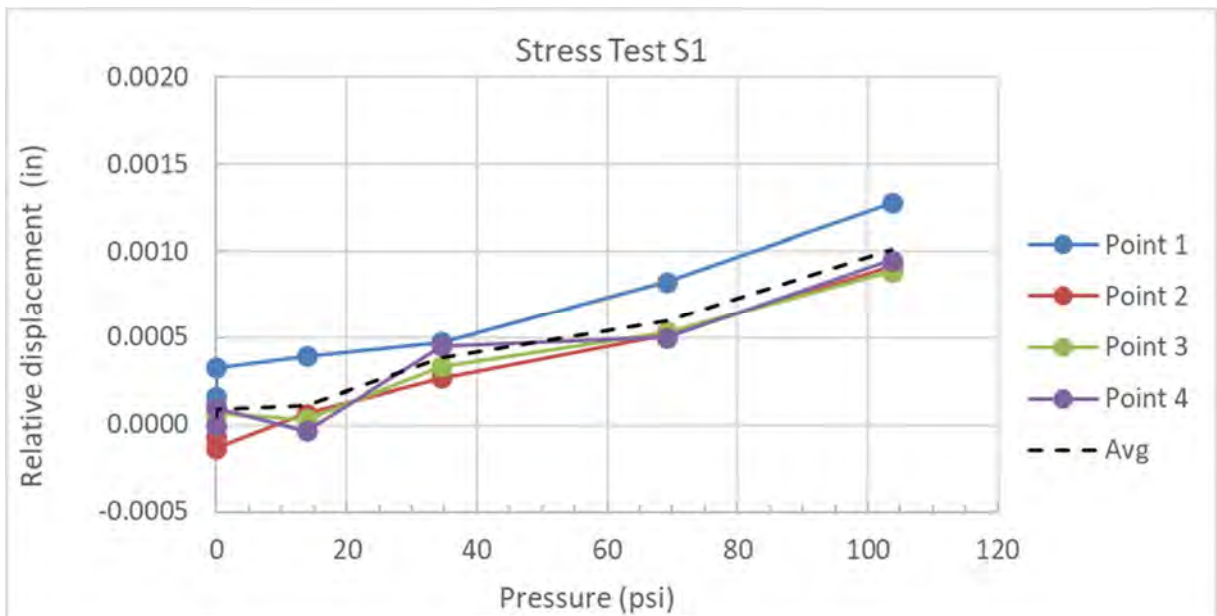


Figure 33. Displacement-stress curves for stress test S1. At this test an initial displacement was not measured following the saw cut. This is an indication of a relatively low compressive stress level at the test area.





Figure 34. Test setup at location S2. Slot was cut through the face of a stone unit.

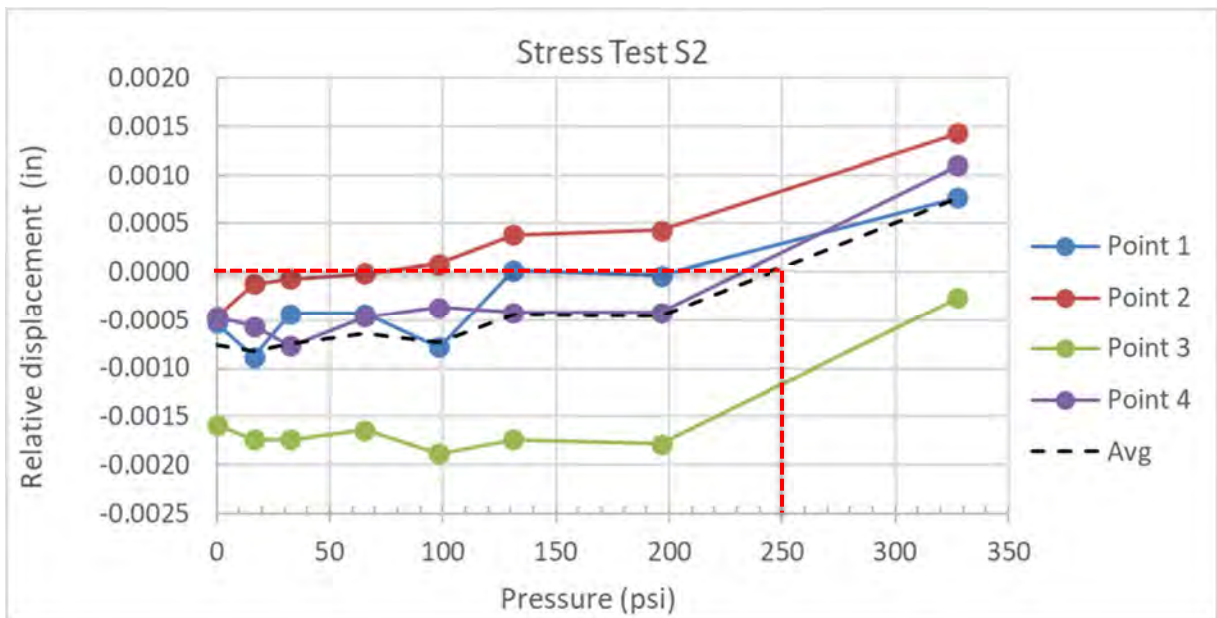


Figure 35. Displacement-stress curves for stress test S2. The compressive stress is approximated based on the average of the four readings to be 250 psi.





Figure 36. Test setup at location S3. Slot was cut through the face of a stone unit.

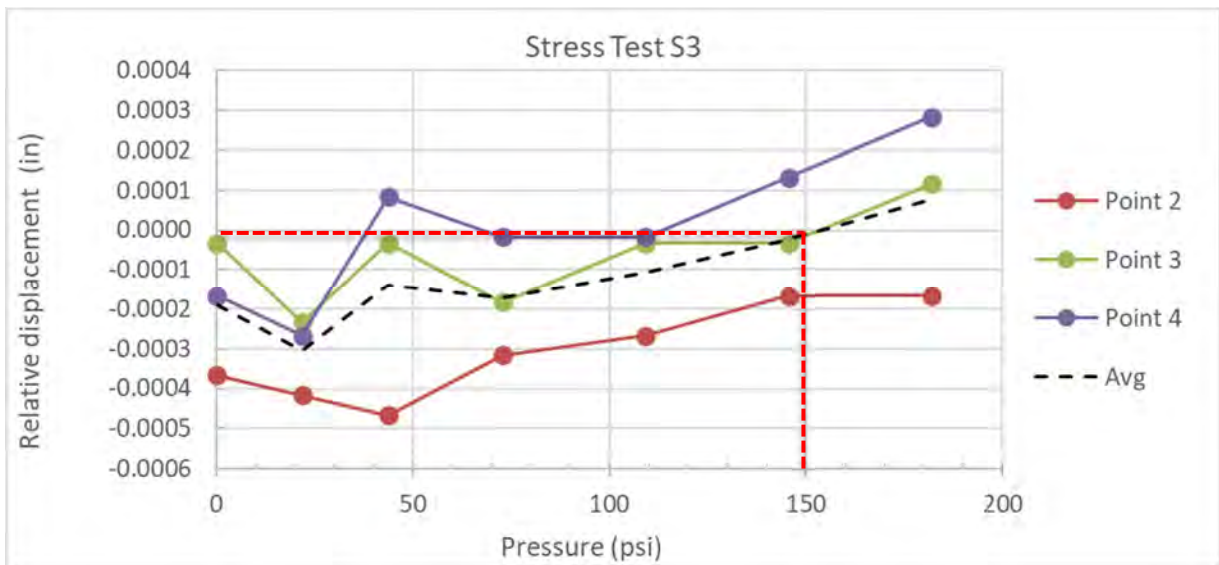


Figure 37. Displacement-stress curves for stress test S3. The compressive stress is approximated based on the average of the four readings to be 150 psi.





Figure 38. Test setup at location S4. Slot was cut through the face of a stone unit.

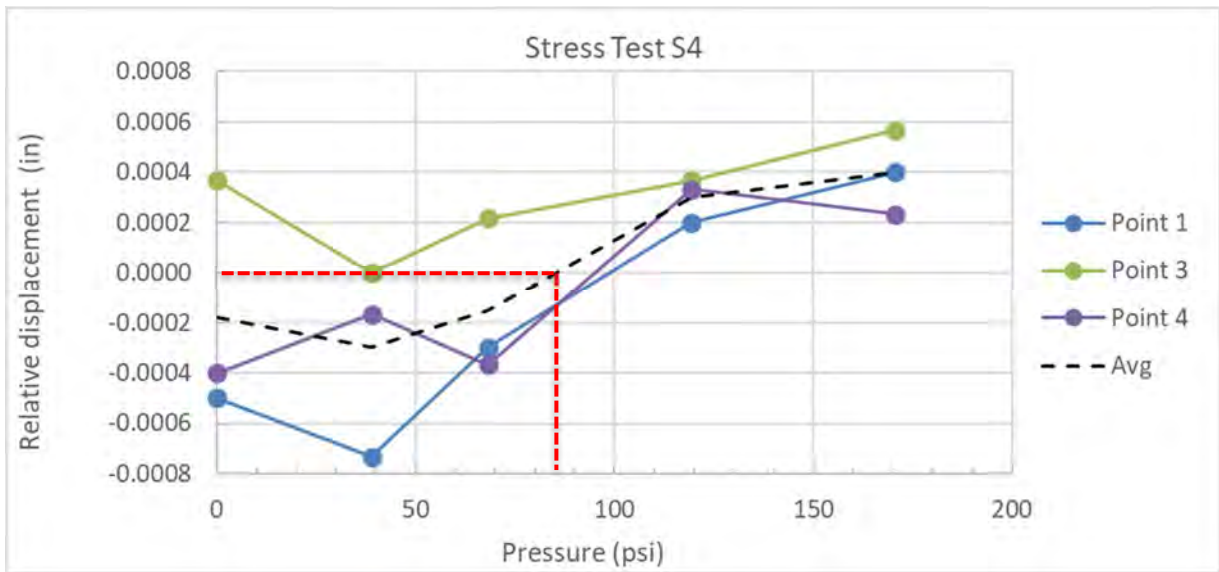


Figure 39. Displacement-stress curves for stress test S4. The compressive stress is approximated based on the average of the three readings to be 85 psi.



Table 2. Summary of results from stress tests.

Test ID	Location	Approx Elevation	Estimated Compressive (psi)	Stone Material
S ₁	Stair Landing #1 – West	175'	-	Marble
S ₂	Stair Landing #24- South	55'	250	Dolostone
S ₃	Ground level-North	5'	150	Dolostone
S ₄	Ground level-East	5'	85	Dolostone

3.3. In-situ Goodman Jack Testing

The elastic modulus of the stone masonry assembly was measured at two locations using a borehole dilatometer (Figure 40). A Roctest Probox model dilatometer was used for the testing. The dilatometer uses a radially expandable membrane that is pressurized within a cylindrical hole drilled into the stone. During the test, the applied pressure and hydraulic volume pumped into the membrane are measured to generate a test curve. As the membrane tightens against the walls of the core and begins to push against the stone, a linear relationship is observed between the volume that can be pumped into the dilatometer (a corollary for the expansion of the core diameter) and the hydraulic pressure. From this linear elastic region, a relationship between the hydraulic volume and pressure is calculated to determine the modulus.

Testing was conducted in two loading cycles. An initial pressurization was performed to an intermediate inflation of the membrane to a load below the estimated maximum strength of the stone or capacity of the test equipment. The membrane was then partially depressurized to approximately the point where the expanded membrane began pressing against the sides of the core. A second pressurization cycle was then run up to the maximum operating pressure or evidence of failure in the stone or specimen was encountered. The failure point of the stone was largely unknown at the start of testing and unpredictable failures of the membrane and stone were encountered. As a result, the pressure level to which the two load cycles were run varied through the testing. In some instances, if failure occurred, only a single load cycle was possible. Plots of test data are included in Appendix D to this report.

Testing was conducted at multiple depths at two cores at the interior of the monument. Testing was conducted at the ground floor of the south wall and from stair landing 26 at the north wall. The membrane on the dilatometer is 18-inches in length such that testing was conducted on a mixture of stone, mortar, and combined substrates. Figure 40 and Figure 41 below provide photos of the Probox test unit and the typical configuration during testing. Figure 42 and Figure 43 provide summaries of where within the two cores tests were conducted. Results of the testing in the form of measured modulus of elasticity are included in Table 3.





Figure 40. Probex dilatometer.



Figure 41. Configuration of goodman jack testing at interior landing 26 on the north wall.



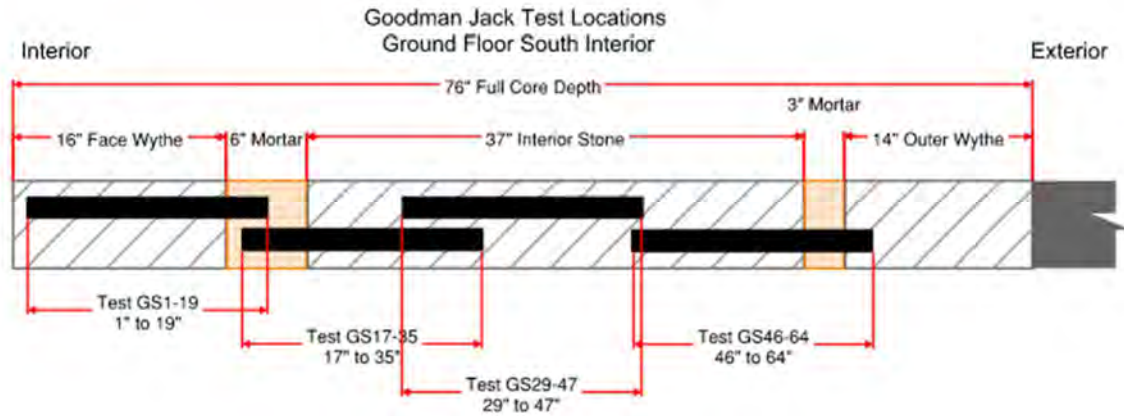


Figure 42. Test locations at ground level on south wall. Tests were conducted sequentially from the interior most test (GS1-19) to the exterior most test (GS46-64).

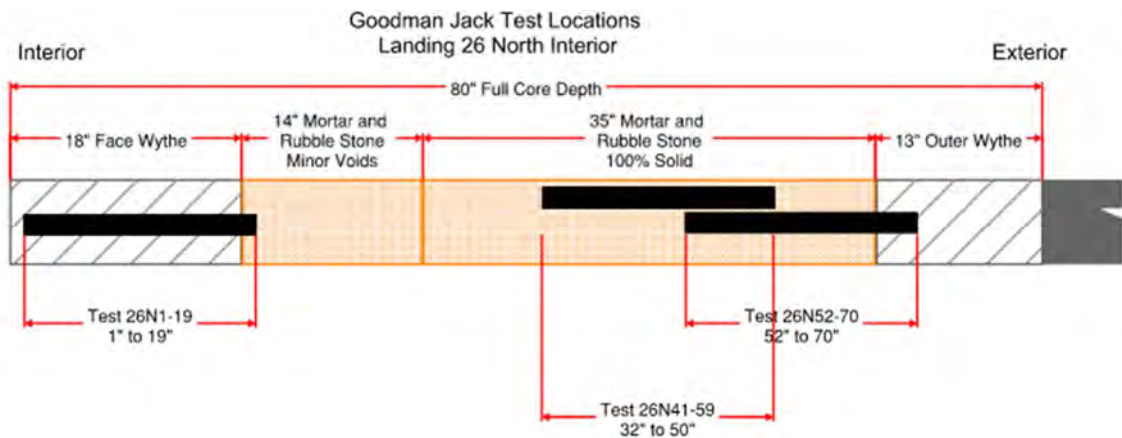


Figure 43. Test locations at landing 26 on the north wall. Tests were conducted sequentially from the interior most test (26N1-19) to the exterior most test (26N52-70).



Table 3. Summary of Goodman Jack Test Data

Test ID	Location	Depth into core (in)	Substrate Description	Measured Modulus of Deformation in (psi)
				2 nd Load Cycle (1 st Load cycle)
GS29-47	South Ground	29" to 47"	18" solid interior wythe stone	1,100,000 (868,000)
26N1-19	Landing 26 North	1" to 19"	17" of interior face wythe stone	N/A^B (1,320,000)
GS1-19	South Ground	1" to 19"	15" of interior face wythe stone with 3" mortar overlap	573,000 (238,000)
GS46-64	South Ground	46" to 64"	13" of interior stone, 3" of mortar, 2" of exterior stone	825,000 (461,000)
GS17-35	South Ground	17" to 35"	13" of interior stone with 5" mortar overlap	N/A^A (N/A)^A
26N52-70	Landing 26 North	52" to 70"	3" of exterior face stone, 15" of solid mortar and rubble stone	192,000 (157,000)
26N41-59	Landing 26 North	41" to 59"	18" of solid mortar and rubble stone	135,000 (116,000)

^AMembrane burst invalidating data

^BFace stone fractured during 1st load cycle; 2nd load cycle not tested to prevent further damage

The above Table 3 is sorted from top to bottom by the percentage of the test area that was in contact with stone instead of collar joint mortar. Because the mortar is significantly weaker than the stone units it is understood that the semi-flexible membrane expanded unevenly across the length of the test specimens where there was a combination of stone and mortar tested. The membrane is understood to have expanded more at the portions of mortar than the portions of stone, thus giving lower measured modulus of deformation when the test area included a collar joint. For many of the tests this was unavoidable due to the membrane being 18" long. There is a clear difference in the measured modulus of deformation between the tests where most or all of the test area was solid stone versus the tests where collar joints were included in the test area.



Tests GS29-47, 26N1-19, GS1-19, and GS46-64 (first four rows in Table 3) are likely more representative of the global modulus of deformation for the walls. This is due to those tests being located either entirely in contact with sound stone or only partially overlapping mortar joints; no rubble areas were included in these four tests. Due to the relative ease for the rubber membrane to expand in softer material (e.g. rubble fill) the measured modulus of deformation can be skewed towards lower values due to the volume of water displacing the membrane into air/rubble cavities instead of deforming the masonry.

Another note is that the Goodman Jack test does not estimate f'_m with the maximum applied test because of the geometry of the test and the direction of the applied load. Instead of applying pure compression forces to a stone specimen, as the flatjack test operates, the Goodman Jack applies load radially from the inside of the core hole. The directionality of the load application is complicated because it is applying a compressive force that creates tension in the stone unit. Think of the left side of the core hole being pushed to the left and the right side of the core hole being pushed right, which applies tension to the stone section at the center of the core hole. Also, all of the observed stone failures during the Goodman Jack tests sounded and looked like tensile fracture failures, rather than compression related crushing failures.

4. LABORATORY STONE MATERIAL TESTING

Six (6) locations throughout the Bennington Battle Monument were selected by ANA, Silman, S&A, and representatives from the State of Vermont for stone cores to be removed for laboratory testing. Core locations were marked on site and Alegrone subsequently used a core drill to extract the samples and turn them over to ANA. Four (4) stone cores were sourced from interior stones and two (2) cores were sourced from exterior stones. All core locations and IDs are included in Appendix B.

Sourced cores were intentionally extracted with the core lengths significantly longer than needed to have sufficient material to follow the test methodology of ASTM C170 for the compressive testing and ASTM C215 for the dynamic modulus testing. Stone material was also recycled such that the dynamic modulus testing was completed first and then the same stone material was further cut to size and gypsum-capped for compressive testing. Dynamic modulus testing is completely nondestructive. A total of fifteen (15) stone specimens were subjected to compressive testing and a total of ten (10) stone specimens were subjected to dynamic modulus testing.

4.1. Compressive Strength Testing

Fifteen (15) stone specimens were sampled in accordance with ASTM C170, *Standard Test Method for Compressive Strength of Dimension Stone*. Figure 44 shows a representative photo of a stone core before and after completion of the compression test.





Figure 44. (left) ASTM C170 test setup for a stone specimen before applying load; (right) stone specimen following compressive failure.

Compressive testing was also separated into two categories of testing, wet and dry. Samples that were tested dry were conditioned for at least 48 hours in a dry oven environment. Samples that were tested wet were conditioned for at least 48 hours in a temperature-controlled water bath. All compressive testing results are shown in Table 4 and Table 5.



Table 4. Compressive testing results for the dry stone specimens.

Specimen ID	Diameter (in.)	Height (in.)	Density (pcf)	Load Direction	Compression Modulus (psi)	Max Pressure (psi)	Stone Type
NORTH-3a	2.75	2.85	164	*	5,442,000	28,310	DOLOSTONE
NORTH-3b	2.75	2.89	165	*	6,057,000	33,540	
SOUTH-4a	2.71	2.99	165	*	5,691,000	31,050	
SOUTH-4b	2.72	2.88	171	*	5,225,000	33,760	
NORTH-5a	2.73	2.70	167	*	**	33,700	
Average (psi)					5,600,000	32,100	
Standard of Deviation (psi)					310,000	2,100	
Coefficient of Variation (%)					6%	7%	
WEST-1a	2.73	2.80	167	Parallel	**	8,730	MARBLE
WEST-1b	2.73	2.81	167	Parallel	**	10,040	
EAST-2a	2.73	2.76	168	Parallel	**	7,750	
Average (psi)					-	8,800	
Standard of Deviation (psi)					-	900	
Coefficient of Variation (%)					-	10%	

Table 5. Compressive testing results for the wet stone specimens.

Specimen ID	Diameter (in.)	Height (in.)	Density (pcf)	Load Direction	Compression Modulus (psi)	Max Pressure (psi)	Stone Type
NORTH-5a	2.75	2.75	172	*	**	26,150	DOLOSTONE
WEST-7a	2.81	2.79	169	*	**	32,090	
EAST-6a	2.76	2.75	167	*	4,094,000	25,740	
EAST-6b	2.73	2.70	175	*	3,860,000	24,920	
Average (psi)					3,980,000	27,200	
Standard of Deviation (psi)					120,000	2,800	
Coefficient of Variation (%)					3%	10%	
WEST-1a	2.77	2.80	165	Parallel	3,214,000	7,780	MARBLE
WEST-1b	2.78	2.75	168	Parallel	3,780,000	9,890	
EAST-2a	2.75	2.73	167	Parallel	3,912,000	10,490	
Average (psi)					3,640,000	9,400	
Standard of Deviation (psi)					300,000	1,200	
Coefficient of Variation (%)					8%	13%	

* Load direction relative to the stone bedding or rift the dolostone samples could not be clearly defined. The dolostone appears more homogenous without a clear bedding or rift direction. All loading of marble samples was applied parallel to stone bedding or rift.

**The Scope of Work did not include running laboratory tests to determine compression modulus of the extracted stone cores. However, ANA opted to test some of the stone specimens for compression modulus by measuring strain during the compression test to compare to results from other in-situ test methods. Not all specimens were tested as such so not every row of the results tables are populated under the compression modulus column.



4.2. Dynamic Modulus Testing

Dynamic modulus testing was conducted by BDI using the stone cores provided by ANA. The testing was in accordance with ASTM C215, *The Standard Test Method for Fundamental Transverse, Longitudinal, and Torsional Frequencies of Concrete Specimen*. Ten (10) stone cores were tested to determine their dynamic modulus and the subsequent static moduli values were estimated using empirical correlations. Test methodology and equations are all included in BDI's report included as Appendix E.

Error! Reference source not found. summarizes BDI's dynamic modulus testing results.

Sample	FL (Hz)	λ (in)	VC (ft/sec)	ρ (lb/ft ³)	Edynamic (psi)	Estatic (psi)	Stone Type
EAST-6a	13250	11.38	12560	168	5,750,000	4,780,000	DOLOSTONE
EAST-6b	11250	11.13	10430	171	4,040,000	3,350,000	
WEST-7	9900	11.63	9591	178	3,540,000	2,940,000	
NORTH-5	12700	11.63	12303	178	5,850,000	4,850,000	
NORTH-3a	9350	11.13	8668	175	2,850,000	2,370,000	
NORTH-3b	11100	11.5	10638	176	4,310,000	3,580,000	
SOUTH-4	9700	11.63	9397	174	3,340,000	2,770,000	
Average (psi)					4,240,000	3,520,000	
Standard Deviation (psi)					1,080,000	900,000	
Coefficient of Variation (%)					25%	26%	
EAST-2	11100	10.75	9944	177	3,800,000	3,150,000	MARBLE
WEST-1a	10000	11.5	9583	169	3,370,000	2,800,000	
WEST-1b	9800	11.63	9494	169	3,290,000	2,730,000	
Average (psi)					3,490,000	2,890,000	
Standard Deviation (psi)					220,000	180,000	
Coefficient of Variation (%)					6%	6%	



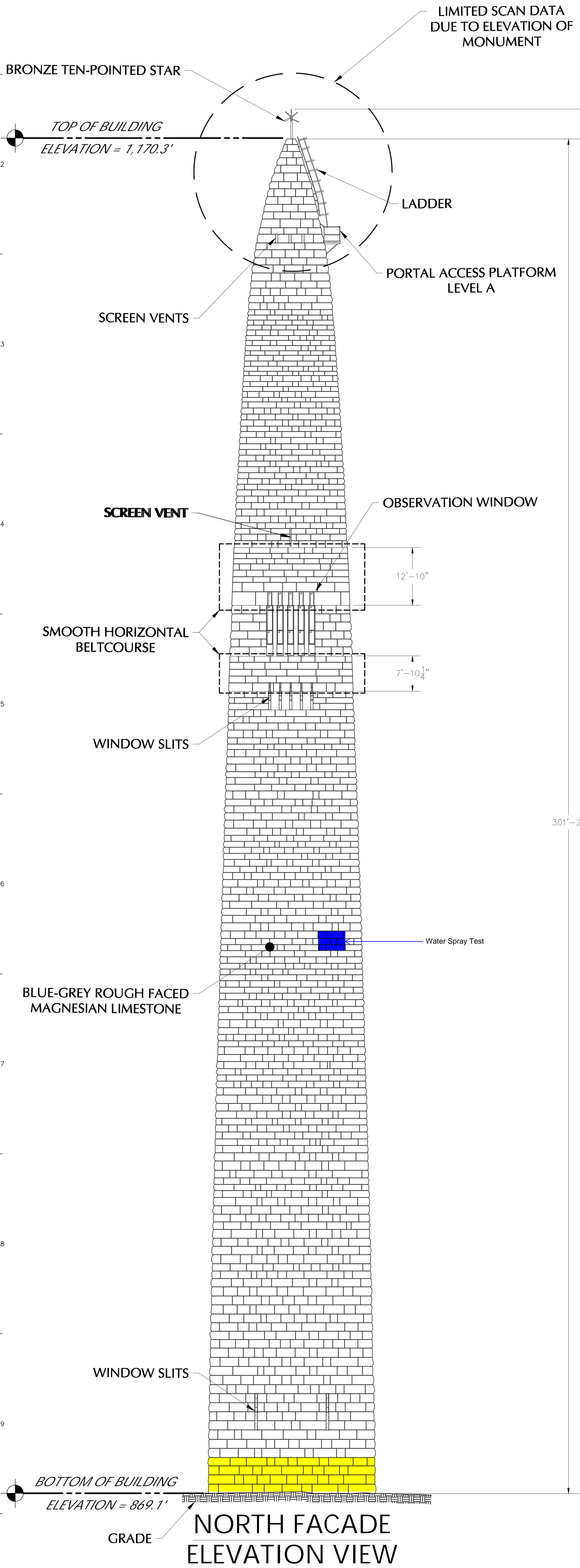
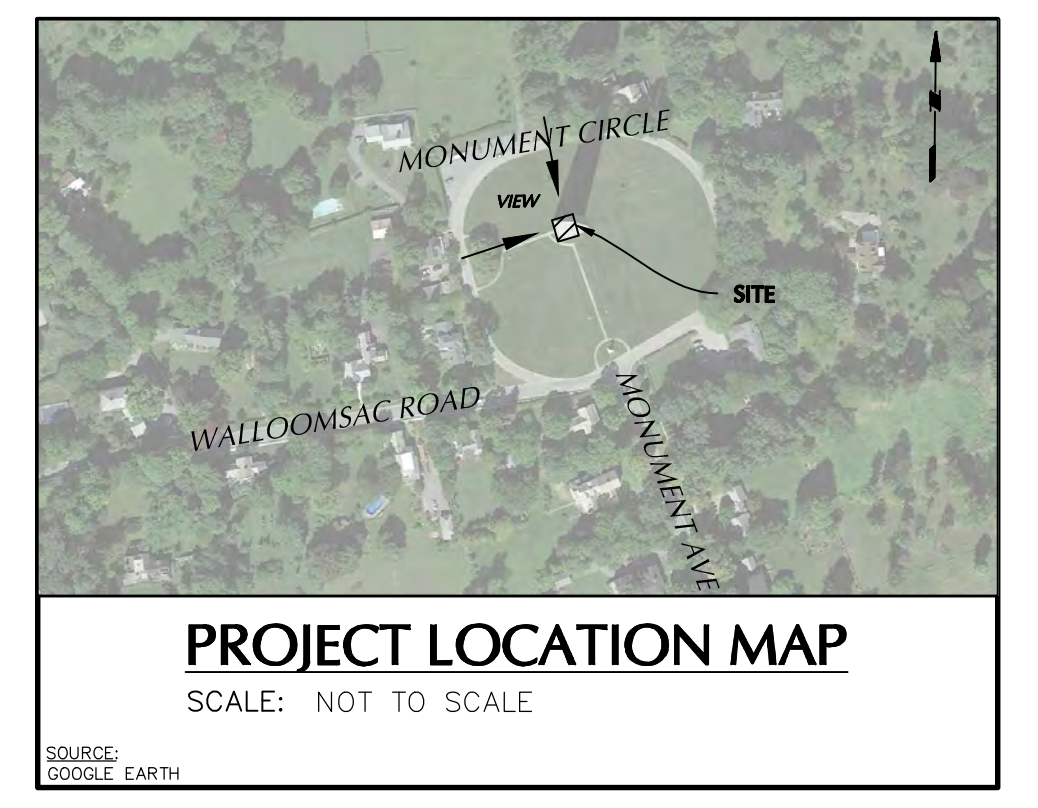
Thank you for the opportunity to work with you on this matter. Please feel free to call if you have any questions.

The information contained in this report is based on the information available or collected at the time that this report was prepared and we reserve the right to modify this report as additional information becomes available. Our services were performed using the degree of skill normally exercised by our professional peers and our findings were reached with a reasonable degree of engineering certainty. The client should be aware that our scope of work was limited to nondestructive evaluation and material testing of stone masonry at the Bennington Battle Monument.

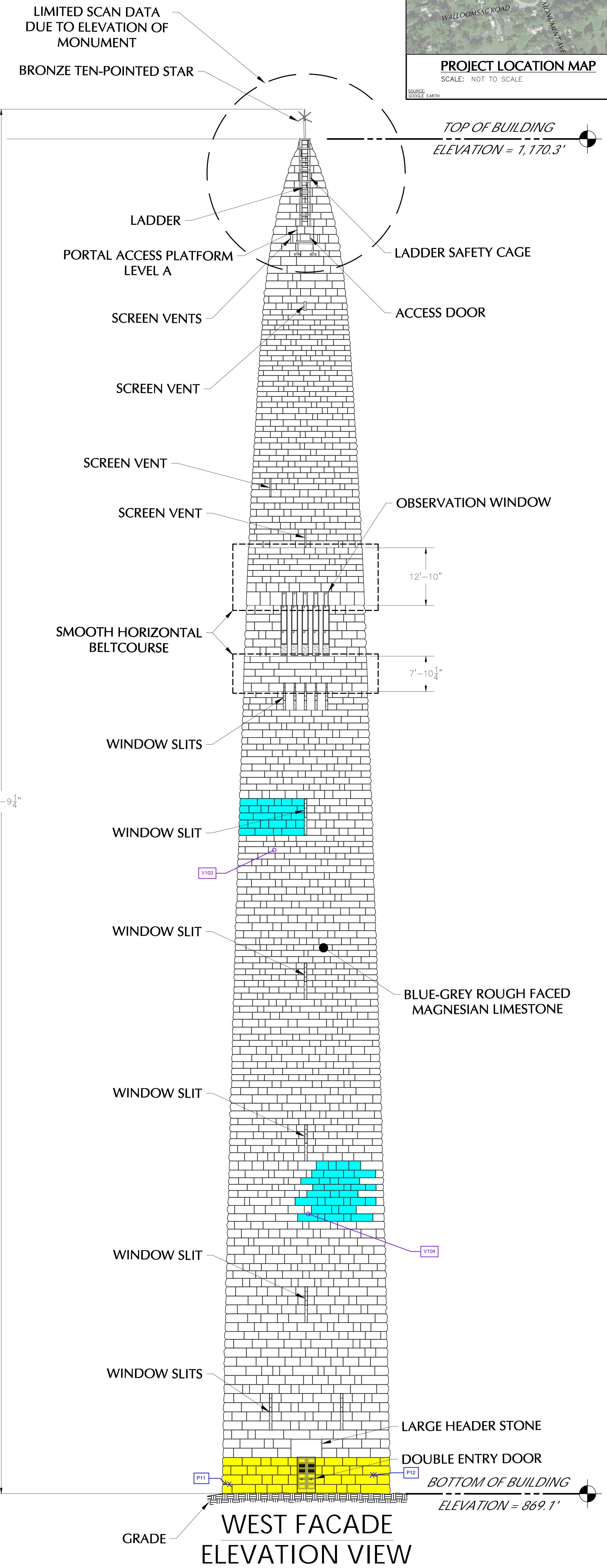


APPENDIX A
NDE Locations





NORTH FACADE ELEVATION VIEW



WEST FACADE ELEVATION VIEW

NOTES:

- THIS SURVEY IS BASED UPON EXISTING PHYSICAL CONDITIONS FOUND AT THE SUBJECT SITE.
- INFORMATION SHOWN HEREON HAS BEEN OBTAINED FROM LASER SCAN DATA COLLECTED BY LANGAN ENGINEERING, ENVIRONMENTAL, SURVEYING AND LANDSCAPE ARCHITECTURE, D.P.C., IN FEBRUARY, 2022.
- ELEVATIONS SHOWN ARE REFERENCED TO THE NORTH AMERICAN VERTICAL DATUM OF 1988.
- ALL UNITS SHOWN HEREON ARE IN U.S. SURVEY FEET.
- THIS PLAN NOT VALID UNLESS EMBOSSED OR BLUE INK STAMPED WITH THE SEAL OF THE PROFESSIONAL LAND SURVEYOR.

ATKINSON-NOLAND & ASSOCIATES
APPENDIX A
August, 2023

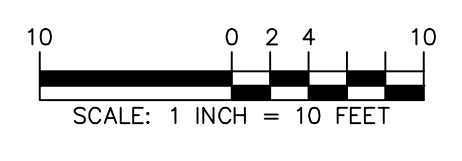
NOTES:
- SCAN AREAS ARE DRAWN SCHEMATICALLY. LOCATIONS AND SIZES OF HATCHWORK ARE APPROXIMATE.
- BACKGROUND DRAWINGS BY OTHERS

Videoscope Hole Location P11 Videoscope Hole Location V1

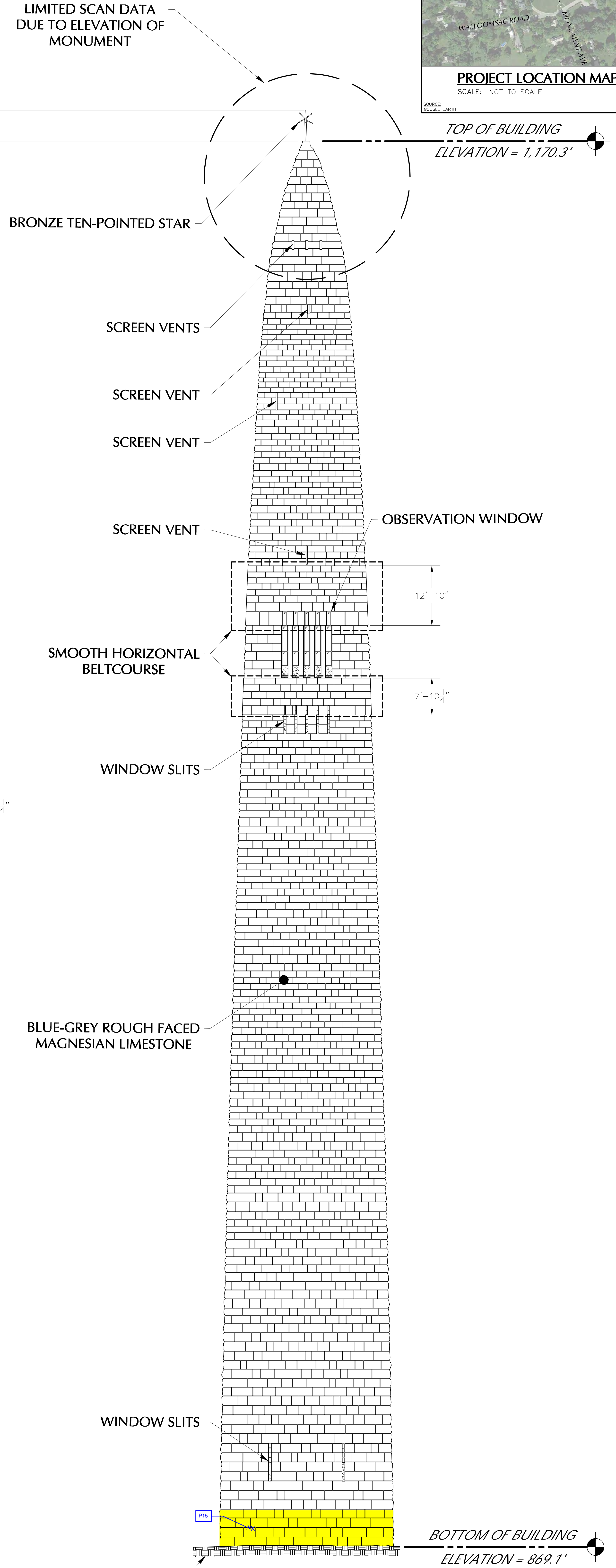
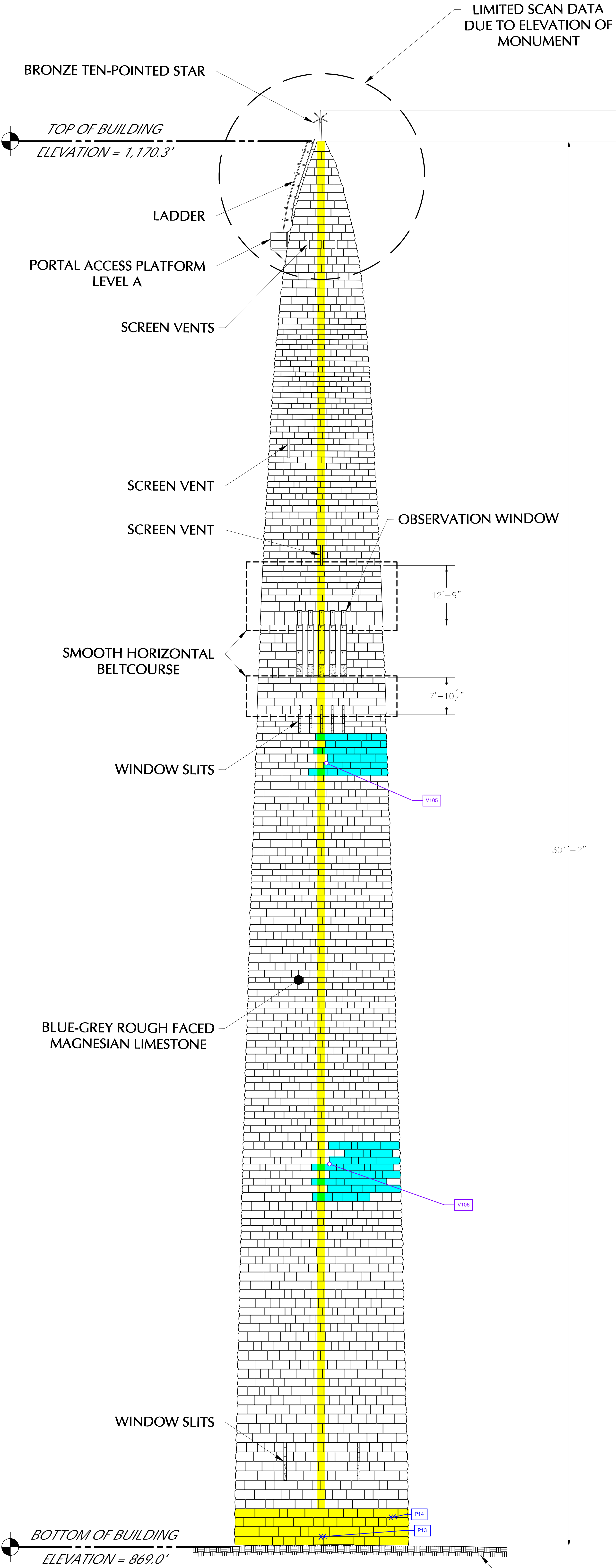
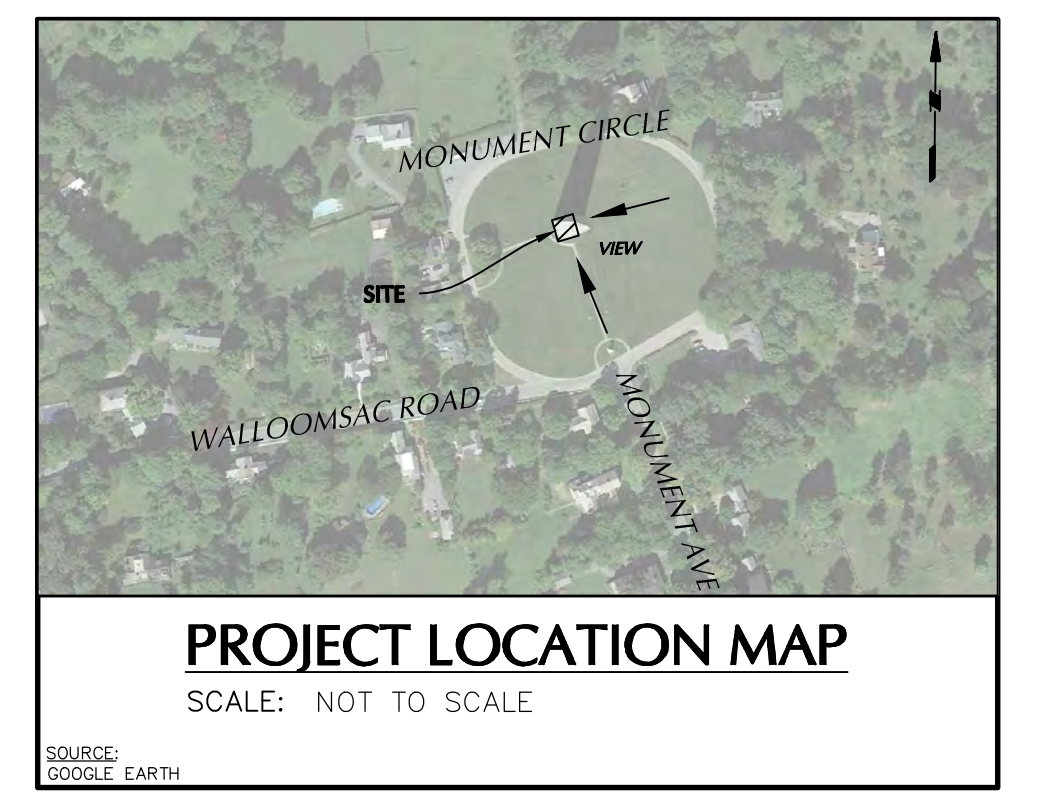
Ultrasound Scan Location Water Spray Test Location

Radar Scan Location Radar Scan Location

PHASE 1 CONTRACT - SEE 6-30-2022 REPORT PHASE 2 CONTRACT - SEE SEPTEMBER 2023 REPORT



<p>LANGAN Langan Engineering and Environmental Services, Inc. 21 Penn Plaza, 360 West 31st Street, 8th Floor New York, NY 10001 T: 212.479.5400 F: 212.479.5444 www.langan.com</p>	<p>Project BENNINGTON BATTLE MONUMENT 15 MONUMENT CIRCLE BENNINGTON, VT BENNINGTON COUNTY VERMONT</p>	<p>Drawing Title ELEVATION PLAN EXTERIOR (NORTH & WEST)</p>	<p>Project No. 170724001</p> <p>Date 05/11/2022</p> <p>Drawn By JFR</p> <p>Checked By PDF</p>	<p>Drawing No. EL-02</p> <p>Sheet 002 of 004</p>
	<p>Filename: \\langan.com\data\NYCData\170724001\Project Data\Discipline\Survey\CAD\Existing\Elevation\170724001-Bennington_Monument_North&West_Elevation.dwg Date: 5/11/2022 Time: 14:29 User: jragrose Style Table: Langan.tbl Layout: ARCH-FR-EL</p>			



SOUTH FACADE ELEVATION VIEW

EAST FACADE ELEVATION VIEW

- NOTES:**
- THIS SURVEY IS BASED UPON EXISTING PHYSICAL CONDITIONS FOUND AT THE SUBJECT SITE.
 - INFORMATION SHOWN HEREON HAS BEEN OBTAINED FROM LASER SCAN DATA COLLECTED BY LANGAN ENGINEERING, ENVIRONMENTAL, SURVEYING AND LANDSCAPE ARCHITECTURE, D.P.C., IN FEBRUARY, 2022.
 - ELEVATIONS SHOWN ARE REFERENCED TO THE NORTH AMERICAN VERTICAL DATUM OF 1988.
 - ALL UNITS SHOWN HEREON ARE IN U.S. SURVEY FEET.
 - THIS PLAN NOT VALID UNLESS EMBOSSED OR BLUE INK STAMPED WITH THE SEAL OF THE PROFESSIONAL LAND SURVEYOR.

ATKINSON-NOLAND & ASSOCIATES
APPENDIX A
August, 2023

NOTES:
- SCAN AREAS ARE DRAWN SCHEMATICALLY. LOCATIONS AND SIZES OF HATCHWORK ARE APPROXIMATE.
- BACKGROUND DRAWINGS BY OTHERS

Videoscope Hole Location P11 V1

Ultrasound Scan Location Water Spray Test Location

Radar Scan Location Radar Scan Location

PHASE 1 CONTRACT - SEE 6-30-2022 REPORT

PHASE 2 CONTRACT - SEE SEPTEMBER 2023 REPORT

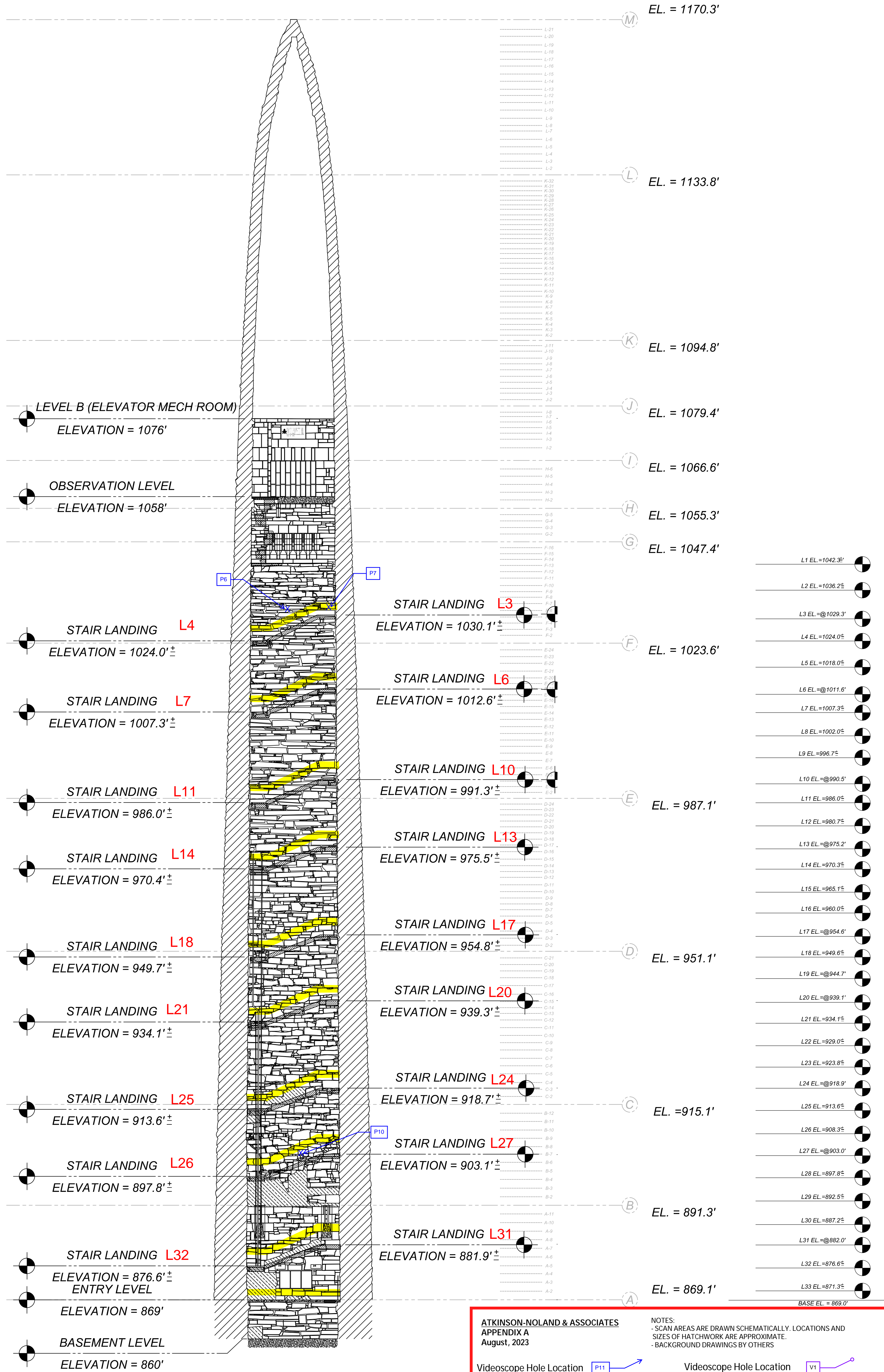
LANGAN
Langan Engineering and Environmental Services, Inc.
21 Penn Plaza, 360 West 31st Street, 8th Floor
New York, NY 10001
T: 212.479.5400 F: 212.479.5444 www.langan.com

Project
BENNINGTON BATTLE MONUMENT
15 MONUMENT CIRCLE
BENNINGTON, VT
BENNINGTON COUNTY VERMONT

Drawing Title
ELEVATION PLAN EXTERIOR (SOUTH & EAST)

Project No. 170724001	Drawing No. EL-01
Date 05/11/2022	Checked By JFR
Drawn By JFR	Sheet 001 of 004
Checked By PDF	





**EAST FACADE
INTERIOR ELEVATION
VIEW**

ATKINSON-NOLAND & ASSOCIATES
APPENDIX A
August, 2023

NOTES:
- SCAN AREAS ARE DRAWN SCHEMATICALLY. LOCATIONS AND SIZES OF HATCHWORK ARE APPROXIMATE.
- BACKGROUND DRAWINGS BY OTHERS

Videoscope Hole Location	P11	Videoscope Hole Location	V1
Ultrasound Scan Location	[Green Hatch]	Water Spray Test Location	[Blue Hatch]
Radar Scan Location	[Yellow Hatch]	Radar Scan Location	[Cyan Hatch]

PHASE 1 CONTRACT - SEE 6-30-2022 REPORT

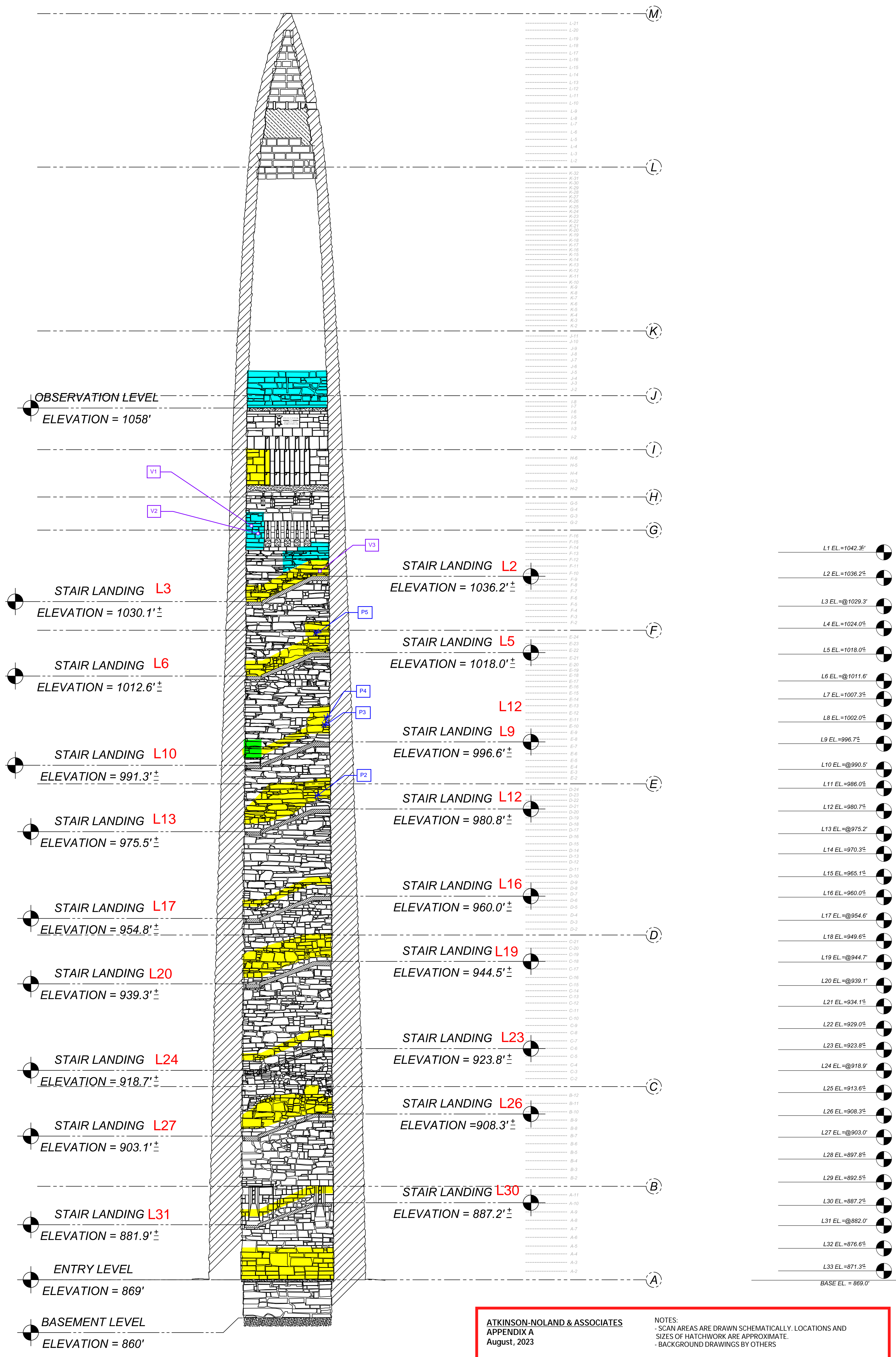
PHASE 2 CONTRACT - SEE SEPTEMBER, 2023 REPORT

SCALE: DATE: SILMAN # JOB # SHEET NO. OF XX	S-201.00
TITLE	EAST INTERIOR ELEVATIONS
REV. NUMBER/REVISION NAME	1 XXXXX
REVISIONS	
SEAL	

**BENNINGTON BATTLE
MONUMENT STRUCTURE**



32 Old Slip, 10th Floor, New York, NY 10005
212 620 7970



**SOUTH FACADE INTERIOR
ELEVATION VIEW**

ATKINSON-NOLAND & ASSOCIATES
APPENDIX A
August, 2023

NOTES:
- SCAN AREAS ARE DRAWN SCHEMATICALLY. LOCATIONS AND SIZES OF HATCHWORK ARE APPROXIMATE.
- BACKGROUND DRAWINGS BY OTHERS

Videoscope Hole Location P11

Ultrasound Scan Location

Radar Scan Location

Videoscope Hole Location V1

Water Spray Test Location

Radar Scan Location

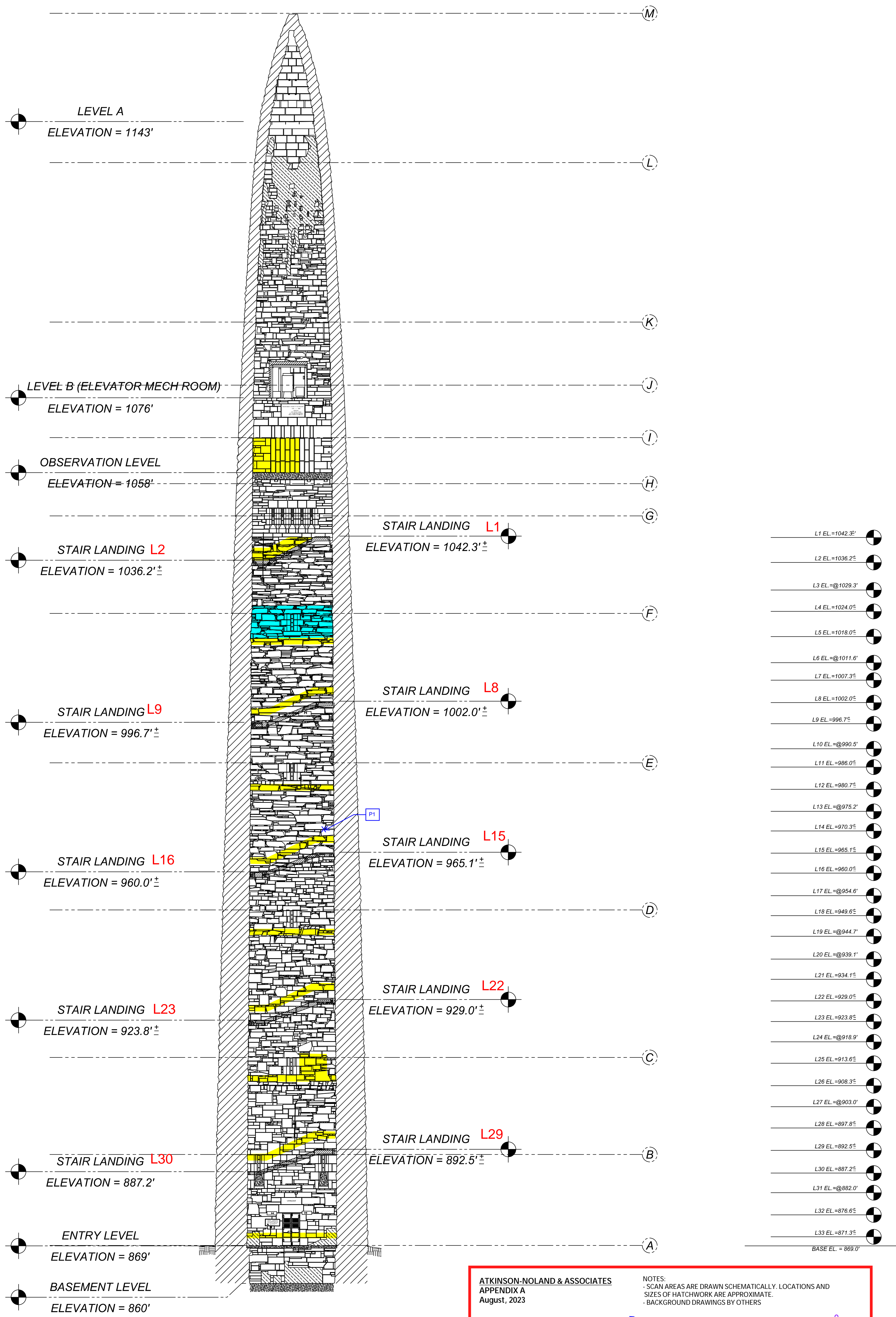
PHASE 1 CONTRACT - SEE 6-30-2022 REPORT

PHASE 2 CONTRACT - SEE SEPTEMBER, 2023 REPORT

SCALE: 1"=0'	S-202.00	SOUTH INTERIOR ELEVATIONS	SHEET NO. OF XX
DATE: 11-07			
SILMAN # JOB #			
REV. NUMBER/REVISION NAME	1	XXXXX	
TITLE	SOUTH INTERIOR ELEVATIONS		
REVISIONS			

**BENNINGTON BATTLE
MONUMENT STRUCTURE**

Silman
32 Old Slip, 10th Floor, New York, NY 10005
212 620 7970



**WEST FACADE
INTERIOR ELEVATION
VIEW**

ATKINSON-NOLAND & ASSOCIATES
APPENDIX A
August, 2023

NOTES:
- SCAN AREAS ARE DRAWN SCHEMATICALLY. LOCATIONS AND SIZES OF HATCHWORK ARE APPROXIMATE.
- BACKGROUND DRAWINGS BY OTHERS

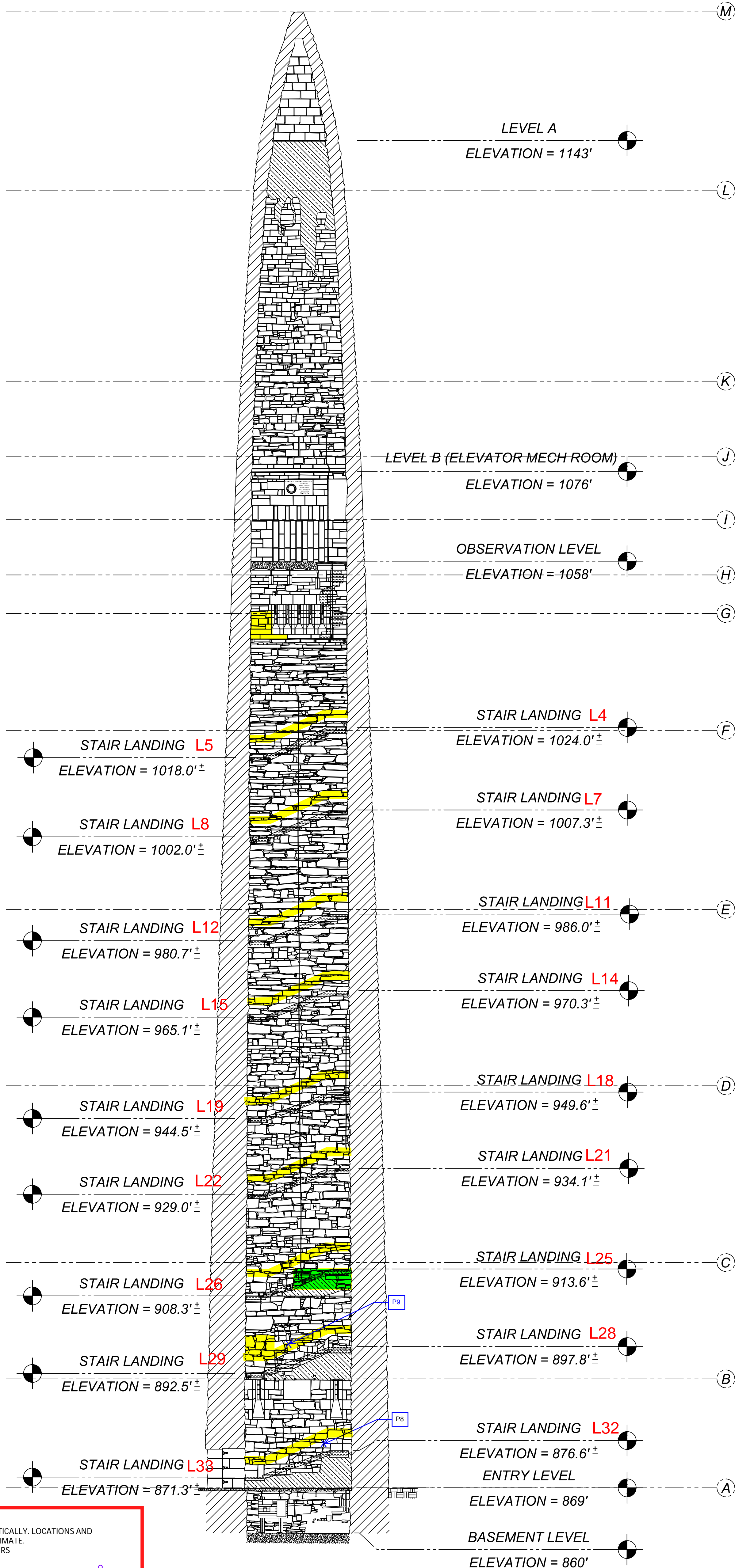
Videoscope Hole Location P11	Videoscope Hole Location V1
Ultrasound Scan Location 	Water Spray Test Location
Radar Scan Location 	Radar Scan Location

PHASE 1 CONTRACT - SEE 6-30-2022 REPORT
PHASE 2 CONTRACT - SEE SEPTEMBER, 2023 REPORT

SCALE: DATE: 0"	SHEET NO. S-203.00	TITLE WEST INTERIOR ELEVATIONS	REV. NUMBER/REVISION NAME	1	XXXXX
SCALE: DATE: 0"				SHEET NO. OF XX	

BENNINGTON BATTLE
MONUMENT STRUCTURE

Silman
32 Old Slip, 10th Floor, New York, NY 10005
212 620 7970



- L1 EL = 1042.3'
- L2 EL = 1036.2'
- L3 EL = 1029.3'
- L4 EL = 1024.0'
- L5 EL = 1018.0'
- L6 EL = 1011.6'
- L7 EL = 1007.3'
- L8 EL = 1002.0'
- L9 EL = 996.7'
- L10 EL = 990.5'
- L11 EL = 986.0'
- L12 EL = 980.7'
- L13 EL = 975.2'
- L14 EL = 970.3'
- L15 EL = 965.1'
- L16 EL = 960.0'
- L17 EL = 954.6'
- L18 EL = 949.6'
- L19 EL = 944.7'
- L20 EL = 939.1'
- L21 EL = 934.1'
- L22 EL = 929.0'
- L23 EL = 923.8'
- L24 EL = 918.9'
- L25 EL = 913.6'
- L26 EL = 908.3'
- L27 EL = 903.0'
- L28 EL = 897.8'
- L29 EL = 892.5'
- L30 EL = 887.2'
- L31 EL = 882.0'
- L32 EL = 876.6'
- L33 EL = 871.3'
- BASE EL = 869.0'

**NORTH FACADE
INTERIOR ELEVATION
VIEW**

ATKINSON-NOLAND & ASSOCIATES
APPENDIX A
August, 2023

NOTES:
- SCAN AREAS ARE DRAWN SCHEMATICALLY. LOCATIONS AND SIZES OF HATCHWORK ARE APPROXIMATE.
- BACKGROUND DRAWINGS BY OTHERS

Videoscope Hole Location P11 Videoscope Hole Location V1
 Ultrasound Scan Location Water Spray Test Location
 Radar Scan Location Radar Scan Location

PHASE 1 CONTRACT - SEE 6-30-2022 REPORT PHASE 2 CONTRACT - SEE SEPTEMBER, 2023 REPORT

REV.	NO.	REVISION
1	XXXXX	

SCALE: 1" = 0'
DATE:
SILMAN # JOB #
SHEET NO. OF XX

S-204.00

NORTH INTERIOR ELEVATIONS

**BENNINGTON BATTLE
MONUMENT STRUCTURE**

Silman
32 Old Slip, 10th Floor, New York, NY 10005
212 620 7970

APPENDIX B

In-situ Test & Core Removal Locations



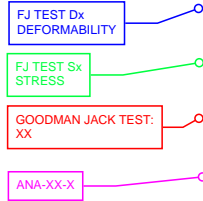
Atkinson-Noland
& Associates

Bennington Battle Monument Phase II Testing

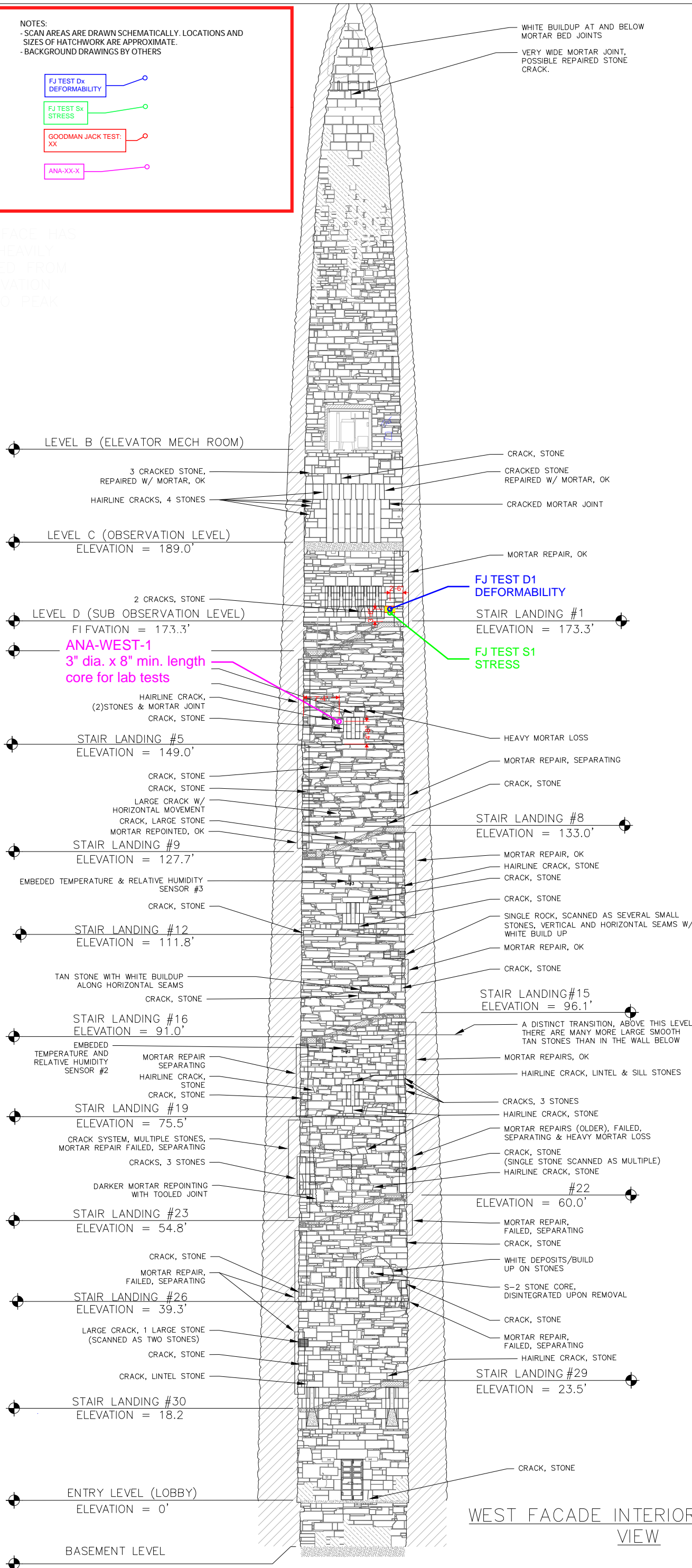
9/20/2023

NOTES:
- SCAN AREAS ARE DRAWN SCHEMATICALLY. LOCATIONS AND SIZES OF HATCHWORK ARE APPROXIMATE.
- BACKGROUND DRAWINGS BY OTHERS

- FLATJACK DEFORMABILITY TEST
- FLATJACK STRESS TEST
- GOODMAN JACK TEST
- LAB TEST CORE LOCATION



INTERIOR FACE HAS BEEN HEAVILY REPOINTED FROM OBSERVATION DECK TO PEAK



WEST FACADE INTERIOR ELEVATION VIEW

BENNINGTON BATTLE MONUMENT
15 MONUMENT CIR, BENNINGTON, VT 05201

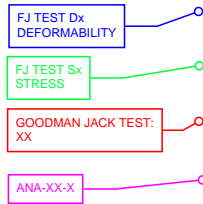
WEST INTERIOR ELEVATION

SCALE: 1"=10' PROJECT# 20-065 DATE: 11/07/2022

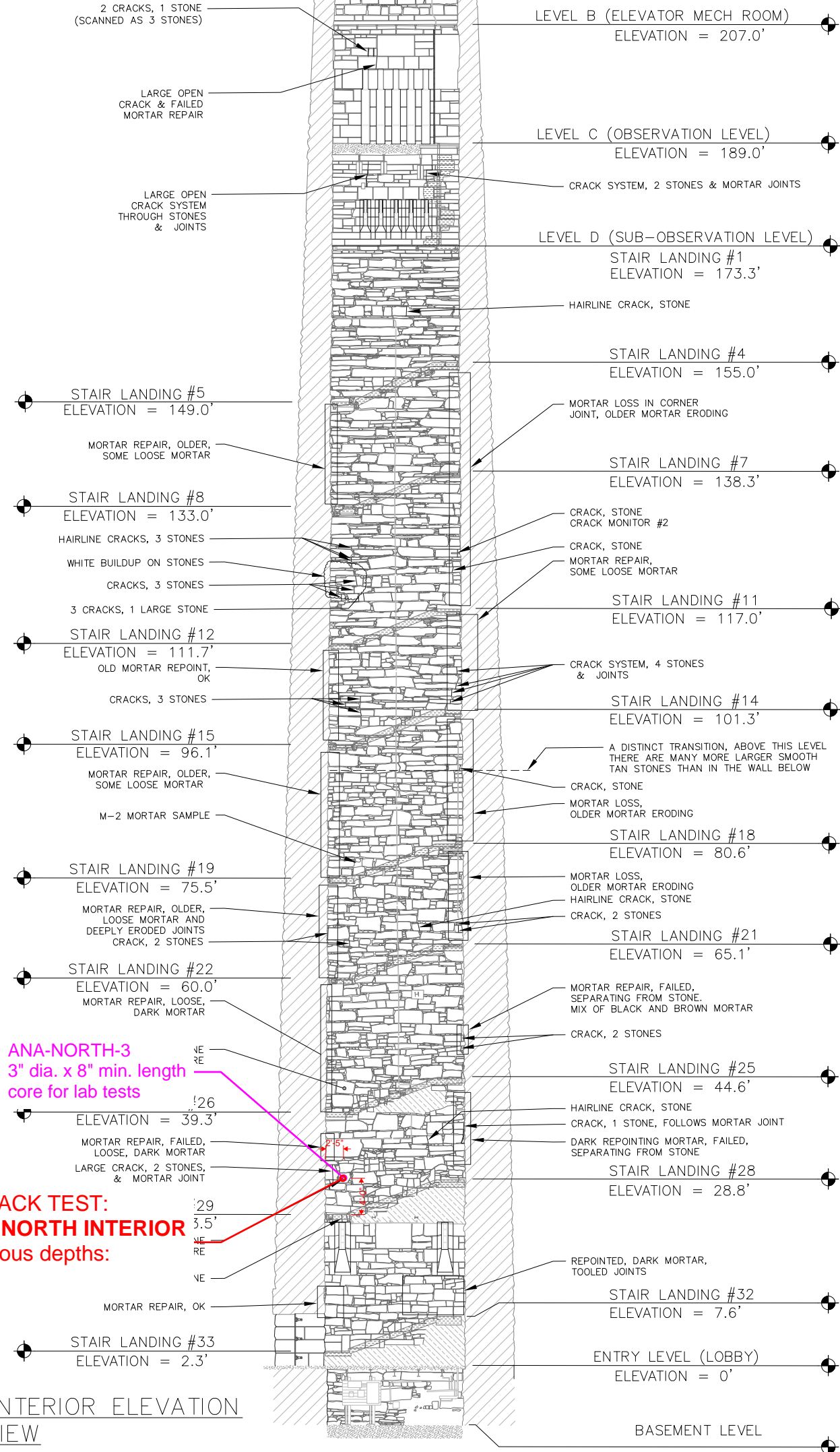
ARCHITECTS | ENGINEERS | LANDSCAPE ARCHITECTS
PH: 802-257-9329 | F: 802-258-3892 | WWW.STEVENS-ASSOC.COM

NOTES:
- SCAN AREAS ARE DRAWN SCHEMATICALLY. LOCATIONS AND SIZES OF HATCHWORK ARE APPROXIMATE.
- BACKGROUND DRAWINGS BY OTHERS

- FLATJACK DEFORMABILITY TEST
- FLATJACK STRESS TEST
- GOODMAN JACK TEST
- LAB TEST CORE LOCATION



INTERIOR FACE HAS BEEN HEAVILY REPOINTED FROM OBSERVATION DECK TO PEAK



NORTH FACADE INTERIOR ELEVATION
VIEW

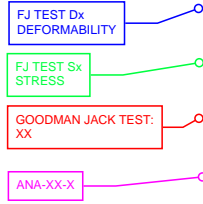
BENNINGTON BATTLE MONUMENT
15 MONUMENT CIR, BENNINGTON, VT 05201

NORTH INTERIOR
ELEVATION

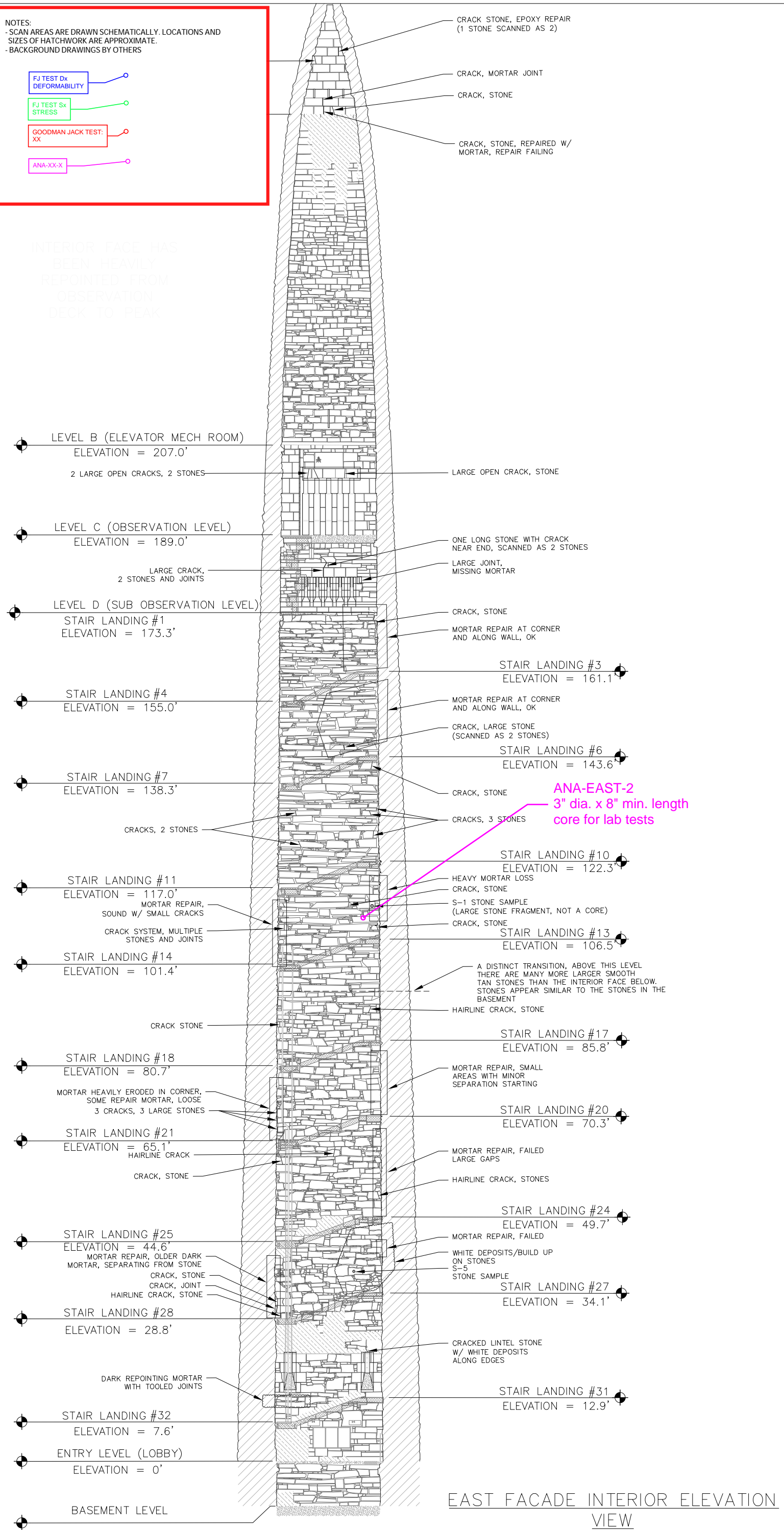
SCALE: 1"=10' PROJECT# 20-065 DATE: 11/07/2022

NOTES:
- SCAN AREAS ARE DRAWN SCHEMATICALLY. LOCATIONS AND SIZES OF HATCHWORK ARE APPROXIMATE.
- BACKGROUND DRAWINGS BY OTHERS

- FLATJACK DEFORMABILITY TEST
- FLATJACK STRESS TEST
- GOODMAN JACK TEST
- LAB TEST CORE LOCATION



INTERIOR FACE HAS BEEN HEAVILY REPOINTED FROM OBSERVATION DECK TO PEAK



EAST FACADE INTERIOR ELEVATION VIEW

BENNINGTON BATTLE MONUMENT
15 MONUMENT CIR, BENNINGTON, VT 05201

EAST INTERIOR ELEVATION

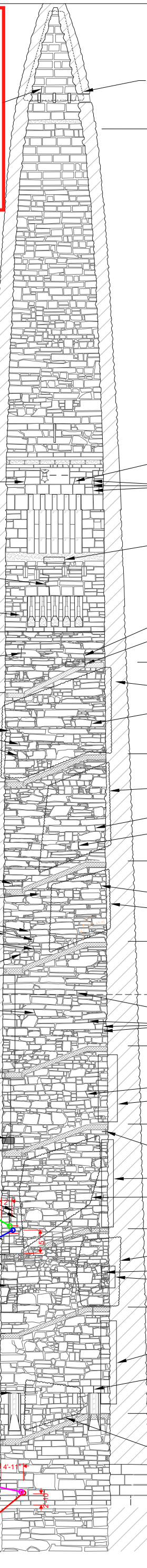
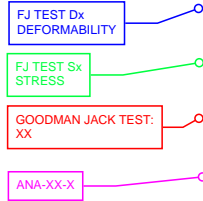


SCALE: 1"=10' PROJECT# 20-065 DATE: 11/07/2022

ARCHITECTS | ENGINEERS | LANDSCAPE ARCHITECTS
PH: 802-257-9329 | F: 802-258-3892 | WWW.STEVENS-ASSOC.COM

NOTES:
 - SCAN AREAS ARE DRAWN SCHEMATICALLY. LOCATIONS AND SIZES OF HATCHWORK ARE APPROXIMATE.
 - BACKGROUND DRAWINGS BY OTHERS

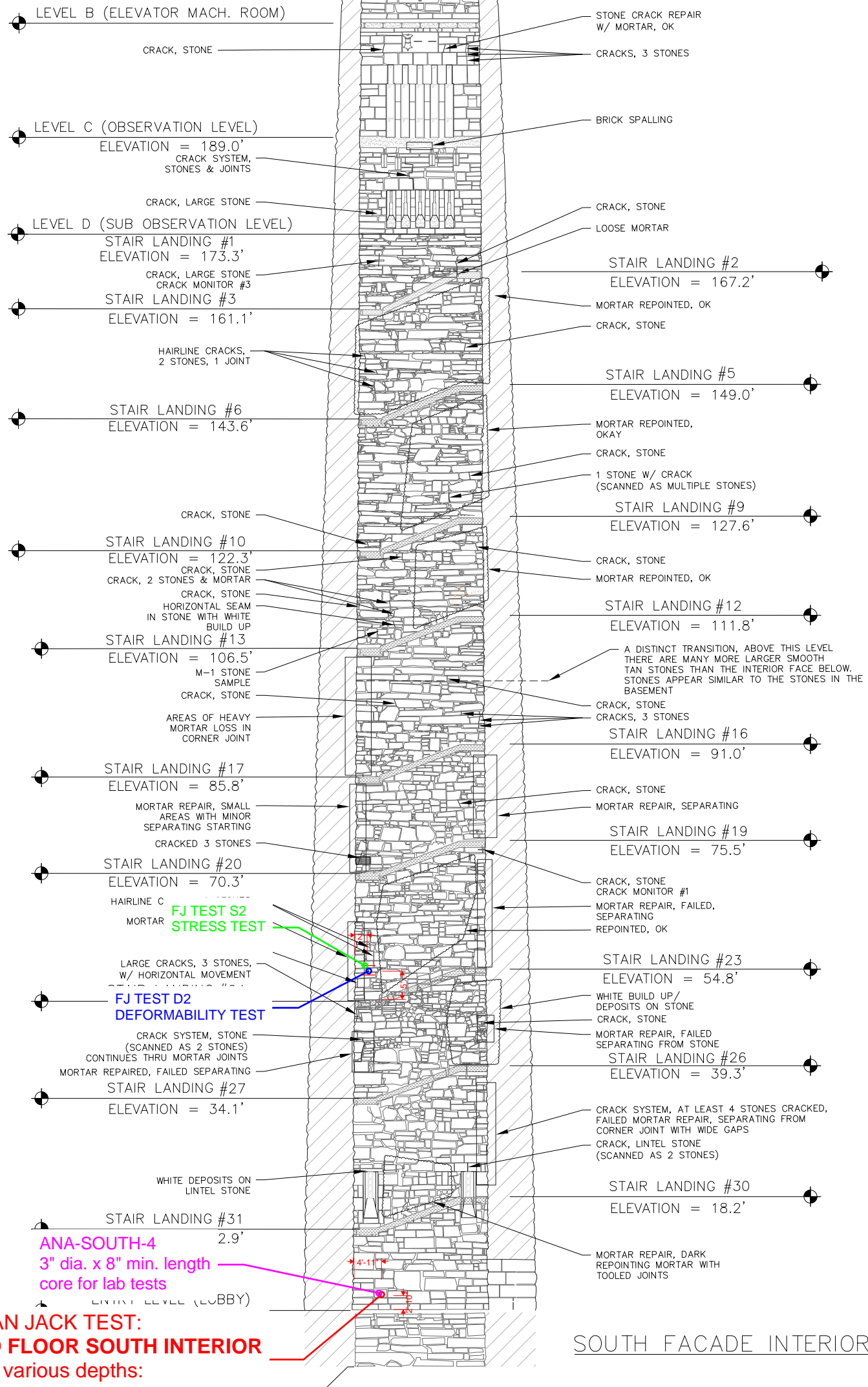
- FLATJACK DEFORMABILITY TEST
- FLATJACK STRESS TEST
- GOODMAN JACK TEST
- LAB TEST CORE LOCATION



WHITE BUILD UP AT AND BELOW MORTAR BED JOINTS, MOST STONES

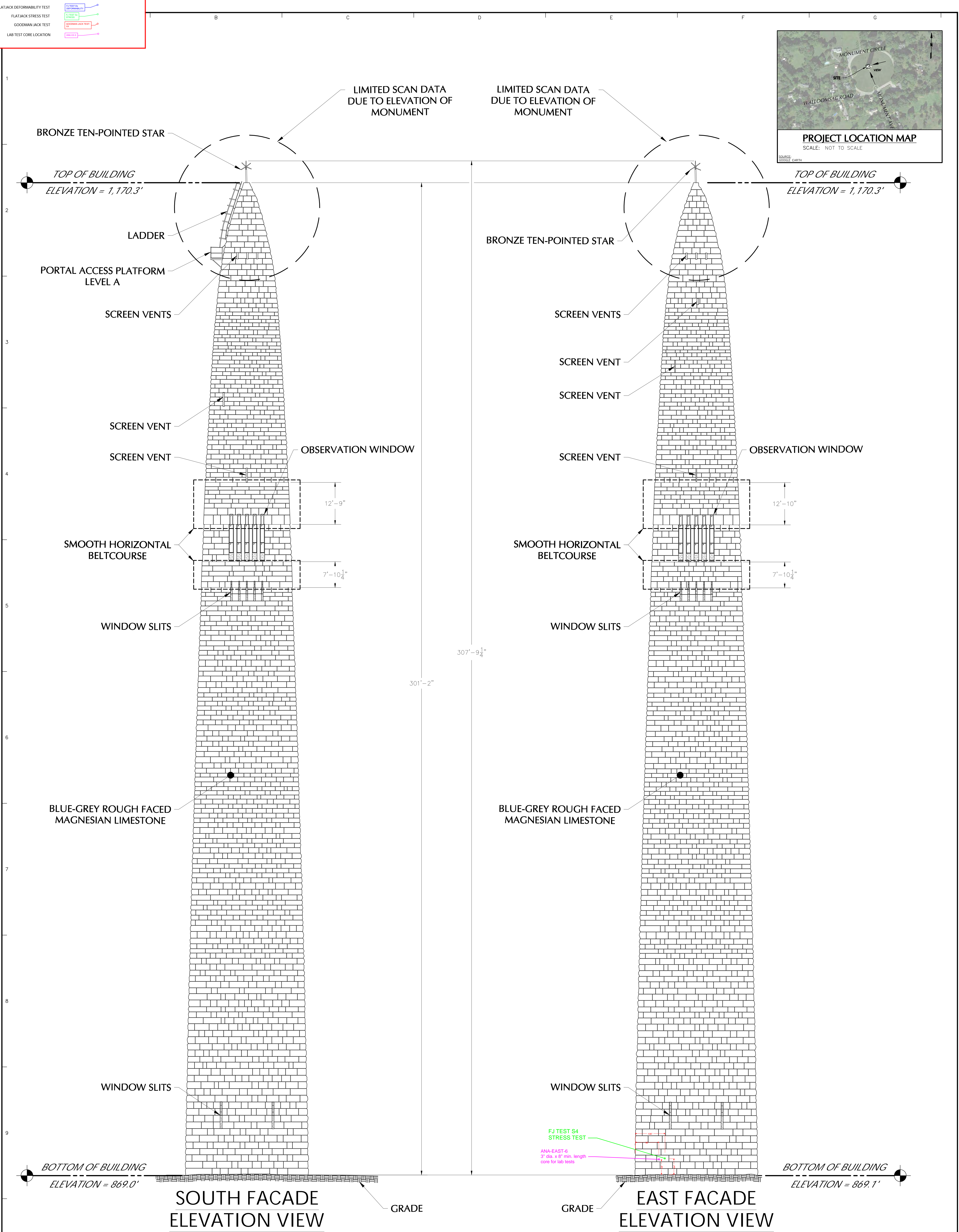
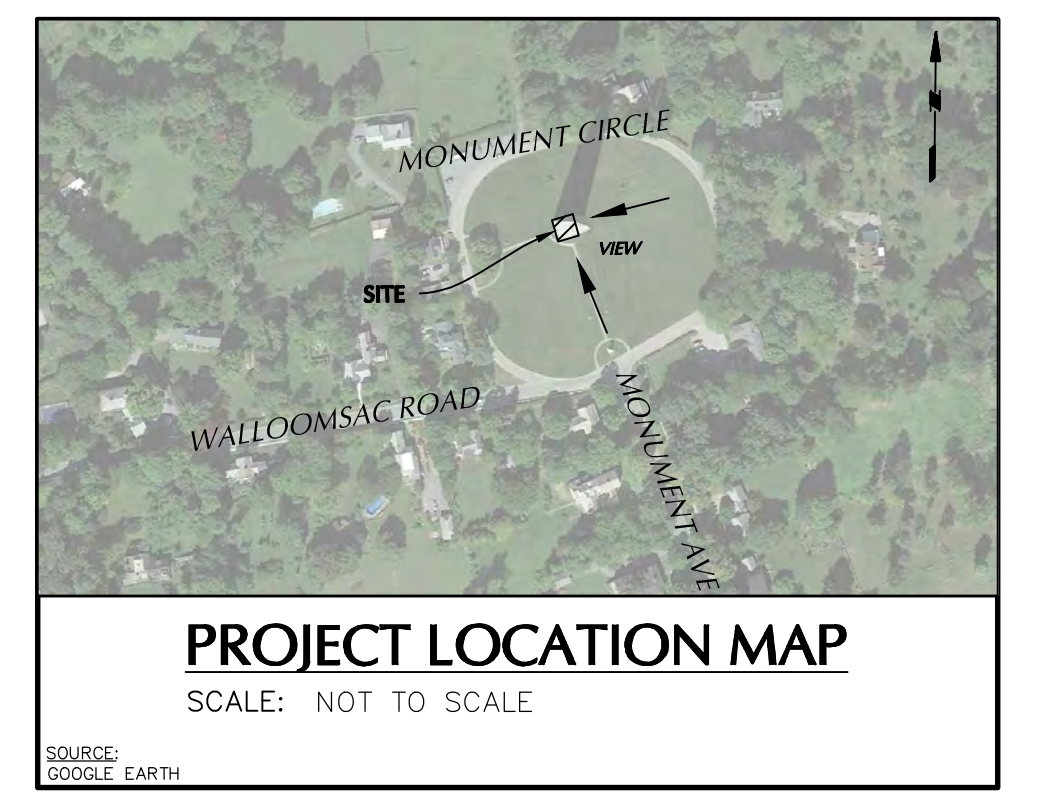
LEVEL A
 ELEVATION = 274.0'

INTERIOR FACE HAS BEEN HEAVILY REPOINTED FROM OBSERVATION DECK TO PEAK

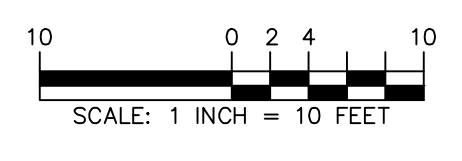


**GOODMAN JACK TEST:
 GROUND FLOOR SOUTH INTERIOR
 4 tests @ various depths:**

SOUTH FACADE INTERIOR ELEVATION VIEW



- NOTES:**
- THIS SURVEY IS BASED UPON EXISTING PHYSICAL CONDITIONS FOUND AT THE SUBJECT SITE.
 - INFORMATION SHOWN HEREON HAS BEEN OBTAINED FROM LASER SCAN DATA COLLECTED BY LANGAN ENGINEERING, ENVIRONMENTAL, SURVEYING AND LANDSCAPE ARCHITECTURE, D.P.C., IN FEBRUARY, 2022.
 - ELEVATIONS SHOWN ARE REFERENCED TO THE NORTH AMERICAN VERTICAL DATUM OF 1988.
 - ALL UNITS SHOWN HEREON ARE IN U.S. SURVEY FEET.
 - THIS PLAN NOT VALID UNLESS EMBOSSED OR BLUE INK STAMPED WITH THE SEAL OF THE PROFESSIONAL LAND SURVEYOR.



<p>LANGAN Langan Engineering and Environmental Services, Inc. 21 Penn Plaza, 360 West 31st Street, 8th Floor New York, NY 10001 T: 212.479.5400 F: 212.479.5444 www.langan.com</p>	Project BENNINGTON BATTLE MONUMENT 15 MONUMENT CIRCLE BENNINGTON, VT BENNINGTON COUNTY VERMONT	Drawing Title ELEVATION PLAN EXTERIOR (SOUTH & EAST)	Project No. 170724001	Drawing No. EL-01
	Date 05/11/2022	Drawn By JFR	Checked By PDF	Sheet 001 of 004

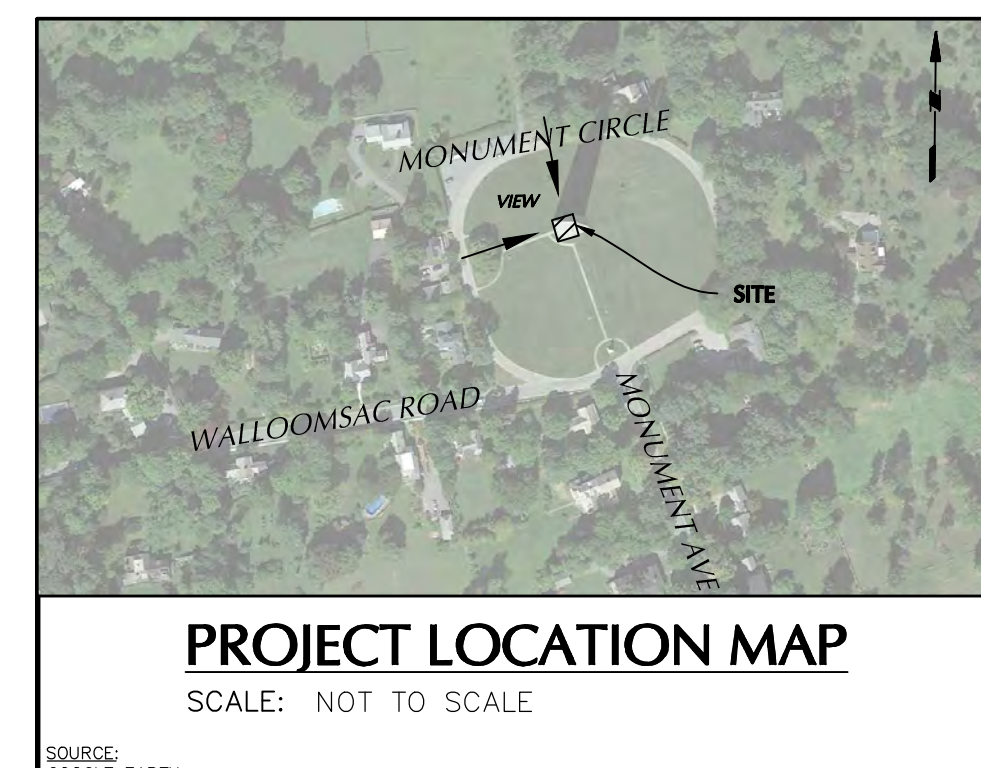
LANGAN PROJECT NO. 170724001

ADRIAN BOLAND & ASSOCIATES
 APPENDIX B
 SEPTEMBER, 2022

NOTE:
 SCAN AREAS ARE DRAWN TO MATHEMATICAL LOCATIONS AND
 SIZE OF FEATURES ARE APPROXIMATE
 BACKGROUND DRAWINGS BY OTHERS

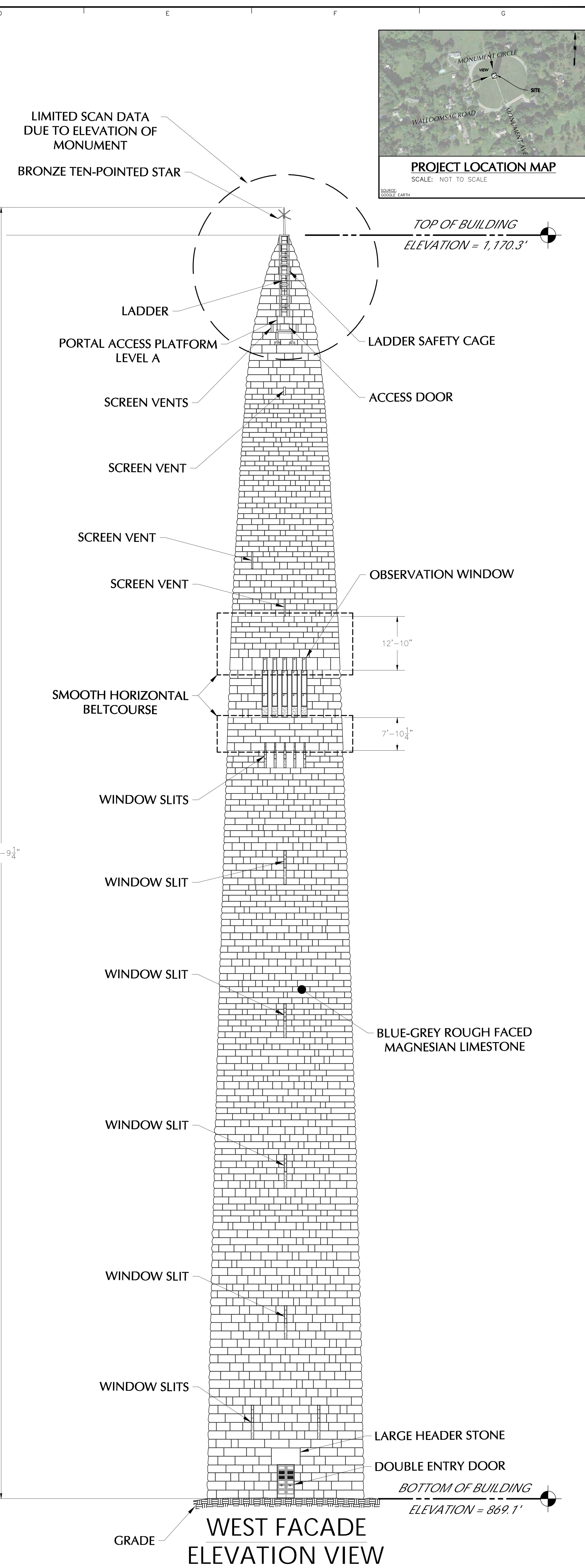
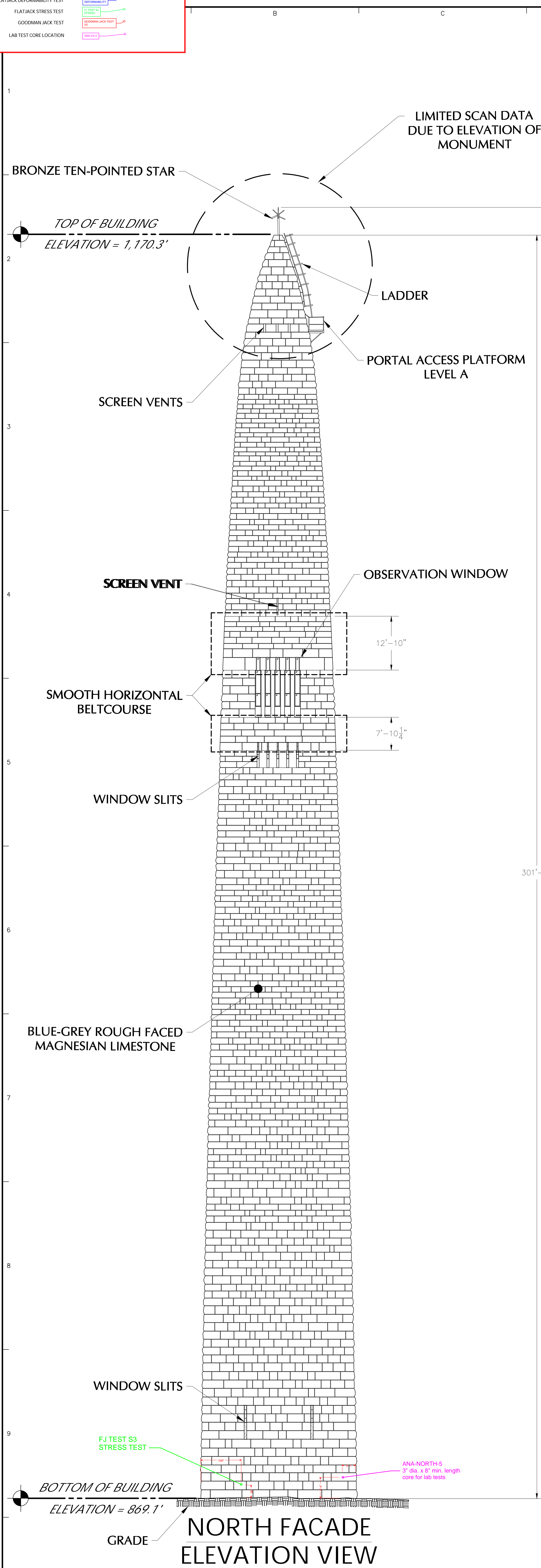
FLATJACK DEFORMABILITY TEST
 FLATJACK STRESS TEST
 GOODMAN JACK TEST
 LAB TEST CORE LOCATION

FJ TEST S3 STRESS TEST
 ANA-NORTH-S
 3" dia. x 8" min. length
 core for lab tests



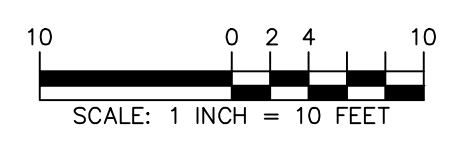
PROJECT NO. 170724001

LANGAN



NOTES:

- THIS SURVEY IS BASED UPON EXISTING PHYSICAL CONDITIONS FOUND AT THE SUBJECT SITE.
- INFORMATION SHOWN HEREON HAS BEEN OBTAINED FROM LASER SCAN DATA COLLECTED BY LANGAN ENGINEERING, ENVIRONMENTAL, SURVEYING AND LANDSCAPE ARCHITECTURE, D.P.C., IN FEBRUARY, 2022.
- ELEVATIONS SHOWN ARE REFERENCED TO THE NORTH AMERICAN VERTICAL DATUM OF 1988.
- ALL UNITS SHOWN HEREON ARE IN U.S. SURVEY FEET.
- THIS PLAN NOT VALID UNLESS EMBOSSED OR BLUE INK STAMPED WITH THE SEAL OF THE PROFESSIONAL LAND SURVEYOR.



<p>LANGAN Langan Engineering and Environmental Services, Inc. 21 Penn Plaza, 360 West 31st Street, 8th Floor New York, NY 10001 T: 212.479.5400 F: 212.479.5444 www.langan.com</p>	Project	BENNINGTON BATTLE MONUMENT	Drawing Title	ELEVATION PLAN EXTERIOR (NORTH & WEST)	Project No.	170724001	Drawing No.	EL-02
		15 MONUMENT CIRCLE BENNINGTON, VT			Date	05/11/2022		
		BENNINGTON COUNTY VERMONT			Drawn By	JFR		
					Checked By	PDF		
								Sheet 002 of 004

Filename: \\langan.com\data\NYC\2021\170724001\Project Data\Discipline\Survey\CAD\Existing\Elevation\170724001-Bennington_Monument_North&West_Elevation.dwg Date: 5/11/2022 Time: 14:29 User: jragones Style Table: Langan.tbl Layout: ARCH-EL

APPENDIX C
Spray Test Results



LEGEND:

APPLIED MOISTURE FROM SPRAY RACK: 1

EXTERIOR MOISTURE FROM RAIN: 9

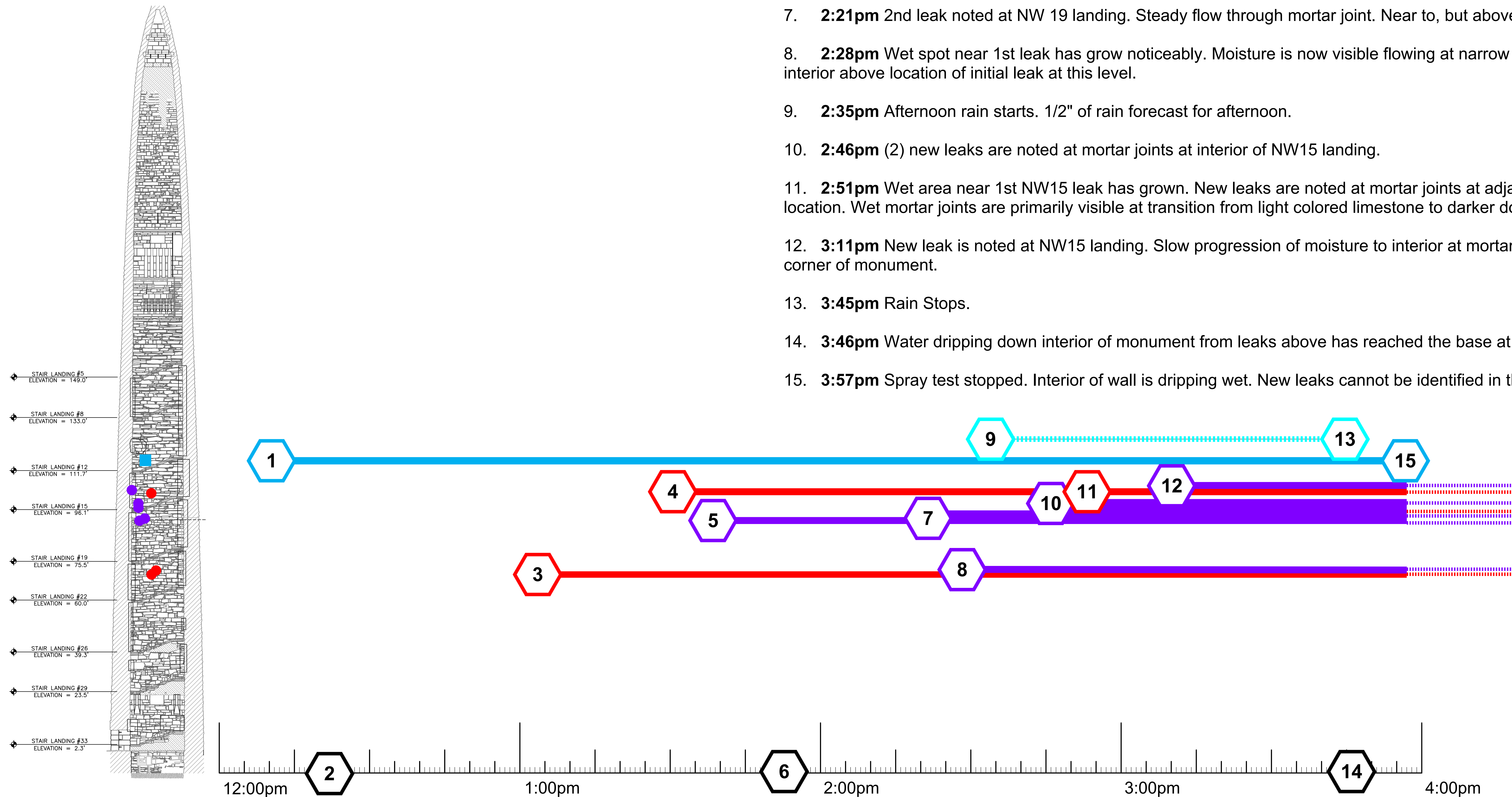
LEAK NOTED AT CRACKED INTERIOR STONE: 3

LEAK NOTED AT INTERIOR MORTAR JOINT: 5

GENERAL OBSERVATION: 2

TIMELINE

1. **12:15pm** Spray testing starts at exterior of NW12 landing.
2. **12:22pm** Water dripping down exterior has reached the base of the monument.
3. **1:08pm** 1st leak noted at NW 22 landing. Water is flowing in a slow, steady drip through cracked stone at interior face of wall and down interior face of monument.
4. **1:35pm** 1st leak noted at NW 15 landing. Slow drip of water at face of water, source appears to be cracked stone or open joint just above visible water flow.
5. **1:43pm** 1st leak noted at NW 19 landing. Small wet spot is visible at face of mortar joint at interior. No crack is visible this location.
6. **1:53pm** Water from first leak at NW22 has washed down wall to NW 26 landing.
7. **2:21pm** 2nd leak noted at NW 19 landing. Steady flow through mortar joint. Near to, but above, 1st leak at this location.
8. **2:28pm** Wet spot near 1st leak has grow noticeably. Moisture is now visible flowing at narrow opening at mortar bed joint at interior above location of initial leak at this level.
9. **2:35pm** Afternoon rain starts. 1/2" of rain forecast for afternoon.
10. **2:46pm** (2) new leaks are noted at mortar joints at interior of NW15 landing.
11. **2:51pm** Wet area near 1st NW15 leak has grown. New leaks are noted at mortar joints at adjacent stones above initial location. Wet mortar joints are primarily visible at transition from light colored limestone to darker dolostone.
12. **3:11pm** New leak is noted at NW15 landing. Slow progression of moisture to interior at mortar joint at interior northwest corner of monument.
13. **3:45pm** Rain Stops.
14. **3:46pm** Water dripping down interior of monument from leaks above has reached the base at the interior.
15. **3:57pm** Spray test stopped. Interior of wall is dripping wet. New leaks cannot be identified in the wash from old.



APPENDIX D

Goodman Jack Test Data and Plots



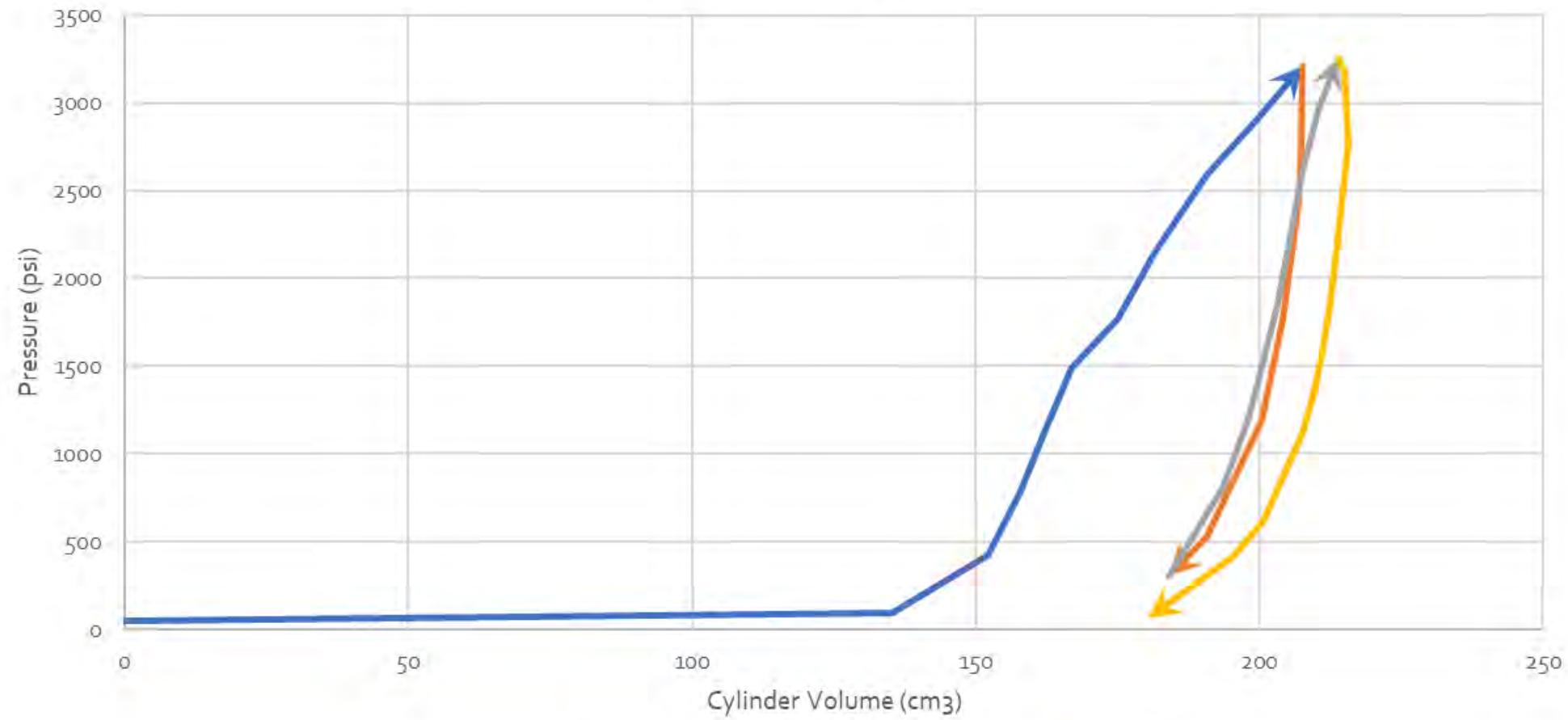
Atkinson-Noland
& Associates

Bennington Battle Monument Phase II Testing

9/20/2023



Test GS1-19



Test GS1-19:
 South Elevation
 Ground Level
 Test Depth = 1" to 19" from interior face

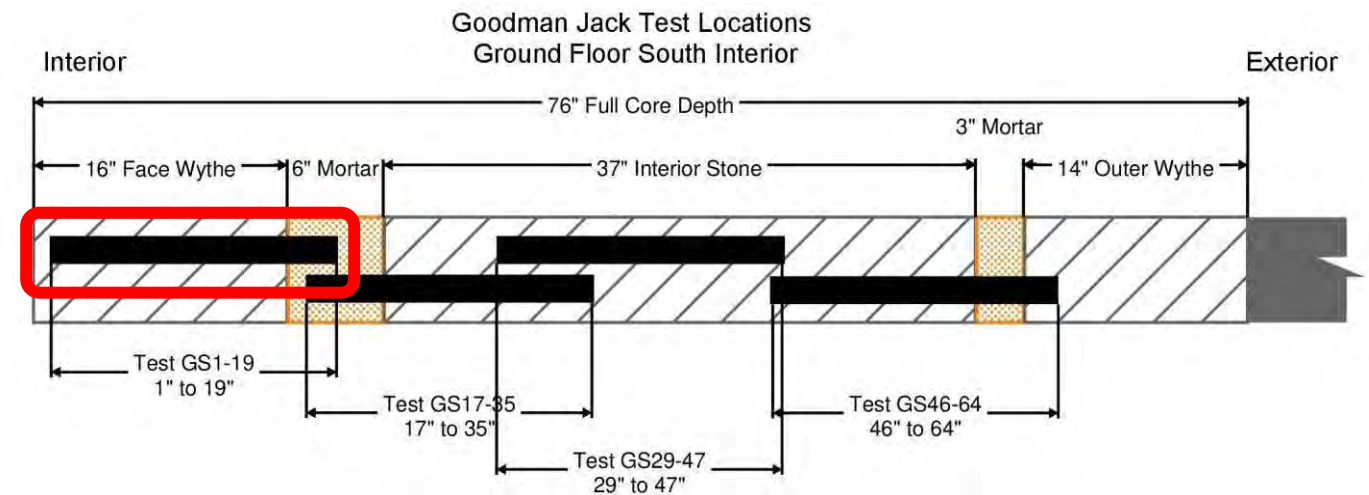
 Test Substrate = 16" of solid stone unit &
 2" of collar joint mortar

Reason for Stopping Test:
 Failure of 16" face wythe
 observed during Load Cycle 1
 and Load Cycle 2 by means of
 vertical cracks opening at
 interior face of wall.

→ Load Cycle 1 → Unload Cycle 1 → Load Cycle 2 → Unload Cycle 2

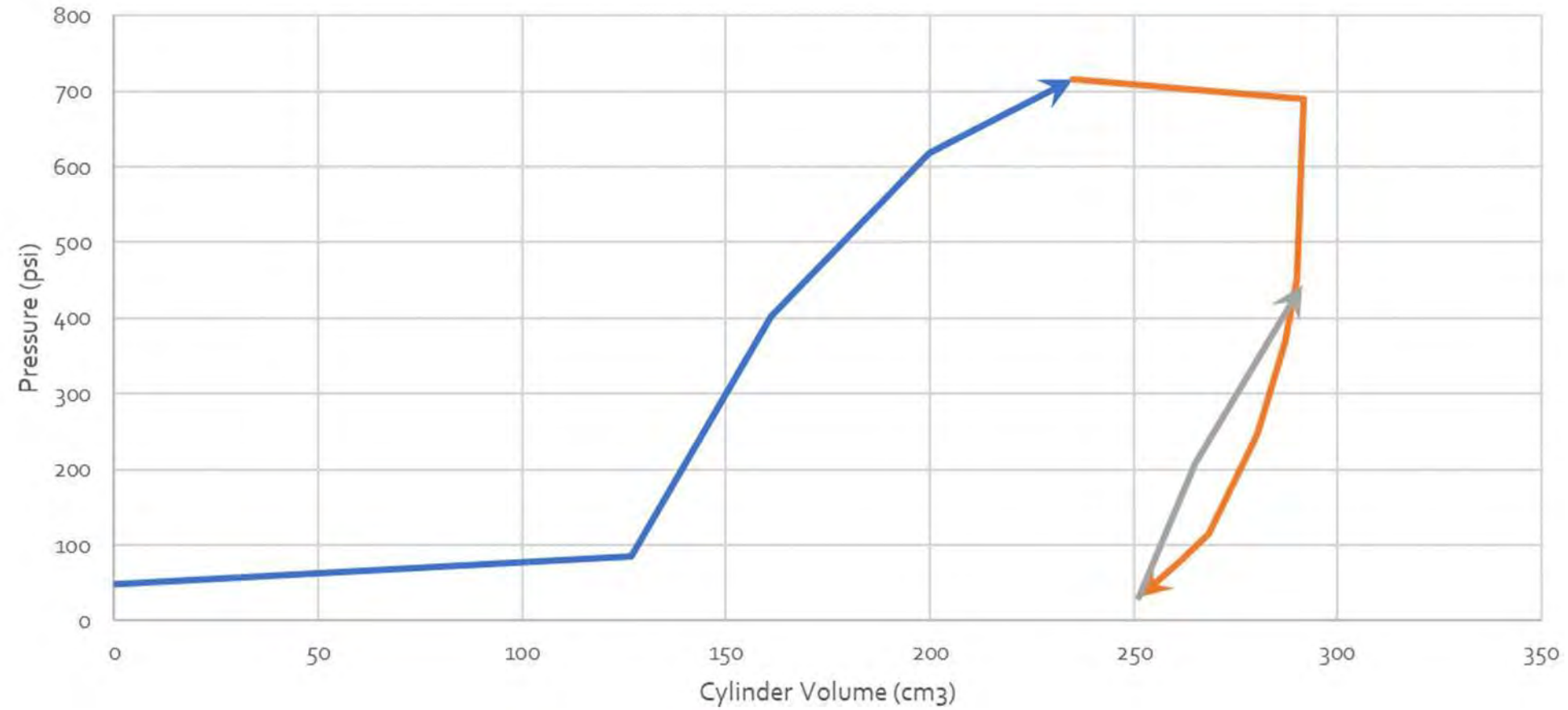
General Test Notes:

- Goodman Jack test data is plotted as pressure (psi) versus volume (cm³)
 - Pressure is exerted radially across the full surface area of the inflatable membrane with dimensions as follows:
 - 18" length x 3" outer diameter
 - Cylinder Volume indicates the amount of water within the inflatable membrane at each load increment and it should correlate with exerted strain on the masonry. Direct strain values are not recorded by the Rocctest Probex Dilatometer.
- Typically, cylinder Volume increases while pressure remains constant at the start of Load Cycle 1 (horizontal portion of the plot). This is due to the inflatable membrane being smaller in diameter than the core hole. Once enough water is pumped into the inflatable membrane and its diameter increases enough to engage the masonry, the pressure begins increasing.
- Typically, two load cycles and two unloading cycles were tested at each Goodman Jack test location, unless there was material failure or equipment failure.





Test GS17-35



Test GS17-35:
South Elevation
Ground Level
Test Depth = 17" to 35" from interior face

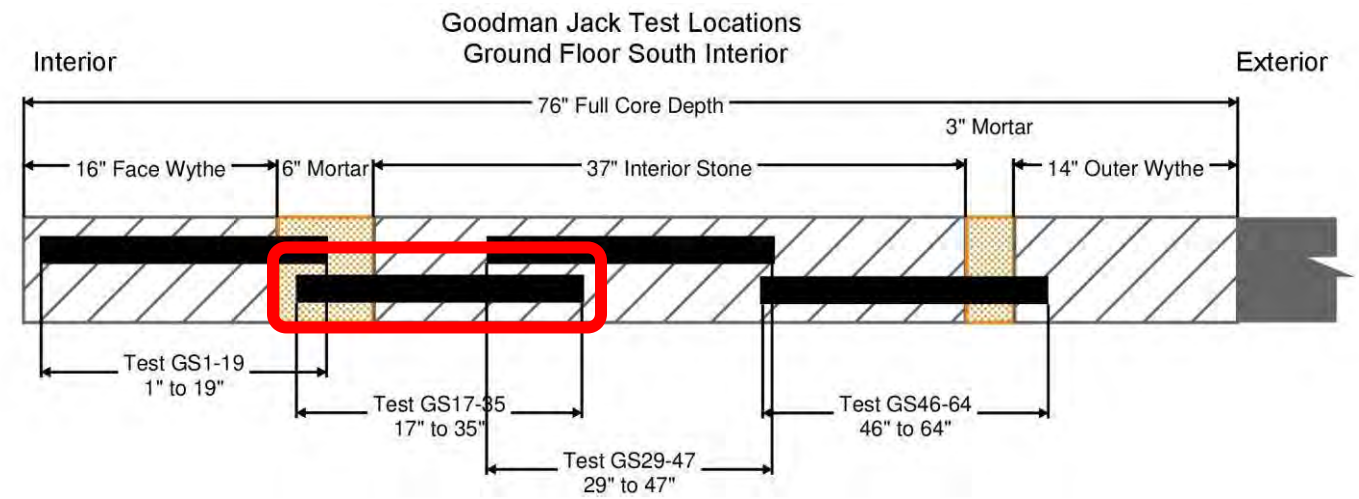
Test Substrate = 13" of solid stone unit & 5" of collar joint mortar

Reason for Stopping Test:
Failure of inflatable membrane during Load Cycle 2; test ended immediately

→ Series1 → Unload Cycle 1 → Load Cycle 2

General Test Notes:

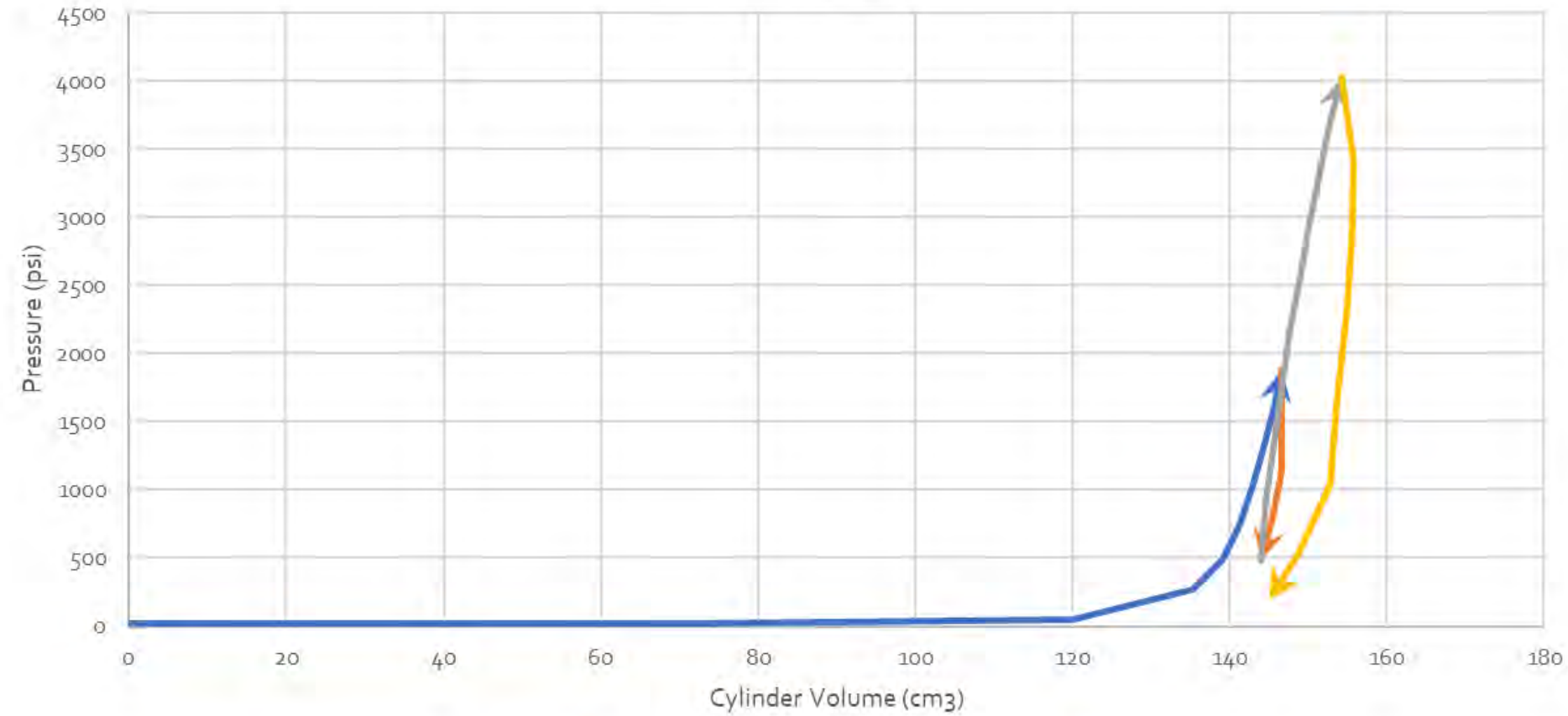
- Goodman Jack test data is plotted as pressure (psi) versus volume (cm³)
 - Pressure is exerted radially across the full surface area of the inflatable membrane with dimensions as follows:
 - 18" length x 3" outer diameter
 - Cylinder Volume indicates the amount of water within the inflatable membrane at each load increment and it should correlate with exerted strain on the masonry. Direct strain values are not recorded by the RocTest Probex Dilatometer.
- Typically, cylinder Volume increases while pressure remains constant at the start of Load Cycle 1 (horizontal portion of the plot). This is due to the inflatable membrane being smaller in diameter than the core hole. Once enough water is pumped into the inflatable membrane and its diameter increases enough to engage the masonry, the pressure begins increasing.
- Typically, two load cycles and two unloading cycles were tested at each Goodman Jack test location, unless there was material failure or equipment failure.





Test GS29-47

Test GS29-47:
South Elevation
Ground Level
Test Depth = 29" to 47" from interior face
Test Substrate = 18" of solid stone unit

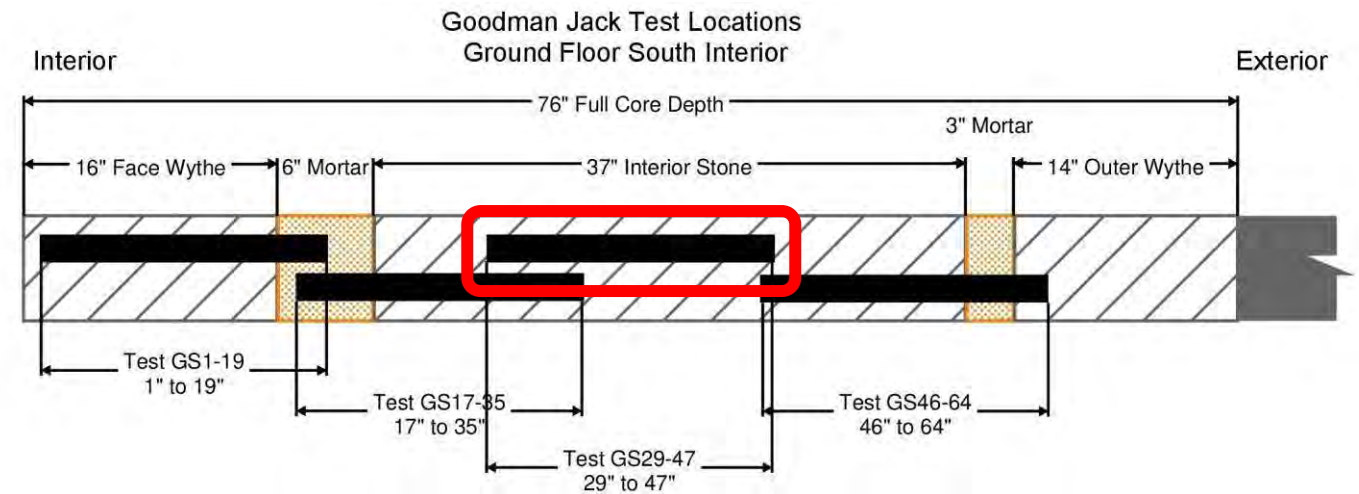


Reason for Stopping Test:
Maximum capacity of equipment reached.

→ Load Cycle 1 → Unload Cycle 1 → Load Cycle 2 → Unload Cycle 2

General Test Notes:

- Goodman Jack test data is plotted as pressure (psi) versus volume (cm³)
 - Pressure is exerted radially across the full surface area of the inflatable membrane with dimensions as follows:
 - 18" length x 3" outer diameter
 - Cylinder Volume indicates the amount of water within the inflatable membrane at each load increment and it should correlate with exerted strain on the masonry. Direct strain values are not recorded by the Roctest Probex Dilatometer.
- Typically, cylinder Volume increases while pressure remains constant at the start of Load Cycle 1 (horizontal portion of the plot). This is due to the inflatable membrane being smaller in diameter than the core hole. Once enough water is pumped into the inflatable membrane and its diameter increases enough to engage the masonry, the pressure begins increasing.
- Typically, two load cycles and two unloading cycles were tested at each Goodman Jack test location, unless there was material failure or equipment failure.

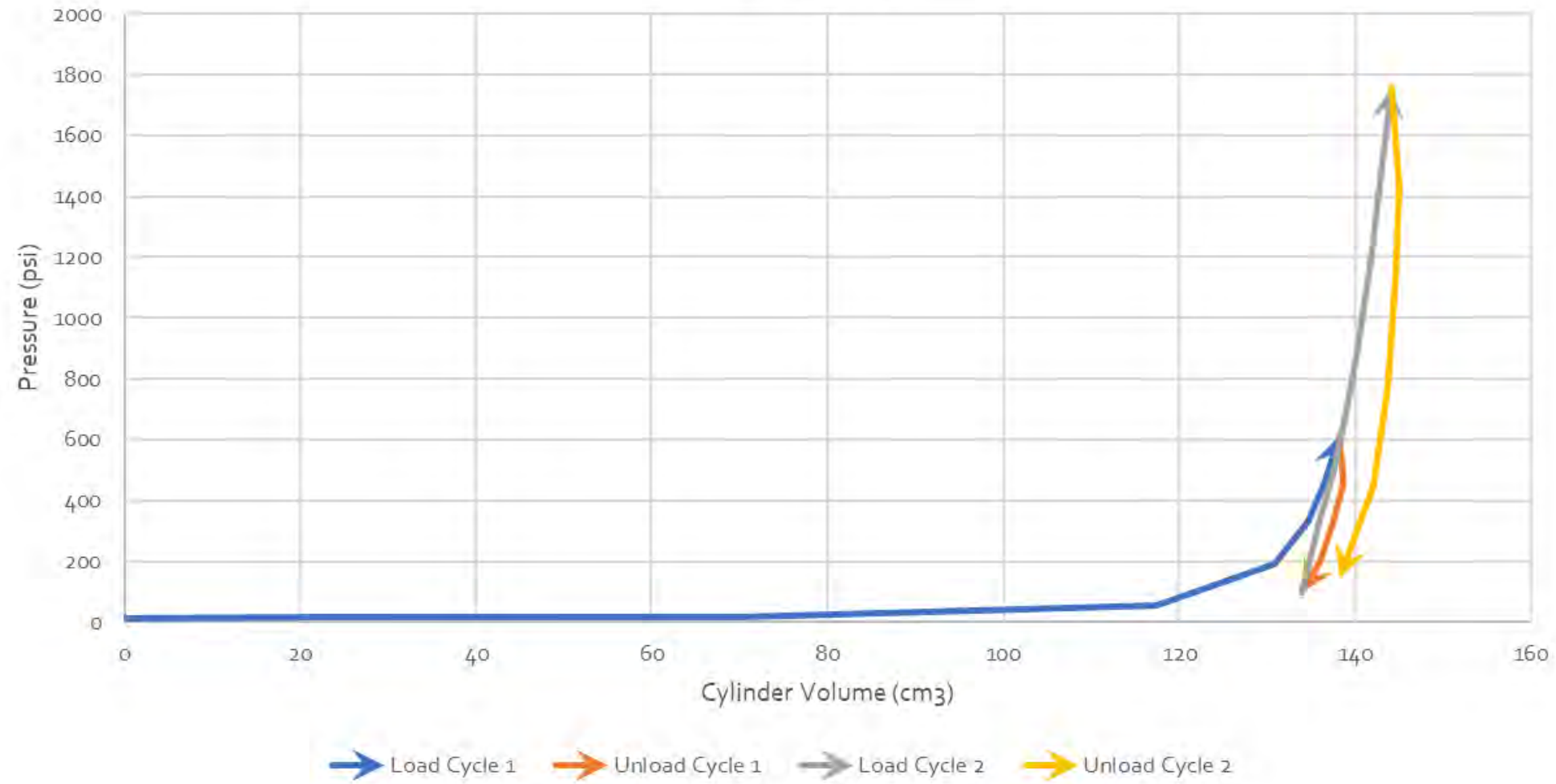




Test GS46-64

Test GS46-64:
South Elevation
Ground Level
Test Depth = 46" to 64" from interior face

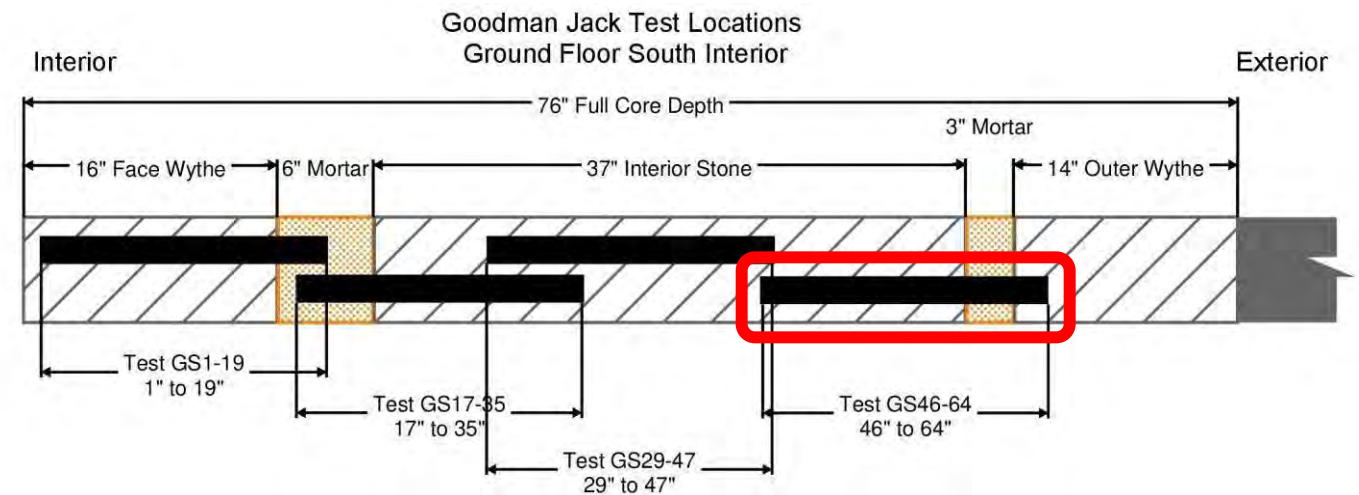
Test Substrate = 15" of solid stone unit & 3" of collar joint mortar



Reason for Stopping Test:
Precautionary stoppage due to concern for a membrane burst at collar joint interface.

General Test Notes:

- Goodman Jack test data is plotted as pressure (psi) versus volume (cm³)
 - Pressure is exerted radially across the full surface area of the inflatable membrane with dimensions as follows:
 - 18" length x 3" outer diameter
 - Cylinder Volume indicates the amount of water within the inflatable membrane at each load increment and it should correlate with exerted strain on the masonry. Direct strain values are not recorded by the RocTest Probex Dilatometer.
- Typically, cylinder Volume increases while pressure remains constant at the start of Load Cycle 1 (horizontal portion of the plot). This is due to the inflatable membrane being smaller in diameter than the core hole. Once enough water is pumped into the inflatable membrane and its diameter increases enough to engage the masonry, the pressure begins increasing.
- Typically, two load cycles and two unloading cycles were tested at each Goodman Jack test location, unless there was material failure or equipment failure.

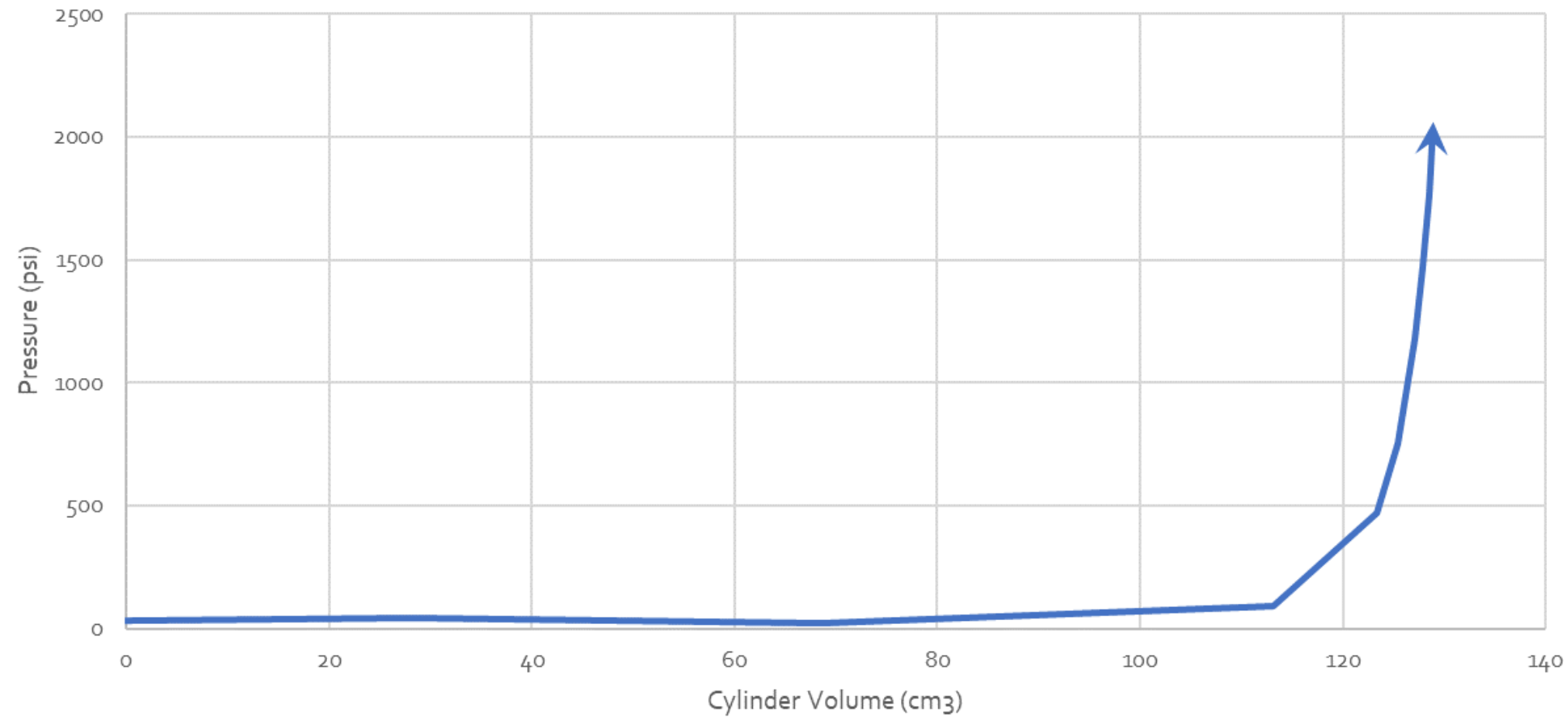




Test 26N1-19

Test 26N1-19:
North Elevation
Landing 26 (~28' above grade)
Test Depth = 1" to 19" from interior face

Test Substrate = 17" of solid stone unit & 1" of collar joint mortar

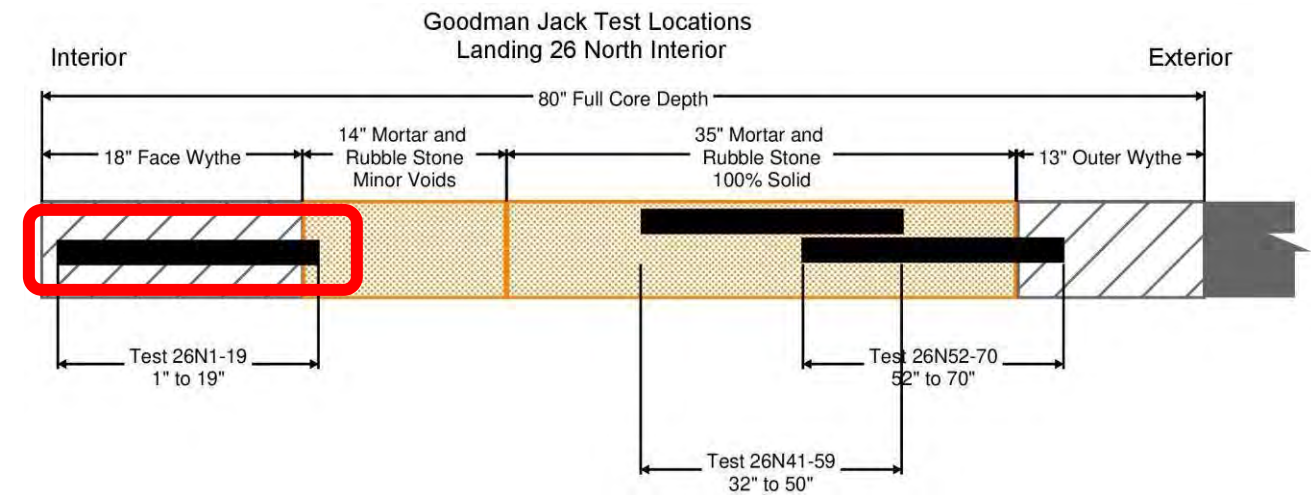


Reason for Stopping Test:
Failure of 18" face wythe observed during Load Cycle 1 and by means of vertical cracks opening for the full depth of the stone unit.

→ Load Cycle 1

General Test Notes:

- Goodman Jack test data is plotted as pressure (psi) versus volume (cm³)
 - Pressure is exerted radially across the full surface area of the inflatable membrane with dimensions as follows:
 - 18" length x 3" outer diameter
 - Cylinder Volume indicates the amount of water within the inflatable membrane at each load increment and it should correlate with exerted strain on the masonry. Direct strain values are not recorded by the Rocctest Probex Dilatometer.
- Typically, cylinder Volume increases while pressure remains constant at the start of Load Cycle 1 (horizontal portion of the plot). This is due to the inflatable membrane being smaller in diameter than the core hole. Once enough water is pumped into the inflatable membrane and its diameter increases enough to engage the masonry, the pressure begins increasing.
- Typically, two load cycles and two unloading cycles were tested at each Goodman Jack test location, unless there was material failure or equipment failure.

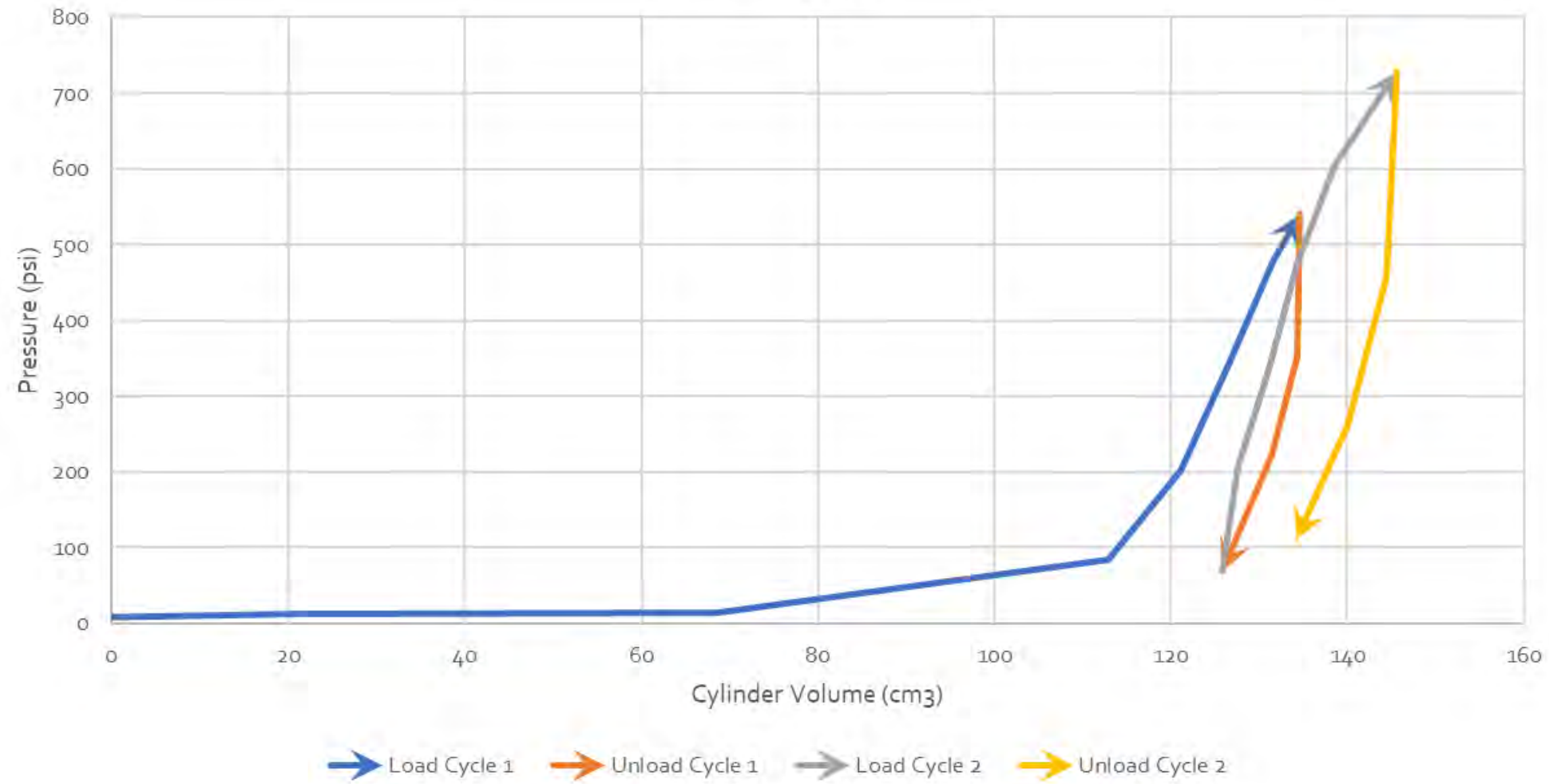




Test GS41-59

Test 26N41-59:
North Elevation
Landing 26 (~28' above grade)
Test Depth = 41" to 59" from interior face

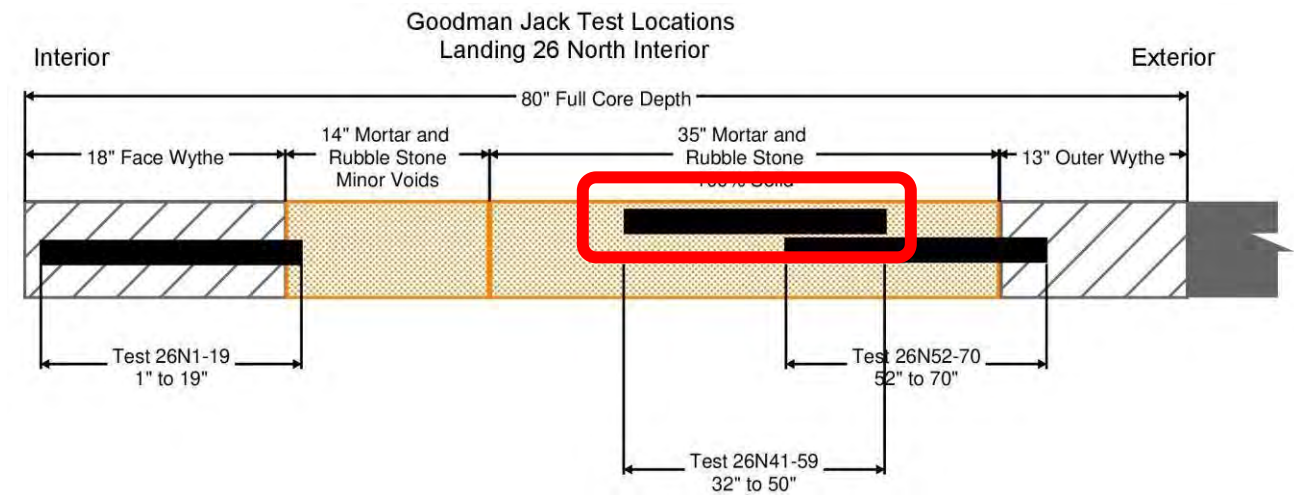
Test Substrate = 18" of mortar and rubble stone masonry, 100% solid before testing



Reason for Stopping Test:
Precautionary stoppage due to concern for a membrane burst at mortar and rubble masonry.

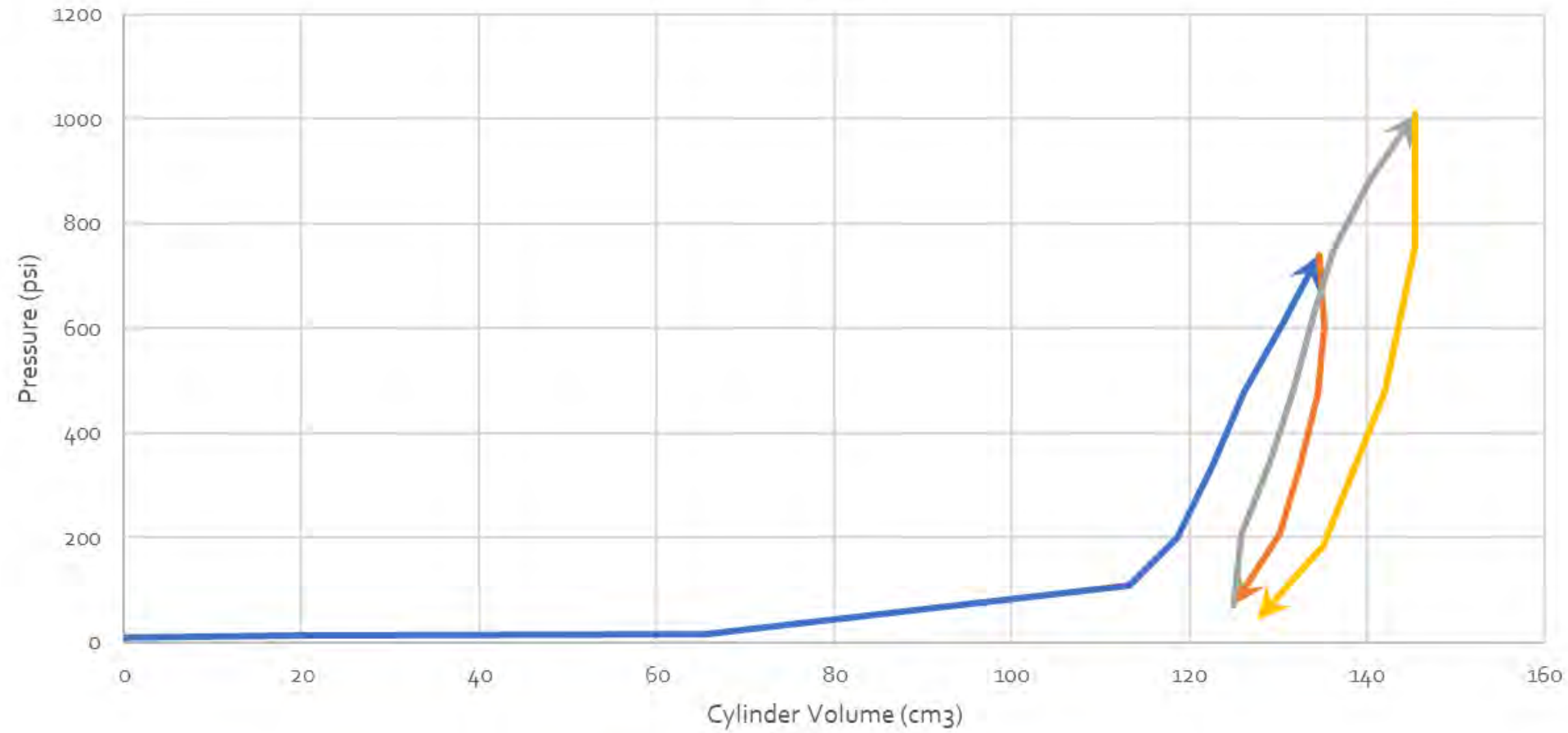
General Test Notes:

- Goodman Jack test data is plotted as pressure (psi) versus volume (cm³)
 - Pressure is exerted radially across the full surface area of the inflatable membrane with dimensions as follows:
 - 18" length x 3" outer diameter
 - Cylinder Volume indicates the amount of water within the inflatable membrane at each load increment and it should correlate with exerted strain on the masonry. Direct strain values are not recorded by the Rocctest Probex Dilatometer.
- Typically, cylinder Volume increases while pressure remains constant at the start of Load Cycle 1 (horizontal portion of the plot). This is due to the inflatable membrane being smaller in diameter than the core hole. Once enough water is pumped into the inflatable membrane and its diameter increases enough to engage the masonry, the pressure begins increasing.
- Typically, two load cycles and two unloading cycles were tested at each Goodman Jack test location, unless there was material failure or equipment failure.





Test GS52-70



Test 26N52-70:

North Elevation
 Landing 26 (~28' above grade)
 Test Depth = 52" to 70" from interior face

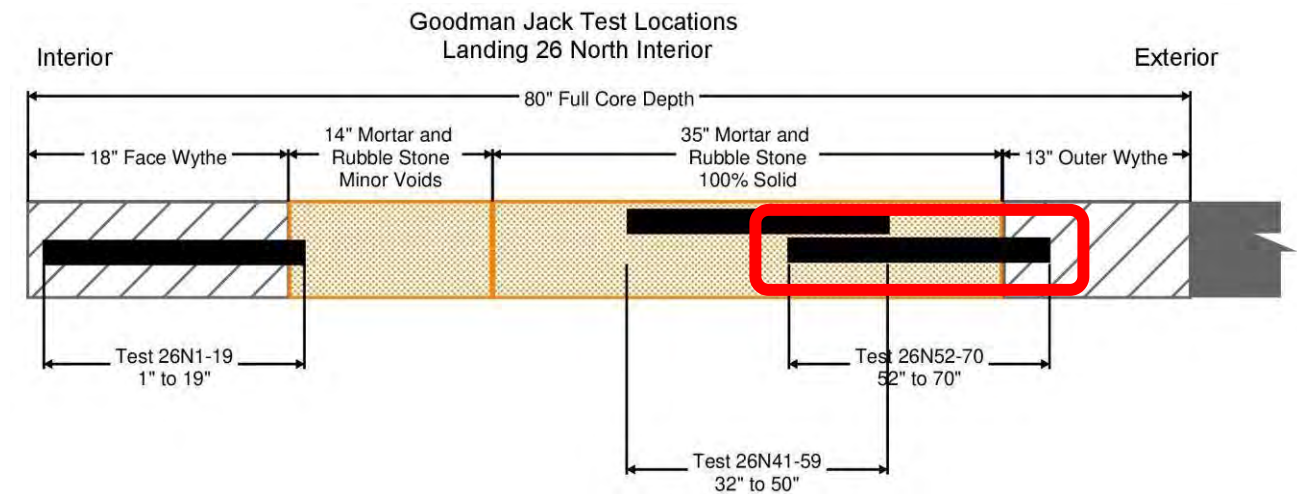
Test Substrate = 15" of mortar and rubble stone masonry, 100% solid before testing & 3" of solid stone unit

Reason for Stopping Test:
 Precautionary stoppage due to concern for a membrane burst at mortar and rubble masonry.

→ Load Cycle 1 → Unload Cycle 1 → Load Cycle 2 → Unload Cycle 2

General Test Notes:

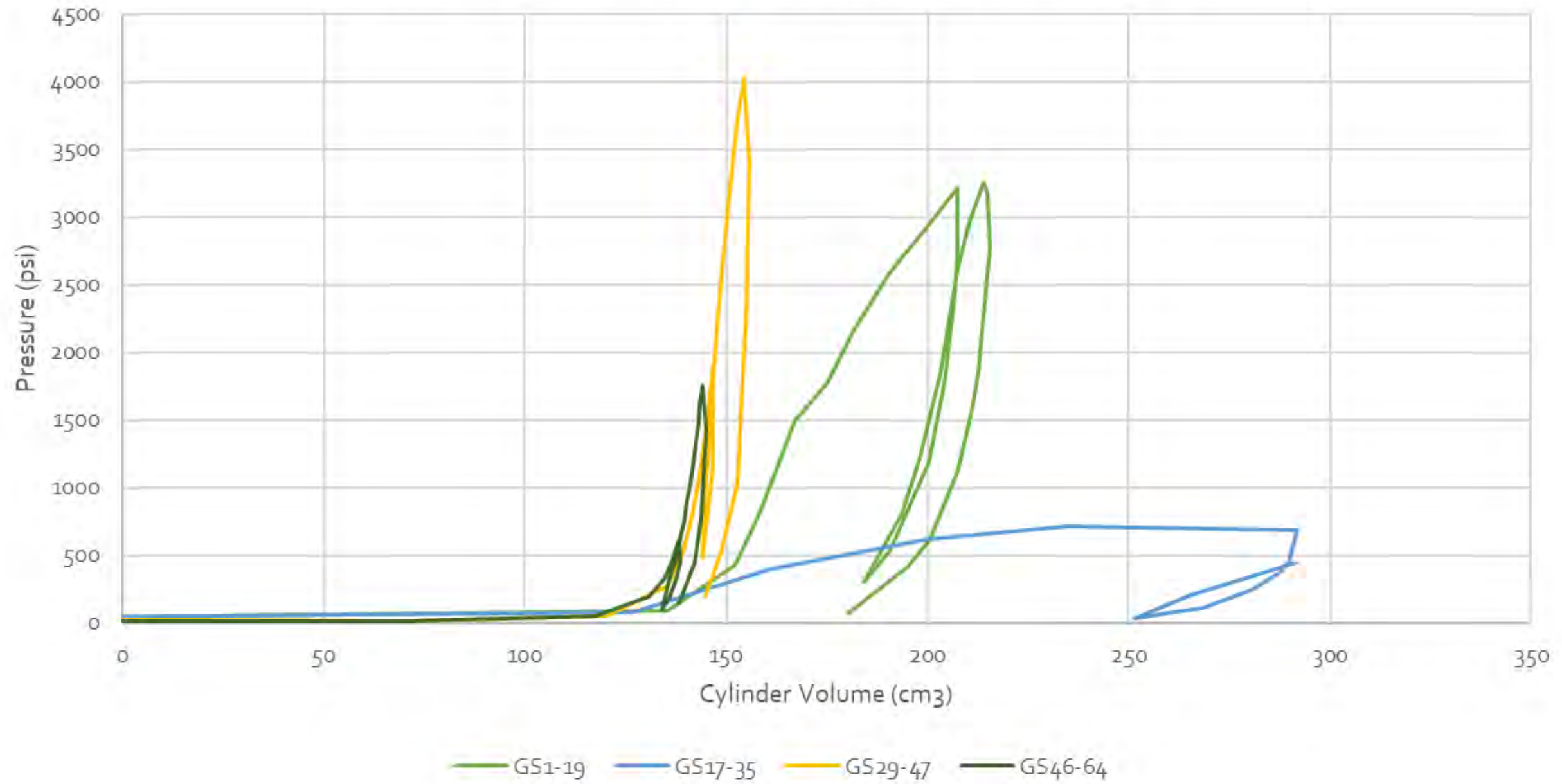
- Goodman Jack test data is plotted as pressure (psi) versus volume (cm³)
 - Pressure is exerted radially across the full surface area of the inflatable membrane with dimensions as follows:
 - 18" length x 3" outer diameter
 - Cylinder Volume indicates the amount of water within the inflatable membrane at each load increment and it should correlate with exerted strain on the masonry. Direct strain values are not recorded by the Rocctest Probex Dilatometer.
- Typically, cylinder Volume increases while pressure remains constant at the start of Load Cycle 1 (horizontal portion of the plot). This is due to the inflatable membrane being smaller in diameter than the core hole. Once enough water is pumped into the inflatable membrane and its diameter increases enough to engage the masonry, the pressure begins increasing.
- Typically, two load cycles and two unloading cycles were tested at each Goodman Jack test location, unless there was material failure or equipment failure.





COMBINED TEST DATA FOR ALL FOUR TESTS AT SOUTH-CORE:

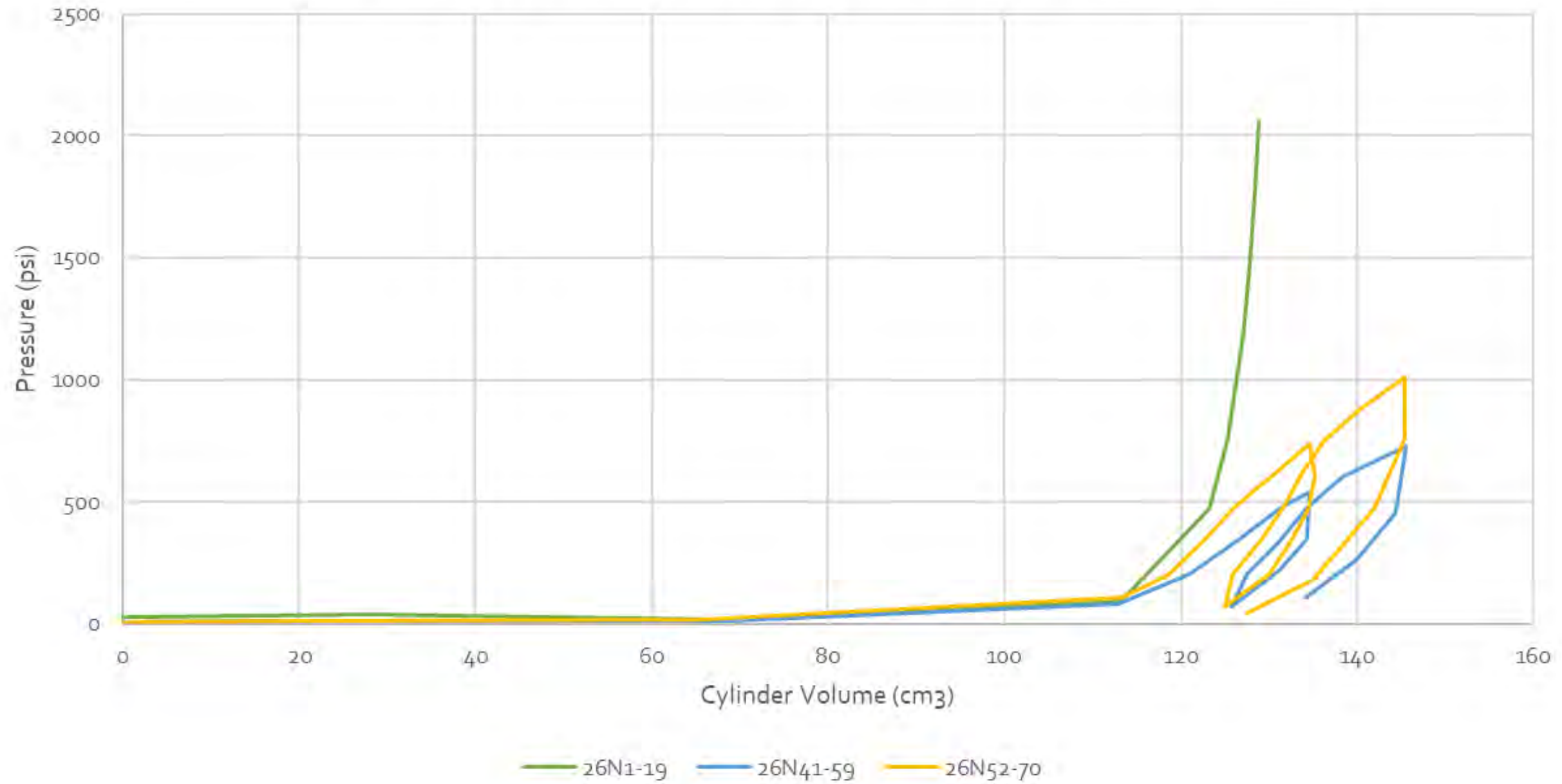
Combined SOUTH-CORE Goodman Jack Test Data





COMBINED TEST DATA FOR ALL THREE TESTS AT NORTH-CORE:

Combined NORTH-CORE Goodman Jack Test Data



APPENDIX E

Dynamic Modulus Test Report (by BDI)



Atkinson-Noland
& Associates

Bennington Battle Monument Phase II Testing

9/20/2023

ATKINSON-NOLAND & ASSOCIATES



SUBMITTED TO:

ATKINSON-NOLAND & ASSOCIATES

32 OLD SLIP, 10TH FLOOR
NEW YORK, NY 10005

SUBMITTED BY:

BDI - CO

740 SOUTH PIERCE AVANUE #15
LOUISVILLE CO 80027 19044

BDI Project No.: **211110-VT**

Report Version: **V1**

Date Submitted: **9/13/2023**



RAW DATA. REFINED RESULTS.

This document contains BDI's Confidential Information and Intellectual Property and is submitted in confidence to the customer and without waiver of BDI's rights to maintain the confidentiality of such information and BDI's ownership of such intellectual property. BDI's methodology disclosed herein is solely included for the interpretation of BDI's results and may not be used for any other purpose, including but not limited to further testing by anyone other than BDI. The submission of the information contained herein shall not be deemed to constitute public disclosure or authorization for disclosure to other parties and may not be used for purposes other than this contract. The information provided is proprietary to BDI and is competitively sensitive. As such, it is protected by federal and state Trade Secrets Acts, 18 U.S.C. §1905, and exempt from disclosure pursuant to 5 U.S.C. § 552(b)(4) and any related state act. Further, BDI's name may not be used in advertising or for promotional purposes without BDI's written consent.

TABLE OF CONTENTS

Executive Summary.....	3
Background	3
Testing Procedures and Results.....	5
References:	7

EXECUTIVE SUMMARY

BDI was contracted by Atkinson-Noland & Associates (ANA) in May 2023 to perform dynamic testing on 10 stone cores. The objective of this testing was to measure the dynamic Young's modulus and calculate the static Young's modulus of each core. The testing was performed in accordance with ASTM C215, the Standard Test Method for Fundamental Transverse, Longitudinal, and Torsional Resonant Frequencies of Concrete Specimen. The acquisition and analysis was performed utilizing standard digital signal processing measures for acoustic waves in solid media.

BACKGROUND

The testing protocol for the FFRC method is explained in detail in ASTM C215 (2014) and involves an impact source, receiver (accelerometer), and digital signal analyzer. The receiver positioning and impact point depends on the desired mode of vibration. Longitudinal vibrations coincide with Young's modulus of elasticity, respectively. After the receivers are positioned, an impact is made at the corresponding impact point and the response time history is recorded with the digital signal analyzer. The time history is then transformed into the frequency domain using an FFT and the first mode fundamental frequency is determined similarly to that of the Impact Echo (IE) method.

The unconstrained longitudinal frequency measured during the FFRC testing is associated with the propagation of normal stress which is related to the unconstrained longitudinal wave, or rod wave, velocity, V_c . The rod wave is related to the dynamic Young's modulus of elasticity. The theory of elasticity governs the relations of the rod wave velocity to the Young's modulus of elasticity:

$$V_c = 2f_iLC_i$$

$$E_d = \rho V_c^2$$

where: V_c = rod wave velocity

f_i = 1st mode unconstrained longitudinal frequency of the specimen

L = length of the specimen

C_i = correction factor that depends on the ratio of the length of the specimen to the diameter of the specimen

E_d = dynamic Young's modulus

ρ = mass density of material

The difference between static and dynamic Young's modulus is of great importance to engineers for several factors. The static Young's modulus is typically assumed to quantify the stiffness of a material during the design phase of a concrete structure. The American Concrete Institute (ACI), Prestress Concrete Institute (PCI), and American Associate of State Highway and Transportation Officials (AASHTO) all suggest methods to calculate the static Young's modulus. Using the equations suggested by each, an engineer could determine an appropriate value of Young's modulus to use in equations to determine deflection, ductility, and other important properties of a designed structure. The dynamic Young's modulus, however, is a measured value. There are currently no accepted design equations from which the dynamic Young's modulus can be calculated. Also, because it can be measured using nondestructive techniques, it is much easier to determine its value on an in-place structure. Due to these differences, there is a growing need for the capability to calculate one moduli from the other.

There has long been a debate concerning the magnitude of the ratio between the static and the dynamic Young's modulus of elasticity and the difference in material behavior required to cause this ratio. Most

literature defines the static Young's modulus of elasticity of concrete as a chord modulus calculated based on an initial strain (typically 0.0005) and a higher strain typically determined as the ultimate compressive stress (typically 40%). These researchers also agree that the dynamic modulus should be considered the initial tangent modulus of a concrete stress-strain curve (Neville 1996; Mesbah et al. 2002; Mehta and Monteiro 2006). Because of the nonlinearity of the stress-strain curve typically measured on concrete specimens, the ratio of static to dynamic Young's modulus is always less than one. Studies have also shown that as the strength of the concrete increases, the stress strain curve becomes more nearly linear. As this happens, the value of the static modulus increases, and the ratio between the dynamic modulus and the static modulus approaches unity (Neville 1996). Although this ratio depends entirely on the specific concrete being measured, studies have been performed in an attempt to quantify the relationship. Several equations have been suggested.

Nagy (1997) obtained moduli measurements on two different concrete mixes and used the results to develop a relationship between the static and dynamic Young's moduli. The relationship is based on the damping ratio of the concrete specimen and is listed as:

$$E_s = \frac{E_d}{1 + \eta^\alpha}$$

where: E_d = dynamic Young's modulus

η = damping ratio,

α = an empirical factor

In his study, Nagy found α to be approximately equal to 0.35. He also found that the ratio between static and dynamic moduli to be approximately 0.80 after a few days of curing. This value is widely accepted as the approximate ratio between static and dynamic Young's moduli and has been reported as 0.83 by Lydon and Balendran in 1986 (Neville 1996). Nagy found his results to be independent of the w/c ratio or cement type. Seely (2005) also studied three concrete mixes and found α to be approximately equal to 0.359, thus validating Nagy's research.

Mesbah et al. (2002) conducted a study on three different high performance concrete mixes. The researchers also concluded that the dynamic modulus is considered to be approximately equal to the initial tangent modulus obtained during a static test. Because the literature reviewed in their research consisted of measurements performed on normal weight concrete, they proposed a formula to convert dynamic to static Young's moduli for high performance concrete:

$$E_s = 9 \times 10^{-11} (65E_d + 1600)^{3.2}$$

where moduli are in units of GPa.

They found that with this formula they were able to accurately predict either the static Young's modulus from the dynamic Young's modulus or vice versa for the three tested mixes. However, they found this formula to be significantly dependent on age of the concrete and it was only held true for the mixes tested.

Han and Kim (2004) performed a study on four concrete mixes cured at various temperatures. The four concrete mixes were composed of two types of cements with two w/c ratios. The four mix designs had a range in compressive strengths based on the curing temperature from 3800 psi to 6500 psi at 28 days. They found that the slope of the initial chord elastic modulus from values of 10×10^{-6} to 50×10^{-6} was more closely related to the dynamic Young's modulus than the initial tangent modulus. They proposed a

formula based on several assumptions. The assumption that as the strength of the concrete increases, the dynamic elastic modulus increases, and the stress-strain curve below 40% of the ultimate compressive strength becomes more linear was made. This led to the assumption that as the linearity of the stress-strain curve increases, the difference between the static and dynamic moduli decreases. Finally, they assumed that when the static modulus is zero, the dynamic modulus is zero.

$$E_s = E_d(1 - ae^{-bE_d})$$

where a and b are constants used to fit the calculated data to the measured data and moduli are in units of GPa.

They found a to range from 0.492 to 1.021 and b to range from 0.0170 to 0.0431. They concluded that since the experimental data had dissimilar ranges at different ages, the comparison between dynamic and static moduli could not be accurately quantified as a function of age. They also concluded that the relationship between dynamic Young's modulus and compressive strength was not significantly affected by cement type or age. In addition, the curing temperature did not have a large influence on the relationship between the initial chord modulus and the dynamic Young's modulus, and cement types did not significantly affect the relationship between static and dynamic Young's moduli. Although the research comparing the static and dynamic moduli appears to be various, most literature agrees that the ratio between the static and dynamic Young's modulus is approximately 0.83, and that this difference is mostly dependent on strength and age (Lydon and Balendran 1986; Neville 1996; Mesbah et al. 2002; Seely 2005; Mehta and Monteiro 2006). Results from other studies also showed that the static Young's modulus could be directly calculated using dynamic Young's modulus and damping ratio measurements (Nagy 1997; Seely 2005). Finally, a majority of the reviewed literature agrees that the dynamic Young's modulus is approximately equal to the initial tangent modulus measured using static tests (Neville 1996; Mesbah et al. 2002; Mehta and Monteiro 2006).

TESTING PROCEDURES AND RESULTS

On July 13 and August 3, 2023, BDI performed dynamic testing in accordance with ASTM C215. All 10 stone cores were suspended at their center by a small chain similar to the concrete core presented in Figure 1. Once suspended, a piezoelectric accelerometer was placed on one end while the other end was struck with a small dynamic force. In this case, the dynamic force was induced with a small ball peen hammer. The acquisition and analysis was performed utilizing National Instruments LabVIEW standard digital signal processing measures for acoustic waves in solid media. The first mode longitudinal frequencies were measured, and dynamic moduli were calculated from those measurements using the equations described above. A typical frequency plot is presented in Figure 2. Finally, the static Young's modulus was calculated as 0.83 of the dynamic moduli. Table 1 presents these results.



Figure 1 – Center Node Suspension of Specimen

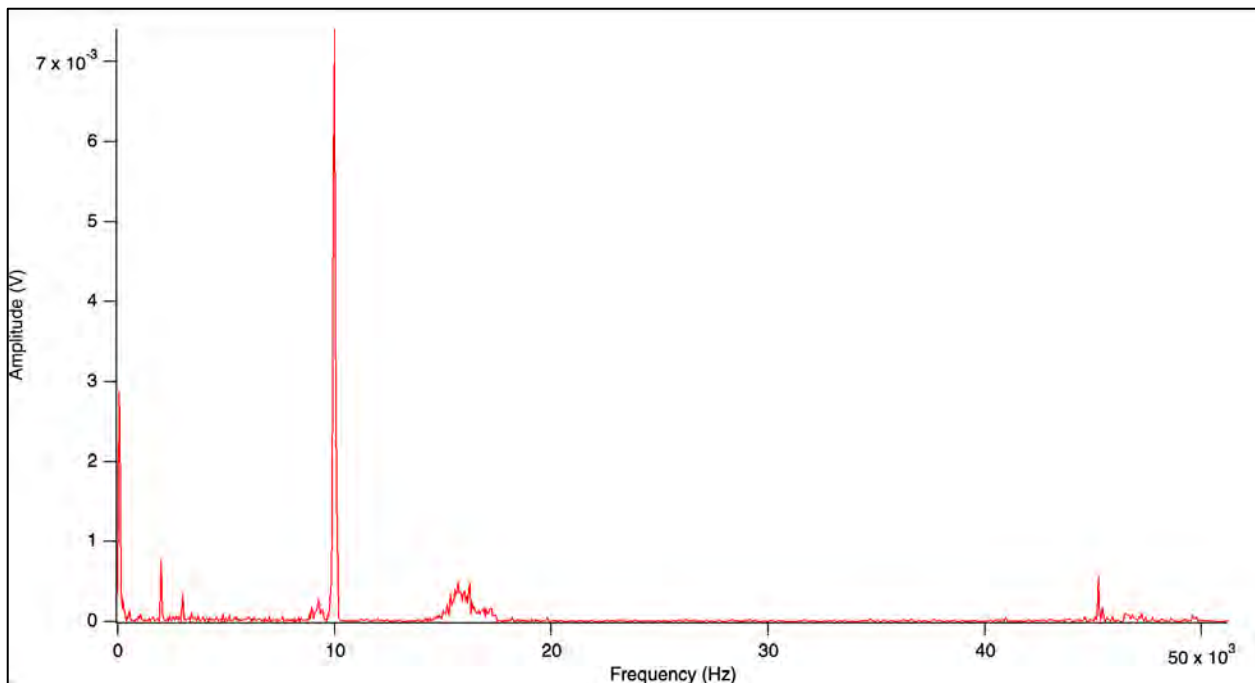


Figure 2 – Typical Frequency Plot

Table 1 - Young's Moduli of Specimen

Sample	Mass (lb)	Volume (in ³)	F_L (Hz)	λ (in)	V_c (ft/sec)	ρ (pcf)	E_d (psi)	E_s (psi)
East 2	3.20	31.15	11100	10.75	9944	177	3.80E+06	3.15E+06
East 6 #1	3.21	32.96	13250	11.38	12560	168	5.75E+06	4.78E+06
East 6 #2	3.20	32.24	11250	11.13	10430	171	4.04E+06	3.35E+06
West 7	3.46	33.69	9900	11.63	9591	178	3.54E+06	2.94E+06
North 5 #1	3.48	33.69	12700	11.63	12303	178	5.85E+06	4.85E+06
West 1 #1	3.27	33.33	10000	11.50	9583	169	3.37E+06	2.80E+06
West 1 #2	3.29	33.69	9800	11.63	9494	169	3.29E+06	2.73E+06
North 3 #1	3.27	32.24	9350	11.13	8668	175	2.85E+06	2.37E+06
North 3 #2	3.39	33.33	11100	11.50	10638	176	4.31E+06	3.58E+06
South 4 #2	3.40	33.69	9700	11.63	9397	174	3.34E+06	2.77E+06

Note that λ corresponds to the wavelength of the wave measured, which is twice the length, L , of the core.

Adequate data collection to determine Poisson's ratio was performed on Samples East 2 (Limestone) and East 6 #1 (Dolostone). The Poisson's ratio determined for these two samples were 0.27 for the Limestone and 0.23 for the Dolostone.

REFERENCES:

1. ASTM C215-14, "The Standard Test Method for Fundamental Transverse, Longitudinal, and Torsional Resonant Frequencies of Concrete Specimen," American Society for Testing and Standards, 2014.
2. Boone, S.D., "A Collection of New Studies Using Existing and Proposed Techniques and Instrumentation for Nondestructive Testing and Analysis of Concrete Materials and Structures," Utah State University School of Graduate Studies, Logan, Utah, 2008.



TEST REPORT
ABSORPTION AND BULK SPECIFIC GRAVITY OF DIMENSION STONE

To: Stevens & Associates
95 Main St
Brattleboro, VT 05301
802-257-9329

Job Name: Bennington
ANA Job No.: 23-222
Date: 11/15/2023

Test Date: 11/15/2023
Tested By: TNM

Sample ID: Stone Cores (light colored)
Date Sample Received: 7/10/2023

Absorption

Specimen ID	Dried Weight (g)	Soaked and Surface-Dried Weight (g)	Water Absorption by Weight (%)
1	475.06	475.87	0.17
2	623.86	624.87	0.16
3	453.38	454.37	0.22

Mean Water Absorption 0.18 %

Bulk Specific Gravity

Specimen ID	Dried Weight (g)	Soaked and Surface-Dried Weight (g)	Soaked and Suspended in Water	Bulk Specific Gravity
1	475.06	475.87	300.01	2.70
2	623.86	624.87	394.01	2.70
3	453.38	454.37	286.41	2.70

Mean Bulk Specific Gravity 2.70

Notes: Samples were tested in accordance with ASTM C97.

TNM
Test Report By

DBW
Reviewed By

Specimen



MATERIALS ANALYSES REPORT

Bennington Battle Monument Bennington, Vermont



Prepared for:
Stevens & Associates, P.C.
95 Main Street
Brattleboro, VT 05301

Prepared by:
Jablonski Building Conservation, Inc.
40 West 27th Street, Floor 12
New York, NY 10001

February 1, 2024

Table of Contents

EXECUTIVE SUMMARY	i
I. INTRODUCTION.....	1
II. METHODOLOGY.....	1
Visual Examination.....	1
Moisture Measurements.....	1
Stone Petrography.....	1
Mortar Analysis	1
Salts Identification	2
III. BRIEF HISTORY AND DESCRIPTION.....	4
V. MATERIALS IDENTIFICATION AND ANALYSES	8
Stone	8
Exterior Moderate Bluish-Gray Stone (Dolomitic Limestone)	8
Interior Pale Yellowish White Stone (Calcitic Marble).....	14
Interior Dark Gray Stone (Dolomitic Breccia)	17
Mortar	20
Potassium Salts	28
Carbonates.....	29
Nitrates.....	29
Contaminants	30
VI. EXISTING CONDITIONS	31
Exterior Conditions.....	31
Spalls and Surface Loss	31
Cracks	35
Open Mortar Joints	38
Calcium Carbonate Deposits.....	42
Biological Soiling	44
Interior Conditions	45
Moisture	45
Cracks	47
Open Joints.....	50
Surface Loss.....	51
Salts.....	52
VII. CONCLUSIONS.....	55

VIII. RECOMMENDATIONS 57

RILEM SURFACE WATER ABSORPTION TESTING 1

 Methodology 1

 Testing Locations..... 1

 Results..... 1

 Conclusions..... 2

APPENDIX A: External Laboratory Reports

APPENDIX B: RILEM Absorption Testing

APPENDIX C: Sampling Location Plan

EXECUTIVE SUMMARY

Jablonski Building Conservation, Inc. was contracted to analyze masonry materials and investigate deteriorated conditions at the Bennington Battle Monument located in Bennington, Vermont. The analysis included an on-site assessment of existing conditions, field testing of moisture properties, and laboratory analyses of stone, mortar, and salt samples removed from the monument. The analysis was performed in order to identify the masonry materials and understand their deterioration mechanisms to inform repair work.

The monument was built using three types of stone including bluish-gray dolomitic limestone on the exterior, and pale yellowish white calcitic marble and dark gray dolomitic breccia on the interior. The exterior dolomitic limestone is Sandy Hill Dolomite quarried in Kingsbury (present-day Hudson Falls), New York. The provenance of interior stones was not determined.

All of the analyzed stone samples were found to be sound and cohesive with relatively low porosity. No significant distress or deterioration was observed in the analyzed samples. However, potential points of weakness were noted in the exterior limestone and interior breccia. Damage observed in situ, including spalling and other forms of surface loss noted in the exterior limestone and cracking observed in the interior breccia, appear to best be explained by the exploitation of these inherent weaknesses in the stone (e.g. stylolites and clayey seams or bedding planes) or geologic phenomena that occurred before construction.

Vertical cracks occurring predominately on the exterior and, to a lesser degree, the interior of the structure are not explained by any geologic features or deterioration of the stone units. The cracks are most likely the result of some structural condition.

The stones of the Bennington Monument were originally bedded in natural cement mortar from Rosendale, New York. Large gaps between the exterior ashlar and the interior rubble walls were filled with a Rosendale natural cement concrete with large aggregate matching the exterior limestone. While the original specifications for the monument called for pointing the exterior in a pigmented Portland cement mortar, no such mortar was found. It may be that multiple repointing campaigns on the exterior removed most traces of the original pointing. It is also possible that natural cement was used in lieu of the specified Portland. Traces of a black-pigmented natural cement mortar found on the monument's interior seem to support the latter possibility. No deficiencies or potential weaknesses were noted in the original mortar samples. However, a minor alkali-aggregate reaction (AAR) was observed in the concrete sample removed from the wall core.

Other than structural cracking, nearly all the deterioration observed in the masonry is related to water infiltration. Large amounts of water entering walls through cracks and open joints has mobilized deleterious salts inherent to the masonry and exposed areas to freeze/thaw damage and frost jacking, propagating still more cracks and open joints. Clay seams in the interior breccia may also swell with prolonged saturation, and cause cracking or spalling. The humid microclimate at the interior of the monument provides an ideal environment for transport and crystallization of salts that would otherwise be rinsed from the masonry by rain wash.

Some previous masonry repairs are inappropriate and serve to exacerbate deterioration. These include non-matching, overly hard, and impermeable re-pointing mortar, the extensive use of caulk in cracks and joints, and poorly executed cementitious patches. Failure of these repairs allows moisture to infiltrate the walls, leading to additional damage.

I. INTRODUCTION

Jablonski Building Conservation, Inc. (JBC) was contracted by Stevens & Associates, P.C. to analyze masonry materials and investigate deteriorated conditions at the Bennington Battle Monument located in Bennington, Vermont. The analysis included an on-site assessment of existing conditions affecting the masonry, field testing of moisture properties, and laboratory analyses of stone, mortar, and salt samples removed from the monument. The analysis was performed to identify the masonry materials and understand their deterioration mechanisms to inform repair work.

II. METHODOLOGY

Visual Examination

The monument was assessed by a trained architectural conservator between June 20-23, 2023. Access was limited to exterior areas accessible from the ground and interior areas accessible from the stairs. Binoculars were used to examine out-of-reach areas. As-found conditions were photographically documented. Additionally, JBC reviewed a comprehensive conditions assessment report and drawings prepared by Vertical Access LLC, dated June 2, 2022.

Moisture Measurements

Relative moisture readings were taken at the interior and exterior stone and mortar using a GE Protimeter MMS meter in pinless/capacitance mode. Relative moisture readings taken on this meter are on a scale ranging from 0 to 1000. Water absorption testing was performed in accordance with RILEM II.4 “Water absorption under low pressure (pipe method)” on the exterior of the monument. Full findings are presented in Appendix B.

Stone Petrography

Eight core samples were removed from the stone masonry by the contractor and transmitted by JBC to Highbridge Materials Consulting, Inc. (Highbridge) for petrographic analysis. Four cores were removed from the exterior and four from the interior. Three cores of the pale yellowish white stone and one core of the dark gray stone were taken from the interior. The samples were petrographically examined following the standard practices contained within ASTM C1721-22 “Standard Guide for Petrographic Examination of Dimension Stone.” Detailed methodology and findings are contained in Appendix A.

Mortar Analysis

Eight mortar samples were removed by JBC. An additional concrete sample was removed from fill present in the collar joint of a wall core extracted by others. The samples were transmitted to Highbridge for petrographic and chemical analysis. Analysis of the eight mortar samples removed by JBC was performed in accordance with the standard practices described in ASTM C1324-20a “Standard Test Method for Examination and Analysis of Hardened Masonry Mortar”. The sample extracted from the wall core contained large rock fragments and was therefore petrographically analyzed according to ASTM C856/C856M-20 “Standard Practice for Petrographic Examination of Hardened Concrete”, with chemical analysis conforming to ASTM C1324-20a. Detailed methodology and findings are contained in Appendix A.

Salts Identification

Seven salt samples were analyzed using X-ray diffraction to identify the water-soluble salts present in the masonry. Five of the samples were scraped from the surface of the masonry by JBC; one sample (BM-01) was extracted using water from a severely deteriorated mortar sample; and one sample was removed from a crust observed on the concrete infill collected from the interior of the wall through core sampling. The samples were transmitted to Highbridge for analysis using proprietary methods. Detailed methodology and findings are contained in Appendix A.

Plans showing the sampling locations are contained in Appendix C. A summary of all samples and the analytical techniques used for each is provided in Table 1 below.

Table 1. Summary of samples and analytical techniques.

SAMPLE ID	LOCATION	ELEVATION	DESCRIPTION	ANALYSES
ANA-South-4	Interior	South	Concrete fill at wall core; Sub-sample of deep core removed for Goodman jack testing by Atkinson-Noland Associates (ANA).	Mortar Analysis (Concrete Petrography), Salts Identification
BM-01	Exterior	South	Friable bedding mortar fragments	Mortar Analysis, Salts Identification
BM-02	Exterior	North	Possible original pointing or bedding mortar from under most recent repointing	Mortar Analysis
BM-05	Interior	Observation Deck, North	Two separate mortars, light buff color is most recent/repointing	Mortar Analysis
JBC-East-2	Interior	East	Light yellowish white stone	Stone Petrography
JBC-East-6	Exterior	East	Moderate bluish gray stone	Stone Petrography
JBC-East-7	Exterior	East	Moderate bluish gray stone	Stone Petrography
JBC-North-5	Exterior	North	Moderate bluish gray stone	Stone Petrography
JBC-North-8	Exterior	North	Moderate bluish gray stone	Stone Petrography
JBC-West-1	Interior	West	Light yellowish white stone	Stone Petrography
JBC-West-3	Interior	West	Light yellowish white stone	Stone Petrography
JBC-West-4	Interior	West	Dark gray stone	Stone Petrography
NE-04	Interior	North	Dark brown mortar	Mortar Analysis
NE-11	Interior	North	Salts removed from light yellowish white stone	Salts Identification
NE-18	Interior	East	Friable mortar fragments	Mortar Analysis
NW-05	Interior	Northwest	Salts on mortar joint	Salts Identification
NW-26	Interior	North	Corner joint	Mortar Analysis
SE-24	Interior	East	Salts removed from dark gray stone	Salts Identification
SW-02	Interior	West	Coarse, buff colored mortar at corner separation	Mortar Analysis
SW-12	Interior	South	Salts removed from crack in light yellowish white stone	Salts Identification
SW-16	Interior	West	Likely original bedding mortar	Mortar Analysis
SW-26	Interior	West	Salts removed from hairline cracks in dark gray stone at rear window	Salts Identification

III. BRIEF HISTORY AND DESCRIPTION¹

The Bennington Battle Monument is a 306-foot-tall unreinforced masonry obelisk designed by Boston architect J. Phillip Rinn and constructed between 1887 and 1891. The monument commemorates the Battle of Bennington, a pivotal victory for American forces during the American Revolution. It is owned by the State of Vermont and managed by the Division of Historic Preservation. The monument is listed on the National Register of Historic Places and is a contributing structure within the Old Bennington National Register District.

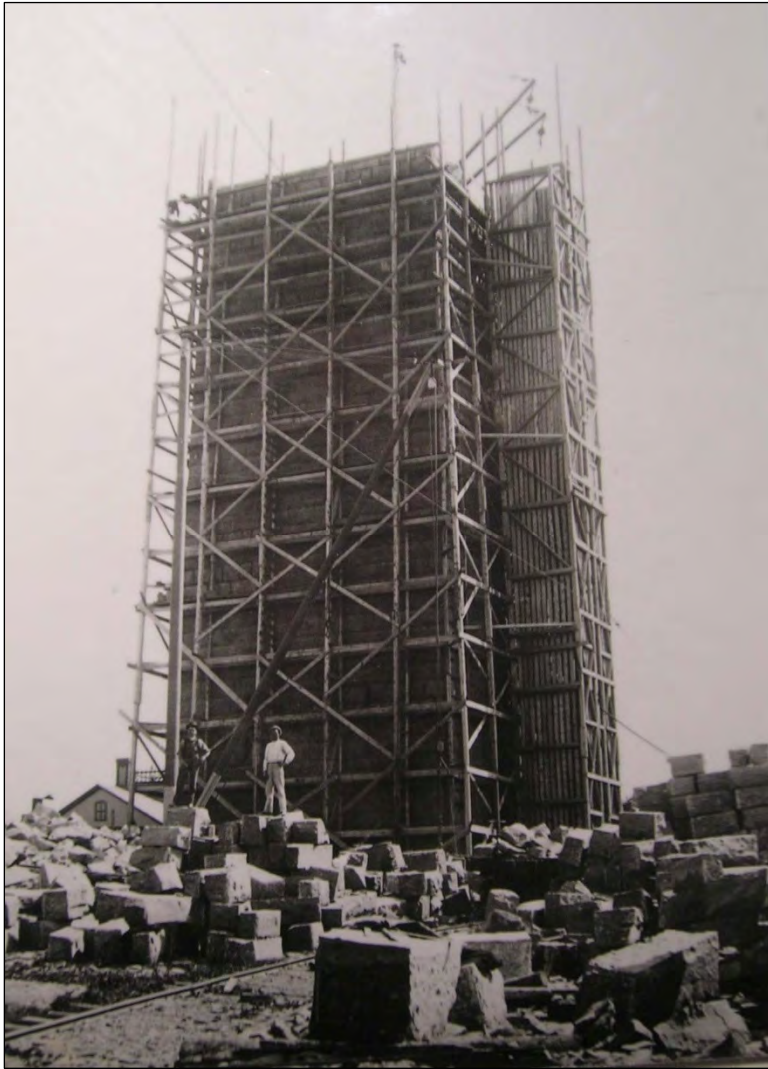


Figure 1. The monument during construction showing blocks of stone being shaped on site (note masons' tools and castoff stone chips in foreground). (Credit: Howard C. Ohlhous, 2008.)

¹ "Bennington Battle Monument," State Historic Sites, Agency of Commerce and Community Development, State of Vermont (accessed Oct. 2023), <https://historicsites.vermont.gov/bennington-monument>.

The monument was built using multiple types of stone. On the exterior, the obelisk was reportedly constructed from Sandy Hill dolomitic limestone quarried near Kingsbury (present-day Hudson Falls), New York. The stones are laid as coursed ashlar with a rock-faced finish (Figure 2) except for two horizontal bands near the observatory level and at window lintels, which have a smooth pointed finish. The interior of the monument was reportedly constructed from a stone local to Bennington. However, visual observation suggests that two stones were used: one pale yellowish white and one dark gray (Figure 3). The use of two distinct stone types was later confirmed through petrographic analysis as discussed below. The interior masonry is laid in a coursed rubble pattern.



Figure 2. Typical exterior rock-faced, coursed Sandy Hill dolomitic limestone ashlar.



Figure 3. Typical interior coursed rubble masonry. Note color difference between stones.

Original specifications for the monument did not stipulate specific stone types, only indicating that the stone be free of defects and how it should be dressed.² However, they did indicate that Portland cement be used for the foundation concrete and pointing mortar in joints between stones and that the masonry should be laid (bedding mortar) in natural cement from Rosendale, New York (Figure 4 and Figure 6). A mix consisting of one part cement to two parts sand was specified for the natural cement mortar but no mix proportions were given for the Portland cement pointing (Figure 5). The specifications did indicate that the pointing should match the color of the stone (Figure 6).

The cements used must be Portland and Rosendale, for the purposes as herein stipulated; must be fresh and very fine ground, and put up in well-made casks.

Figure 4. Excerpt from original specifications, indicating that Portland and Rosendale natural cement be used.

by the Architect before being used in the work. All mortar to be used in the work is to be Rosendale cement and sand of the qualities before specified, mixed in the proportion of one part of cement, by measure, to two parts of sand. In measuring cement, it

Figure 5. Excerpt from original specifications indicating mix design for natural cement mortar.

Pointing. The outside pointing is to be done as the work progresses. Rake out the joints not less than 2 1/2 in. deep, directly after setting of stone, and pack in solid with Portland cement, coarse sand, and a small portion of water. Make concave joint the color of the ^{STONE} ~~stones~~, and smoothly tooled.

Figure 6. Excerpt from original specifications describing pointing with Portland cement matching the color of the stone.

Although a complete history of repair interventions at the monument was not available to JBC, we have reviewed a repair timeline summarized in a report by Silman.³ Following the fall of a stone from the top of the monument in the early 1950s, the upper 100 feet of the obelisk were repointed and bronze cramps (effectively staples for stone) were used to repair cracks, apparently throughout the exterior. In 1959, the upper 30 feet of the monument were repointed and the stone was reportedly “waterproofed” with a silicone coating. In the 1960s and 70s, an engineering consultant from the Vermont State Department of Administration prepared a report entitled, “A Restoration

² “Contract and Specification for the Bennington Battle Monument, March 1887” (digital reproduction provided to JBC by client).

³ Silman, “Structural Engineering Evaluation” report dated December 15, 2022: 7-8.

Program for the Bennington Battle Monument,” in which the author noted cracking masonry near the corners of the obelisk, localized vertical cracking in the stone, efflorescence on interior walls, and disintegration of the interior mortar—conditions that continue to affect the monument today. While the author made recommendations for repairs, it is unknown whether any of the work was performed. The monument underwent further repairs in the early 1980s that included repointing and crack repairs at the upper portions and the application of a water-repellant coating to the entire exterior. However, by the end of the decade, additional repointing work was apparently required and was performed. Finally, in 2005, bids were solicited for repairs that included repointing, among other work. However, it is not known if this work was performed.

V. MATERIALS IDENTIFICATION AND ANALYSES

Stone

Petrographic analysis of samples removed from the monument determined that the structure was built using three geologically distinct types of stone: a bluish-gray dolomitic limestone on the exterior and pale yellowish white calcitic marble and dark gray dolomitic breccia on the interior. Findings are discussed below with additional details of the analyses contained in Appendix A.⁴

Exterior Moderate Bluish-Gray Stone (Dolomitic Limestone)



Figure 7. Exterior dolomitic limestone

The exterior stone was identified as dolomitic limestone derived from biopelmicrite. *Biopelmicrite* is a form of limestone containing calcareous mud pellets and marine fossils cemented together by calcite. Some of these fossils remain visible. This rock underwent a secondary process known as dolomitization wherein the original calcitic material is replaced by crystalline magnesian carbonate. The four examined samples exhibit varying degrees of dolomitization, though the majority of the stone has been recrystallized. Because dolomitization is incomplete, the stone is classed as a dolomitic limestone rather than dolomite. Unlike calcareous limestones, the rather high degree of dolomitization makes this stone dense, hard, and resistant to acid attack. Medium silt to fine sand consisting mostly of quartz with a minor amount of feldspar is distributed throughout the stone in varying concentrations. This sediment is intermixed with clay.

At the microscale, the structure of the stone is fairly uniform. Sedimentary bedding planes are not evident in most places, though all samples contain cleavage in the form of stylolites (Figure 8). *Stylolites* are seams within a rock mass where minerals have been dissolved via pressure dissolution. Minerals that are insoluble in water, such as clays, pyrite, and oxides, as well as insoluble organic matter, remain within the seams. With the scarcity of sedimentary bedding planes

⁴ Excerpt from Ryan-Biggs & Associates report dated 1988, reprinted in Atkinson-Noland & Associates, Inc., “Stone Masonry Nondestructive Evaluation” report dated June 30, 2022: [17].

visible in the samples, it is primarily through the appearance of stylolites that we are able to determine the orientation of the original rock from which the stones were cut. Of the four stones sampled, three were apparently face-bedded, i.e. oriented in the wall so that the natural bedding planes run parallel to the face of the wall rather than horizontally as they occur in nature.

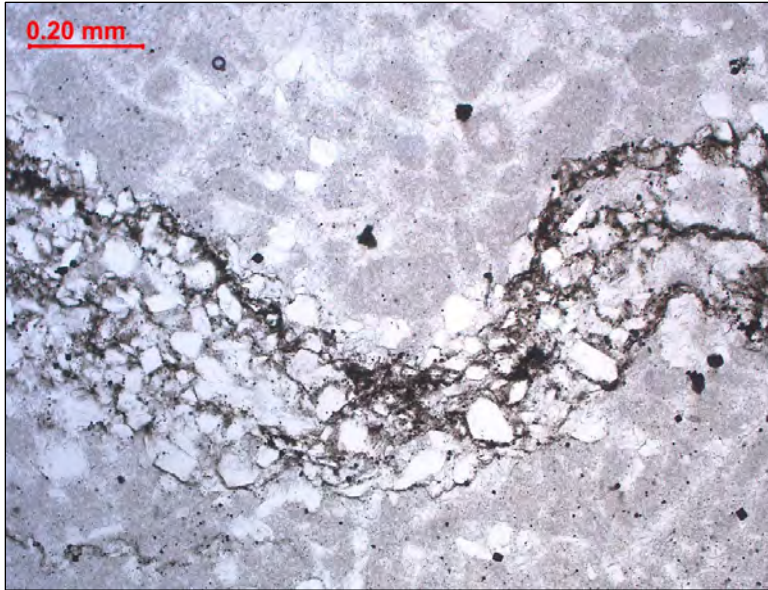


Figure 8. Photomicrograph of a stylolite (wave form running left to right) comprised of mostly quartz and sulfide grains in Sample JBC-East-6 (Plain polarized light, Credit: Highbridge).

In situ however, sedimentary bedding planes are more pronounced (Figure 9). The majority of stones are naturally-bedded, with approximately one third face-bedded, and a limited number of edge-bedded stones (i.e. stones oriented with their natural bedding planes running vertically and perpendicular to the face of the wall). Best practice dictates that sedimentary stones be naturally-bedded in most instances for maximum compressive strength and resistance to weathering. While face bedding results in a more uniform appearance and is not uncommon, it leaves the stones susceptible to dramatic failure through delamination.

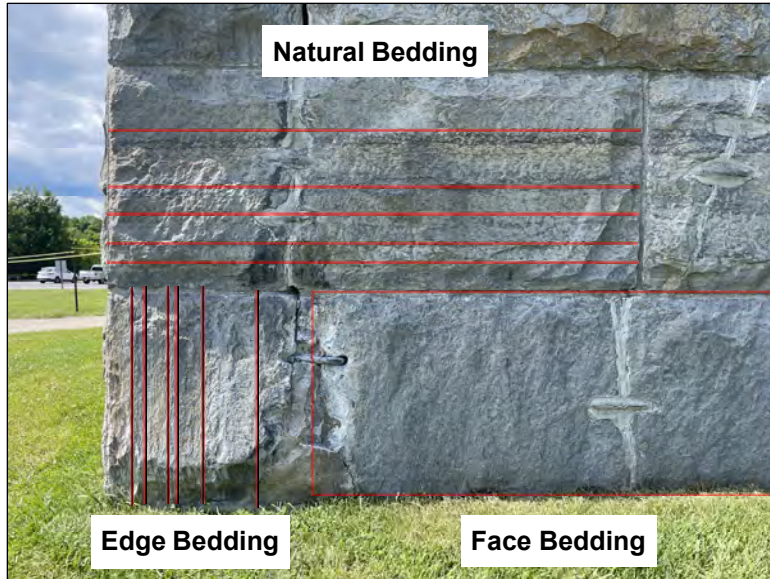


Figure 9. Corner of monument showing stones in three different orientations: natural bedding, face bedding, and edge bedding (bedding planes indicated).

Styolites represent a potential weakness in building stone as these seams of concentrated clays, organics, and other fine insoluble matter can be susceptible to swelling and shrinking during wet and dry cycles and frost jacking during freezing events. However, this is not the case in the examined samples. All styolites appear tight and impermeable with no evidence to suggest that they represent a durability concern. While no deterioration associated with styolites was identified in the analyzed samples, which were removed from relatively intact stone at the bottom of the monument, it is possible that styolites contribute to deterioration in other locations, such as at the top of the monument where delamination is more prevalent. Geologic cracking (i.e. cracking that naturally occurred in the rock before the stone was quarried) might also help to explain delamination observed in situ. However, cracking is minor in the examined samples and limited to a few hairline cracks that are oriented at shallow angles away from the surface of the stone. No cracking from damage occurring in service was observed in the samples.

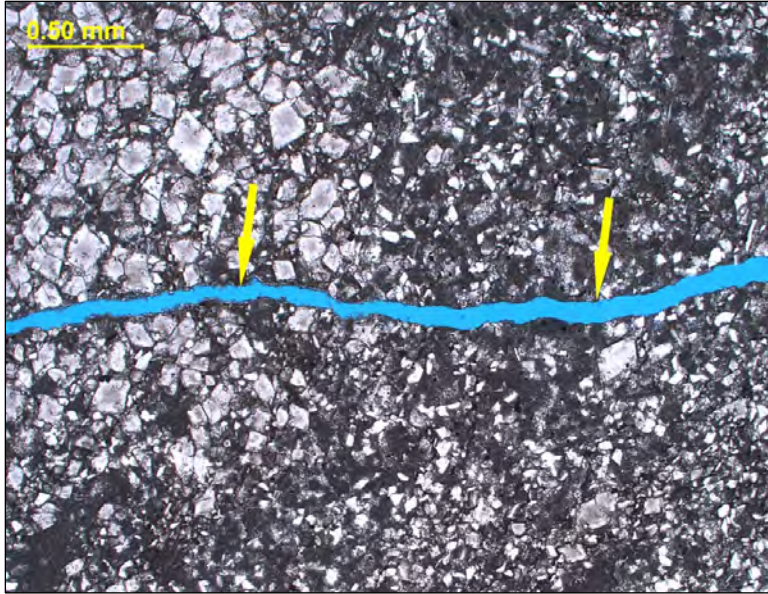


Figure 10. Photomicrograph of a microcrack filled with blue epoxy in Sample JBC-North-5 (Plain polarized light, Credit: Highbridge).

Overall, the exterior stone samples were found to be cohesive, hard, impermeable, and sound. Only superficial surface weathering consistent with age and the location of the stone on the structure was observed under the microscope. In two samples, chemical weathering or possibly some past chemical cleaning campaign has dissolved acid-soluble carbonate minerals in the outer portion of the stone, leaving the acid-insoluble minerals raised proud on the surface (Figure 11). This explains the rough and uneven surface texture of the stone in situ (Figure 12). No evidence of past reported water-repellant coatings was observed. Pyrite was identified as a constituent mineral through petrographic examination (Figure 13). While the iron sulfide present in pyrite is known to oxidize and cause reddish brown staining on the exposed surface of similar pyrite-bearing stone, no such staining was observed in the samples, and the pyrite appears stable.

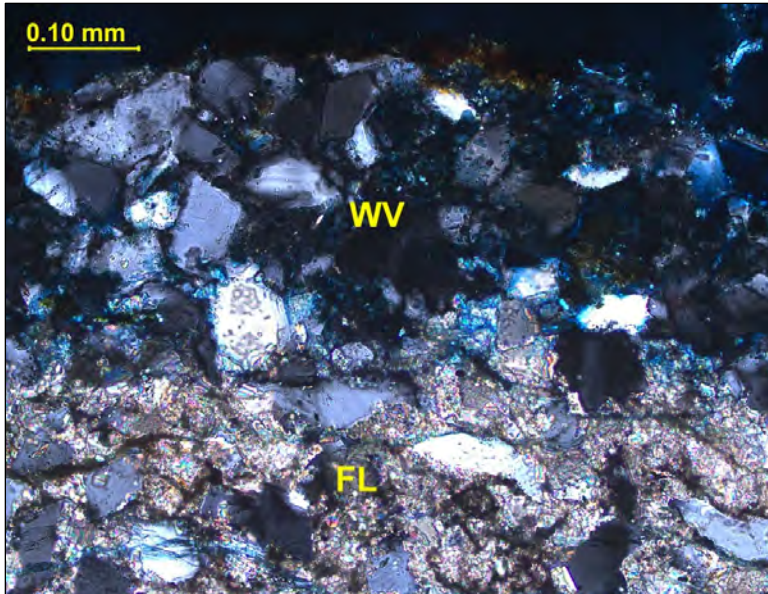


Figure 11. Photomicrograph of a cross-section through the exposed face (oriented to image top) of Sample JBC-East-7, showing carbonate minerals present in the fresh limestone (FL) that have preferentially dissolved within the weathered veneer (WV) leaving voids filled with blue epoxy (Crossed-polarized light, Credit: Highbridge).



Figure 12. Exterior stone showing an uneven surface texture caused by preferential weathering of acid-soluble carbonate material. A fossilized ammonite, the extinct relative of sea creatures such as the modern nautilus, is visible at image center.

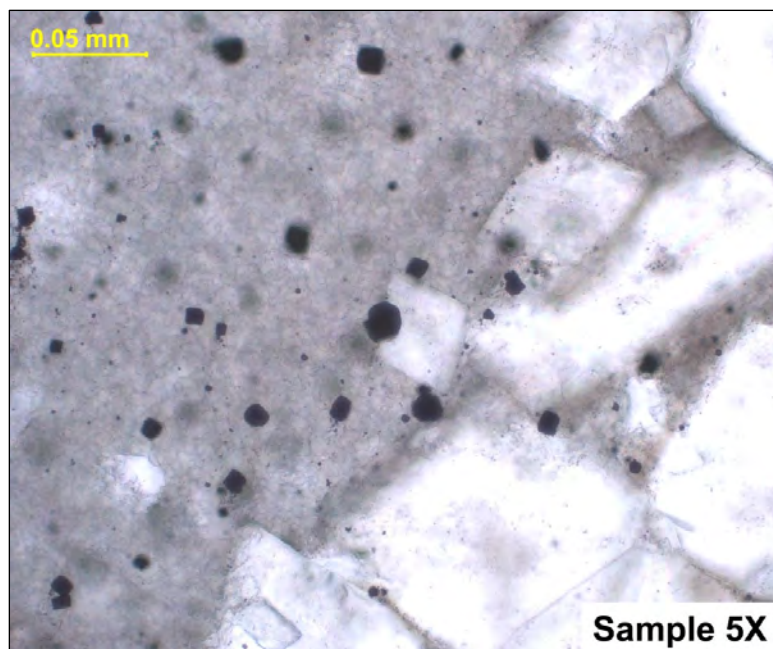


Figure 13. Photomicrograph of dark-colored iron sulfide particles (pyrite) dispersed throughout the matrix in Sample JBC-North-5 (Plane polarized light, Credit: Highbridge).

Numerous anecdotal reports indicate that the exterior stone is Sandy Hill “dolomite” originally quarried near Kingsbury (present-day Hudson Falls), New York. While samples of stone from any suspected quarry would have to be analyzed to verify this claim, George P. Merrill’s 1897 *Stones for Building and Decoration* describes stone quarried in the area around Kingsbury as dark blue-black magnesian limestone that is fine-grained and compact, with large fossils.⁵ This description is consistent with the samples removed from the monument. Further still, John C. Smock’s 1888 *Building Stone in the State of New York*, notes that stone from the Sandy Hill Quarry Company “is being used... for the base of the Bennington Monument in Vermont”.⁶ Smock describes the stone, which was readily extracted in large blocks due to the geologic features of the quarry, as being specially adapted to use in heavy masonry and notes its usage in several engineering structures including bridges and elements of the Croton Aqueduct.

⁵ Gorge P Merrill, *Stones for Building and Decoration* (New York: John Wiley & Sons, 1897), 220.

⁶ John C. Smock, *Building Stone in the State of New York*, Bulletin of the New York State Museum of Natural History No. 3 (Albany, NY: Charles Van Benthuyzen & Sons, 1888), 100.

Interior Pale Yellowish White Stone (Calcitic Marble)



Figure 14. Interior calcitic marble (stone at image center).

The interior pale yellowish white stone was identified as a fine-grained calcitic marble. *Marble* is a metamorphic rock that is formed in nature when limestone is subjected to intense heat and pressure. This metamorphic process causes a complete recrystallization of the original limestone into an interlocking mosaic of calcite and/or dolomite crystals depending on the mineralogy of the limestone. The temperatures and pressures necessary to form marble usually destroy any fossils and sedimentary textures present in the original rock. The characteristic swirls and veins of many marble varieties are usually due to various mineral impurities which were originally present as grains or layers in the limestone. These various impurities have been mobilized and recrystallized by the intense pressure and heat of the metamorphism.

At the microscale, the stone is dense and uniform with diffuse, orange-toned veining (Figure 15). The stone consists almost entirely of calcite and no accessory minerals were identified. Quartz and white mica are present in only trace quantities. Microcracks and hairline cracks run along the veins but are likely geologic features predating construction of the monument.

In situ, the exposed surface of the stone has an orange hue while freshly broken surfaces of the samples appear warm white in color. This surface discoloration is a patina likely due to oxidation of trace amounts of iron present in the matrix. Microscopically, the patina appears as an ultrafine clay-like veneer (Figure 16). While the composition of the patina could not be determined through petrographic examination, it likely consists of iron oxides or iron oxide-hydroxides. Pure calcitic marbles are not expected to contain much iron. However, it is possible that trace amounts of iron present in the calcite crystal structure are freed and become oxidized when acidic corrosion occurs along exposed surfaces. The source of the acid may be natural, such as soft water or water enriched with carbon dioxide from the atmosphere leaching through the walls of the monument, or it may

have been an acid-based cleaning chemical.⁷ No history of past cleaning campaigns was available, and it is not possible to distinguish between these possibilities petrographically. However, acid attack is further supported by presence of eroded calcite grains observed microscopically along exposed surfaces (Figure 17).

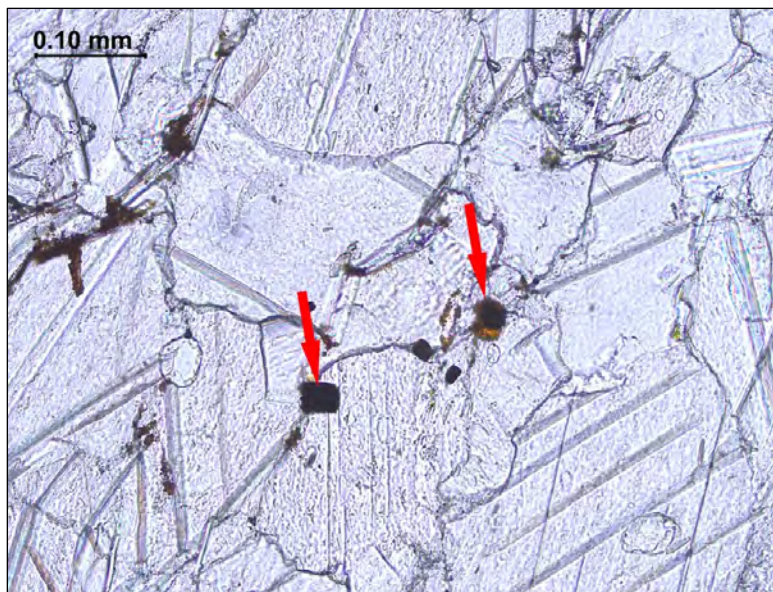


Figure 15. Photomicrograph of Sample JBC-East-2 in plane polarized light showing reddish brown iron oxide particles (indicated) responsible for the diffuse orange veining (Credit: Highbridge).

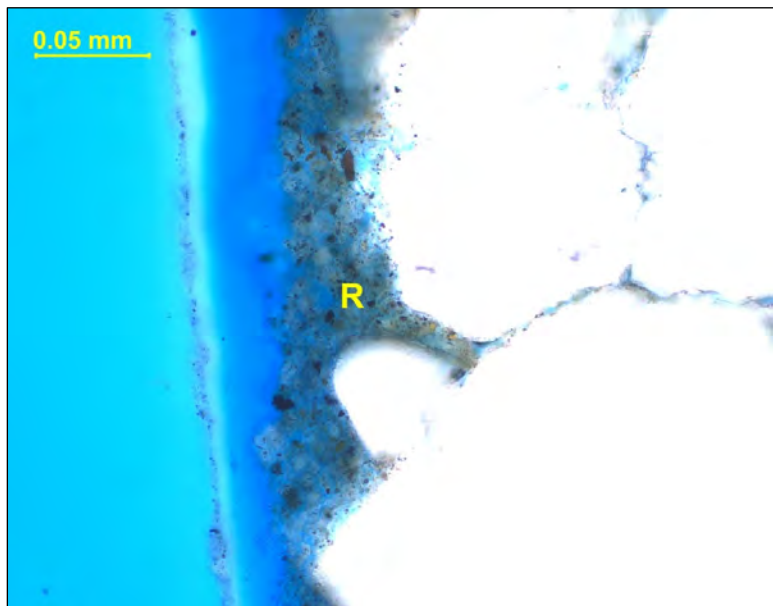


Figure 16. Photomicrograph taken at the outer, exposed surface of Sample JBC-West-3 in plane polarized light, showing the stone's patina comprised of ultrafine reddish brown particles (R), believed to be iron oxide (Credit: Highbridge).

⁷ Sulfur dioxide from industrial pollutants is excluded as a source of acid since its reaction with calcitic marble would have produced gypsum which is absent in the samples examined.

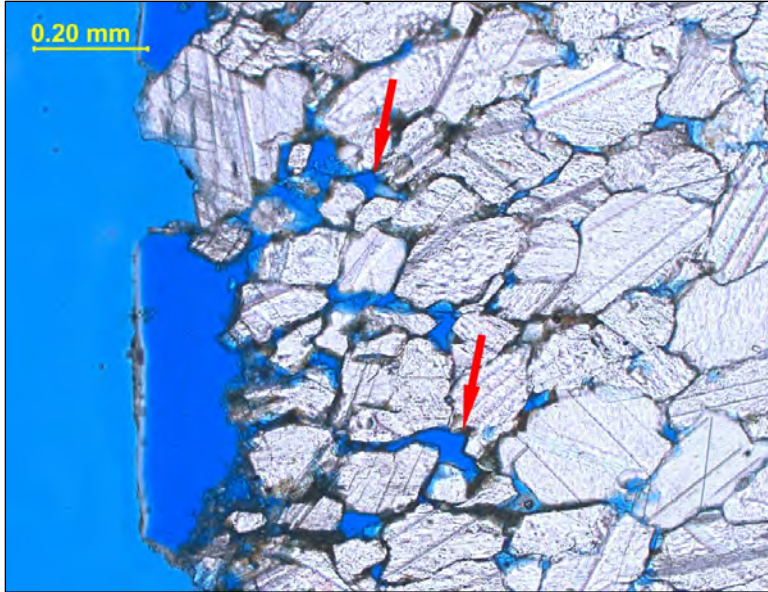


Figure 17. Photomicrograph taken at the outer, exposed surface of Sample JBC-West-1 in plane polarized light, showing open pores (indicted) created by acid dissolution of the constituent calcite grains (Credit: Highbridge).

Calcitic marbles are particularly susceptible to a form of surface loss known as granular disaggregation, or “sugaring”. *Sugaring* is the detachment of individual grains from the exposed surface of white marble and is attributed to thermal cycling and the highly anisotropic coefficient of thermal expansion of calcite. It has also been attributed to dissolution of grain boundaries by acid attack. No evidence of sugaring was detected in the examined samples or observed in the field. The stone is located on the interior of the monument where thermal cycles are relatively mild. It also appears that the microtexture of the stone, particularly its modest grain size variation and a significant amount of physical interlocking between adjacent calcite crystals, provide resistance to sugaring.

Anecdotal reports mistakenly identified this stone as a locally quarried dolomitic limestone. While it is certainly not dolomitic, it remains possible that the stone may originate from Vermont. Based on the geology of the southern part of the state, it is possible that the marble came from a local quarry. However, it was not possible to identify a source based on petrographic analysis of the samples alone.

Interior Dark Gray Stone (Dolomitic Breccia)



Figure 18. Interior dolomitic breccia (stone at image center).

The interior dark gray stone was identified as a silicified dolomitic breccia consisting of clasts of uniform dolostone bound by recrystallized quartz (Figure 19). *Breccia* is a rock composed of clasts, or large angular fragments of minerals or rocks, cemented together by a fine-grained matrix. In this case, the rock fragments consist of dolostone (a rock comprised almost entirely of dolomite)

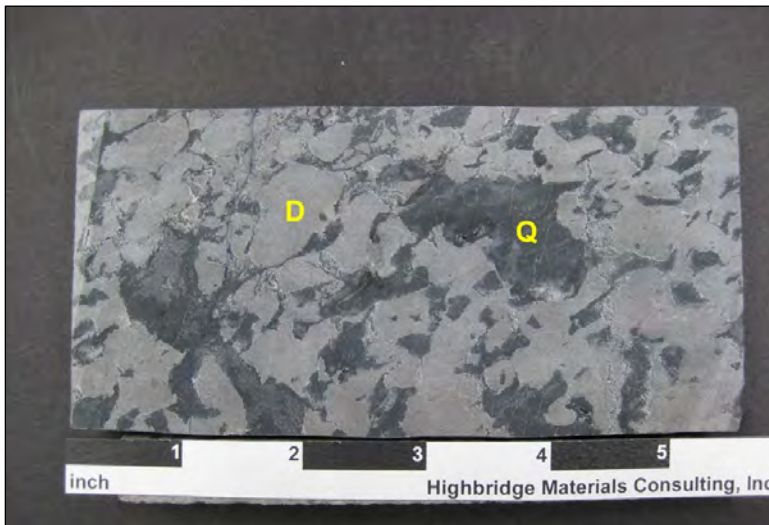


Figure 19. Freshly cut section through breccia showing angular dolostone fragments (D) in a matrix of recrystallized quartz (Q) (Sample JBC-West-4, Credit: Highbridge).

At the microscale, the dolomitic breccia has no significant porosity and is quite dense. No stylolites, cracks, or other planes of preferential weakness were identified within the bulk of the stone. However, the face of the masonry and the rear of the core sample contain secondary veining that consists of partly preserved slivers of limestone that are stained red by iron oxide (hematite)

(Figure 20). This veining may represent a potential point of weakness in the stone due to the expansive potential of iron oxide when exposed to wet/dry cycles.

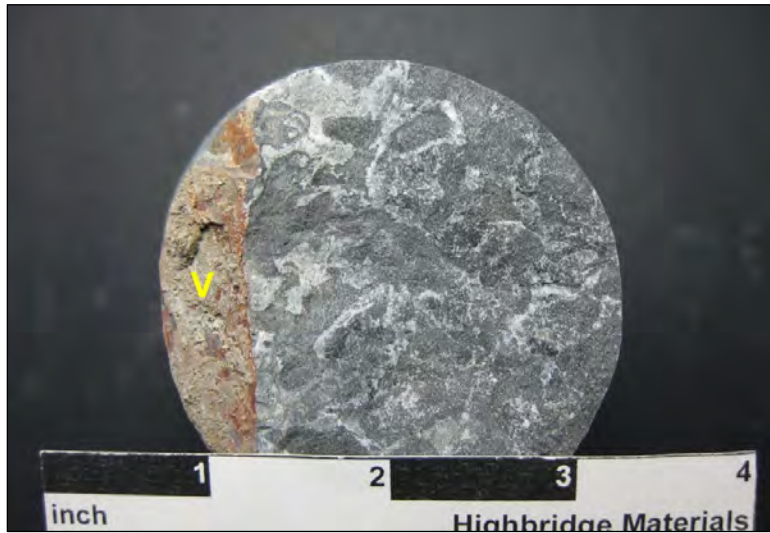


Figure 20. Breccia core showing bisected vein (V) stained reddish brown by iron oxide (Sample JBC-West-4, Credit: Highbridge).

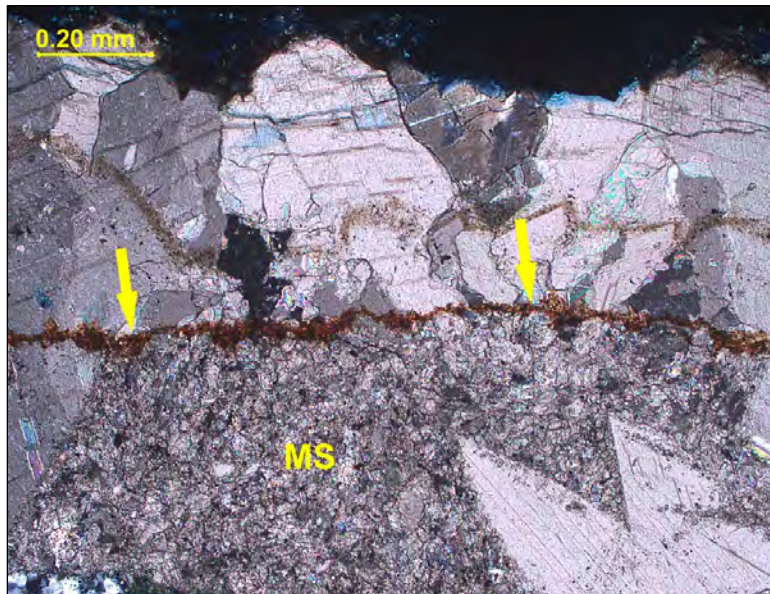


Figure 21. Photomicrograph of a section through a vein showing its reddish-brown iron oxide lining (hematite, indicated) surrounded by dolomite crystals and a sliver of microsparite (MS) that has not been completely replaced by dolomite (Cross-polarized light, Credit: Highbridge).

Sparse carbonaceous⁸ clay deposits are present in the interstices between dolomite crystals (Figure 22) and as discontinuous “floating” seams in the quartz matrix (Figure 23). Clay pockets or seams can present a point of weakness in a rock matrix if they are susceptible to swelling in contact with water. However, the clay deposits observed in the sample are unlikely to present a point of weakness due to their low abundance and distribution in the matrix.

⁸ Carbonaceous materials are organic matter consisting of the preserved residue of plant or animal tissue.

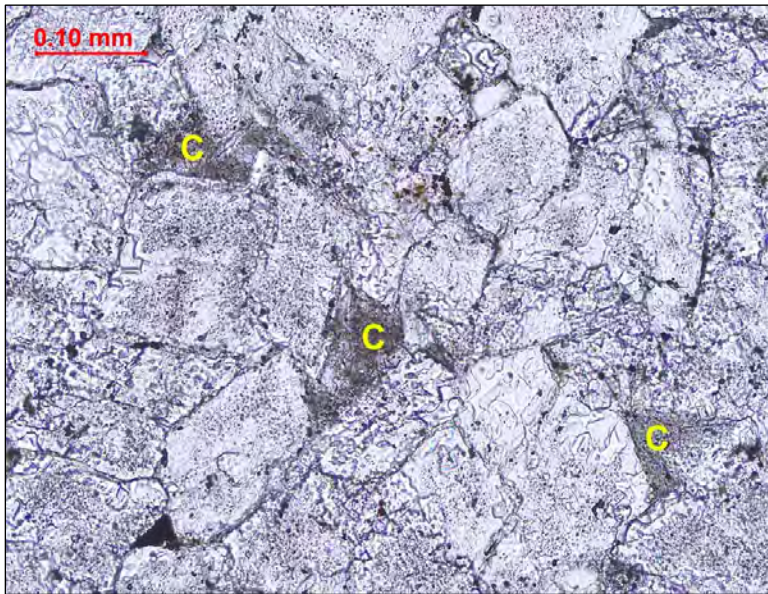


Figure 22. Photomicrograph showing clay filling interstices between dolomite crystals (Plane polarized light, Credit: Highbridge).

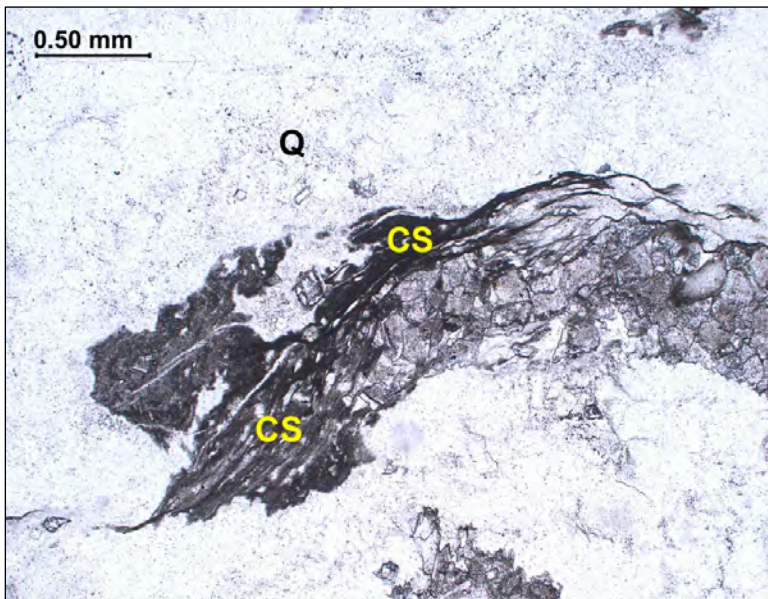


Figure 23. Photomicrograph of clay seam surrounded by quartz (Plane polarized light, Credit: Highbridge).

Orthogonal cracking (so called “checkerboard” cracking) was observed in limited units of this stone in situ (Figure 24). Occurrences of this type of cracking appeared random with no clear relationship to other deteriorated conditions or the orientation of the stone in the wall. While it is possible that this cracking is related to the iron-rich veining, the morphology of the cracks and veins do not appear to correspond. Cracking is also not clearly related to sparse clay pockets and seams present in the stone matrix. The examined sample was removed from sound material and no cracking was observed by the petrographer. An additional sample removed by plunge-cutting the face of the masonry was provided to JBC by the client for the purpose of investigating the orthogonal cracking, but again, no such cracks were observed in the bulk sample and further

analysis of this sample was not performed. Without petrographic examination of the cracking, it is only possible to speculate. Based on the morphology of cracks, their limited and apparently random occurrence, and cracking observed in similar stones in other structures, we suspect that orthogonal cracking in the breccia is geologic, predating construction of the monument. Water moving through the walls of the monument has traveled through the cracks, depositing calcium and salts from other materials. These white-colored deposits outline the cracks, making them more apparent. While waterborne salts may have enlarged any pre-existing cracks, salts are unlikely to have caused the cracking.



Figure 24. Orthogonal cracks (indicated) in an interior breccia unit. White efflorescence or carbonate deposits occur along the cracks.

Anecdotal reports initially identified this stone as a locally quarried dolomitic limestone. The reported stone type comports with our analysis; however, no provenance could be determined from the analyzed sample alone. Given the geology of neighboring areas, it is possible the stone was quarried in Vermont or New York.

Mortar

Compositional analysis of nine mortar samples determined that the masonry was originally built using natural cement mortar and concrete fill. Findings are summarized in Table 2 and discussed below with additional details of the analyses contained in Appendix A.

Seven samples (Samples BM-01, NE-04, NE-18, NW-26, SW-02, SW-16, and ANA-South-4) represent mixes that date to the original construction (Table 2). These samples all contain natural cement binder with microtextural and chemical characteristics that are consistent with material quarried in the vicinity of Rosendale, New York, and manufactured in the nineteenth century. The six mortar samples from this natural cement cohort (excluding ANA-South-4, a concrete) all have similar medium-grained natural sands. Most of these mortars are estimated to have binder to sand ratios in the 1 : 1 to 1 : 2 range that was historically typical for natural cement mortars. This is in accordance with the 1887 specifications which called for masonry to be laid in Rosendale mortar with a 1 : 2 (binder : sand) mix ratio (Figure 5 above).

Table 2. Summary of mortar analyses findings.

SAMPLE ID	BINDER TYPE	ESTIMATED ASTM C270 MIX	ESTIMATED BINDER : SAND RATIO (by volume)
BM-01	Natural cement	n/a	> 1 : 1.9
NE-04	Natural cement (w/ black pigment)	n/a	1 : 1.2
NE-18	Natural cement	n/a	1 : 1.3
NW-26	Natural cement	n/a	1 : 1.1
SW-02	Natural cement	n/a	1 : 1.1
SW-16	Natural cement	n/a	1 : 2.7
BM-05	Gray portland cement and dry hydrated lime	Type N	1 : 3.1
BM-02	Masonry cement (gray Portland cement and crushed limestone)	Type M	1 : 3.2
ANA-South-4	Natural cement	n/a	n/a

The natural cement mortars contain no lime as was typical of the time period. Six mortars are unpigmented and have a pale brown color that is inherent to the cement (Figure 25). However, Sample NE-04, removed from an interior window return, contains a black pigment (possibly carbon black) that is crudely incorporated (Figure 26 and Figure 27). This pigmented mortar is also likely original with cement paste and aggregate characteristics similar to the other natural cement samples. The 1887 specifications indicated that pointing mortar was to be made the same color as the stone (Figure 6 above), suggesting an intent to pigment the mortar. Indeed, probes performed on the monument exposed an earlier, black-colored mortar, and the same mortar is also found at some interior window returns (Figure 28).

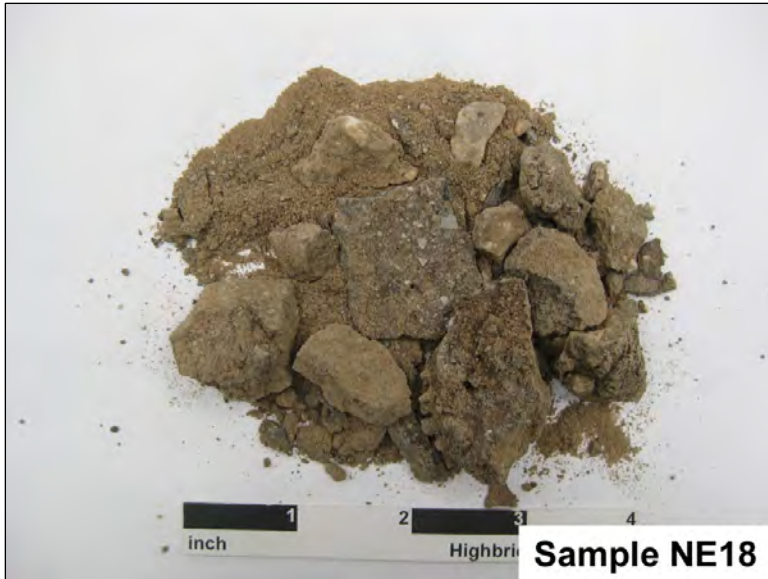


Figure 25. Sample NE-18 has a brown color typical of Rosendale natural cement mortars (Credit: Highbridge).

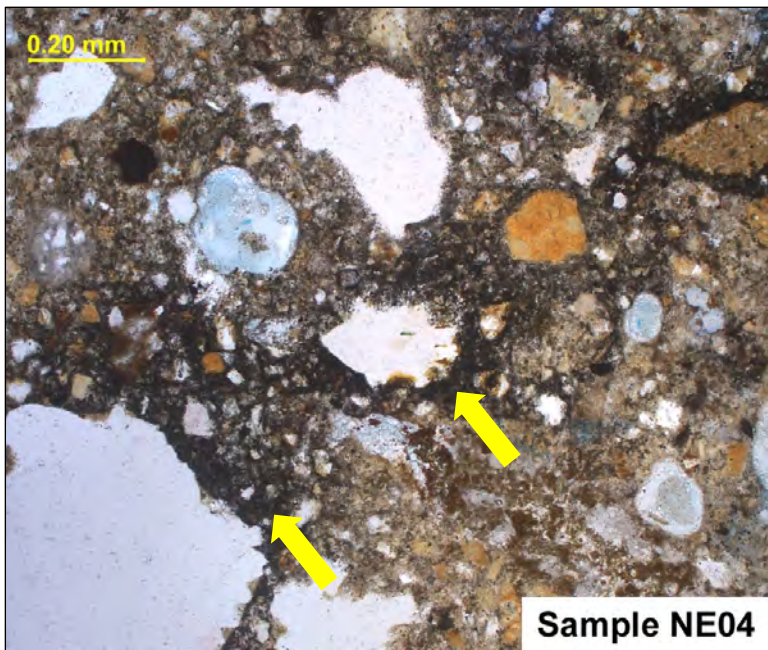


Figure 26. Photomicrograph of sample NE-04 in section showing streak of black pigment (indicated), with pigment particles too fine to be discerned at the scale of the light microscope (Cross-polarized light, Credit: Highbridge).

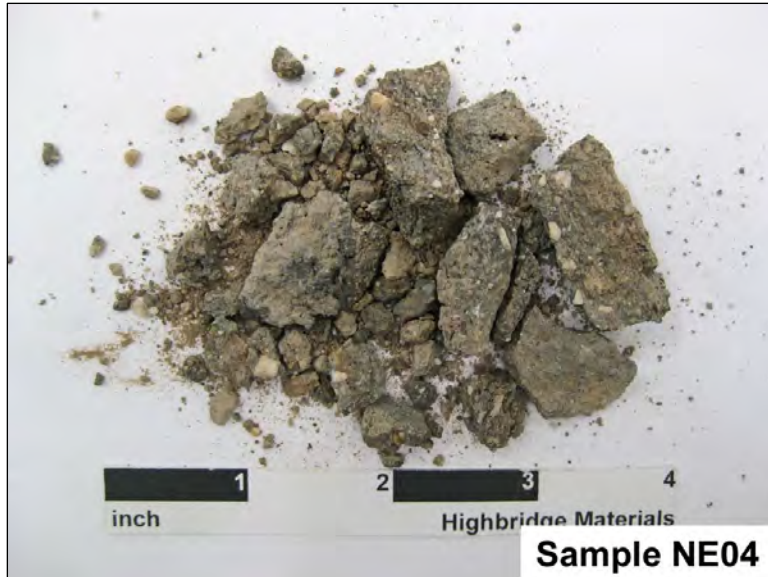


Figure 27. Sample NE-04 has a color ranging from brown and greenish gray due to the uneven incorporation of black pigment.



Figure 28. Black-colored pointing mortar (indicated) at interior window return is likely original pointing mortar.

The 1887 specifications also indicated that the mortar joints were to be raked and repointed using Portland cement mortar after the stones had been laid in natural cement. The practice of using lime or natural cement mortar for bedding masonry, followed by raking and pointing joints with a Portland-based mortar that was believed to be more durable, was certainly not uncommon in the late 19th century. However, no evidence of any Portland cement mortar contemporary to the date of construction was found. While the two remaining samples (BM-02 and BM-05) are both Portland cement mixes, the characteristics of the cement are more consistent with twentieth century material. These two samples most likely represent separate twentieth century repointing campaigns. Sample BM-05 is a Portland cement-lime mortar with proportions in the range of a modern ASTM C270 Type N mix. It also contains an iron additive that has oxidized, resulting in

fine reddish-brown spots within the otherwise light brownish gray mortar (Figure 29). Sample BM-02 is a much stronger mix containing masonry cement (a modified Portland cement mixture) in approximately Type M mix proportions and has a more neutral gray color (Figure 30).

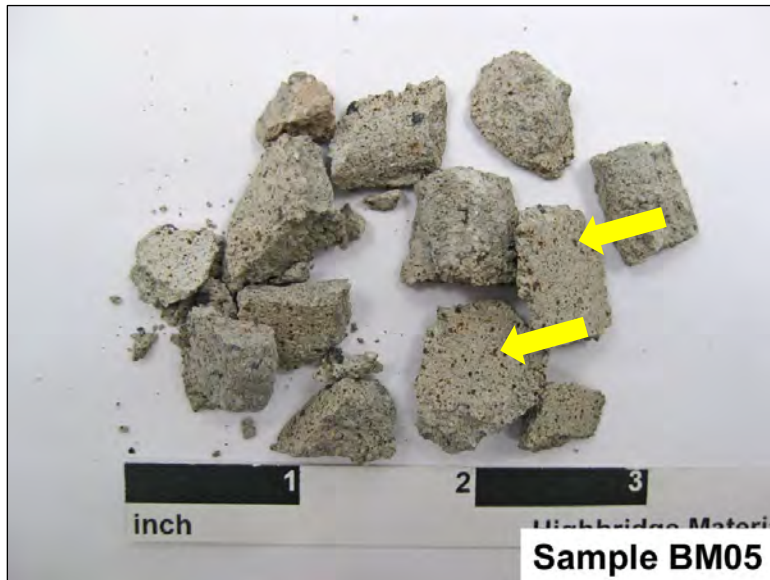


Figure 29. Sample BM-05 with reddish brown iron oxide spots indicated (Credit: Highbridge).

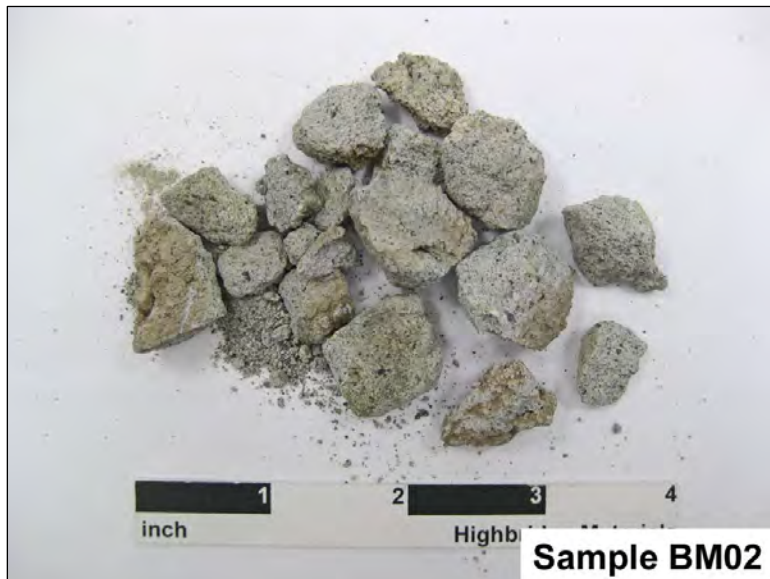


Figure 30. Sample BM-02 (Credit: Highbridge).

Most of the mortar samples are cohesive and intact. The original natural cement mortars tend to have a moderate hardness and high permeability. The two later Portland cement-based mortars are also relatively permeable despite their cement-rich compositions. Regardless, the examined mortars appear to be in mostly sound condition with only minor cracking and secondary salt deposition as the result of water infiltration. Sample BM-01 is the exception. This sample was removed from a deteriorated, open joint as damp, small, and friable fragments and exhibits signs of extensive water infiltration as expected (Figure 31 and Figure 32).

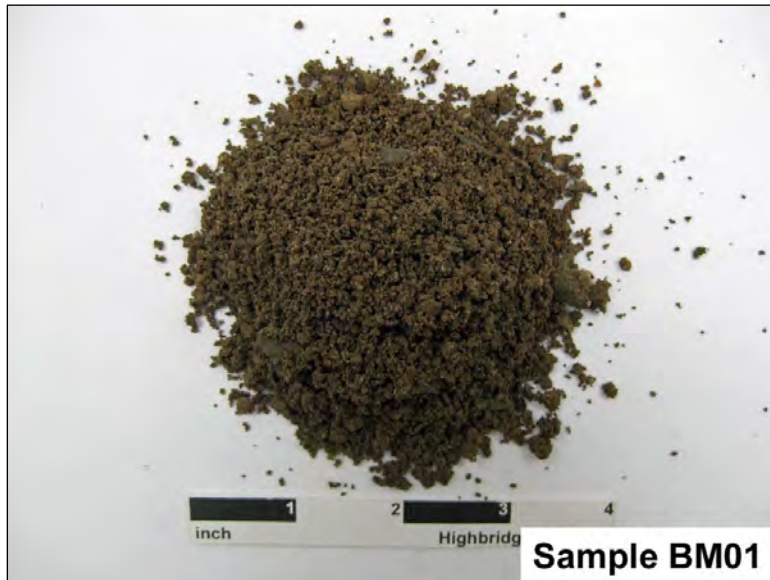


Figure 31. Sample BM-01 showing deteriorated condition of mortar (Credit: Highbridge).



Figure 32. Sampling location for BM-01 (open joint).

Sample ANA-South-4, removed from fill present at the wall core, was identified as a natural cement concrete with no Portland cement or lime additions. Like the natural cement mortars, the physical and chemical characteristics of the cement paste are consistent with cements produced in the vicinity of Rosendale during the nineteenth century. The chemical signature of the cement is nearly identical to that of mortar sample NE-18. The fine aggregate is a coarse-grained and broadly graded natural sand derived from the same source as that used in the other natural cement mortars. The coarse aggregate consists primarily of crushed dolomitic limestone with a top size of 2-inches and few particles passing the 1/2-inch sieve (approximately consistent with a No. 4 or No. 357 gradation profile). The limestone is the same as that used for the exterior masonry and may be repurposed castoffs from dressing the exterior stones on site. The material proportions are

estimated to be consistent with a 1 : 2 : 3 or a 1 : 2 : 4 (cement : sand : coarse aggregate) mix by volume.

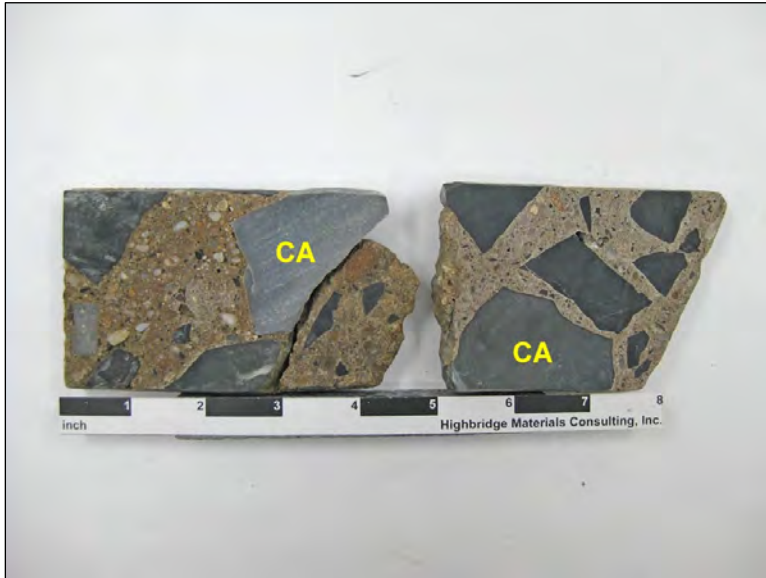


Figure 33. Section through sample ANA-South-4 showing large, crushed limestone aggregate (CA) surrounded by a paste of fine aggregate and cement.

While the petrographic analysis identified no major workmanship issues in Sample ANA-South-4 and the concrete is in sound condition for its age, a very minor incipient alkali-aggregate reaction (AAR) has occurred between the cement paste and the coarse limestone aggregate. AAR is a reaction that can occur between a highly alkaline cement paste and certain constituents of the aggregate in concrete or mortar. This reaction can cause expansion of the altered aggregate, leading to expansion, cracking, and spalling of the concrete. A few aggregate grains in the sample contain microscopic or hairline cracks and several cracks are also observed in the cement paste (Figure 34). Despite the cracks, the sample remains cohesive. There are very sparse occurrences of reaction gel within some of the aggregate cracks. Most notably, there is a visible white coating of layered reaction gel that lines a formed surface of the core sample (Figure 35). This white coating was further analyzed using X-ray diffraction (see “Salt Identification” section below).

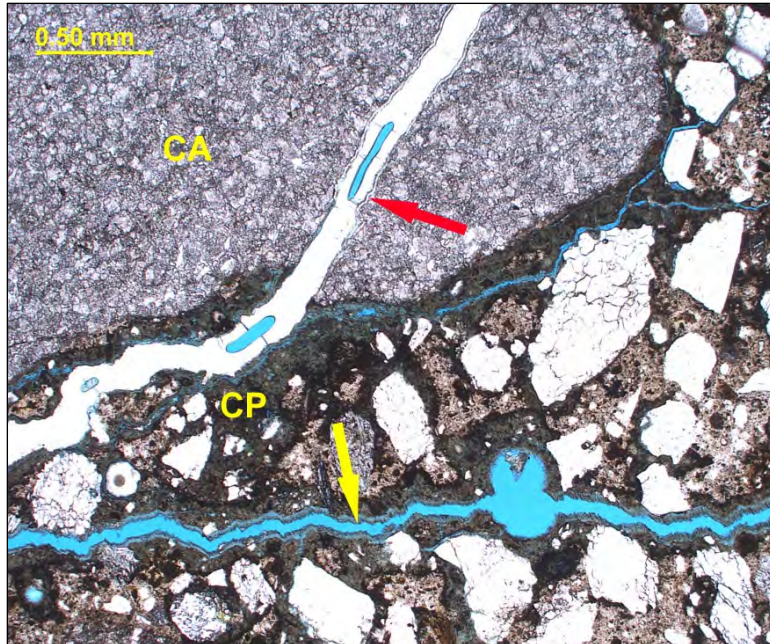


Figure 34. Photomicrograph of sample ANA-South-4 showing a crack (red arrow) transecting a coarse aggregate particle (CA). While this crack is mostly filled with colorless epoxy, a thin veneer of reaction gel lines the crack surfaces. The crack (yellow arrow) extends into the cement paste (CP). (Cross polarized light, Credit: Highbridge.)



Figure 35. Formed end of core sample ANA-South-4 showing a thin white residue consisting of alkali-aggregate reaction gel.

While AAR is potentially destructive, the small degree of reaction observed in this particular sample is unlikely to present durability issues. Assuming that this sample is representative of all infill concrete, the durability risk to the overall structure should be considered quite low. There is very little reaction gel present within the concrete itself despite the coating along the formed face on the outside of the sample. As the petrographer notes, given that natural cement behaves in part as a calcined clay, it would be reasonable to expect that any potential AAR expansion and cracking

are mitigated.⁹ The petrographer has observed a large number of nineteenth century natural cement concrete samples and has never encountered an advanced alkali-aggregate reaction even where aggregates would otherwise be considered highly susceptible in Portland cement paste. Still, it is possible that AAR is present and more advanced in other areas of the structure that were not sampled, and that severe AAR could contribute to cracking observed in stones.

Salt Identification

Seven salt samples were identified using X-ray diffraction. The results of this analysis are summarized in Table 3.

Table 3. Summary of identified salts and their percent concentration.

SAMPLE ID	SALT		TOTAL EXTRACTED SALT CONCENTRATION (% by wt.)
	Major (>10% by wt.)	Minor (<10% by wt.)	
NW-05	Aphthitalite, kalicinite	Calcite	6.5
NE-11	Calcite, arcanite	Aphthitalite, cristobalite	N/A
SE-24	Kalicinite, arcanite	Calcite	16.6
SW-12	Aphthitalite, kalicinite, calcite	Sylvite	0.4
SW-26	Aphthitalite, kalicinite	Vanthoffite	7.9
BM-01	Niter, magnesium nitrate hexahydrate, gypsum	-	5.6
ANA-South-4	Calcite, aragonite, dolomite	Quartz	N/A

Potassium Salts

Most of the samples were loose surface scrapings containing some variety of potassium salt. Most are sulfates (aphthitalite and arcanite), though some bicarbonate (kalicinite) is also present. It is difficult to isolate a particular source of these salts since the potassium ion is easily solubilized and transported in most of its forms. However, there are two sources of sulfate ion that are more likely than others. The first is from the remobilization of gypsum or epsomite formed by reaction between the masonry and acids, such as sulfuric acid dissolved in rainwater. The second is from sulfate additions to cements. By the late nineteenth century, gypsum was an additive in both Portland and natural cement.

While JBC is unfamiliar with the morphology of the particular salt species identified, sulfates can be quite damaging to masonry due to their tendency to crystallize within its pores (cryptoflorescence) or within cracks and crevices in the masonry assembly. The expansive force

⁹ See Highbridge Materials Analysis, Inc., “Concrete Analysis Report” SL1846-05, pg. 7 reprinted in Appendix A. Numerous studies have concluded that AAR in Portland cement concretes is mitigated by addition of calcined clays: Quang Dieu Nguyen, T. Kim, A. Castel, “Mitigation of Alkali-Silica Reaction by Limestone Calcined Clay Cement (LC3),” *Cement and Concrete Research* 137 (2020); James Sarfo-Ansah, E. Atiemo, K. Boakye, D. Adjei, and A. Adjaottor, “Calcined Clay Pozzolan as an Admixture to Mitigate the Alkali-Silica Reaction in Concrete,” *Journal of Materials Science and Chemical Engineering* 2 (2010): 20-26.

of cryptoflorescing salts can cause surface loss like that seen on the interior of the monument and enlarge hairline cracks and contribute to spalling.

Carbonates

Calcite is found throughout the samples, along with some aragonite in Sample ANA-South-4. Calcite is one of several crystalline forms of the chemical compound, calcium carbonate (CaCO_3), which forms rocks such as limestone and marble, and is present in cementitious masonry materials derived from these rocks.

Calcite is typically deposited from water that has passed through calcium hydroxide-bearing material including, in this case, the natural cement and Portland cement in mortars and concrete used to construct the masonry. When exposed to significant amounts of water, the free calcium hydroxide in these materials dissolves. This calcium-hydroxide solution may be transported to the face of the masonry through capillary action or may seep through voids or cracks in the masonry. Once the solution reaches the surface, the water evaporates and, upon exposure to carbon dioxide in the atmosphere, the calcium hydroxide carbonates to form calcium carbonate. Calcium carbonate is not water soluble and repeated deposition of calcium hydroxide results in thick, brittle encrustations forming on the surface of affected masonry. Thin calcite residues and thick crusts are present throughout the monument and are typically found along cracks and below open joints where large volumes of water have preferentially travelled. The crusts are typically white in color, with some dark colored crusts resulting from contamination with dirt, atmospheric pollutants, or, in the case of some interior stone, stained red by iron oxide inherent in the stone.

Although unsightly, calcite deposits do not typically damage masonry. Rather, it is the underlying water infiltration causing the deposits that is likely to contribute to damage. Abundant calcite deposits also indicate depletion of the cementitious binder in mortar and concrete, though the weakening effect is typically negligible in relation to damage caused by water infiltration. Calcite can fill pores within masonry units (often at the surface) and impede the movement of moisture through the unit. This phenomenon is potentially damaging to porous masonry, such as sandstone, but is unlikely to affect dense stones used in the monument. Though not a direct effect of calcite deposits, damage can occur when the deposits are removed using inappropriate means such as grinding the face of masonry unit or aggressive cleaning with strong acids.

Nitrates

Two forms of nitrate (niter, also known as potassium nitrate, and magnesium nitrate hexahydrate) are found in the one mortar sample analyzed for salts, BM-01, which was sampled as a disaggregated and water-logged mortar from the bottom of the monument. Nitrates typically derive from the decomposition of organic materials. In this context, these can include fertilizers used in adjacent landscaping or bird excrement. One of the nitrates is magnesium-based. As this sample contains natural cement, a magnesium-based binder, the cement may be the source of detected magnesium.

Niter is highly soluble in water. The humidity level at which this salt changes from liquid to crystalline form increases with lower temperatures. As a consequence of this effect, there is a danger of supersaturated salt solutions filling masonry pores in cold weather and subsequent crystallization and damage during dry periods and higher temperatures. While nitrates may

contribute to deterioration of the monument masonry, their contribution is likely limited and confined to the base of the monument and areas contaminated with bird or bat excrement.

Contaminants

An amorphous component noted in analysis results for the concrete infill sample (ANA-South-4) may relate to minor reaction gels produced from alkali-aggregate reactions in the concrete (see “Mortar” section above). Some amorphous material is also indicated in Sample NE-11 though its nature is less certain.

VI. EXISTING CONDITIONS

JBC did not perform a comprehensive conditions assessment survey of the masonry. However, based on our observations and those reported by Vertical Access in their comprehensive exterior survey¹⁰, the Bennington Battle Monument is in fair overall condition. Deteriorated conditions include spalls, cracks, open and deteriorated joints, dampness/active water infiltration, efflorescence, calcium carbonate deposits, and biological soiling. The structure also exhibits multiple repairs, some of which employed inappropriate materials.

Exterior Conditions

The most serious conditions affecting the exterior masonry include spalling/surface loss, cracking, and open mortar joints. Many of these conditions have been repaired and some of those repairs have now failed. Calcium carbonate residues and biological soiling are also present.

Spalls and Surface Loss

The majority of the spalls in the exterior masonry occur at the upper portions of the monument. These range in size from small fragments measuring approximately 1 to 2-inches across to large pieces measuring from 10 to 60 square inches in size.¹¹ Spalls, or fragments that have cracked and detached from individual masonry units, generally occur as the result of a buildup of stresses below the surface. When the stresses become significant enough to fracture the material, pieces disengage from the body. These internal stresses may result from corrosion of metallic anchors embedded in the masonry assembly, subsurface crystallization of water-soluble salts, frost jacking, or freeze/thaw or other thermal cycling. In some cases, weaknesses inherent to a particular stone, such as some styolites, veins, or clay seams, may also result in spalling. The cause of spalling in the exterior stone was not apparent from field observations or petrographic analysis. However, clayey styolites observed in the examined samples represent a potential plane weakness that may contribute to this condition. Spalls observed in geologically similar stone at other sites (e.g. the dolomitic limestone anchorages of the Brooklyn Bridge) suggest that this type of stone may be pre-disposed to spalling.

¹⁰ Vertical Access, “Exterior Investigation” report dated June 2, 2022.

¹¹ Vertical Access, Draft letter re. removals from the monument, dated June 2, 2023.



Figure 36. Spall removed from the exterior stone masonry (Credit: Vertical Access).



Figure 37. Spall removed from the exterior stone masonry (Credit: Vertical Access).

In some areas, spalls have been repaired with cementitious patching material that has subsequently cracked and failed. In some cases, patches appeared to have been well executed with bolts embedded in the host stone and a wire armature to support the patching materials (Figure 38). In other cases, patching was poorly executed with the cementitious material spread thinly without sufficient preparation of the substrate (Figure 39). While JBC did not perform a close visual examination of failed patches (which occur at the upper portions of the monument requiring specialized rope access), photos taken by Vertical Access show extensive cracking, scaling, and

white residues. These suggest that failure was the result of freeze/thaw weathering and/or water-soluble salts, where not obviously related to poor workmanship.



Figure 38. Cracked and spalled cementitious patch repair (Credit: Vertical Access).



Figure 39. Cracked and failed parge coat applied over the face of a stone (Credit: Vertical Access).

In addition to spalls, other forms of stone surface loss, including delamination and scaling, were reported by Vertical Access in very limited areas at the upper portions of the monument. Delamination is a process affecting stones with a layered structure (mostly sedimentary rocks and some metamorphic rocks), wherein portions of the stone detach from the main body along the stone's laminae or natural bedding planes (Figure 40). Delamination can be caused by the swelling and shrinking of hygroscopic clays present between laminae during wetting and drying cycles, or it can result from the expansive forces of frost jacking or crystallization of soluble salts between

laminae. The thickness of delaminated material is usually dictated by the depth of the stone's bedding planes with detachment typically occurring in sheets. Face-bedded sedimentary stones (i.e. those with bedding planes oriented parallel with the face of the wall) are particularly susceptible to delamination as the outermost laminae is unrestrained by adjacent stones and mortar. This condition is not widespread.



Figure 40. Delamination in a stone at the upper portion of the monument (Credit: Vertical Access).

Unlike delamination, scaling, or the detachment of flakes of material near and parallel to the surface of the stone, does not following any stone structure (Figure 41). The thickness of a scale is generally millimetric to centimetric and is negligible compared to its surface dimension. The cause (or causes) of scaling may be varied but is often related to an accumulation of water-soluble salts or other minerals at the face of the stone. Some have also speculated that thermal or hygric cycling may contribute to the condition. Still, scaling on the exterior of the monument was not observed at the lower portions inspected by JBC and was noted in only very limited areas by Vertical Access.



Figure 41. Scaling (indicated) in a stone at the upper portion of the monument (Credit: Vertical Access).

Cracks

Vertical cracks are abundant on all exterior elevations. The majority of these are hairline cracks (< 1/16-inch wide) through individual stones, running the full height of the unit, and located directly below a vertical mortar joint from the masonry above (Figure 42 and Figure 43). As with spalls, cracks form in masonry to relieve stresses. Though, unlike spalls where the stressing forces occur within a masonry unit, cracks are most often related to stresses occurring external to a particular unit such as excessive shear, compressive, or tensile loads. These may occur locally or may be the result of overall structural issues such as settlement. Localized cracking may result from corrosion of metallic anchors embedded in the masonry assembly, frost jacking, other thermal cycling. Deleterious salts and freeze-thaw weathering tend to create erosion, crumbling, or a series of small cracks, and do not typically result in discrete cracks unless they are exploiting a natural weakness in the stone. While some localized cracking is present the vast majority of the cracks appear to be structural in nature. We suspect that they may be due to uneven load distribution along the horizontal plane of the stones (e.g. point loading). This is supported by the cracks' regular occurrence below vertical mortar joints, many of which are open or were (open and) previously repointed or caulked and may have acted as a sort of vertical fault line. The cracks are not explained by features inherent to the stone such as bedding planes or stylolites.



Figure 42. Exterior crack (indicated, repaired with caulk) showing typical vertical orientation and location below mortar joint.



Figure 43. Exterior of monument with cracks highlighted in red. Note that most cracks fall below a vertical mortar joint.

If cracks remain open, water infiltrating the cracks can lead to widening of cracks, additional cracking, or other forms of deterioration. Many of the exterior cracks in the monument have been repaired, some more than once. Repairs included patching with cementitious mortar or surface-applied epoxy or sealing with elastomeric caulking. In some cases, cracks were additionally stabilized using bronze cramps embedded in the face of the stone, with the cramps sealed with mortar or caulk (Figure 44). Some cracks have repropagated in stones that were previously repaired and fresh cracks with no previous repairs were observed, indicating the condition is active (Figure 45). In many locations, cementitious crack repairs have detached and failed (Figure 46).

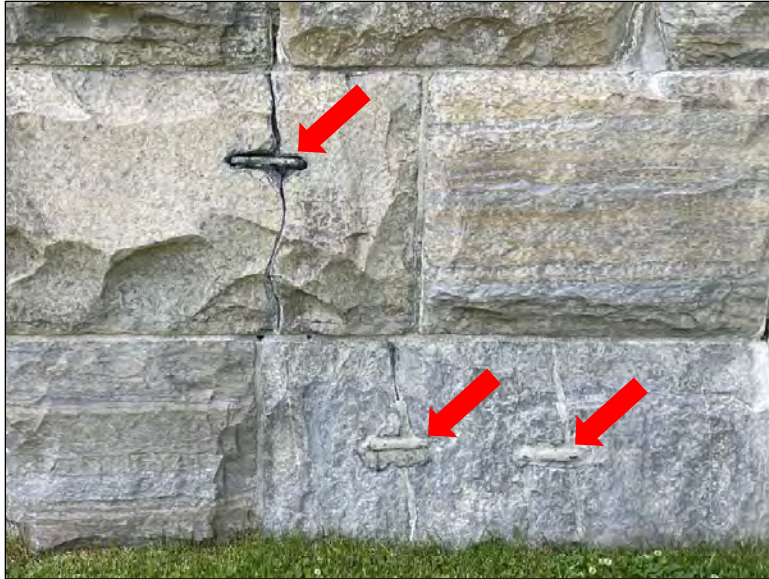


Figure 44. Bronze cramps (indicated) used to stabilize cracks at the base of the monument. Lower cramps have been sealed with elastomeric caulk.



Figure 45. A previously repaired crack with a fresh hairline crack (indicated) extending from the repair.



Figure 46. Detached and failed cementitious crack repair (Credit: Vertical Access).

Open Mortar Joints

Mortar loss is typical throughout the exterior and, like the conditions noted above, is most severe at the upper portions of the monument. These joints typically manifest as open vertical joints where the outer inch or more of mortar is missing and the remaining mortar in the joint is disaggregated (Figure 47). In many locations, the mortar loss has occurred at the lower portion of the joint, leaving the upper portion intact (Figure 48 and Figure 49). Moderately eroded joints were also observed. However, this condition is typical for the age of the structure and natural weathering and is not concerning.



Figure 47. Detail of a typical open joint showing accumulation of crumbly mortar and debris at bottom of joint.



Figure 48. Typical open joint at upper portion of monument. Note mortar at top of joint is deteriorated but remains firmly in place. (Credit: Vertical Access.)



Figure 49. Typical open joint at upper portion of monument. Note mortar at top of joint is deteriorated but remains firmly in place. (Credit: Vertical Access.)

Mortar loss can occur for a number of reasons including movement of the masonry assembly, poor mortar mix design and/or installation, erosion and weathering, water infiltration, freeze-thaw damage, salt contamination, or acid attack. Once the joints have failed, water will enter the masonry assembly and cause additional deterioration. Mortar loss at the monument bears signs of being largely related to water infiltration. The majority of losses occur in vertical joints (or in horizontal joints immediately adjacent to the vertical) where water preferentially travels as it moves down the tall structure. Saturated mortar at the bottom of vertical joints is vulnerable to freeze/thaw damage. Crumbling mortar behind surface losses and white calcium carbonate material leached from deteriorated joints (see “Calcium Carbonate Deposits” section below) both

indicate that high amounts of water are moving through the assembly and have done so over a long period of time.

In other cases, deteriorated joints are likely the result of the use of incompatible joint materials such as overly hard or impermeable mortar or the use of caulk in lieu of mortar. Many loose mortar fragments were removed by Vertical Access from the upper portions of the monument. Images show gray colored repointing mortar that has detached from the cheeks of the joint (Figure 50 and Figure 51). While we were unable to access these locations, the color and texture of the mortar, along with its particular deterioration pathology, suggest that these joints may have been pointed with an overly hard Portland cement-rich mortar. Such mortar is likely insufficiently permeable to allow moisture to escape the masonry assembly and, instead, traps water behind the pointing where it causes deterioration. We also note that Portland cement mortars applied over natural cement mortar have a tendency to fail, possible as a result of incompatibilities in the thermal or hygric coefficients of expansion between the two materials.¹²



Figure 50. Failed mortar joint at upper portion of monument, possibly resulting from the use of incompatible repointing mortar (Credit: Vertical Access).

¹² Helen Thomas-Haney, “Battle of the Cements: Portland Cement Repairs and Original Natural Cement Mortars,” virtual presentation, Association for Preservation Technology International – Northeast Chapter, June 8, 2022.



Figure 51. Failed mortar joint at upper portion of monument removed (Credit: Vertical Access).

The use of elastomeric caulk in mortar joints can also trap moisture in the assembly. Mortar serves as the primary path of escape for moisture in the masonry. Impervious caulking prevents the joints from draining, instead trapping the moisture and causing adjacent masonry units to become saturated and, eventually, deteriorate. Unlike mortar, which should remain attached but will gradually erode with age, sealants typically shrink and detach from the cheeks of joints or crack as they age, permitting water into the joint. Caulking mortar joints also interferes with future repointing campaigns, preventing mortar from bonding properly to the masonry units and setting mortar as residue from the caulk fills the pores of the masonry, reducing suction, and acting as a bond-breaker. In limited locations at the base of the monument, JBC noted sealant residues present below detached pointing mortar (Figure 52).



Figure 52. Residue from a previous caulking campaign (indicated) observed below a repointing campaign employing hard, Portland cement-rich mortar that has detached and failed.

Calcium Carbonate Deposits

White-colored calcium carbonate deposits are found along cracks (Figure 53), around previous repairs (Figure 54), and along and below open or deteriorated mortar joints (Figure 55). This is a typical condition present throughout the exterior. Calcium carbonate deposits occur due to large amounts of water passing through the masonry over a long period of time (see detailed explanation in “Salts” section above). Water most likely enters the masonry through the abundant open joints and cracks. Analysis of deposits at the monument indicates that these are primarily composed of the mineral calcite. While these deposits are relatively innocuous and primarily only aesthetically detracting, they serve as an indicator of serious water infiltration issues.



Figure 53. White-colored calcium carbonate deposit along hairline crack.

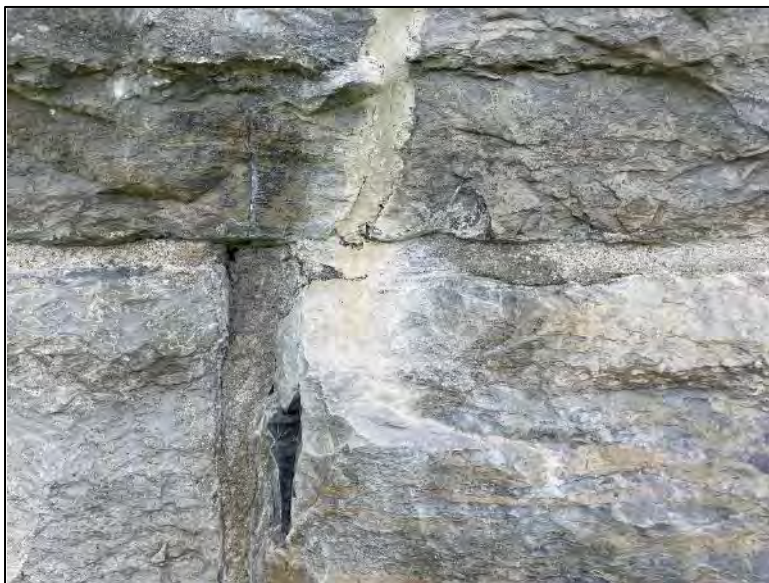


Figure 54. Carbonate deposit (white material) below an epoxy crack repair.



Figure 55. Heavy accumulation of carbonate material leached from a cracked and deteriorated mortar joint.

Biological Soiling

Biological soiling is typical across the exterior of the monument but appears to be concentrated most heavily at stones with coarser surface texture (Figure 56), the top third of the monument, and the northwest and southwest corners. Biological soiling is the presence of micro-flora such as algae, moss, lichen, or mold growing on the surface of a building element and often occurs in shaded areas. It is a symptom of excess moisture. Biological soiling is primarily a cosmetic issue; however, as a symptom of moisture infiltration, it can be indicative of larger issues. Biological soiling can be damaging in and of itself. Bacteria and lichen produce oxalic acids that damage carbonate-based masonry. Biological growths can fill pores in masonry surfaces, blocking the path for water to escape and contributing to deterioration of the substrate. The degree of biological soiling at the monument is minor and no damage related to the soiling was observed.



Figure 56. Biological soiling (dark colored material) on surface of an exterior stone.

Interior Conditions

Deteriorated conditions affecting the interior masonry include, in order of severity, cracking, open or otherwise deteriorated mortar joints, efflorescence, surface loss, and calcium carbonate deposits. Other than cracks that are not well explained by moisture, most of this deterioration is attributable to high moisture levels in the masonry.

Moisture

JBC measured the relative moisture content of the stone and mortar at different levels across the height of the interior of the structure in June of 2023 (Figure 57). The walls were damp to fully saturated despite several days of relatively warm and dry weather immediately preceding the measurements (Table 4). Moisture was concentrated at the corners and bottom third of the monument where stone readings measured 400 to 800 relative moisture content (out of 1000), and mortar readings were 600 to 1000. At the observation level, high moisture levels were limited to the corners and near the window openings (Figure 58). Concentration of moisture at interior corners may relate to the greater mass of the masonry or extensive cracking noted in those locations (see “Cracks” section below) or, it may simply be an effect of how air circulates through the structure and water evaporates from the stone. High moisture levels at the lower portion of the monument suggest that rising damp may be an issue. It should also be noted that moisture levels within the structure are likely impacted by hygroscopic salts and that moisture readings taken with either conductance or capacitance -type meters will be skewed higher by their presence.



Figure 57. A high, 600 moisture reading taken at the interior stone.

Table 4. Daily precipitation in Bennington for the month preceding moisture measurements on June 21, 2023. (Source: NOWData - NOAA Online Weather Data, Bennington Morse State Park AP Station, <https://www.weather.gov/wrh/climate?wfo=aly>)

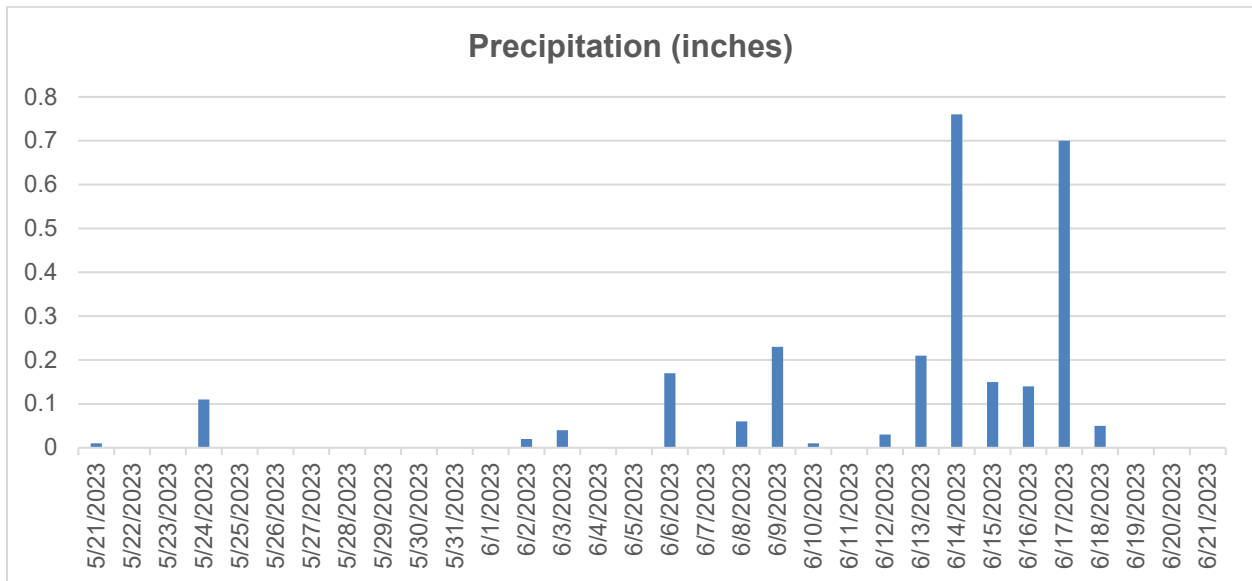




Figure 58. Discoloration due to dampness in the corners of the observation platform.

JBC attempted to perform RILEM surface water absorption tests on the interior masonry in order to understand and measure the porosity of the stone. However, all attempts failed because soiling, the friable surfaces of the stone and mortar, and the moisture already present in these materials prevented the adhesive putty required to hold the measuring tube in place from sticking to the surface.

Cracks

Cracking on the interior of the monument includes vertical cracks through one or more stones, horizontal cracks that run along the bedding planes of a stone, and orthogonal cracking in individual stones. Cracks occur in both the breccia and marble.

Large cracks through the stone and mortar separating from the cheeks of joints were noted at the interior corners and extend the full height of the monument (Figure 59). In some locations, the cracks are very deep, extending into the wall at least 8 inches. This cracking is most likely structural in nature.



Figure 59. Typical crack (indicated) at interior corner.

Most other cracks are isolated to one stone unit and occur as single vertical cracks (Figure 60 and Figure 61). These are likely the result of excessive shear, compressive or tensile loads on the affected unit.

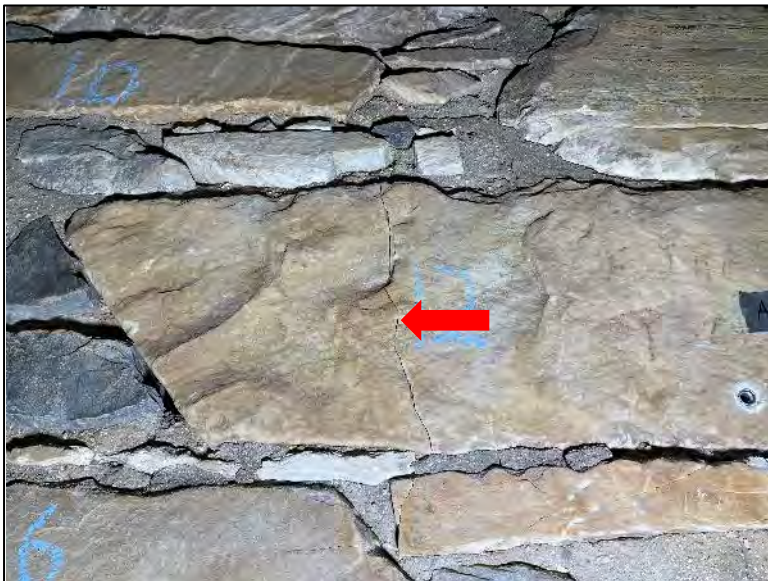


Figure 60. Typical interior vertical crack (indicated) isolated to one stone.



Figure 61. A hairline crack (indicated) through a window lintel resulting from the load of the masonry carried above.

Orthogonal cracking is limited to the interior dolomitic breccia (Figure 24 above and Figure 62 below). This type of cracking manifests in single stones as an interconnected network of fine cracks at approximate right angles to one another, forming a rectilinear pattern. The depth of the cracks is unknown. The pattern appears somewhat related to the structure of the affected stones (e.g. tracing bedding planes) and may have been present in the rock formation when the stone was quarried. The orthogonal cracks are typically outlined by white carbonate and other salt deposits carried through the cracks by water. Cyclical hydration and recrystallization of water-soluble salts within cracks may serve to widen them.



Figure 62. Orthogonal cracks (indicated) in an interior breccia unit.

Similar to the orthogonal cracking, horizontal cracks observed in interior marble units appear to follow the natural foliation of the stone (Figure 63). As with orthogonal cracks, many of the

horizontal cracks in the marble are filled with calcium carbonate and other salts (Figure 64). These seams may represent weaker material that has been precipitated out of the stone matrix or is otherwise preferentially exploited by water moving through the stone. Horizontal cracks in the marble are a geologic feature that predates construction but may have been enlarged by moisture-related deterioration.



Figure 63. A single, horizontal crack follows the natural foliation of an interior marble unit.

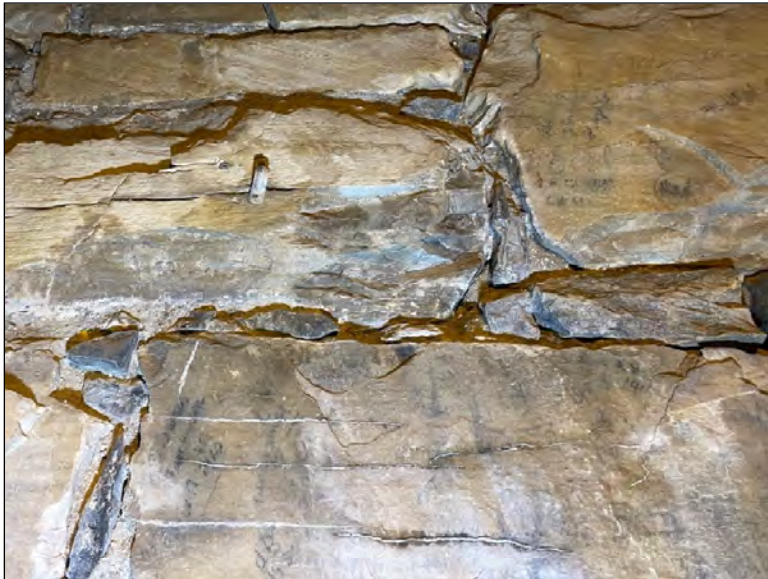


Figure 64. A series of horizontal cracks in an interior marble unit are filled with salts.

Open Joints

Open and deteriorated joints are present throughout the interior of the monument but are most prevalent below the observation level where joints have either not been repointed or were repointed less frequently. Open joints included large, deep voids between the roughhewn rubble stones

(Figure 65). At other joints, the outer surface of the mortar was friable with disaggregated mortar debris accumulating on the projecting surfaces of stones below (Figure 66). Monument staff reported cleaning this debris from the stairs regularly, though it reappears quickly. Disaggregated mortar is most severe at the bottom third of the monument where high moisture levels were also recorded. Disaggregation of interior joints is consistent with damage from water-soluble salts and freeze-thaw weathering.



Figure 65. Large void between two interior stones.



Figure 66. Light brown disaggregated mortar (indicated) coats projecting surfaces of interior stones.

Surface Loss

In several locations, the breccia exhibits differential surface loss, leaving behind small, raised portions that retain the stone's original surface patina (Figure 67). As with interior mortar joints, this damage is the result of contamination with water-soluble salts. This is evidenced by the white

salt residues observed coating the surfaces of the lost portion of the stone (Figure 68). Petrographic analysis identified the breccia as containing fragments of dolostone bound in matrix of quartz. The raised portions are likely harder, denser pockets of quartz that have resisted attack by crystallizing salts.



Figure 67. Differential surface loss in the interior breccia.

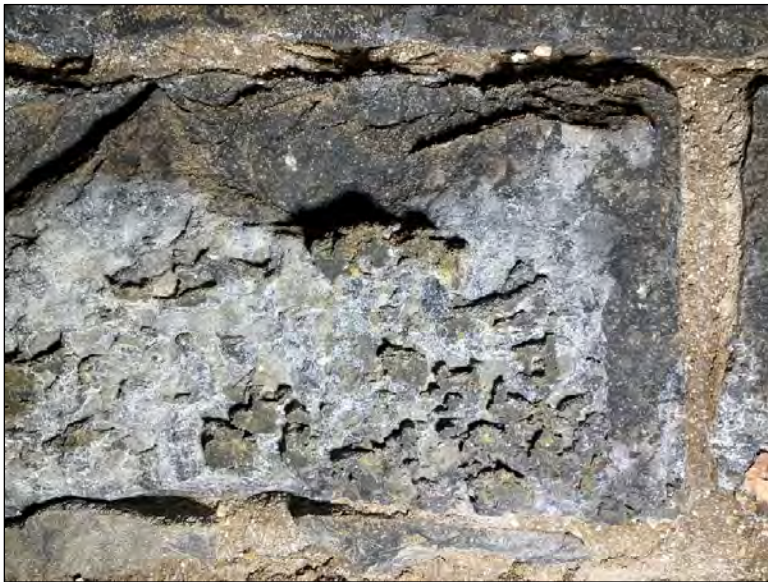


Figure 68. Detail showing white salt residue coating the lost portion of a breccia surface.

Salts

Both efflorescing and calcium carbonate salts are found along many of the cracks, mortar joints, and on the surface of interior stones (Figure 69). As with the exterior, interior calcium carbonate deposits are caused by water infiltrating the masonry and leaching calcium hydroxide from cementitious materials used in the masonry construction. Water infiltration also contributes to the formation of efflorescence, or surface blooms of deliquescent salts. The interior of the monument

was notably damp at the time of inspection and apparently stays so throughout most of the year, which is ideal for salt transport. Analysis of salt samples found both sulfate and nitrate salts in addition to carbonates. The sulfates may originate from constituents of the mortar and concrete, while nitrates, which affect the bottom of the monument, are likely from bird guano or fertilizers used in the adjacent landscape. The presence of high moisture levels and salts at the base of the monument could be indicative of a rising damp condition. While insoluble calcium carbonate deposits are largely innocuous other than their unsightly appearance, water soluble efflorescence can cause serious damage including surface loss or complete disintegration of stones. Salt solutions will preferentially travel along any cracks present in stones and, as water evaporates, the salts will crystallize within and along the surface of the crack. This can result in granular disintegration of the stone along the crack.



Figure 69. Efflorescence and/or carbonate crusts along cracks and mortar joints.

Efflorescence and associated disaggregated mortar resulting from salt damage are most severe at the bottom third of the monument where elevated moisture levels were also detected. Monument staff reportedly clean the disaggregated material off the ramps in these locations, but the debris reappears quickly (Figure 70).



Figure 70. White colored efflorescence on the surface of the stone and mortar joints. Note light brown dust (mortar debris disaggregated by crystallizing salts) accumulating on projections from the stone.

VII. CONCLUSIONS

The Bennington Battle Monument was built using three types of stone including bluish-gray dolomitic limestone on the exterior, and pale yellowish white calcitic marble and dark gray dolomitic breccia on the interior. The exterior dolomitic limestone is Sandy Hill Dolomite quarried in Kingsbury (present-day Hudson Falls), New York. The provenance of interior stones was not determined.

All of the stone samples examined petrographically were found to be sound and cohesive with relatively low porosity. While potential points of weakness were noted in the exterior limestone and interior breccia, no significant distress or deterioration was observed in thin section. That being said, it should be noted that these observations pertain to the specific samples examined and do not exclude distress and deterioration in stones that were not sampled. Deterioration observed in situ including, spalling and other forms of surface loss noted in the exterior limestone and cracking observed in the interior breccia, appears to best be explained by the exploitation of inherent weaknesses in the stone (e.g. stylolites and clayey seams or bedding planes) by infiltrating water and salts or geologic cracking that occurred before construction.

Vertical cracks occurring predominately on the exterior and, to a lesser degree, the interior of the structure cannot be explained by any geologic features or deterioration of the stone units. The cracks are most likely the result of some structural condition (e.g. movement or uneven load distribution).

The stones of the Bennington Monument were originally bedded in natural cement mortar from Rosendale, New York. Large gaps between the exterior ashlar and the interior rubble walls were filled with a Rosendale natural cement concrete with large aggregate matching the exterior limestone. While the original specifications for the monument called for pointing the exterior in a pigmented Portland cement mortar, no such mortar was found. It may be that multiple repointing campaigns conducted on the exterior have removed most traces of the original pointing. It is also possible that natural cement was used in lieu of the specified Portland. Traces of a black-pigmented natural cement pointing mortar found on the monument's interior seem to support the latter possibility.

No deficiencies or potential weaknesses were noted in the original mortar samples. However, minor AAR was observed in the concrete sample removed from the wall core. While AAR can be destructive in its advanced stages, the level of reaction observed in the sample was minor. AAR, or at least the minor degree of AAR seen in the examined sample, does not readily explain cracking and other forms of deterioration observed in the monument masonry. Further, we are not aware of any remedial action that could be taken to address this condition other than repairing the exterior envelope to prevent further moisture infiltration.

Other than structural cracking, nearly all of the deterioration observed in the masonry materials of the Bennington Monument is related to water infiltration. Large amounts of water entering walls through cracks and open joints has mobilized deleterious salts inherent to the masonry and exposed areas to freeze/thaw damage and frost jacking, propagating still more cracks and open joints. The

humid microclimate at the interior of the monument provides an ideal environment for the transport of salts to the interior face of the masonry.

Some previous masonry repairs are inappropriate and serve to exacerbate deterioration. These include non-matching, overly hard, and impermeable re-pointing mortar, the extensive use of caulking in cracks and joints, and poorly executed cementitious patches. Failure of these repairs allows moisture to infiltrate the walls, leading to additional damage.

VIII. RECOMMENDATIONS

The following recommendations are based on the results of JBC's analysis. They are intended to address issues relating to the historic masonry materials that are within JBC's limited scope and do not purport to address structural issues or the preservation of non-masonry historic elements. As the Bennington Battle Monument is listed on the National Register of Historic Places, all work must follow the "Preservation" treatment approach defined in the Secretary of the Interior's Standards for the Treatment of Historic Properties as: "...the act or process of applying measures necessary to sustain the existing form, integrity, and materials of an historic property." Work should focus on the repair of historic materials and features rather than extensive replacement. The removal of distinctive materials or alteration of features that characterize the property should be avoided. The recommendations below are presented in order of priority, with work necessary to prevent further deterioration listed first, followed by repairs to correct damage and address aesthetic issues.

1. Repoint mortar joints.

1.1. All exterior joints should be raked to depths equal to 2-1/2 times the width of the joints, or to sound mortar, and repointed.

1.1.1. Joints should be repointed to the depths necessary to eliminate any voids in the masonry assembly that may serve as conduits for water movement within walls. Deep repointing (repointing for the full depth of masonry units) will be necessary in some locations.

1.1.2. Based on available evidence a natural cement mortar with a mix ratio of 1 : 2 (cement : sand) is appropriate. Mortar aggregate should be sourced to replicate the aggregate extracted from the original mortar (samples available from JBC). The owner should consider whether this mortar should be pigmented black to match original pointing mortar located on the interior. While a pigmented mortar may be appropriate, no definite evidence that a pigmented mix was used on the exterior was found.

1.2. All open or severely eroded interior joints should be to depths equal to 2-1/2 times the width of the joints, or to sound mortar, and repointed.

1.2.1. Based on available evidence a natural cement mortar with a mix ratio of 1 : 2 (cement : sand) is appropriate. This mortar should be pigmented black to match the color of existing original samples. Mortar aggregate should be sourced to replicate the aggregate extracted from the original mortar (samples available from JBC).

2. Repair cracks.

2.1. Vertical cracks in exterior stones should be repaired by pinning across the crack with stainless steel rod driven into holes drilled at opposing angles from either side of the crack and set in epoxy. The crack should then be routed to remove all traces of previous sealant

or epoxy repairs that may interfere with mortar adhesion, pointed with mortar matching the color of the stone, and grouted with modified natural cement grout.

- 2.1.1. The recommendation may be superseded by those of the structural engineer.
- 2.1.2. We note that pinning all of the exterior vertical cracks is an aggressive intervention. However, we believe that it is warranted in this case because the cracks remain active (as evidenced by failed previous repairs and reoccurring cracking) and the specific cause of cracking has not been identified to date.
- 2.2. Cracks in interior stones may remain (no repair). Cracked lintels may be removed and repaired with concealed pins if determined necessary by the structural engineer.
- 2.3. Sealant should not be used in cracks unless active movement is anticipated.
3. Repair spalls, losses, and failed or inappropriate previous patching repairs.
 - 3.1. Failed or inappropriate repairs, including those repairs that have cracked or separated from the masonry and repairs that detract from the aesthetics of the monument, should be removed and replaced.
 - 3.2. Spalls and losses with a large surface area should be repaired with a dutchman prepared from the same or petrographically similar stone indented into the face of the damaged stone, bonded with epoxy, and supported by stainless steel pins.
 - 3.3. Spalls and losses up to 6 inches in diameter may be repaired with composite patching material matching the color of the stone in which it is installed.
 - 3.4. Small spalls, scaling, and surface losses that do not expose the masonry to moisture infiltration or do not detract from the aesthetics of the monument may remain (no repair).
 - 3.5. Bronze cramps used in previous crack repairs may remain but should be inspected and re-grouted as necessary.
4. Remediate salts.
 - 4.1. Salts should be removed from interior walls by brushing and vacuuming. No water or acids should be used.
 - 4.2. High interior humidity levels should be mitigated by either de-humidifying the air or circulating outside air through the interior. As humidity levels drop and air circulation is increased, efflorescent blooms will appear. Clean new efflorescence per 4.1 above. This may have to be performed several times as the walls dry.
5. Monitor deteriorated conditions.
 - 5.1. Vertical cracks, particularly cracks at the interior corners of the structure should be monitored for movement.

5.2. Alkali-aggregate reaction (AAR) observed in the concrete infill at the wall core cannot be readily monitored. However, this condition should be noted in the record for the benefit of future preservation efforts. JBC does not believe that additional destructive probes to investigate the extent of AAR in the concrete are necessary at this time.

6. Clean exterior.

6.1. The monument may be cleaned, if desired, to remove biological soiling and calcium carbonate deposits. Cleaning products and procedures should be tested prior to full-scale use.

6.1.1. Acidic cleaning chemicals should be avoided. While the exterior dolomitic limestone and interior breccia are acid resistant limestones, the interior marble is not and will be etched by acidic cleaners.

6.1.2. Heavy calcium carbonate deposits can be very tenacious, frequently requiring mechanical removal using chisels or micro-air abrasive blasting and strong acids. Acids should not be used for this purpose.

Application of water-repellant coatings to the exterior masonry is not recommended. This analysis determined that the exterior stone is not sufficiently porous to pose any sort of waterproofing issue. Past coating applications were likely ineffective.

Appendix A
External Laboratory Reports

Bennington Battle Monument
Bennington, Vermont

Petrographic Examination of Interior Marble

Bennington Battle Monument

15 Monument Circle, Bennington, VT 05201



Prepared for
Jablonski Building Conservation, Inc.

Client ID
JABL001

Report No.
SL1846-01

Report Date
08/26/23



Confidentiality

This report presents the results of laboratory testing requested by the client to satisfy specific project requirements. As such, the client has the right to use this report as necessary in any commercial matters related to the referenced project. Any reproduction of this report must be done in full. In offering a more thorough analysis, it may have been necessary for Highbridge to describe proprietary laboratory methods or present opinions, concepts, or original research that represent the intellectual property of Highbridge Materials Consulting and its successors. These intellectual property rights are not transferred in part or in full to any other party. Presentation of any or all of the data or interpretations for purposes other than those necessary to satisfy the goals of the investigation are not permitted without the express written consent of the author. The findings may not be used for purposes outside those originally intended. Unauthorized uses include but are not limited to internet or electronic presentation for marketing purposes, presentation of findings at professional venues, or submission of scholarly articles.

Standard of Care

Highbridge has performed its services in conformance with the care and skill ordinarily exercised by reputable members of the profession practicing under similar conditions at the same time. No other warranty of any kind, expressed or implied, in fact or by law, is made or intended. Interpretations and results are based strictly on samples provided and/or examined.

Cover Image

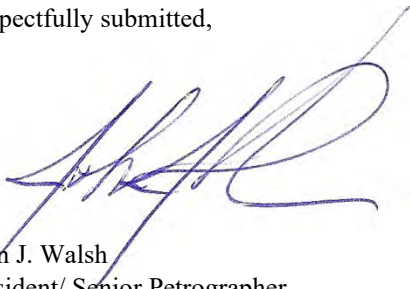
The Bennington Battle Monument in Bennington, VT. Image downloaded August 26, 2023 without modification.

Photo credit: King of Hearts

https://commons.wikimedia.org/wiki/File:Bennington_Battle_Monument_October_2021_001.jpg

Under Creative Commons License CC BY-SA 4.0 - <https://creativecommons.org/licenses/by-sa/4.0/deed.en>

Respectfully submitted,



John J. Walsh
President/ Senior Petrographer
Highbridge Materials Consulting, Inc.

1. Executive Summary

This report presents the results of a petrographic examination on three dimension stone samples taken from the interior of the Bennington Battle Monument, Bennington, VT. These are described by the client as the light yellowish white stone.

All three samples are identified as fine-grained calcitic marble. There are no distinctive accessory minerals and no potentially unstable minerals such as pyrite. There is no significant variation in mineralogy or microtexture between the three samples. Diffuse orange-toned veins are variably distributed throughout the core samples. All are nearly parallel to the core axes. Microcracks and hairline cracks coincide with some of the veins and these are interpreted to predate the construction.

The marble exhibits no incipient granular disaggregation (i.e., sugaring). A modest grain size variation and a predominance of interpenetrating grain boundaries provide resistance to this type of decay. Excluding the fine cracks, the stone is cohesive and sound. No potential durability issues are identified.

The exposed surfaces of the three marble cores exhibit an orange discoloration. This seems to correlate with some chemical corrosion of calcite crystals and the development of a fine veneer with possible iron-rich particulates. Though it was not possible to fully investigate the surface weathering petrographically, it is certainly superficial. The discoloration is interpreted to be a natural patina or residue related to iron release and oxidation within the stone itself. It does not appear to be an extrinsic deposit.

2. Introduction

On July 6 and 7, 2023, Highbridge received a total of eight stone masonry cores from Ms. Danielle Pape of Jablonski Building Conservation, Inc. According to Ms. Pape, the samples were recovered from the Bennington Battle Monument, Bennington, VT. The monument is a stone obelisk completed in 1889.

The client indicates that four of the samples were taken from the interior and four from the exterior. A summary of the samples and their identifications are presented in Table 2.1. Photographs provided by the client indicate the cores to have been taken horizontally through individual masonry units. The orientation of the vertical plane was not indicated on the samples.

Table 2.1: Summary of Received Samples

The laboratory has assigned shortened sample identifications to simplify reporting and these identifications will be used throughout all reports. The laboratory identification is shown in the "HMC ID" column.

Client ID	HMC ID	Description from client transmittal
JBC-West-1	1N	Interior, light yellowish white stone, theoretically from a local quarry
JBC-East-2	2N	Interior, light yellowish white stone, theoretically from a local quarry
JBC-West-3	3N	Interior, light yellowish white stone, theoretically from a local quarry
JBC-West-4	4N	Interior, dark gray stone, theoretically from a local quarry
JBC-North-5	5X	Exterior, moderate bluish gray dolomitic limestone quarried from Hudson Falls, NY
JBC-East-6	6X	Exterior, moderate bluish gray dolomitic limestone quarried from Hudson Falls, NY
JBC-East-7	7X	Exterior, moderate bluish gray dolomitic limestone quarried from Hudson Falls, NY
JBC-North-8	8X	Exterior, moderate bluish gray dolomitic limestone quarried from Hudson Falls, NY

At the client's request, a petrographic examination is performed on each sample. The testing includes a characterization of the mineralogy and microtexture of the stone. The client has mentioned a cracking condition described as "checkerboard" cracking that is usually accompanied by some type of salt run or efflorescence. While there is a desire to investigate the nature of this cracking, the author has suggested that a careful description of the crack geometry and a sample that includes a good representation of the cracking would be necessary to approach this issue.

This report presents the results for the three interior marble samples (1N, 2N, and 3N). Results for the other samples will be presented under separate cover.

3. Methods of Examination

The petrographic examination was conducted in accordance with the standard practices contained within ASTM C1721-22. Data collection is performed or supervised by a degreed geologist who by nature of their education is qualified to operate the analytical equipment employed. Analysis and interpretation are performed or directed by a supervising petrographer who satisfies the qualifications as specified in Section 4 of ASTM C856/C856M-20.

The following personnel contributed to the examination:

Technicians:	M. Pattie A. Ledwitch
Petrographer:	J. Walsh

4. Petrographic Findings and Discussion

4.1 - Lithology

The material represented by Samples 1N, 2N, and 3N is a fine-grained calcitic marble. All samples clearly represent the same source rock. The marble texture is moderately seriate, xenoblastic, and moderately interlobate meaning that there is some variation in grain size, crystal faces are not distinct, and grain boundaries have somewhat irregular profiles. The marble has a foliation produced by a slight flattening of the constituent calcite crystals. The stone consists almost entirely of calcite. No dolomite is detected. Quartz and white mica (probably muscovite) are found in trace quantity. No accessory minerals are identified. There are traces of iron alteration products and these are usually associated with the mica. No iron sulfide minerals are detected.

The marble exhibits a diffuse orange-toned veining to varying degree. The veining has a centimeter spacing and is oriented approximately parallel to the core axis in each sample. The veining typically correlates with areas very slightly more enriched in quartz and mica. However, these trace minerals are quite sparse and do not form discrete seams. There is a greater concentration of iron alteration product present within the veins. This is responsible for the warm tone of these features.

Hairline cracking and microcracking are present to varying degree with the most regular cracking observed in Sample 2N. Crack spacing is anywhere from one to several centimeters. The cracking parallels the metamorphic fabric and coincides with the diffuse veins. Much if not all of this cracking is likely to have predated the installation.

A non-cohesive tensile joint is present in Sample 3N. The joint has a dip of about 55° relative to the metamorphic fabric. The minimum distance from the exterior core surface is 3.5". The author does not know whether the joint intersects the face of the stone somewhere outside of the corehole. A veneer of iron-rich clay coats the joint surface.

4.2 - Secondary Service Effects

Assuming the cracks are pre-existing geological structures, all observed secondary effects are superficial weathering features. The bulk of the marble is sound and no incipient intergranular failures are identified in any of the three samples. No deleterious salts are identified at the scale of the light microscope. Of course, it is always possible for submicroscopic salts to be present with the stone capillaries. Other instrumental analysis would be required to identify these.

Samples 1N and 3N exhibit very minor grain corrosion within the outermost millimeter or two, and this has resulted in an increase in the surface microporosity. In Sample 1N, the corrosion is characterized by a rounding of grain boundaries. In Sample 3N, a jagged comb-like etching has occurred along grain surfaces. In either case, the corrosion has resulted in the development of micropores at the junction between adjacent calcite crystals.

All three samples have outer surfaces that display an orange-hued discoloration. Microscopically, there is an ultrafine clay-like deposit or residue on the surfaces and sometimes within the subsurface pores created by the grain boundary corrosion. The fine material contains some reddish particulates that likely consist of iron oxides or iron oxide-hydroxides. The full composition of the fine-grained veneer cannot be determined through the qualitative petrographic examination. Scanning electron microscopy and electron dispersive spectroscopy would be necessary for a more thorough characterization of the surface weathering.

4.3 - Discussion

The protolith of the marble would have been a highly pure calcitic limestone. The veined areas represent depositional events for which there was a slight influx of terrigenous quartz and clay sediment. However, these were not major flood depositions that resulted in a continuous layer or seam of siliceous sediment. It would seem reasonable that the marble would have come from one of the many marble quarries in Vermont. However, the mineralogy and microtexture are highly nondescript and not diagnostic of a particular quarry source.

The microscopic grain corrosion observed along exposed surfaces is of a type that usually results from the interaction of carbonate minerals with acidic agents. These can be natural acids such as soft water or water enriched in carbon dioxide from the atmosphere. When sulfur dioxide is present from industrial pollution, the dissolved calcium can react with the sulfate to form gypsum. No gypsum is observed in association with any of the surface weathering. Mild acids can also be present in cleaning agents. Distinguishing between these possibilities cannot be accomplished through a routine petrographic examination.

The author has not visited the site. However, the client has provided a photograph of the area where Sample 1N was taken. All of the marble in this vicinity has a uniform orange discoloration along the entirety of each exposed face. Adjacent gray limestone is completely free of any warm discoloration. This suggests that the discoloration is not a deposit but rather a residue or patina. In fact, the surface color is very similar to that of the natural veining observed within the fresh stone. It is also noted that there is no unaltered iron sulfide present anywhere within the three marble cores. The discoloration cannot be the result of the oxidation of microscope pyrite, marcasite, or pyrrotite.

Similar patinas are sometimes developed in dolomitic marble probably due to trace amounts of iron within the dolomite crystal structure that are freed and become oxidized when acidic corrosion occurs along exposed surfaces. Metamorphic calcite is not expected to contain as much iron. Nevertheless, the author has encountered at least one other example of orange discoloration in pure calcitic marble where etching from acid-based cleaners released iron from the calcite to produce an amorphous iron-stained veneer. The veneer identified in this study is qualitatively similar.

The most common decay mode in marble is granular disaggregation. In marble dimension stone, this is the cause of so-called "sugaring". The three samples exhibit good grain cohesion and there is no incipient granular failure anywhere in the stone. Several mineralogical and textural features of marble dictate how susceptible any particular marble may be to this phenomenon. With regard to mineralogy, calcitic marbles are generally more susceptible than dolomitic marbles due to the highly anisotropic coefficient of thermal expansion in calcite. The marbles in this study are calcitic and therefore more susceptible to grain boundary stresses during diurnal thermal cycling. However, within the spectrum of grain boundary textures, these marbles have a modest grain size variation and a significant amount of interpenetration between adjacent calcite crystals. The microtexture provides resistance to granular disaggregation and this counteracts any susceptibility caused by the mineralogy.

The client has described a type of cracking that the project members are referring to as "checkerboard cracking". The client has provided two photographs of the dark interior limestone illustrating these cracks. These show an orthogonal crack pattern characterized by continuous and approximately equidistant horizontal cracks and occasional vertical cracks that truncate against the horizontal structures. While the marble contains some horizontal cracking coincident with veins, there are no photographs showing any significant vertical cracks. Furthermore, the limestone cracking is sharp and the crack intersections appear to be flush with the face of the stone. Instead, the crack intersections in the marble appear to be recessed along the face. This suggests pre-existing cracks along which subsequent chemical weathering had localized. Based on the petrographic observations, the marble cracks are interpreted to predate the construction.

5. Petrographic Data

Table 5.1: Petrographic Data

Sample ID	JBC-West-1
As-received description	
Dimensions	The sample consists of one intact core sample with a 2.75" diameter and a 13.0" length. Orientations were not included with the sample. However, the marble fabric is perpendicular to the face of the stone suggesting a naturally-bedded masonry orientation. For the analysis, the stone was cross-sectioned perpendicular to this fabric. The outer direction is apparent from the surface weathering.
Appearance and fabric	The material is a dense uniform white marble with a diffuse orange-toned veining that is faintly visible along the core circumference. The stone is fine-grained and equigranular. The fresh color observed along the rear break is warm white (Munsell color code approximately N9). The weathered color is light salmon (Munsell color code approximately 7.5YR 7/3).
Structure	A series of broadly en echelon cracks or seams are parallel or subparallel to the veining. These appear to be slowly water-permeable.
Outer surface	The surface is ruggedly planar with a shallow elephant-skin texture. Low spots coincide with the cracking and possibly also the veining. There are some local high spots that may coincide with less-soluble siliceous minerals. The surface is uniformly weathered to a light salmon color.
Inner surface	The inner face is a clean, artificial drilling break exposing fresh marble.
Lithological identification	
Description	The stone is identified a fine-grained calcitic marble with a seriate xenoblastic interlobate grain texture and a planar foliation.
Mineralogy	
Calcite	The stone consists almost entirely of calcite. Grain sizes range from approximately 0.1 to 0.6 millimeters in length. All crystals exhibit deformation twins with two orientations visible in most grains in thin section. The twin planes are mostly planar though there are rare occurrences of slightly curved twins. The twin planes have moderate thickness. Though not quantified, the distribution of twin plane orientations appears to be anisotropic with a greater abundance of twins oriented at a low angle to the metamorphic fabric.
Quartz	Quartz is a trace constituent that occurs as very fine, equidimensional, anhedral crystals usually no more than a few tens of microns in diameter. These occur between adjacent calcite crystals. Though distributed throughout the stone, these tend to be somewhat more concentrated within diffuse veins and near open seams.
Mica	White mica is a trace phase. Some of it is present as discrete crystal platelets oriented parallel to the marble fabric. Others occur in very fine rounded "lumps" usually several tenths of a millimeter in diameter. These are intermixed with iron alteration products and likely represent a higher grade mineral that had been replaced as a retrograde metamorphic reaction. The mica occurs primarily within diffuse veins and near open seams.
Iron alteration product	Exceptionally fine iron alteration products are observed in association with mica or sometimes alone. As with the mica, the iron alterations tend to be concentrated within the orange-toned veins.
Microtexture	
Grain texture	The marble exhibits an interlocking grain texture typical of marble. Technically, the microtexture is classified as moderately seriate, xenoblastic, and moderately interlobate meaning that there is some variety of grain sizes, crystal surfaces are not well-defined, and there is some irregular interpenetration of adjacent crystals. Grain boundaries are generally sutured but subgrains are rare.
Fabric	There is a slight grain flattening with long axes that lie approximately 5° from the core axis. Thin sections were only prepared in a vertical orientation perpendicular to the wall surface. As such, it is not clear whether the fabric is defined by a lineation as well as a foliation. There is a diffuse orange-toned veining that parallels the primary metamorphic fabric. This coincides with a slight increase in noncarbonate minerals but this is barely detectable.

Table 5.1 (cont'd.): Petrographic Data

Sample ID	JBC-West-1
Microtexture (cont'd.)	
Grain size	The marble is fine-grained on average. The majority of crystal lengths range from about 0.1 to 0.6 millimeters.
Pore structure	Excluding discrete cracks or seams, there is no microporosity visible at the scale of the light microscope. Polarized light microscopy is only capable of distinguishing micropores on the order of 0.001 millimeters and greater. It is assumed that the marble contains a normal distribution of submicroscopic pore space even if no visible pores are apparent.
Secondary geological effects	
Plastic deformation	Crystal plastic strain is apparent in all grains in the form of deformation twinning, grain flattening, and grain boundary migration.
Brittle deformation	Several cracks are present within the core that are interpreted to be features that pre-exist the stone installation. The cracks are oriented at an approximately 5° angle from the core axis and tend to coincide with or run adjacent to the diffuse veins. Any single crack that extends along the length of the core is actually a series of cracks of several centimeters length that overlap at their crack tips in a shallow en echelon arrangement. The crack spacing is at least a centimeter though several centimeters may be more typical. Microscopically, the crack profile is jagged and more often follows grain boundaries than transects grains. There are often a few closely-spaced parallel microcracks constituting what appears to be a single crack visually. Crack openings are mostly microscopic.
Alteration	The rock is fresh and no significant secondary alteration is observed.
Veins	No discrete mineralized veins or other type of secondary geological mineralization is identified.
Masonry details	
Finish	The finish is rough based on the small area examined in hand sample.
Masonry orientation	The masonry appears to be normally-bedded as the metamorphic fabric is roughly parallel to the core axis. However, no directional arrow was present on the sample and all that can be technically stated is that the metamorphic fabric is perpendicular to the face of the stone.
Secondary service effects	
Cracking	The cracks or seams identified petrographically all appear to represent pre-existing geological features. Within the outermost 5 millimeters, some of the cracks show moderately increased opening thicknesses up to about 0.04 millimeters.
Grain boundary cohesion	No evidence for granular disaggregation is observed throughout the bulk of the marble.
Salt deposition	No significant salt deposits are observed petrographically at the scale of the light microscope. It should be stressed that salts present within submicroscopic capillaries may not be readily viewed petrographically and these are usually better assessed through chemical analysis.
Weathering	The marble exhibits a weathering veneer that extends a maximum of 2 millimeters from the surface but with most notable effects to a depth of only 0.5 millimeters maximum. Within this rind, most of the calcite has been partly dissolved along grain boundaries to produce a secondary microporosity. Past 0.5 millimeters, isolated pores parallel to the metamorphic fabric extend to about 2 millimeters depth. The pores are lined or filled with an ultrafine-grained weathering product that is not resolvable at the scale of the light microscope. Fine reddish particulates within the clay-sized product suggest some iron content.
Soiling	None observed
Biogrowth	None observed

Table 5.2: Petrographic Data

Sample ID		JBC-East-2
As-received description		
Dimensions	The sample consists of one intact core sample with a 2.75" diameter and a 11.5" maximum length. Orientations were not included with the sample. However, the marble fabric is perpendicular to the face of the stone suggesting a naturally-bedded masonry orientation. For the analysis, the stone was cross-sectioned perpendicular to this fabric. The outer direction is apparent from the surface weathering.	
Appearance and fabric	The material is a dense uniform white marble with a diffuse orange-toned veining that is faintly visible along the core circumference and very clear along the rear of the core. The stone is fine-grained and equigranular. The fresh color observed along the rear break is warm white to very light gray (Munsell color code approximately N9 to N8). The weathered color is salmon (Munsell color code approximately 7.5YR 6-6.5/4).	
Structure	A series of broadly en echelon cracks or seams are parallel or subparallel to the veining. These appear to be variably water-permeable.	
Outer surface	The surface is ruggedly planar and uniformly weathered to a salmon color. One of the cracks is visible along the face of the stone.	
Inner surface	The inner face is a clean, artificial drilling break exposing fresh marble. The surface has a stepped pattern due to its intersection with cracks and veins that are perpendicular to the face.	
Lithological identification		
Description	The stone is identified a fine-grained calcitic marble with a seriate xenoblastic interlobate grain texture and a planar foliation.	
Mineralogy		
Calcite	The stone consists almost entirely of calcite. Grain sizes range from approximately 0.1 to 0.6 millimeters in length. All crystals exhibit deformation twins with two orientations visible in most grains in thin section. The twin planes are mostly planar though there are minor occurrences of slightly curved twins. The twin planes have moderate thickness. Though not quantified, the distribution of twin plane orientations appears to be anisotropic with a greater abundance of twins oriented at a low angle to the metamorphic fabric.	
Quartz	Quartz is a trace constituent that occurs as very fine to fine, equidimensional, anhedral crystals or sometimes as small crystal clusters usually no more than about 0.1 millimeters in diameter. These occur between adjacent calcite crystals or within fine mica concentrations. The quartz is concentrated within diffuse veins and near open seams.	
Mica	White mica is a trace phase. A minor proportion of it is present as discrete crystal platelets oriented parallel to the marble fabric. More of the mica occurs in very fine rounded "lumps" usually several tenths of a millimeter in diameter. These are intermixed with iron alteration products and likely represent a higher grade mineral that had been replaced as a retrograde metamorphic reaction. There are also discontinuous seamlets of contorted mica with intermixed iron alteration products. These are found to a maximum size of about 3 millimeters length. All mica occurs within the diffuse veins and near open seams.	
Iron alteration product	Fine iron alteration products are observed in association with mica or sometimes alone. As with the mica, the iron alterations are concentrated within the orange-toned veins.	
Microtexture		
Grain texture	The marble exhibits an interlocking grain texture typical of marble. Technically, the microtexture is classified as moderately seriate, xenoblastic, and moderately interlobate meaning that there is some variety of grain sizes, crystal surfaces are not well-defined, and there is some irregular interpenetration of adjacent crystals. Grain boundaries are generally sutured but subgrains are rare.	
Fabric	There is a slight grain flattening with long axes that lie approximately parallel to the core axis. Thin sections were only prepared in a vertical orientation perpendicular to the wall surface. As such, it is not clear whether the fabric is defined by a lineation as well as a foliation. There is a diffuse orange-toned veining that parallels the primary metamorphic fabric. This coincides with a modest increase in noncarbonate minerals.	

Table 5.2 (cont'd.): Petrographic Data

Sample ID	JBC- East-2
Microtexture (cont'd.)	
Grain size	The marble is fine-grained on average. The majority of crystal lengths range from about 0.1 to 0.6 millimeters. Grain size tends to be finest within the veins.
Pore structure	Excluding discrete cracks or seams, there is no microporosity visible at the scale of the light microscope. Polarized light microscopy is only capable of distinguishing micropores on the order of 0.001 millimeters and greater. It is assumed that the marble contains a normal distribution of submicroscopic pore space even if no visible pores are apparent.
Secondary geological effects	
Plastic deformation	Crystal plastic strain is apparent in all grains in the form of deformation twinning, grain flattening, and grain boundary migration.
Brittle deformation	Several cracks are present within the core that are interpreted to be features that pre-exist the stone installation. The cracks are oriented approximately parallel to the core axis and tend to coincide with or run adjacent to the diffuse veins. Any single crack that extends along the length of the core is actually a series of cracks of several centimeters length that overlap at their crack tips in a shallow en echelon arrangement. The crack spacing is about 2 to 3 centimeters near the face of the stone and about 1 centimeter deeper within the interior. Microscopically, the crack profile is jagged and more often follows grain boundaries than transects grains. Crack openings are all microscopic.
Alteration	The rock is fresh and no significant secondary alteration is observed.
Veins	No discrete mineralized veins or other type of secondary geological mineralization is identified.
Masonry details	
Finish	The finish is somewhat rough based on the small area examined in hand sample.
Masonry orientation	The masonry appears to be normally-bedded as the metamorphic fabric is roughly parallel to the core axis. However, no directional arrow was present on the sample and all that can be technically stated is that the metamorphic fabric is perpendicular to the face of the stone.
Secondary service effects	
Cracking	The cracks or seams identified petrographically all appear to represent pre-existing geological features. Other than this, there is a very minor occurrence of grain boundary microcracking about 1 to 2 grains deep that mostly parallels the outer face
Grain boundary cohesion	No evidence for granular disaggregation is observed throughout the bulk of the marble.
Salt deposition	No significant salt deposits are observed petrographically at the scale of the light microscope. It should be stressed that salts present within submicroscopic capillaries may not be readily viewed petrographically and these are usually better assessed through chemical analysis.
Weathering	No distinctive weathering veneer is observed along the outer face in thin section. There are traces of an ultrafine-grained weathering product that is not resolvable at the scale of the light microscope that is sometimes observed at calcite grain boundaries. Fine reddish particulates within this clay-sized product suggest some iron content.
Soiling	None observed
Biogrowth	None observed

Table 5.3: Petrographic Data

Sample ID	
JBC-West-3	
As-received description	
Dimensions	The sample consists of 2.75" diameter core received in two contiguous pieces with a total length of 12.5". Orientations were not included with the sample. However, the marble fabric appears to be perpendicular to the face of the stone suggesting a naturally-bedded masonry orientation. For the analysis, the stone was cross-sectioned perpendicular to this fabric. The outer direction is apparent from the surface weathering. The core break occurs along a sharp pre-existing crack or structure at a distance between 3.5" and 5.5" from the outer face. If the assumed orientation is correct, the break strikes parallel to the face of the stone, and dips approximately 55° either toward or away from the front surface.
Appearance and fabric	The material is a dense uniform white marble with a diffuse orange-toned veining that is faintly visible along the core circumference. The stone is fine-grained and equigranular. The fresh color observed along the rear break is white (Munsell color code approximately N9). The weathered color is masked by grayish soiling but appears salmon.
Structure	The core break is roughly planar with an orange-brown weathering veneer containing fine brownish specks. There is also one faint crack is visible toward the rear of the core. This is parallel to the veining.
Outer surface	The surface is ruggedly planar and uniformly weathered to a salmon color. The color is masked by some uniform grayish soiling.
Inner surface	The inner face is a clean, artificial drilling break exposing fresh marble.
Lithological identification	
Description	The stone is identified a fine-grained calcitic marble with a seriate xenoblastic interlobate grain texture and a planar foliation.
Mineralogy	
Calcite	The stone consists almost entirely of calcite. Grain sizes range from approximately 0.1 to 0.6 millimeters in length. All crystals exhibit deformation twins with two orientations visible in most grains in thin section. The twin planes are mostly planar though there are rare occurrences of slightly curved twins. The twin planes have moderate thickness. Though not quantified, the distribution of twin plane orientations appears to be anisotropic with a greater abundance of twins oriented at a low angle to the metamorphic fabric.
Quartz	Quartz is a trace constituent that occurs as very fine, equidimensional, anhedral crystals usually no more than a few tens of microns in diameter. These occur between adjacent calcite crystals. Though distributed throughout the stone, these tend to be somewhat more concentrated within diffuse veins and near open seams.
Mica	White mica is a trace phase. Some of it is present as discrete crystal platelets oriented parallel to the marble fabric. Others occur as very fine lens-shaped mica fish that sometimes exhibit additional rotational shear. These are sometimes intermixed with iron alteration products. The mica occurs primarily within diffuse veins and near open seams.
Iron alteration product	Exceptionally fine iron alteration products are observed in association with mica or sometimes alone. As with the mica, the iron alterations tend to be concentrated within the orange-toned veins.
Microtexture	
Grain texture	The marble exhibits an interlocking grain texture typical of marble. Technically, the microtexture is classified as moderately seriate, xenoblastic, and moderately interlobate meaning that there is some variety of grain sizes, crystal surfaces are not well-defined, and there is some irregular interpenetration of adjacent crystals. Grain boundaries are generally sutured but subgrains are rare.
Fabric	There is a slight grain flattening with long axes that lie approximately 5° from the core axis. Thin sections were only prepared in a vertical orientation perpendicular to the wall surface. As such, it is not clear whether the fabric is defined by a lineation as well as a foliation. There is a very diffuse orange-toned veining that parallels the primary metamorphic fabric. This coincides with a slight increase in noncarbonate minerals but this is barely detectable.

Table 5.3 (cont'd.): Petrographic Data

Sample ID	JBC-West-3
Microtexture (cont'd.)	
Grain size	The marble is fine-grained on average. The majority of crystal lengths range from about 0.1 to 0.6 millimeters.
Pore structure	Excluding discrete cracks or seams, there is no microporosity visible at the scale of the light microscope. Polarized light microscopy is only capable of distinguishing micropores on the order of 0.001 millimeters and greater. It is assumed that the marble contains a normal distribution of submicroscopic pore space even if no visible pores are apparent.
Secondary geological effects	
Plastic deformation	Crystal plastic strain is apparent in all grains in the form of deformation twinning, grain flattening, and grain boundary migration.
Brittle deformation	There is a highly planar joint surface at a distance between 3.5" and 5.5" from the outer face. The joint has a dip of approximately 55°. An ultrafine-grained orange-colored weathering product lines the joint face and likely includes some iron alteration phases. There is also some exceptionally minor cracking that tends to coincide with the diffuse orange veins toward the rear of the core. Any cracking identified is incipient and barely detectable at the scale of the light microscope.
Alteration	The rock is fresh and no significant secondary alteration is observed.
Veins	No discrete mineralized veins or other type of secondary geological mineralization is identified.
Masonry details	
Finish	The finish is rough based on the small area examined in hand sample.
Masonry orientation	The masonry appears to be normally-bedded as the metamorphic fabric is roughly parallel to the core axis. However, no directional arrow was present on the sample and all that can be technically stated is that the metamorphic fabric is perpendicular to the face of the stone.
Secondary service effects	
Cracking	The cross-cutting joint is interpreted to represent a pre-existing geological feature. No obvious service-related cracking is evident.
Grain boundary cohesion	No evidence for granular disaggregation is observed throughout the bulk of the marble.
Salt deposition	No significant salt deposits are observed petrographically at the scale of the light microscope. It should be stressed that salts present within submicroscopic capillaries may not be readily viewed petrographically and these are usually better assessed through chemical analysis.
Weathering	The marble exhibits a weathering veneer that extends less than 1 millimeter from the surface. Within this rind, most of the calcite has been chemically etched along crystal boundaries. The etching has a distinctive comb-like texture, at least in a two-dimensional section. The loss of carbonate has resulted in an increased microporosity within this weathered rind. Along the outer surface, there is an ultrafine-grained weathering product that fills in the microscopic embayments between adjacent calcite crystals. The weathering product is not resolvable at the scale of the light microscope. However, minor reddish particulates within the clay-sized product suggest some iron content.
Soiling	None observed
Biogrowth	None observed

Appendix I: Photographs and Photomicrographs

Microscopic examination is performed on an Olympus BX-51 polarized/reflected light microscope and an Olympus SZ40 stereoscopic microscope. The polarized light microscope is fitted with a Tucsen MIchrome 5 Pro 5MP digital camera. The stereoscopic microscope is used for simple magnification. Sample types examined under this microscope include fractured surfaces, fine constituents extracted through chemical or physical means, or honed or polished cross sections. The polarized light microscope (PLM) magnifies but also employs principles of optical crystallography. The most common sample preparation for the PLM is the petrographic thin section. For this preparation, cross-sectioned samples are mounted to glass slides and are milled to a thickness sufficient to allow light to be transmitted through the material. These are usually prepared without water and with minimal heat to avoid altering minerals that are water or temperature-sensitive. In many cases, the samples are impregnated with a low-viscosity, blue-dyed epoxy. When so treated, blue areas represent some type of void space (e.g., air-voids, capillary pores, cracks, etc.). The polarized light photomicrographs are taken using a variety of optical settings chosen to best demonstrate the feature(s) of interest. These are distinguished as follows:

Plane polarized light (abbreviated as PPL)

This method uses the refractive power of different constituents to produce an artificial sense of surface relief. Otherwise, the method is the closest to a simple magnification of the material. The setting is often used to demonstrate granular relationships or microstructure. Pore spaces and cracks are observable with this setting if the blue-dyed epoxy is used.

Conoscopic polarized light (abbreviated as CPL)

In this setting, the transmitted light is condensed just before passing through the thin section. The method tends to bring colors or finer particulates into higher contrast at the expense of image sharpness. The setting is often used to image grain boundary failures in dimension stone, pigment particulates in binders, or gel phases in the micropores of cement pastes.

Cross polarized light (abbreviated as XPL)

The setting places the thin section between two pieces of polarizing film oriented at 90° to one another. In isotropic materials (e.g., glasses, simple salts), all light is absorbed and the materials appear black. In anisotropic crystals, two light rays traveling at different speeds are produced within the thin section and these offset waves interfere at the upper polarizing film. The interference produces a color that can be used to calculate properties of the crystal structure and aid in identification of mineral species. In essence, the colors are artificial. It should be noted that color is a function of orientation and color differences do not necessarily indicate material differences.

Compensator plates

When in XPL mode, full-wave or quarter-wave compensator plates may be inserted into the light path to add or subtract interference. Technically, these methods are used to calculate properties of the crystal structure. However, they can also be used to alter the image appearance to help improve contrast between different constituents. They can also reveal preferred orientations in some materials (e.g., oriented residual crystallinity in fired ceramics).

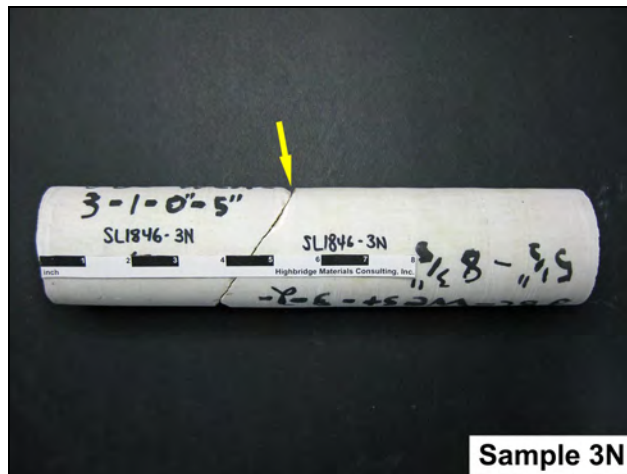
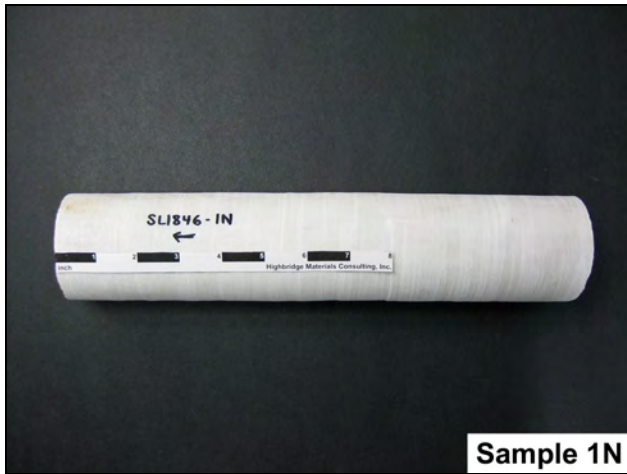


Figure 1: Photographs of the three interior marble cores provided to Highbridge for petrographic examination. The cores are shown in side view with their outer surfaces oriented toward the left of each image. The arrow shows a non-cohesive geological joint in Sample 3N.

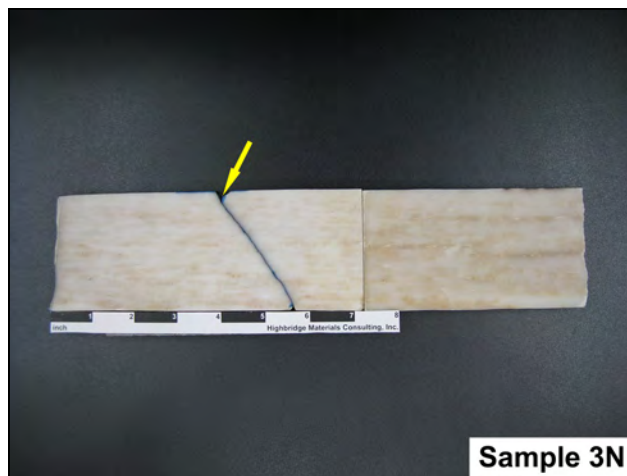
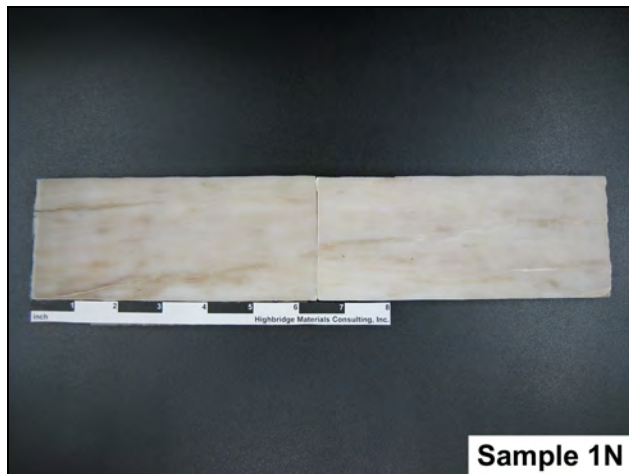


Figure 2: Photographs of honed sections of the three marble cores. These are oriented the same as in the last figure. Note that the marble is uniform with the exception of diffuse orange-toned veins. The joint in Sample 3N is again indicated by an arrow.

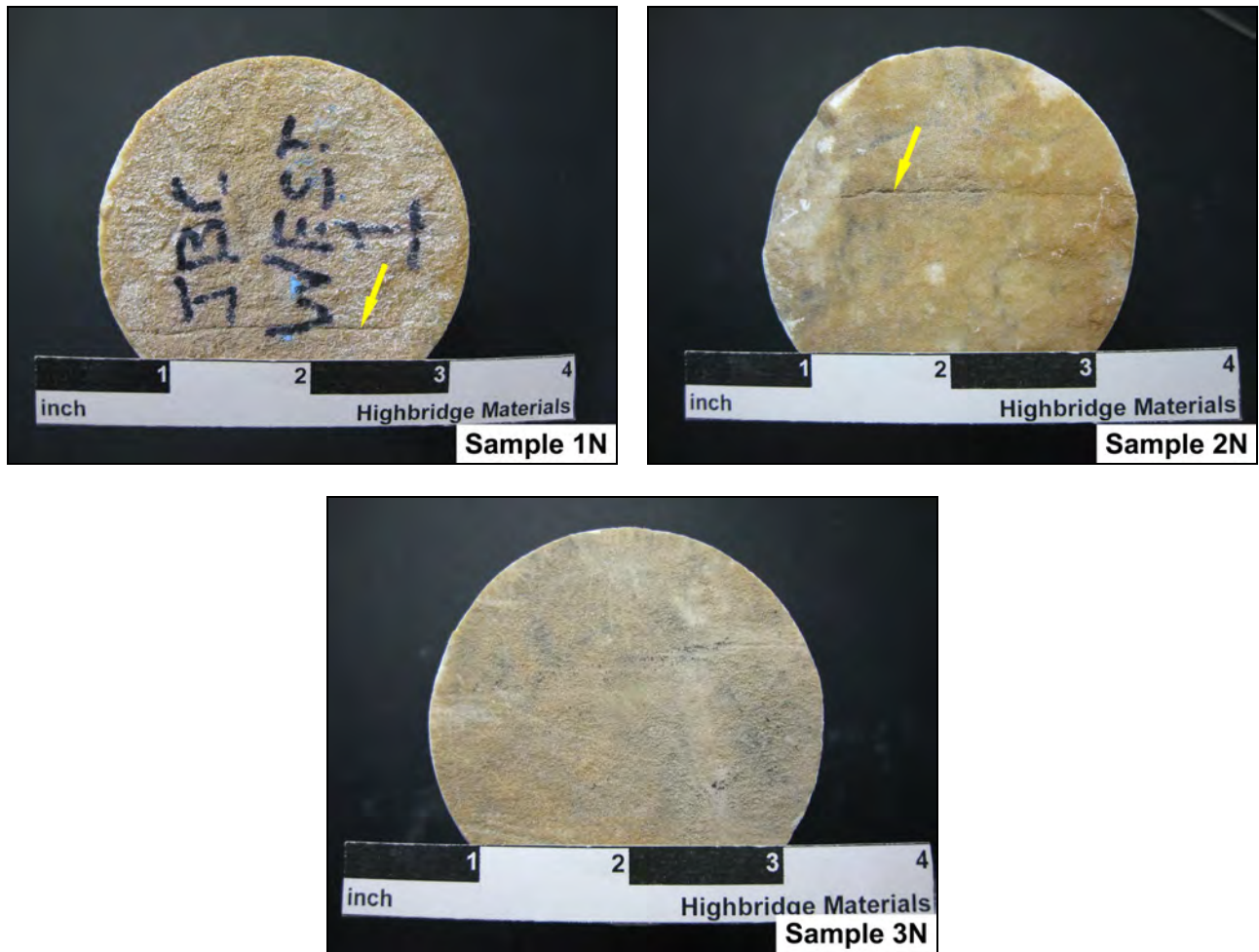


Figure 3: Photographs of the outer cores surfaces. Note that all have an orange-hued discoloration. A few fine cracks intersect the outer surfaces (arrows). These are interpreted to predate the construction.

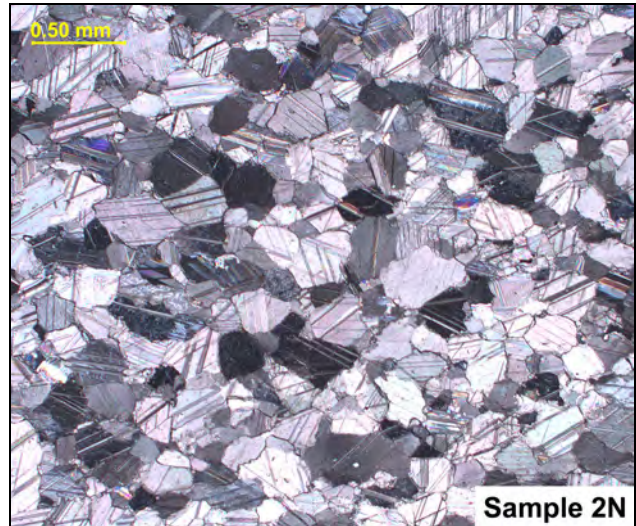
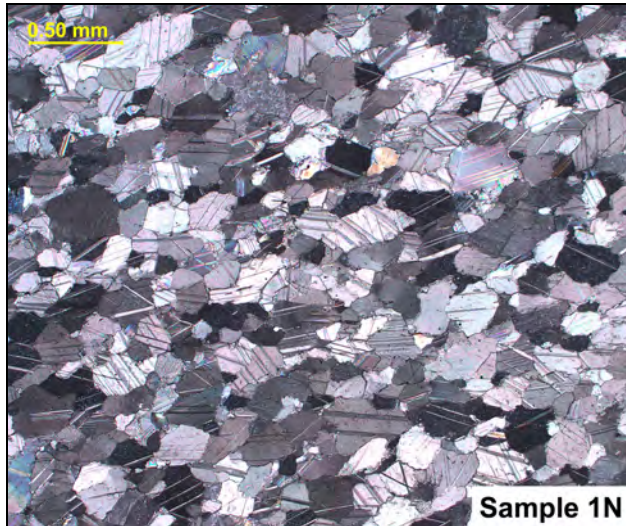


Figure 4: XPL photomicrographs illustrating the mineralogy and microtexture of the marble. The stone consists of a mosaic of calcite crystals. There is a modest grain size variation and a slight grain flattening. Grain boundaries are mostly irregular and interlobate.

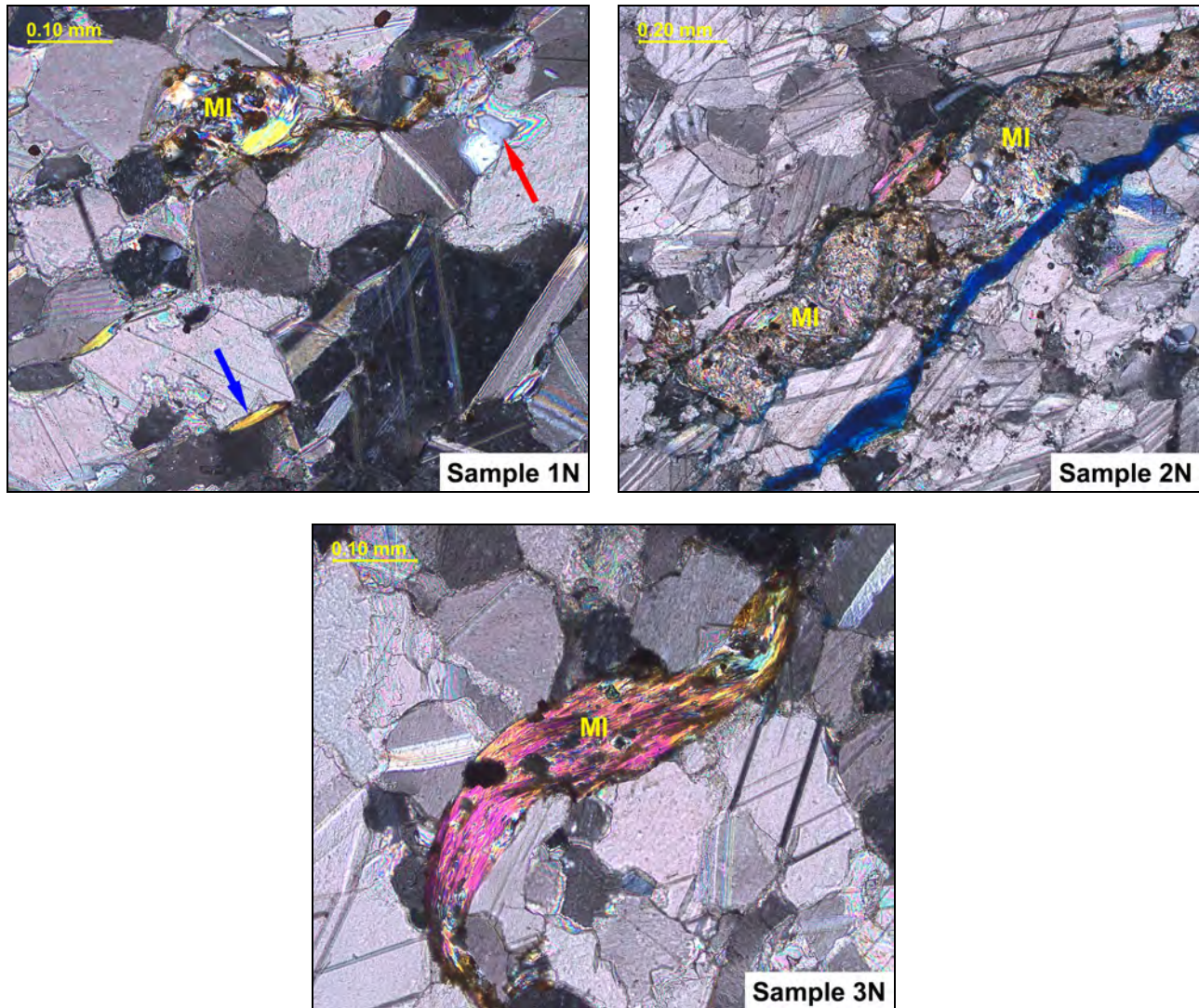


Figure 5: XPL photomicrographs illustrating the trace mineralogy of the marble. Mica crystals are shown (MI and blue arrow). The mica exhibits different morphologies. The blue arrow in the upper left image shows a typical platelet. The other mica in this image is a fine cluster of contorted crystals intermixed with some iron oxide. The mica in the upper left image occurs in a fine discontinuous seamlet of contorted crystals. In the lower image, a mica "fish" is slightly sheared. The red arrow in the upper left image indicates a fine quartz grain.

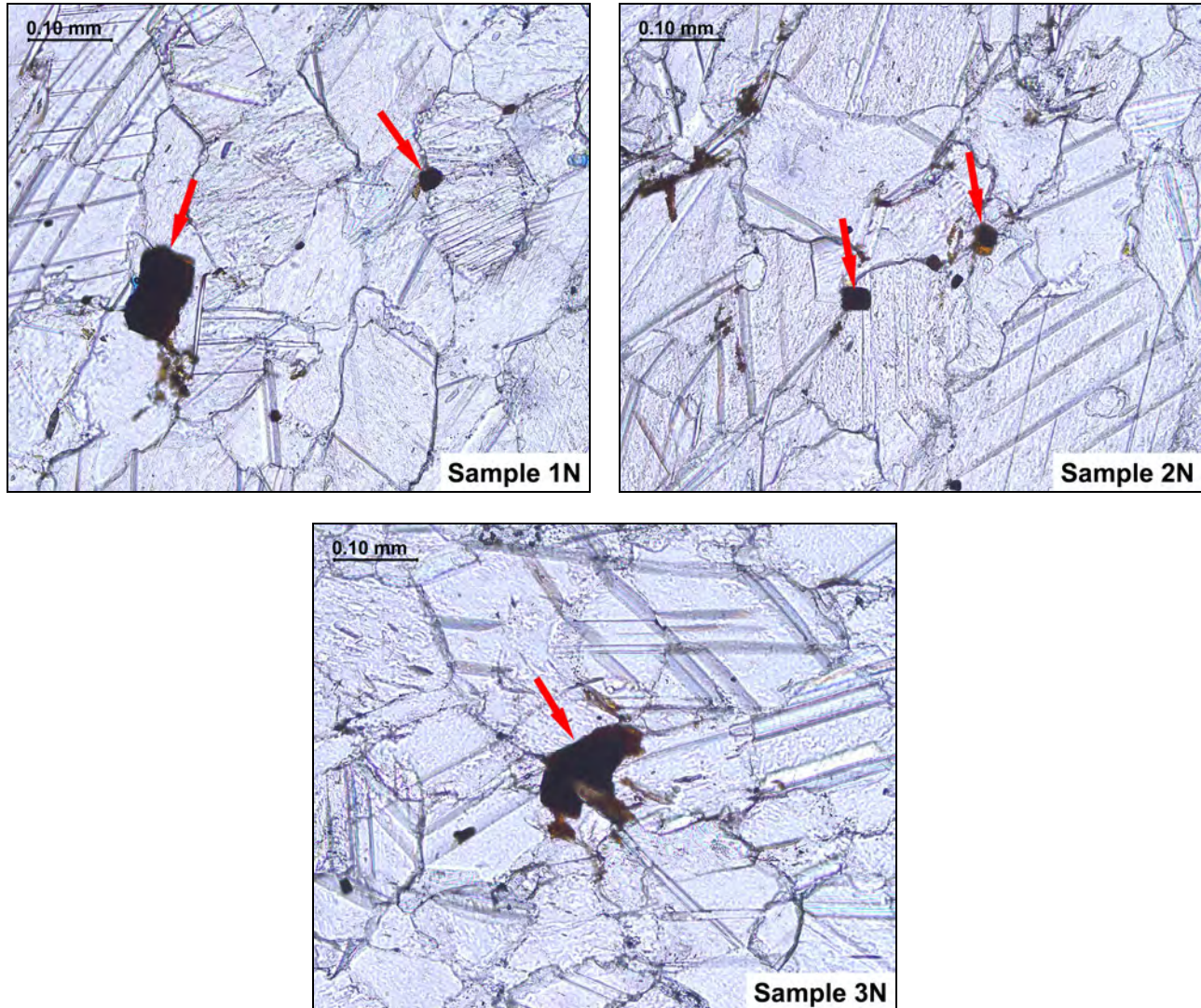


Figure 6: PPL photomicrographs. The arrows indicate fine iron alteration products. These sparse grains are responsible for the diffuse orange hue of the veins.

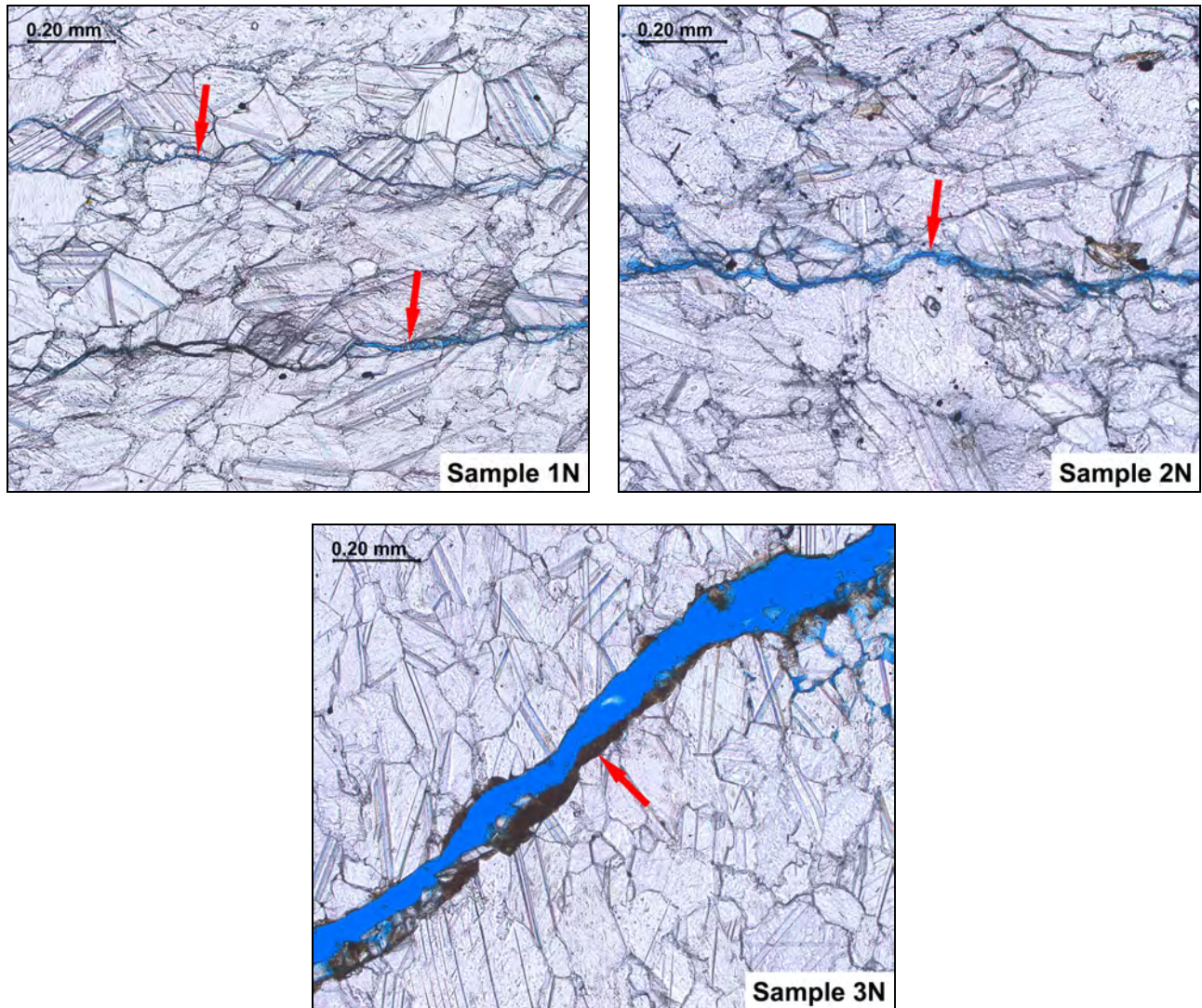


Figure 7: PPL photomicrographs. (Upper images) The arrows indicate fine microcracks that coincide with the veins. These likely predate the construction and relate to the very slight mineralogical and textural differences within these planes. No deleterious salts are identified within the cracks. (Lower image) The arrow indicates the tensile joint in Sample 3N. Note that the joint is lined with a very fine alteration product rich in iron oxide.

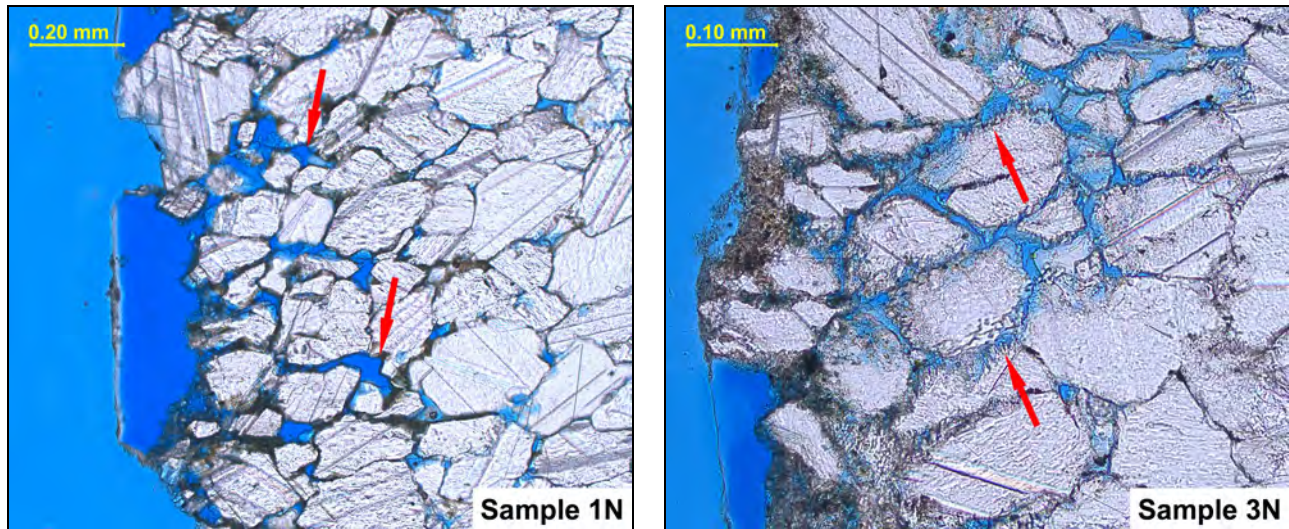


Figure 8: PPL photomicrographs taken at the outer surfaces of Samples 1N and 3N. Note that the images are taken at different magnifications. The arrows indicate pore spaces created through the acidic etching of constituent calcite crystals. The grain corrosion is more uniform in Sample 1N. In Sample 3N, the etching has produced fine jagged comb-like structures.

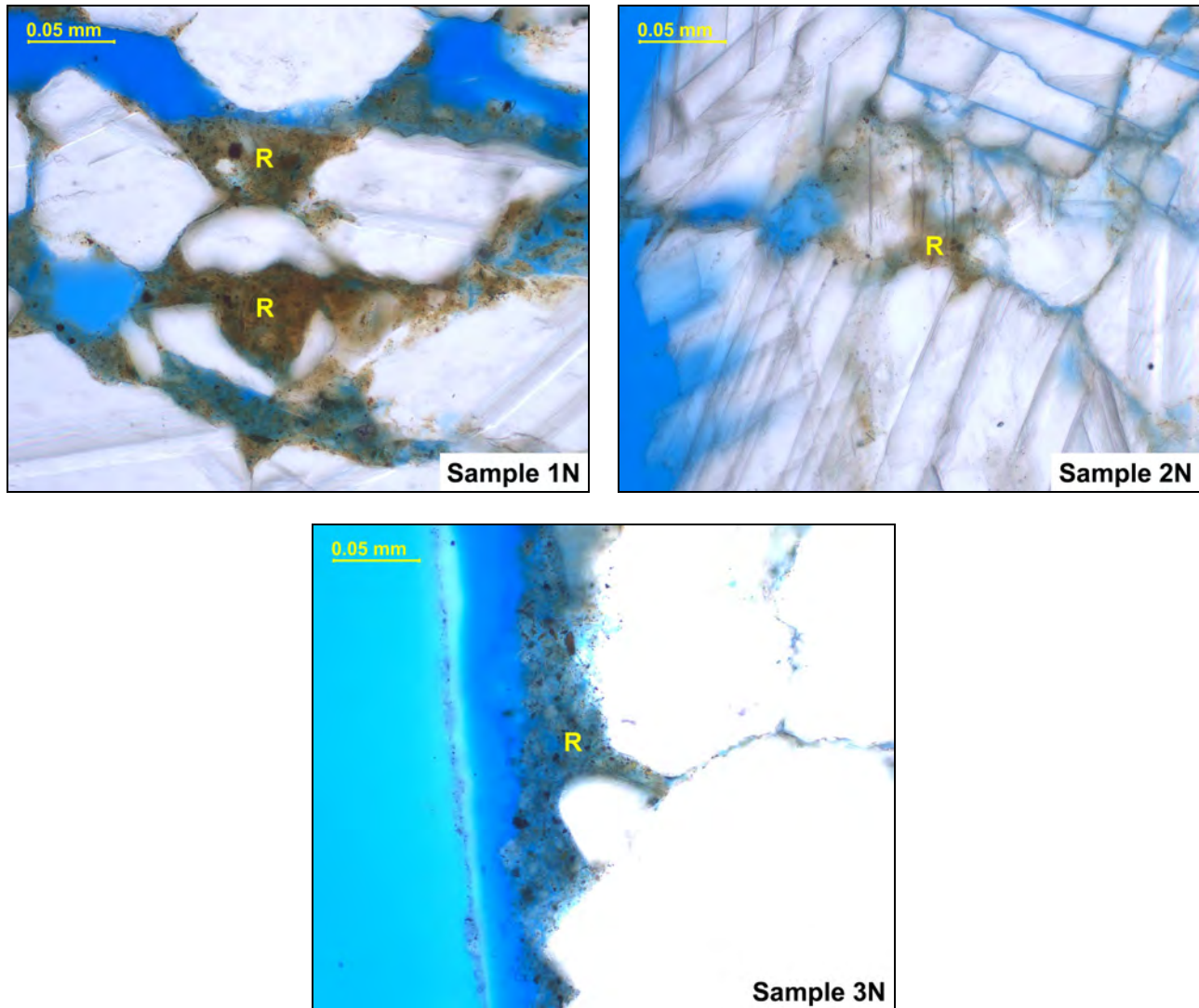
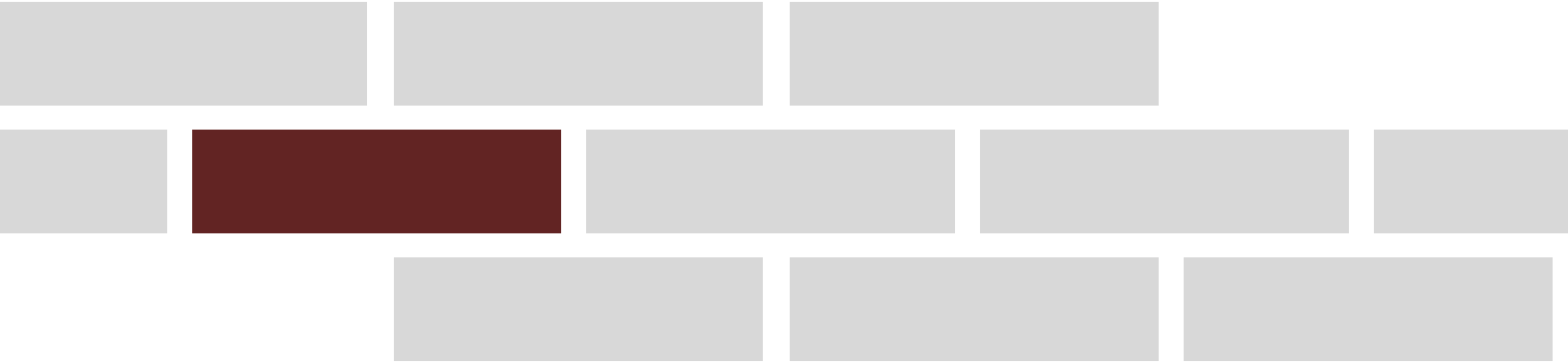


Figure 9: CPL photomicrographs taken at the outer surfaces of all three samples. The outer surface and some subsurface pores are lined with a residue (R) containing ultrafine-grained reddish particulates believed to consist of iron oxides. These residues are interpreted to be responsible for the orange discoloration on each surface. The iron may have been released through the corrosion of the surface calcite.

Petrographic Examination of Interior Limestone

Bennington Battle Monument

15 Monument Circle, Bennington, VT 05201



Prepared for
Jablonski Building Conservation, Inc.

Client ID
JABL001

Report No.
SL1846-02

Report Date
08/28/23



Confidentiality

This report presents the results of laboratory testing requested by the client to satisfy specific project requirements. As such, the client has the right to use this report as necessary in any commercial matters related to the referenced project. Any reproduction of this report must be done in full. In offering a more thorough analysis, it may have been necessary for Highbridge to describe proprietary laboratory methods or present opinions, concepts, or original research that represent the intellectual property of Highbridge Materials Consulting and its successors. These intellectual property rights are not transferred in part or in full to any other party. Presentation of any or all of the data or interpretations for purposes other than those necessary to satisfy the goals of the investigation are not permitted without the express written consent of the author. The findings may not be used for purposes outside those originally intended. Unauthorized uses include but are not limited to internet or electronic presentation for marketing purposes, presentation of findings at professional venues, or submission of scholarly articles.

Standard of Care

Highbridge has performed its services in conformance with the care and skill ordinarily exercised by reputable members of the profession practicing under similar conditions at the same time. No other warranty of any kind, expressed or implied, in fact or by law, is made or intended. Interpretations and results are based strictly on samples provided and/or examined.

Cover Image

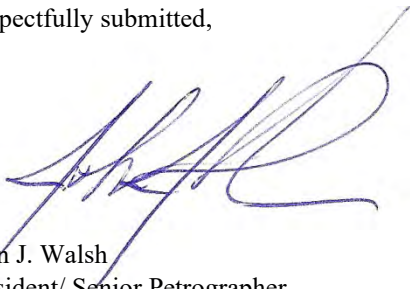
The Bennington Battle Monument in Bennington, VT. Image downloaded August 26, 2023 without modification.

Photo credit: King of Hearts

https://commons.wikimedia.org/wiki/File:Bennington_Battle_Monument_October_2021_001.jpg

Under Creative Commons License CC BY-SA 4.0 - <https://creativecommons.org/licenses/by-sa/4.0/deed.en>

Respectfully submitted,



John J. Walsh
President/ Senior Petrographer
Highbridge Materials Consulting, Inc.

1. Executive Summary

This report presents the results of a petrographic examination on one dimension stone sample taken from the interior of the Bennington Battle Monument, Bennington, VT. The material is described by the client as the dark gray stone.

The material is identified as a silicified dolomitic breccia. It consists of centimeter-scale clasts of uniform dolostone bound by a matrix of recrystallized quartz. A minor amount of clay from the original limestone is encapsulated within the densely recrystallized rock. The stone is hard, non-porous, and monolithic.

The material is considered sound and durable. No potential weaknesses are identified within the bulk of the stone. However, residues of secondary veins are present along the front and back of the stone. These could be seen as potential weaknesses if they were present within the stone rather than on the faces of the masonry unit. The reddish color of the vein material is an intrinsic iron oxide naturally present within the vein. No secondary weathering is identified that can be attributed to the service environment.

2. Introduction

On July 6 and 7, 2023, Highbridge received a total of eight stone masonry cores from Ms. Danielle Pape of Jablonski Building Conservation, Inc. According to Ms. Pape, the samples were recovered from the Bennington Battle Monument, Bennington, VT. The monument is a stone obelisk completed in 1889.

The client indicates that four of the samples were taken from the interior and four from the exterior. A summary of the samples and their identifications are presented in Table 2.1. Photographs provided by the client indicate the cores to have been taken horizontally through individual masonry units. The orientation of the vertical plane was not indicated on the samples.

Table 2.1: Summary of Received Samples

The laboratory has assigned shortened sample identifications to simplify reporting and these identifications will be used throughout all reports. The laboratory identification is shown in the "HMC ID" column.

Client ID	HMC ID	Description from client transmittal
JBC-West-1	1N	Interior, light yellowish white stone, theoretically from a local quarry
JBC-East-2	2N	Interior, light yellowish white stone, theoretically from a local quarry
JBC-West-3	3N	Interior, light yellowish white stone, theoretically from a local quarry
JBC-West-4	4N	Interior, dark gray stone, theoretically from a local quarry
JBC-North-5	5X	Exterior, moderate bluish gray dolomitic limestone quarried from Hudson Falls, NY
JBC-East-6	6X	Exterior, moderate bluish gray dolomitic limestone quarried from Hudson Falls, NY
JBC-East-7	7X	Exterior, moderate bluish gray dolomitic limestone quarried from Hudson Falls, NY
JBC-North-8	8X	Exterior, moderate bluish gray dolomitic limestone quarried from Hudson Falls, NY

At the client's request, a petrographic examination is performed on each sample. The testing includes a characterization of the mineralogy and microtexture of the stone. The client has mentioned a cracking condition described as "checkerboard" cracking that is usually accompanied by some type of salt run or efflorescence. While there is a desire to investigate the nature of this cracking, the author has suggested that a careful description of the crack geometry and a sample that includes a good representation of the cracking would be necessary to approach this issue.

This report presents the results for the one interior limestone sample (4N). Results for the other samples will be presented under separate cover.

3. Methods of Examination

The petrographic examination was conducted in accordance with the standard practices contained within ASTM C1721-22. Data collection is performed or supervised by a degreed geologist who by nature of their education is qualified to operate the analytical equipment employed. Analysis and interpretation are performed or directed by a supervising petrographer who satisfies the qualifications as specified in Section 4 of ASTM C856/C856M-20.

The following personnel contributed to the examination:

Technicians:	M. Pattie A. Ledwitch
Petrographer:	J. Walsh

4. Petrographic Findings and Discussion

4.1 - Lithology

Sample 4N consists of a fine-grained, bluish-gray dolomitic breccia. The dolomitic portion of the stone consists of irregular centimeter-scale fragments that are surrounded by regions of fine to medium-grained recrystallized quartz. The dolomite has a grain size of about 0.1 to 0.2 millimeters. The quartz ranges in size from 0.01 to 0.5 millimeters. Carbonaceous clay is present in the microscopic interstices between dolomite crystals. The clay also occurs as discontinuous seams that "float" in the quartz. The carbonaceous component is exceptionally fine-grained and it is not clear whether the carbon is present as a hydrocarbon or as finely disseminated graphite. With the exception of the clay seams, none of the original limestone microtexture is preserved.

At the scale of the core sample, the stone is completely monolithic with no obvious bedding structure or other sedimentary texture. The sparse and discontinuous clay seams likely parallel the original sedimentary bedding. These are oriented at an angle of approximately 45° from the masonry surface. As the core was not oriented, the disposition of the bedding orientation relative to the construction cannot be determined.

There is no significant porosity and the stone is quite dense. No stylolites, cracks, or other planes of preferential weakness are identified within the bulk of the stone. However, the face of the masonry and the rear of the core sample contain secondary vein structures. It is not known if these are complete or if there would have been a much greater thickness of crystallized material attached to what is present in the core. The veins contain slivers of partly preserved limestone with a microsparite texture. The veins are stained red by hematite (iron oxide) that lines the vein surfaces and the limestone slivers. The hematite indicates geological fluid flow along the vein structure. Similarly, there is some minor secondary dissolution of the dolomite just adjacent to the vein resulting in secondary pores along the grain boundaries.

4.2 - Secondary Service Effects

The sample provided for examination is sound, and no deleterious service effects are identified petrographically. No cracking, crumbling, or other physical distress is observed. No deleterious salts are identified at the scale of the light microscope. Of course, it is always possible for submicroscopic salts to be present with the stone capillaries. Other instrumental analysis would be required to identify these.

4.3 - Discussion

The stone is thoroughly recrystallized and it is not possible to determine what the original rock might have been in detail other than an argillaceous limestone. The manner in which the dolomitic regions are distributed suggests that the apparent fragmentation of the original limestone was tectonic rather than depositional. Additionally, sparsely distributed clay seams all share a similar orientation that precludes the random deposition of sedimentary particles. Whatever the case, all of the fragmentation appears to predate the dolomitization and silicification of the rock. These secondary mineralogical overprints nearly obliterate all but the basic structure of the breccia.

The mass of dolomite and quartz is essentially a monolith with no regions or planes of relative weakness. The only planes are the iron-rich veins that are found at the front and rear of the stone. A photograph provided by the client illustrates that the vein remnants are present as a patchy reddish residue on the face of the masonry unit. The iron itself is intrinsic to the vein and does not represent weathering of the stone in service. The veins would represent weaker horizons if they were present within the stone and favorably oriented. The author does not know how widespread these features might be.

The client has described a type of cracking that the project members are referring to as "checkerboard cracking". The client has provided two photographs of the dark interior limestone illustrating these cracks. These show an orthogonal crack pattern characterized by continuous and approximately equidistant horizontal cracks and occasional vertical cracks that truncate against the horizontal structures. The crack pattern is not evident in the photograph for this particular sample location. Furthermore, in the sample examined for this report, there is no evidence for any orthogonal cracking or any pre-existing structure that might give rise to this type of cracking. No further commentary may be offered regarding this crack pattern without examining samples that include the structure.

5. Petrographic Data

Table 5.1: Petrographic Data

Sample ID	JBC-West-4
As-received description	
Dimensions	The sample consists of 2.75" diameter core received in two contiguous pieces with a total maximum length of 11.75". Orientations were not included with the sample. The outer direction is apparent from the surface weathering. However, there is no sedimentary or structural fabric that might help understand the stone orientation and plan a cross-section. The core break occurs at approximately 6.5" from the face of the stone. The break appears to have occurred along fresh limestone. There is no evidence to suggest that this might be a pre-existing structure.
Appearance and fabric	The material is a dense bluish-gray dolostone with a centimeter-scale mottling. Dark areas are finer-grained and light areas are sparry. The fresh color along core breaks is dark bluish-gray (Munsell color code approximately 5PB 4.25/0.75). Most of the weathered face is coated by a mineralized vein. Small windows through the vein are either medium gray or an ochre yellow.
Sedimentary features	The stone appears monolithically bedded with a centimeter-scale nodular texture. No bedding planes or laminations are visible in the core sample.
Structure	The front and rear of the sample contain very thin mineralized veins. The one on the face is roughly perpendicular to the core axis and at least 50% complete. The one at the rear is about 45° to the core axis and covers only about 20% of the surface. Both veins are stained pink to rich red.
Outer surface	The surface is ruggedly planar and contains a mineralized vein as discussed above. The remainder of the surface is mostly lightly soiled.
Inner surface	The inner face is a clean, artificial drilling break exposing fresh limestone.
Lithological identification	
Description	The rock is a dolomitic breccia with quartzose matrix.
Lithological components	
Carbonate matrix	A fine carbonaceous clay matrix occurs as an interstitial phase between intergrown dolomite crystals. In thin section, the clay appears within the mostly triangular-shaped interstices between adjacent dolomite crystals. The clay also "dots" the contacts between pairs of adjacent crystals that are in more complete contact.
Bioclasts	None observed
Peloids	None observed
Ooids	None observed
Intraclasts	None observed
Non-carbonate constituents	In addition to the interstitial clay described above, approximately 30% of the rock consists of quartz that occurs interstitially to irregular centimeter-scale "fragments" of dolostone. The quartz is very fine to medium-grained. The very fine material consists of subgrains formed through deformation of the quartz. The medium-grained quartz exhibits grain boundary suturing resulting from grain boundary migration processes. Included within the quartz are sparse discontinuous seams and truncated fragments of carbonaceous clay. The clay seams sometime grade into muscovite. The quartz also includes traces of very fine-grained hematite clusters that are replacements for pyrite. These are generally associated with the clay. No unaltered pyrite is detected.
Grain size	Dolomite crystals are uniformly fine-grained with crystal sizes ranging from 0.1 to 0.2 millimeters. Though somewhat bimodal, the quartz is much more variable in size with grains from 0.01 to 0.5 millimeters in diameter.
Grain shape	The dolomite is rhombic in shape and crystals are euhedral to subhedral. Where well-formed crystal faces are observed, these are often curved. The quartz is equidimensional and anhedral.
Pore structure	There is no significant microporosity visible at the scale of the light microscope throughout most of the dolostone. Only just adjacent to the vein is there some very local secondary porosity developed within the dolomitic portion of the stone. With that said, note that polarized light microscopy is only capable of distinguishing micropores on the order of 0.001 millimeters and greater. It is assumed that the dolostone contains a normal distribution of submicroscopic pore space even if no visible pores are apparent.

Table 5.1 (cont'd.): Petrographic Data

Sample ID	JBC-West-4
Sedimentary fabric	
Grain or matrix support	The dolostone is fully grain-supported. All matrix is interstitial.
Grain-shape preferred orientation	None observed
Sedimentary lags	None observed
Bedding structure	There is no obvious bedding structure preserved in the dolostone. The discontinuous clay seams contained within the quartzose regions are oriented at an angle of roughly 45° to the face of the masonry. However, the core was not oriented when recovered so it is not clear how this angle relates to the installation.
Masonry orientation	Unknown
Diagenetic effects	
Compaction	Dolomite crystals exhibit a minor to modest grain suturing without any significant grain deformation.
Cementation	None observed
Dolomitization	The entirety of the stone is dolomitized leaving only non-carbonate phases unaffected.
Secondary geological structure	
Brittle cracks	A very minor amount of microcracking is observed to transect some of the quartzose regions. These are well-spaced and all are geologically healed.
Bulk grain deformation	No grain flattening is identified.
Deformation twinning	None observed
Stylolites	No stylolitic structures are obvious. However, some of the clay seams may have been the site of minor pressure solution processes before the stone was recrystallized.
Veins	As described in the "As-received description" section, vein structures are present at the front and rear of the core. The outermost vein was included in petrographic thin section. This is a maximum of about 2 millimeters in thickness. It contains slivers of calcitic microsparite that is partly dolomitized. Hematite lines the internal surfaces of the veins providing the bright red color of the structure. Some of the dolomitic matrix was partly solubilized within 1 to 2 millimeters of the vein resulting in grain boundaries that are somewhat microporous. A yellowish limonitic stain lines the grain boundaries in this location.
Secondary service effects	
Cracking	No cracking is obvious in the core sample. The core break is interpreted to be a sampling artifact.
Grain boundary cohesion	No loss of cohesion around grain boundaries is noted.
Salt deposition	No salt deposits are identified at the scale of the light microscope. It should be stressed that salts present within submicroscopic capillaries may not be readily viewed petrographically and these are usually better assessed through chemical analysis.
Soiling	None significant. Any debris identified petrographically appears to consist of unrinsed drilling slurry from the sample removal.
Biogrowth	None observed

Appendix I: Photographs and Photomicrographs

Microscopic examination is performed on an Olympus BX-51 polarized/reflected light microscope and an Olympus SZ40 stereoscopic microscope. The polarized light microscope is fitted with a Tucsen MIchrome 5 Pro 5MP digital camera. The stereoscopic microscope is used for simple magnification. Sample types examined under this microscope include fractured surfaces, fine constituents extracted through chemical or physical means, or honed or polished cross sections. The polarized light microscope (PLM) magnifies but also employs principles of optical crystallography. The most common sample preparation for the PLM is the petrographic thin section. For this preparation, cross-sectioned samples are mounted to glass slides and are milled to a thickness sufficient to allow light to be transmitted through the material. These are usually prepared without water and with minimal heat to avoid altering minerals that are water or temperature-sensitive. In many cases, the samples are impregnated with a low-viscosity, blue-dyed epoxy. When so treated, blue areas represent some type of void space (e.g., air-voids, capillary pores, cracks, etc.). The polarized light photomicrographs are taken using a variety of optical settings chosen to best demonstrate the feature(s) of interest. These are distinguished as follows:

Plane polarized light (abbreviated as PPL)

This method uses the refractive power of different constituents to produce an artificial sense of surface relief. Otherwise, the method is the closest to a simple magnification of the material. The setting is often used to demonstrate granular relationships or microstructure. Pore spaces and cracks are observable with this setting if the blue-dyed epoxy is used.

Conoscopic polarized light (abbreviated as CPL)

In this setting, the transmitted light is condensed just before passing through the thin section. The method tends to bring colors or finer particulates into higher contrast at the expense of image sharpness. The setting is often used to image grain boundary failures in dimension stone, pigment particulates in binders, or gel phases in the micropores of cement pastes.

Cross polarized light (abbreviated as XPL)

The setting places the thin section between two pieces of polarizing film oriented at 90° to one another. In isotropic materials (e.g., glasses, simple salts), all light is absorbed and the materials appear black. In anisotropic crystals, two light rays traveling at different speeds are produced within the thin section and these offset waves interfere at the upper polarizing film. The interference produces a color that can be used to calculate properties of the crystal structure and aid in identification of mineral species. In essence, the colors are artificial. It should be noted that color is a function of orientation and color differences do not necessarily indicate material differences.

Compensator plates

When in XPL mode, full-wave or quarter-wave compensator plates may be inserted into the light path to add or subtract interference. Technically, these methods are used to calculate properties of the crystal structure. However, they can also be used to alter the image appearance to help improve contrast between different constituents. They can also reveal preferred orientations in some materials (e.g., oriented residual crystallinity in fired ceramics).

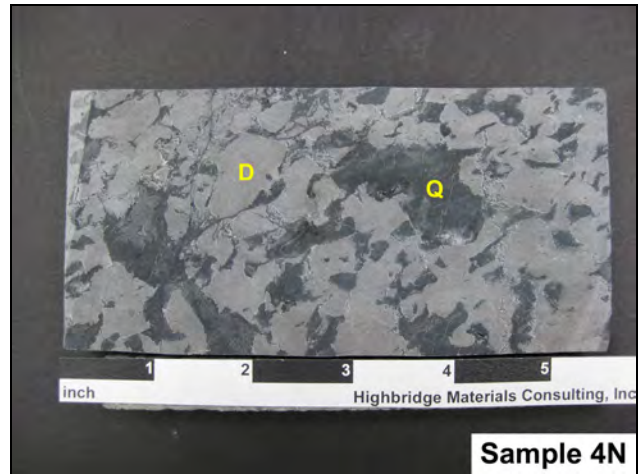
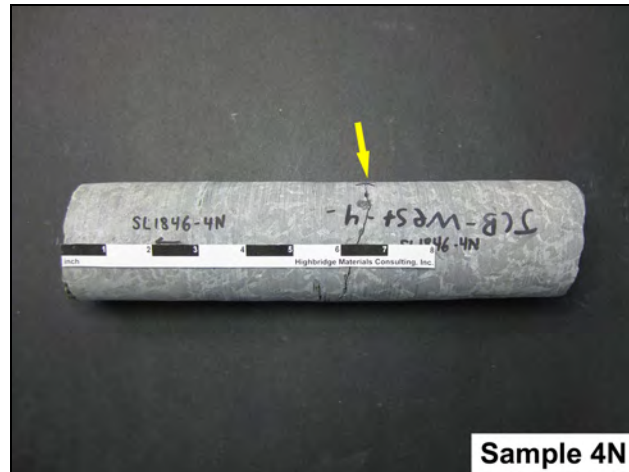


Figure 1: (Upper image) Photograph of the interior limestone core provided to Highbridge for petrographic examination. The core is shown in side view with the outer surface oriented toward the left of the image. The arrow shows a core break that is interpreted to be an artifact of sampling. (Lower left image) A honed cross section of the core is shown having the same orientation as the full core in the preceding image. (Lower right image) A portion of the cross section was acid-etched to highlight the texture. Irregular fragments of dolostone (D) are embedded in a matrix of recrystallized quartz (Q).

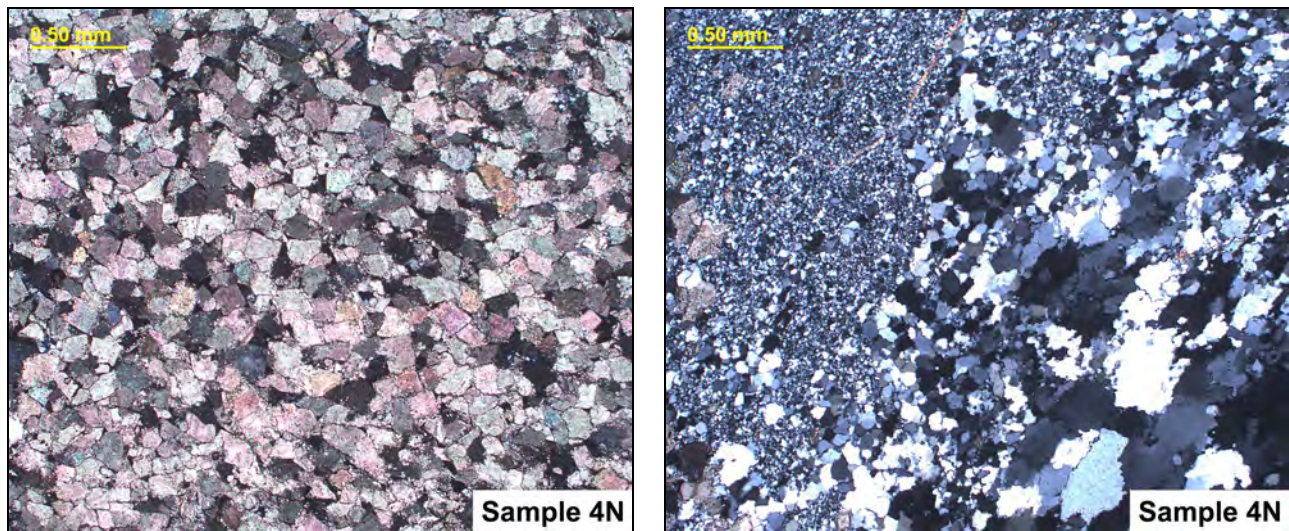


Figure 2: XPL photomicrographs illustrating the overall texture of the two main lithological regions of the stone. (Left) The dolomitic portion of the stone consists of uniformly fine-grained dolomite crystals. These have rhombic shapes and often display crystal faces. (Right) The grains in shades of gray consist of recrystallized quartz. The quartz exhibits a greater range of grain sizes.

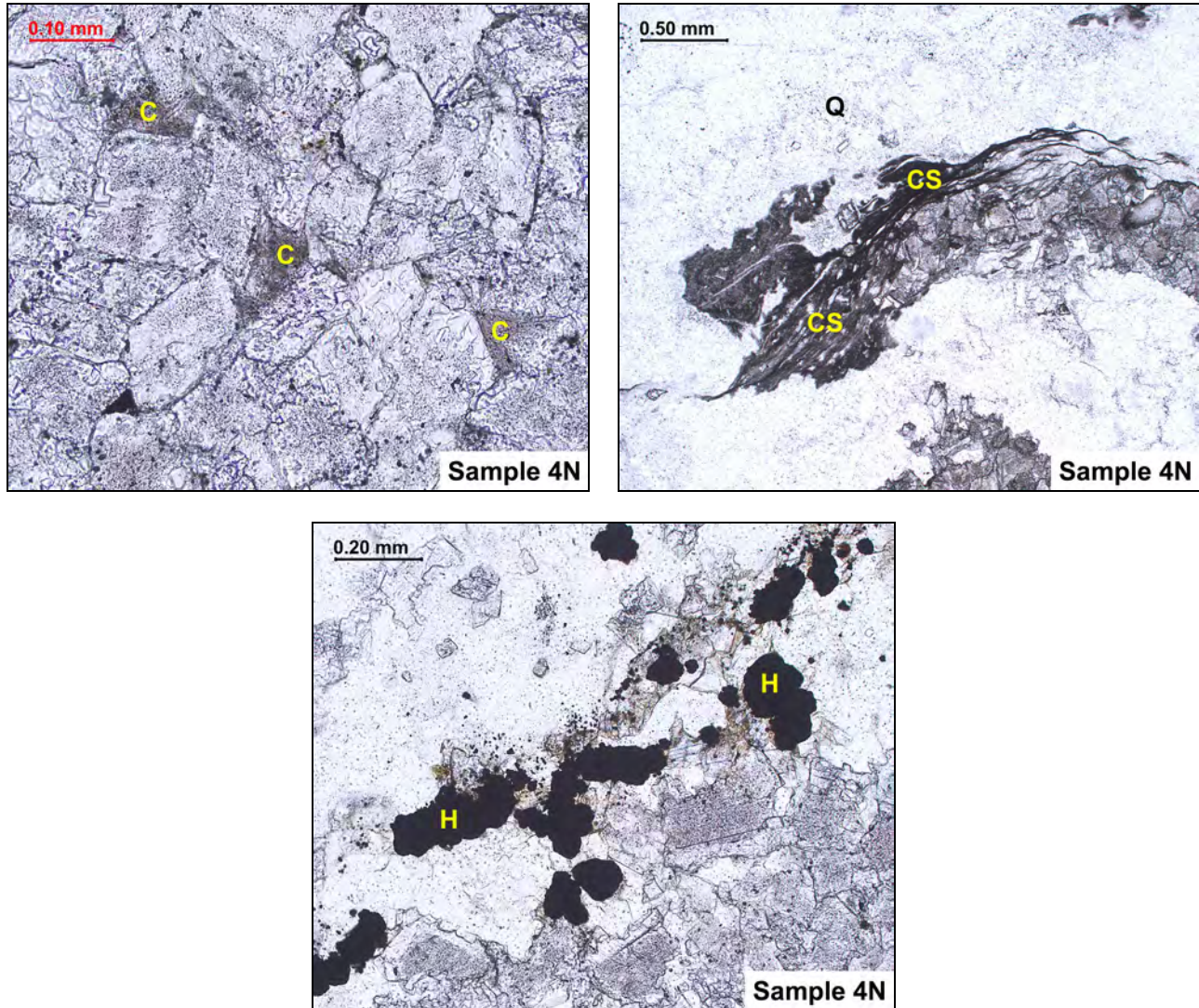


Figure 3: PPL photomicrographs illustrating the lesser constituents of the stone. (Upper left) Carbonaceous clay (C) is often found at the angular interstices between adjacent dolomite crystals. (Upper right) A clay seam (CS) is truncated and embedded in a quartzose region (Q). (Lower) Very fine hematite crystals (H) are a replacement of original pyrite crystals.

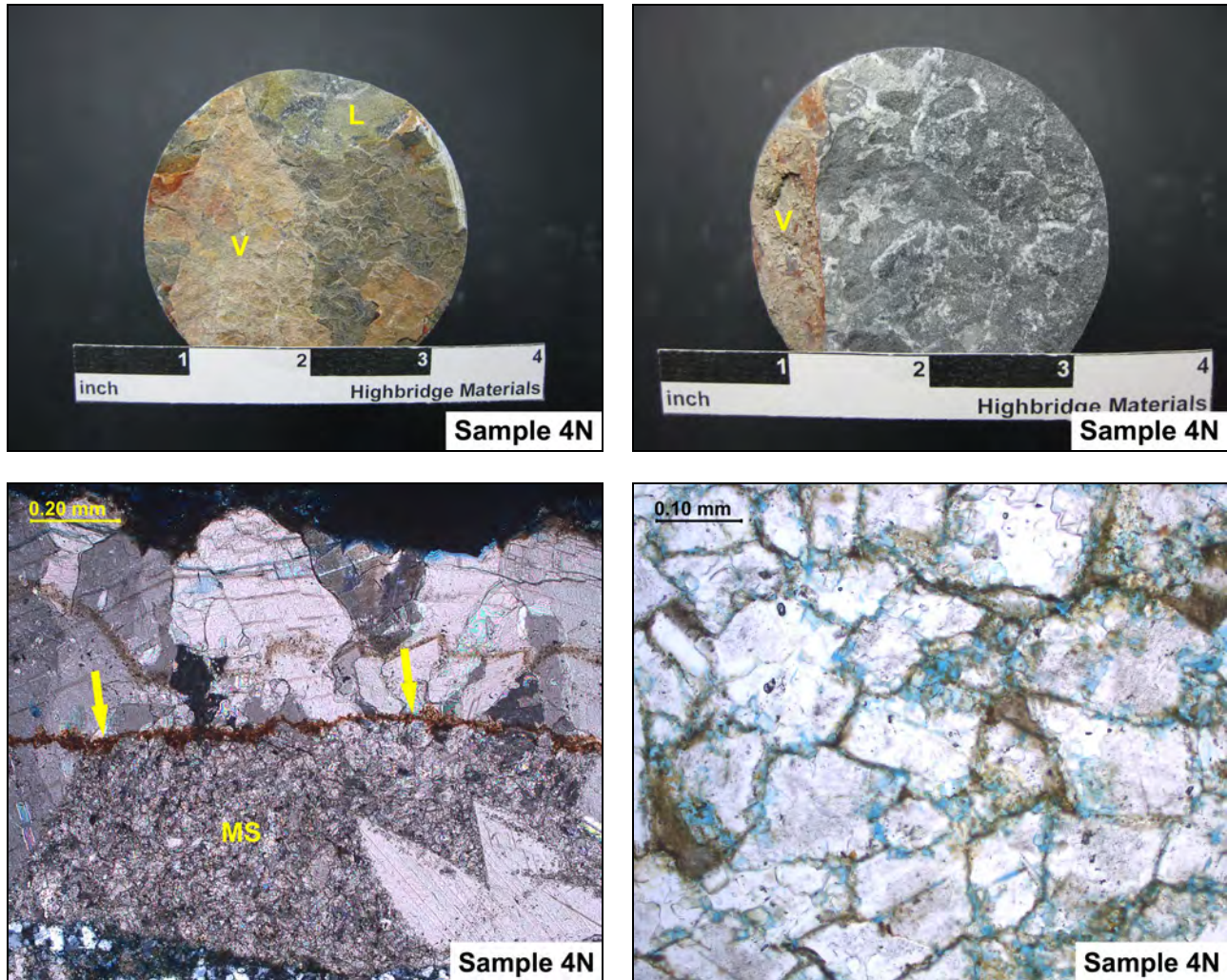


Figure 4: (Upper left) The outer surface of the core is shown. Much of the face is covered by a thin geological vein (V). Beyond the vein, some of the dolostone is yellow in color due to limonite lining the grain boundaries (L). (Upper right) A similar vein is intersected along the rear surface. (Lower left XPL image) The outer vein contains a sliver of microsparite (MS) that is not completely replaced by dolomite. Thin hematite linings (arrows) are responsible for the reddish color seen in hand sample. (Lower right CPL image) This photomicrograph was taken just beyond the outer vein. The bluish color represents pore spaces where there has been some solubilization of the dolomite locally. Note the yellowish brown linings around individual crystals. These contain limonite or iron oxide-hydroxide.

Petrographic Examination of Exterior Limestone

Bennington Battle Monument

15 Monument Circle, Bennington, VT 05201



Prepared for
Jablonski Building Conservation, Inc.

Client ID
JABL001

Report No.
SL1846-03

Report Date
09/17/23



Confidentiality

This report presents the results of laboratory testing requested by the client to satisfy specific project requirements. As such, the client has the right to use this report as necessary in any commercial matters related to the referenced project. Any reproduction of this report must be done in full. In offering a more thorough analysis, it may have been necessary for Highbridge to describe proprietary laboratory methods or present opinions, concepts, or original research that represent the intellectual property of Highbridge Materials Consulting and its successors. These intellectual property rights are not transferred in part or in full to any other party. Presentation of any or all of the data or interpretations for purposes other than those necessary to satisfy the goals of the investigation are not permitted without the express written consent of the author. The findings may not be used for purposes outside those originally intended. Unauthorized uses include but are not limited to internet or electronic presentation for marketing purposes, presentation of findings at professional venues, or submission of scholarly articles.

Standard of Care

Highbridge has performed its services in conformance with the care and skill ordinarily exercised by reputable members of the profession practicing under similar conditions at the same time. No other warranty of any kind, expressed or implied, in fact or by law, is made or intended. Interpretations and results are based strictly on samples provided and/or examined.

Cover Image

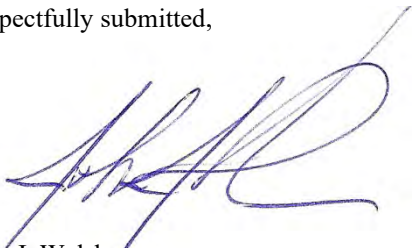
The Bennington Battle Monument in Bennington, VT. Image downloaded August 26, 2023 without modification.

Photo credit: King of Hearts

https://commons.wikimedia.org/wiki/File:Bennington_Battle_Monument_October_2021_001.jpg

Under Creative Commons License CC BY-SA 4.0 - <https://creativecommons.org/licenses/by-sa/4.0/deed.en>

Respectfully submitted,



John J. Walsh
President/ Senior Petrographer
Highbridge Materials Consulting, Inc.

1. Executive Summary

This report presents the results of a petrographic examination on four dimension stone samples taken from the exterior of the Bennington Battle Monument, Bennington, VT. The material is described by the client as a moderate bluish-gray dolomitic limestone quarried from Hudson Falls, NY.

Petrographically, all four samples have a clear affinity. Where not masked by fine well-formed dolomite crystals, the original rock is observed to have been composed of densely-packed carbonate mud pellets (peloids) and sparsely distributed fossil fragments (mostly echinoderms and trilobites). The stone would have been classified as a biopelmicrite. Dolomitization has recrystallized the majority of the stone in three of the samples, and virtually all of the stone in Sample 7X. Fine quartzose sediment is found throughout the rock and occasionally concentrated into planar bands. These are the only indications of sedimentary bedding as the peloids and bioclasts appear more as a jumbled mass. Pressure solution has produced stylolitic cleavage in some of the stone and this has concentrated fine iron sulfides that are present throughout all of the stone.

Secondary service effects are limited to minor superficial weathering. The bulk of the stone is found to be cohesive, indurate, impermeable, and sound. The only features that might be considered potential durability issues would include the presence of pyrite, minor geological microcracks, and stylolites. However, none are found to have caused any distress or aesthetic deficiencies in these particular samples.

2. Introduction

On July 6 and 7, 2023, Highbridge received a total of eight stone masonry cores from Ms. Danielle Pape of Jablonski Building Conservation, Inc. According to Ms. Pape, the samples were recovered from the Bennington Battle Monument, Bennington, VT. The monument is a stone obelisk completed in 1889.

The client indicates that four of the samples were taken from the interior and four from the exterior. A summary of the samples and their identifications are presented in Table 2.1. Photographs provided by the client indicate the cores to have been taken horizontally through individual masonry units. The orientation of the vertical plane was not indicated on the samples.

Table 2.1: Summary of Received Samples

The laboratory has assigned shortened sample identifications to simplify reporting and these identifications will be used throughout all reports. The laboratory identification is shown in the "HMC ID" column.

Client ID	HMC ID	Description from client transmittal
JBC-West-1	1N	Interior, light yellowish white stone, theoretically from a local quarry
JBC-East-2	2N	Interior, light yellowish white stone, theoretically from a local quarry
JBC-West-3	3N	Interior, light yellowish white stone, theoretically from a local quarry
JBC-West-4	4N	Interior, dark gray stone, theoretically from a local quarry
JBC-North-5	5X	Exterior, moderate bluish gray dolomitic limestone quarried from Hudson Falls, NY
JBC-East-6	6X	Exterior, moderate bluish gray dolomitic limestone quarried from Hudson Falls, NY
JBC-East-7	7X	Exterior, moderate bluish gray dolomitic limestone quarried from Hudson Falls, NY
JBC-North-8	8X	Exterior, moderate bluish gray dolomitic limestone quarried from Hudson Falls, NY

At the client's request, a petrographic examination is performed on each sample. The testing includes a characterization of the mineralogy and microtexture of the stone. The client has mentioned a cracking condition described as "checkerboard" cracking that is usually accompanied by some type of salt run or efflorescence. While there is a desire to investigate the nature of this cracking, the author has suggested that a careful description of the crack geometry and a sample that includes a good representation of the cracking would be necessary to approach this issue.

This report presents the results for the four exterior limestone samples (5X, 6X, 7X, and 8X). Results for the other samples will be presented under separate cover.

3. Methods of Examination

The petrographic examination was conducted in accordance with the standard practices contained within ASTM C1721-22. Data collection is performed or supervised by a degreed geologist who by nature of their education is qualified to operate the analytical equipment employed. Analysis and interpretation are performed or directed by a supervising petrographer who satisfies the qualifications as specified in Section 4 of ASTM C856/C856M-20.

The following personnel contributed to the examination:

Technicians:	M. Pattie A. Ledwitch
Petrographer:	J. Walsh

4. Petrographic Findings and Discussion

4.1 - Lithology

The four exterior samples all derive from the same geological source despite any variation between samples. The material is a dense, bluish-gray limestone that weathers light gray. When taken as a whole, the rock is a biopelmicrite with variable amounts of silty and fine sandy sediment. The original carbonate rock has been appreciably dolomitized. Biopelmicrite indicates a limestone that is dominated by cemented carbonate mud pellets with a fairly sparse distribution of marine fossil debris. Dolomitization is a secondary process whereby the original calcitic microtexture is replaced by crystalline magnesian carbonate.

The original rock fabric is detectable in places where dolomitization is not complete. The background texture consists of densely distributed and well sorted peloids with diameters ranging from about 0.075 to 0.20 millimeters. These are cemented together with calcite microspar. In Sample 6X, some of the peloids exhibit faint internal texture suggesting that the peloids may not have been amorphous originally. Nonetheless, virtually all now consist of a dense, ultrafine-grained carbonate mud.

Bioclasts (invertebrate fossil fragments) are sparsely distributed throughout the peloidal mass. Debris from echinoderms and trilobites are observed in all. Gastropods, brachiopods, and sponges are also identified in some samples though much less frequently. Impressions of ammonites are visible on the outer surface of Sample 7X though none are included within the stone itself. Other fossil forms are evident but are undifferentiated due to the masking effect of the dolomitization.

Siliceous sediment is distributed throughout the limestone in varying concentration. This includes medium silt to fine sand consisting mostly of quartz with a minor amount of feldspar. Clays may be intermixed but these are not present as discrete mud-filled seams. Bands that are more concentrated in quartzose sediment are noted toward the interior of Sample 5X and all throughout Sample 7X. In all cases, the siliceous sediment is intermixed with carbonate minerals.

Sedimentary bedding is not especially evident in most places. Only the banding of quartz-rich sediment provides unequivocal evidence of the original depositional orientation. In most places, the orientation of elongate fossil forms is not sufficiently constant to indicate the original horizontal plane. In fact, it is suspected that the limestone represents some sort of structureless debris-flow deposit or a sedimentary deposit for which there had been significant reworking through bioturbation or similar process. With that said, the banded quartz deposits likely represent intermittent storm deposits. All samples contain solution cleavage in the form of stylolites. Assuming these all formed in the same orientation, it is then possible to determine the sedimentary orientation in the samples that do not contain obvious quartzose banding. With that said, Samples 5X, 6X, and 7X are interpreted to represent face-bedded masonry units. Sample 8X is the only naturally-bedded unit of the sample set.

The original limestone was heavily dolomitized. In fact, though the original limestone was a biopelmicrite, the rock is now classified as a dolomitic limestone or even a dolostone. There is at least a 50% recrystallization by volume in Samples 5X, 6X, and 8X. Sample 7X is almost completely dolomitized. The dolomite occurs as well-formed rhombic crystals that range in size from 0.05 to 0.25 millimeters. Associated with the dolomitization is the formation of copious iron sulfide (likely pyrite) throughout the stone. The association is typical of the reducing environments that favor the formation of dolomite. Most of the sulfide is dispersed and extremely fine-grained. As such, it is a relatively minor component volumetrically despite its ubiquity in the stone.

Secondary deformation of the dolostone is mostly limited to the formation of stylolites. These are pressure-solution seams along which the carbonate has dissolved under pressure leaving behind an accumulation of less soluble quartz, pyrite, and possibly some clay. There is no porosity or secondary cracking observed within the stylolites. These are most abundant throughout Sample 5X and within the interior half of Sample 6X. Stylolites are relatively scarce in Sample 8X. In Sample 7X, there are no continuous stylolites though there is incipient pressure solution evident abundantly throughout the core.

Geological cracking is minor in the examined samples. These are limited to a few hairline cracks that are oriented at a shallow angle to the core axis. Most of the cracking has remained cohesive though the structures are not healed with any secondary mineralization. These likely represent late-stage joints within the rock formation. While quarry joints are often avoided, these were likely too fine to result in rejection.

4.2 - Secondary Service Effects

Weathering effects are identified along the outer surface of each core. However, all of these are superficial and exceptionally minor. None are a cause for concern with respect to the continued serviceability or durability of the stone. All samples exhibit microscopic scaling cracks none of which extend more than about 0.5 millimeters from the existing surface. Sample 7X and 8X have a microscopic veneer in which the carbonate minerals have dissolved due to interaction with environmental acids (e.g., acid rain or certain types of microbiota). The insoluble minerals are left proud along the surface. In Sample 8X, this has made the stylolitic cleavages visible in relief. In Sample 7X, negative impressions of ammonites are apparent and these effectively overshadow any weathering effects.

Beyond any surface weathering effects, the samples provided for examination are sound, and no deleterious service effects are identified petrographically. No significant cracking, crumbling, or other physical distress is observed. No deleterious salts are identified at the scale of the light microscope. Of course, it is always possible for submicroscopic salts to be present with the stone capillaries. Other instrumental analysis would be required to identify these.

4.3 - Discussion

The four stone units provided for examination represent a fairly narrow range of lithological characteristics. Assuming the samples were selected randomly, then it may be reasonably safe to assume that these are representative of the exterior construction. Of course, if only grade-height material was selected, then it cannot be said for certain that the same quarry benches were used throughout the elevation. Nevertheless, the samples examined for this report are dense, cohesive, dolostones (or dolomitic limestones) the bulk of which are hard, impermeable, and sound. There are only three features of the stone that may be considered potential weaknesses and none of these appear to detract from the stone quality based on the samples provided for examination.

Finely disseminated iron sulfides are present throughout all stone. There are building stones with similar distributions of fine pyrite (e.g., the Hardyson quartzite in Pennsylvania) for which exposure of freshly dressed surfaces cause a rapid oxidation of the pyrite resulting in a rusty or reddish veneer across the face of the stone. There is no evidence within this particular stone to suggest a similar instability. Given the long history of the monument, there is no reason to suspect any future patination substantially different than that currently present. Unless there are other areas on the monument where iron bleed is evident, there should be no concern over the sulfide mineralogy.

Natural microcracks or joints are identified in all samples with the exception of Sample 7X. These are mostly oriented at a shallow angle to the core axis meaning that these likely transect the outer surface of the masonry unit outside the diameter of the core sample. Technically, these cracks may be considered potentially permeable to moisture and the ingress of salts. However, there is no evidence for any decalcification, secondary mineralization, or subsidiary cracking within these relatively minor structures.

Stylolites are very common in Paleozoic limestone. Because these tend to concentrate clays, organics, and other fine insoluble matter, then can be susceptible to swelling during wet/dry cycles, and to frost wedging during saturated freezing events. This is especially the case where stone is unrestrained in a skyward-facing application (e.g., sills or copings) or where the stylolites are parallel to the wall face. The former does not apply to these particular samples. However, all but Sample 8X is oriented such that stylolites are parallel to the face of the masonry unit. Despite this, there is no evidence of any secondary openings or "unpacking" along any of the observed structures. All stylolites appear tight and impermeable. Nothing in this examination suggests that these stylolites may represent a durability concern.

5. Petrographic Data

Table 5.1: Petrographic Data

Sample ID	JBC-North-5
As-received description	
Dimensions	The sample consists of 2.75" diameter core received in three contiguous pieces with a total maximum length of 10.75". Orientations were not included with the sample. The sedimentary structure indicates that the masonry unit was face-bedded and this prevents an educated guess on the original masonry orientation. The outer direction is apparent from the surface weathering. The core breaks occur at approximately 4" and 8" from the face of the stone. The breaks appear to have occurred along fresh limestone. There is no evidence to suggest that these might be pre-existing structures.
Appearance and fabric	The material is a dense bluish-gray limestone with complex internal structure. The fresh color along core breaks is dark bluish-gray with splotches of light gray (Munsell color code approximately 5PB 4/0.5). The weathered color is medium gray on average (Munsell color code approximately 5PB 5/0.5). However, there are faint mottles more greenish in hue.
Sedimentary features	The stone appears monolithically bedded. The interior of the bed is defined by lighter-colored deformed nodules separated by darker, presumably argillaceous regions.
Structure	Incipient clay-rich stylolites are observed with a multiple-centimeter spacing mostly deeper within the core. These do not appear porous. A single veinlet is observed roughly perpendicular to the masonry face.
Outer surface	The surface is roughly planar and weathered. Sparse fine-grained fossil forms stand out in shallow relief.
Inner surface	The inner face is a clean, artificial drilling break exposing fresh limestone.
Lithological identification	
Description	The original rock was a variably sandy pelmicrite to biopelmicrite that has been appreciably dolomitized.
Lithological components	
Matrix	Very little original matrix is identified. All micrite occurs as part of particulate materials (i.e., micritic peloids). Any material interstitial to the peloids has recrystallized to a microspar.
Bioclasts	The limestone is sparsely bioclastic. Dolomitization obscures a significant amount of the microstructure so that some fossil forms are not readily identifiable. However, obvious groups include echinoderms and trilobites. The echinoderm fragments consist of single calcite crystals as is characteristic for these forms. The trilobites exhibit the typical sweeping extinction under crossed polars. All other fossil forms exhibit significant sparry recrystallization. Most bioclasts are one to several millimeters in size.
Peloids	Wherever micritic calcite is preserved, the microtexture consists of tightly packed peloids usually about 0.075 to 0.20 millimeters in diameter.
Ooids	None observed
Intraclasts	While much of the microtexture is obscured by the secondary dolomitization, a few centimeter-scale intraclasts are identified. These are micritic and sometimes sparsely fossiliferous.
Siliceous sediment (sand and silt)	Siliceous sediment is a minor component. Most of the sediment consists of quartz though some alkali feldspar is also detected. The sediment includes subangular particles from medium silt to very fine sand size. For most of the core, the sediment is variably dispersed throughout the limestone and is concentrated only within thin stylolites. Toward the interior of the core, there are irregular regions or bands more concentrated in siliceous sediment.
Siliceous sediment (clay)	Very little clay material is positively identified except within the silty areas near the rear of the core. Though there are stylolites in which fine material has been concentrated, most of this appears to be finely disseminated iron sulfide.
Other components	Iron sulfide (probably pyrite) is found throughout the limestone in minor concentration. Much of it is in the form of extremely fine-grained crystals sparsely distributed throughout the matrix. Less commonly, relatively coarser crystals are found in small clusters. The sulfide is most concentrated within stylolitic cleavage.

Table 5.1 (cont'd.): Petrographic Data

Sample ID	JBC-North-5
Lithological components (cont'd.)	
Grain size	There is a wide range of grain sizes. Calcitic micrite within peloids and in the interstices between dolomite crystals is submicroscopic. Peloids range in size from 0.075 to 0.20 millimeters. Bioclasts are mostly one to several millimeters in length. Dolomite crystals are generally between 0.05 and 0.25 millimeters.
Grain shape	Micrite, peloids, and dolomite crystals are all equidimensional though varied in shape. Many of the fossil forms tend to be elongate.
Pore structure	There is no microporosity visible at the scale of the light microscope. Polarized light microscopy is only capable of distinguishing micropores on the order of 0.001 millimeters and greater. It is assumed that the limestone contains a normal distribution of submicroscopic pore space even if no visible pores are apparent.
Sedimentary fabric	
Grain or matrix support	The limestone is grain supported.
Grain-shape preferred orientation	There is not a strong grain-shape preferred orientation. Though not consistently so, some of the coarsest fossils are oriented vertically to subvertically relative to the core orientation.
Sedimentary lags	No discrete lags are identified. There is some local concentration of siliceous sediment.
Bedding structure	Despite what appears to be some variation in sedimentary character throughout the core section, there is not a strong bedding structure apparent behind the dolomitic overprint. In fact, the more or less random orientation of fossil forms and disruption of continuity in silt-rich horizons suggests that either the sediment was reworked while unconsolidated or the whole mass represents a jumbled debris deposit.
Masonry orientation	The represented masonry unit appears to be face-bedded based on what appears to be the original sedimentary orientation.
Diagenetic effects	
Compaction	Compaction is evident in the presence of interpenetrated bioclasts and discrete stylolites. Grain flattening is not a significant feature.
Cementation	A microspar cement binds the copious peloids. The peloidal matrix and its cementation represent the majority of the relict limestone texture. A coarser calcite recrystallization is observed within bioclasts.
Dolomitization	A significant volume of the stone is dolomitized. The dolomitization coincides with the darker gray portions of the stone. The dolomite occurs as euhedral rhombs with lengths ranging from 0.075 to 0.20 millimeters. Dolomite crystals often have dusty interiors and clear margins.
Secondary geological structure	
Brittle cracks	An exceptionally fine crack is found at an oblique angle to the core axis. This extends several inches within the core section. The crack is unhealed and does not respond substantially to local structure.
Bulk grain deformation	No grain flattening is identified.
Deformation twinning	Deformation twins are not especially abundant.
Stylolites	Stylolites are common throughout the stone core with an approximately centimeter-scale spacing. The morphology is mostly sutured-type with some wave-type. Stylolites occur as single planes and multiple anastomosing planes. The thickest packets of stylolites are about 1 millimeter. It is assumed that the structures are horizontal with respect to bedding. However, the sedimentary bedding orientation is not especially well-defined. The stylolites contain concentrations of quartz and iron sulfide. Dolomite crystallization also appears to favor the stylolite structures.
Veins	None detected

Table 5.1 (cont'd.): Petrographic Data

Sample ID	JBC-North-5
Secondary service effects	
Cracking	Very minor scaling microcracks are found at the exposed surface of the stone to a depth no greater than 0.5 millimeters. No mineralizations are found in association.
Grain boundary cohesion	No loss of cohesion around grain boundaries is noted.
Salt deposition	No salt deposits are identified at the scale of the light microscope. It should be stressed that salts present within submicroscopic capillaries may not be readily viewed petrographically and these are usually better assessed through chemical analysis.
Soiling	None observed petrographically
Biogrowth	None observed petrographically

Table 5.2: Petrographic Data

Sample ID	JBC-East-6
As-received description	
Dimensions	The sample consists of 2.75" diameter core received in two possibly contiguous pieces with a total maximum length of 12.25". There is a suspected fit between the two pieces though it is not certain. Orientations were not included with the sample. The sedimentary structure indicates that the masonry unit was face-bedded and this prevents an educated guess on the original masonry orientation. The outer direction is apparent from the surface weathering. The core break occurs at approximately 6.5" from the face of the stone. The break appears to have occurred along fresh limestone. However, a wedge of material was lost in the recovery. The contact with the interior part of the core is a roughly planar surface at an approximately 45° angle from the core axis.
Appearance and fabric	The material is a dense bluish-gray limestone with complex internal structure. The fresh color along core breaks is dark bluish-gray with splashes of light gray (Munsell color code approximately 5PB 4/0.5). The weathered color is medium gray on average (Munsell color code approximately 5PB 6/0.75).
Sedimentary features	The stone appears monolithically bedded. The interior of the bed is defined by lighter-colored deformed nodules separated by darker, presumably argillaceous regions.
Structure	Incipient clay-rich stylolites are observed with a centimeter to multiple-centimeter spacing mostly deeper within the core. These do not appear porous.
Outer surface	The surface is roughly planar and weathered. Sparse fine-grained fossil forms stand out in shallow relief.
Inner surface	The inner face is a clean, artificial drilling break exposing fresh limestone.
Lithological identification	
Description	The original rock was a variably sandy pelmicrite to biopelmicrite that has been appreciably dolomitized.
Lithological components	
Matrix	Very little original matrix is identified. All micrite occurs as part of particulate materials (i.e., micritic peloids). Any material interstitial to the peloids has recrystallized to a microspar.
Bioclasts	The limestone is sparsely bioclastic. Dolomitization obscures a significant amount of the microstructure so that some fossil forms are not readily identifiable. However, obvious groups include echinoderms and trilobites. Some larger recrystallized shell fragments appear to represent brachiopods. The echinoderm fragments consist of single calcite crystals as is characteristic for these forms. The trilobites exhibit the typical sweeping extinction under crossed polars. All other fossil forms exhibit significant sparry recrystallization. Most bioclasts are one to several millimeters in size. There are a few fossils coarser than a centimeter.
Peloids	Wherever micritic calcite is preserved, the microtexture consists of tightly packed peloids usually about 0.075 to 0.20 millimeters in diameter. A minor proportion of the peloids exhibit some type of faint structure suggesting these were not originally amorphous.
Ooids	None observed
Intraclasts	None observed
Siliceous sediment (sand and silt)	Siliceous sediment is a minor component. Most of the sediment consists of quartz though some alkali feldspar is also detected. The sediment includes subangular particles from medium silt to very fine sand size. For most of the core, the sediment is variably dispersed throughout the limestone and is concentrated only within thin stylolites. The stylolites themselves are more concentrated within the interior half of the provided core.
Siliceous sediment (clay)	Very little clay material is positively identified. Though there are stylolites in which fine material has been concentrated, most of this appears to be finely disseminated iron sulfide.
Other components	Iron sulfide (probably pyrite) is found throughout the limestone in minor concentration. Much of it is in the form of extremely fine-grained crystals sparsely distributed throughout the matrix. Less commonly, relatively coarser crystals are found in small clusters. The sulfide is most concentrated within stylolitic cleavage.

Table 5.2 (cont'd.): Petrographic Data

Sample ID	JBC-East-6
Lithological components (cont'd.)	
Grain size	There is a wide range of grain sizes. Calcitic micrite within peloids and in the interstices between dolomite crystals is submicroscopic. Peloids range in size from 0.075 to 0.20 millimeters. Bioclasts are mostly one to several millimeters in length. Dolomite crystals are generally between 0.05 and 0.25 millimeters.
Grain shape	Micrite, peloids, and dolomite crystals are all equidimensional though varied in shape. Many of the fossil forms tend to be elongate.
Pore structure	There is no microporosity visible at the scale of the light microscope. Polarized light microscopy is only capable of distinguishing micropores on the order of 0.001 millimeters and greater. It is assumed that the limestone contains a normal distribution of submicroscopic pore space even if no visible pores are apparent.
Sedimentary fabric	
Grain or matrix support	The limestone is grain supported.
Grain-shape preferred orientation	There is not a strong grain-shape preferred orientation. Though not consistently so, some of the coarsest fossils are oriented vertically to subvertically relative to the core orientation.
Sedimentary lags	No discrete lags are identified.
Bedding structure	Despite what appears to be some variation in sedimentary character throughout the core section, there is not a strong bedding structure apparent behind the dolomitic overprint. In fact, the more or less random orientation of fossil forms suggests that either the sediment was reworked while unconsolidated or the whole mass represents a jumbled debris deposit.
Masonry orientation	The represented masonry unit appears to be face-bedded based on what appears to be the original sedimentary orientation.
Diagenetic effects	
Compaction	Compaction is evident in the presence of interpenetrated bioclasts and discrete stylolites. Grain flattening is not a significant feature.
Cementation	A microspar cement binds the copious peloids. The peloidal matrix and its cementation represent the majority of the relict limestone texture. A coarser calcite recrystallization is observed within bioclasts.
Dolomitization	A significant volume of the stone is dolomitized. The dolomitization coincides with the darker gray portions of the stone. The dolomite occurs as euhedral rhombs with lengths ranging from 0.075 to 0.20 millimeters. Dolomite crystals often have dusty interiors and clear margins.
Secondary geological structure	
Brittle cracks	An exceptionally fine crack is found at an oblique angle to the core axis. This extends several inches within the core section. The crack is unhealed and does not respond substantially to local structure. The crack is responsible for the lost wedge of limestone near the center of the core section.
Bulk grain deformation	No grain flattening is identified.
Deformation twinning	Deformation twins are not especially abundant.
Stylolites	Stylolites are common throughout the inner half of the stone core and sparse within the outer half. The stylolites have less than a centimeter-scale spacing where most common. The morphology is mostly sutured-type with some wave-type. Stylolites occur as single planes and multiple anastomosing planes. The thickest packets of stylolites are about 1 millimeter. It is assumed that the structures are horizontal with respect to bedding. However, the sedimentary bedding orientation is not especially well-defined. The stylolites contain concentrations of quartz and iron sulfide. Dolomite crystallization also appears to favor the stylolite structures.
Veins	None detected

Table 5.2 (cont'd.): Petrographic Data

Sample ID	JBC-East-6
Secondary service effects	
Cracking	Very minor scaling microcracks are found at the exposed surface of the stone to a depth no greater than 0.5 millimeters. No mineralizations are found in association. Some loss of cohesion is observed in the geological crack discussed earlier. The crack itself is not interpreted to be service-related.
Grain boundary cohesion	No loss of cohesion around grain boundaries is noted.
Salt deposition	No salt deposits are identified at the scale of the light microscope. It should be stressed that salts present within submicroscopic capillaries may not be readily viewed petrographically and these are usually better assessed through chemical analysis.
Soiling	None observed petrographically
Biogrowth	None observed petrographically

Table 5.3: Petrographic Data

Sample ID	JBC-East -7
As-received description	
Dimensions	The sample consists of one intact core sample with a 2.75" diameter and a 12.25" maximum length. Orientations were not included with the sample. The sedimentary structure indicates that the masonry unit was face-bedded and this prevents an educated guess on the original masonry orientation. The outer direction is apparent from the surface weathering.
Appearance and fabric	The material is a dense bluish-gray limestone with complex internal structure. The fresh color along the core break is dark bluish-gray (Munsell color code approximately 5PB 3.7/0.75). The weathered color is medium brownish-gray on average (Munsell color code approximately 2.5Y 5/0.75). However, centimeter-scale ammonite fossils in relief on the surface are neutral medium gray.
Sedimentary features	The stone appears monolithically bedded. The interior of the bed is defined by lighter-colored deformed nodules separated by darker, presumably argillaceous regions. Fossil-rich horizons appear to be more frequent with depth in the core.
Structure	The core just barely grazed two stylolite structures that appear to be roughly parallel to one another. For the analysis, the stone was cross-sectioned perpendicular to this fabric.
Outer surface	The surface is roughly planar and weathered. Centimeter-sized ammonite fossils stand out in shallow relief.
Inner surface	The inner face is a clean, artificial drilling break exposing fresh limestone.
Lithological identification	
Description	The rock is a sandy dolostone. The original limestone lithology is uninterpretable due to the dolomitic overprinting.
Lithological components	
Matrix	Very little original matrix is identified. There are fine interstices between adjacent dolomite crystals. These are mostly filled with sulfide minerals though clays may also be present.
Bioclasts	Ammonite fossil impressions are apparent at the outer surface of the core. However, these appear to be impressions of fossils present in the adjacent rock within the original stratigraphic section. No ammonites are observed within the core itself. Very sparse fossils that have not been dolomitized occur occasionally throughout the core section. Most of the obvious ones are fragments of echinoderms. Some brachiopods shell fragments may also be present. Most bioclasts are about 0.5 to a few millimeters in size.
Peloids	None observed
Ooids	None observed
Intraclasts	None observed
Siliceous sediment (sand and silt)	Siliceous sediment is dispersed in varying concentration throughout the core section. There is a notable banding of differing sediment concentrations that relate to original bedding. Most of the sediment consists of quartz though some alkali feldspar is also detected. The sediment includes subangular particles from medium silt to very fine sand size.
Siliceous sediment (clay)	Very little clay material is positively identified. However, clay may be interspersed with the fine sulfides present throughout the interstitial space between dolomite crystals.
Other components	Iron sulfide (probably pyrite) is found throughout the limestone in modest concentration. Much of it is in the form of extremely fine-grained crystals sparsely distributed throughout the matrix.

Table 5.3 (cont'd.): Petrographic Data

Sample ID	JBC-East -7
Lithological components (cont'd.)	
Grain size	The rock is generally fine-grained and dominated by the dolomitic texture. Dolomite crystals range in size from about 0.05 to 0.20 millimeters. Quartz sediment is finer and calcite spar within fossils is coarser.
Grain shape	The dolomite is rhombic in shape and crystals are euhedral to subhedral. Where well-formed crystal faces are observed, these are often curved. The quartz is equidimensional and anhedral.
Pore structure	There is no microporosity visible at the scale of the light microscope. Polarized light microscopy is only capable of distinguishing micropores on the order of 0.001 millimeters and greater. It is assumed that the limestone contains a normal distribution of submicroscopic pore space even if no visible pores are apparent.
Sedimentary fabric	
Grain or matrix support	The dolostone is fully grain-supported. All matrix is interstitial.
Grain-shape preferred orientation	None observed
Sedimentary lags	No discrete lags are identified. There is some local concentration of siliceous sediment.
Bedding structure	There is a mostly planar banding of quartzose sediment that defines the bedding orientation of the dolostone.
Masonry orientation	The represented masonry unit is face-bedded.
Diagenetic effects	
Compaction	Dolomite crystals exhibit a minor to modest grain suturing without any significant grain deformation.
Cementation	None observed
Dolomitization	The majority of the stone volume is dolomitized. The dolomite occurs as euhedral rhombs with lengths ranging from 0.075 to 0.20 millimeters. Dolomite crystals often have dusty interiors and clear margins.
Secondary geological structure	
Brittle cracks	None observed
Bulk grain deformation	No grain flattening is identified.
Deformation twinning	None observed
Stylolites	Incipient stylolites are observed to varying degree throughout the core section. However, there are no continuous structures identified.
Veins	None detected
Secondary service effects	
Cracking	Very minor scaling microcracks are found at the exposed surface of the stone to a depth no greater than 0.5 millimeters. No mineralizations are found in association.
Grain boundary cohesion	No loss of cohesion around grain boundaries is noted.
Salt deposition	No salt deposits are identified at the scale of the light microscope. It should be stressed that salts present within submicroscopic capillaries may not be readily viewed petrographically and these are usually better assessed through chemical analysis.
Soiling	None observed petrographically
Biogrowth	A greenish biogrowth is observed along the outer face.
Other	There is a microscopic veneer along the core surface where the carbonate has preferentially dissolved leaving only the acid-insoluble quartz sand.

Table 5.4: Petrographic Data

Sample ID	JBC-North-8
As-received description	
Dimensions	The sample consists of 2.75" diameter core received in two contiguous pieces with a total maximum length of 12.0". Orientations were not included with the sample. However, suspected sedimentary structure suggests that the masonry unit was naturally-bedded. For the analysis, the stone was cross-sectioned perpendicular to this fabric. The outer direction is apparent from the surface weathering. The core is broken along two surfaces. One of these is in the rear portion of the core. This is at a high angle to suspected bedding and parallel to the core axis. The other is perpendicular to the face of the stone at approximately 5.75" depth. The breaks appear to have occurred along fresh limestone. There is no physical evidence to suggest that these might be pre-existing structures though the stone is clearly breaking along weaknesses.
Appearance and fabric	The material is a dense bluish-gray limestone with complex internal structure. The fresh color along core breaks is dark bluish-gray (Munsell color code approximately 5PB 3.75/0.75). The weathered color is medium gray with yellowish-gray mottles (average Munsell color code approximately 2.5Y 5.5/0.5)
Sedimentary features	The stone appears monolithically bedded. The interior of the bed is defined by lighter-colored deformed nodules separated by darker, presumably argillaceous regions.
Structure	No secondary structure is obvious in hand sample.
Outer surface	The surface has a rugged profile. The surface is weathered with sedimentary laminations standing out in shallow relief.
Inner surface	The inner face is a clean, artificial drilling break exposing fresh limestone.
Lithological identification	
Description	The original rock was a variably sandy pelmicrite to biopelmicrite that has been appreciably dolomitized.
Lithological components	
Matrix	Very little original matrix is identified. All micrite occurs as part of particulate materials (i.e., micritic peloids). Any material interstitial to the peloids has recrystallized to a microspar.
Bioclasts	The limestone is sparsely bioclastic. Dolomitization obscures a significant amount of the microstructure so that some fossil forms are not readily identifiable. However, obvious groups include echinoderms and trilobites. A few gastropods are positively identified. One sponge spicule is noted in thin section. The echinoderm fragments consist of single calcite crystals as is characteristic for these forms. The trilobites exhibit the typical sweeping extinction under crossed polars. All other fossil forms exhibit significant sparry recrystallization. Most bioclasts are one to several millimeters in size. There are a few fossils coarser than a centimeter.
Peloids	Wherever micritic calcite is preserved, the microtexture consists of tightly packed peloids usually about 0.075 to 0.20 millimeters in diameter.
Ooids	None observed
Intraclasts	None observed
Siliceous sediment (sand and silt)	Siliceous sediment is a minor component. Most of the sediment consists of quartz though some alkali feldspar is also detected. The sediment includes subangular particles from medium silt to very fine sand size. For most of the core, the sediment is variably dispersed throughout the limestone and is concentrated only within thin stylolites.
Siliceous sediment (clay)	Very little clay material is positively identified. Though there are stylolites in which fine material has been concentrated, most of this appears to be finely disseminated iron sulfide.
Other components	Iron sulfide (probably pyrite) is found throughout the limestone in minor concentration. Much of it is in the form of extremely fine-grained crystals sparsely distributed throughout the matrix. Less commonly, relatively coarser crystals are found in small clusters. The sulfide is most concentrated within stylolitic cleavage.

Table 5.4 (cont'd.): Petrographic Data

Sample ID	JBC-North-8
Lithological components (cont'd.)	
Grain size	There is a wide range of grain sizes. Calcitic micrite within peloids and in the interstices between dolomite crystals is submicroscopic. Peloids range in size from 0.075 to 0.20 millimeters. Bioclasts are mostly one to several millimeters in length. Dolomite crystals are generally between 0.05 and 0.25 millimeters.
Grain shape	Micrite, peloids, and dolomite crystals are all equidimensional though varied in shape. Many of the fossil forms tend to be elongate.
Pore structure	There is no microporosity visible at the scale of the light microscope. Polarized light microscopy is only capable of distinguishing micropores on the order of 0.001 millimeters and greater. It is assumed that the limestone contains a normal distribution of submicroscopic pore space even if no visible pores are apparent.
Sedimentary fabric	
Grain or matrix support	The limestone is grain supported.
Grain-shape preferred orientation	There is not a strong grain-shape preferred orientation. Though not consistently so, some of the coarsest fossils are oriented horizontally to subhorizontally relative to the core orientation.
Sedimentary lags	No discrete lags are identified.
Bedding structure	Despite what appears to be some variation in sedimentary character throughout the core section, there is not a strong bedding structure apparent behind the dolomitic overprint. In fact, the more or less random orientation of fossil forms suggests that either the sediment was reworked while unconsolidated or the whole mass represents a jumbled debris deposit.
Masonry orientation	The represented masonry unit appears to be naturally-bedded based on what appears to be the original sedimentary orientation.
Diagenetic effects	
Compaction	Compaction is evident in the presence of interpenetrated bioclasts and discrete stylolites. Grain flattening is not a significant feature.
Cementation	A microspar cement binds the copious peloids. The peloidal matrix and its cementation represent the majority of the relict limestone texture. A coarser calcite recrystallization is observed within bioclasts.
Dolomitization	A significant volume of the stone is dolomitized. The dolomitization coincides with the darker gray portions of the stone. The dolomite occurs as euhedral rhombs with lengths ranging from 0.075 to 0.20 millimeters. Dolomite crystals often have dusty interiors and clear margins.
Secondary geological structure	
Brittle cracks	Two hairline cracks are observed that have a subhorizontal orientation with respect to the assumed bedding. The cracks are cohesive but open. The crack path is highly meandering.
Bulk grain deformation	No grain flattening is identified.
Deformation twinning	Deformation twins are not especially abundant.
Stylolites	Stylolites are sparse throughout the core section. The morphology is mostly sutured-type with some wave-type. Stylolites occur as single planes and multiple anastomosing planes. The thickest packets of stylolites are about 1 millimeter. It is assumed that the structures are horizontal with respect to bedding. However, the sedimentary bedding orientation is not especially well-defined. The stylolites contain concentrations of quartz and iron sulfide. Dolomite crystallization also appears to favor the stylolite structures.
Veins	None detected

Table 5.4 (cont'd.): Petrographic Data

Sample ID	JBC-North-8
Secondary service effects	
Cracking	Very minor scaling microcracks are found at the exposed surface of the stone to a depth no greater than 0.5 millimeters. No mineralizations are found in association. There is one vertical crack near the rear of the core that terminates against the central core break. It is not clear whether this was a pre-existing crack or if it developed during core removal.
Grain boundary cohesion	No loss of cohesion around grain boundaries is noted.
Salt deposition	No salt deposits are identified at the scale of the light microscope. It should be stressed that salts present within submicroscopic capillaries may not be readily viewed petrographically and these are usually better assessed through chemical analysis.
Soiling	None observed petrographically
Biogrowth	A greenish biogrowth is observed along the outer face.
Other	There is a microscopic veneer along the core surface where the carbonate has preferentially dissolved leaving the stylolites in positive relief along the face.

Appendix I: Photographs and Photomicrographs

Microscopic examination is performed on an Olympus BX-51 polarized/reflected light microscope and an Olympus SZ40 stereoscopic microscope. The polarized light microscope is fitted with a Tucsen M1chrome 5 Pro 5MP digital camera. The stereoscopic microscope is used for simple magnification. Sample types examined under this microscope include fractured surfaces, fine constituents extracted through chemical or physical means, or honed or polished cross sections. The polarized light microscope (PLM) magnifies but also employs principles of optical crystallography. The most common sample preparation for the PLM is the petrographic thin section. For this preparation, cross-sectioned samples are mounted to glass slides and are milled to a thickness sufficient to allow light to be transmitted through the material. These are usually prepared without water and with minimal heat to avoid altering minerals that are water or temperature-sensitive. In many cases, the samples are impregnated with a low-viscosity, blue-dyed epoxy. When so treated, blue areas represent some type of void space (e.g., air-voids, capillary pores, cracks, etc.). The polarized light photomicrographs are taken using a variety of optical settings chosen to best demonstrate the feature(s) of interest. These are distinguished as follows:

Plane polarized light (abbreviated as PPL)

This method uses the refractive power of different constituents to produce an artificial sense of surface relief. Otherwise, the method is the closest to a simple magnification of the material. The setting is often used to demonstrate granular relationships or microstructure. Pore spaces and cracks are observable with this setting if the blue-dyed epoxy is used.

Conoscopic polarized light (abbreviated as CPL)

In this setting, the transmitted light is condensed just before passing through the thin section. The method tends to bring colors or finer particulates into higher contrast at the expense of image sharpness. The setting is often used to image grain boundary failures in dimension stone, pigment particulates in binders, or gel phases in the micropores of cement pastes.

Cross polarized light (abbreviated as XPL)

The setting places the thin section between two pieces of polarizing film oriented at 90° to one another. In isotropic materials (e.g., glasses, simple salts), all light is absorbed and the materials appear black. In anisotropic crystals, two light rays traveling at different speeds are produced within the thin section and these offset waves interfere at the upper polarizing film. The interference produces a color that can be used to calculate properties of the crystal structure and aid in identification of mineral species. In essence, the colors are artificial. It should be noted that color is a function of orientation and color differences do not necessarily indicate material differences.

Compensator plates

When in XPL mode, full-wave or quarter-wave compensator plates may be inserted into the light path to add or subtract interference. Technically, these methods are used to calculate properties of the crystal structure. However, they can also be used to alter the image appearance to help improve contrast between different constituents. They can also reveal preferred orientations in some materials (e.g., oriented residual crystallinity in fired ceramics).

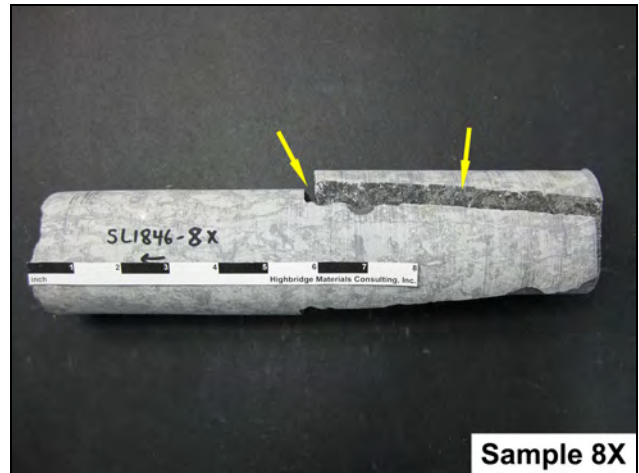
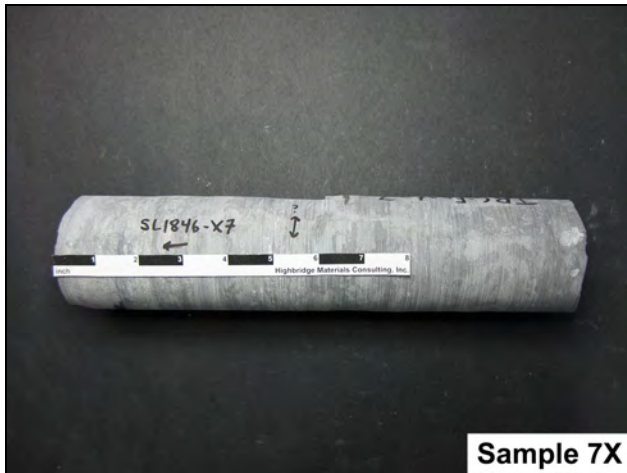
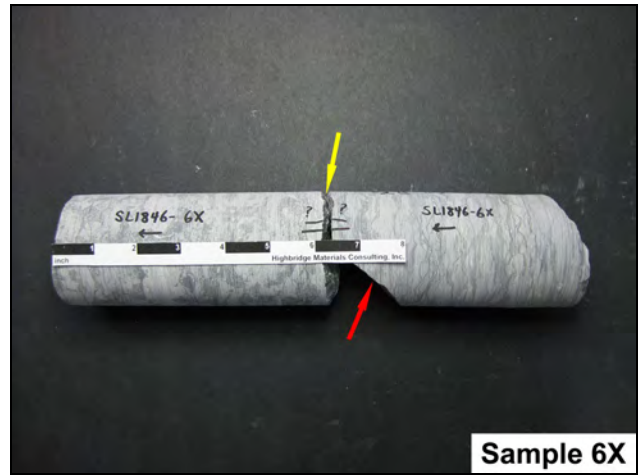
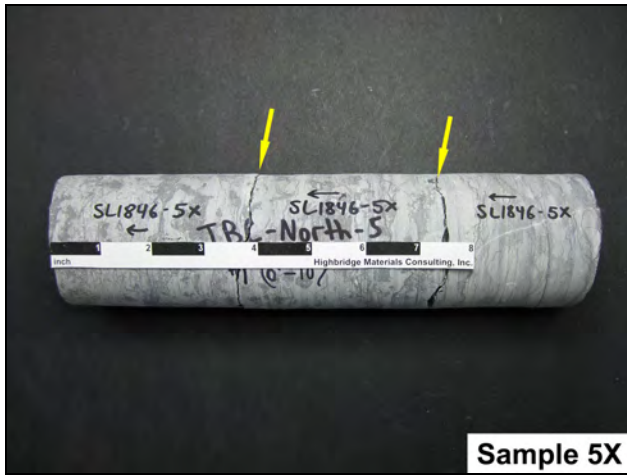


Figure 1: Photographs of the four exterior limestone cores provided to Highbridge for petrographic examination. The cores are shown in side view with their outer surfaces oriented toward the left of each image. The yellow arrows show core breaks that were present in the samples as-delivered. The red arrow shown for Sample 6X indicates a wedge of limestone lost in the sample recovery.

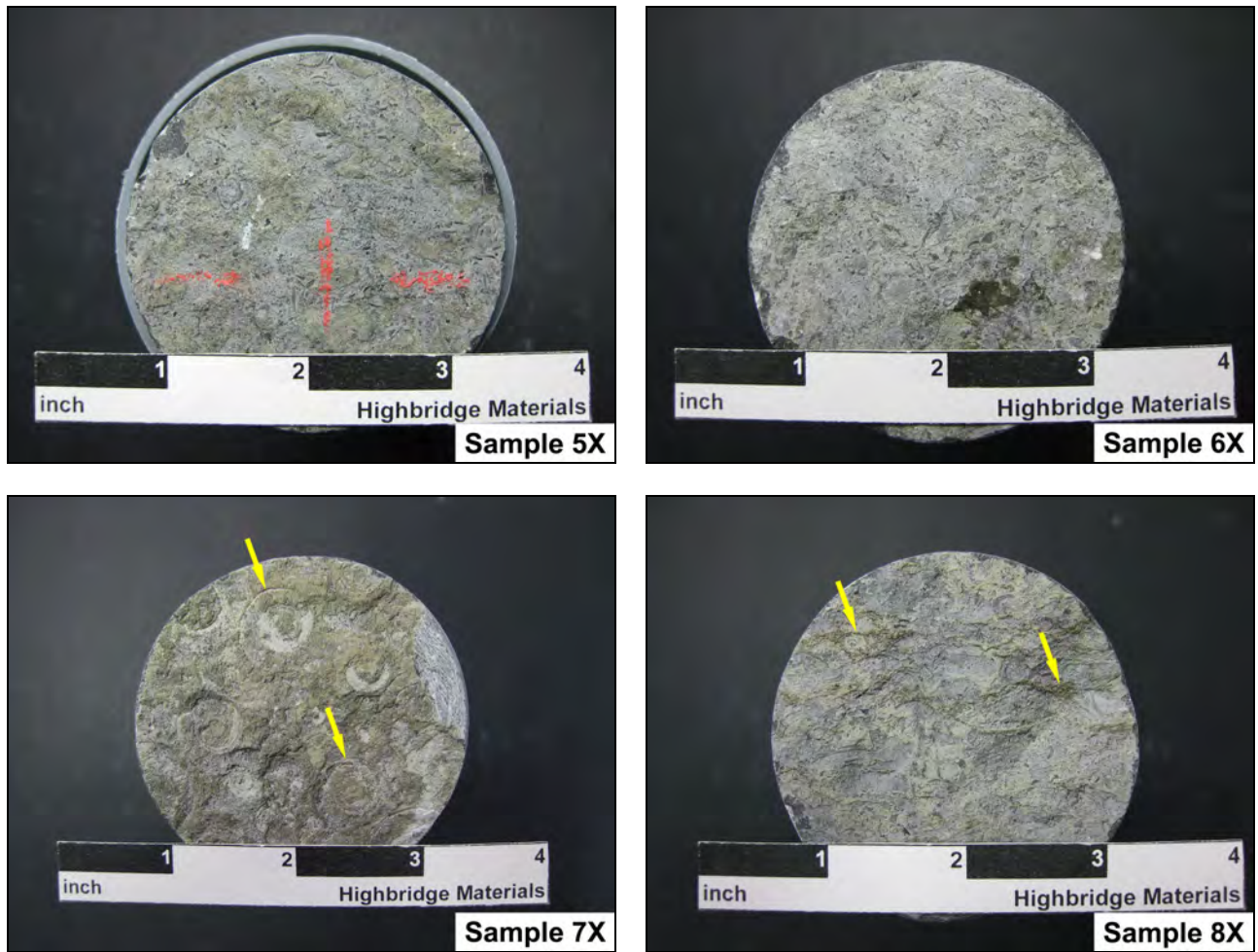


Figure 2: Photographs of the outer core surfaces. In the image for Sample 7X, the arrows show impressions of fossil ammonites. For Sample 8X, the arrows indicate where quartz-rich stylolites stand out in relief due to chemical weathering.

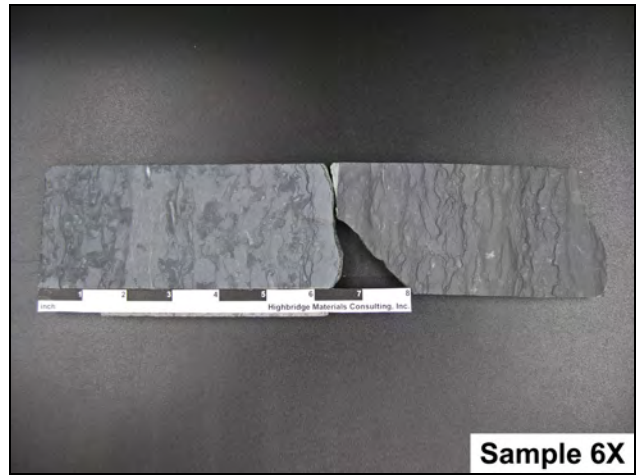
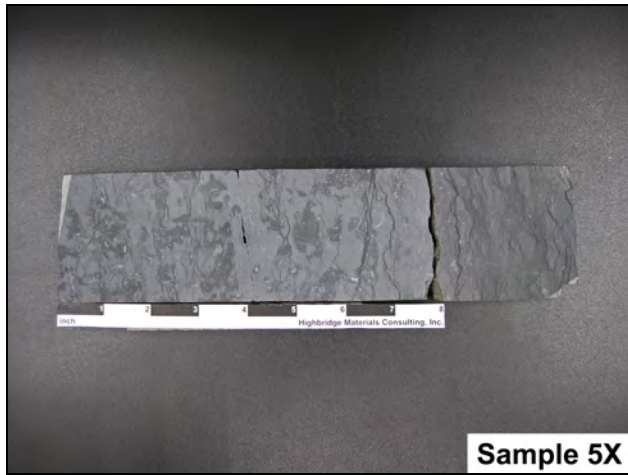


Figure 3: Photographs of honed sections of the four limestone cores. These are oriented the same as in Figure 1. Note that the primary fabric parallels the face of the masonry unit in the first three samples. In contrast, the fabric runs parallel to the core axis in Sample 8X.

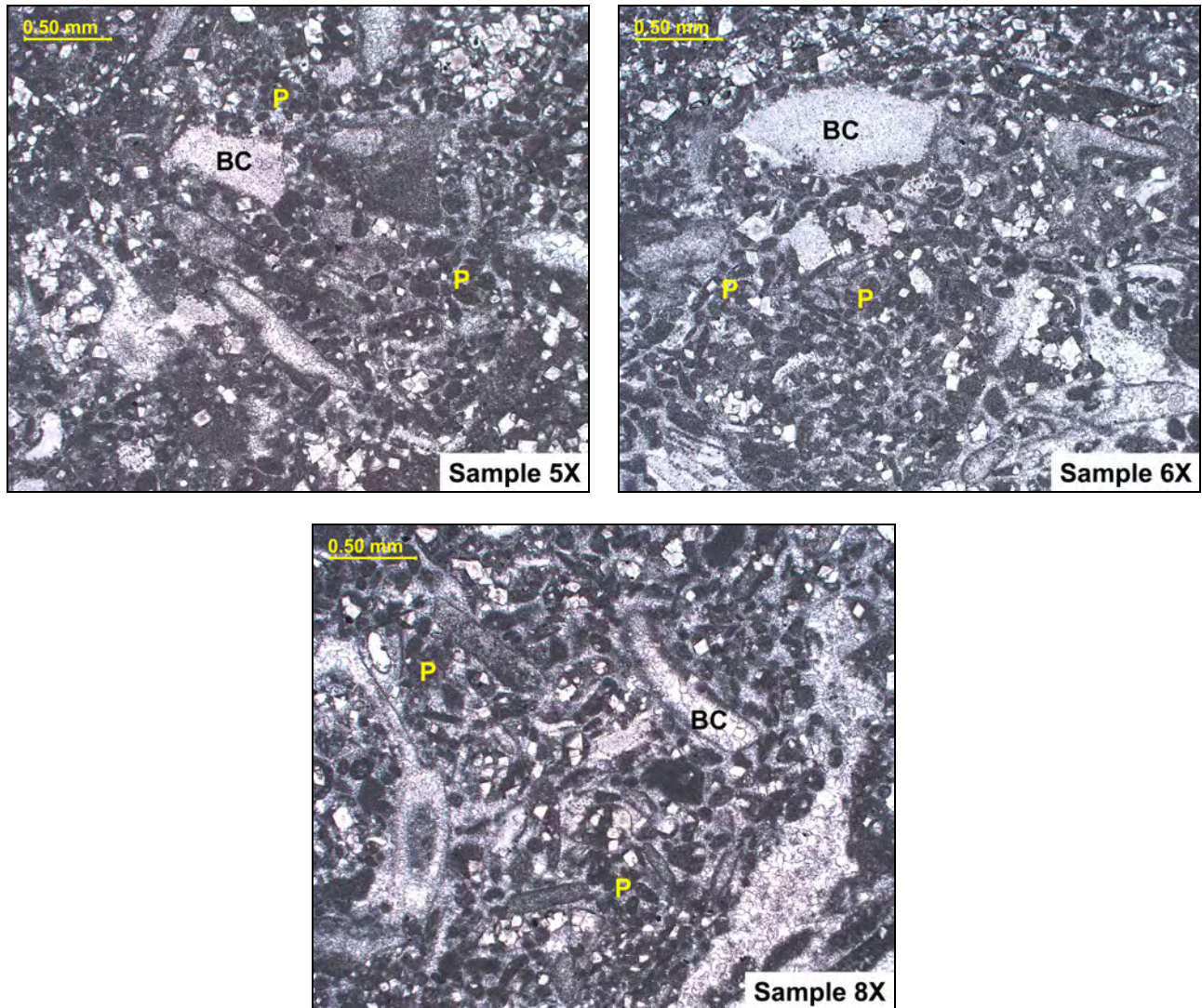


Figure 4: PPL photomicrographs illustrating the original limestone fabric prior to the dolomitization of the stone. The matrix consists of densely packed peloids (P). These consist of micrite (fine carbonate mud) and are cemented by a microscopic calcite spar. Bioclasts (BC) are sparsely distributed throughout the peloidal mass. The most easily identifiable of these include debris from echinoderms and trilobites. Note that this original fabric is not observable in Sample 7X.

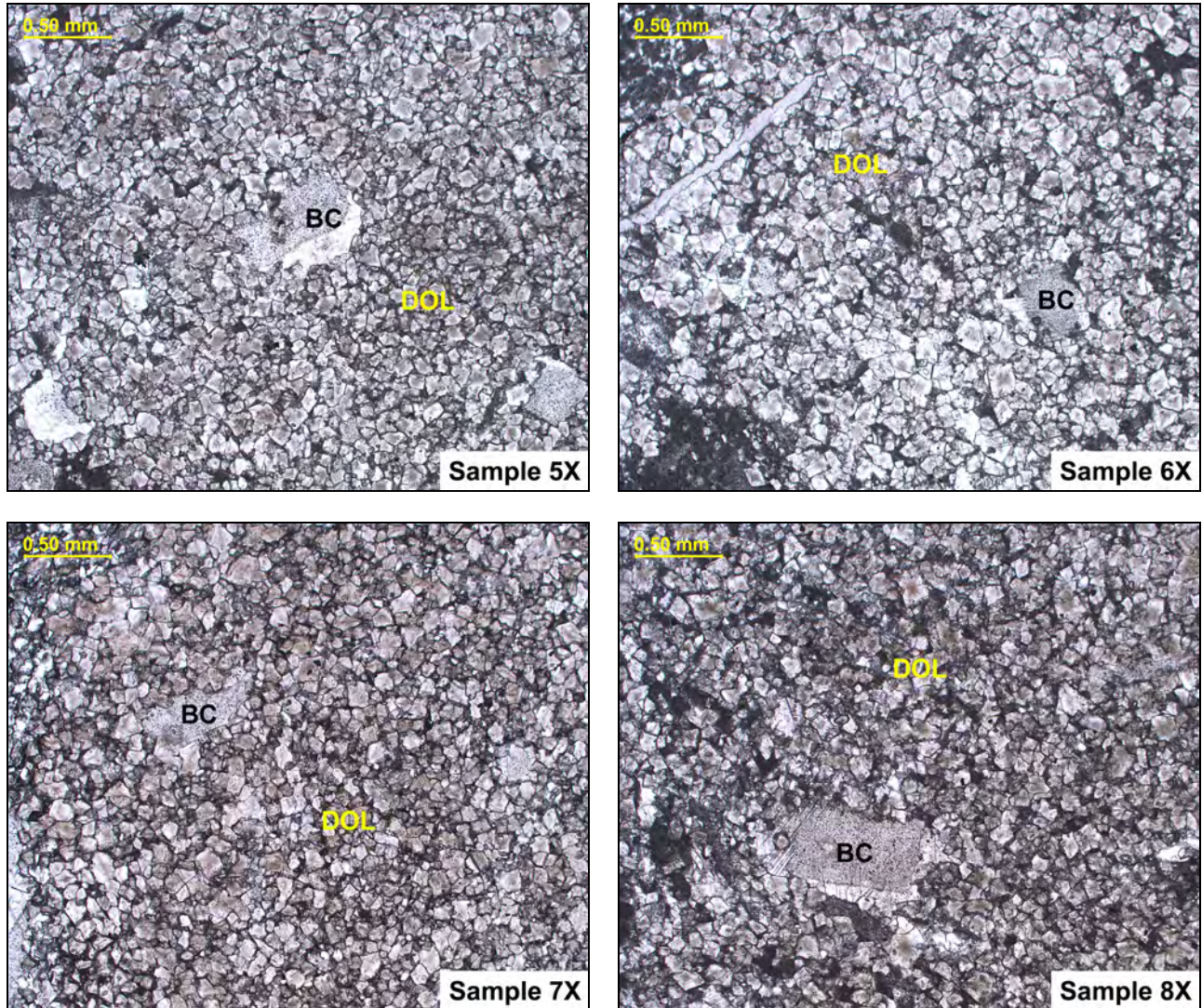


Figure 5: PPL photomicrographs. The majority of the stone is diagenetically recrystallized and this masks much of the original sedimentary texture. The recrystallized portions contain a network of well-formed fine-grained rhombic dolomite crystals (DOL). Some of the bioclasts (BC) are preserved within the matrix but these are largely overprinted.

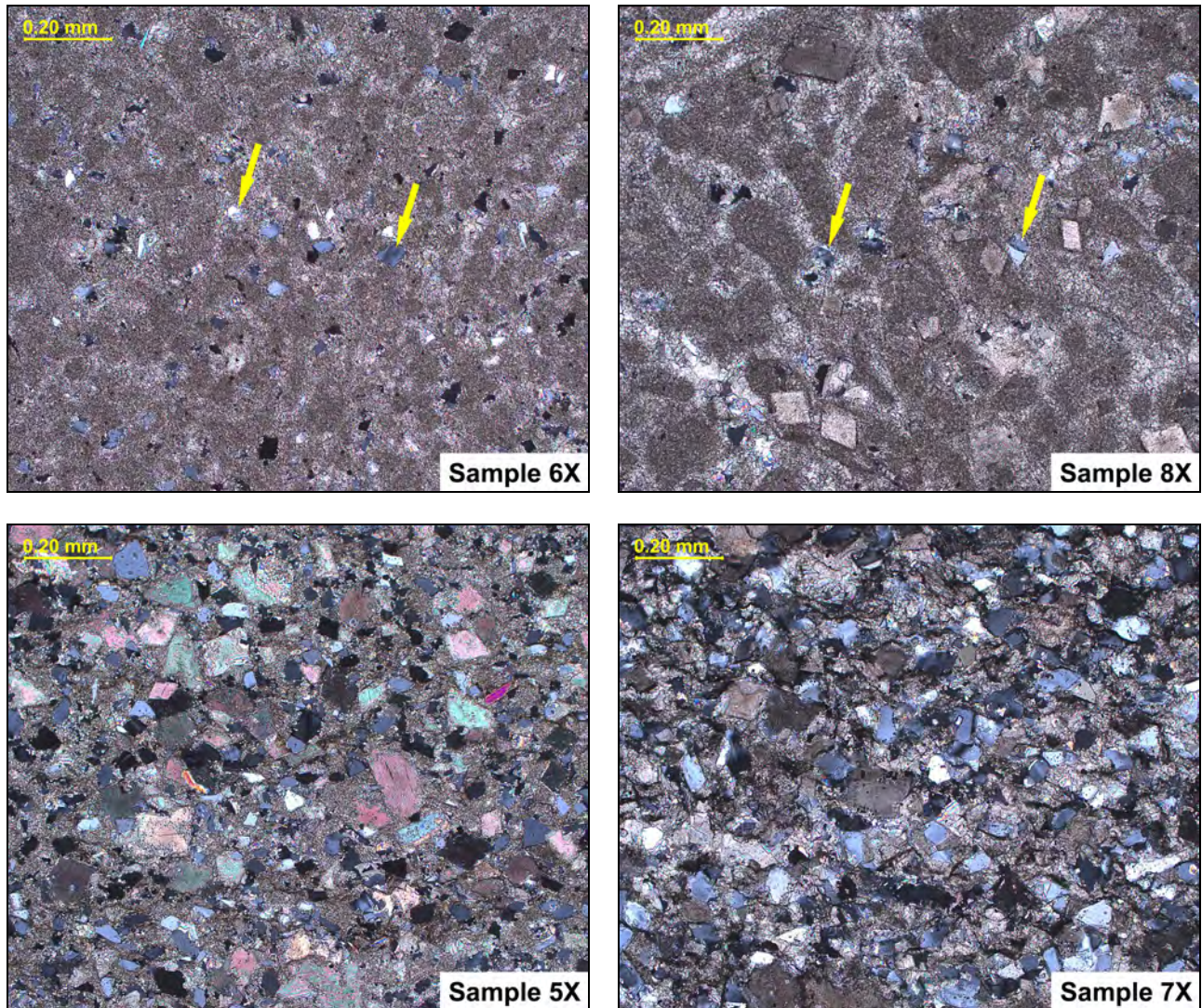


Figure 6: PPL photomicrographs. (Upper images) Fine sediment is distributed throughout all of the stone. The arrows show silt-sized grains of quartz and feldspar in two of the samples. (Lower images) Bands enriched in quartz are found in Samples 5X and 7X. In these images, the quartz and feldspar are represented by the white and gray particulates. The sediment-rich bands are the only planar sedimentary structures discernible in the limestone. Other planar fabrics are structural rather than sedimentary.

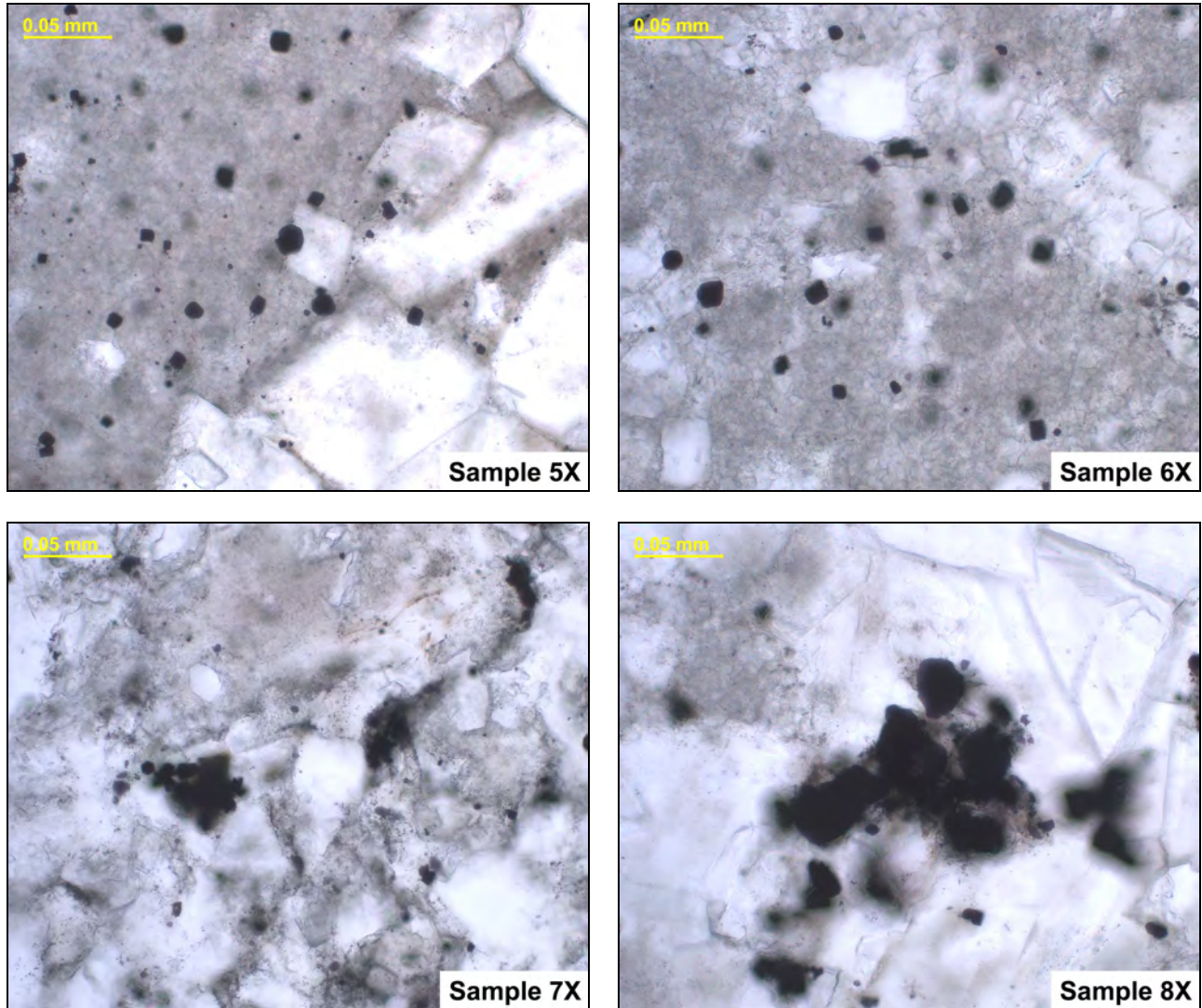


Figure 7: CPL photomicrographs. The black grains are iron sulfides found ubiquitously throughout the stone. Virtually all of the sulfide is fresh and unoxidized. The grains are finer than the thickness of the thin section. In part, this causes the grains to appear blurry.

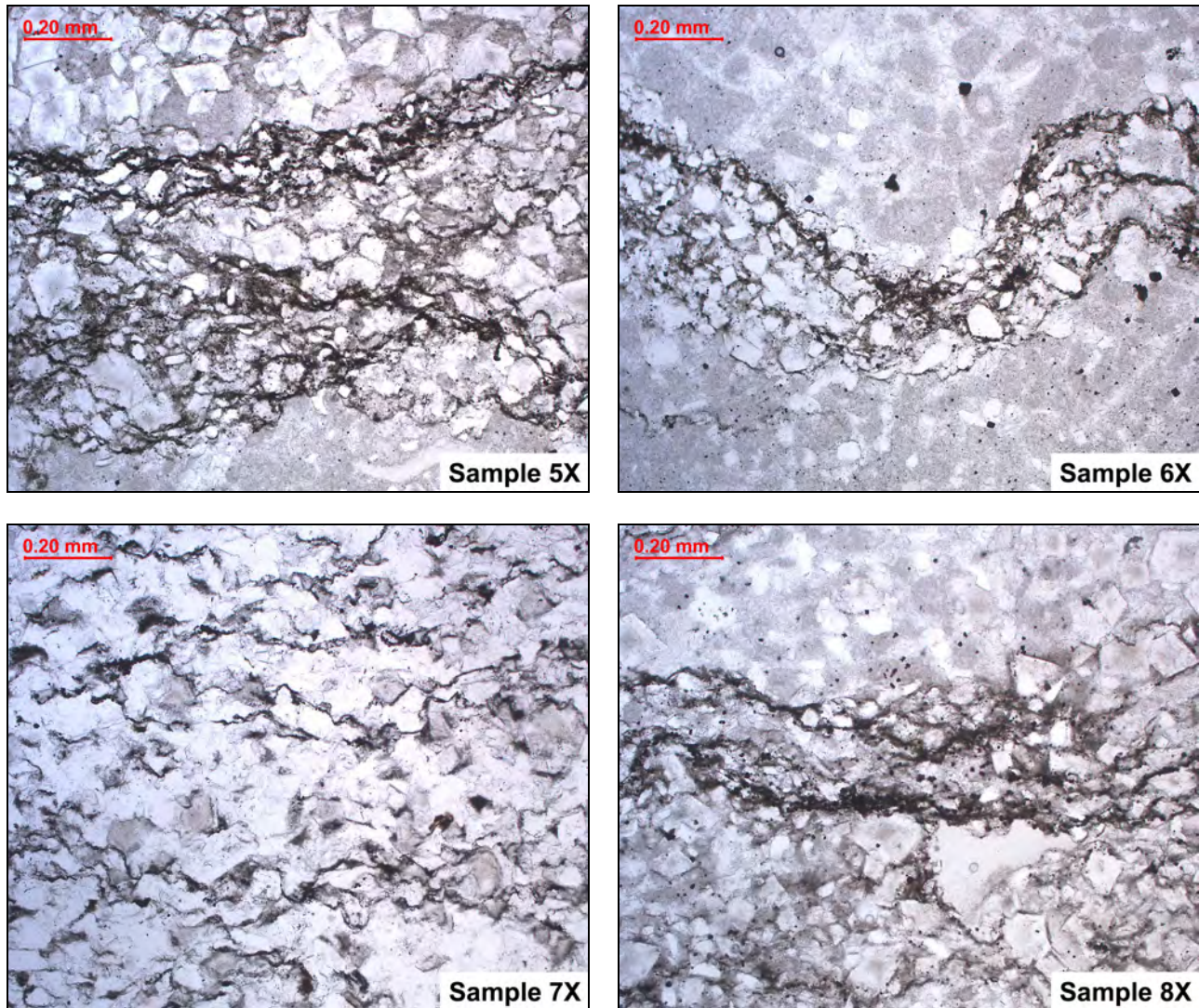


Figure 8: CPL photomicrographs. The dark streaks running left to right in the images are concentrations of quartz and sulfide grains in pressure solution cleavages called stylolites. These are sites along which the carbonate has dissolved under geological pressure leaving behind insoluble materials. While these can sometimes be permeable and represent planes of preferential weakness, all appear tight and indurate in the sample set. Note that there are no continuous stylolites in Sample 7X. All are incipient in this sample.

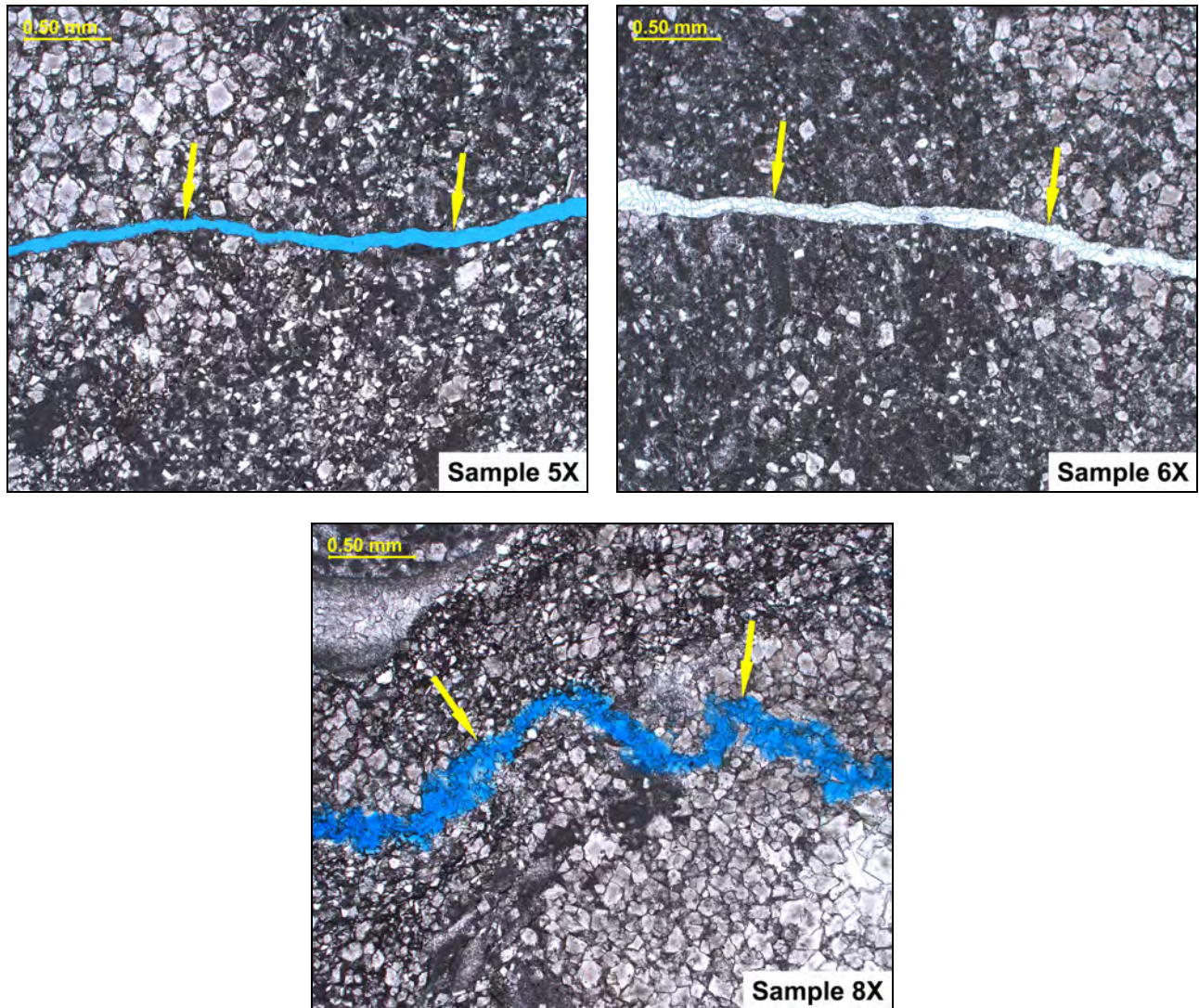


Figure 9: The arrows in these PPL photomicrographs indicate hairline cracks in three of the samples that are interpreted to have formed geologically. Two are filled with a blue-dyed epoxy. The crack in Sample 8X was cut at an oblique angle resulting in a less sharp character in cross section. No dissolution, mineralizations, or subsidiary cracking is found in association with these minor cracks.

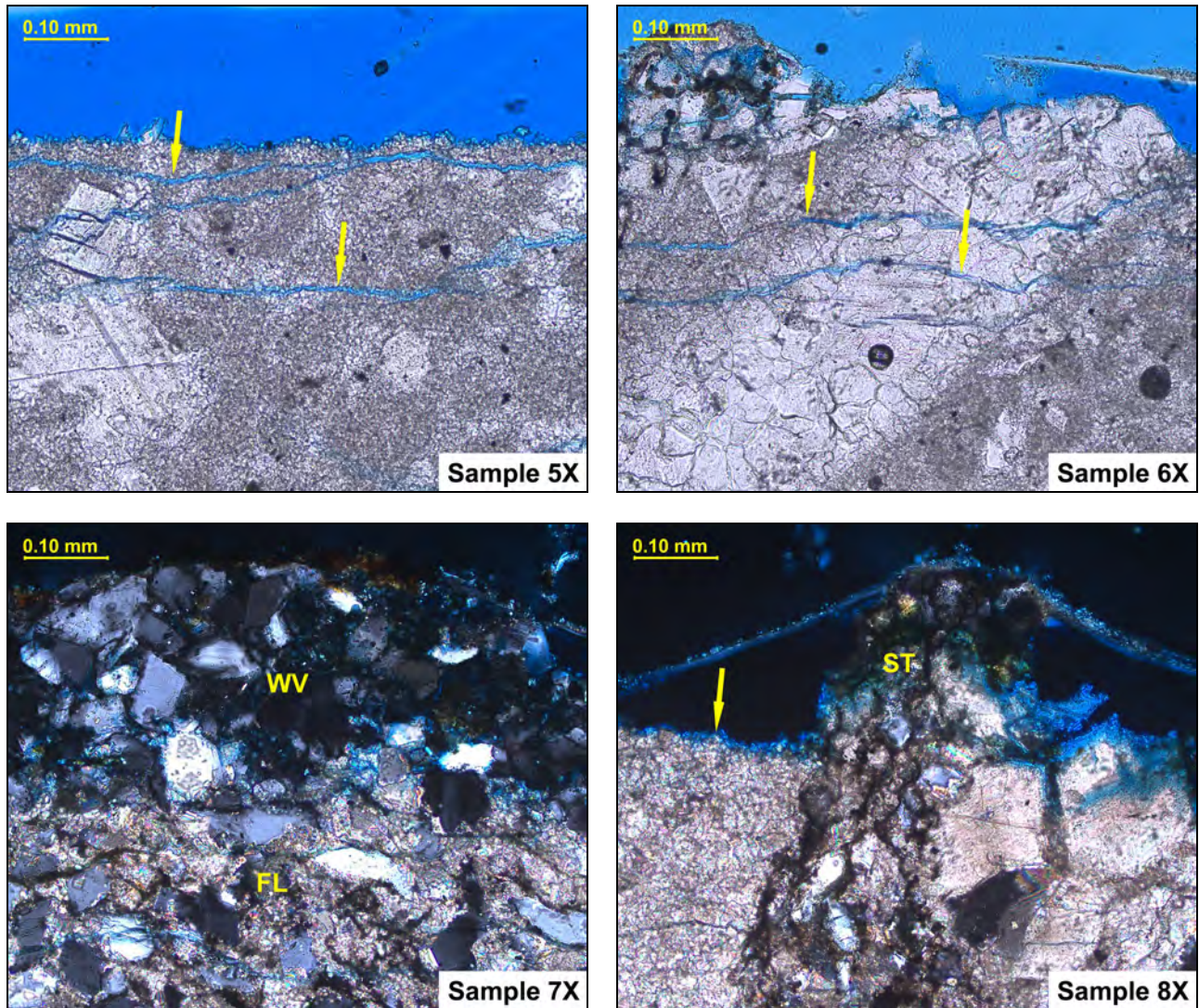


Figure 10: These PPL photomicrographs were taken at the outer surface of each core. The surfaces are oriented toward the top of each image. In the upper two images, the arrows indicate exceptionally minor scaling cracks. At lower left, the carbonate minerals are present in the fresh limestone (FL) of Sample 7X but, have preferentially dissolved within the weathered veneer (WV). Insoluble quartz remains proud along the weathered face. At lower right, a stylolite (ST) remains proud over the weathered-back carbonate (arrow) of Sample 8X. All of the observed weathering in the four samples is considered superficial and innocuous.

X-ray Diffraction Analysis Report

Bennington Battle Monument

15 Monument Circle, Bennington, VT 05201



Prepared for

Jablonski Building Conservation, Inc.

Client ID

JABL001

Report No.

SL1846-04

Report Date

12/17/23

HIGHBRIDGE



MATERIALS CONSULTING, INC.

Confidentiality

This report presents the results of laboratory testing requested by the client to satisfy specific project requirements. As such, the client has the right to use this report as necessary in any commercial matters related to the referenced project. Any reproduction of this report must be done in full. In offering a more thorough analysis, it may have been necessary for Highbridge to describe proprietary laboratory methods or present opinions, concepts, or original research that represent the intellectual property of Highbridge Materials Consulting and its successors. These intellectual property rights are not transferred in part or in full to any other party. Presentation of any or all of the data or interpretations for purposes other than those necessary to satisfy the goals of the investigation are not permitted without the express written consent of the author. The findings may not be used for purposes outside those originally intended. Unauthorized uses include but are not limited to internet or electronic presentation for marketing purposes, presentation of findings at professional venues, or submission of scholarly articles.

Standard of Care

Highbridge has performed its services in conformance with the care and skill ordinarily exercised by reputable members of the profession practicing under similar conditions at the same time. No other warranty of any kind, expressed or implied, in fact or by law, is made or intended. Interpretations and results are based strictly on samples provided and/or examined.

Cover Image

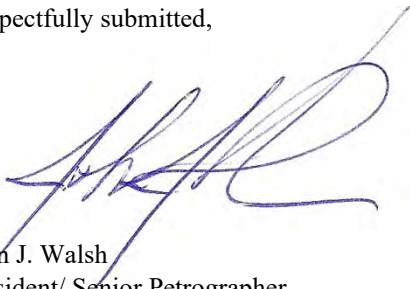
The Bennington Battle Monument in Bennington, VT. Image downloaded August 26, 2023 without modification.

Photo credit: King of Hearts

https://commons.wikimedia.org/wiki/File:Bennington_Battle_Monument_October_2021_001.jpg

Under Creative Commons License CC BY-SA 4.0 - <https://creativecommons.org/licenses/by-sa/4.0/deed.en>

Respectfully submitted,



John J. Walsh
President/ Senior Petrographer
Highbridge Materials Consulting, Inc.



Heather Hartshorn
Senior Chemist
Highbridge Materials Consulting, Inc.

1. Executive Summary

This report presents the results of x-ray diffraction analysis on salts sampled from various portions of the masonry at the Bennington Battle Monument, Bennington, VT. These are described by the client as the light yellowish white stone.

Most of the samples were provided as loose surface scrapings. These all contain some type of potassium salt. Most are sulfates, though some bicarbonate is also present. Due to the high solubility of most of its compounds, potassium is highly mobile and can have derived from most anywhere. However, the sulfates are likely from pollutants in the environment, or additives in the cements present in the masonry.

One of the samples is a degraded and water-logged mortar from near grade. The soluble salts in this sample are rich in nitrates likely derived either from bird excrement or fertilizers. Some magnesium in the salts may derive from natural cement in the mortar.

A thin salt veneer along the formed face of a concrete infill core contains calcite and impurities from the aggregate. However, an amorphous component is noted in the XRD spectrum. This may relate to minor reaction gels produced from aggregate reactions in the concrete. Some amorphous material is also indicated in Sample NE11 though its nature is less certain.

2. Introduction

On November 2, 2023, a set of masonry samples were delivered to the laboratory by Mr. Edward FitzGerald of Jablonski Building Conservation, Inc. According to Mr. FitzGerald, these represent materials sampled from the Bennington Battle Monument, Bennington, VT. The monument is a stone obelisk completed in 1889. The client has requested that the laboratory perform materials analysis on a subset of the samples as summarized in Table 2.1 below. The choice of samples to analyze are based on priorities set by Mr. FitzGerald with some additional input by the laboratory.

Table 2.1: Summary of Received Samples

This table includes only those samples selected for analysis. The laboratory made some nominal amendments to sample identifications for consistency and simplicity in reporting. These are shown in the "HMC ID" column. These identifications will be used throughout all reports.

Client ID	HMC ID	Client description on sample bag or verbally	Analytical scope requested
NW5	NW05	Salts on mortar joint	Water-soluble salts
NE11	NE11	Buff stone salts	Water-soluble salts
SE24-NE25	SE24	Salts, dark gray stone	Water-soluble salts
SW12	SW12	Salts in crack, buff stone	Water-soluble salts
SW26	SW26	Rear window, dark gray stone, salts in HC	Water-soluble salts
BM-01	BM01	South elev., ext. sand mortar bedding	Mortar analysis, water-soluble salts
BM-02	BM02	South ext. elev., org. point/bed? Under most recent repointing	Mortar analysis
BM-05	BM05	Observation deck, 2 mortars, light buff on top, flat & flush	Mortar analysis
NE4	NE04	Dark brown mortar	Mortar analysis
NE18	NE18	Interior, crumbly mortar near dark gray stone	Mortar analysis
NW26	NW26	Corner joint	Mortar analysis
SW2	SW02	Int. coarse, buff color at corner separation	Mortar analysis
SW16	SW16	Org. bedding	Mortar analysis
(none)	CF	Concrete infill	Concrete petrography, mortar analysis, salts

The requested testing includes the following:

- **X-ray diffraction analysis of salts or mineralizations**

The client has requested the qualitative identification of salts for seven samples. Five of the samples were provided as scrapings of variable purity. One sample (BM01) consists of water-logged mortar debris with no salts visible. One sample (CF) consists of a salt crust along the formed face of a concrete infill layer. The samples were analyzed either as-found, or after extraction and redeposition. X-ray diffraction analysis (XRD) is used to identify the phases present.

- **Compositional mortar analysis**

The client has requested that Highbridge perform compositional mortar analysis on eight of the provided samples. The testing includes a petrographic examination and chemical analysis to identify constituents, estimate proportions, and assess overall condition. Chemical digestions to extract sand samples for description and gradation are also included.

- **Petrographic examination and partial compositional analysis of infill concrete**

Petrographic examination is used to examine the infill concrete. The purpose is to identify constituents, assess condition, and investigate potential causes of any observed distress. A compositional analysis is performed on the mortar fraction of the concrete to evaluate the proportions of binder and sand using the same techniques described above for mortar.

This report presents the results of the qualitative salt identification. Results for the other analyses will be presented under separate cover when complete.

3. Methods of Examination

X-ray diffraction analysis was performed using proprietary methods. Sample preparation was performed at Highbridge's laboratory facility. Instrumentation was performed by H&M Analytical Services in Hamilton, NJ. Additional information on methods is presented in Section 4 of this report.

The following personnel contributed to the examination:

Technician:	M. Pattie
Analysts:	M. Cortez J. Adametz (H&M Analytical)
Chemist:	H. Hartshorn
Petrographer:	J. Walsh

4. X-Ray Diffraction Analysis of Salt Deposits and Water-Soluble Salts

Table 4.a: Characteristics of Provided Samples

Sample ID	Description
NW05	The sample consists of white crumbs along with mortar residues. Much of the material appears very reflective. Marble debris may be included.
NE11	The sample appears fairly pure and consists mostly of bright white flakes and crumbs of a compact, moderately reflective material.
SE24	Approximately equal parts of a compact, greasy-lustered white salt, and what appears to be soiling and other brownish debris.
SW12	The sample contains at least one large piece of marble, along with pinkish granules and brownish soiling. Most of the granules appear to be marble as well.
SW26	Fragments of compact white material along with some dark fragments (limestone?). The sample size is very small.
BM01	Light brown mortar sample weighing a total of 56 grams (after subsampling). The mortar consists mostly of very small fragments and an abundance of granules and powder.
CF	A white salt coating lines the formed surface of a concrete infill core sample. The salts were transferred from the surface for analysis.

4.1 - Laboratory Methods

Three types of sample preparation were used to concentrate salts for x-ray diffraction analysis (XRD) as follows.

A. Water extraction

Most of the fragmental samples contained too many impurities to analyze in their "as-found" condition. These included Samples NW05, SE24, SW12, and SW26. Sample BM01 is essentially a crumbled mortar sample and this was also treated by water extraction. For these, the samples were all prepared by crushing any larger particles to roughly sand-sized pieces in an agate mortar and pestle. Each sample was added to a 1 L beaker to which approximately 500 mL of distilled water was added. Each beaker was placed on a hot plate, and the suspension was boiled for 5 minutes. The samples were then left to digest at room temperature for approximately 1 week. Following the digestion period, each mixture was vacuum-filtered through a fine-textured (Q2) filter paper. Several rinsings of the residue were similarly filtered. The filtrate was transferred to a 1 L beaker and evaporated on a hot plate set to 180°C until the filtrate was reduced to approximately 25 to 50 mL. The reduced filtrate was then transferred to a glass petri dish and placed in a laboratory oven set to 55°C to finish evaporating to dryness. The precipitated salts were transferred from the petri dish, viewed under low-powered magnification to record their characteristics (see Table 4.a), and then gently ground in an agate mortar and pestle.

B. "As-found"

Sample NE11 was sufficiently pure as-received. This sample was simply ground in an agate mortar and pestle before analysis.

C. Transfer

The formed surface of Sample CF is coated with a thin veneer of white salts. The laboratory prepared a flexible slide with a piece of double-sided adhesive tape and pressed this against the deposit to collect a sufficient quantity of the mineralization for direct analysis.

Table 4.1a: Characteristics of Extracted Salts

Sample ID	Description	Deliquescent
NW05	Thin white film with no distinguishable crystals	No
SE24	Mass of opaque, white salts	No
SW12	Thin translucent film, no distinguishable crystals	No
SW26	Thin translucent film, no distinguishable crystals	No
BM01	Thin film of fine white crystals. The mass was pale orange-brown after scraping from the petri dish.	Very slightly

With the exception of the sample adhered to the flexible slide, all of the samples were transferred to glassine envelopes. All seven samples were sent to H&M Analytical in Hamilton, NJ for instrumental analysis. According to Ms. Jessica Adametz, the loose powders were loaded into the wells of zero-background sample holders, and the slide was affixed directly to a similar holder. All samples were then placed into a Panalytical X'pert Powder diffractometer using Cu radiation at 45kV/40mA. The scans were run over a 2θ range of 6° to 80° , with a step size of 0.0131° and an accumulated counting time of 250 seconds per step. Once the patterns had been collected, the crystalline phases were identified with the aid of the Powder Diffraction File published by the International Centre for Diffraction Data or the Inorganic Crystal Structure Database.

4.2 - Laboratory Findings

The identified phases are described in Tables 4.2b and 4.2c. The original spectra from which these phases are interpreted are presented in Appendix I.

Table 4.2a: Extracted Salt Recovery

For the soluble salts extracted through water digestion, the total percentage of extracted salt is shown. These values are only relative to the provided sample. They do not necessarily represent the degree of contamination within the associated masonry component.

Sample ID	Sample wgt. (g)	Extracted salt wgt. (g)	Percentage of extracted salts (%)
NW05	0.3507	0.0229	6.5
SE24	1.7499	0.2911	16.6
SW12	1.4150	0.0061	0.4
SW26	0.0852	0.0067	7.9
BM01	15.3013	0.8513	5.6

Table 4.2b: XRD - Interpreted Phases

Rietveld refinement is not applied to these spectra and a formal quantification of the phases would not be meaningful. The major and minor categories given here are rough approximations based on the strength of any given signal relative to the most intense peak. Two of the spectra exhibited a broad hump that is generally attributable to the presence of some non-crystalline or otherwise amorphous material.

Sample ID	Major (> 10% by weight)	Minor to trace (< 10% by weight)	Signal notes
NW05	Aphthitalite, kalicinite	Calcite	-
NE11	Calcite, arcanite	Aphthitalite, cristobalite	Amorphous hump
SE24	Kalicinite, arcanite	Calcite	-
SW12	Aphthitalite, kalicinite, calcite	Sylvite	-
SW26	Aphthitalite, kalicinite	Vanthoffite	-
BM01	Niter, magnesium nitrate hexahydrate, gypsum	-	-
CF	Calcite, aragonite, dolomite	Quartz	Amorphous hump

Table 4.2c: Chemical Formulas

Mineral name	Chemical formula
Aphthitalite	$K_3Na(SO_4)_2$
Aragonite	$CaCO_3$
Arcanite	K_2SO_4
Calcite	$CaCO_3$
Cristobalite	SiO_2
Dolomite	$CaMg(CO_3)_2$
Gypsum	$CaSO_4 \cdot 2H_2O$
Kalicinite	$KH(CO_3)$
Magnesium nitrate hexahydrate	$Mg(NO_3)_2 \cdot 6(H_2O)$
Niter	KNO_3
Quartz	SiO_2
Sylvite	KCl
Vanthoffite	$Na_6Mg(SO_4)_4$

4.3 - Discussion

The following commentary may be offered regarding the phases identified through x-ray diffraction analysis:

Potassium salts

All of the loose scrapings provided by the client are enriched in potassium salts including sulfates (aphthitalite and arcanite) and bicarbonate (kalicinite). As an alkali, potassium is a highly mobile element that is easily solubilized and transported in most of its forms. As such, it is difficult to isolate a particular source. With that said, there are two sources of sulfate ion that are more likely than others. The first is from the remobilization of gypsum or epsomite formed by reaction between the masonry and environmental acids (e.g., sulfuric acid dissolved in rainwater). The second is from sulfate additions to cements used in the construction. By the late nineteenth century, gypsum was an additive in both portland and natural cement.

Carbonates

Calcite is found throughout the sample set as well as some aragonite in Sample CF. These carbonates are innocuous phases that typically precipitate from water that has passed through any calcium-bearing material.

Nitrates

Two forms of nitrate are found in the one mortar sample understood to have been collected near grade. Nitrates typically derive from the decomposition of organic materials. In this context, these can include fertilizers used in the adjacent landscaping or bird excrement. One of the nitrates is magnesium-based. As will be discussed in a forthcoming mortar analysis report, this sample contains natural cement, a magnesium-based binder. The cement may be the source of magnesium in this sample.

Aggregate impurities

In addition to carbonate salts, the surface deposit in the concrete infill sample contains a little bit of quartz and dolomite. These are both components of the aggregate in this particular concrete. The aggregates are likely sources for these signals.

Amorphous humps

The spectra for Samples NE11 and CF (reference) contain broad "humps" at low 2θ . Though broad noise can sometimes be attributable to preferential orientation of crystals, these well-defined humps indicate the presence of some type of non-crystalline material. As will be discussed in a forthcoming petrographic examination for Sample CF, there are traces of amorphous reaction gel possibly associated with minor reaction of the dolostone coarse aggregate. A thin veneer of this gel is noted along the same surface from which the salt sample was collected. Sample NE11 may contain some of the same reaction product. However, petrography has been performed for this sample.

Vanhoffite

There are several very minor peaks in the spectrum for Sample SW26 that are not fully explained by the potassium sulfates. The peaks could be explained by a trace quantity of the sodium-magnesium sulfate salt, vanhoffite. However, it should be stressed that the presence of this phase is highly uncertain. It would not be inappropriate to draw any conclusions from this tentative identification.

Appendix I: X-Ray Diffraction Spectra

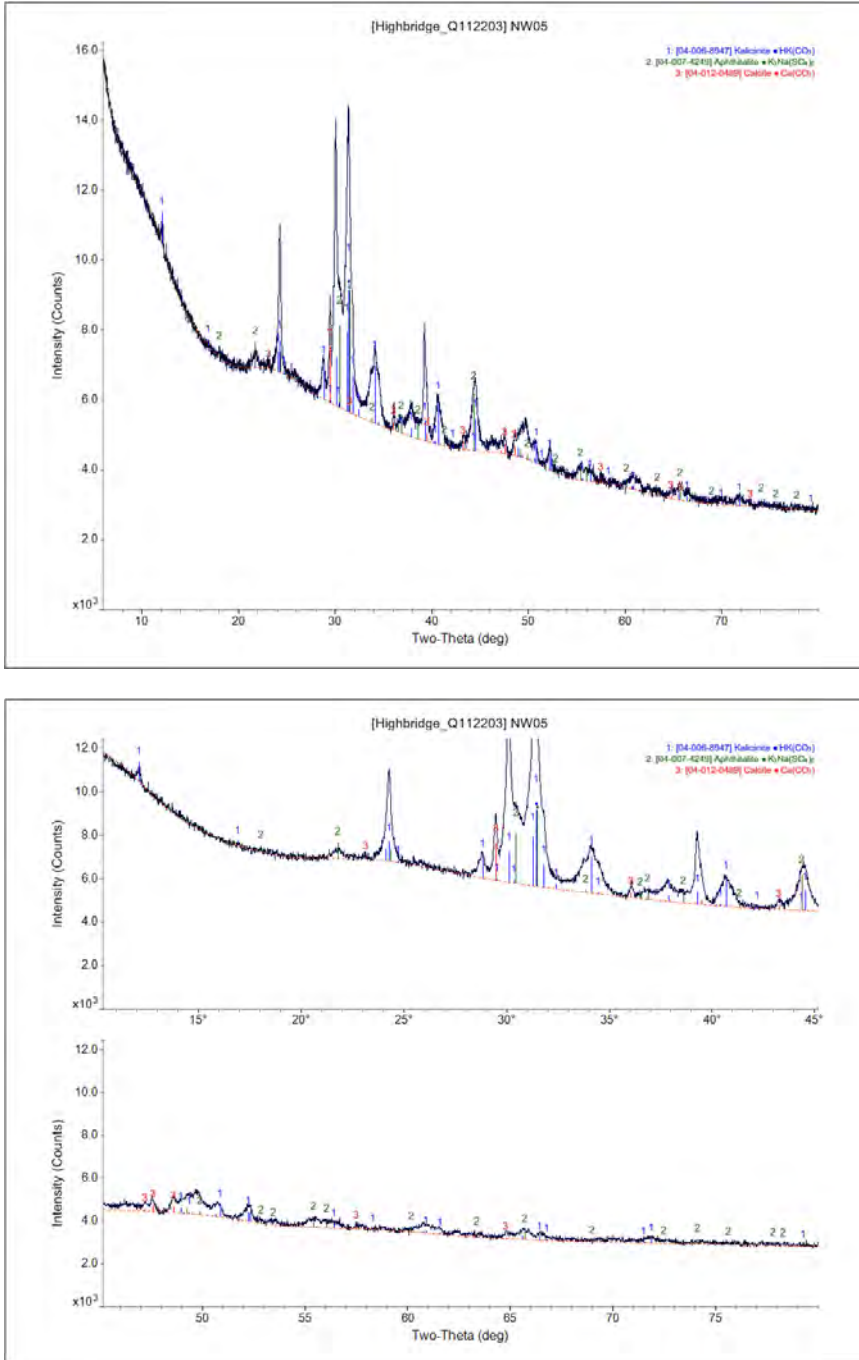


Chart I.1: X-ray diffraction spectrum for Sample NW05. The salts were extracted by water digestion from surface scrapings provided by the client. The full spectrum is shown at top and an exploded view at bottom.

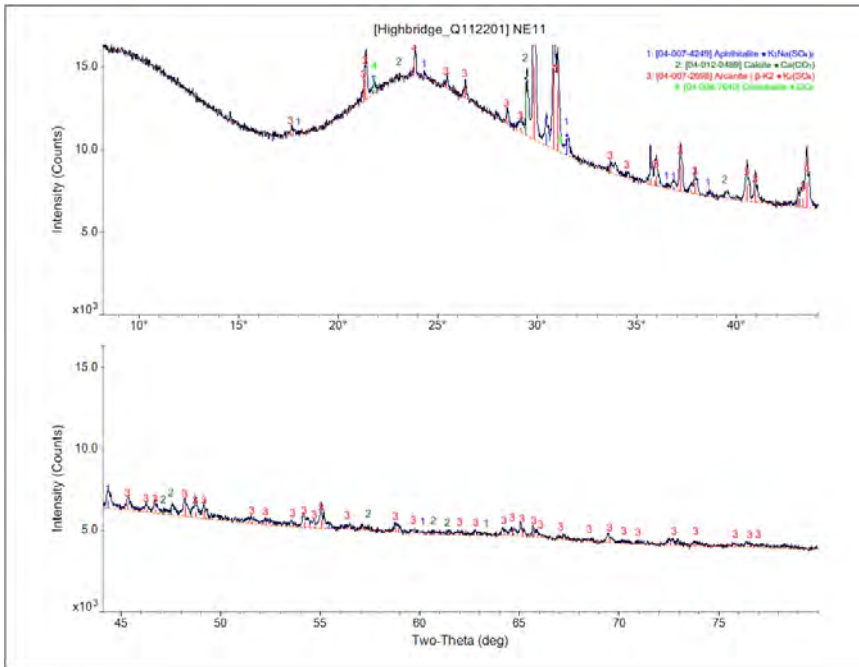
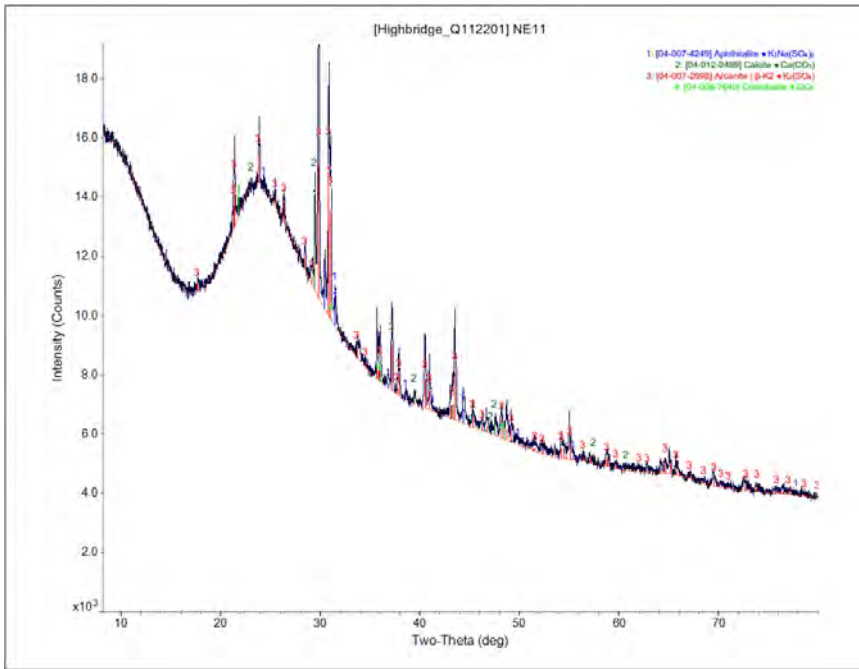


Chart I.2: X-ray diffraction spectrum for Sample NE11. The surface scraping provided by the client was ground and measured "as-found". The full spectrum is shown at top and an exploded view at bottom. Note the broad hump at 2θ between about 20° and 30° . This is indicative of an amorphous material.

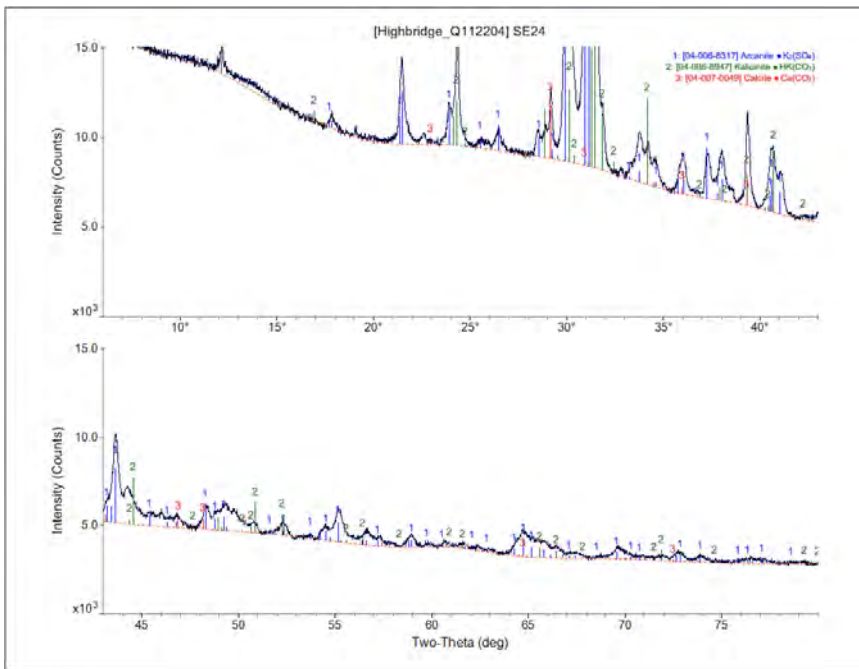
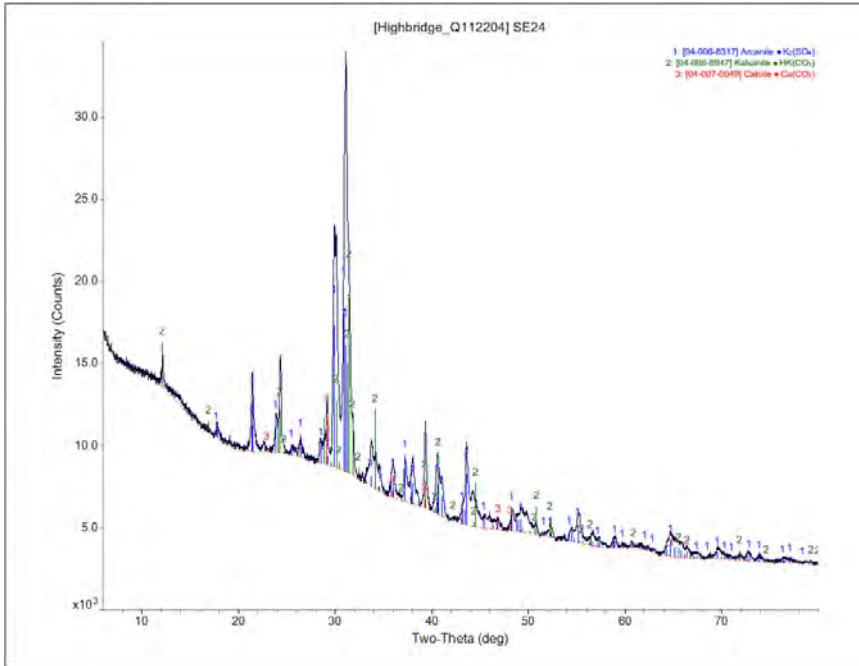


Chart I.3: X-ray diffraction spectrum for Sample SE24. The salts were extracted by water digestion from surface scrapings provided by the client. The full spectrum is shown at top and an exploded view at bottom.

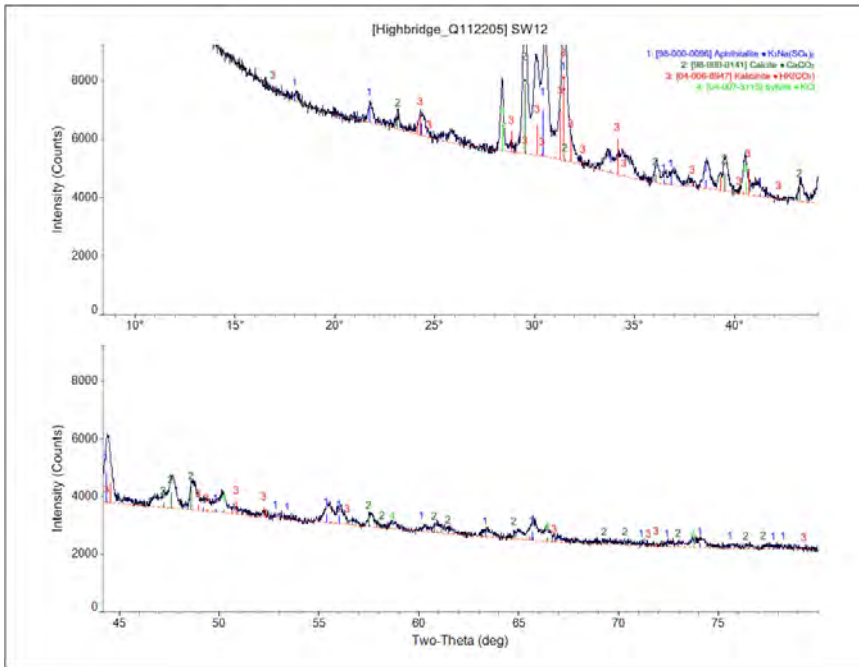
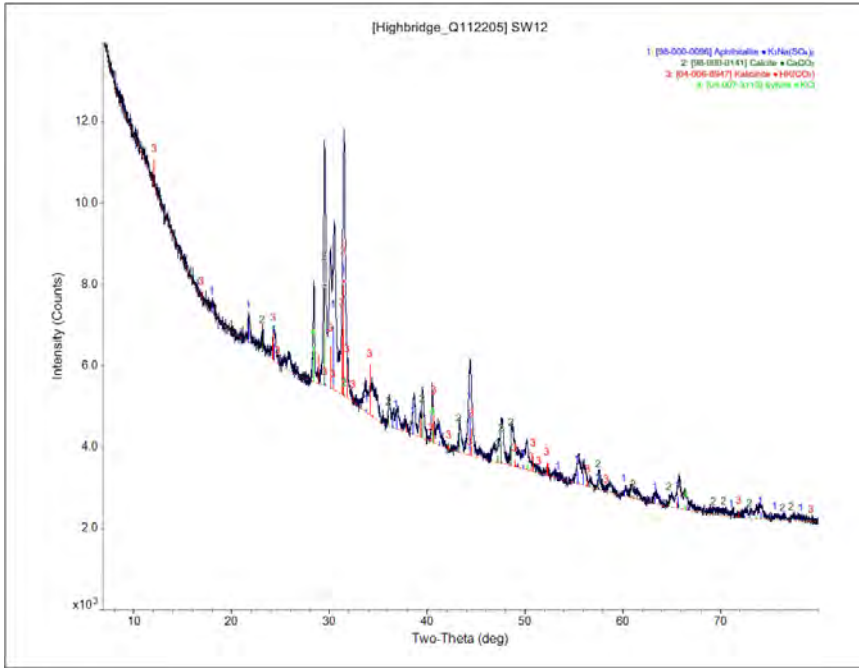


Chart I.4: X-ray diffraction spectrum for Sample SW12. The salts were extracted by water digestion from surface scrapings provided by the client. The full spectrum is shown at top and an exploded view at bottom.

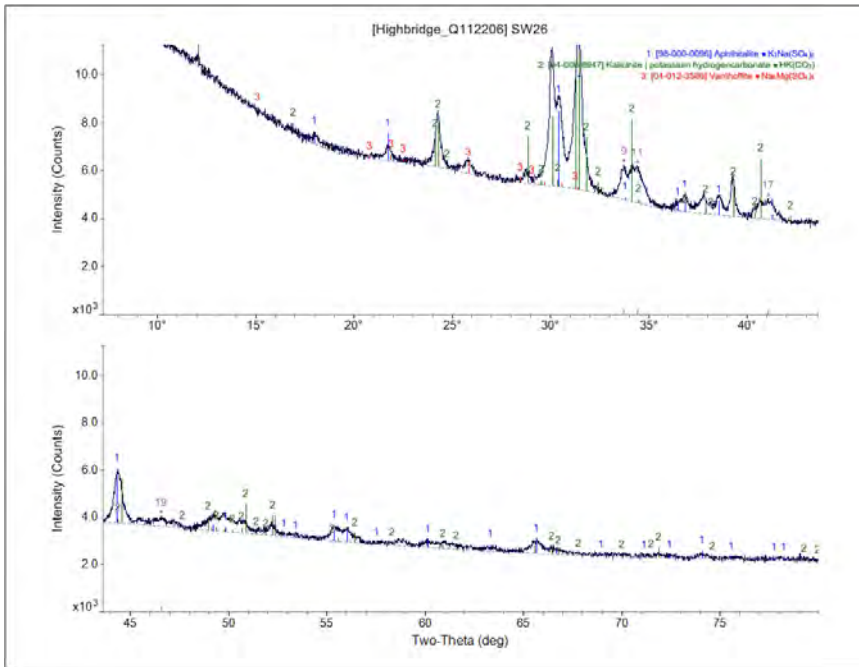
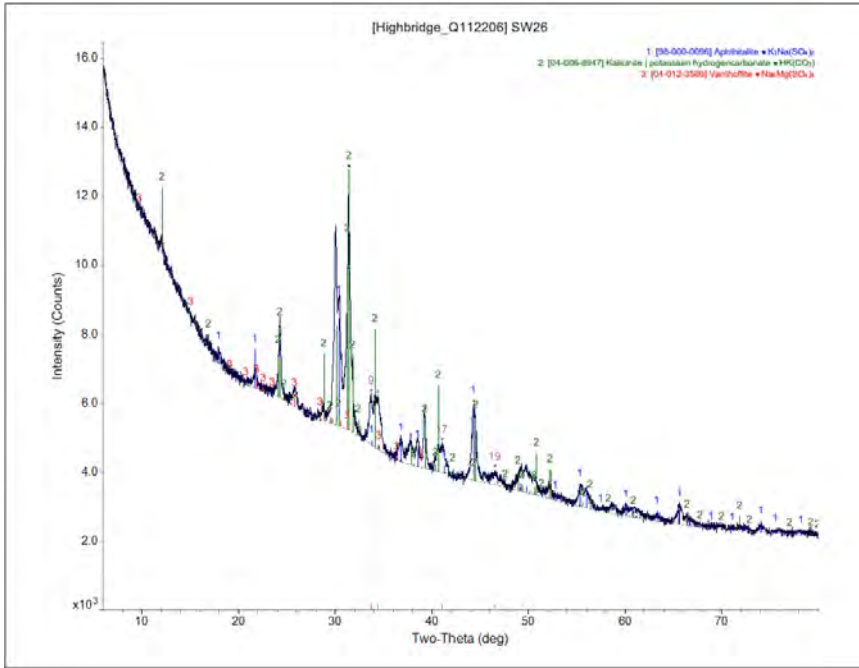


Chart I.5: X-ray diffraction spectrum for Sample SW26. The salts were extracted by water digestion from surface scrapings provided by the client. The full spectrum is shown at top and an exploded view at bottom.

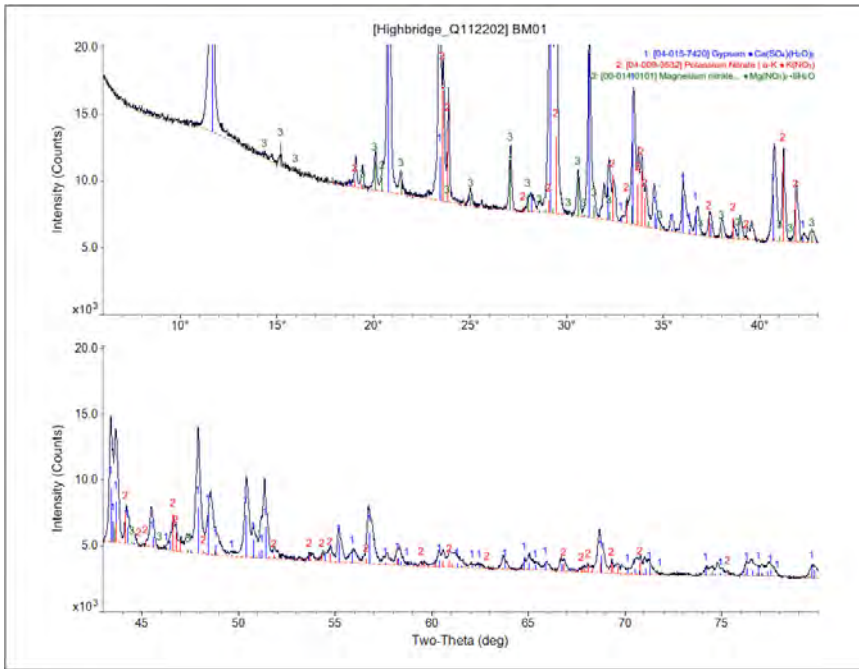
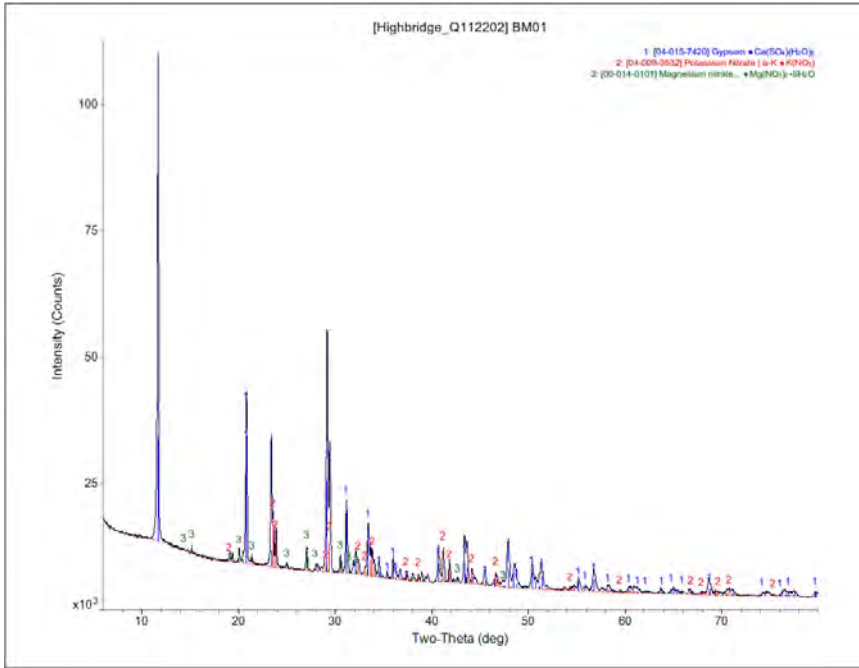


Chart I.6: X-ray diffraction spectrum for Sample BM01. The salts were extracted by water digestion from degraded mortar debris provided by the client. The full spectrum is shown at top and an exploded view at bottom.

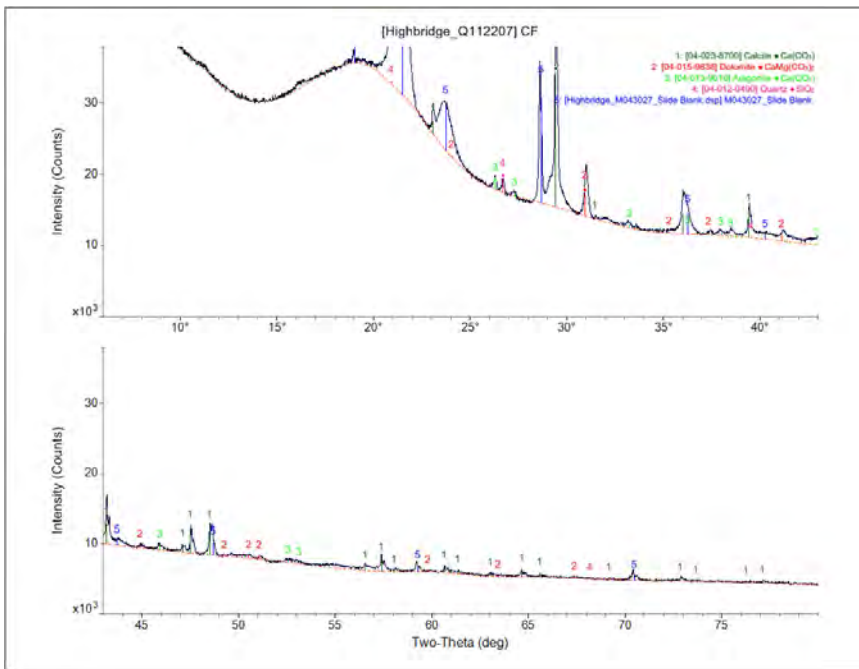
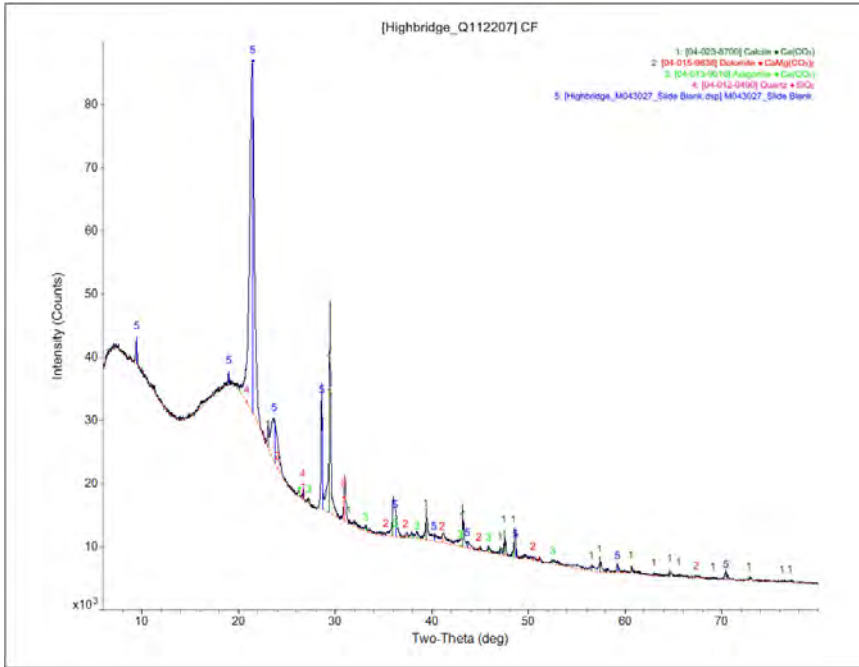


Chart I.7: X-ray diffraction spectrum for Sample CF. The salts were directly transferred from a mineralized veneer present along a formed surface of concrete infill. The full spectrum is shown at top and an exploded view at bottom. Note the broad hump at 2θ centered about 20°. This is indicative of an amorphous material.

Appendix II: Photographs

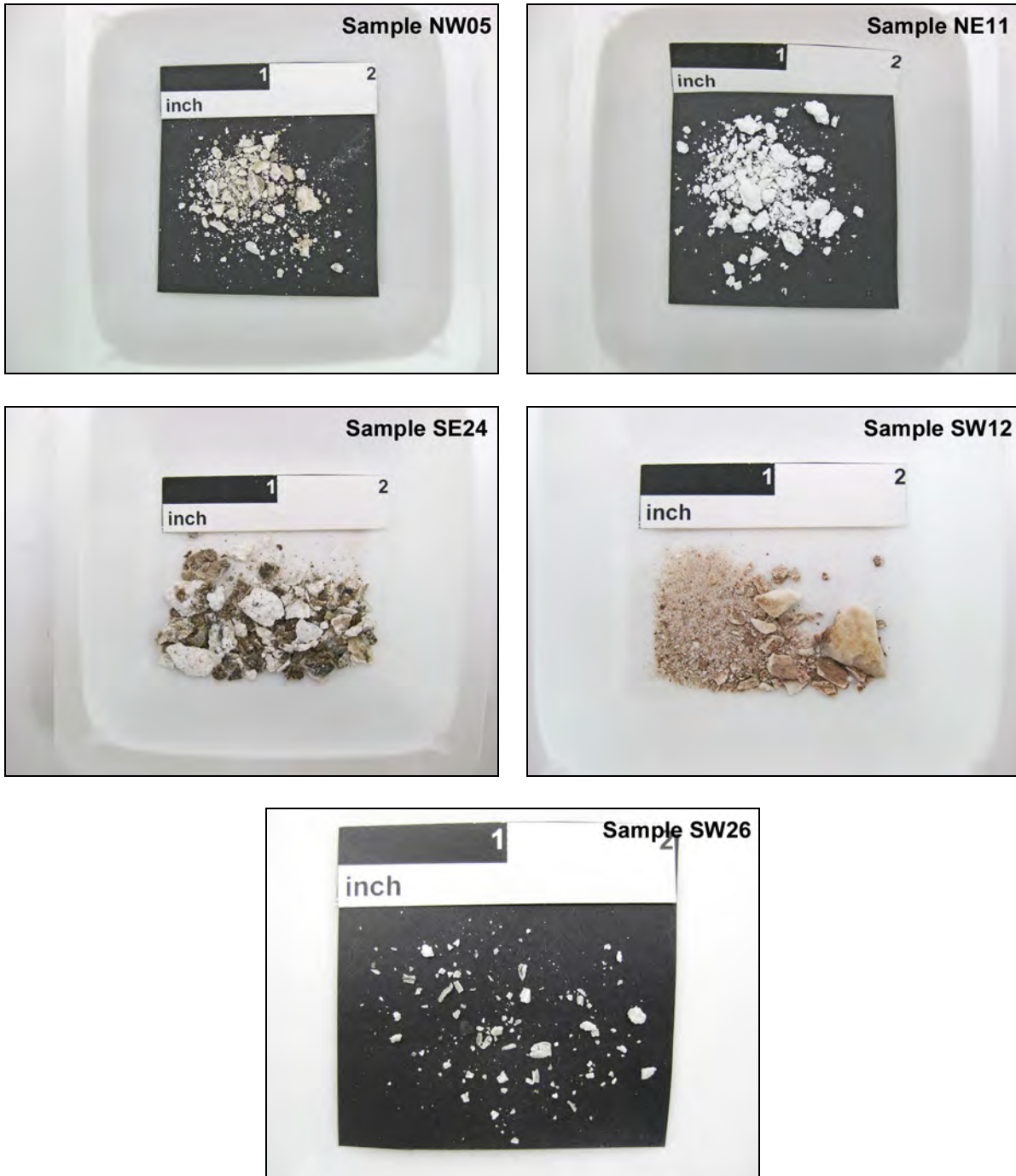


Figure 1: Photographs of the five samples consisting of salt deposits scraped from masonry surfaces by the client and provided to the laboratory for analysis. Four of these were subjected to a water extraction process to concentrate the salt from other debris. Only Sample NE11 was measured in its "as-found" condition.

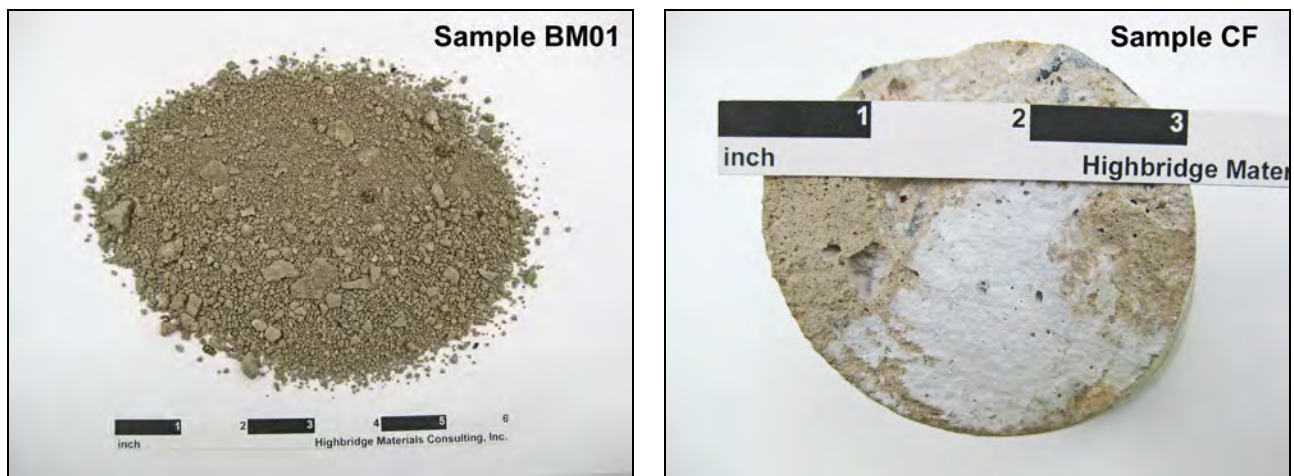


Figure 2: Photographs of Samples BM01 and CF as received. BM01 is a degraded mortar sample from which salts were extracted through water digestion. Sample CF was taken from the formed surface of a concrete infill sample where there was a veneer deposit of secondary salts.

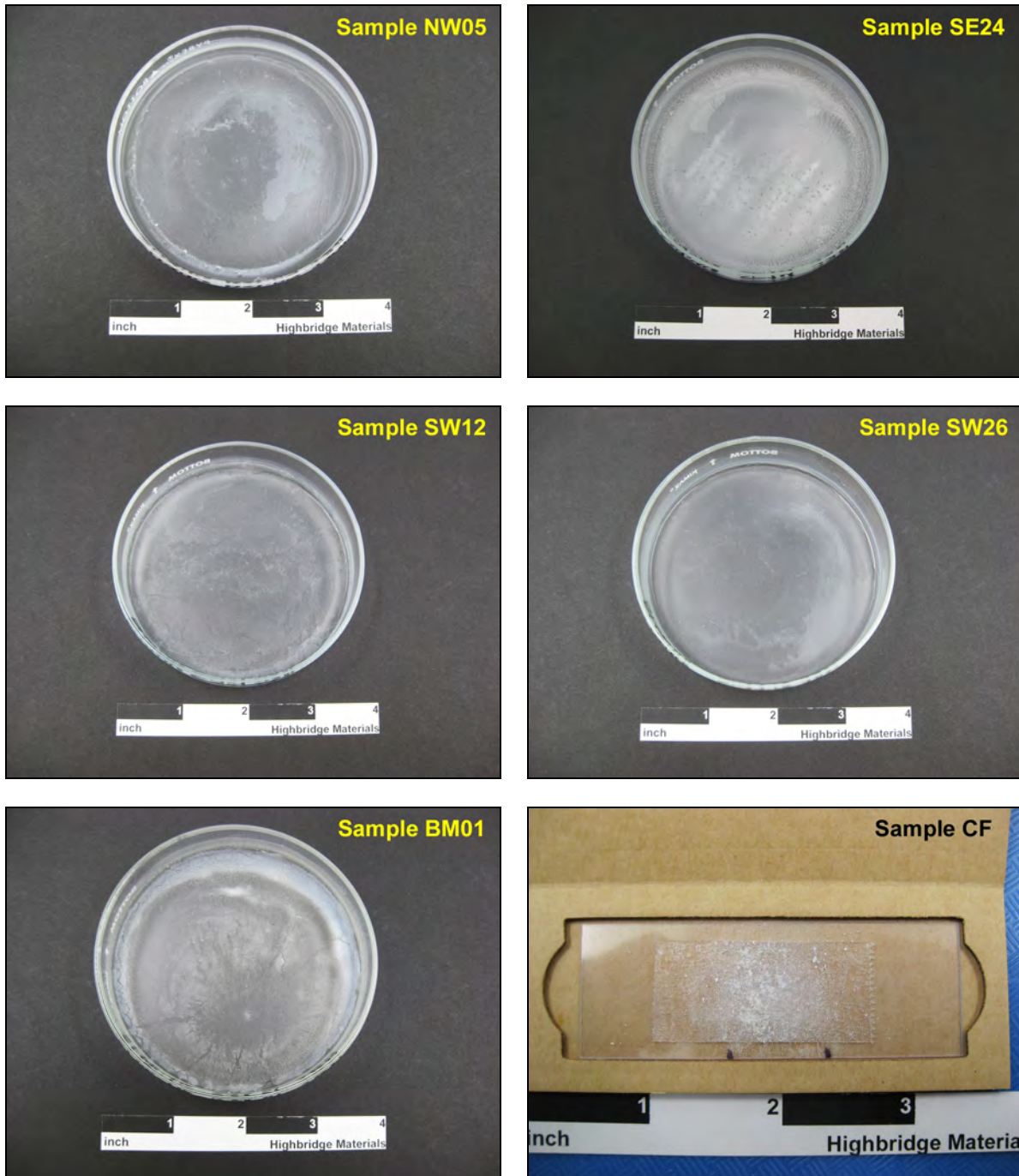


Figure 3: Photographs of the water-extracted salts after redeposition in the petri dishes through evaporation, and the one salt sample transferred on a flexible slide. All were analyzed using XRD. Sample NE11 is not shown here as it was run directly as-found.

Concrete Analysis Report

Bennington Battle Monument

15 Monument Circle, Bennington, VT 05201



Prepared for

Jablonski Building Conservation, Inc.

Client ID

JABL001

Report No.

SL1846-05

Report Date

12/26/23

HIGHBRIDGE



MATERIALS CONSULTING, INC.

Confidentiality

This report presents the results of laboratory testing requested by the client to satisfy specific project requirements. As such, the client has the right to use this report as necessary in any commercial matters related to the referenced project. Any reproduction of this report must be done in full. In offering a more thorough analysis, it may have been necessary for Highbridge to describe proprietary laboratory methods or present opinions, concepts, or original research that represent the intellectual property of Highbridge Materials Consulting and its successors. These intellectual property rights are not transferred in part or in full to any other party. Presentation of any or all of the data or interpretations for purposes other than those necessary to satisfy the goals of the investigation are not permitted without the express written consent of the author. The findings may not be used for purposes outside those originally intended. Unauthorized uses include but are not limited to internet or electronic presentation for marketing purposes, presentation of findings at professional venues, or submission of scholarly articles.

Standard of Care

Highbridge has performed its services in conformance with the care and skill ordinarily exercised by reputable members of the profession practicing under similar conditions at the same time. No other warranty of any kind, expressed or implied, in fact or by law, is made or intended. Interpretations and results are based strictly on samples provided and/or examined.

Cover Image

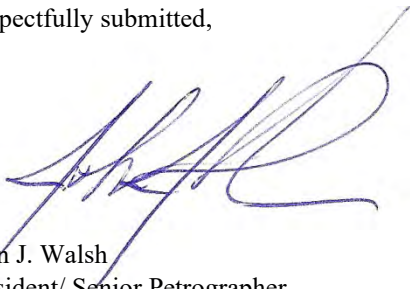
The Bennington Battle Monument in Bennington, VT. Image downloaded August 26, 2023 without modification.

Photo credit: King of Hearts

https://commons.wikimedia.org/wiki/File:Bennington_Battle_Monument_October_2021_001.jpg

Under Creative Commons License CC BY-SA 4.0 - <https://creativecommons.org/licenses/by-sa/4.0/deed.en>

Respectfully submitted,



John J. Walsh
President/ Senior Petrographer
Highbridge Materials Consulting, Inc.



Heather Hartshorn
Senior Chemist
Highbridge Materials Consulting, Inc.

1. Executive Summary

This report presents the results of petrographic and chemical analysis of an infill concrete sample recovered from the masonry at the Bennington Battle Monument, Bennington, VT.

The mixture is a normal weight, natural cement concrete with no portland cement or lime additions. The mix water content was sufficient to provide a fresh mix with adequate workability. The fine aggregate is a coarse-grained and broadly graded natural sand. The coarse aggregate is primarily a crushed limestone with a particle size distribution approximately consistent with a No. 4 or No. 357 gradation profile. The stone is the same as that used for the exterior masonry. The material proportions are estimated to be consistent with a 1 : 2 : 3 or a 1 : 2 : 4 mix by volume. There are no major workmanship issues identified petrographically.

The concrete is in sound condition for its age. A very minor incipient alkali-aggregate reaction has occurred between the cement paste and the limestone coarse aggregate. A thin white veneer along one formed surface represents a gel phase produced by this reaction. No major durability concerns are indicated if based strictly on the observations of this one core. Of course, field observations should be used to confirm this interpretation.

2. Introduction

On November 2, 2023, a set of masonry samples were delivered to the laboratory by Mr. Edward FitzGerald of Jablonski Building Conservation, Inc. According to Mr. FitzGerald, these represent materials sampled from the Bennington Battle Monument, Bennington, VT. The monument is a stone obelisk completed in 1889. The client has requested that the laboratory perform materials analysis on a subset of the samples as summarized in Table 2.1 below. The choice of samples to analyze are based on priorities set by Mr. FitzGerald with some additional input by the laboratory.

Table 2.1: Summary of Received Samples

This table includes only those samples selected for analysis. The laboratory made some nominal amendments to sample identifications for consistency and simplicity in reporting. These are shown in the "HMC ID" column. These identifications will be used throughout all reports.

Client ID	HMC ID	Client description on sample bag or verbally	Analytical scope requested
NW5	NW05	Salts on mortar joint	Water-soluble salts
NE11	NE11	Buff stone salts	Water-soluble salts
SE24-NE25	SE24	Salts, dark gray stone	Water-soluble salts
SW12	SW12	Salts in crack, buff stone	Water-soluble salts
SW26	SW26	Rear window, dark gray stone, salts in HC	Water-soluble salts
BM-01	BM01	South elev., ext. sand mortar bedding	Mortar analysis, water-soluble salts
BM-02	BM02	South ext. elev., org. point/bed? Under most recent repointing	Mortar analysis
BM-05	BM05	Observation deck, 2 mortars, light buff on top, flat & flush	Mortar analysis
NE4	NE04	Dark brown mortar	Mortar analysis
NE18	NE18	Interior, crumbly mortar near dark gray stone	Mortar analysis
NW26	NW26	Corner joint	Mortar analysis
SW2	SW02	Int. coarse, buff color at corner separation	Mortar analysis
SW16	SW16	Org. bedding	Mortar analysis
(none)	CF	Concrete infill	Concrete petrography, mortar analysis, salts

The requested testing includes the following:

- **X-ray diffraction analysis of salts or mineralizations**

The client has requested the qualitative identification of salts for seven samples. Five of the samples were provided as scrapings of variable purity. One sample (BM01) consists of water-logged mortar debris with no salts visible. One sample (CF) consists of a salt crust along the formed face of a concrete infill layer. The samples were analyzed either as-found, or after extraction and redeposition. X-ray diffraction analysis (XRD) is used to identify the phases present.

- **Compositional mortar analysis**

The client has requested that Highbridge perform compositional mortar analysis on eight of the provided samples. The testing includes a petrographic examination and chemical analysis to identify constituents, estimate proportions, and assess overall condition. Chemical digestions to extract sand samples for description and gradation are also included.

- **Petrographic examination and partial compositional analysis of infill concrete**

Petrographic examination is used to examine the infill concrete. The purpose is to identify constituents, assess condition, and investigate potential causes of any observed distress. A compositional analysis is performed on the mortar fraction of the concrete to evaluate the proportions of binder and sand using the same techniques described above for mortar.

This report presents the results of the infill concrete analysis. Results for the other analyses will be presented under separate cover when complete.

3. Methods of Examination

The petrographic examination was conducted in accordance with the standard practices contained in ASTM C856/C856M-20. Data collection is performed or supervised by a degreed geologist who by nature of their education is qualified to operate the analytical equipment employed. Analysis and interpretation are performed or directed by a supervising petrographer who satisfies the qualifications as specified in Section 4 of ASTM C856.

Chemical analysis was performed in general accordance with the procedures outlined in ASTM C1324-20a. Water, carbon dioxide, and aggregate weight percentages are determined gravimetrically. Oxide weight percentages are determined by inductively coupled plasma - optical emission spectroscopy (ICP-OES). While ASTM classifies C1324 as a test method, it is intended to serve as a guideline for qualified practitioners with ample experience in the various materials under consideration. Section 10.2 indicates the need for discretion on the part of the laboratory to ensure that methods are tailored to specific mortar compositions. As such, Highbridge chooses specific digestion methods, supplementary tests, instrumentation protocols, and mathematical models to best characterize each individual mortar under consideration. Many of these are proprietary methods that have been researched internally.

The following personnel contributed to the examination:

Technicians:	M. Pattie J. Negron
Analyst:	M. Cortez
Chemist:	H. Hartshorn
Petrographer:	J. Walsh

4. Petrographic Findings and Discussion

4.1 - Materials

The sample is identified as a normal weight natural cement concrete prepared to a workable consistency without an excess of mix water. The natural cement is a dolomitic product having microtextural and chemical characteristics consistent with cements produced in the Rosendale, NY region during the nineteenth century. The chemical signature of the cement is nearly identical with that of mortar sample NE18 described in Highbridge Report SL1846-06. No portland cement, lime, or supplementary cementitious materials are identified in the concrete.

The fine aggregate is a clean natural sand consisting primarily of metaquartzite. The sand derives from the same source used for the natural cement mortars in the monument. The material is hard, inelastic, and nonporous, and is physically suitable for use in concrete mixtures. The particle size distribution is quite broad. With over 25% retained on the No. 8 sieve, the aggregate would not comply with the permissible gradation limits of the modern standard for concrete sand (ASTM C33/C33M-18). However, the coarse aggregate contains little below the 1/2" sieve, and the 10% of fine aggregate retained on the No. 4 sieve helps to fill in the gap between the two aggregate additions.

The coarse aggregate is a crushed stone consisting of dolomitic limestone. A few grains of white calcitic marble are also detected. The aggregate has a nominal top size of about 2", and there is little passing a 1/2" sieve. Though difficult to estimate at the available sample size, the gradation profile would probably comply with a modern No. 4 or No. 357 stone. Most particles are sharp-textured and equidimensional. The limestone is essentially the same as that used for the exterior masonry (Highbridge Report SL1846-03). It is possible that waste material from the masonry was incorporated into the infill concrete. Being hard, inelastic, and non-porous, the rock type is physically suitable for use in concrete mixtures. Furthermore, the stone would not be flagged as chemically unsound for use in concrete having a 100-year service life expectancy. Nonetheless, there is some evidence for a minor incipient alkali-aggregate reaction as discussed later in this report.

4.2 - Component Proportions

Based strictly on the petrographic observations, the concrete has material distributions that would be found in a typical 1 : 2 : 3 or 1 : 2 : 4 mixture as specified prior to ca. 1920. The ratios refer to volumes of dry cement, sand, and stone, respectively. The three components are all present at a volume that should allow for adequate consolidation of the mixture without rock pockets or sand lenses.

With that said, a portion of the mortar was subsampled from the concrete to perform a compositional analysis on a fraction excluding the stone. Another portion was subsampled to extract an aggregate sample for visual description and gradation. The weight percentage of aggregate extracted for the gradation sample is about 54%. For this particular sample, an aggregate content of 54% would indicate a cement to sand ratio of roughly 1 : 1.5 or so. This is consistent with the visual estimate. However, the smaller subsample used for chemical analysis yielded an insoluble residue of about 78%. This is unusually high for natural cement mortars. Even if the original sand is assumed to have had a higher bulk density due to its coarseness and broad gradation, the cement to sand ratio could be no more than about 1 : 3.6. This is clearly sandier than suggested by the petrographic observations. It is suspected that the small sample size needed to avoid any coarse aggregate resulted in an overestimate of the coarsest sand particles.

4.3 - Original Placement and Hydration

Based on the examined core sections, the concrete constituents were reasonably well-mixed, adequately deposited, and thoroughly cured. The mix water is estimated to have been adequate to provide sufficient slump to the fresh mixture. Two core sections were provided for analysis. The shorter of the two is densely consolidated with little entrapped air. There is a formed surface on one side that is complete and lacks any forming defects. The concrete represented by the longer piece is compact but less well consolidated at the fine scale. The mortar tends to be clumpy adjacent to the stone. Ponding of mix water in these regions resulted in a somewhat higher permeability locally. This type of texture is not unusual for an infill concrete and should not be considered a major deficiency.

4.4 - Secondary Service Effects

The author does not know the structural requirements of the concrete and would always defer to an engineer regarding the mechanical suitability of a concrete mix to its application. From a nonstructural materials perspective, the concrete has not suffered any significant decay over the course of its service.

The only secondary effect worthy of note is a minor incipient alkali-aggregate reaction between the dolomitic limestone coarse aggregate and the natural cement paste. A few aggregate grains contain microscopic or hairline cracks. Several cracks are also observed in the cement paste. All of these remain cohesive. There are very sparse occurrences of reaction gel within some of the aggregate cracks. Most notably, there is a visible white coating of layered reaction gel that lines the one formed surface in the shorter core section. This is the same layer tested for salt content in Highbridge Report SL1846-04. The layered gel observed petrographically is consistent with the so-called amorphous hump identified in the XRD spectrum. A similar hump was detected in Sample NE18. It is not known whether this relates to an infill concrete.

The degree of reaction observed in this particular sample is not concerning. There is very little reaction gel present within the concrete itself despite the coating along the formed face. There is no published literature regarding the susceptibility of aggregates to alkali-aggregate reaction when in the presence of natural cement. Given that natural cement behaves in part as a calcined clay, it would be reasonable to expect that any potential reactivity is mitigated. The author has observed a fair number of nineteenth century natural cement concrete samples and has never encountered an advanced alkali-aggregate reaction even where aggregates would be considered highly susceptible in portland cement paste.

Assuming this sample is representative of all infill concrete, the durability risk would be considered quite low. Still, the potential threat should be reviewed by others more familiar with the material distribution within the monument. If this infill concrete is a major component that is sufficiently restrained by the masonry, then it would be prudent to ensure that any cracking observed along the masonry is unrelated to any more advanced aggregate reaction.

5. Petrographic Data

Table 5.1: Petrographic Data

Sample ID	CF
As-received description	
Dimensions/details	The sample consists of two non-contiguous core sections. Both have 2.75" diameters. The longer piece is approximately 6" in length. The shorter piece is approximately 3.5" in length.
Surfaces (longer section)	One side is a somewhat clumpy placement face oriented at a high angle to the core axis. The other surface is also clumpy but appears to mostly coincide with a large aggregate socket.
Surfaces (shorter section)	One surface is a clean, artificial drilling break. The other is a highly planar formed face at a modest angle to the core axis. This surface is fully coated with a thin deposit of matte white salt.
Core circumference	The larger piece exhibits a preferential loss of mortar along the cored circumference. The smaller piece has a circumference that is smooth and untextured.
Embedded items	None
Visible cracks	None observed
Coarse aggregate	
Type	Carbonate crushed stone
Estimated volume	The core sections are small relative to the aggregate size preventing an accurate estimate of the coarse aggregate content. However, the distribution appears moderate and consistent with aggregate volumes of 30% to 35% by hardened concrete volume.
Lithology	The stone is primarily a dolomitic limestone. The original sedimentary texture consists of a peloidal partly bioclastic limestone. The dolomitic overprint is partial and consists of fine euhedral rhombic crystals. A few grains of white calcitic marble are also detected.
Nominal top size	2" with most if not all passing
Grading	The gradation profile is difficult to estimate given the small sample size. The majority of the aggregate volume in the two core pieces appears to be coarser than 1" in diameter. There is virtually nothing that would pass a 1/2" sieve. Based on the limited volume observed, the particle size distribution would be closest to a modern No. 4 or No. 357 gradation profile.
Roundness	Subangular to angular
Aspect	Equant to slightly subequant
Coatings and rims	None significant
Cracks	None significant
Fine aggregate	
Type	Siliceous natural sand
Estimated volume	Approximately 35-40% by hardened mortar fraction
Lithology	The sand consists primarily of a fine-grained metaquartzite. Much of it is nearly pure quartz though there are also micaceous grains. Granite is a minor component and ironstone is found in trace abundance.
Nominal top size	No. 4 sieve
Grading	The sand is very broadly graded with a peak abundance just a little finer than the No. 30 sieve. There is a modest amount of material passing the No. 100 sieve.
Roundness	Subangular to angular
Aspect	Mostly equant
Clay coatings or friable materials	None significant
Organic impurities	None identified

Table 5.1 (cont'd.): Petrographic Data

Sample ID	CF
Cement paste	
Hand sample qualities	Intentional fractures are somewhat crumbly and deflect around aggregate particles. The freshly exposed cement paste is brown with a moderately dull luster. The paste is moderate in hardness and rapidly water-absorptive.
Paste microstructure	There is some heterogeneity in the paste primarily due to occasional clumpiness of the mortar fraction. Locally, the paste is more porous wherever consolidation is less complete. Elsewhere, the paste is dense and well-formed with a relatively low capillary porosity.
Calcium hydroxide Evidence for admixtures¹	None preserved No admixtures are obvious based on indirect petrographic evidence.
Residual cement²	Residual natural cement particles are abundant throughout the cementitious paste. Most grains are finer than approximately 0.25 millimeters. The cement exhibits complex microtextures consistent with the low-temperature firing of an argillaceous dolomitic limestone. Finer "grit" is densely distributed throughout the paste including ferruginous and siliceous residue that did not combine during firing. Fine agglomerates of inert clinker phases are also present.
SCMs³	None identified
Other inclusions	None identified
Variations	Except where microporosity is higher due to less complete consolidation of the mortar, the paste hydration characteristics are uniform throughout the examined cross section.
W/cm estimate⁴	The water to cement ratio is estimated to have been moderately low though sufficient for adequate placement.
Air-void system	
Entrained air	None present
Entrapped air	Entrapped air voids are present at approximately 2-3% by volume. All voids are relatively fine in size. There are no honeycombs or other coarse void structures.
Paste-aggregate interfaces	
Description	In the larger core section, the mortar is somewhat clumpy around coarse aggregate particles. This resulted in microporous zones and weakened paste-aggregate bonds. The mortar is better consolidated around the stone in the smaller core section.
Original placement features	
Mixing of dry ingredients	There are no cement lumps, sand streaks, or aggregate concentrations. All constituents are estimated to have been well mixed.
Mix water	The mix water was well incorporated into the fresh mixture and there is no evidence for inappropriate retempering.
Consolidation/ compaction	The concrete mixture was moderately well-consolidated.
Segregations	None observed
Preferential orientations	None observed
Bleed water features	None observed
Cold joints/ other contacts	None observed
Laitance	Not applicable
Forming	There is one formed face present in the smaller core section. The concrete is compact against this surface. No forming defects are evident.
Finish	Not applicable
Curing	The natural cement is thoroughly cured and the cementitious paste is well-developed.

Table 5.1 (cont'd.): Petrographic Data

Sample ID	CF
Secondary service effects	
Surface erosion/weathering	Not applicable
Carbonation	The cement paste is isotropic in the smaller core piece though the pH is found to be near 9. In the larger core piece, carbonation is only observed along air-void perimeters within less consolidated cement paste.
Cracking	Some hairline cracking is evident in the smaller core piece. This does not exhibit any particular pattern.
Chemical alteration in paste	The cement paste itself does not exhibit any outward sign of chemical attack.
Mineral deposits	Traces of ettringite are observed within air-voids. Crack surfaces are sometimes lined with fine carbonate deposits. A thin white veneer is present along the formed face in the shorter core section. This is observed to be a layered siliceous gel deposit. Traces of this gel are also observed within coarse aggregate cracks.
Aggregate reactivity	A trace alkali-aggregate reaction is observed within the dolomitic aggregate. A few microcracks are observed transecting the stone. As described above, there are trace occurrences of reaction gel within the aggregate, and a layer of exuded gel along the formed face of the concrete.
Other	No other secondary effects are noted.

Notes:

1. Organic admixtures or soluble inorganic additives cannot be detected petrographically, though their effects on concrete microstructure can sometimes be discerned.
2. The presence of unhydrated cement grains does not necessarily indicate poor hydration of the binder. A greater abundance of unhydrated cement is typical with reduced w/cm.
3. SCMs = supplementary cementitious materials.
4. Water to cementitious materials ratio (w/cm) cannot be quantified petrographically. Estimates are made qualitatively based on many characteristics of the hardened cement paste including behavior of the paste when fractured, capillary porosity, concentration of residual unhydrated cement, and microtextural features of the primary calcium hydroxide formed during the cement hydration. The estimates are complicated by the presence of SCMs, organic additives, or through chemical changes that occur with age.

6. Aggregate Sieve Analysis

The fine aggregate was extracted from the mortar portion of the concrete by digesting the sample in a solution sufficient to decompose the binder. The following procedure was used:

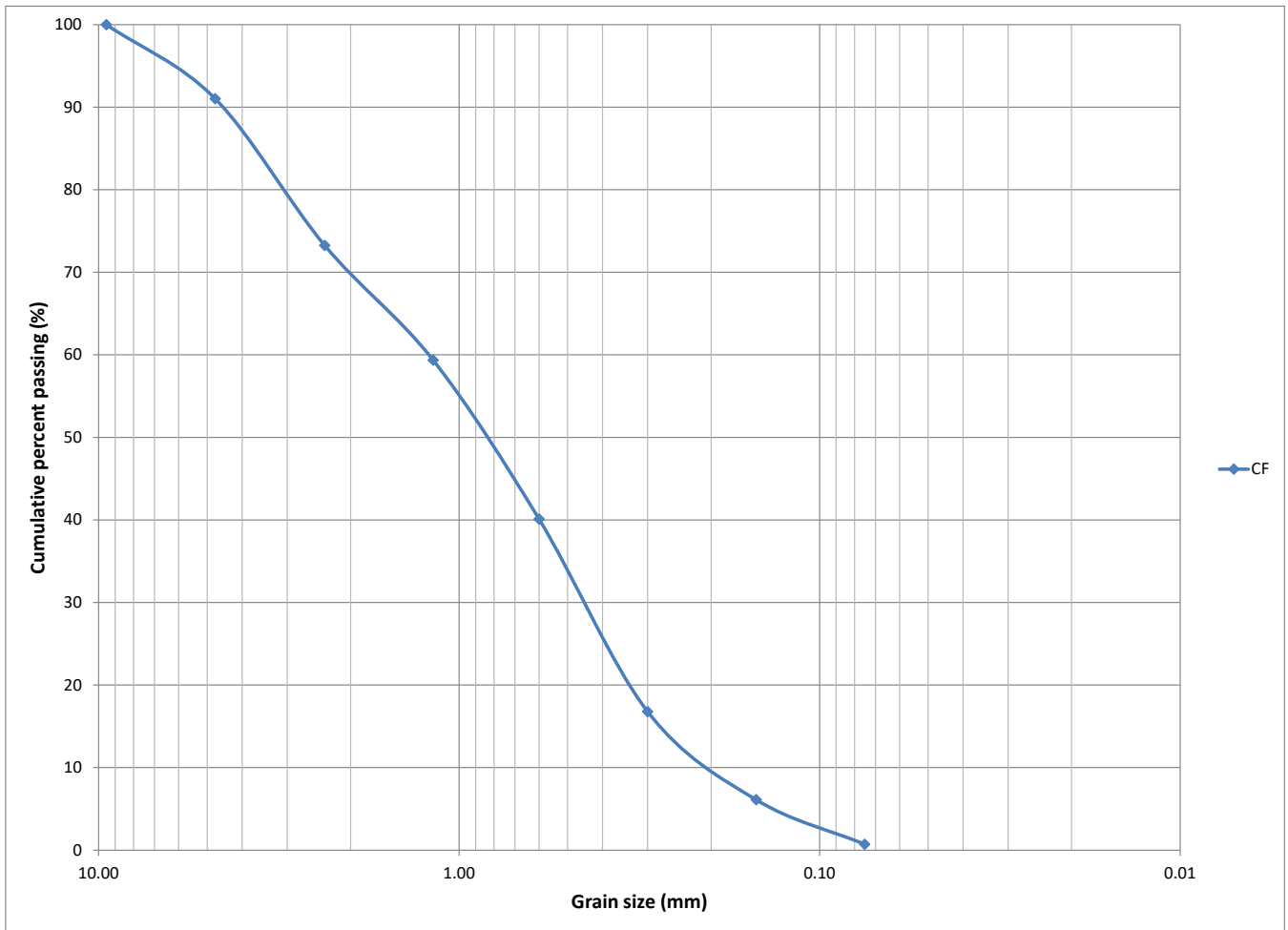
- A portion of the concrete was broken up with a hammer to produce pieces that could be further reduced with a tile nipper.
- Smaller pieces were broken away in an effort to exclude any of the limestone coarse aggregate.
- Approximately 60 grams of mortar was recovered. This subsample was placed in a 400 mL low-form glass beaker and digested in a 33% v/v hydrochloric acid solution.
- Once the binder was largely decomposed, the beaker was agitated to suspend fines or low-density material. After allowing for the settling of aggregate above the silt and clay sizes, the material remaining in suspension was decanted into a 1-quart polyethylene pail. Several rinsings of the settled aggregate were performed until the water ran clear. The suspended fines produced by each rinsing were transferred to the larger pail.
- The sand in the original beaker was transferred to a 1-pint wide-mouth polypropylene container. The sand was scrubbed with bare fingers to release any residual natural cement from the surfaces of the sand grains. This was again transferred to the polyethylene pail.
- The cleaned sand was dried in an oven at 45°C. The dried sand was photographed, described, and graded through a standard sieve stack.
- The suspended fines in the 1-quart container were allowed to settle and the supernatant was decanted. The fines were transferred to a 250 mL Nalgene beaker and digested in a 10g/L NaOH solution at a temperature just below boiling to decompose any cementitious residues. The fines were rinsed several times and then dried.
- The cleaned fines were observed in petrographic grain mount. It was found that most of this material still consisted of inert, insoluble components of the natural cement. As such, all of this fraction was excluded from the gradation calculation. The exclusion of any silt from the sand is considered a negligible error.

Table 6.1: Acid Digestion Data

Sieve size	Retention (g)	Cumulative passing (%)	Cumulative retained (%)
3/8"	0.00	100.0	0.0
No. 4	2.91	91.0	9.0
No. 8	5.77	73.3	26.7
No. 16	4.51	59.3	40.7
No. 30	6.24	40.1	59.9
No. 50	7.57	16.8	83.2
No. 100	3.47	6.1	93.9
No. 200	1.75	0.7	99.3
Pan	0.23	0.0	100.0
Fineness modulus			3.13

Chart 6.1: Aggregate Sieve Analysis

The following chart presents the particle size distribution curve for the extracted sand sample. The chart plots the data from the cumulative passing values in Table 6.1. The fine end of the curve is terminated at the No. 200 sieve. Any silt and clay components are not graded beyond this point.



7. Chemical Analysis

Table 7.1: Chemical Analysis Results

Proprietary modifications were made to the chemical digestion procedure described by ASTM C1324 to more effectively decompose the natural cement binder. This included a digestion in warm, dilute hydrochloric acid solution prior to the alkaline digestion subprocedures. The insoluble residue was determined directly from the initial digestion rather than through the digestion of a separate aliquot.

Sample ID	CF
Component (wgt. %)	
SiO ₂	2.84
CaO	6.13
MgO	3.40
Al ₂ O ₃	0.68
Fe ₂ O ₃	0.65
Insoluble residue	77.68
LOI to 110°C	0.43
LOI 110°C-550°C	2.47
LOI 550°C-950°C	5.57
Measured totals	99.84

The following features of the total measured chemistry should be noted:

- The total yield at nearly 100% indicates that the analysis is self-consistent.
- The insoluble residue at 78% is exceptionally high for a typical natural cement mortar. Since the analysis is self-consistent, any error must be associated with sampling. It is suspected that efforts to avoid sampling the coarse aggregate resulted in an oversampling of the No. 4 sieve fine aggregate. It should be stressed that errors in aggregate sampling should have no effect on the measured proportion of chemical components of the cement.

Table 7.2: Estimated Natural Cement Chemistry

The binder in the concrete sample consists of natural cement with no other additives. As such, the natural cement chemistry can be estimated from the total chemical analysis presented in Table 7.1. The five major oxides in the binder are normalized to a 92% weight yield. The residual 8% is assumed to represent minor uncombined silt and clay from the natural cement binder. CaO/SiO₂ and CaO/MgO ratios are calculated directly from the data. Important chemical indices are calculated as follows:

$$\begin{aligned} \text{Hydraulic index} &= (\text{SiO}_2 + \text{Al}_2\text{O}_3) / \text{CaO} \\ \text{Cementation index} &= (2.8 \cdot \text{SiO}_2 + 1.1 \cdot \text{Al}_2\text{O}_3 + 0.7 \cdot \text{Fe}_2\text{O}_3) / (\text{CaO} + 1.4 \cdot \text{MgO}) \end{aligned}$$

An estimated chemistry for mortar sample NE18 is provided for comparison (Highbridge Report SL1846-06). Also provided for comparison is an average chemistry for historical Rosendale cements calculated from fifteen individual analyses presented in Eckel's *Cements, Limes and Plasters*.

Sample ID	CF	NE18	Historical Average
Component (wgt. %)			
SiO ₂	19.1	18.8	26.8
CaO	41.1	40.4	35.0
MgO	22.8	24.3	18.7
Al ₂ O ₃	4.6	4.6	8.3
Fe ₂ O ₃	4.3	3.9	3.2
Other	8.0	8.0	8.0
CaO/SiO₂	2.2	2.2	1.3
CaO/MgO	1.8	1.7	1.9
Hydraulic index	0.58	0.58	1.00
Cementation index	0.84	0.81	1.41

The following features of the cement chemistry are important to note:

- Samples CF and NE18 have exceptionally similar cement chemistries in every regard. Not only does this suggest that both analyses are robust, it indicates that the same source of cement was used for these two materials.
- Except for the those of Rosendale, NY, very few historical cements would have MgO content as high as those measured for these samples.
- Though it is clear that these cements were manufactured in Rosendale, NY, they deviate from the average composition. Specifically, they are richer in CaO and deficient in SiO₂. This results in lower hydraulic and cementation indices.

Table 7.3: Calculated Mortar Composition

When calculating the sand content of a masonry mortar, it is customary to assume the sand has a bulk density of 80 lbs./ft.³. This is a reasonable estimate for damp, loose sand that passes the gradation requirements of ASTM C144. The first column below uses this density when calculating the cement to sand ratio. However, the fine aggregate is quite coarse and broadly graded (Section 6). It is safe to assume that this aggregate would have been appreciably denser than a typical masonry sand. For the second column below, it is assumed that the fine aggregate has a bulk density of 100 lbs./ft.³. This would be a better assumption for torpedo sand.

Regardless of the assumed sand density, the measured insoluble residue is clearly higher than is typical of natural cement mixtures. As described earlier, it is assumed that the unusually high residue results from some type of sampling error. As such, none of the proportions presented in this table are considered accurate. Alternative estimates are discussed in Section 4.2 above.

Sample ID	CF	CF
Component	$\rho = 80 \text{ pcf}$	$\rho = 100 \text{ pcf}$
Natural cement (wgt. %)	16	16
Sand (wgt. %)	84	84
Cement : sand ratio (by volume)	1 : 4.9	1 : 3.9

Notes:

- The natural cement weight is calculated assuming the five measured oxides represent 92% of the natural cement by weight. The sand weight is taken directly from the acid-insoluble residue. The cement and sand weights are then normalized to 100% to return the materials to a dry weight basis. Volumetric ratios are calculated assuming a natural cement bulk density of 75 lbs./ft.³. Two different sand densities are used to calculate a range of proportions (i.e., 80 and 100 lbs./ft.³, respectively).

References

Eckel, Edwin C. *Cements, Limes, and Plasters. Their Materials, Manufacture, and Properties*. New York: Robert Drummond, 1905.

Appendix I: Photographs and Photomicrographs

Microscopic examination is performed on an Olympus BX-51 polarized/reflected light microscope and an Olympus SZ40 stereoscopic microscope. The polarized light microscope is fitted with a Tucsen MIchrome 5 Pro 5MP digital camera. The stereoscopic microscope is used for simple magnification. Sample types examined under this microscope include fractured surfaces, fine constituents extracted through chemical or physical means, or honed or polished cross sections. The polarized light microscope (PLM) magnifies but also employs principles of optical crystallography. The most common sample preparation for the PLM is the petrographic thin section. For this preparation, cross-sectioned samples are mounted to glass slides and are milled to a thickness sufficient to allow light to be transmitted through the material. These are usually prepared without water and with minimal heat to avoid altering minerals that are water or temperature-sensitive. In many cases, the samples are impregnated with a low-viscosity, blue-dyed epoxy. When so treated, blue areas represent some type of void space (e.g., air-voids, capillary pores, cracks, etc.). The polarized light photomicrographs are taken using a variety of optical settings chosen to best demonstrate the feature(s) of interest. These are distinguished as follows:

Plane polarized light (abbreviated as PPL)

This method uses the refractive power of different constituents to produce an artificial sense of surface relief. Otherwise, the method is the closest to a simple magnification of the material. The setting is often used to demonstrate granular relationships or microstructure. Pore spaces and cracks are observable with this setting if the blue-dyed epoxy is used.

Conoscopic polarized light (abbreviated as CPL)

In this setting, the transmitted light is condensed just before passing through the thin section. The method tends to bring colors or finer particulates into higher contrast at the expense of image sharpness. The setting is often used to image grain boundary failures in dimension stone, pigment particulates in binders, or gel phases in the micropores of cement pastes.

Cross polarized light (abbreviated as XPL)

The setting places the thin section between two pieces of polarizing film oriented at 90° to one another. In isotropic materials (e.g., glasses, simple salts), all light is absorbed and the materials appear black. In anisotropic crystals, two light rays traveling at different speeds are produced within the thin section and these offset waves interfere at the upper polarizing film. The interference produces a color that can be used to calculate properties of the crystal structure and aid in identification of mineral species. In essence, the colors are artificial. It should be noted that color is a function of orientation and color differences do not necessarily indicate material differences.

Compensator plates

When in XPL mode, full-wave or quarter-wave compensator plates may be inserted into the light path to add or subtract interference. Technically, these methods are used to calculate properties of the crystal structure. However, they can also be used to alter the image appearance to help improve contrast between different constituents. They can also reveal preferred orientations in some materials (e.g., oriented residual crystallinity in fired ceramics).

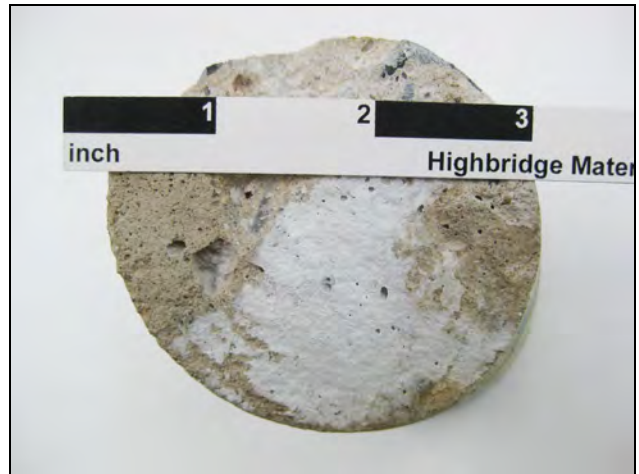


Figure 1: Photographs of the concrete infill sample provided to Highbridge for examination. The sample is shown in side view in the upper image. The core was provided in two non-contiguous pieces. Most of the coarse aggregate consists of limestone (LS). There are a few grains of white marble as well (M). End surfaces are shown in the two lower images. The surface in the lower left image terminates at an aggregate socket. Note that the brown mortar is somewhat clumpy in the socket. A planar formed face is shown at lower right. Note the white veneer consisting primarily of an alkali-aggregate reaction gel.

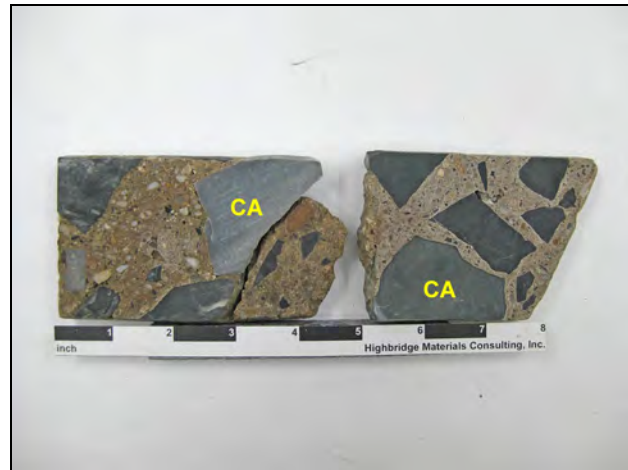


Figure 2: Photographs illustrating the aggregate size and gradation. (Upper image) A honed cross section of the concrete is shown. The size and distribution of the carbonate crushed stone aggregate (A) is visible at this scale. The angular stone has a top size of 2" and few particles passing the 1/2" sieve. (Lower left) The fine aggregate is shown after extraction from the mortar through chemical digestion. (Lower right) The extracted fine aggregate is shown after gradation through a standard sieve stack. The fine aggregate is coarse-grained and quite broadly graded.

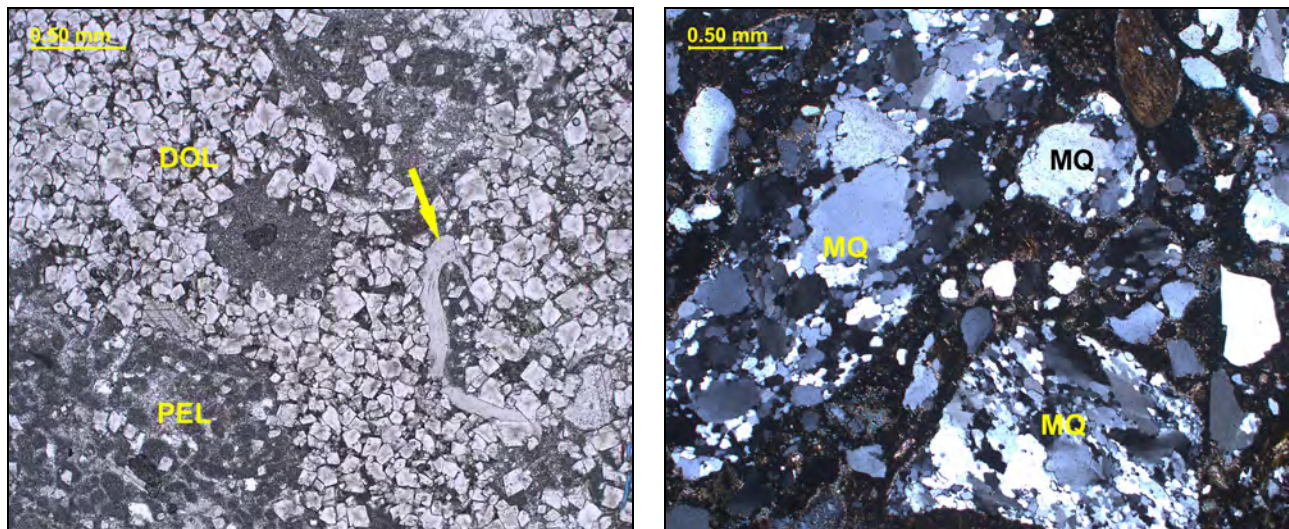


Figure 3: Photomicrographs illustrating the main aggregate types. (Left PPL image) The coarse aggregate is a dolomitic limestone. Part of the limestone is dolomitized (DOL). Where the original rock texture is preserved, much of it is peloidal (PEL). There are also bioclastic grains such as the trilobite fragment shown by the arrow. These features are identical to those identified in the exterior masonry stone. (Right XPL image) A group of metaquartzite grains are shown (MQ). These grains make up the majority of the fine aggregate.

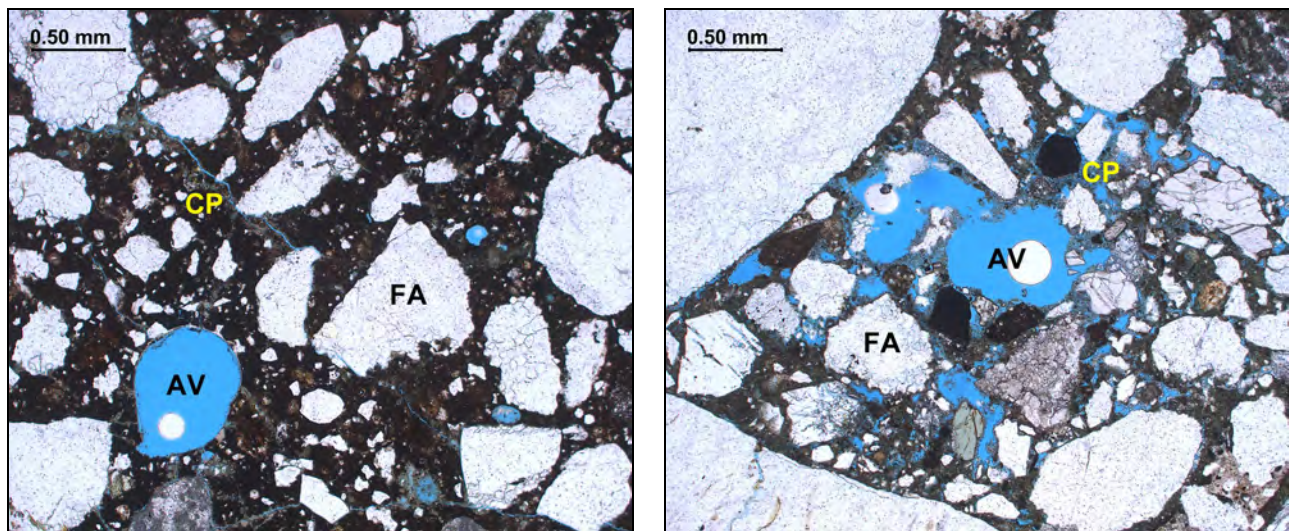


Figure 4: PPL photomicrographs illustrating the overall microtexture of the concrete. The left image is typical of most of the concrete. The right image is more typical of clumpier areas adjacent to coarse aggregate grains in the longer core section. In all, the fine aggregate (FA) is evenly distributed throughout the matrix. The spacing of aggregate particles indicates a fairly cement-rich composition typical of natural cement-based materials. The cement paste (CP) is uniformly developed. As shown by the differing absorption of the blue-dyed epoxy used in the sample preparation, the clumpier areas have a higher microporosity. Everywhere else, the cement paste is denser and more compact. Air-voids (AV) are a little more abundant in the right image where the paste is less compact.

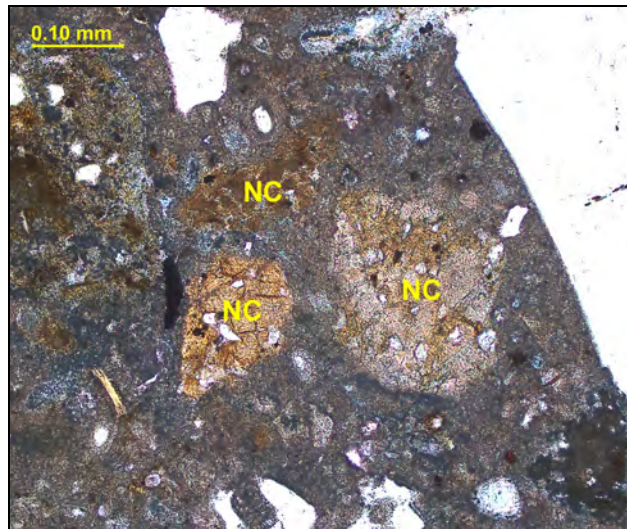


Figure 5: PPL photomicrograph. A cluster of residual natural cement grains are shown (NC). These have microtextures consistent with the low-temperature firing of an argillaceous dolostone. The microscopic and chemical characteristics are typical of those of the Rosendale natural cements.

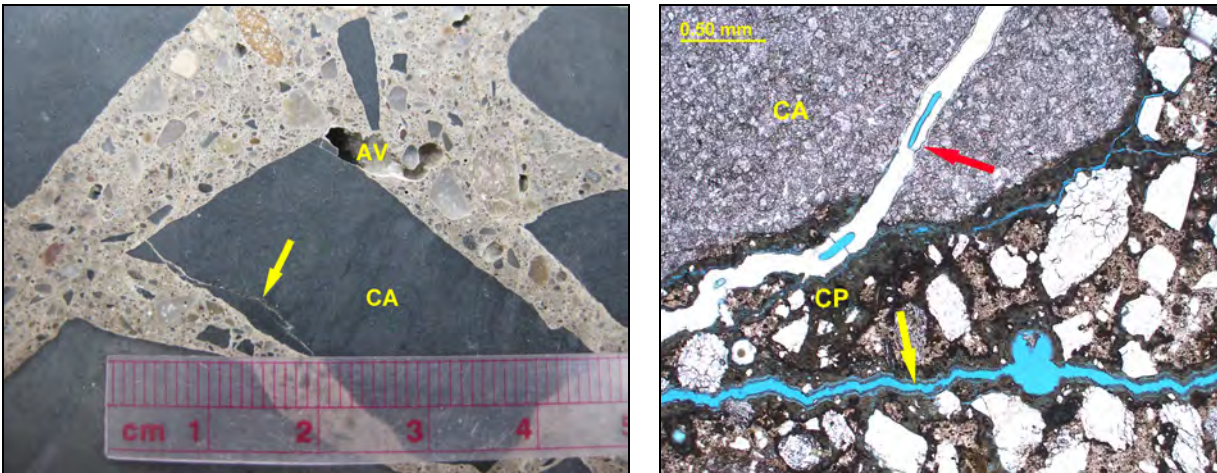


Figure 6: (Left) A close-up is shown of the honed cross section. A coarse aggregate particle (CA) contains a hairline crack (arrow). An adjacent air-void (AV) is thinly lined with some reaction gel. (Right) PPL photomicrograph. A crack (red arrow) transects a coarse aggregate particle (CA). This crack opened in preparation and is now mostly filled with colorless epoxy. Still, a thin veneer of reaction gel lines the crack surfaces. The crack extends into the cement paste (CP). Cracks are also observed transecting the mortar fraction (yellow arrow).

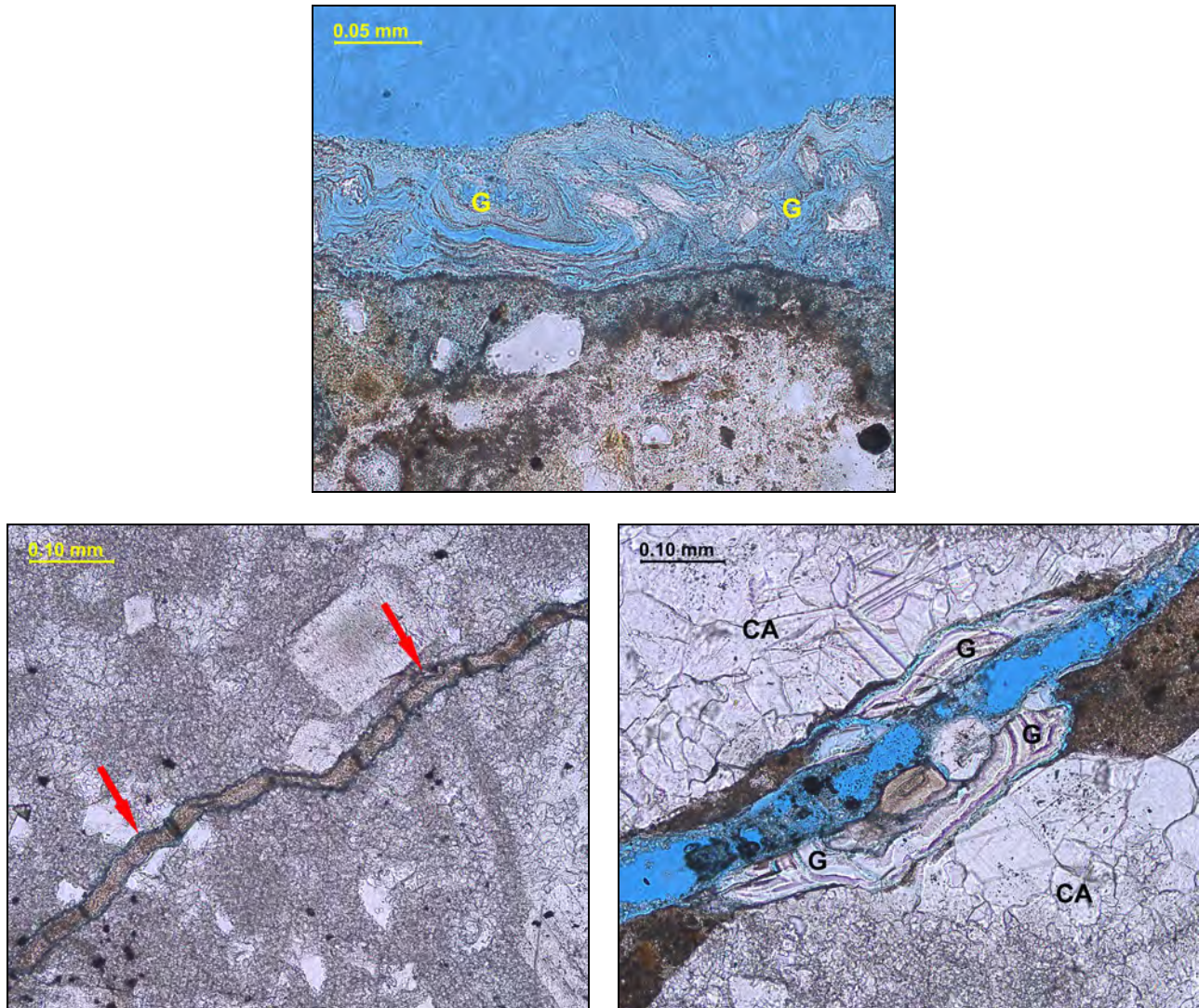


Figure 7: PPL photomicrographs. (Upper image) The white veneer lining the planar formed surface shown in Figure 1 consists mostly of a layered reaction gel (G). (Lower left) The arrows indicate a microcrack within a coarse aggregate grain completely filled with secondary reaction gel. (Lower right) A more open crack within a coarse aggregate grain (CA) contains a deposit of layered gel (G).

Mortar Analysis Report

Bennington Battle Monument

15 Monument Circle, Bennington, VT 05201



Prepared for

Jablonski Building Conservation, Inc.

Client ID

JABL001

Report No.

SL1846-06

Report Date

12/28/23

HIGHBRIDGE



MATERIALS CONSULTING, INC.

Confidentiality

This report presents the results of laboratory testing requested by the client to satisfy specific project requirements. As such, the client has the right to use this report as necessary in any commercial matters related to the referenced project. Any reproduction of this report must be done in full. In offering a more thorough analysis, it may have been necessary for Highbridge to describe proprietary laboratory methods or present opinions, concepts, or original research that represent the intellectual property of Highbridge Materials Consulting and its successors. These intellectual property rights are not transferred in part or in full to any other party. Presentation of any or all of the data or interpretations for purposes other than those necessary to satisfy the goals of the investigation are not permitted without the express written consent of the author. The findings may not be used for purposes outside those originally intended. Unauthorized uses include but are not limited to internet or electronic presentation for marketing purposes, presentation of findings at professional venues, or submission of scholarly articles.

Standard of Care

Highbridge has performed its services in conformance with the care and skill ordinarily exercised by reputable members of the profession practicing under similar conditions at the same time. No other warranty of any kind, expressed or implied, in fact or by law, is made or intended. Interpretations and results are based strictly on samples provided and/or examined.

Cover Image

The Bennington Battle Monument in Bennington, VT. Image downloaded August 26, 2023 without modification.

Photo credit: King of Hearts

https://commons.wikimedia.org/wiki/File:Bennington_Battle_Monument_October_2021_001.jpg

Under Creative Commons License CC BY-SA 4.0 - <https://creativecommons.org/licenses/by-sa/4.0/deed.en>

Respectfully submitted,



Heather Hartshorn
Senior Chemist
Highbridge Materials Consulting, Inc.



John J. Walsh
President/ Senior Petrographer
Highbridge Materials Consulting, Inc.

1. Executive Summary

This report presents the results of the petrographic and chemical analysis of eight (8) mortar samples reportedly recovered from the Bennington Battle Monument, an 1889 stone obelisk in Bennington, VT.

Six of the mortars (Samples BM01, NE04, NE18, NW26, SW02, and SW16) likely represent mixes from the original late nineteenth construction. These samples all contain mixtures of Rosendale natural cement and similar medium-grained natural sands. Most of these mortars are estimated to have binder to sand ratios in the 1 : 1 to 1 : 2 range that was typical for historical natural cement mortars. It should be noted that Sample BM01 was received in an incredibly degraded condition, and the proportional estimates for this sample should be considered approximate. Five of the six mortars have pale brown colors in hand sample. However, Sample NE04 also contains a black pigment that is somewhat streakily incorporated, giving it mottles of more greenish-gray color.

The other two samples are interpreted to represent twentieth century construction campaigns. Sample BM05 is a portland cement-lime mortar with proportions in the range of a modern Type N mix. It also contains an iron additive that has oxidized, resulting in fine reddish-brown spots within the otherwise light brownish gray mortar. Sample BM02 is a masonry cement mortar that has a more neutral gray color.

Most of the mortar samples are cohesive and intact. The original natural cement mortars tend to have a moderate hardness and high permeability. The two later portland cement-based mortars are also relatively permeable despite their cement-rich compositions. Regardless, the examined mortars appear to be in mostly sound condition with only minor cracking and secondary salt deposition. Of course, Sample BM01 is the exception. It is much more degraded and exhibits signs of extensive moisture infiltration.

Table 1.1: Summary of Calculated Mortar Designs

Sample ID	Binder type	Estimated binder proportions	Estimated binder to sand ratio (by volume)
BM01	Natural cement	n/a	> 1 : 1.9
NE04	Natural cement (with a black pigment addition)	n/a	1 : 1.2
NE18	Natural cement	n/a	1 : 1.3
NW26	Natural cement	n/a	1 : 1.1
SW02	Natural cement	n/a	1 : 1.1
SW16	Natural cement	n/a	1 : 2.7
BM05	Gray portland cement and dry hydrated lime	Type N	1 : 3.1
BM02	Masonry cement (gray portland cement and crushed limestone)	Type M	1 : 3.2

2. Introduction

On November 2, 2023, a set of masonry samples were delivered to the laboratory by Mr. Edward FitzGerald of Jablonski Building Conservation, Inc. According to Mr. FitzGerald, these represent materials sampled from the Bennington Battle Monument, Bennington, VT. The monument is a stone obelisk completed in 1889. The client has requested that the laboratory perform materials analysis on a subset of the samples as summarized in Table 2.1 below. The choice of samples to analyze are based on priorities set by Mr. FitzGerald with some additional input by the laboratory.

Table 2.1: Summary of Received Samples

This table includes only those samples selected for analysis. The laboratory made some nominal amendments to sample identifications for consistency and simplicity in reporting. These are shown in the "HMC ID" column. These identifications will be used throughout all reports.

Client ID	HMC ID	Client description on sample bag or verbally	Analytical scope requested
NW5	NW05	Salts on mortar joint	Water-soluble salts
NE11	NE11	Buff stone salts	Water-soluble salts
SE24-NE25	SE24	Salts, dark gray stone	Water-soluble salts
SW12	SW12	Salts in crack, buff stone	Water-soluble salts
SW26	SW26	Rear window, dark gray stone, salts in HC	Water-soluble salts
BM-01	BM01	South elev., ext. sand mortar bedding	Mortar analysis, water-soluble salts
BM-02	BM02	South ext. elev., org. point/bed? Under most recent repointing	Mortar analysis
BM-05	BM05	Observation deck, 2 mortars, light buff on top, flat & flush	Mortar analysis
NE4	NE04	Dark brown mortar	Mortar analysis
NE18	NE18	Interior, crumbly mortar near dark gray stone	Mortar analysis
NW26	NW26	Corner joint	Mortar analysis
SW2	SW02	Int. coarse, buff color at corner separation	Mortar analysis
SW16	SW16	Org. bedding	Mortar analysis
(none)	CF	Concrete infill	Concrete petrography, mortar analysis, salts

The requested testing includes the following:

- **X-ray diffraction analysis of salts or mineralizations**

The client has requested the qualitative identification of salts for seven samples. Five of the samples were provided as scrapings of variable purity. One sample (BM01) consists of water-logged mortar debris with no salts visible. One sample (CF) consists of a salt crust along the formed face of a concrete infill layer. The samples were analyzed either as-found, or after extraction and redeposition. X-ray diffraction analysis (XRD) is used to identify the phases present.

- **Compositional mortar analysis**

The client has requested that Highbridge perform compositional mortar analysis on eight of the provided samples. The testing includes a petrographic examination and chemical analysis to identify constituents, estimate proportions, and assess overall condition. Chemical digestions to extract sand samples for description and gradation are also included.

- **Petrographic examination and partial compositional analysis of infill concrete**

Petrographic examination is used to examine the infill concrete. The purpose is to identify constituents, assess condition, and investigate potential causes of any observed distress. A compositional analysis is performed on the mortar fraction of the concrete to evaluate the proportions of binder and sand using the same techniques described above for mortar.

This report presents the results of the compositional mortar analysis. Results for the other analyses will be presented under separate cover when complete.

3. Methods of Examination

The petrographic examination is conducted in accordance with the standard practices contained within ASTM C1324-20a. Data collection is performed or supervised by a degreed geologist who by nature of their education is qualified to operate the analytical equipment employed. Analysis and interpretation are performed or directed by a supervising petrographer who satisfies the qualifications as specified in Section 4 of ASTM C856/C856M-20.

Chemical analysis is performed in general accordance with the procedures outlined in ASTM C1324-20a. Water, carbon dioxide, and aggregate weight percentages are determined gravimetrically. Oxide weight percentages are determined by inductively coupled plasma - optical emission spectroscopy (ICP-OES). While ASTM classifies C1324 as a test method, it is intended to serve as a guideline for qualified practitioners with ample experience in the various materials under consideration. Section 10.2 indicates the need for discretion on the part of the laboratory to ensure that methods are tailored to specific mortar compositions. As such, Highbridge chooses specific digestion methods, supplementary tests, instrumentation protocols, and mathematical models to best characterize each individual mortar under consideration. Many of these are proprietary methods that have been researched internally.

The following personnel contributed to the examination:

Technicians:	M. Pattie
	J. Negron
Analyst:	M. Cortez
Chemist/Petrographer:	H. Hartshorn
Supervisor:	J. Walsh

4. Laboratory Findings and Discussion (Natural Cement Mortars)

4.1 - Overall Appearance and Quality (Natural Cement Mortars)

Six of the mortars (Samples BM01, NE04, NE18, NW26, SW02, and SW16) are mixtures of natural cement and medium-grained metaquartzite sand. In most of the samples the mortar has a light brown to medium brown color (Munsell code approximately 10YR 5-6/2-3). However, the mortar in Sample SW16 is slightly lighter colored, likely due to its higher sand content. In Sample NE04, the mortar also contains a black pigment that is not always evenly mixed. The result is a mortar with a mixture of cocoa brown and greenish gray colors (Munsell code approximately 5Y 4/1.5 on average).

In Samples NE18, NW26, SW02, and SW16, the cured product is cohesive with a moderate hardness and high permeability. Sample NE04 is comparatively harder and more indurate with a low permeability. The qualities of Sample BM01 cannot be evaluated since it was provided to the laboratory as only fine mortar debris without any significant intact fragments to examine.

4.2 - Materials (Natural Cement Mortars)

All six natural cement mortars contain natural sands consisting primarily of metaquartzite with a lesser granitic component. Though the aggregate gradations are not identical between the six samples, all of these were likely derived from the same local source. Notably, the sand in these mortars appears to also derive from the same source as the fine aggregate used in the concrete filled examined for Highbridge Report SL1846-05. The aggregate in each is clean with no clay linings, friable particles, or organic materials that would be expected to increase the water demand or decrease the bond between the aggregate and the cement paste. The sands are all considered hard, non-porous, and durable for use in masonry mortars.

A sample of the aggregate was extracted from each mortar through chemical digestion. The recovered materials are mildly to moderately variegated with a light brownish gray color overall (Munsell code approximately 2.5Y 7/1). Grain shapes are somewhat sharp-textured. The extracted sands are all medium-grained with nominal top sizes at the No. 8 or No. 4 mesh. All of the sands are also broadly graded with peak abundances between the No. 30 and No. 50 sieves. Details of the quantified gradation profile are presented in Section 7. Technically, the sands are all coarser than ones that would be compliant with modern masonry gradations as specified in ASTM C144-18. That said, the overall gradation is quite broad and is considered generally appropriate for most masonry mortars.

The sole binder in each of these mortars is a domestic natural cement. No lime or other binder additions are detected. Microtextural characteristics are consistent with those produced in the Rosendale, NY manufacturing district during the nineteenth century. The presence of Rosendale natural cement in each is confirmed by the measured binder chemistry (Table 8.1c). The use of this type of cement is consistent with the reported 1889 construction date and location not far up the Hudson River from Rosendale. The following trends are observed with regard to the natural cement binders in these samples.

- The natural cement chemistries are nearly identical in Samples NE04, NW26, SW02, and SW16. This suggests the same batch of natural cement was used in these four mortars and these samples represent contemporaneous mixes.
- Although the cement in Sample NE18 has a different chemistry than the other samples, its composition is practically identical to the natural cement measured in the concrete infill (see Highbridge Report SL1846-05).
- In Sample BM01, the measured binder has a chemical signature in the general range expected for a natural cement although it is technically more calcium-rich than expected for a typical Rosendale cement. That said, the measured chemistry is not expected to reflect the original cement composition since the provided sample was incredibly degraded and contained contaminants from the masonry and other organic materials.

Sample NE04 also contains a black pigment addition. The black pigment is present as ultrafine-grained particulates that are barely discernible at the scale of the light microscope. Petrographically, the pigment is not uniformly distributed throughout the mortar, which results in fine streaks of color within the mortar sample. The pigment is suspected to be carbon black. While the type of black pigment would normally be evaluated chemically, the natural cement binder acts as a major interference that does not allow for further characterization in this particular sample.

4.3 - Component Proportions (Natural Cement Mortars)

Material proportions for the six natural cement mortars are estimated from the chemical analysis presented in Section 8.1. Samples NE04, NE18, NW26, and SW02 have binder to sand ratios estimated between 1 : 1.1 and 1 : 1.3 by volume. Sample BM01 technically has a calculated cement to sand ratio near 1 : 2. However, it is likely that the sand content is overestimated in Sample BM01 due to the incredibly degraded quality of the provided mortar sample. While the sand contents in these five mortars may seem to be exceptionally rich mixtures, domestic natural cement mortars performed better with lower sand contents. Historical mix designs generally ranged from 1 : 1 to 1 : 2.

Sample SW16 has a cement to sand ratio estimated at 1 : 2.7 by volume. This represents a dense sanding for a mortar with a pure natural cement binder. That said, the gradation of the aggregate in this sample is quite broad, which allows for a more economical packing of the sand grains and a lower volume of interstitial binder paste to fill the space between the aggregate.

As mentioned above, Sample NE04 also contains a black pigment addition. Although original pigment contents cannot be determined accurately for natural cement mixtures, it is still possible to set maximum constraints based on the chemical analysis. As a point of reference, ASTM C270 currently recommends a maximum pigment dosage as 10% of dry portland cement weight. Though it is possible to calculate a pigment dosage as high as 22% by weight of dry natural cement in this sample, the original pigment content was probably much lower than the estimated maximum due to the intermixing of insoluble silt and clay from the cement binder. That said, the pigment distribution is moderately dense throughout the binder paste and could have represented a higher content than the recommended dosage for modern portland cement-based mixtures.

4.4 - Condition and Service Performance (Natural Cement Mortars)

There are no major workmanship defects identified in Samples NE18, NW26, SW02, and SW16. The mortar constituents are well-blended, and the mix water was fully incorporated into the fresh mixture. The sand content is notably dense in Sample SW16, and it was likely necessary to increase the original mix water content in order to achieve a workable fresh mix. This appears to have been the case, as evidenced by the higher microporosity of the cement paste in this sample compared to the others. Regardless, each of these four mortars is compact and well-consolidated. The cured products are all cohesive, and the binder paste has a moderate hardness and high permeability. These features are within the range expected for historical natural cement mortars.

In Sample NE04, though the natural cement and aggregate are well-mixed, the black pigment is not evenly distributed throughout the binder matrix. This results in streaks of more heavily pigmented paste that give the mortar a mottled appearance when freshly broken. The carbon black pigment may have increased the water demand of the fresh mix, and this is supported by the denser cement paste in this sample compared to that in the other four natural cement mortars described above. On the whole, the mortar in Sample NE04 is compact and well-consolidated. However, the fresh mix appears to have reached freezing temperatures before it hardened. This is evidenced by the occurrence of microscopic ice crystal impressions that form splays of planar voids throughout the binder paste. Where present, these may have reduced the strength and increased the permeability relative to unfrozen areas of the mortar. Still, the integrity of the examined mortar is not significantly compromised, and the general properties are within the range expected for a natural cement mortar. The cured product is hard, indurate, and slowly water-absorptive.

For Sample BM01, the qualities of the original mixing and place of the mortar cannot be evaluated since the provided sample included only fine debris and no intact mortar pieces. In this sample, the natural cement paste is fully decalcified and there is secondary carbonate lining surfaces and fine cracks. This suggests that there has been a high degree of moisture infiltration in the location from which this sample was taken.

Samples NE04, NE18, NW26, SW02, and SW16 are all fully carbonated, which is a normal and desirable consequence of long-term curing. There is no evidence of any paste degradation. However, all of the mortars exhibit some minor cracking and secondary mineralizations. In Sample NE 18, the cracking is more extensive and there is also an abundance of isotropic salt observed filling the cracks. However, the examined mortar pieces still remain cohesive and intact.

5. Laboratory Findings and Discussion (Sample BM05)

5.1 - Overall Appearance and Quality (Sample BM05)

The mortar in Sample BM05 is interpreted to represent a twentieth century repointing mortar. It is a portland cement-lime mix with a medium-grained natural sand. The mortar has a light brownish gray color (Munsell code approximately 2.5Y 6.75/1). There are also some visible rust-spots due to an addition of metallic iron particles. The cured product is hard and indurate yet somewhat rapidly water-absorptive.

5.2 - Materials (Sample BM05)

The aggregate is a medium-grained natural sand that is a mixture of metaquartzite and lesser marble rock. Although the sand is clearly distinct from that employed in the original natural cement mortars, the aggregate in this sample could also be derived from a local deposit. The sand is free of clay linings and friable particles, and the aggregate is considered hard, non-porous, and durable for use in masonry mortars.

There is a minor addition of metallic iron flakes that have sizes in the range of the sand particles and are distributed in relatively low abundance throughout the binder matrix. Historically, iron flakes have been added to cementitious materials as a surface hardener or a shrinkage compensator. However, the purpose of this additive is unknown to the author within the context of this particular mortar.

A sample of the siliceous portion of the original sand along with the iron flakes was extracted from the mortar through chemical digestion. The extracted material has a mildly variegated appearance with a light brownish gray color overall (Munsell code approximately 2.5Y 6.5/1). Note that the marble grains dissolved during the sand extraction, and the marble may have contributed some more light gray, opaque particles to the original aggregate.

The aggregate grains are somewhat sharp-textured. The sand is medium-grained and broadly graded. The nominal top size is estimated at the No. 8 mesh, and the peak abundance is retained between the No. 30 and No. 50 sieves. Details of the gradation profile are presented in Section 7. The siliceous portion of the aggregate would comply with the permissible limits in the modern standard for masonry sands (ASTM C144-18). The petrographic distribution of the marble particles suggests the original sand was slightly coarser than the extracted siliceous portion alone. However, the particle size distribution of the original aggregate still may have complied with the modern standard.

The binder consists of portland cement and dry hydrated lime. No supplementary cementitious materials or pigment additions are detected. The portland cement is a gray variety, as indicated petrographically by the iron-bearing ferrite observed petrographically (Table 9.7) and the low $\text{SiO}_2/\text{Fe}_2\text{O}_3$ ratio measured chemically (Table 8.2b). The microtextures of the cement are most consistent with a product manufactured in the mid-twentieth century. Similarly, the lime has a particulate texture that is typical of a prepackaged dry hydrate product. This indicates a vintage no earlier than ca. 1910, when prepackaged dry hydrated limes became commercially available in the United States. The chemical analysis (Table 8.2b) also indicates that the lime is a dolomitic variety, which is common for prepackaged dry hydrated limes. Given the binder microtextures, this mortar is suspected to represent a twentieth century repointing or repair.

5.3 - Component Proportions (Sample BM05)

The chemical analysis presented in Section 8 is used to calculate the proportions of the original mix. The cement to lime ratio is estimated near 1 : 1 and the binder to sand ratio near 1 : 3 by volume. These mix proportions are consistent with a Type N formulation as specified in the modern standard for masonry mortars (ASTM C270-19a^{e1}). Historical versions of the same standard would have classified this mix as a Type B formulation. However, this mortar could predate even the historical version of the standard.

5.4 - Condition and Service Performance (Sample BM05)

Based on the examined sample pieces, the mortar was well-mixed with no sand streaks or coarse binder inclusions. The mix water was thoroughly incorporated, and the cement was well-hydrated and cured. The mortar is compact and adequately consolidated. The cured product is hard and indurate, though the paste is somewhat rapidly water-absorptive. These characteristics are within the range expected for the estimated composition.

The mortar is fully carbonated, which is a normal result of long-term service. The pieces remain intact with no evidence of any significant cracking distress, paste degradation, or deleterious salt mineralizations. The most notable service effect is the leaching of iron oxide from the metallic iron addition into the surrounding binder paste. This contributes to fine iron oxide spots that are visible on the joint face of the provided mortar pieces. However, there is no evidence of any expansive distress related to this feature.

6. Laboratory Findings and Discussion (Sample BM02)

6.1 - Overall Appearance and Quality (Sample BM02)

The mortar in Sample BM02 is interpreted to represent a twentieth century repointing mortar. It is a mixture of masonry cement and relatively fine-grained sand. The mortar has a gray color (Munsell code approximately N7.5). The cured product is relatively indurate, though the paste is soft and highly permeable.

6.2 - Materials (Sample BM02)

The aggregate consists primarily of fine-grained, clastic sedimentary rock particles. The sand is clean with no clay linings or friable materials. Grain shapes are moderately soft-textured, and the particles are mostly equant to subequant. Overall, the sand is considered relatively hard and reasonably durable for use in cementitious mixtures. Some of the clay-rich rock grains may be susceptible to expansion upon saturation and freeze-thaw cycling. However, there is no evidence of any such distress in the examined sample.

A sample of the aggregate was extracted from the mortar through chemical digestion. The extracted sand is mostly uniform and opaque with a medium gray color (Munsell code approximately 2.5Y 5/0.5). The sand is relatively fine-grained and somewhat narrowly graded with a nominal top size at the No. 8 mesh and 70% of the material centered around the No. 50 sieve. Details of the quantified gradation profiles are presented in Section 7. The aggregate is finer and more narrowly graded than one that would comply with the modern standard for masonry sands (ASTM C144-18).

The binder is interpreted to represent a prepackaged masonry cement (or mortar cement). It contains a mixture of portland cement, crushed limestone, and an air-entraining agent. The cement is identified as a gray portland and its hydration is highly advanced. The chemical analysis indicates that the crushed limestone is a high-calcium variety. The limestone is added to masonry cements as a plasticizer in lieu of hydrated lime. The abundance of spherical air-voids with fine diameters indicates that the mortar was intentionally air-entrained. This is a typical feature of prepackaged masonry cements and mortar cements. The use of an air-entrained masonry cement indicates that the mortar dates no earlier than ca. 1940, and likely represents a twentieth century repointing or repair material.

6.3 - Component Proportions (Sample BM02)

Prepackaged masonry cements are specified by their physical properties rather than through the proportions of their ingredients. These properties are tested in preproduction using standardized mixing, molding, and curing methods. As such, it is never possible to determine the typing of a masonry cement mixture unless it is available as a dry powder. Nevertheless, it is still useful to calculate the weight and volume proportions of the mix in this sample in order to better understand its performance. These calculated proportions are presented in Table 8.3c.

The binder is estimated to contain roughly 75% portland cement by weight. Guidance provided by ASTM C1324 suggests that this proportioning is closer to that often used in masonry cement blends that satisfy a Type M property. The binder to sand ratio is estimated at 1 : 3.2 by volume. The mortar is technically slightly oversanded compared to mixes specified in the modern standard for masonry mortars (ASTM C270-19a^{e1}), which only allows up to three parts sand for each part binder.

6.4 - Condition and Service Performance (Sample BM02)

Based on the examined sample pieces, the constituents of the mortar were thoroughly-blended. The mortar is compact. Although the sand distribution is somewhat dense due to the moderately high content of narrowly graded aggregate grains, the mortar mix is still adequately consolidated and entrapped air-voids are not overly abundant. Much of the air-void structure consists of very fine, spherical air-voids that are the result of the air-entraining admixture in the prepackaged masonry cement binder.

The cured product is relatively indurate. However, the paste is soft and highly water-absorptive. The paste qualities are softer and more permeable than would be expected for a Type M masonry cement mortar, and this could be due to the use of a high original mix water content. The relatively high content of narrowly graded sand would have increased the amount of mix water needed to create a workable mix, and the additional water would have increased the capillary porosity in the binder paste compared to a similar mortar mixed with a lower water content.

Despite the softness and permeability of the mortar, the examined sample pieces appear sound. No significant deleterious service effects are identified petrographically. The most notable secondary reaction is the full carbonation of the binder paste, which is a normal and desirable consequence of aging.

7. Aggregate Sieve Analysis

Aggregate samples were extracted from the eight mortars by digesting each sample in an acid sufficient to decompose the binder. The following procedure was used for each sample:

- A subsample of the mortar was placed in a 400-mL low-form glass beaker and digested in a 25% v/v hydrochloric acid solution. For the six natural cement mortars, the acid was replenished with a 33% v/v hydrochloric acid solution over the course of the digestion.
- Once the binder was decomposed, the beaker was agitated to suspend fines or low-density material. After allowing for the settling of aggregate above the silt and clay sizes, the material remaining in suspension was decanted into a 1-quart polyethylene pail. Several rinsings of the settled aggregate were performed until the water ran clear. The suspended fines produced by each rinsing were transferred to the larger pail.
- The sand in the original beaker was transferred to a 1-pint wide-mouth polypropylene container. The sand was scrubbed with bare fingers to release any hydrous silica gel or additional fines from the surfaces of the sand grains. The silica is a byproduct of the incongruent dissolution of hydraulic cement. These were again transferred to the polyethylene pail.
- The cleaned sand was dried in an oven at 45°C. The dried sand was photographed, described, and graded through a standard sieve stack.
- The suspended fines in the 1-quart container were allowed to settle and the supernatant was decanted. The fines were then digested below boiling in a 10g/L NaOH solution to decompose any hydrous silica from the portland cement. The fines were rinsed several times and then dried.
- Both the undecanted material passing the No. 200 sieve and the decanted fines passing the No. 200 sieve were viewed in petrographic grain mount to decide what should be included in the gradation analysis.
 - For the natural cement mortars, all of the undecanted material consists of silt and clay from the aggregate. The decanted fines are found to consist mostly of undigested clays from the natural cement binder. The decanted fines from Sample NE04 also contain a black pigment. As such, all of the decanted material is excluded from the gradation analysis. The exclusion of any silt and clay from the aggregate that was also captured in the decanted fraction is considered to represent a minor error.
 - For Samples BM05 and BM02, both the undecanted and decanted fractions are derived from the aggregate. Since there are no significant binder residuals, all of the extracted material is included in the gradation analysis.
- It should be noted that Sample BM05 contains some marble aggregate that was digested during the sand extraction. The gradation presented below represents only the siliceous portion of the aggregate. The marble appears to mostly be concentrated in the medium to coarse sand sizes with only a lower proportion passing the No. 50 sieve.

Table 7.1: Chemical Digestion Data - Weight Retention (g)

Sieve size	BM01	NE04	NE18	NW26	SW02	SW16	BM05	BM02
	Natural cement-based						Portland cement-based	
3/8"	0.00	0.00	0.00	0.00	0.00	0.00	0.00	0.00
No. 4	0.14	0.00	0.00	0.19	0.80	1.40	0.00	0.00
No. 8	0.78	0.80	0.88	1.41	1.27	1.39	0.00	0.11
No. 16	0.97	0.89	1.37	2.29	2.47	1.63	0.48	0.53
No. 30	1.26	1.91	2.18	3.21	5.43	2.94	1.05	1.44
No. 50	1.20	2.11	3.24	3.26	6.68	4.95	1.44	4.46
No. 100	0.57	0.64	1.27	0.97	1.86	2.58	0.71	4.29
No. 200	0.20	0.20	0.19	0.17	0.45	0.70	0.39	1.40
Pan	0.02	0.03	0.03	0.03	0.04	0.08	0.27	0.28

Table 7.2: Chemical Digestion Data - Cumulative Passing (%)

Sieve size	BM01	NE04	NE18	NW26	SW02	SW16	BM05	BM02
	Natural cement-based						Portland cement-based	
3/8"	100.0	100.0	100.0	100.0	100.0	100.0	100.0	100.0
No. 4	97.3	100.0	100.0	98.4	95.8	91.1	100.0	100.0
No. 8	82.2	87.9	90.4	86.1	89.1	82.2	100.0	99.1
No. 16	63.3	74.4	75.4	66.3	76.1	71.8	88.9	94.8
No. 30	38.7	45.3	51.7	38.5	47.5	53.1	64.7	83.3
No. 50	15.3	13.2	16.2	10.2	12.4	21.5	31.5	47.7
No. 100	4.3	3.5	2.4	1.8	2.6	5.0	15.1	13.4
No. 200	0.4	0.4	0.3	0.3	0.2	0.5	6.2	2.3
Pan	0.0	0.0	0.0	0.0	0.0	0.0	0.0	0.0

Table 7.3: Chemical Digestion Data - Cumulative Retained (%)

Sieve size	BM01	NE04	NE18	NW26	SW02	SW16	BM05	BM02
	Natural cement-based						Portland cement-based	
3/8"	0.0	0.0	0.0	0.0	0.0	0.0	0.0	0.0
No. 4	2.7	0.0	0.0	1.6	4.2	8.9	0.0	0.0
No. 8	17.8	12.1	9.6	13.9	10.9	17.8	0.0	0.9
No. 16	36.7	25.6	24.6	33.7	23.9	28.2	11.1	5.2
No. 30	61.3	54.7	48.3	61.5	52.5	46.9	35.3	16.7
No. 50	84.7	86.8	83.8	89.8	87.6	78.5	68.5	52.3
No. 100	95.7	96.5	97.6	98.2	97.4	95.0	84.9	86.6
No. 200	99.6	99.6	99.7	99.7	99.8	99.5	93.8	97.7
Pan	100.0	100.0	100.0	100.0	100.0	100.0	100.0	100.0
Fineness modulus	2.99	2.76	2.64	2.99	2.77	2.75	2.00	1.62

Chart 7.1: Aggregate Sieve Analysis (Natural Cement Mortars)

The following chart presents the particle size distribution curves for the sand samples extracted from the natural cement mortars. The chart plots the data from the cumulative passing values in Table 7.2. The fine end of the curve is terminated at the No. 200 sieve, and any silt and clay components are not graded beyond this point. The material passing the No. 200 sieve may be underestimated since some undigested clay and silt from the aggregate may have been captured in the decanted material that was excluded from the gradation profile. Any resulting error in the estimated fines content is considered to be minor.

Note that, although none of the gradation curves are identical, the general shapes of the curves are similar. However, the sand in Sample SW16 is slightly coarser and more broadly graded compared to the sands in the other five natural cement mortars.

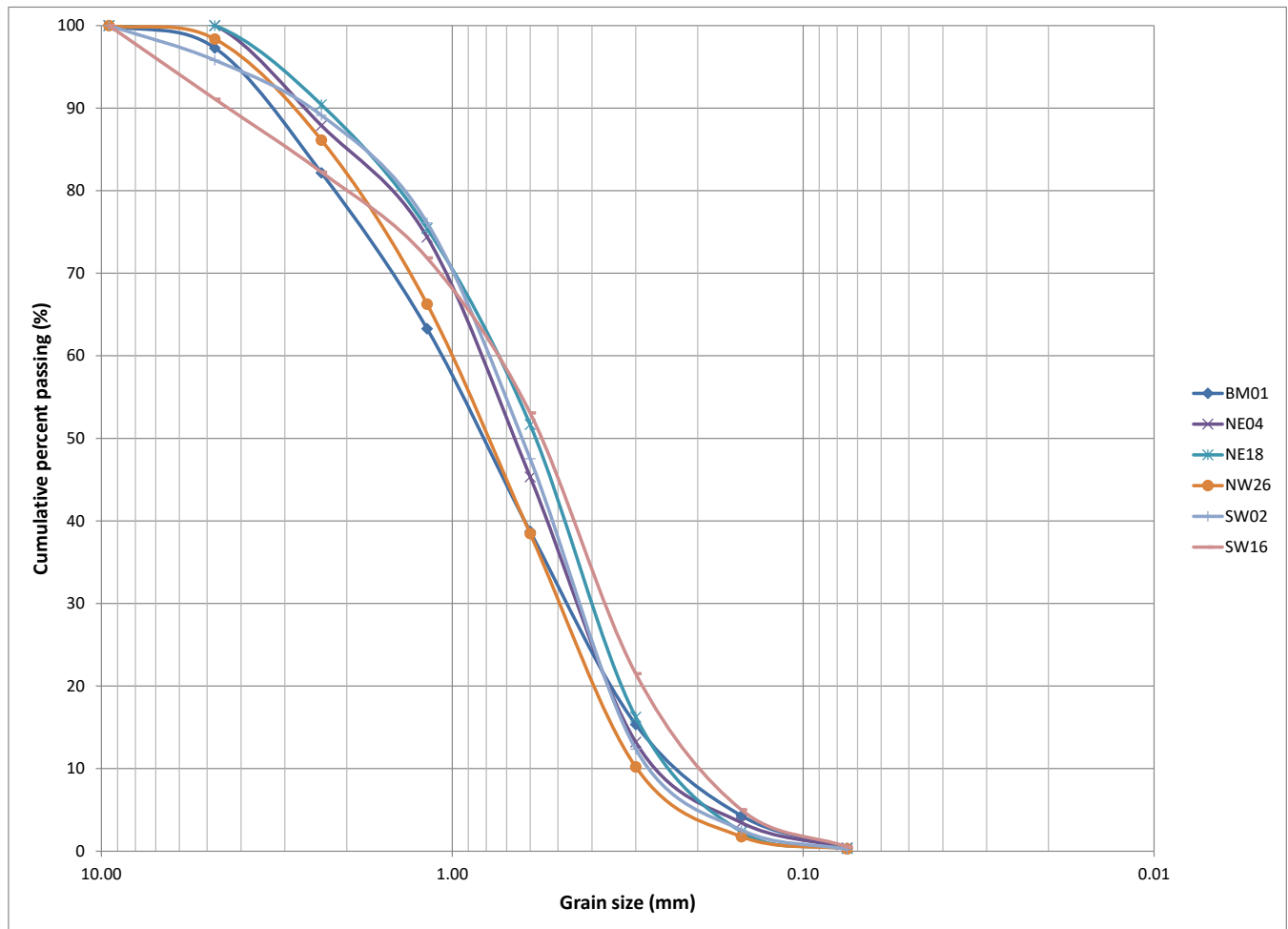
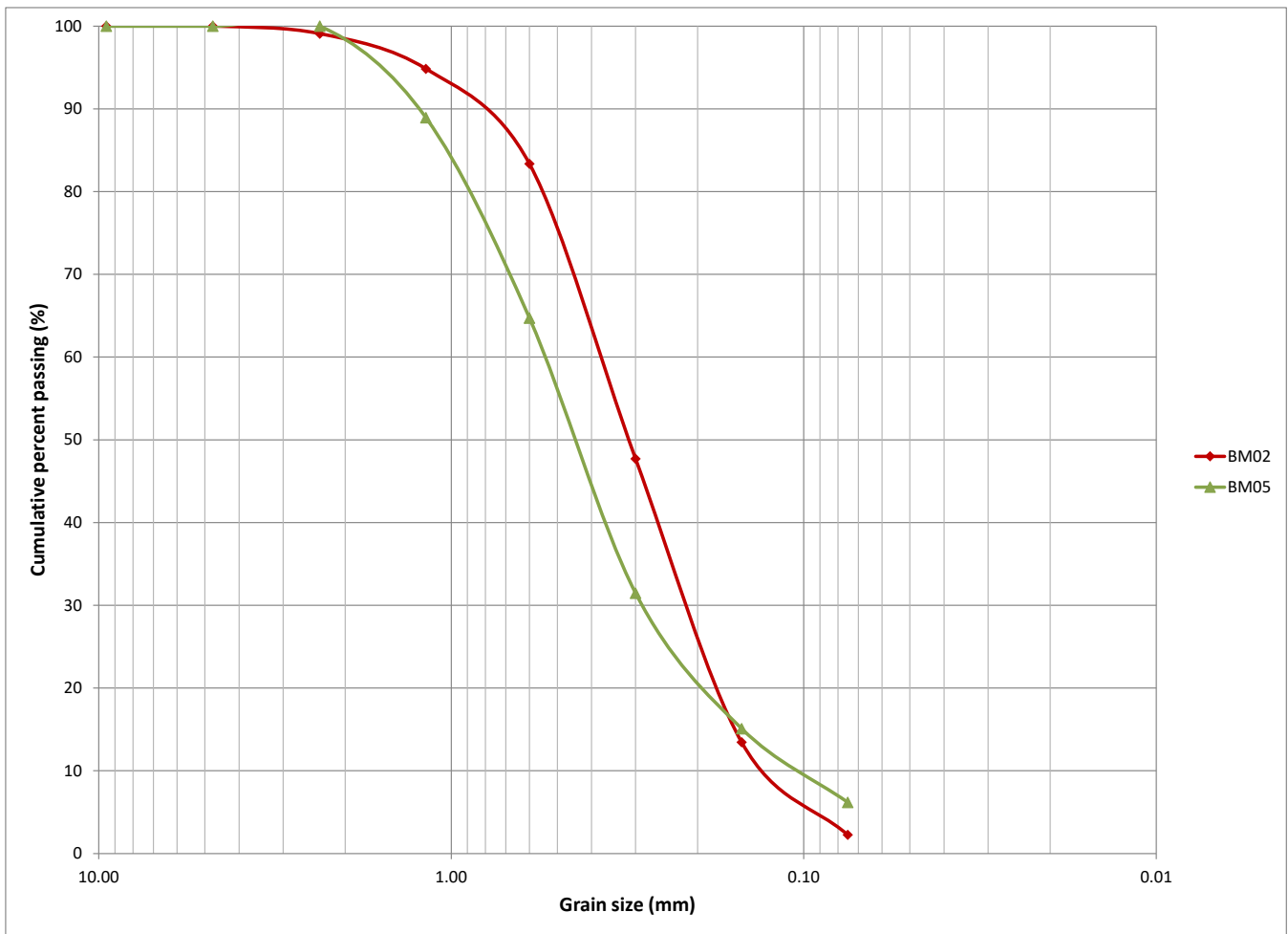


Chart 7.2: Aggregate Sieve Analysis (Portland Cement-Based Mortars)

The following chart presents the particle size distribution curves for the sand samples extracted from Samples BM05 and BM02. The chart plots the data from the cumulative passing values in Table 7.2. The fine end of the curve is terminated at the No. 200 sieve, and any silt and clay components are not graded beyond this point.

It should be noted that the gradation curve does not include the marble portion of the aggregate in the Sample BM05. The marble appears to mostly be present in the particle sizes above the No. 50 sieve, and the gradation curve plotted below may be slightly narrower and finer than that of the original aggregate.



8. Chemical Analysis

8.1 - Chemical Analysis of Natural Cement Mortars

Table 8.1a: Chemical Analysis Results (Natural Cement Mortars)

For Samples BM01, NE04, NE18, NW26, SW02, and SW16, proprietary modifications were made to the chemical digestion procedure described by ASTM C1324 to most effectively decompose the natural cement binder while minimizing any leaching of components from the aggregate. The procedure included a warm digestion in dilute hydrochloric acid solution (20% v/v) followed by a heated digestion in alkaline solution (10 g/L NaOH). The method was also modified to determine the insoluble residue directly from the aliquot used for the soluble oxide analysis rather than through the digestion of a separate subsample.

Sample ID	BM01	NE04	NE18	NW26	SW02	SW16
Component (wt. %)						
SiO ₂	5.63	7.50	6.04	8.95	9.00	5.72
CaO	13.03	11.66	13.01	13.58	14.12	8.45
MgO	4.21	7.21	7.81	7.78	8.23	4.91
Al ₂ O ₃	0.97	1.27	1.49	1.50	1.42	0.97
Fe ₂ O ₃	0.85	1.04	1.26	1.29	1.13	0.87
Insoluble residue	60.00	49.88	43.30	42.96	44.99	65.35
LOI to 110°C	1.56	3.28	5.64	5.57	3.84	2.58
LOI 110°C-550°C	3.04	5.31	8.36	4.99	4.53	2.67
LOI 550°C-950°C	11.39	10.45	10.09	11.83	12.23	7.70
Measured total	100.68	97.59	97.01	98.46	99.50	99.22

Table 8.1b: Estimate of Pigment Content (Sample NE04)

The insoluble residue contains both sand and pigment. In cementitious mixes such as this, the pigment particles are often finer than the aggregate and can be isolated by size or density in sand extraction (Section 7). The extracted material that was decanted and treated with NaOH solution is found to consist of a mixture of pigment and undigested residues from the natural cement binder. Still, the weight of this fraction can be directly compared to the total weight of material extracted for the aggregate analysis. The weight percent of pigment as a percentage of the chemically-extracted sand can then be compared to the insoluble residue from the chemical analysis to estimate the maximum pigment content of the original mix.

Sample ID	NE04
Extracted pigment wgt. (g)	1.18
Total extracted material wgt. (g)	8.88
Pigment as wgt. % of extracted material	13.28
Maximum pigment as wgt. % of the total mortar	7.60

Table 8.1c: Estimated Binder Chemistry (Natural Cement Mortars)

In Samples BM01, NE04, NE18, NW26, SW02, and SW16, the binder is interpreted to consist of natural cement with no other additives. As such, the cement chemistry is estimated from the total chemical analysis presented in Table 8.1a. The five major oxides in the binder are normalized to a 92% weight yield, assuming the other 8% consists of trace and insoluble constituents of the natural cement binder. This is compared to a normalized example of historical Rosendale natural cement presented in the righthand column. The presented Rosendale cement chemistry was taken from Table 115 in Edwin Eckel's *Cements, Limes, and Plasters* where it is referenced as an analysis from "F.O. Norton". Important chemical indices are calculated for all of the samples as follows:

$$\begin{aligned} \text{Hydraulic index} &= (\text{SiO}_2 + \text{Al}_2\text{O}_3) / \text{CaO} \\ \text{Cementation index} &= (2.8 \cdot \text{SiO}_2 + 1.1 \cdot \text{Al}_2\text{O}_3 + 0.7 \cdot \text{Fe}_2\text{O}_3) / (\text{CaO} + 1.4 \cdot \text{MgO}) \end{aligned}$$

Sample ID	BM01	NE04	NE18	NW26	SW02	SW16	Historical Rosendale
Component (wgt. %)							
SiO ₂	21.0	24.1	18.8	24.9	24.4	25.2	26.1
CaO	48.5	37.4	40.4	37.7	38.3	37.2	34.8
MgO	15.7	23.1	24.3	21.6	22.3	21.6	21.0
Al ₂ O ₃	3.6	4.1	4.6	4.2	3.9	4.3	6.2
Fe ₂ O ₃	3.1	3.3	3.9	3.6	3.1	3.8	3.8
Other	8.0	8.0	8.0	8.0	8.0	8.0	8.0
CaO/MgO	3.1	1.6	1.7	1.7	1.7	1.7	1.7
CaO/SiO ₂	2.3	1.6	2.2	1.5	1.6	1.5	1.3
SiO ₂ /Al ₂ O ₃	5.8	5.9	4.0	6.0	6.3	5.9	4.2
SiO ₂ /Fe ₂ O ₃	6.7	7.2	4.8	7.0	8.0	6.6	6.8
Hydraulic index	0.51	0.75	0.58	0.77	0.74	0.79	0.93
Cementation index	0.92	1.06	0.81	1.13	1.08	1.16	1.28

The following features are worth noting:

- In five of the six mortars (Samples NE04, NE18, NW26, SW02, and SW16), the measured binder chemistry is consistent with that expected for a nineteenth century natural cement manufactured in the Rosendale district of New York. This is further demonstrated by the clustering of these samples on the ternary diagram in Chart 8.1c below.
- The cement chemistry measured for Samples NE04, NW26, SW02, and SW16 is practically identical. This suggests that these four mortars contain the same batch of Rosendale natural cement and are likely contemporaneous with one another.
- The measured binder in Sample BM01 has a higher CaO content than recorded for historical Rosendale natural cements. This is clearly demonstrated by the higher CaO/MgO and CaO/SiO₂ ratios compared to the other five mortars and the example of historical Rosendale cement. The higher CaO content is not suspected to be due to a lime addition, since there is no clear evidence of lime observed petrographically. Of course, this mortar sample was provided as fine debris rather than intact pieces, and it is difficult to confirm the absence of lime from the small fragments included in thin section. That said, there is an abundance of secondary calcite precipitated within cracks and along the edges of the fragments. If this deposit is the result of leaching from other materials in the assembly, it certainly could have enriched the examined mortar in CaO. Either way, the measured chemistry is not suspected to accurately represent the composition of the original cement in this sample.

Chart 8.1c: Ternary Diagram (Natural Cement Mortars)

This ternary diagram plots the SiO₂, CaO, and MgO contents measured in each of the six mortars. The three oxides are normalized to 100% prior to plotting. Samples NE04, NW26, SW02, and SW16 are all tightly clustered on the ternary diagram, demonstrating the use of the same batch of cement in these four mortars. Sample NE18 has a distinctly different cement chemistry that is still in the range expected for Rosendale natural cements. As mentioned above, the chemistry measured for Sample BM01 is more CaO-rich and is likely not representative of the original cement composition due to the quality and condition of the provided sample.

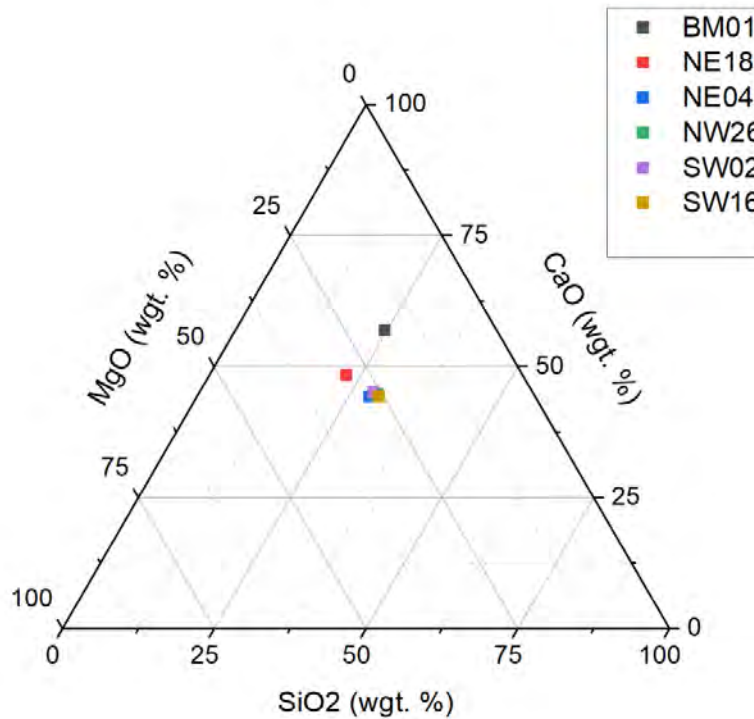


Table 8.1d: Calculated Components (Natural Cement Mortars)

The binder in Samples BM01, NE04, NE18, NW26, SW02, and SW16 is interpreted to consist solely of natural cement with no lime addition. All of the proportions presented in the table below are calculated as follows.

- The five soluble oxides are assumed to represent roughly 92% of the natural cement binder by weight.
- The sand is represented by the insoluble residue measurement.
- Sample NE04 also contains a pigment addition. The maximum weight of pigment has been subtracted from the insoluble residue in order to estimate the original sand content of these mixes.
- The natural cement and sand are assumed to have bulk densities of 75 lbs./ft.³ and 80 lbs./ft.³.

The presented proportions are calculated assuming the original natural cement contained roughly 8% insoluble silt and clay. However, Rosendale natural cements historical could have contained up to 15% insoluble material. If alternate calculations were performed assuming this higher insoluble content, then the estimated sand contents are reduced slightly. Still, none of the samples would be estimated to contain less than one part sand for each part cement, and Sample SW16 would be estimated to have a cement to sand ratio of 1 : 2.5 by volume.

It should be noted that Sample BM01 was provided as fine debris rather than as intact mortar pieces. The mortar in this sample also appears to have been subjected to moisture infiltration and secondary deposition of calcite. Due to the quality and condition of this sample, the estimated proportions below are considered to be a less accurate representation of the original mortar mix.

The pigment content in Sample NE04 is estimated using the data presented in Table 8.1b. In the chemical analysis, the pigment and the aggregate are measured together as the acid-insoluble residue. However, since the pigment is less dense than the sand, it was possible to mostly separate these two components physically during the chemical digestion used to extract the sand. The proportional weight of the pigment was subtracted from the insoluble residue before performing the other calculations described above. The pigment is reported as a maximum weight since there is some insoluble silt and clay from the natural cement binder is still intermixed. It is reported by weight of cement since this is the industry standard for evaluating pigment dosages. In any case, it should be stressed that it is never advisable to match pigment weights determined through compositional analysis as color intensities must be assumed to vary between different sources. It is always best to match color through a mock-up process. Factors including mix water content, tooling methodology, and weather conditions may all affect final color.

Sample ID	BM01	NE04	NE18	NW26	SW02	SW16
Component						
Natural cement (wgt. %)	33	44	43	46	45	26
Sand (wgt. %)	67	56	57	54	55	74
Pigment (as max. wgt. % of cement)	n/a	22.5	n/a	n/a	n/a	n/a
Cement : sand ratio (by volume)	1 : 1.9	1 : 1.2	1 : 1.3	1 : 1.1	1 : 1.1	1 : 2.7

8.2 - Chemical Analysis of Portland Cement-Lime Mortar

Table 8.2a: Chemical Analysis Results (Sample BM05)

Chemical analysis was performed in general accordance with methods contained within ASTM C1324. The method was modified to determine the insoluble residue directly from the aliquot used for the soluble oxide analysis rather than through the digestion of a separate subsample.

The high total yield is attributed to the double measurement of the marble sand. The dolomitic portion would have been measured completely in the insoluble residue and partially (as volatile CO₂) in the losses on ignition.

Sample ID	BM05
Component (wt. %)	
SiO ₂	2.78
CaO	18.37
MgO	2.11
Al ₂ O ₃	1.03
Fe ₂ O ₃	0.87
Insoluble residue	56.28
LOI to 110°C	0.89
LOI 110°C-550°C	2.30
LOI 550°C-950°C	18.78
Measured total	103.41

Table 8.2b: Normalized Binder Chemistry (Sample BM05)

The binder in Sample BM05 consists of a combination of portland cement and lime. As such, it is not possible to accurately determine the original chemistry of any one product. Nevertheless, it is useful to normalize the chemical analysis to observe the combined composition of these binders. The five major oxides reported in Table 8.2a are normalized to a 100% weight basis to produce the following table.

Sample ID	BM05
Component (wgt. %)	
SiO ₂	11.0
CaO	73.0
MgO	8.4
Al ₂ O ₃	4.1
Fe ₂ O ₃	3.5
CaO/SiO ₂	6.6
SiO ₂ /MgO	1.3
SiO ₂ /Fe ₂ O ₃	3.2

The following features of the binder chemistry are worth noting:

- The SiO₂/Fe₂O₃ ratio indicates a higher Fe₂O₃ content than expected for gray portland cement. For reference, gray portland cements typically have SiO₂/Fe₂O₃ ratios near 7 while white cements have SiO₂/Fe₂O₃ ratios closer to 20. The higher Fe₂O₃ content is attributed to soluble iron from the iron oxides that have emanated into the binder matrix from the metallic iron particles in the mortar.
- The SiO₂/MgO ratio is lower than those expected for gray portland cement alone (typically near 7). This indicates that the lime contributes some MgO to the measured binder chemistry and is a dolomitic variety. This assumption is used to calculate the proportions as described in the following table.
- The CaO/SiO₂ ratio is higher than expected for a gray portland cement (typically near 3), indicating the presence of other sources of CaO. In this mortar, these are interpreted to be the dolomitic lime as well as any calcite that was dissolved from the marble aggregate particles.

Table 8.2c: Calculated Components (Sample BM05)

As mentioned in Table 8.2b, the measured CaO content of the mortar is likely elevated from that of the original cement-lime binder due to the dissolution of some calcite from marble in the sand addition. This can be corrected for mathematically to estimate the proportions of the original mortar. The following assumptions are made in order to calculate the proportions presented in the table below.

- The gray portland cement has a typical chemistry with a CaO/SiO₂ ratio of 3.0 and a SiO₂/MgO ratio of 7.0.
- The lime is a purely dolomitic variety with a CaO/MgO ratio of 1.4.
- Any excess CaO is attributed to digested portions of the marble sand. This excess amount of CaO is converted to CaCO₃ by molecular weight conversion and added back to the insoluble residue to represent the total original sand content.
- The portland cement, dry hydrated lime, and sand are estimated to have bulk densities of 94 lbs./ft.³, 40 lbs./ft.³, and 80 lbs./ft.³ respectively.

The mortar is estimated to have proportions near a 1 : 1 : 6 mix. The estimated mix design would be in the range of a Type N mortar when compared to the modern standard for masonry mortars (ASTM C270-19a^{e1}). In historical versions of the same standard, this would have been categorized as a Type B mortar.

It should be noted that where volume proportions are given, these are based on estimated original bulk densities of the materials. However, limes are subject to great variation in volume due to factors such as settling or “fluffing” in dry powders. The table also presents the weight percentages of the dry ingredients (portland cement, dry hydrated lime, and sand). These are more accurate as they represent direct measurements of material mass and are not based on assumptions of bulk density. Of course, all of these discussions may be academic since it is usually desirable to modify the original design if modern materials will be used to replace their historic counterparts. The findings of a mortar analysis are best used to constrain possible repair designs rather than as a prescription for a specific formulation.

Sample ID	BM05
Component	
Portland cement (wgt. %)	15
Lime expressed as dry hydrate (wgt. %)	6.4
Sand (wgt. %)	79
Cement : lime ratio (by volume)	1 : 1.0
Binder : sand ratio (by volume)	1 : 3.1

8.3 - Chemical Analysis of Masonry Cement Mortar

Table 8.3a: Chemical Analysis Results (Sample BM02)

Chemical analysis was performed in general accordance with methods contained within ASTM C1324. The method was modified to determine the insoluble residue directly from the aliquot used for the soluble oxide analysis rather than through the digestion of a separate subsample.

Sample ID	BM02
Component (wt. %)	
SiO ₂	3.34
CaO	13.11
MgO	0.59
Al ₂ O ₃	0.87
Fe ₂ O ₃	0.44
Insoluble residue	69.33
LOI to 110°C	0.98
LOI 110°C-550°C	2.11
LOI 550°C-950°C	10.68
Measured total	101.44

Table 8.3b: Estimated Binder Chemistry (Sample BM02)

The binder in Sample BM02 is a masonry cement that contains a mixture of portland cement and crushed limestone plasticizer. As such, it is not possible to accurately determine the original chemistry of any one product in this mortar sample. Nevertheless, it is useful to normalize the chemical analysis to observe the combined composition of these binders. The five major oxides reported in Table 8.3a are normalized to a 100% weight basis to produce the following table.

Sample ID	BM02
Component (wt. %)	
SiO ₂	18.2
CaO	71.5
MgO	3.2
Al ₂ O ₃	4.7
Fe ₂ O ₃	2.4
CaO/SiO ₂	3.9
SiO ₂ /MgO	5.7
SiO ₂ /Fe ₂ O ₃	7.6

The following features of the binder chemistry are worth noting:

- The binder has a CaO/SiO₂ ratio greater than expected for a gray portland cement alone (typically near 3). This is consistent with the presence of a plasticizer addition.
- The SiO₂/Fe₂O₃ ratio indicates the use of a gray rather white portland cement. Gray portland cements typically have SiO₂/Fe₂O₃ ratios near 7 while white cements have SiO₂/Fe₂O₃ ratios closer to 20.
- The SiO₂/MgO ratio is near that expected for a gray portland cement alone (typically near 7), suggesting that the plasticizer is a high-calcium variety.

Table 8.3c: Calculated Components (Sample BM02)

ASTM C1324 provides calculation methods for masonry cements. However, these solve for the masonry cement weight by subtracting all other estimated components from 100%. Wherever possible, the laboratory prefers to calculate each component independently and then check where errors might be present. For this specific mixture, the following assumptions were used to calculate the proportions reported in the table:

- All SiO₂ derives from portland cement with an original SiO₂ content of 21%.
- The crushed limestone plasticizer can be calculated through molecular weight conversion from the measured CaO and after subtracting sufficient CaO and MgO to satisfy the calculated cement content (63.5% and 3%, respectively).
- The sand is represented by the insoluble residue measurement.
- Volumetric ratios are calculated from the weights using standard assumptions of the bulk weights of individual ingredients. Given the portland cement content within the prepackaged binder, the bulk density used for the masonry cement is based on guidance in ASTM C1324 for masonry cement products.

The mortar is estimated to have a moderately high sand content. Based on the guidance provided in ASTM C1324, the content of plasticizer in the masonry cement is estimated to be consistent with a Type M product. That said, masonry cements are specified by their properties when tested in preproduction rather than by their proportions. As such, any proportional estimates made do not necessarily determine a mortar type.

Sample ID	BM02
Component	
Portland cement (wgt. %)	18
Masonry cement (wgt. %)	24
Sand (wgt. %)	76
Cement content in masonry cement (wgt. %)	74
Binder : sand ratio (by volume)	1 : 3.2

References

Eckel, Edwin C. *Cements, Limes, and Plasters. Their Materials, Manufacture, and Properties.* New York: Robert Drummond, 1905.

9. Petrographic Data

Table 9.1: Petrographic Data - Sample BM01

Sample ID	BM01
As-received description	
Description	The sample consists of 56 grams of mortar debris and contaminants such as stone flakes and beetle parts. There is also some damp moss left behind in the sample bag. The sample was separated into three parts: Retained on the No. 8 sieve (9 grams), retained between the No. 8 and No. 16 sieves (19 grams), passing the No. 16 sieve (11 grams).
Retained on No. 8 sieve	This fraction includes large flakes of dark gray stone and rounded pebbles of white stone. The mortar is brownish, clumpy, and perhaps sandy. It is mostly dusty, and the features of the mortar are difficult to view. There is no obviously dense mortar. Insect fragments are common along with one or two whole ladybugs.
Retained between No. 8 and No. 16 sieves	This fraction consists of dusty brown grains that are mostly friable (Munsell code approximately 10YR 5/2). This material is probably mostly mortar and sand, though some stone chips and bugs are also included.
Passing No. 16 sieve	This fraction consists of material that is similar to but finer than that retained between the No. 8 and No. 16 sieves.
Sand	
Lithology	The aggregate is a natural sand consisting of a mixture of fine-grained metaquartzite and granite. Much of it is nearly pure quartz though there are also micaceous grains and a minor assembly of metamorphic accessory minerals. Trace carbonate rock particles are also detected.
Appearance	The sand has a moderately variegated appearance. It mostly consists of semi-translucent particles with a light brownish gray color overall (Munsell code approximately 2.5Y 7.5/1). The moderate visual variegation is due to a mixture of opaque particles in the fraction coarser than the No. 16 mesh. These include a mixture of dark gray, white, and tan particles.
Gradation	The recovered sand is medium-grained and broadly graded. The nominal top size is at the No. 4 sieve though most particles pass this mesh. The peak abundance is around the No. 30 sieve, and the fines content is relatively low.
Shape/aspect ratio	Particles are mostly equidimensional with fewer subequant grains. Particle shapes are subangular on average.
Clay coatings/friable materials	No significant clay linings or undispersed clay lumps are detected.
Binder matrix	
Paste uniformity	The cured paste has a heterogeneous microtexture due to secondary reactions in the mortar.
Capillary porosity	The capillary porosity is mostly high though there are some areas of the more intact examined pieces where the binder matrix has a relatively low capillary microporosity.
Microscopic shrinkage cracking	None detected
Residual calcium hydroxide	Calcium hydroxide from the initial hydration of the cement has been fully depleted from the binder matrix.
Evidence for admixtures¹	None

Table 9.1 (cont'd.): Petrographic Data - Sample BM01

Sample ID	BM01 (cont'd.)
Binder residuals	
Binder type	Domestic natural cement
Hydraulic cement	Residual natural cement particles are identified in moderate abundance throughout the paste matrix. Most grains are finer than approximately 0.25 millimeters. These exhibit complex microtextures consistent with the low-temperature firing of an argillaceous dolomitic limestone with a low abundance of quartz silt. There is a moderately low proportion of finer "grit" distributed throughout the paste, including partly fused quartz silt and other refractory elements that did not fully combine during firing.
Lime	None detected
Pozzolans/SCMs²	None detected
Other	There are traces of cinder that likely represent fuel used in the production of the natural cement binder.
Pigment	
Details	There are rare pieces of the debris that contain some ultrafine black particulates. These could represent a carbon black pigment similar to that observed in Sample NE04. However, the evidence is scarce and there is no consistent pigmentation observed throughout the examined debris.
Other materials	
Details	The sample consists entirely of debris. Although most is mortar, there are also some contaminants from the masonry units and from organic materials including plant matter and insect fragments.
Placement features	
Constituent distribution	There are no intact mortar pieces to evaluate. However, the material within the small pieces of debris does not appear to contain any sand streaks or coarse binder inclusions.
Mix water	There is no evidence for inappropriate retempering.
Compaction/consolidation	The compaction and consolidation of the mortar cannot be evaluated since only fine mortar debris is included in the sample.
Estimated air content/structure	The air content of the mortar cannot be evaluated since only fine mortar debris is included in the sample.
Paste-sand interfaces	Sand grains appear to be well-coated with binder
Other	None
Secondary effects	
Carbonation	The paste is uncarbonated throughout all of the mortar debris.
Paste alteration	The paste is decalcified and areas of the mortar have a heightened microporosity.
Cracking	There are splays sharp, randomly-oriented microscopic cracks observed within the mortar debris.
Mineral deposits	The fine cracks described above are often filled with secondary calcite. There are also deposits of more coarsely crystalline carbonate on the surfaces of the mortar debris.
Surface erosion/weathering	No joint face was included in the provided sample.

Notes:

1. Organic admixtures or soluble inorganic additives cannot be detected petrographically, though their effects on paste microstructure can sometimes be discerned.
2. SCMs = supplementary cementitious materials.

Table 9.2: Petrographic Data - Sample NE04

Sample ID	NE04
As-received description	
Description	The sample consists of multiple surface mortar fragments with a moderate abundance of granules and powder weighing a total of 34 grams. The mortar is compact with a texture dominated by No. 8 sized white and pale orange coarse sand grains.
Surfaces	Joint faces are ruggedly planar with low to moderate relief, coarse sand exposure. The weathered face is generally pale brown. Other surfaces are compact and dusty. Some of the rear surfaces are clumpy.
Appearance	Fresh surfaces have a subvitreous to moderately dull luster. The paste is an intermixed mass of cocoa brown and dark greenish-gray. The latter dominates with an overall color having a Munsell code of approximately 5Y 4/1.5.
Hardness/friability	The paste is hard, and the mortar is indurate.
Absorptivity	The mortar matrix is slowly water-absorptive.
Other details	One of the sample pieces has some randomly distributed microcracks that transect the joint face. No other cracks or any binder grains or mineral deposits are visible in hand sample.
Sand	
Lithology	The aggregate is a natural sand derived primarily from a fine-grained metaquartzite rock and lesser granite. It consists mostly of quartz with lesser feldspar. Minor constituents include mica and an assembly of metamorphic accessory minerals. Trace carbonate rock particles are also detected.
Appearance	The sand is mildly variegated and mostly semi-translucent with a light brownish gray color (Munsell code approximately 2.5Y 7/0.5). Some minor visual variegation is produced by opaque particles mostly coarser than the No. 16 sieve. These grains are often white or light gray, though fewer are dark gray or rust-colored.
Gradation	The recovered sand is medium-grained and broadly graded. The nominal top size is at the No. 4 mesh with all particles passing, and the peak abundance between the No. 30 and No. 50 sieves. The fines content is moderate.
Shape/aspect ratio	Particles are mostly equidimensional with fewer subequant grains. Particle shapes are subangular to angular.
Clay coatings/friable materials	No significant clay linings or undispersed clay lumps are detected.
Binder matrix	
Paste uniformity	The cured paste is mostly uniform.
Capillary porosity	The capillary porosity is moderately low.
Microscopic shrinkage cracking	None detected
Residual calcium hydroxide	Fully consumed in carbonation reactions.
Evidence for admixtures¹	None

Table 9.2 (cont'd.): Petrographic Data - Sample NE04

Sample ID	NE04 (cont'd.)
Binder residuals	
Binder type	Domestic natural cement
Hydraulic cement	Residual natural cement particles are identified in high abundance throughout the paste matrix. Most grains are finer than approximately 0.5 millimeters, and many are finer than 0.25 millimeters. These exhibit complex microtextures consistent with the low-temperature firing of an argillaceous dolomitic limestone with a low abundance of quartz silt. There is also a relatively high proportion of finer "grit" distributed throughout the paste, including partly fused quartz silt and other refractory elements that did not fully combine during firing.
Lime	None detected
Pozzolans/SCMs²	None detected
Other	There are traces of cinder that likely represent fuel used in the production of the natural cement binder.
Pigment	
Concentration	Pigment particles are detected in mostly low density throughout the binder matrix. However, there are submillimeter areas and streaks within the binder paste where the pigment is much more heavily concentrated.
Composition	The pigment is likely carbon-based, but this is not confirmed petrographically.
Particle size	The pigment is very finely ground. Particles are ultrafine-grained and barely resolved at the scale of the light microscope.
Color of extracted pigment	A sample of the fines extracted through chemical digestion has a dark gray color (Munsell color code approximately 2.5Y4.25/1). However, the original pigment was likely a black color and the dark gray color is a result of the pigment intermixed with light brown residues from the natural cement binder.
Other materials	
Details	None detected
Placement features	
Constituent distribution	The constituents are well-mixed with no sand streaks or coarse binder inclusions.
Mix water	There is no evidence for inappropriate retempering.
Compaction/consolidation	The mortar is compact and well-consolidated.
Estimated air content/structure	The total air content is estimated at approximately 3-5% by volume. Voids are mostly rounded to subrounded in shape and are typically no more than 0.5 millimeters in diameter.
Paste-sand interfaces	Sand grains are well-coated with binder
Other	Splays of locally subparallel planar partings disrupt the binder paste in half of the mortar pieces observed petrographically. These partings represent ice crystal impressions that formed while the cement paste was unhardened.
Secondary effects	
Carbonation	The paste is fully carbonated throughout the sample pieces examined.
Paste alteration	None observed
Cracking	One of the examined pieces has a low abundance of sharp, randomly-oriented microscopic cracks.
Mineral deposits	There are traces of secondary carbonate lining air-voids and partings in the cement paste.
Surface erosion/weathering	There is no degradation of the paste at the joint face. However, the surfaces are covered with a microscopically-thin veneer of secondary mineralizations including calcite, gypsum, and some isotropic salts.

Notes:

- Organic admixtures or soluble inorganic additives cannot be detected petrographically, though their effects on paste microstructure can sometimes be discerned.
- SCMs = supplementary cementitious materials.

Table 9.3: Petrographic Data - Sample NE18

Sample ID	NE18
As-received description	
Description	The sample consists of several irregular mortar fragments and abundant fine powder weighing a total of 85 grams.
Surfaces	There are no obvious tooled faces or bed contacts.
Appearance	Fresh surfaces have a dull luster, and the color is varying shades of brown that is sometimes streaky (Munsell code ~10YR 5.75/2.75 though some areas are as dark as 10YR 4.25/2.5).
Hardness/friability	The paste ranges from having a moderate hardness to being moderately soft. The mortar is cohesive and nonfriable.
Absorptivity	The mortar matrix is rapidly water-absorptive.
Other details	There are some pieces with white sand exposure that may represent crack faces. Otherwise, there are no obvious cracks. No binder grains or mineralizations are visible in hand sample.
Sand	
Lithology	The aggregate is a natural sand derived primarily from a fine-grained metaquartzite rock and lesser granite. It consists mostly of quartz with lesser feldspar. Minor constituents include mica and an assembly of metamorphic accessory minerals. Trace ironstone and carbonate rock particles are also detected.
Appearance	The sand is mildly variegated and mostly semi-translucent with a light brownish gray color (Munsell code approximately 2.5Y 7.5/1). Some minor visual variegation is produced by opaque particles mostly coarser than the No. 16 sieve. These grains are often white or light gray, though fewer are dark gray, greenish-gray, or rust-colored.
Gradation	The recovered sand is medium-grained and broadly graded. The nominal top size is at the No. 4 mesh with all particles passing, and the peak abundance between the No. 30 and No. 50 sieves. The fines content is relatively low.
Shape/aspect ratio	Particles are mostly equidimensional with fewer subequant grains. Particle shapes are subangular on average.
Clay coatings/friable materials	No significant clay linings or undispersed clay lumps are detected.
Binder matrix	
Paste uniformity	The cured paste is uniform.
Capillary porosity	The capillary porosity is moderately low.
Microscopic shrinkage cracking	None detected
Residual calcium hydroxide	Fully consumed in carbonation reactions.
Evidence for admixtures¹	None

Table 9.3 (cont'd.): Petrographic Data - Sample NE18

Sample ID	NE18 (cont'd.)
Binder residuals	
Binder type	Domestic natural cement
Hydraulic cement	Residual natural cement particles are identified in moderately high abundance throughout the paste matrix. Most grains are finer than approximately 0.5 millimeters, and many are finer than 0.25 millimeters. These exhibit complex microtextures consistent with the low-temperature firing of an argillaceous dolomitic limestone with a low abundance of quartz silt. There is a moderately low proportion of finer "grit" distributed throughout the paste, including partly fused quartz silt and other refractory elements that did not fully combine during firing.
Lime	None detected
Pozzolans/SCMs²	None detected
Other	There are traces of glassy clinker particles, all with diameters finer than 0.5 millimeters. These could represent clinkered material from the cement manufacturing process. There are also traces of cinder that likely represent fuel used in the production of the natural cement binder. Finally, there are traces of cellular plant fiber within the binder matrix. This likely represents a minor contaminant from when the mortar was freshly mixed.
Pigment	
Concentration	None detected
Composition	n/a
Particle size	n/a
Color of extracted pigment	n/a
Other materials	
Details	None detected
Placement features	
Constituent distribution	The constituents are well-mixed with no sand streaks or coarse binder inclusions.
Mix water	There is no evidence for inappropriate retempering.
Compaction/consolidation	The mortar is compact and well-consolidated.
Estimated air content/structure	The total air content is estimated at approximately 2-4% by volume. Voids are mostly rounded to amoeboid in shape and are typically no more than one millimeter in diameter.
Paste-sand interfaces	Sand grains are well-coated with binder
Other	None
Secondary effects	
Carbonation	The paste is fully carbonated throughout the sample pieces examined.
Paste alteration	None observed
Cracking	There is a moderately low abundance of sharp, randomly-oriented microscopic cracks distributed throughout the examined pieces.
Mineral deposits	There is a high abundance of secondary mineralizations that are isotropic and could potentially represent chloride salts. These are observed lining some of the pieces and also within some of the adjacent cracks described above.
Surface erosion/weathering	No joint face was included in the provided sample.

Notes:

1. Organic admixtures or soluble inorganic additives cannot be detected petrographically, though their effects on paste microstructure can sometimes be discerned.
2. SCMs = supplementary cementitious materials.

Table 9.4: Petrographic Data - Sample NW26

Sample ID	NW26
As-received description	
Description	The sample consists of several mortar fragments weighing a total of 80 grams. Some of the pieces are irregular and elongate as if these represent joint mortar.
Surfaces	There are no obvious tooled surfaces or bed contacts included in the sample.
Appearance	Fresh surfaces have a dull luster and a brown color (Munsell code ~10YR 6/2). Coarse white sand is part of the aesthetic though the sand is sparse.
Hardness/friability	The paste has moderate hardness. The mortar is cohesive and indurate.
Absorptivity	The mortar matrix is rapidly water-absorptive.
Other details	No cracks, binder inclusions, or mineralizations are visible in hand sample. Trace black coal cinder is observed in fresh surfaces.
Sand	
Lithology	The aggregate is a natural sand derived primarily from a fine-grained metaquartzite rock and lesser granite. It consists mostly of quartz with lesser feldspar. Minor constituents include mica and an assembly of metamorphic accessory minerals. Carbonate rock particles and chert are also present in minor to trace abundance.
Appearance	The sand has a moderately variegated appearance. It mostly consists of semi-translucent to semi-opaque particles with a light brownish gray color overall (Munsell code approximately 2.5Y 7/1). The moderate visual variegation is due to a mixture of opaque particles in the fraction coarser than the No. 16 mesh. These include a mixture of light gray, white, dark gray, tan, and fewer reddish-brown and greenish-gray particles.
Gradation	The recovered sand is medium-grained and broadly graded. The nominal top size is at the No. 4 sieve though most particles pass this mesh. The peak abundance is around the No. 30 sieve, and the fines content is relatively low.
Shape/aspect ratio	Particles are mostly equidimensional with fewer subequant grains. Particle shapes are subangular on average.
Clay coatings/friable materials	No significant clay linings or undispersed clay lumps are detected.
Binder matrix	
Paste uniformity	The cured paste is mostly uniform.
Capillary porosity	The capillary porosity is moderately low.
Microscopic shrinkage cracking	None detected
Residual calcium hydroxide	Fully consumed in carbonation reactions.
Evidence for admixtures¹	None

Table 9.4 (cont'd.): Petrographic Data - Sample NW26

Sample ID	NW26 (cont'd.)
Binder residuals	
Binder type	Domestic natural cement
Hydraulic cement	Residual natural cement particles are identified in high abundance throughout the paste matrix. Most grains are finer than approximately 0.5 millimeters, and many are finer than 0.25 millimeters. These exhibit complex microtextures consistent with the low-temperature firing of an argillaceous dolomitic limestone with a low abundance of quartz silt. There is also a relatively high proportion of finer "grit" distributed throughout the paste, including partly fused quartz silt and other refractory elements that did not fully combine during firing.
Lime	None detected
Pozzolans/SCMs²	None detected
Other	There are traces of cinder that likely represent fuel used in the production of the natural cement binder.
Pigment	
Concentration	None detected
Composition	n/a
Particle size	n/a
Color of extracted pigment	n/a
Other materials	
Details	None detected
Placement features	
Constituent distribution	The constituents are well-mixed with no sand streaks or coarse binder inclusions.
Mix water	There is no evidence for inappropriate retempering.
Compaction/consolidation	The mortar is compact and well-consolidated.
Estimated air content/structure	The total air content is estimated at approximately 2-3% by volume. Voids are mostly subrounded to amoeboid in shape and are typically no more than 0.5 millimeters in diameter.
Paste-sand interfaces	Sand grains are well-coated with binder
Other	There are trace discontinuous partings that typically occur at the boundary between the sand and the paste. These are soft-textured and appear to represent plastic cracks that occurred prior to the hardening of the mortar.
Secondary effects	
Carbonation	The paste is fully carbonated throughout the sample pieces examined.
Paste alteration	None observed
Cracking	There is a low abundance of discontinuous, randomly-oriented microscopic cracks distributed throughout the examined pieces.
Mineral deposits	Secondary carbonate deposits are often observed filling the cracks described above.
Surface erosion/weathering	No joint face was included in the provided sample.

Notes:

- Organic admixtures or soluble inorganic additives cannot be detected petrographically, though their effects on paste microstructure can sometimes be discerned.
- SCMs = supplementary cementitious materials.

Table 9.5: Petrographic Data - Sample SW02

Sample ID	SW02
As-received description	
Description	The sample consists mostly of pointing mortar pieces weighing a total of 421 grams. The joints are wide, and there are instances of coarse limestone aggregate and aggregate sockets at the rear of the pieces.
Surfaces	The joint face is wavy planar and very lightly soiled with low relief, coarse sand exposure of white to pale orange sand grains. The rear surfaces are compact.
Appearance	Fresh surfaces have a dull waxy luster and a variably orangish-brown color (Munsell code ~10YR 6/2 to 10YR 5/3).
Hardness/friability	The paste has moderate hardness, and the mortar is indurate.
Absorptivity	The mortar matrix is rapidly water-absorptive.
Other details	No cracks, binder grains, or mineral deposits are visible in hand sample.
Sand	
Lithology	The aggregate is a natural sand derived primarily from a fine-grained metaquartzite rock and lesser granite. It consists mostly of quartz with lesser feldspar. Minor constituents include mica and an assembly of metamorphic accessory minerals. Trace ironstone and carbonate rock particles are also detected.
Appearance	The sand has a moderately variegated appearance. It mostly consists of semi-translucent to semi-opaque particles with a light brownish gray color overall (Munsell code approximately 2.5Y 7/1). The moderate visual variegation is due to a mixture of opaque particles in the fraction coarser than the No. 16 mesh. These include a mixture of light gray, white, dark gray, tan, and fewer reddish-brown and greenish-gray particles.
Gradation	The recovered sand is medium-grained and broadly graded. The nominal top size is at the No. 4 mesh, and the peak abundance between the No. 30 and No. 50 sieves. The fines content is relatively low.
Shape/aspect ratio	Particles are mostly equidimensional with fewer subequant grains. Particle shapes are subangular to angular.
Clay coatings/friable materials	No significant clay linings or undispersed clay lumps are detected.
Binder matrix	
Paste uniformity	The cured paste is uniform.
Capillary porosity	The capillary porosity is moderately low.
Microscopic shrinkage cracking	None detected
Residual calcium hydroxide	Fully consumed in carbonation reactions.
Evidence for admixtures¹	None

Table 9.5 (cont'd.): Petrographic Data - Sample SW02

Sample ID	SW02 (cont'd.)
Binder residuals	
Binder type	Domestic natural cement
Hydraulic cement	Residual natural cement particles are identified in high abundance throughout the paste matrix. Most grains are finer than approximately 0.5 millimeters, and many are finer than 0.25 millimeters. These exhibit complex microtextures consistent with the low-temperature firing of an argillaceous dolomitic limestone with a low abundance of quartz silt. There is also a relatively high proportion of finer "grit" distributed throughout the paste, including partly fused quartz silt and other refractory elements that did not fully combine during firing.
Lime	None detected
Pozzolans/SCMs²	None detected
Other	There are traces of cinder that likely represent fuel used in the production of the natural cement binder. There are also traces of cellular plant fiber within the binder matrix. This likely represents a minor contaminant from when the mortar was freshly mixed.
Pigment	
Concentration	None detected
Composition	n/a
Particle size	n/a
Color of extracted pigment	n/a
Other materials	
Details	None detected
Placement features	
Constituent distribution	The constituents are well-mixed with no sand streaks or coarse binder inclusions.
Mix water	There is no evidence for inappropriate retempering.
Compaction/consolidation	The mortar is compact and well-consolidated.
Estimated air content/structure	The total air content is estimated at approximately 3-5% by volume. Voids are mostly subrounded with fewer amoeboid in shape and are typically no more than 0.5 millimeters in diameter.
Paste-sand interfaces	Sand grains are well-coated with binder
Other	None
Secondary effects	
Carbonation	The paste is mostly carbonated throughout the sample pieces examined.
Paste alteration	None observed
Cracking	There is a low abundance of sharp, randomly-oriented microscopic cracks distributed throughout the examined pieces. These often coincide with paste-aggregate boundaries adjacent to the red bed sedimentary sand grains.
Mineral deposits	There are traces of some undifferentiated mineralizations lining the cracks described above.
Surface erosion/weathering	No joint face was included in the prepared thin section.

Notes:

1. Organic admixtures or soluble inorganic additives cannot be detected petrographically, though their effects on paste microstructure can sometimes be discerned.
2. SCMs = supplementary cementitious materials.

Table 9.6: Petrographic Data - Sample SW16

Sample ID	SW16
As-received description	
Description	The sample consists of multiple small, irregular, shard-like mortar fragments weighing a total of 67 grams.
Surfaces	There are no obvious joint faces or bed surfaces.
Appearance	Fresh surfaces have a dull luster and a light brown color (Munsell code ~10YR 6.75/2).
Hardness/friability	The paste has a moderate hardness, and the mortar is cohesive.
Absorptivity	The mortar matrix is rapidly water-absorptive.
Other details	No cracks, binder grains, or mineralizations are visible in hand sample.
Sand	
Lithology	The aggregate is a natural sand derived primarily from a fine-grained metaquartzite rock and lesser granite. It consists mostly of quartz with lesser feldspar. Minor constituents include mica and an assembly of metamorphic accessory minerals. Trace ironstone, carbonate rock particles, and chalcedony are also detected. Within the metaquartzite rock, there are rare corroded particles from which the quartz and feldspar appears to be mostly absent and only traces of cellular organic material remain.
Appearance	The sand has a moderately variegated appearance. It mostly consists of semi-translucent to semi-opaque particles with a light brownish gray color overall (Munsell code approximately 2.5Y 7/1). The moderate visual variegation is due to a mixture of opaque particles in the fraction coarser than the No. 16 mesh. These include a mixture of mostly white and fewer light gray, rust-colored, purplish particles.
Gradation	The recovered sand is medium-grained and broadly graded. The nominal top size is at the No. 4 mesh, and the peak abundance between the No. 30 and No. 50 sieves. The fines content appears to have been at least moderate though it is hard to distinguish the fine sand particles from the quartz silt in the natural cement.
Shape/aspect ratio	Particles are mostly equidimensional with fewer subequant grains. Particle shapes are subangular to angular.
Clay coatings/friable materials	No significant clay linings or undispersed clay lumps are detected.
Binder matrix	
Paste uniformity	The cured paste is mostly uniform.
Capillary porosity	The capillary porosity is moderate.
Microscopic shrinkage cracking	None detected
Residual calcium hydroxide	Fully consumed in carbonation reactions.
Evidence for admixtures¹	None

Table 9.6 (cont'd.): Petrographic Data - Sample SW16

Sample ID	SW16 (cont'd.)
Binder residuals	
Binder type	Domestic natural cement
Hydraulic cement	Residual natural cement particles are identified in high abundance throughout the paste matrix. Most grains are finer than approximately 0.5 millimeters, and many are finer than 0.25 millimeters. These exhibit complex microtextures consistent with the low-temperature firing of an argillaceous dolomitic limestone with a low abundance of quartz silt. There is also a relatively high proportion of finer "grit" distributed throughout the paste, including partly fused quartz silt and other refractory elements that did not fully combine during firing.
Lime	None detected
Pozzolans/SCMs²	None detected
Other	There are traces of cinder that likely represent fuel used in the production of the natural cement binder.
Pigment	
Concentration	None detected
Composition	n/a
Particle size	n/a
Color of extracted pigment	n/a
Other materials	
Details	None detected
Placement features	
Constituent distribution	The constituents are well-mixed despite the relatively dense distribution of the sand grains. There are no sand streaks or coarse binder inclusions.
Mix water	There is no evidence for inappropriate retempering.
Compaction/consolidation	The mortar is compact and well-consolidated.
Estimated air content/structure	The total air content is estimated at approximately 4-6% by volume. Voids are mostly rounded in shape and are typically no more than 0.5 millimeters in diameter.
Paste-sand interfaces	Sand grains are well-coated with binder
Other	None
Secondary effects	
Carbonation	The paste is mostly carbonated throughout the sample pieces examined.
Paste alteration	None observed
Cracking	There is a trace abundance of sharp, randomly-oriented microscopic cracks distributed throughout the examined pieces. These often coincide with paste-aggregate boundaries adjacent to the red bed sedimentary sand grains.
Mineral deposits	None significant
Surface erosion/weathering	No joint face was included in the provided sample.

Notes:

- Organic admixtures or soluble inorganic additives cannot be detected petrographically, though their effects on paste microstructure can sometimes be discerned.
- SCMs = supplementary cementitious materials.

Table 9.7: Petrographic Data - BM05

Sample ID	BM05
As-received description	
Description	The sample consists of several small surface mortar fragments weighing a total of 23 grams.
Surfaces	Tooled faces are planar to slightly convex. The tooling is mostly cream with a vitreous luster, though it is dotted with fine rust spots less than one millimeter in diameter. The other faces are compact and fresh.
Appearance	Fresh surfaces have a moderately subvitreous luster and a light brownish gray color (Munsell code ~2.5Y 6.75/1).
Hardness/friability	The paste is hard, and the mortar is indurate.
Absorptivity	The mortar matrix is somewhat rapidly water-absorptive.
Other details	No cracks, binder grains, or mineral deposits are visible in hand sample.
Sand	
Lithology	The aggregate is a natural sand consisting primarily of quartz and metaquartzite rock grains. Lesser constituents include marble, feldspar, and phyllite.
Secondary Additive	There is a lesser to minor component of iron-based metallic particles from which iron oxide has leached into the surrounding binder paste.
Appearance	The sand extracted through acid digestion is mildly variegated and semi-translucent to semi-opaque with a light brownish gray color (Munsell code approximately 2.5Y 6.5/1). Some minor visual variegation is due to more opaque particles, mostly coarse than the No. 16 mesh, that have dark gray, light gray, tan, white, and reddish-brown colors.
Gradation	The recovered sand is medium-grained and broadly graded. The nominal top size is found at the No. 8 mesh with all grains passing, and the peak abundance is retained between the No. 30 and No. 50 sieves. The fines content is moderate.
Shape/aspect ratio	Particles are mostly equidimensional with fewer subequant grains. Particle shapes are subangular on average, though individual particle shapes range from subrounded to angular.
Clay coatings/friable materials	No significant clay linings or undispersed clay lumps are detected.
Binder matrix	
Paste uniformity	The cured paste is uniform.
Capillary porosity	The capillary porosity of the binder matrix is moderately high.
Microscopic shrinkage cracking	A low abundance of discontinuous shrinkage cracks are observed.
Residual calcium hydroxide	None observed
Evidence for admixtures¹	None
Binder residuals	
Binder type	Gray portland cement and dry hydrated lime
Hydraulic cement	The cement hydration is advanced and virtually all hydraulic calcium silicate is consumed in hydration reactions. Nevertheless, residual portland cement grains are observed in moderately high concentration, mostly as agglomerates of former belite and lesser alite with a residual skeleton of interstitial iron-bearing ferrite. The belite within the agglomerates is consistently fine-grained. Many of the agglomerates would have been retained on a No. 200 sieve with some approaching the No. 100 mesh.
Lime	Undispersed lime grains are present in moderate abundance as internally nondescript particulates that are mostly finer than 150 µm in diameter. Virtually all of the lime grains are fully carbonated.
Pozzolans/SCMs²	None detected
Other	None detected

Table 9.7 (cont'd.): Petrographic Data - BM05

Sample ID	BM05 (cont'd.)
Pigment	
Concentration	None detected
Composition	n/a
Particle size	n/a
Color of extracted pigment	n/a
Other materials	
Details	None detected
Placement features	
Constituent distribution	The constituents are well-mixed with no sand streaks or coarse binder inclusions.
Mix water	There is no evidence for inappropriate retempering.
Compaction/consolidation	The mortar is compact and well-consolidated.
Estimated air content/structure	In some pieces, the voids are mostly rounded to subrounded and estimated to represent approximately 7% to 9% by volume of the hardened mortar.
Paste-sand interfaces	Sand grains are well-coated with binder.
Other	None
Secondary effects	
Carbonation	The binder paste is fully carbonated in the examined mortar pieces.
Paste alteration	None observed
Cracking	None detected
Mineral deposits	None detected
Surface erosion/weathering	None detected. There is no evidence of any weathering at the surface, and all of the sand grains remain coated with binder paste.

Notes:

1. Organic admixtures or soluble inorganic additives cannot be detected petrographically, though their effects on paste microstructure can sometimes be discerned.
2. SCMs = supplementary cementitious materials.

Table 9.8: Petrographic Data - BM02

Sample ID	BM02
As-received description	
Description	The sample consists of multiple small mortar fragments and minor granules and powder weighing a total of 40 grams.
Surfaces	The mortar pieces have mostly fresh surfaces. There are a few slightly yellowed faces with low relief sand exposure. However, there are no obvious tooled faces or bed contacts.
Appearance	Fresh surfaces have a dull luster and a gray color (Munsell code ~N7.5).
Hardness/friability	The paste is soft, though the mortar is relatively indurate.
Absorptivity	The mortar matrix is rapidly water-absorptive.
Other details	No cracks, binder inclusions, or mineral deposits are visible in hand sample.
Sand	
Lithology	The aggregate consists mostly of argillaceous, fine-grained sedimentary rocks including argillites and siltstones. Quartz and feldspar are lesser constituents. Minor carbonate rock particles, opaque minerals, and accessory mineral grains are also detected.
Appearance	The sand extracted through acid digestion is mostly uniform and opaque with a gray color (Munsell color code approximately 2.5Y 5/0.5).
Gradation	The recovered sand is relatively fine-grained and somewhat narrowly graded with a nominal top size at the No. 8 mesh and roughly 70% of the material retained in the intervals around the No. 50 sieve. The fines content is moderately low.
Shape/aspect ratio	Particles are equant to subequant. Grain shapes are mostly subrounded though fewer particles are subangular in shape.
Clay coatings/friable materials	No significant clay linings or undispersed clay lumps are detected.
Binder matrix	
Paste uniformity	The cured paste is uniform.
Capillary porosity	The capillary porosity of the binder matrix is moderately high.
Microscopic shrinkage cracking	None observed
Residual calcium hydroxide	Fully consumed in carbonation reactions.
Evidence for admixtures¹	The size distribution and abundance of fine spherical voids indicates the use of an air-entraining agent.
Binder residuals	
Binder type	Masonry cement (or mortar cement) consisting of gray portland cement and crushed limestone plasticizer
Hydraulic cement	The cement hydration is extremely advanced and all hydraulic calcium silicate is consumed in hydration reactions. Still, residual portland cement grains are observed distributed throughout the paste in moderate concentration. Most are fine-grained agglomerates of former calcium silicate with a residual skeleton of interstitial iron-bearing ferrite (Hadley grains). In some cases, even the ferrite has been consumed and only "ghosts" of former cement grains are observed. Most of the agglomerates would have passed a No. 200 sieve.
Lime	None detected
Other plasticizer	Fine angular carbonate particulates are present in moderate concentration.
Pozzolans/SCMs²	None detected
Other	None detected

Table 9.8 (cont'd.): Petrographic Data - BM02

Sample ID	BM02 (cont'd.)
Pigment	
Concentration	None detected
Composition	n/a
Particle size	n/a
Color of extracted pigment	n/a
Other materials	
Details	None detected
Placement features	
Constituent distribution	The constituents are well-mixed with no sand streaks or coarse binder inclusions.
Mix water	There is no evidence for inappropriate retempering.
Compaction/consolidation	The mortar is compact and well-consolidated.
Estimated air content/structure	There are entrained air-voids that are typically spherical and less than 0.25 millimeters in diameter. These are estimated to represent approximately 6% to 8% of the hardened mortar by volume. Additionally, there are some subrounded to amoeboid-shaped consolidated voids that are typically finer than one millimeter in diameters. These are estimated to add approximately 4% to 6% to the total air content.
Paste-sand interfaces	Sand grains are well-coated with binder
Other	None
Secondary effects	
Carbonation	The binder paste is fully carbonated in the examined mortar pieces.
Paste alteration	None observed
Cracking	None significant
Mineral deposits	Thin deposits of secondary calcite line the edges and adjacent air-voids within some of the mortar pieces.
Surface erosion/weathering	No joint face was included in the provided sample.

Notes:

1. Organic admixtures or soluble inorganic additives cannot be detected petrographically, though their effects on paste microstructure can sometimes be discerned.
2. SCMs = supplementary cementitious materials.

Appendix I: Photographs and Photomicrographs

Microscopic examination is performed on an Olympus BX-51 polarized/reflected light microscope and an Olympus SZ40 stereoscopic microscope. The polarized light microscope is fitted with a Tucsen MIchrome 5 Pro 5MP digital camera. The stereoscopic microscope is used for simple magnification. Sample types examined under this microscope include fractured surfaces, fine constituents extracted through chemical or physical means, or honed or polished cross sections. The polarized light microscope (PLM) magnifies but also employs principles of optical crystallography. The most common sample preparation for the PLM is the petrographic thin section. For this preparation, cross-sectioned samples are mounted to glass slides and are milled to a thickness sufficient to allow light to be transmitted through the material. These are usually prepared without water and with minimal heat to avoid altering minerals that are water or temperature-sensitive. In many cases, the samples are impregnated with a low-viscosity, blue-dyed epoxy. When so treated, blue areas represent some type of void space (e.g., air-voids, capillary pores, cracks, etc.). The polarized light photomicrographs are taken using a variety of optical settings chosen to best demonstrate the feature(s) of interest. These are distinguished as follows:

Plane polarized light (abbreviated as PPL)

This method uses the refractive power of different constituents to produce an artificial sense of surface relief. Otherwise, the method is the closest to a simple magnification of the material. The setting is often used to demonstrate granular relationships or microstructure. Pore spaces and cracks are observable with this setting if the blue-dyed epoxy is used.

Conoscopic polarized light (abbreviated as CPL)

In this setting, the transmitted light is condensed just before passing through the thin section. The method tends to bring colors or finer particulates into higher contrast at the expense of image sharpness. The setting is often used to image grain boundary failures in dimension stone, pigment particulates in binders, or gel phases in the micropores of cement pastes.

Cross polarized light (abbreviated as XPL)

The setting places the thin section between two pieces of polarizing film oriented at 90° to one another. In isotropic materials (e.g., glasses, simple salts), all light is absorbed and the materials appear black. In anisotropic crystals, two light rays traveling at different speeds are produced within the thin section and these offset waves interfere at the upper polarizing film. The interference produces a color that can be used to calculate properties of the crystal structure and aid in identification of mineral species. In essence, the colors are artificial. It should be noted that color is a function of orientation and color differences do not necessarily indicate material differences.

Compensator plates

When in XPL mode, full-wave or quarter-wave compensator plates may be inserted into the light path to add or subtract interference. Technically, these methods are used to calculate properties of the crystal structure. However, they can also be used to alter the image appearance to help improve contrast between different constituents. They can also reveal preferred orientations in some materials (e.g., oriented residual crystallinity in fired ceramics).

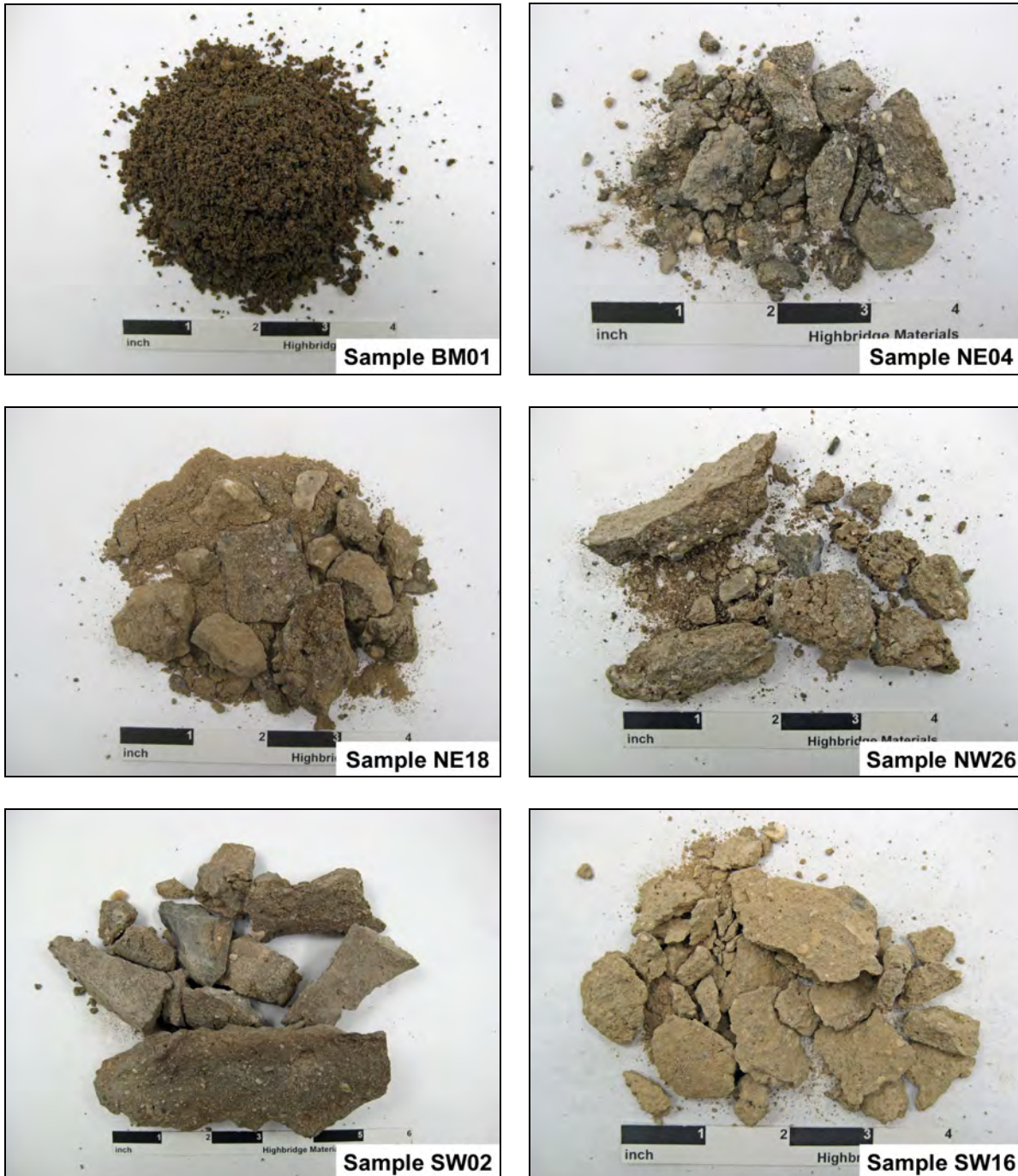


Figure 1: Photographs of the six natural cement mortar samples provided to Highbridge for compositional analysis. Sample BM01 was received as a damp pile of brownish debris. The mortar in Sample NE04 has a mixture of cocoa brown and greenish gray colors due to the uneven incorporation of black pigment. This mortar is relatively hard with a low permeability. The other four mortars all have light to medium brown colors, and their cured products have a moderate hardness and high permeability.

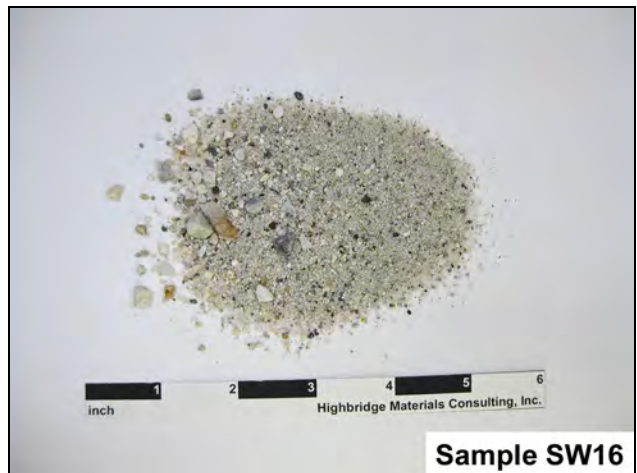
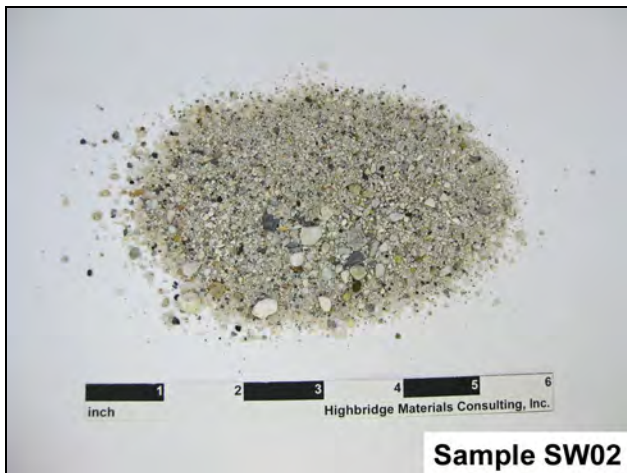
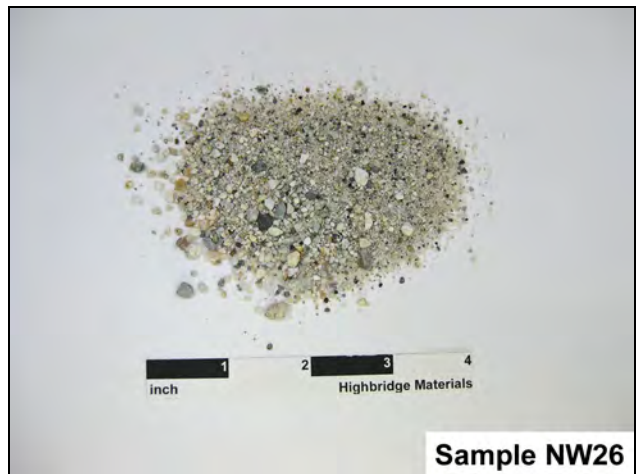
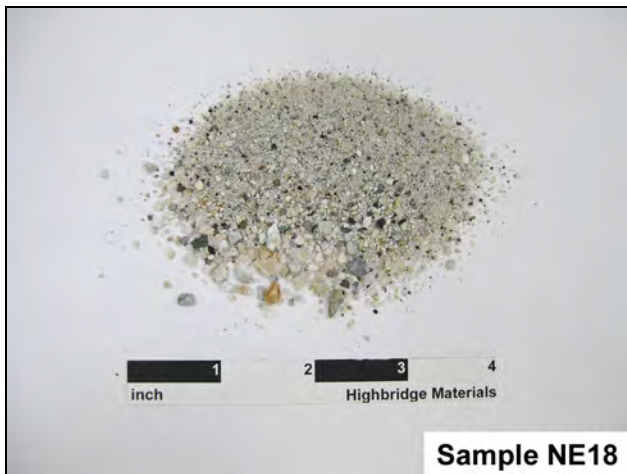
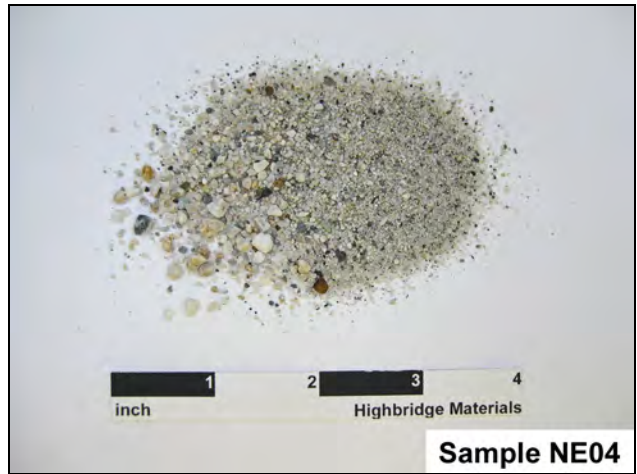
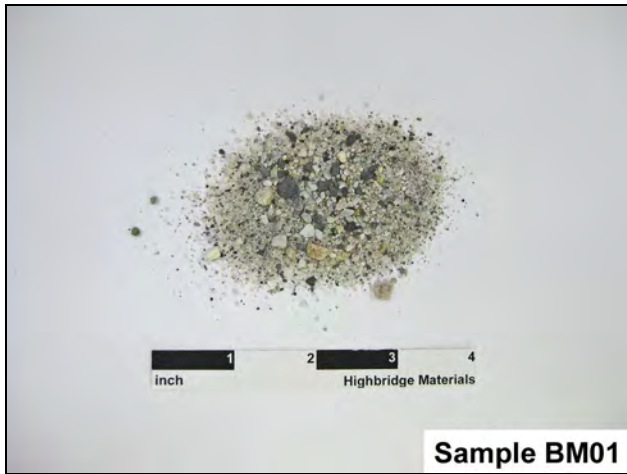


Figure 2: Photographs of the aggregates extracted from the six natural cement mortars through chemical digestion. The total recovery is shown for each.

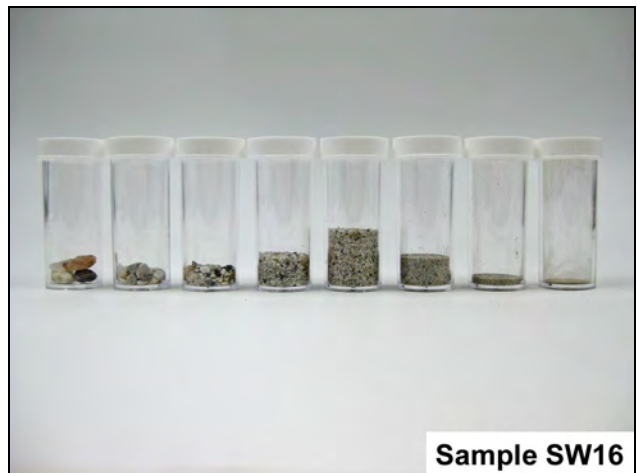
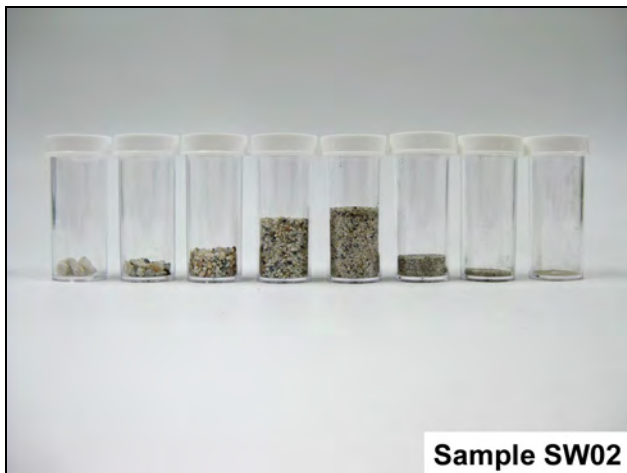
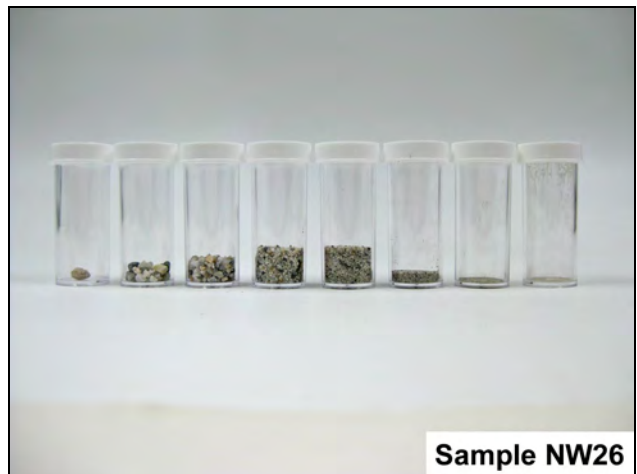
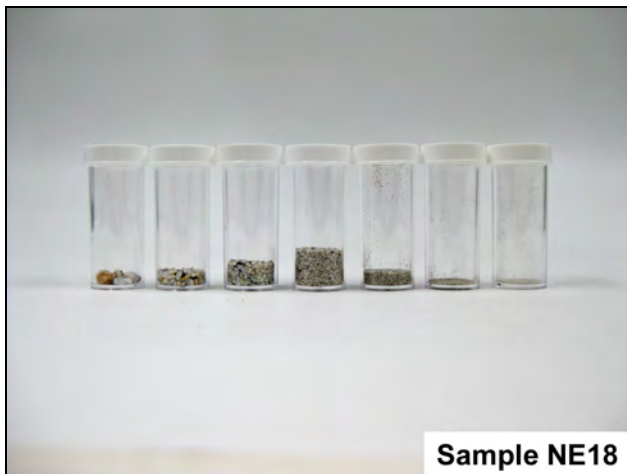
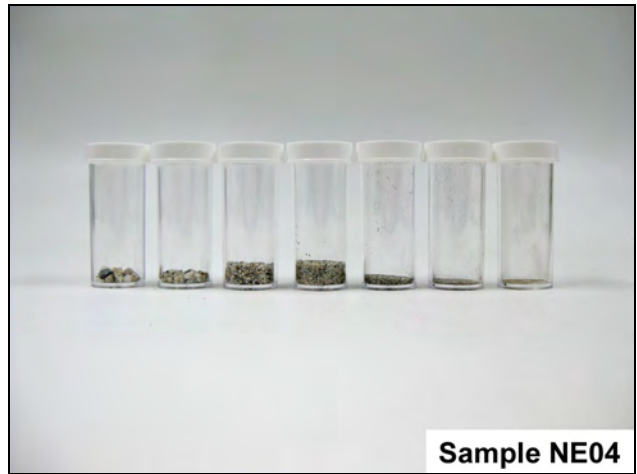
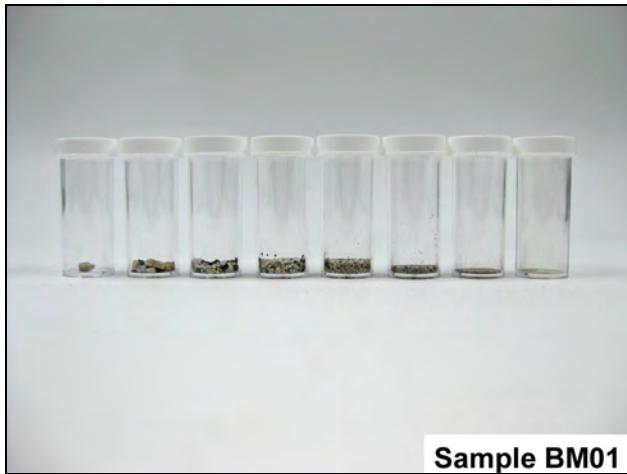


Figure 3: Photographs of the aggregates extracted from the six natural cement mortars through chemical digestion. Each extracted sand is shown after gradation through a standard sieve stack.

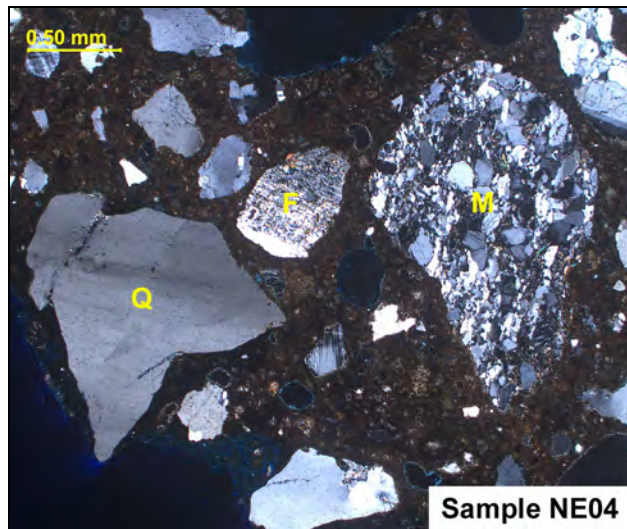


Figure 4: XPL photomicrograph illustrating the lithology of the aggregates used in the six natural cement mortars. The sand in each consists primarily of metaquartzite (M). There is also a lesser granitic component, as demonstrated by the constituent quartz (Q) and feldspar (F) in this image.

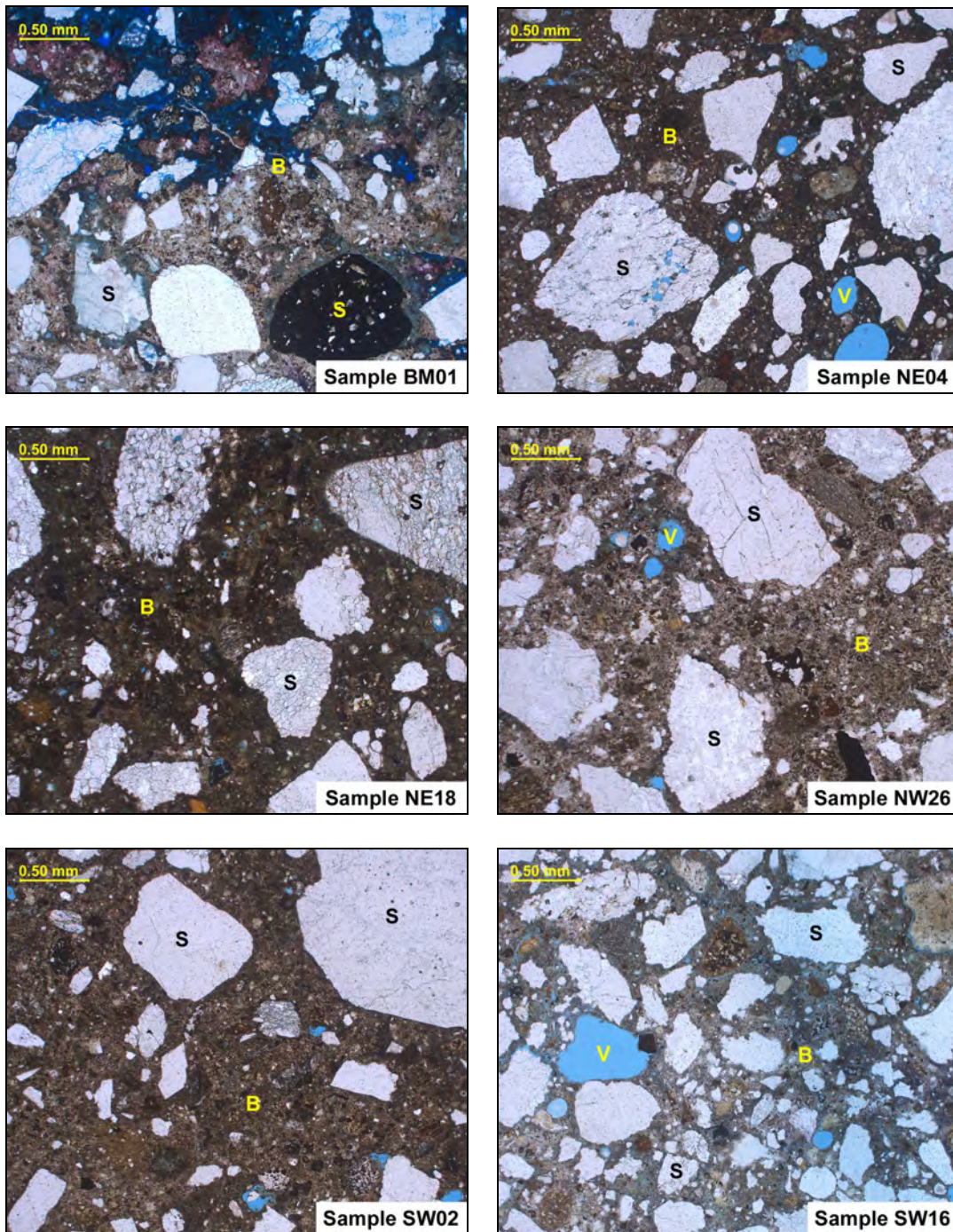


Figure 5: PPL photomicrographs illustrating the microtexture of the natural cement mortar samples. The binder matrix (B) is uniformly developed in each. The capillary porosity of the binder paste is demonstrated by the degree of absorption of the blue-dyed epoxy used in the sample preparation. Sample SW16 has a comparatively higher microporosity, likely due to a higher original mix water content. In Sample BM01, there are areas of heightened microporosity and much of the binder is decalcified. The sand (S) in each is somewhat sharp-textured, medium-grained, and broadly-graded. The sand is somewhat sparsely distributed throughout most of the samples. However, there is a higher sand content in Sample SW16. All of the natural cement mortars appear to have been well-consolidated and air-voids (V) are not excessive.

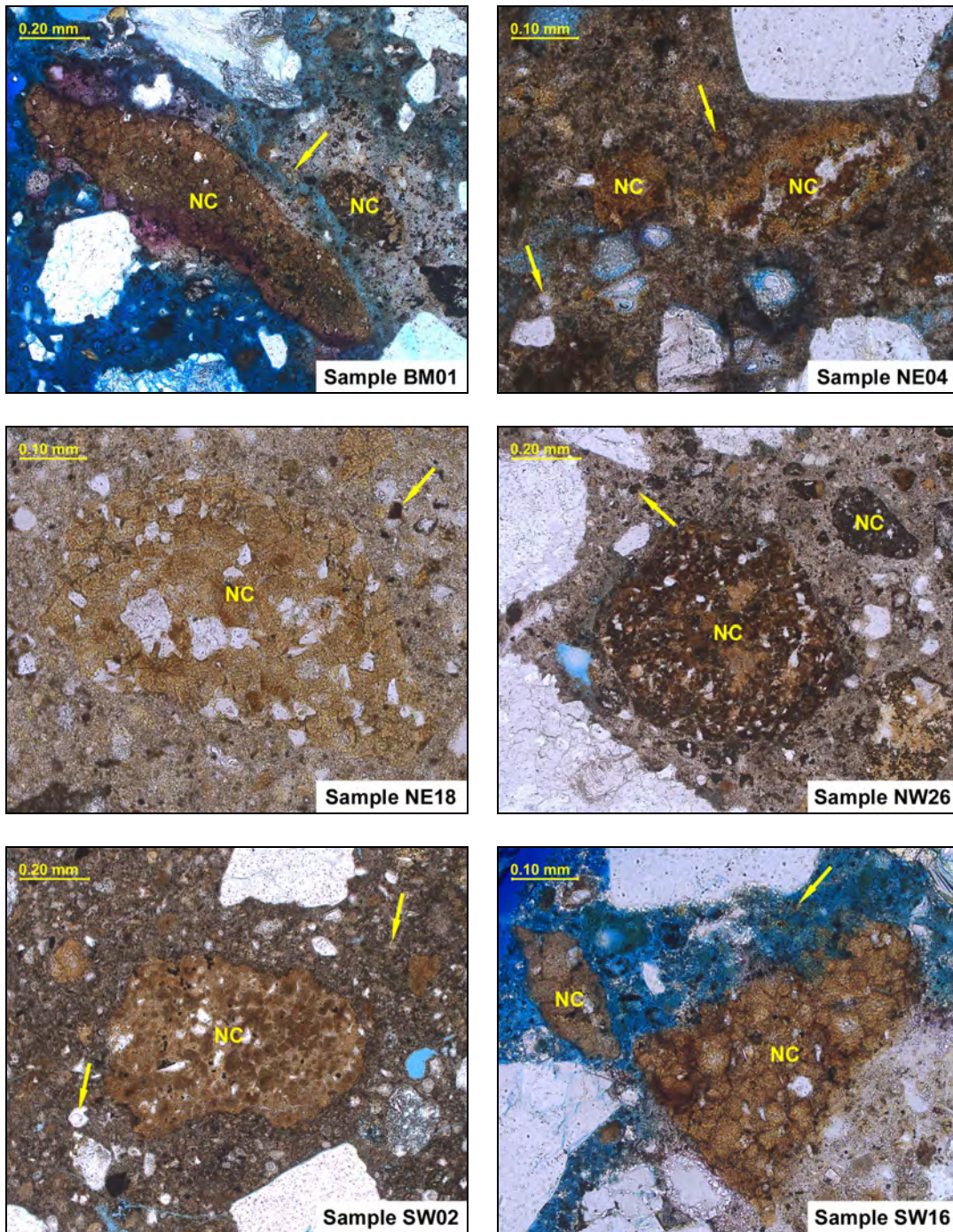


Figure 6: PPL photomicrographs illustrating characteristics of the natural cement binder in six of the mortar samples. Natural cement residuals (NC) are abundant throughout the hydrated paste in each sample. These have microtextural characteristics consistent with cements from Rosendale, New York. There is also a relatively high abundance of inert "grit" from the natural cement that is distributed throughout the binder matrix, as indicated by the arrows.

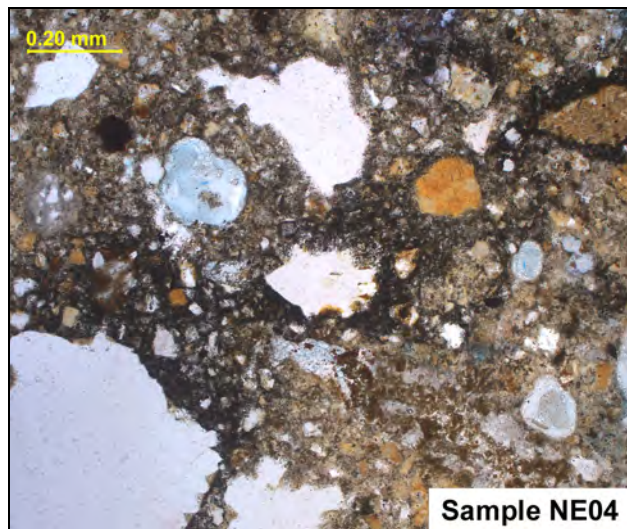
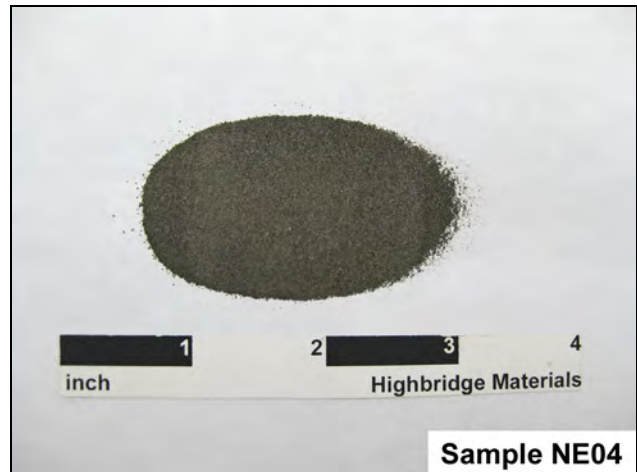


Figure 7: Images illustrating the pigment addition in Sample NE04. (Upper left photograph) The mortar contains a black pigment that is not always evenly incorporated and gives the fresh surfaces a mottled appearance. (Upper right photograph) A sample of the pigment was extracted along with the sand sample through chemical digestion. The dark gray material shown here consists of black pigment intermixed with residues from the natural cement binder. (Lower CPL photomicrograph) The pigment is ultrafine-grained and individual particles are barely resolved at the scale of the light microscope. Though there is pigment throughout the binder paste, there are streaks with a higher concentration of the black pigment as shown in this image.

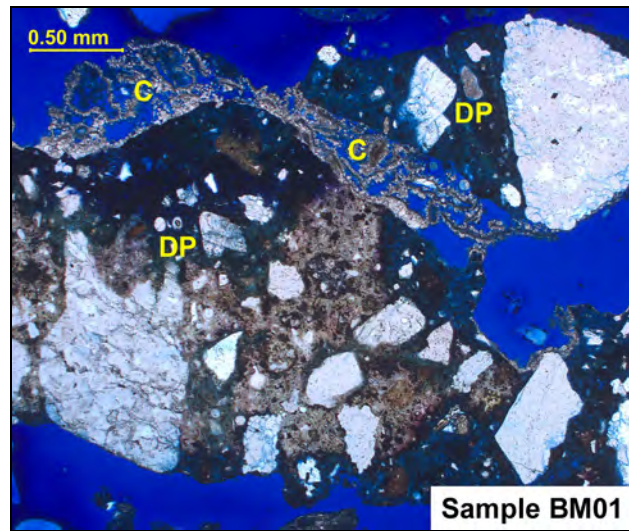


Figure 8: PPL photomicrograph showing the degraded condition of Sample BM01. The sample consists of fine pieces of mortar debris. The few intact fragments consist mostly of decalcified paste (DP), and secondary deposits of calcium carbonate (C) are abundant. These features suggest the mortar has been subject to a high degree of water infiltration.

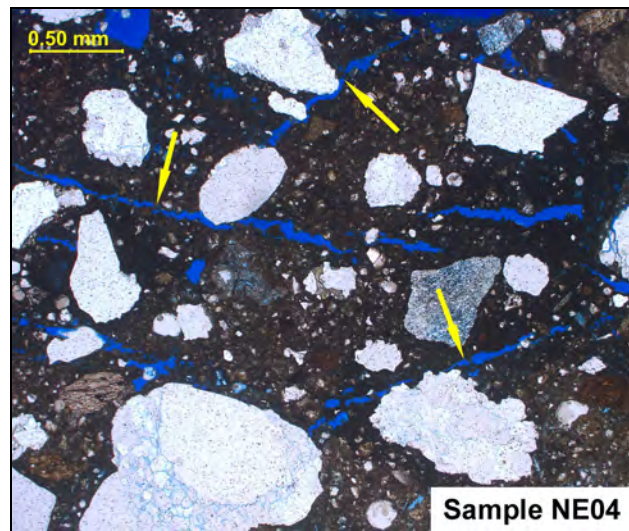


Figure 9: PPL photomicrograph illustrating the splays of ice crystal impressions (arrows) observed in Sample NE04. These indicate that the mortar froze before hardening and suggest the mortar was placed during cold weather.

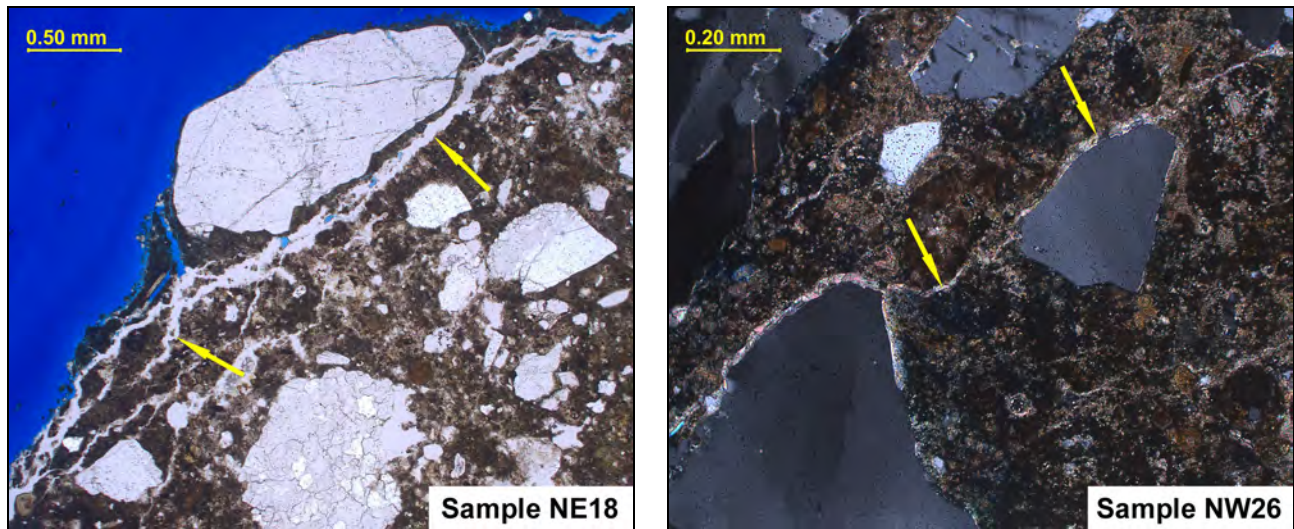


Figure 10: PPL photomicrograph illustrating the fine cracks (arrows) in Samples NE18 and NW26. In Sample NE18, these are filled with an undifferentiated, isotropic salt (potentially chlorides). In Sample NW26, these are often filled with secondary carbonate deposits.

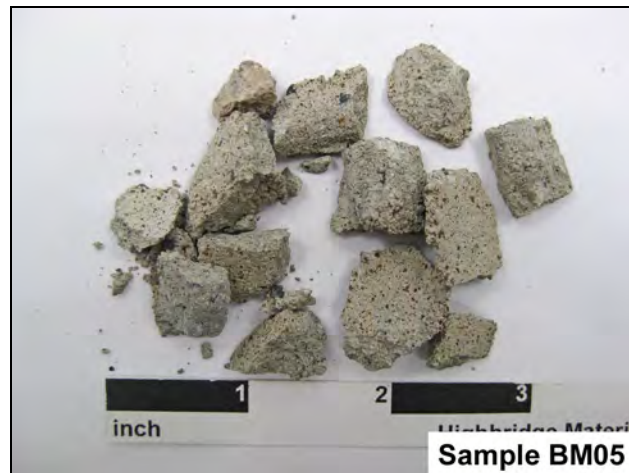


Figure 11: Photograph of Sample BM05 provided to Highbridge for compositional analysis. This is a cement-lime mortar that has a light brownish gray color overall and some fine dark spots due to an iron additive. The mortar is hard and indurate though the paste is somewhat rapidly water-absorptive.

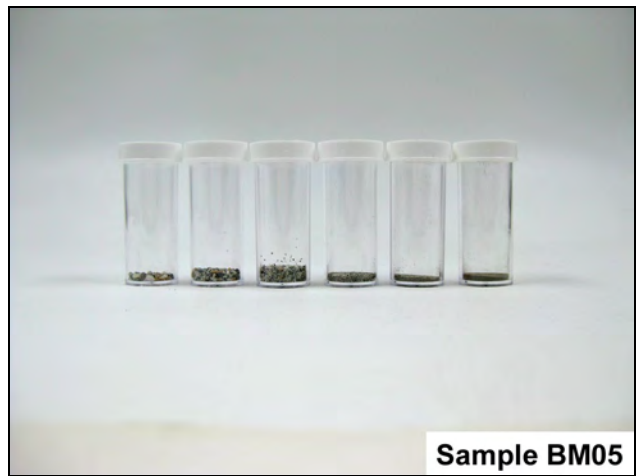
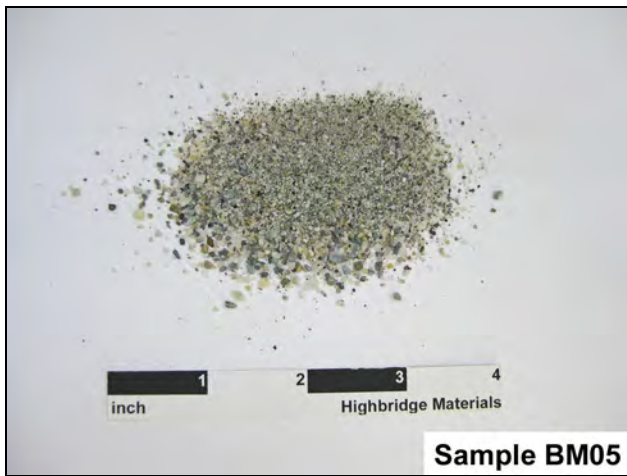


Figure 12: Photographs of the aggregates extracted from Sample BM05 through chemical digestion. (Left image) The total recovery is shown. (Right image) The extracted sand is shown after gradation through a standard sieve stack.

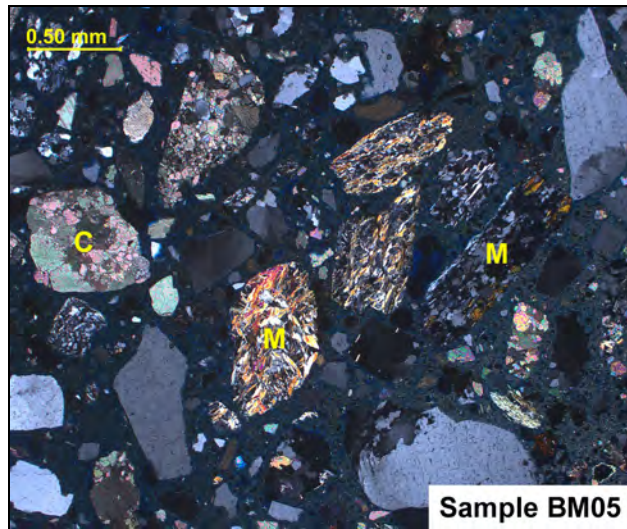


Figure 13: XPL photomicrograph illustrating the lithology of the aggregate used in Sample BM05. The sand consists of a mixture of metaquartzite (M) and lesser carbonate rock (C).

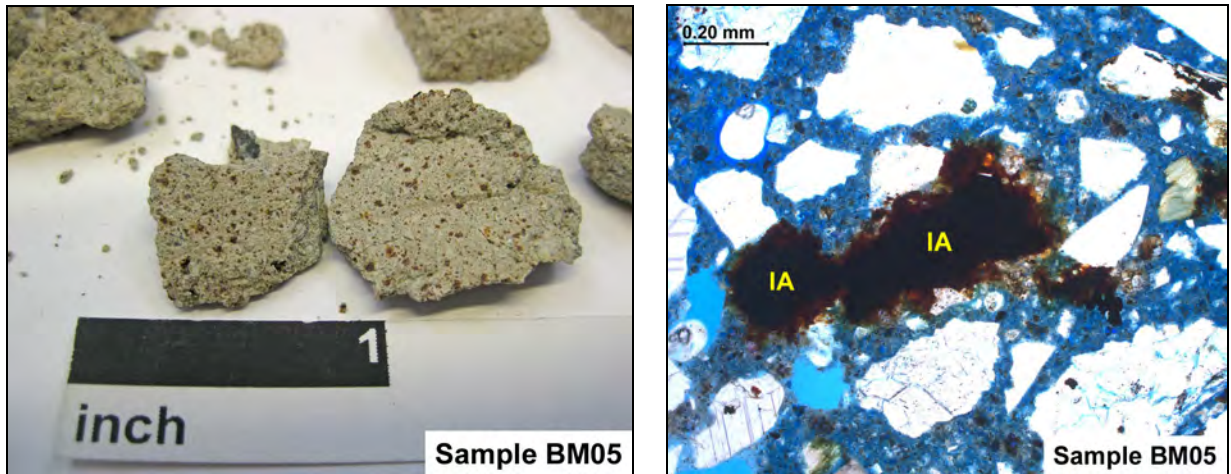


Figure 14: Images illustrating the metallic iron addition within Sample BM05. (Left photograph) The iron particles have oxidized producing fine rust spot, as viewed here on the tooled surface of the mortar. (Right CPL photomicrograph) The iron additive (IA) was added as sand-sized particles from which iron oxides have now emanated into the surrounding binder paste.

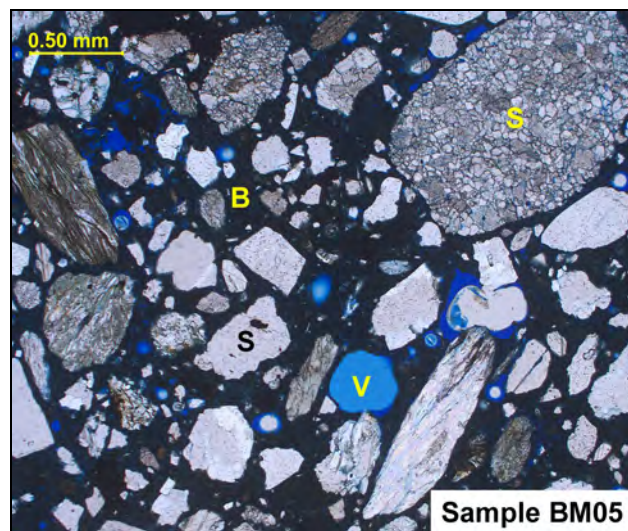


Figure 15: PPL photomicrograph illustrating the microtexture of the mortar in Sample BM05. The binder matrix (B) has a moderately high microporosity, as indicated by the absorption of the blue-dyed epoxy used in the sample preparation. The sand (S) is somewhat sharp-textured, broadly-graded, and evenly distributed. The mortar was well consolidated and air-voids (V) are not excessive.

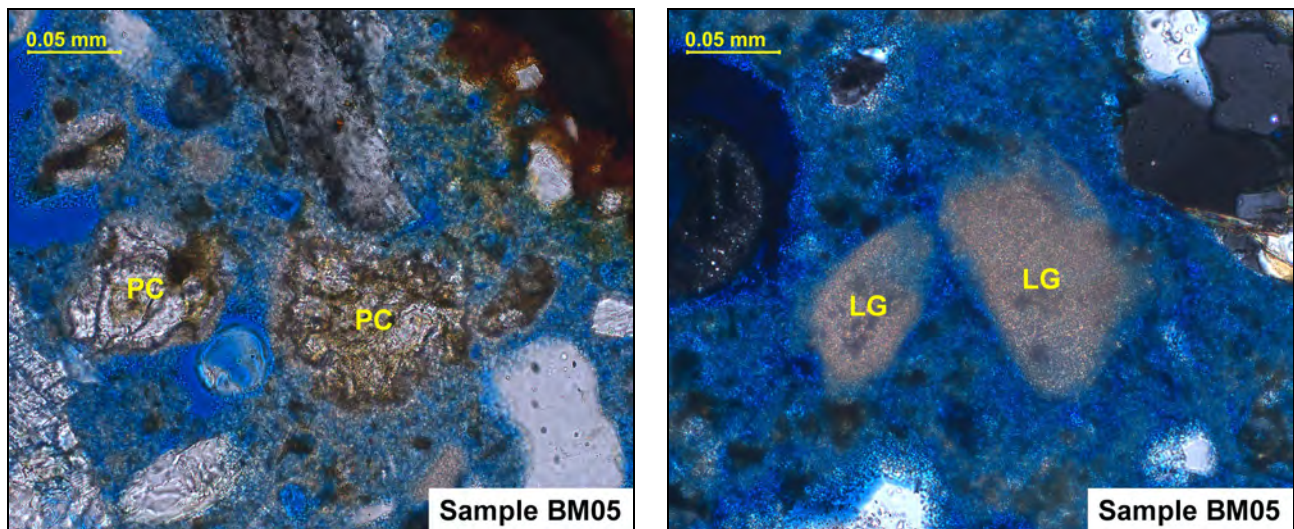


Figure 16: Photomicrographs illustrating the constituents of the cement-lime binder in Sample BM05. (Left PPL image) Portland cement residuals (PC) consist of relatively fine-grained agglomerates of former calcium silicate. Only the brown ferrite phase remains and this ferrite skeleton outlines the sites of former hydraulic minerals. The iron-bearing ferrite identifies the cement as a gray variety. (Right XPL image) Undispersed lime grains are moderately abundant. These are all carbonated, and the particulate texture is consistent with the use of a prepackaged dry hydrate.

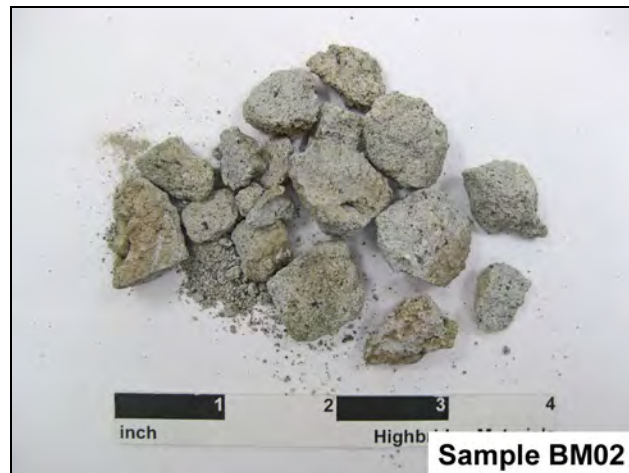


Figure 17: Photograph of Sample BM02 provided to Highbridge for compositional analysis. This is a masonry cement mortar that has a medium gray color overall. The cured product indurate though the paste is soft and rapidly water-absorptive.

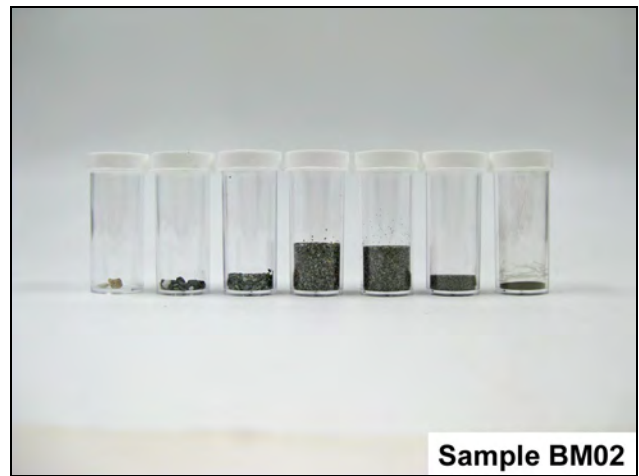
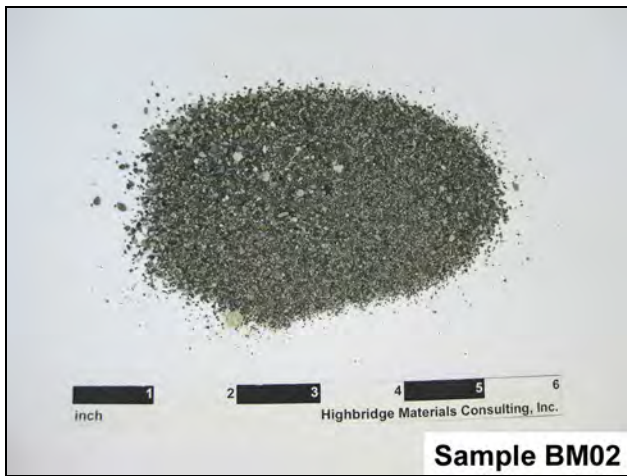


Figure 18: Photographs of the aggregates extracted from Sample BM02 through chemical digestion. (Left image) The total recovery is shown. (Right image) The extracted sand is shown after gradation through a standard sieve stack.

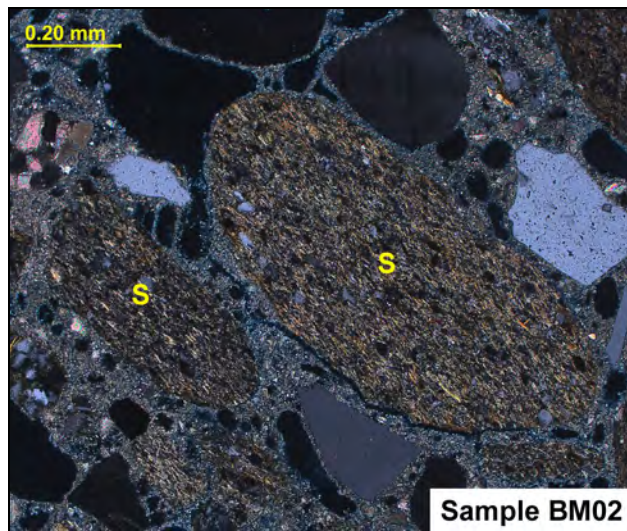


Figure 19: XPL photomicrograph illustrating the lithology of the aggregate used in Sample BM02. The sand consists mostly of fine-grained sedimentary clastic rock particles (S).

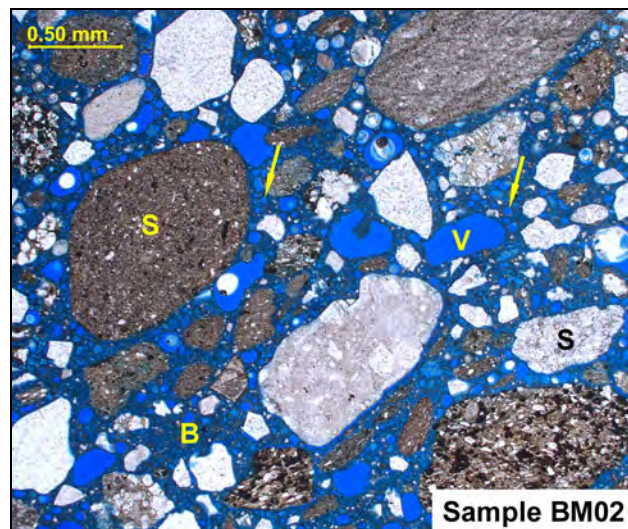


Figure 20: PPL photomicrograph illustrating the microtexture of the mortar in Sample BM02. The binder matrix (B) has a high microporosity, as indicated by the absorption of the blue-dyed epoxy used in the sample preparation. The sand (S) in each is somewhat soft-textured, broadly-graded, and evenly distributed. The mortar was well consolidated with only minor entrapped air-voids (V). The majority of the air structure consists of fine, spherical voids (arrows) that indicate the use of an air-entraining admixture, which is a typical component of prepackaged masonry cements.

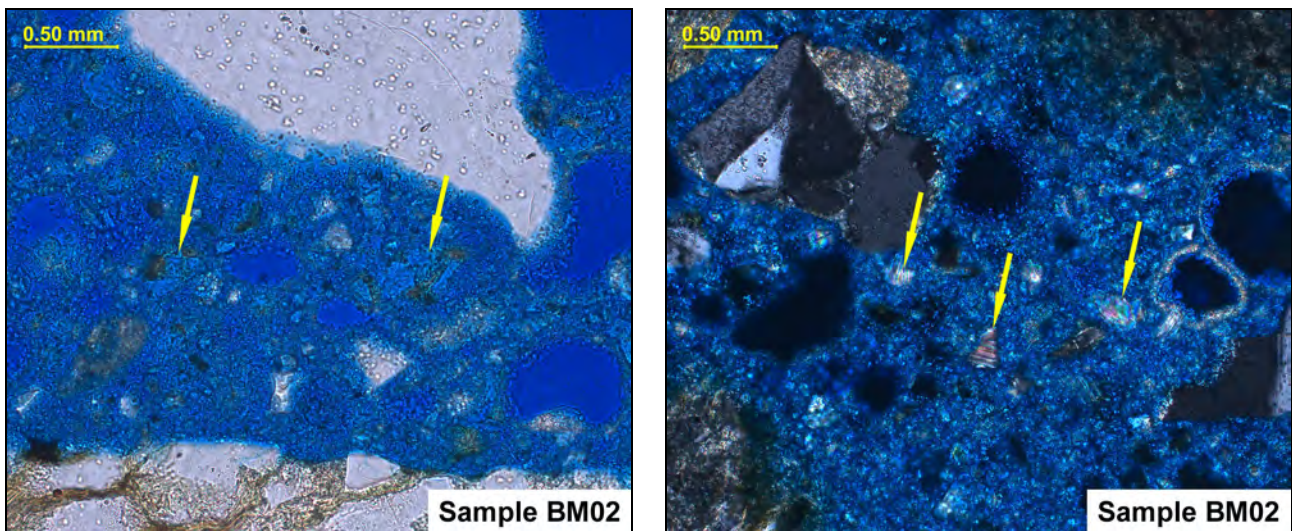


Figure 21: Photomicrographs illustrating the microtexture of the masonry cement binder constituents in Sample BM02. (Left PPL image) Portland cement residuals (arrows) are relatively abundant. These exhibit a high degree of hydration and only the dark-colored ferrite skeleton remains within the cement agglomerates. The ferrite identifies the cement as a gray variety. (Right XPL image) The arrows indicate crushed limestone particulates. These are used as a plasticizer in lieu of hydrated lime in prepackaged masonry cements.

Appendix B
RILEM Absorption Testing

Bennington Battle Monument
Bennington, Vermont

RILEM SURFACE WATER ABSORPTION TESTING

Jablonski Building Conservation, Inc. (JBC) performed RILEM surface water absorption tests on the exterior and interior of the Bennington Battle Monument. RILEM tests were performed to determine if any inconsistencies between the water absorption of the exterior versus interior stone. Tests were only able to be performed on the exterior stone, however. The interior stone was completely saturated.

Methodology

RILEM Test Method 11.4 measures the rate at which water moves through porous materials like masonry. The interior structure of a masonry material is a system of fine interconnected pores. Wetting by liquid water involves capillary conduction (suction) through this pore system, proceeding along both vertical and horizontal pathways. The wetting rate and pattern of each material are directly related to its capillary structure and pore size distribution.

A pipe-like apparatus is used to measure the rate at which water is absorbed. Its flat, circular brim (at the bottom end of the pipe) is affixed to the masonry surface by interposing a piece of putty. The vertical tube is graduated from 0 to 5mL, with an open end on top.

Four tests were performed on the exterior stone:

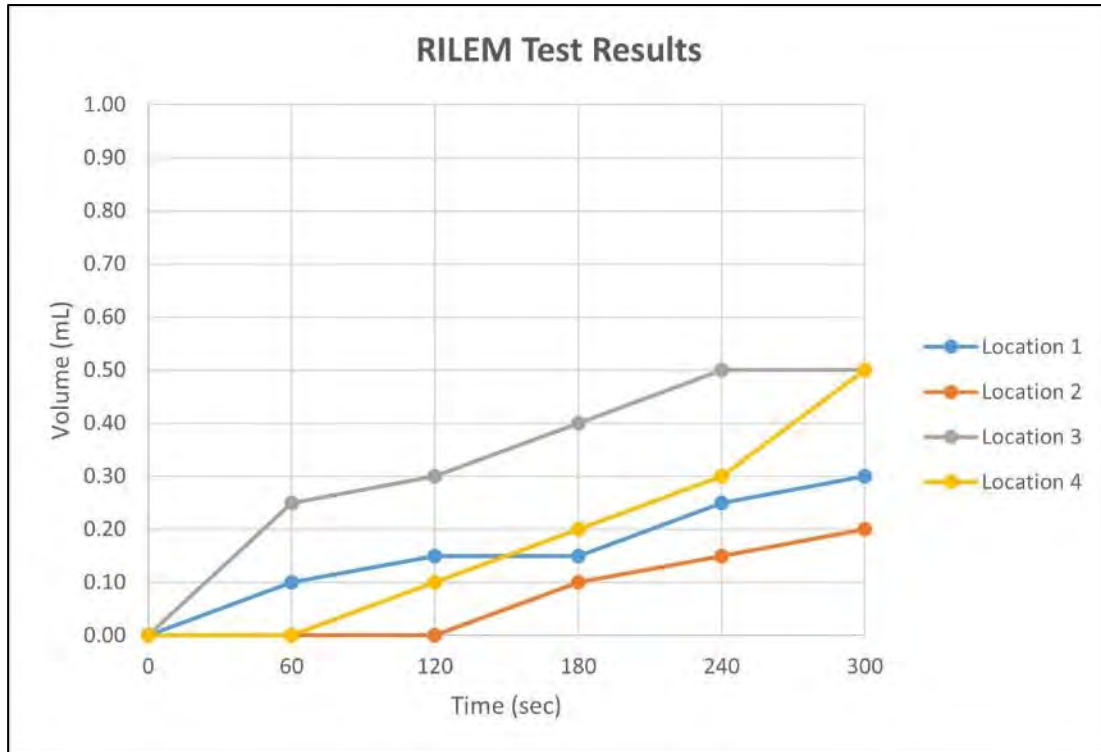
1. The RILEM tube was affixed to the sample using putty between the flat, circular brim of the pipe and the surface of the sample. The tube was pressed into the surface of the sample to ensure adhesion.
2. Water was then added through the upper, open end of the pipe until the water reached the 0 gradation mark.
3. The quantity of water absorbed by the masonry was read from the graduated tube every minute for five minutes.
4. The results of the measurements are presented in the form of a graph with the volume of water absorbed in milliliters (mL) reported as a function of time in seconds.

Testing Locations

Testing was performed in four locations on the exterior limestone of the Bennington Battle Monument. All locations could be reached from grade. Locations 1 and 2 were from stone units that were face bedded. Location 3 was a stone unit with exposed fossils on the surface, and Location 4 was a naturally bedded unit.

Results

The exterior testing locations absorbed 1 ml or less of water over five minutes. The testing apparatuses were left on the stone units while other work was being performed for close to two hours with less than 2 ml of water absorption.

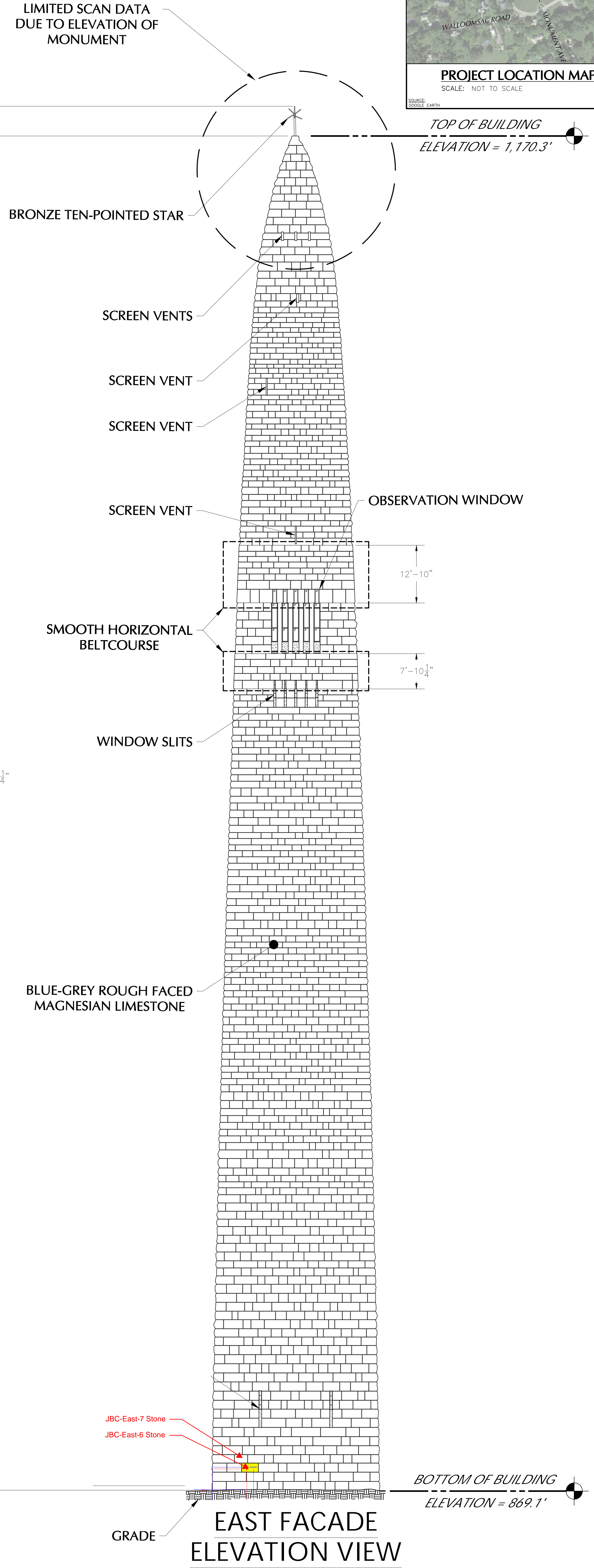
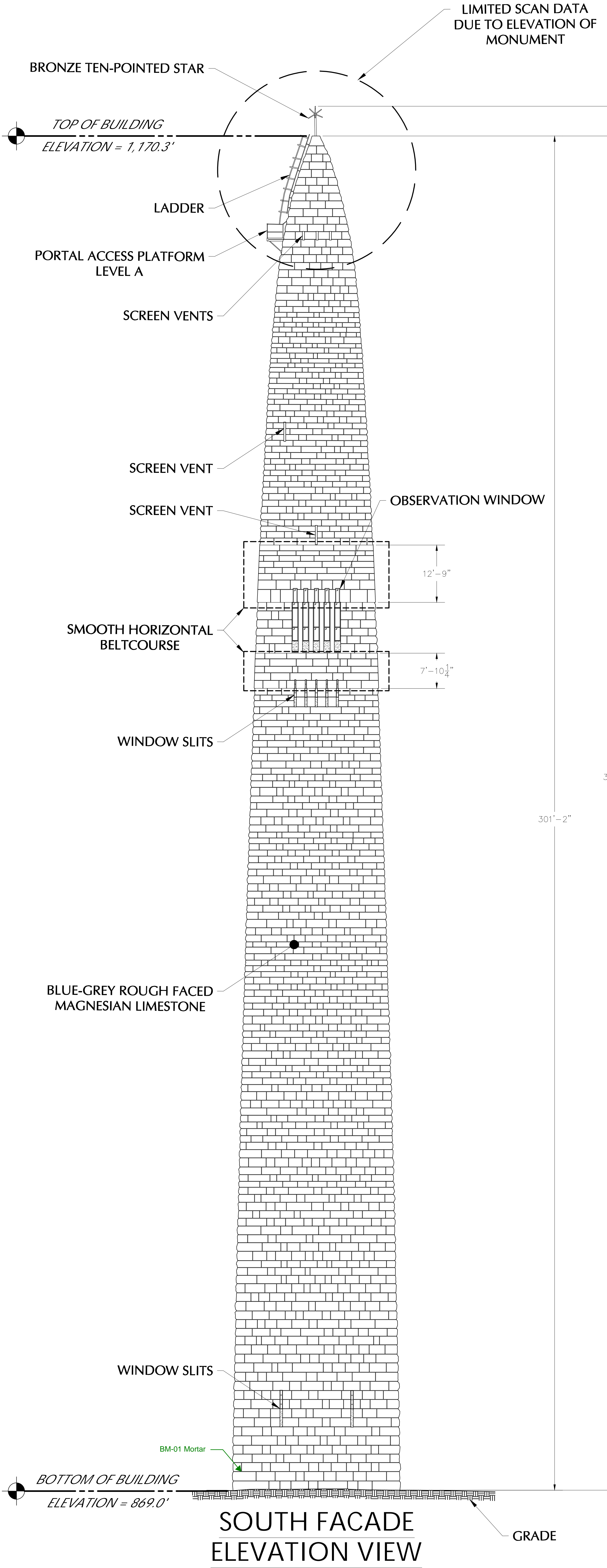
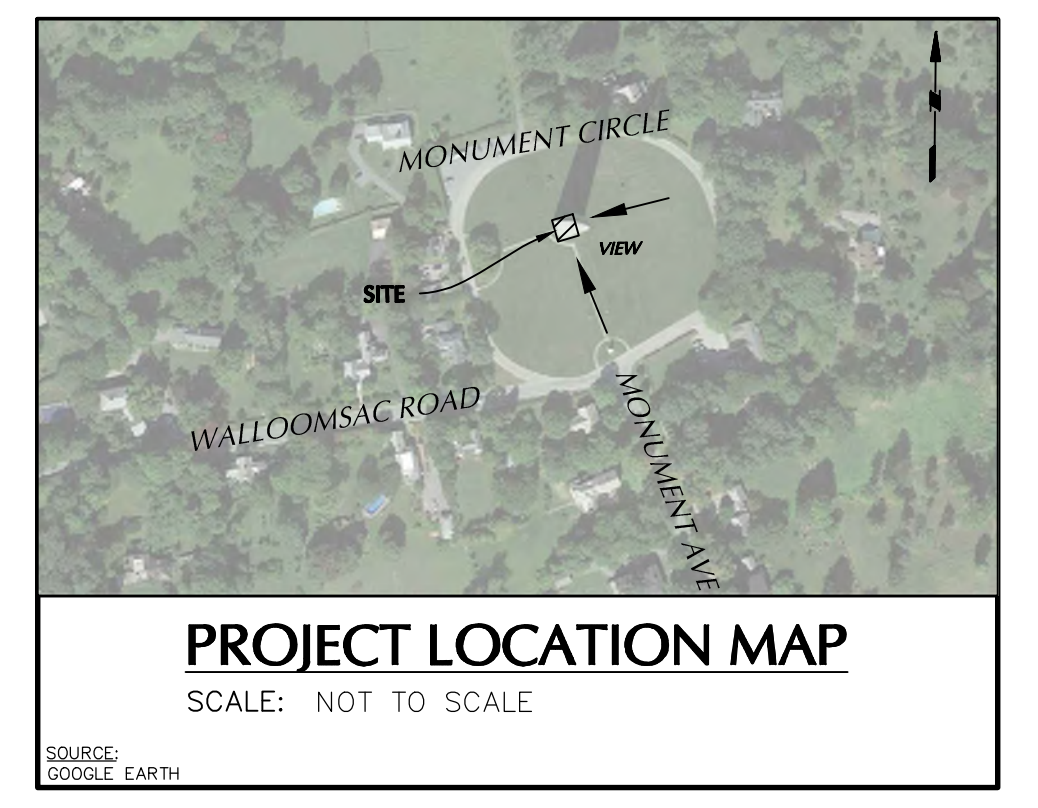


Conclusions

All four testing locations were minimally absorbent. The two face bedded units absorbed slightly less water compared to the naturally bedded unit and unit with surface exposure. Dolomitic limestones are typically very dense and allow minimal water absorption. There were no substantial differences in the exterior stone versus the mortar. Water is likely infiltrating at failed mortar joints and cracks.

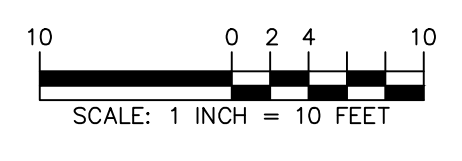
A p p e n d i x C
S a m p l i n g L o c a t i o n P l a n

Bennington Battle Monument
Bennington, Vermont

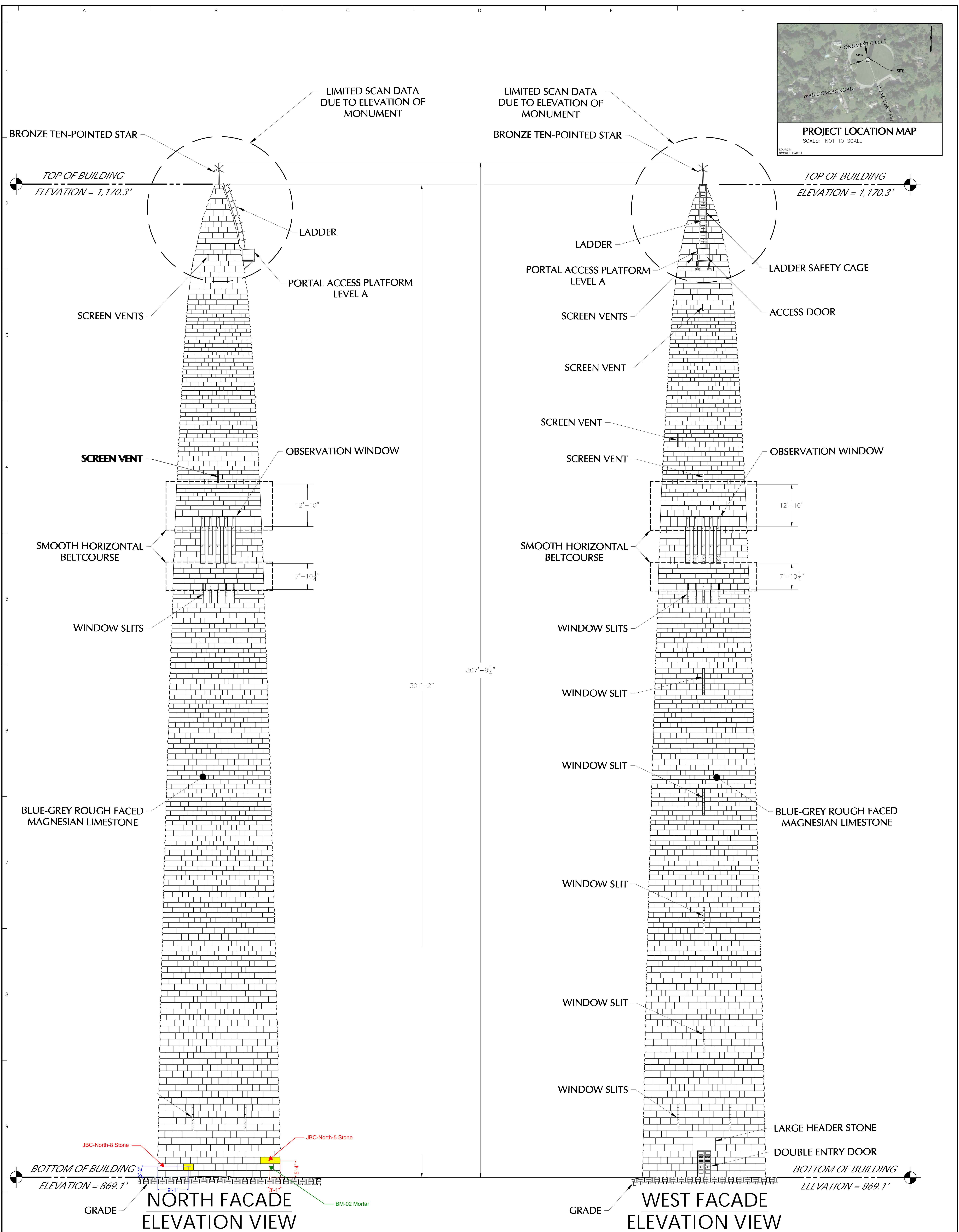
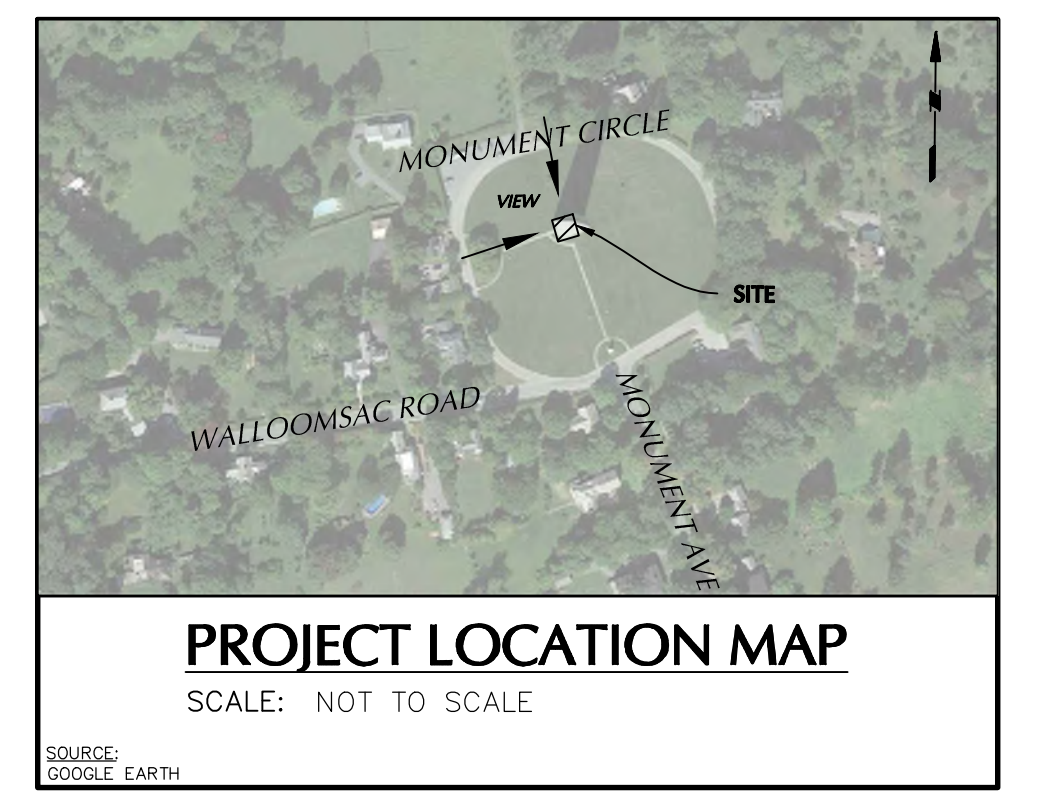


SAMPLING LOCATION PLAN

- NOTES:**
1. THIS SURVEY IS BASED UPON EXISTING PHYSICAL CONDITIONS FOUND AT THE SUBJECT SITE.
 2. INFORMATION SHOWN HEREON HAS BEEN OBTAINED FROM LASER SCAN DATA COLLECTED BY LANGAN ENGINEERING, ENVIRONMENTAL, SURVEYING AND LANDSCAPE ARCHITECTURE, D.P.C., IN FEBRUARY, 2022.
 3. ELEVATIONS SHOWN ARE REFERENCED TO THE NORTH AMERICAN VERTICAL DATUM OF 1988.
 4. ALL UNITS SHOWN HEREON ARE IN U.S. SURVEY FEET.
 5. THIS PLAN NOT VALID UNLESS EMBOSSED OR BLUE INK STAMPED WITH THE SEAL OF THE PROFESSIONAL LAND SURVEYOR.



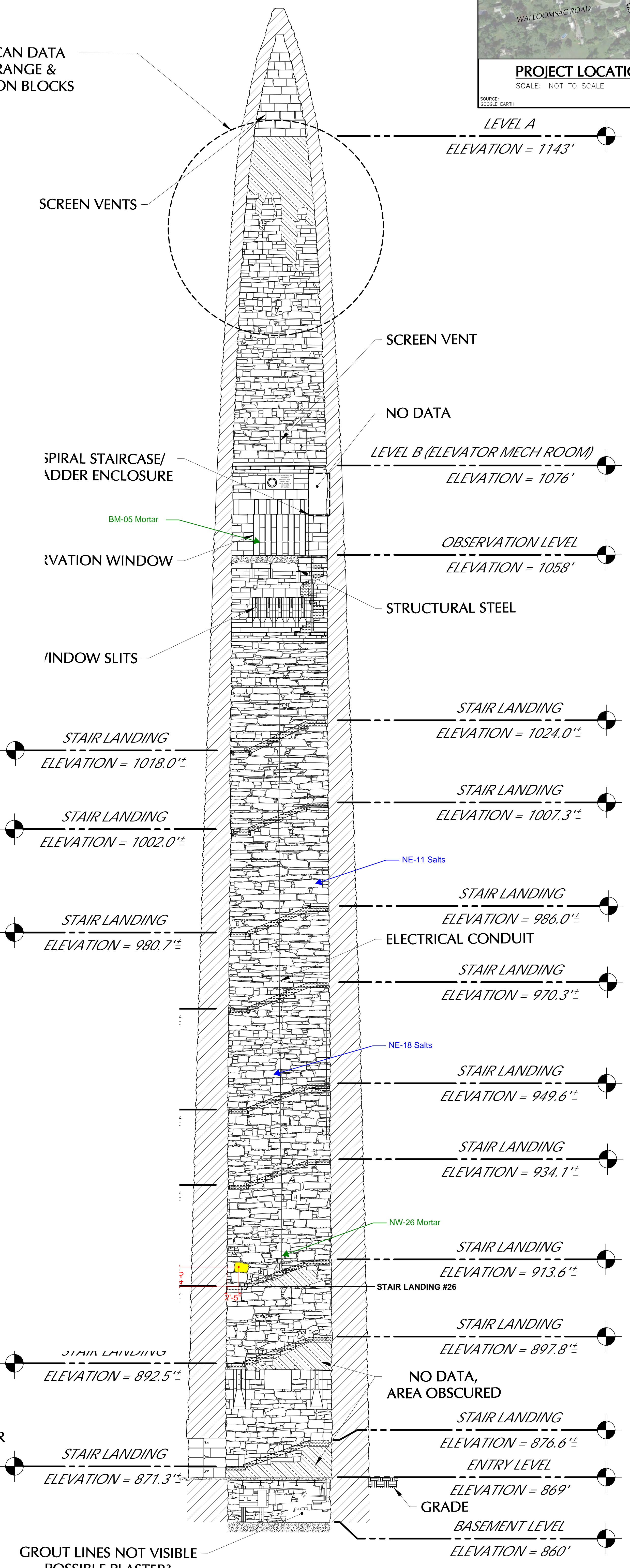
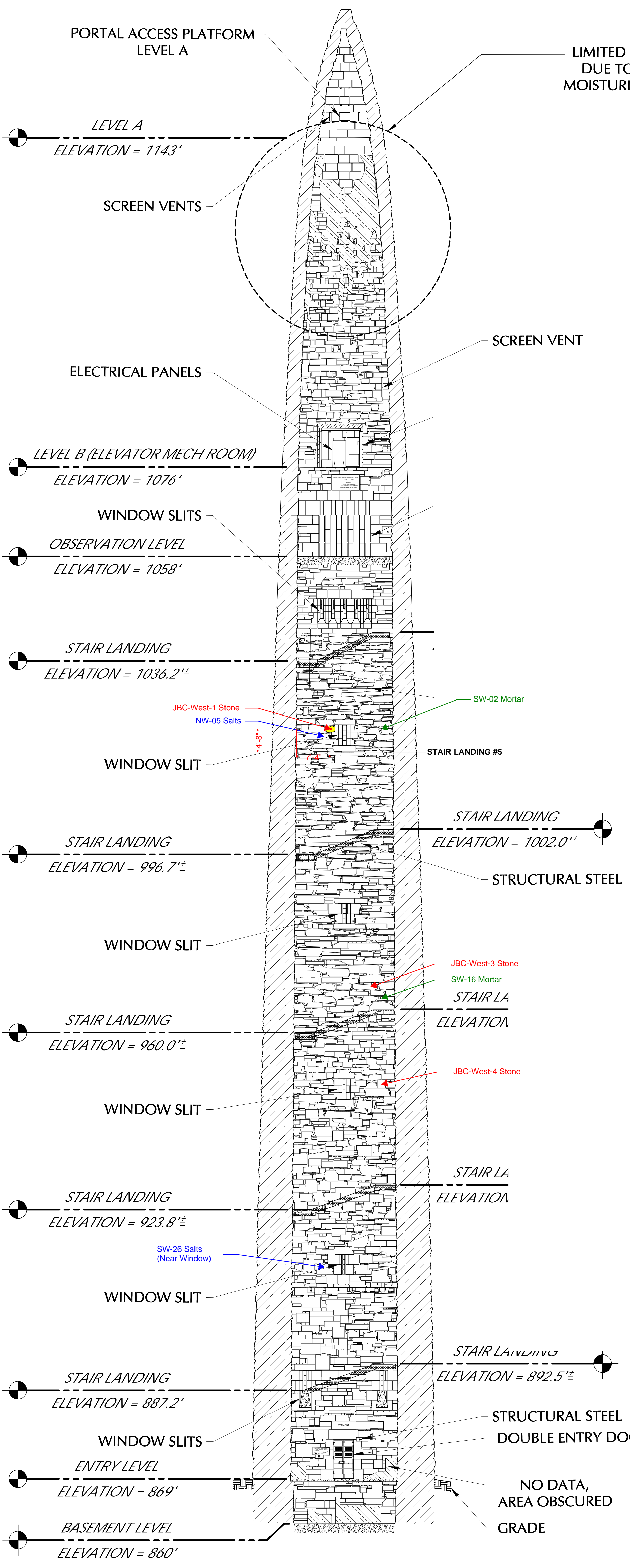
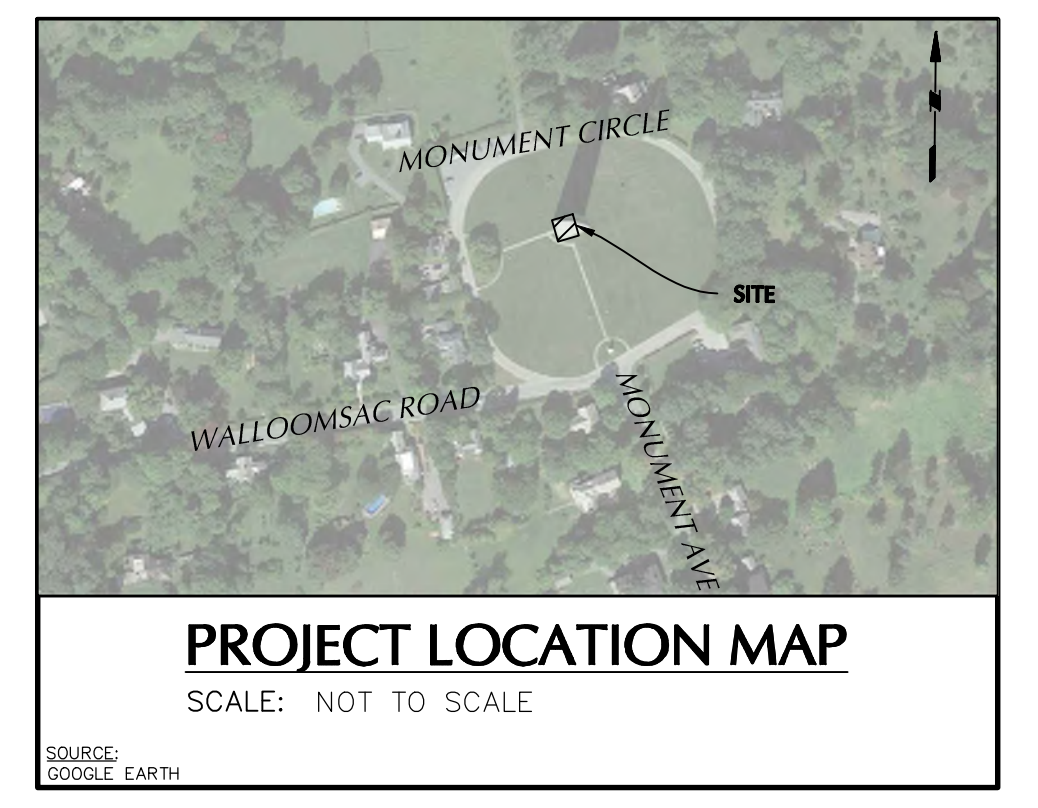
LANGAN Langan Engineering and Environmental Services, Inc. 21 Penn Plaza, 360 West 31st Street, 8th Floor New York, NY 10001 T: 212.479.5400 F: 212.479.5444 www.langan.com	Project BENNINGTON BATTLE MONUMENT 15 MONUMENT CIRCLE BENNINGTON, VT BENNINGTON COUNTY VERMONT	Drawing Title ELEVATION PLAN EXTERIOR (SOUTH & EAST)	Project No. 170724001	Drawing No. EL-01
	Date 05/11/2022	Drawn By JFR	Checked By PDF	Sheet 001 of 004



- NOTES:**
1. THIS SURVEY IS BASED UPON EXISTING PHYSICAL CONDITIONS FOUND AT THE SUBJECT SITE.
 2. INFORMATION SHOWN HEREON HAS BEEN OBTAINED FROM LASER SCAN DATA COLLECTED BY LANGAN ENGINEERING, ENVIRONMENTAL, SURVEYING AND LANDSCAPE ARCHITECTURE, D.P.C., IN FEBRUARY, 2022.
 3. ELEVATIONS SHOWN ARE REFERENCED TO THE NORTH AMERICAN VERTICAL DATUM OF 1988.
 4. ALL UNITS SHOWN HEREON ARE IN U.S. SURVEY FEET.
 5. THIS PLAN NOT VALID UNLESS EMBOSSED OR BLUE INK STAMPED WITH THE SEAL OF THE PROFESSIONAL LAND SURVEYOR.

SAMPLING LOCATION PLAN

<p>LANGAN Langan Engineering and Environmental Services, Inc. 21 Penn Plaza, 360 West 31st Street, 8th Floor New York, NY 10001 T: 212.479.5400 F: 212.479.5444 www.langan.com</p>	<p>Project BENNINGTON BATTLE MONUMENT 15 MONUMENT CIRCLE BENNINGTON, VT BENNINGTON COUNTY VERMONT</p>	<p>Drawing Title ELEVATION PLAN EXTERIOR (NORTH & WEST)</p>	<p>Project No. 170724001</p>	<p>Drawing No. EL-02</p>
	<p>Date 05/11/2022</p>	<p>Drawn By JFR</p>	<p>Checked By PDF</p>	<p>Sheet 002 of 004</p>



WEST FACADE INTERIOR ELEVATION VIEW

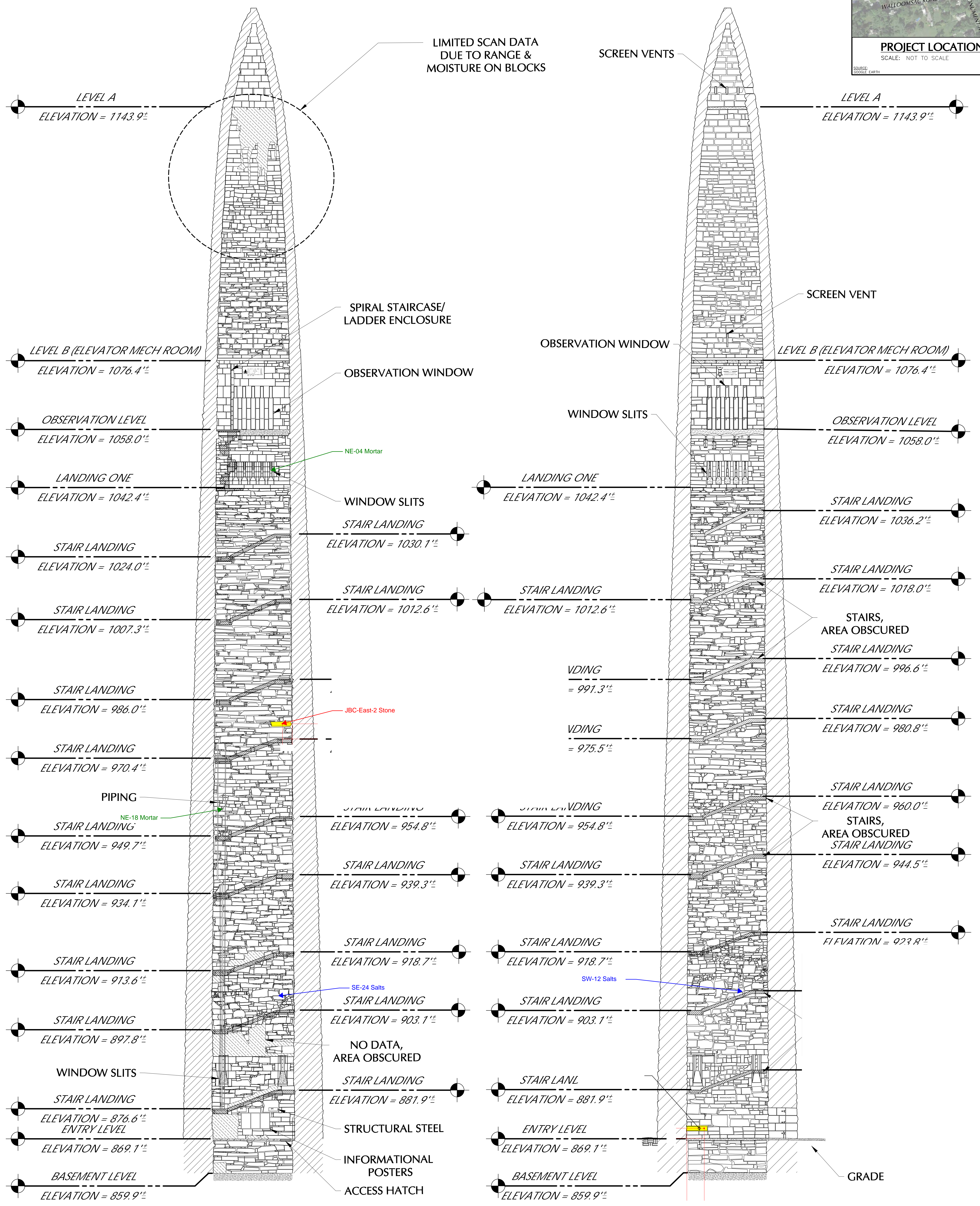
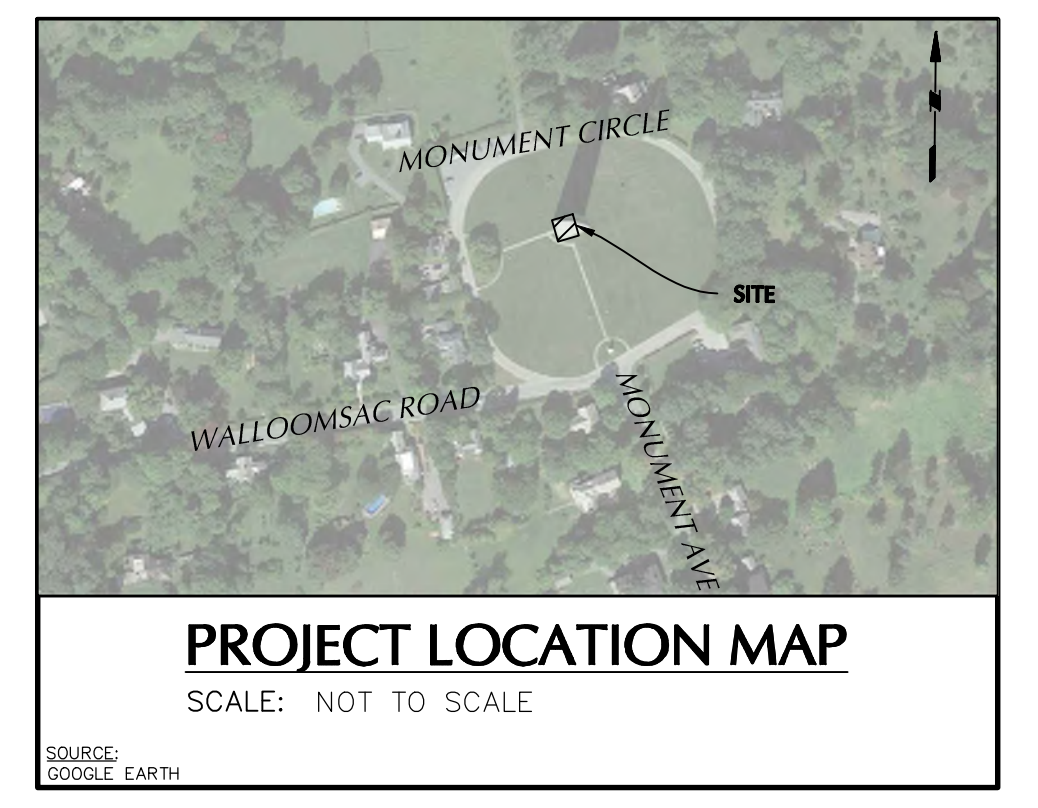
NORTH FACADE INTERIOR ELEVATION VIEW

SAMPLING LOCATION PLAN

- NOTES: 1. THIS SURVEY IS BASED UPON EXISTING PHYSICAL CONDITIONS FOUND AT THE SUBJECT SITE. 2. INFORMATION SHOWN HEREON HAS BEEN OBTAINED FROM LASER SCAN DATA COLLECTED BY LANGAN ENGINEERING, ENVIRONMENTAL, SURVEYING AND LANDSCAPE ARCHITECTURE, D.P.C., IN FEBRUARY, 2022. 3. ELEVATIONS SHOWN ARE REFERENCED TO THE NORTH AMERICAN VERTICAL DATUM OF 1988. 4. ALL UNITS SHOWN HEREON ARE IN U.S. SURVEY FEET. 5. THIS PLAN NOT VALID UNLESS EMBOSSED OR BLUE INK STAMPED WITH THE SEAL OF THE PROFESSIONAL LAND SURVEYOR.



LANGAN Langan Engineering and Environmental Services, Inc. 21 Penn Plaza, 960 West 31st Street, 8th Floor New York, NY 10001 T: 212.479.5400 F: 212.479.5444 www.langan.com Project BENNINGTON BATTLE MONUMENT 15 MONUMENT CIRCLE BENNINGTON, VT BENNINGTON COUNTY VERMONT Drawing Title ELEVATION PLAN INTERIOR (NORTH & WEST) Project No. 170724001 Date 05/11/2022 Drawn By JFR Checked By PDF Drawing No. EL-03 Sheet 003 of 004

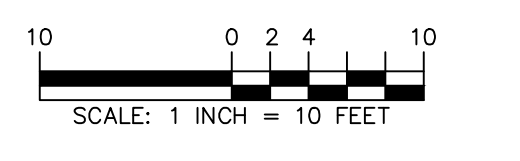


EAST FACADE INTERIOR ELEVATION VIEW

SOUTH FACADE INTERIOR ELEVATION VIEW

- NOTES:**
1. THIS SURVEY IS BASED UPON EXISTING PHYSICAL CONDITIONS FOUND AT THE SUBJECT SITE.
 2. INFORMATION SHOWN HEREON HAS BEEN OBTAINED FROM LASER SCAN DATA COLLECTED BY LANGAN ENGINEERING, ENVIRONMENTAL, SURVEYING AND LANDSCAPE ARCHITECTURE, D.P.C., IN FEBRUARY, 2022.
 3. ELEVATIONS SHOWN ARE REFERENCED TO THE NORTH AMERICAN VERTICAL DATUM OF 1988.
 4. ALL UNITS SHOWN HEREON ARE IN U.S. SURVEY FEET.
 5. THIS PLAN NOT VALID UNLESS EMBOSSED OR BLUE INK STAMPED WITH THE SEAL OF THE PROFESSIONAL LAND SURVEYOR.

SAMPLING LOCATION PLAN



LANGAN Langan Engineering and Environmental Services, Inc. 21 Penn Plaza, 960 West 31st Street, 8th Floor New York, NY 10001 T: 212.479.5400 F: 212.479.5444 www.langan.com	Project BENNINGTON BATTLE MONUMENT 15 MONUMENT CIRCLE BENNINGTON, VT BENNINGTON COUNTY VERMONT	Drawing Title ELEVATION PLAN INTERIOR (SOUTH & EAST)	Project No. 170724001	Drawing No. EL-04
	Date 5/11/2022	Drawn By JFR	Checked By PDF	Sheet 004 of 004

**Bennington Battle Monument
Bennington, VT**

**CONDITION ASSESSMENT AND TREATMENT RECOMMENDATIONS
FOR
ENVIRONMENTAL CONDITIONS INSIDE MONUMENT**



Prepared By:

Landmark Facilities Group, Inc.
252 East Avenue
Norwalk, CT 06855
203-866-4626

Draft: January 10, 2024

Final:

Contents

INTRODUCTION	2
PHYSICAL DESCRIPTION OF EXISTING CONDITIONS	3
1. HVAC Systems.....	3
2. Electrical.....	5
ISSUES TO CONSIDER FOR PLANNING PURPOSES	7
1. Building-Related Issues	7
a. Sources of Moisture within the monument.....	8
b. Monitoring Data.....	8
c. Reduce Water Penetration.....	10
d. Potential volume of water in the monument.....	10
2. Heating, Ventilating, and Air Conditioning (HVAC) Systems	10
a. Sustainability.....	10
b. Humidity Control.....	10
c. Sources of Heat.....	12
RECOMMENDATIONS	12
1. Building-Related Recommendations	12
2. HVAC System Recommendations.....	12

INTRODUCTION

The Bennington Battle Monument is a 300-foot-high stone obelisk located in Bennington, Vermont. The monument commemorates the Battle of Bennington during the American Revolutionary War.

The monument's cornerstone was laid in 1887, and it was completed in November 1889. It is constructed of Sandy Hill Dolomite. The walls at the base of the monument are more than seven feet thick and narrow to about three feet thick near the peak

The Bennington Battle Monument is a Vermont State Historic Site.

The interior of the monument contains an elevator to the observatory level at 200 feet and stairs from ground level up to the elevator machine room. There is a basement space below the ground level that is accessible by a hatch in the floor.

This report presents existing conditions, issues that should be considered when planning treatments for the building and recommended treatment options.

PHYSICAL DESCRIPTION OF EXISTING CONDITIONS

1. HVAC Systems.

There are no functional HVAC systems in the monument. There are remains of a heating system that has been abandoned ()



Figure 1. Remnants of abandoned heating system in monument

The heating system was fed steam from a boiler in the visitor's center. The boiler has been removed, but the old piping has been cut and capped where it came through the foundation wall. () The steam piping and steam condensate piping was buried between the buildings. The piping passed through a pit on the north side of the monument and entered the monument basement from the pit.



Figure 2. Former boiler room in visitor's center. Note piping cut and capped

The steam piping and steam condensate piping was buried between the buildings. The piping passed through a pit on the north side of the monument and entered the monument basement from the pit. The abandoned piping is still visible in the pit. ()



Figure 3. Abandoned piping in pit adjacent to monument

2. Electrical.

Electric Service

There a 200A 120/240 electrical service to the site. The meter and main switch are located on the west side of the drive surrounding the monument. () The electric service runs underground to the monument.



Figure 4. Electric Service

There is an electrical panel located in the basement of the monument.



Figure 5. Main Electrical Panel in monument basement

It is a 30 position, 200 amp, 120/208 volt panel with a 175 amp main circuit breaker. According to the panel directory, the panel serves lights and the elevator in the monument.

There is a circuit breaker panel located in the elevator machine room. ()



Figure 6. Elevator machine room panel

It is a 12 position, 100 amp, 120/240 volt panel with a 60 amp main circuit breaker. According to the panel directory, the panel primarily serves the heat in the machine room.

The electrical equipment all appears to be in good condition.

ISSUES TO CONSIDER FOR PLANNING PURPOSES

The interior of the monument is experiencing high relative humidity conditions that are leading to stone damage and corrosion and deterioration of iron and steel members.

There are a variety of issues to consider for planning purposes that are related to the building envelope and potential mechanical systems. The issues include:

1. Building-Related Issues

a. Sources of Moisture within the monument

There are two likely sources for the moisture found within the interior of the monument.

1. The first source is from water passing through the stone from the rain penetrating the exterior.
2. The second likely source is from condensation on the stone interior during certain periods of the year. Since the stone has a large thermal mass, it likely stays cold enough to be below the outside air dew point well into the spring and summer. Since moisture in air behaves like a gas, the moisture content of the air inside the monument will respond quickly to changes outside. As the higher dew point air hits the cold stone, it condenses.

b. Analysis of Monitoring Data

The data provided by Atkinson-Noland Associates shows the stone temperature within 9” of the interior surface of the stone and the interior space temperatures are very closely correlated. It reaches a high temperature of about 75°F in August and a low temperature of about 10°F for a short period in February. The cyclical range of temperature over the seasons also correlates closely with the range of temperature of the outside air. This is not surprising considering saturated stone offers very little insulating value (even when 84” thick!).

The monitoring data for the interior air in the monument shows the relative humidity experiences wide swings from lows of 30% to highs of 100%. These swings are occurring very rapidly, most likely in response to changes in weather. Starting in Late May through September, the RH swings are less dramatic and have lower peaks and higher troughs. The highs are down around 85% and the lows stay above 40%. The RH reduction starts roughly when the stone reaches about 70°F in late May and continues until the stone temperature drops below 60° in the fall.

The fact that the RH peak values drop as the space warms seems to indicate that the moisture content of the air inside the monument is somewhat stable and that the saturated stone is not an unlimited source of moisture that causes continuous saturated air inside the monument.

We looked at the required moisture removal rate from two perspectives:

1. The first calculation is based on a formula for estimating the rate of evaporation from poured concrete. The formula was developed by Paul J. Uno based on the Menzel formula and uses the air temperature, material temperature and the air RH to predict the pounds of moisture per square foot of surface area. As expected, the evaporation rate is very near zero when the stone is cold (at or below the dewpoint of the air in the monument) and increases rapidly as the stone is warmed. Based on this formula, and using the data collected by ANA, we arrived at 2 estimates:
 - Average evaporation rate: 14 gallons per hour
 - Peak summer evaporation rate: 61 gallons per hour
2. The second approach was based on analysis of the temperature and relative humidity data collected by ANA and converting the readings into the humidity ratio. The humidity ratio is defined as the ratio of the mass of water vapor in humid air over the mass of dry air in a body of air. The result is the pounds of water in the air per pound of dry air. The approximate volume of air in the monument is roughly 96,000 cubic feet, and the density of dry air equals 0.078 pounds/cubic foot, so the mass of dry air in the monument is roughly 7,500 pounds. Since the humidity ratio (W) is known from the T & RH data, the pounds of moisture in the air can be calculated by multiplying the pounds of dry air by the humidity ratio. Judging from the T & RH data, the desired humidity ratio for drying out the stone is approximately 0.0038 pounds of water in the air per pound of dry air. On a peak day this is roughly

109 lbs of water or about 13 gallons of water. Assuming the monument has an air exchange rate of about once an hour when the entry door is open, the moisture removal rate to dry the stone calculates to a removal rate of about roughly 13 gallons per hour.

c. Reduce Water Penetration.

The monument is exposed to weather-driven rain and snow that is being wicked into the stone exterior. Controlling the water penetrating the exterior is a prerequisite to any measures to reduce the interior relative humidity.

d. Potential volume of water in the monument.

The testing to date has determined that the stone walls of the monument are saturated with water. The team has estimated the volume of stone comprising the monument roughly 150,000 cubic feet with roughly 5% of the volume being void spaces. If the stone is saturated as is believed, the water volume could be as high as 55,000 gallons.

2. Heating, Ventilating, and Air Conditioning (HVAC) Systems

a. Sustainability

Any new HVAC systems proposed for monument need to be reliable, easy to maintain and energy efficient. The design of these systems should endeavor to minimize impact on the environment by being energy efficient and, if mechanical cooling for dehumidification is utilized, using refrigerants that do not deplete the ozone.

b. Humidity Control

There are two primary means of removing moisture from the interior of the monument:

Natural Ventilation. Ventilation would involve introducing air at lower elevation of the monument and exhausting it at a high elevation of the monument.

Ideally this would be accomplished using the stack effect. Stack effect is the movement of air into and out of buildings and chimneys and is driven by air buoyancy. Buoyancy occurs due to a difference in indoor-to-outdoor air density resulting from temperature and moisture differences. The result is either a positive or negative buoyancy force. The greater the thermal difference and the height of the structure, the greater the buoyancy force, and thus the stack effect. If the air in the building is warmer than the outside, this warmer air will float out the top opening, being replaced with cooler air from outside. If the air inside is cooler than that outside, the cooler air will drain out the low opening, being replaced with warmer air from outside.

In order to develop a predictable ventilation rate in the winter, it may be necessary to introduce some heat within the monument to create a buoyant force.

Mechanical ventilation. Mechanical ventilation would require the use of a fan to exhaust the air from the structure. The most practical method would be to have a fan above the observation level drawing air from the below the observation level and pressurizing the space above the observation level so air was pushed out of the vents to the exterior.

The challenges related to introducing ventilation are:

- The observation level creates an obstruction to free ventilation between the bottom 200' of the monument and the roughly 100' above the observation level.

- The ventilation would need to be controlled by monitoring inside air conditions and outside air conditions and only ventilating when the outside air had a lower moisture content than the inside air.

Dehumidification. Dehumidification would require a mechanical system to reduce the moisture content of the air and drain the moisture away from the interior. It may be possible to locate numerous dehumidifiers on the various stair landings below the observation level.

c. Sources of Heat

If it is determined that adding heat to the air in the monument to create a more predictable buoyant force for natural ventilation, the potential heat sources include Fuel Fired Boiler and Geothermal Heat Pumps.

Fuel Fired Boiler. A fuel-fired boiler would have to be located remotely and steam or hot water piped underground to the monument-similar to what done in the past.

Geothermal Heat Pumps. It may be feasible to locate water-to-water heat pumps in the basement of the monument tied to a geothermal loop field in the ground surrounding the monument. Geothermal heat pumps are an efficient way to produce heat.

RECOMMENDATIONS

1. Building-Related Recommendations

- a. Immediate Measures
 - i. Reduce rain water penetration into the stone.

2. HVAC System Recommendations

a. Immediate Measures

i. Install dehumidifiers on various stair landings throughout the monument to begin the drying process for the stone walls. The recommended dehumidifiers would be similar to Hi-E Dry model 195 which have a rated moisture removal rate of 205 pints (~25 gallons) per day at 70°F, 80%. Using a desired removal rate of 13 gallons per hour (312 gallons per day), approximately 12 of these units would be required throughout the monument. In order to achieve both good air distribution and the needed moisture removal rate, we recommend the following locations:

1. Basement: 1 unit
2. Entry: 3 units
3. Each Elevator Landing: 2 units (4 total)
4. Observation level: 2 units
5. Elevator MER: 1 units
6. Observation Level: 1 unit

The humidifiers are equipped with a set point controller which we recommend initially be set at 50%.

Each dehumidifier will require a dedicated 15 amp 120 volt single phase power circuit. The electric service to the monument is a 3 phase service rated for 175 amperes at 120/208 volts and has 12 spare positions in it. The main electrical load in the monument is the elevator which is fed by a 100 amp 3 pole breaker.

The dehumidifiers will also require a drain line to the exterior. A common non-ferrous pipe riser running vertically from the elevator machine level to the basement with taps for each dehumidifier is recommended. Each dehumidifier has a built in pump and 25 feet of hose to connect to the drain riser.

The dehumidifiers should be operated when the air temperature inside the monument is above 40°F and when the main entry door is closed.

- ii. Install additional T & RH monitoring for the air inside the monument at different levels for additional study. We recommend a monitoring point every 50 feet in elevation up to the elevator machine room and including one temperature and relative monitor for the exterior conditions. The run time for each dehumidifier should also be logged by the monitoring system. The data collected would be used to determine if a passive ventilation system, or a reduced dehumidifier count, could be implemented once the indoor moisture conditions are stable

b. Long Range Plan

- i. Evaluate the additional data when dehumidification is active to determine the potential for a more passive ventilation system:
 - 1. Determine a pathway for air to pass from below the observation level to the chamber above the observation level.
- ii. Consider installing a water-to-water geothermal heat pump system to provide a low level of heat to the monument to induce natural ventilation with draft.
- iii. Utilize a digital controller to operate a ventilation system.

APPENDIX

HI-E DRY 195

High-Efficiency Dehumidifier

Hi-E DRY 195 dehumidifiers are designed and built with emphasis on efficiency and durability. Today's Hi-E DRY 195 dehumidifiers remove up to seven pints of water per kilowatt hour, while the industry average remains at only two to three pints.

The high-efficiency design of Hi-E DRY 195 dehumidifiers offer more than just dramatically reduced utility costs. The larger water removal capacity from a smaller, more efficient refrigeration system eliminates the need for 220 volt circuits in many applications. The smaller refrigeration system allows Hi-E DRY 195 dehumidifiers to cost less than other commercial dehumidifiers of equal capacity.

The Hi-E DRY 195 high efficiency dehumidifier utilizes refrigeration to cool the incoming air stream below its dew point as it passes through the dehumidification (evaporator) coil. This cooling results in the removal of moisture (latent heat) and reduction in temperature (sensible heat). The cooled and dried air is used to pre-cool the incoming air stream resulting in up to a 200 percent increase in overall efficiency. After the pre-cooling stage the processed air is reheated by passing through the condenser coil. The latent heat removed by the evaporator coil is returned to the air stream at this stage as sensible heat, resulting in an overall temperature increase from the incoming air.



Features:

- Controlled by a dehumidistat with settings from 20 to 80 percent relative humidity and a positive "on" and "off" setting.
- Contains a blower switch that permits continuous blower operation independent of dehumidification.
- Portable and provided with four casters.
- Contains an internal condensate pump capable of lifting condensate 17 feet and 20 feet of condensate hose.
- Wiring is through a factory installed six foot power cord; 115 volt with ground.

Water Removal Rates (Pints/Day)

320 pints	90°F, 90%
245 pints	80°F, 80%
192 pints	80°F, 60% (AHAM)
205 pints	70°F, 80%
150 pints	70°F, 60%
162 pints	60°F, 80%
99 pints	60°F, 60%
81 pints	50°F, 80%
40 pints	50°F, 60%

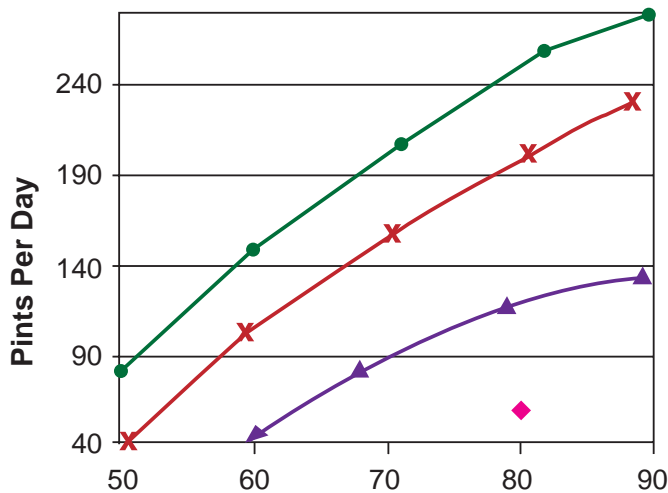


HI-E DRY 195

High-Efficiency Dehumidifier

Capacity; Pints per Day

		Relative Humidity					
		30	40	50	60	70	80
Air temp	50				40	65	81
	60		30	60	99	110	162
	70		65	120	150	180	205
	80		110	150	192	205	245
	85		115	160	198	230	262
	90		127	175	210	252	285



Minimum Performance at Set Conditions

	70° 60%	80° 60%
Intake Air	70° 60%	80° 60%
Water removal/day	156 Lbs	200 Lbs
Pints/KWH	5.4	5.9

ETL Listed



Specifications

Part Number	4030060
Power	115 VAC 12 amps
Kilowatts	1.25 (80° 60%)
Water Removal	192 pints (80°, 60%)
Blower	540 CFM
Operating Range	33°F–110°F
Filters	16"x16"x2" Pleated Media, (P/N 4021799) MERV-8

Warranty

Five years:
1st year 100% of Parts and Labor
2nd-5th year 100% of Parts of sealed refrigerant system

Dimensions

	Unit	Shipping
Width:	36.6"	39.25"
Height:	40"	48.75"
Depth:	19"	30"
Weight:	180 lbs	214 lbs

Accessories and Replacement Air Filters

4021799	16" x 16" x 2" Pleated Media Filter MERV-8
4023684	Duct Kit, Optional
4020175	115V Remote Dehumidistat, Optional



Date: 12 January, 2024

To: Stevens & Associates
95 Main Street
Battleboro, VT 05301

From: Andrew Piedl

Re: Bennington Battle Monument – Masonry Wall Moisture Analysis

Background:

The Bennington Battle Monument is a 306-foot-tall, circa 1891 stone masonry obelisk. A study is currently underway to assess the condition of the monument.

Steven Winter Associates (SWA) was engaged to analyze the hygrothermal properties of the masonry walls of the monument, which are currently saturated. SWA performed an analysis of the masonry wall to study options to promote drying of the masonry.

Methods:

Methods include visual observation, desk top research, review of relevant documents and use of WUFI software to analyze hygrothermal properties of the masonry. SWA also visited the site on 25 May 2023 to review existing conditions.

SWA reviewed available documents relevant to the hygrothermal analysis that include:

- Structural Engineering Evaluation, prepared by Silman and dated December 15, 2022
- Materials Examination Report prepared by Jablonski Building Conservation, Inc., (JBC) dated October 2023
- Stone Masonry Evaluation prepared by Atkinson-Noland & Associates, Inc. (ANA), dated September 20, 2023
- Monitoring Data Summary, prepared by ANA, dated March 4, 2023.

WUFI Pro 6.7 software was used to simulate the existing masonry wall assembly and options to promote drying. These options may include reducing water infiltration, lowering interior relative humidity, and increasing interior winter air temperature.

WUFI software simulates one-dimensional dynamic models; as described by its developer, it "allows realistic calculation of the transient coupled one- and two-dimensional heat and moisture transport in walls and other multi-layer building components exposed to natural weather". This software is typically used to analyze and optimize hygrothermal properties of proposed exterior wall assemblies and is used here to evaluate how climate may be manipulated to optimize drying of the currently saturated masonry.

Observations:

The walls at the base of the monument are more than seven feet thick and comprised of three wythes of stone. At the top of the structure, the walls diminish in thickness to two wythes of stone with a thickness of less than three feet. The stone masonry at the exterior is weathered, with severe deterioration at the upper portion of the monument. Existing conditions include cracks, failed mortar joints and spalling.

The stone masonry at the interior has signs of deterioration; existing conditions include cracks, deteriorated mortar joints, and elevated moisture content. The masonry conditions, including results of various repair campaigns are well documented in greater detail; refer to the reports listed above in the 'Methods' section.

The Materials Examination Report prepared by JBC identifies the stone at the exterior as Sandy Hill dolomite, a silicified dolomitic breccia limestone quarried in Hudson Falls NY. At the interior, there is a mix of locally quarried light-colored, fine grained calcitic marble and dark silicified dolomitic breccia. There appears to be a higher concentration of light-colored stone at the upper portion of the monument interior.

Original mortar at bed joints appears to be lime and Portland cement-based mortar formulation comparable to Type K mortar.

Available documentation suggests that collar joints and voids are filled with Portland cement-based mortar with large aggregate more similar to concrete than mortar.

Visual observation by SWA and water testing performed by others indicate that liquid water readily infiltrates the exterior surface and presents at the interior. At the lower portion of the structure, the interior surfaces of the masonry walls are visibly wet.

There are three active temperature / humidity monitors placed within the monument with more than one year of recorded data. Two of the monitors are sealed within the interior side of the stone masonry walls, located approximately 90 and 120 feet above grade. The third monitor, which records the ambient temperature and humidity of the interior climate, is located approximately 15 feet above grade.

Both monitors that are sealed within the masonry have recorded at or near 100 percent relative humidity (RH) since being installed. The interior climate monitor readings are relatively high, with an average of approximately 72 percent RH, varying between a low of 15% RH and a high of 100% RH. Regarding temperature, data from all three monitors exhibit a comparable pattern of fluctuation, but with the interior climate typically being a few degrees cooler than the temperature of the monitors embedded in the interior of the stone masonry.

A comparison of the interior climate relative humidity compared to the exterior weather relative humidity recorded at William H. Morse State Airport shows some similarity but varies by as much as 40%. In some instances, interior humidity is higher than exterior humidity; at other times interior humidity is lower than exterior humidity.

Bennington VT is in the International Building Code Climate Zone 6b (cold humid). The temperature typically varies from a high of approximately 80°F to a low of 14°F and rarely below above 86°F or -4°. During spring and autumn, the average monthly rainfall is between two to three inches. During summer, average rainfall is between three to four inches. In winter, the average snowfall is approximately ten inches.

There is no recognizable correlation between interior humidity, exterior humidity, and precipitation. Refer to Combined Relative Humidity, Exterior RH, Precipitation graph on page 12 of Monitoring Data Summary, prepared by ANA, dated March 4, 2022.

There are masonry openings with windows at two observation levels located approximately two-thirds up the height of the monument. Existing drawings also note pairs of slit windows at each elevation near the base, a column of four slit windows spaced approximately 35 feet vertically at the west elevation and approximately 20 screen vents located at the upper third of the monument.

WUFI Software Analysis

The intent of the WUFI analysis is to first establish a model of the existing configuration and climatic condition ('existing model') and then manipulate the climatic conditions to study their impact upon drying the stone masonry walls.

The exterior wall assembly used in the WUFI model is based upon the information obtained by one of the cores made by ANA for their Goodman Jack tests from the core hole made at the south wall (Ground Floor South Interior core, Core ID = ANA-SOUTH-4).

WUFI software has a material library that includes a limited number of stone types. The properties of the material library may be manipulated and customized for specific applications, but since there is little data for the physical properties of the stone used in the monument, materials from within the WUFI data base were used in the model.

For both the grey stone at the exterior and the dark stone at the interior, Georgian Bay Limestone was selected for the model because of its high resistance to water vapor transmission and similarity to the dolomitic limestone.

The Georgian Bay UNESCO Geopark's web site (<https://georgianbaygeopark.com/>) states that the "Georgian Bay Formation represents sediments collected far from the newly emerging Taconic Mountains. At High Falls, we can see shaley facies in the lower parts of the outcrop transition upwards into dolomitic limestones." To the best of our knowledge, this is the closest material to the silicified dolomitic breccia limestones used in the construction of the monument.

To further verify the material selection and calibrate the existing condition model, alternate stone materials were used in various models. The Georgian Bay Limestone produced results that were most consistent with observed conditions.

For exterior climate, a weather file for Albany NY was used in the model as being the closest available data for the climate for the Bennington VT location.

For interior climate, data for a full year of recorded interior relative humidity and temperature was reviewed and entered into the model. The recorded interior climate data, which includes daily fluctuation of temperature and humidity cannot be entered directly into the model, as the software only accepts averages and overall fluctuation as data.

The existing model also includes a 'moisture source' at the exterior material layer. This additional moisture source simulates water infiltration into the stone masonry wall due to naturally occurring precipitation. The actual amount of water infiltration is unknown, but a standard value based upon ANSI/ASHRAE standard 160, which is a 1% fraction of the rain load was used in the existing model.

The duration of the model is typically a default setting for a three-year period. Initial conditions are also a default setting beginning with relative humidity elevated to 80% uniformly distributed across all material layers.

Generally, the total water content within the full thickness of the masonry wall trends upward for the three-year model period. The model indicates that moisture content at the inner wythe of stone increases at a higher rate than the middle wythe, while water content at the exterior wythe decreases (refer to Appendix A - WUFI Analysis, Existing South Masonry Wall model, Pages 3-5). The moisture content within the modeled material layers is consistent with the observable conditions of the masonry wall.

Of all the variables that were manipulated, reduction of interior climate relative humidity was most effective for reducing masonry total water content (refer to Appendix A - WUFI Analysis, South Masonry Wall - No Added Moisture + Reduced Interior RH models, Pages 9-14).

This model includes a combination of both the elimination of additional moisture source and reduction of interior relative humidity from the existing 72% RH with a 50% amplitude to 60% RH with a 20% amplitude. The elimination of additional moisture source represents repair of exterior masonry wall surfaces: repointing existing open mortar joints and repairing cracks that facilitate water infiltration. As water infiltration through the masonry wall is a primary contributor to elevated interior humidity, eliminating the additional moisture source is necessary to reduce interior relative humidity. The results of other models that simulate the manipulation of additional moisture source without reduction of interior humidity are described below.

A peculiar result of the No Added Moisture + Reduced Interior RH model is that the middle wythe of masonry showed modest *increase* in water content during the three-year period, while total water content and water content at the inner wythe showed reduced moisture content.

To better understand both this peculiar increase of moisture at the middle wythe and the length of time necessary to reach full saturation of the interior wythe of masonry for the existing model, some models were run for a ten-year period. Interestingly, for the model with reduced relative humidity and water infiltration, water content within the middle wythe initially increases slightly for the first three years and then begins to decrease during remainder of the ten-year period (refer to Appendix A - WUFI Analysis, South Masonry Wall - No Added Moisture + Reduced Interior RH models, Page 13). For the existing model, moisture content at the interior wythe reaches 95% RH at approximately seven years, tapers off but continues to increase for the remaining ten years.

To better understand the effect of water infiltration on the masonry wall, two models simulated variations on the 1% fraction of the rain load ANSI/ASHRAE standard 160 used in the existing model. One model simulated the wall with no additional moisture source and a second model simulated the wall with 3% fraction of rain load moisture source. Both models indicate some change in moisture content. The model with no additional moisture shows modest change in moisture content at outer, middle and interior wythes of masonry (refer to Appendix A - WUFI Analysis, Existing South Masonry Wall - Without Added Moisture, Pages 15-17). When additional moisture source is increased to 3%, there is some, but only a modest increase in water content across the material layers (refer to Appendix A - WUFI Analysis, Existing South Masonry Wall - With Increased Moisture, Pages 18-19).

To better understand the effect of interior air temperature on the masonry wall, a model simulated interior climate with increased ambient air temperature. The model was based upon the existing model, but with 60° F with fluctuation of 20° F; and 72% RH with a 50% amplitude instead of the 55° F with fluctuation with 25° F existing condition. The model with increased interior air temperature shows modest change in moisture content at outer, middle and interior wythes of masonry (refer to Appendix A - WUFI Analysis, Existing South Masonry Wall - With Increased Ambient Temperature, Pages 20-21).

Conclusions:

- A. The existing WUFI model indicates elevated moisture content in the masonry wall, particularly at the inner wythe. This modeled condition is consistent with observations and recorded data. Excessive moisture content within a masonry structure is always concerning, but especially in northern climates where freeze-thaw cycles may occur.

A freeze-thaw cycle occurs when air temperature drops below freezing, then increases allowing ice to thaw again. This weathering process accelerates deterioration when saturated masonry freezes as the temperature drops. As the ice expands, it pushes the masonry apart. When the temperature rises, the ice melts, and water fills enlarged voids or cracks within the masonry. The water freezes again as the temperature falls, and the

expansion of the ice causes further expansion to the crack. The saturated condition of the masonry puts the entire structure at risk.

- B. The WUFI analysis generally indicates that for all models, the moisture content of the outer wythe, which begins with 80% RH, generally trends downward. A moisture content in masonry below 80% RH is generally safe. However, moisture content within the middle and inner wythes of masonry trend toward increased moisture content. These upward trends for the inner portions of the masonry are a concern. While the inner portions of the masonry wall are generally warmer than the exterior part of the wall, there are times when the temperature at the middle and inner wythe drop below freezing. At the same time freezing occurs, relative humidity is above 80% RH; conditions where deterioration of the stone may occur.
- C. Reducing water infiltration reduces water content within the masonry, but not as effectively as reducing interior relative humidity. However, to reduce interior humidity, the first step will be to reduce water infiltration which is the primary source for interior atmospheric humidity. Water that readily infiltrates the masonry walls produces an interior climate that is perpetually damp with relative humidity at the interior often higher than exterior relative humidity, especially during cold weather. WUFI analysis suggests that interior elevated relative humidity produces increased moisture content within the inner portion of the masonry wall and that this moisture content slowly dries toward the exterior through the full thickness of the masonry assembly.
- D. Introduction of a minimal amount of heat to increase the average interior air temperature by five degrees Fahrenheit does very little to reduce total water content within the masonry wall assembly. This increase in air temperature slows down but does not reverse the trend toward increased moisture content within the masonry wall assembly.

Recommendations:

- 1. While reducing interior elevated humidity is the primary recommendation to reverse the increasing moisture trend in the stone masonry, this cannot be achieved without first substantially reducing water infiltration through the masonry walls.
- 2. To reduce water infiltration through the masonry walls, repair of the exterior masonry walls is required. Design repairs to minimize infiltration of liquid water while maximizing water vapor transmission to enhance outward drying of the masonry walls. Specific recommendations for exterior masonry repair are within the scope of work of other design team members, but generally these will include:
 - a. Raking and repointing existing open, cracked, and deteriorated mortar joints with appropriate mortar.
 - b. Repairing open cracks in the stone masonry.
 - c. Where possible, remove and avoid water vapor-impermeable products such as epoxies, bituminous mastic, and impermeable sealants, coatings and sealers in repairing the exterior surface of the masonry.
 - d. Limit use of impermeable water control products such as sealants and metal flashing or joint covers to upward facing, horizontal surfaces.
 - e. Prior to any masonry cleaning, make necessary repairs or temporary measures to minimize water infiltration into the masonry because of the cleaning process.
- 3. Consider providing some type of temporary protection against water infiltration as soon as possible; assuming that the structure will be scaffolded during restoration, it may be

possible to incorporate some type of temporary 'roof' and enclosure at exterior walls to reduce water uptake in the masonry. This could also serve as an opportunity for 'signage' or a simple but decorative temporary enclosure to transmit a message to the public regarding the extraordinary restoration occurring at the monument.

4. Reduce interior elevated humidity by optimizing ventilation. This may be achieved by passive or mechanical methods during optimal weather conditions, such as when exterior relative humidity is lower than interior relative humidity (generally during spring, winter and autumn). Consider strategies to improve ventilation and reduce humidity for temporary period before repair campaign commences, temporarily during construction and by more permanent methods after completion of construction.
5. If budgets allow, perform additional material testing to verify the hygrothermal properties of each type of stone present in the monument. These would allow for more accurate analysis and include:
 - Physical property – inch pound units (metric/SI units)
 - Bulk density – lbs/ft³ (kg/m³)
 - Porosity - ft³ /ft³ (m³/m³)
 - Specific Heat Capacity – Btu/lb °F (J/kg K)
 - Thermal Conductivity – Btu/h ft °F (W/mK)
 - Permeability – perm inch (Water Vapor Diffusion Resistance Factor)
6. Continue monitoring interior climate (relative humidity and temperature). In addition, consider adding monitors at the upper portion of the monument to record temperature and relative humidity at both the inner wythe of stone and the ambient interior climate.

End of written report

South Masonry Wall Analysis

Table of Contents:

Page 1	Table of Contents	Page 12	South Masonry Wall - No Added Moisture + Reduced Interior RH: Total Water Content + Water Content Limestone Layer 1 (Ten Year Period):
Page 2	South Masonry Wall Analysis: Introduction	Page 13	South Masonry Wall - No Added Moisture + Reduced Interior RH: Water Content Limestone Layer 2 + Water Content Limestone Layer 3 (Ten Year Period):
Page 3	Existing South Masonry Wall: Total Water Content + Water Content Limestone Layer 1	Page 14	South Masonry Wall - No Added Moisture + Reduced Interior RH: Temperature / RH at Monitor 3 + Temperature / Dew Point at Monitor 3 (Ten Year Period):
Page 4	Existing South Masonry Wall: Water Content Limestone Layer 2 + Water Content Limestone Layer 3	Page 15	South Masonry Wall - Without Added Moisture: Total Water Content + Water Content Limestone Layer 1
Page 5	Existing South Masonry Wall: Temperature / Relative Humidity (RH) at Monitor 3 + Temperature / Dew Point at Monitor 3	Page 16	South Masonry Wall - Without Added Moisture: Water Content Limestone Layer 2 + Water Content Limestone Layer 3
Page 6	Existing South Masonry Wall (Ten Year Period): Total Water Content + Water Content Limestone Layer 1	Page 17	South Masonry Wall - Without Added Moisture: Temperature / RH at Monitor 3 + Temperature / Dew Point at Monitor 3
Page 7	Existing South Masonry Wall (Ten Year Period): Water Content Limestone Layer 2 + Water Content Limestone Layer 3	Page 18	South Masonry Wall - With Increased Moisture: Total Water Content + Water Content Limestone Layer 1
Page 8	Existing South Masonry Wall (Ten Year Period): Temperature / Relative Humidity (RH) at Monitor 3 + Temperature / Dew Point at Monitor 3	Page 19	South Masonry Wall - With Increased Moisture: Water Content Limestone Layer 2 + Water Content Limestone Layer 3
Page 9	South Masonry Wall - No Added Moisture + Reduced Interior RH: Total Water Content + Water Content Limestone Layer 1	Page 20	South Masonry Wall - With Increased Ambient Temperature: Total Water Content + Water Content Limestone Layer 1
Page 10	South Masonry Wall - No Added Moisture + Reduced Interior RH: Water Content Limestone Layer 2 + Water Content Limestone Layer 3	Page 21	South Masonry Wall - With Increased Ambient Temperature: Water Content Limestone Layer 2 + Water Content Limestone Layer 3
Page 11	South Masonry Wall - No Added Moisture + Reduced Interior RH: Temperature / RH at Monitor 3 + Temperature / Dew Point at Monitor 3		

South Masonry Wall Analysis

Introduction

Intent

The intent of the WUFI analysis is to first establish a model of the existing configuration and climatic condition (referred to as the 'existing model') and then manipulate the climatic conditions to study their impact upon drying the stone masonry walls.

Model Description

WUFI Pro Version 6.7 software, as described by its developer, "allows realistic calculation of the transient coupled one- and two-dimensional heat and moisture transport in walls and other multi-layer building components exposed to natural weather". The software was used to model the existing proposed skylight assemblies.

Existing Assembly

The exterior wall assembly used in the WUFI model is based upon the information obtained by one of the cores made by Atkinson-Noland & Associates, Inc. for their Goodman Jack tests from the core hole made at the south wall (Ground Floor South Interior core, Core ID = ANA-SOUTH-4).

Weather location for the model was Albany NY as being the closest available data for the climate for the Bennington VT location.

The existing model includes a 'moisture source' at the exterior material layer. This additional moisture source simulates water infiltration into the stone masonry wall due to naturally occurring precipitation, based upon ANSI/ASHRAE standard 160, which is a 1% fraction of the rain load was used in the existing model.

For interior climate, data for a full year of recorded interior relative humidity and temperature was reviewed and entered into the model as 55° F with fluctuation of 25° F; and 72% RH with a 50% amplitude

Hygrothermal Behavior Summary

For the Existing Assembly, the WUFI model indicates that generally, the total water content within the full thickness of the masonry wall trends upward for the three-year model period. The model indicates that moisture content at the inner wythe of stone increases at a higher rate than the middle wythe, while water content at the exterior wythe decreases (Existing South Masonry Wall model, Pages 3-8). The moisture content within the modeled material layers is consistent with the observable conditions of the masonry wall.

Of all the variables that were manipulated, reduction of interior climate relative humidity was most effective for reducing masonry total water content (South Masonry Wall - No Added Moisture + Reduced Interior RH models, Pages 9-14). This model used an interior climate with 60% RH with a 20% amplitude with 55° F with fluctuation of 25° F

One model simulated the wall with no additional moisture source and a second model simulated the wall with 3% fraction of rain load moisture source. Both models indicate some change in moisture content. The model with no additional moisture shows modest change in moisture content at outer, middle and interior wythes of masonry (Existing South Masonry Wall - Without Added Moisture, Pages 15-17). When additional moisture source is increased to 3%, there is some, but only a modest increase in water content across the material layers (Existing South Masonry Wall - With Increased Moisture, Pages 18-19).

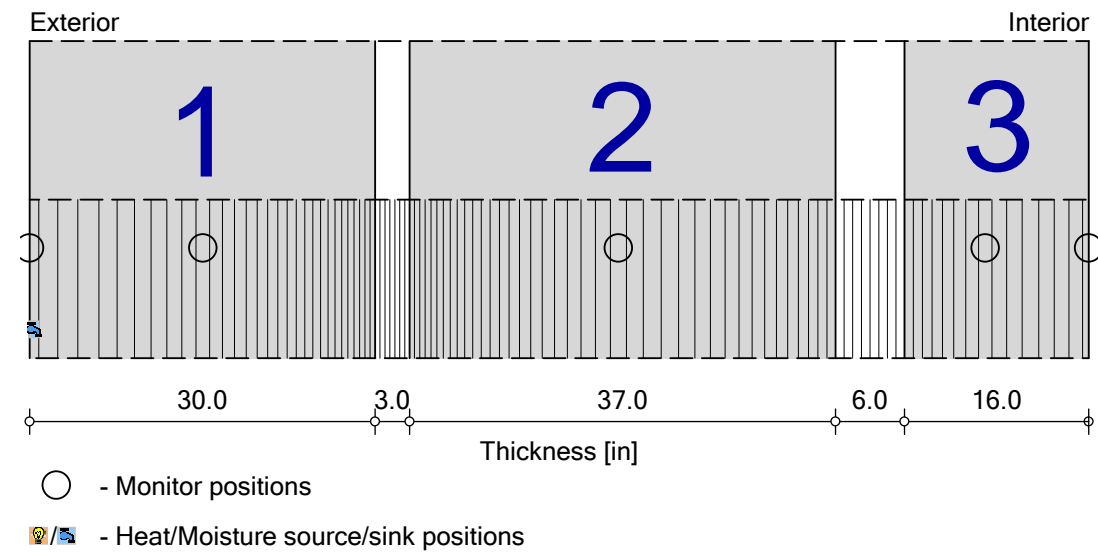
One model simulated interior climate with increased ambient air temperature with 60° F with fluctuation of 20° F; and 72% RH with a 50% amplitude instead of the 55° F with fluctuation of 25° F existing condition. The model with increased interior air temperature shows modest change in moisture content at outer, middle and interior wythes of masonry (Existing South Masonry Wall - With Increased Ambient Temperature, Pages 20-21).

South Masonry Wall Analysis

Existing South Masonry Wall

Boundary Conditions

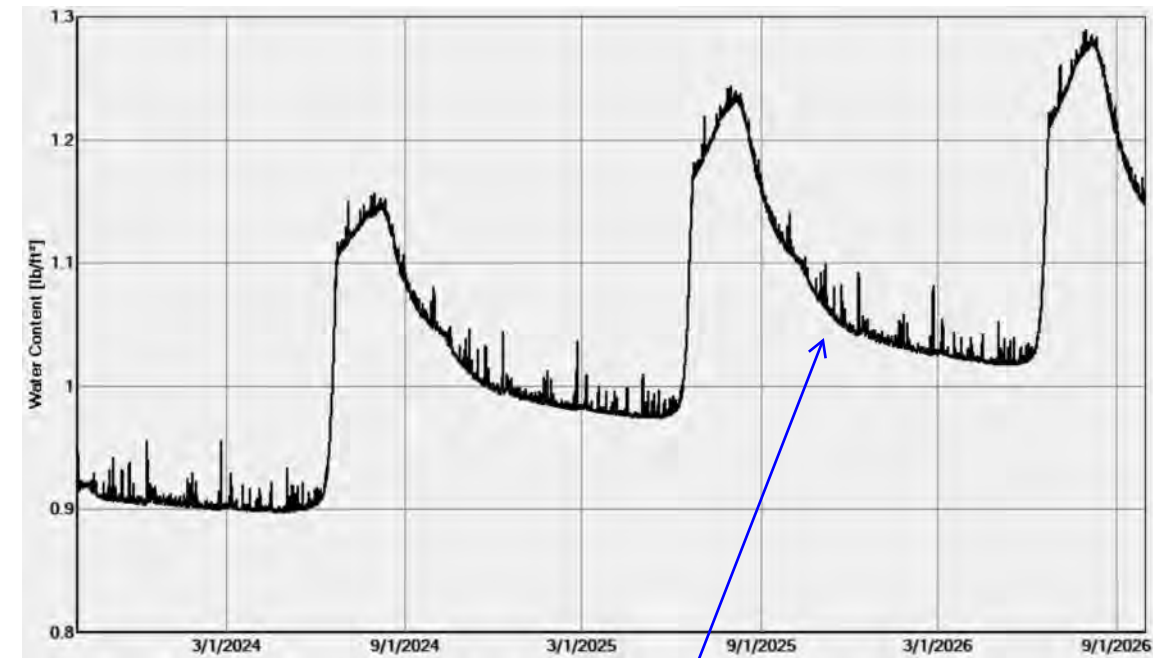
Exterior (left side) Albany, NY
 Interior (right side) 55° F with fluctuation of 25° F; and 72% RH with a 50% amplitude
 Moisture Source Exterior Limestone Layer - 1% (ANSI/ASHRAE standard 160)



Materials:

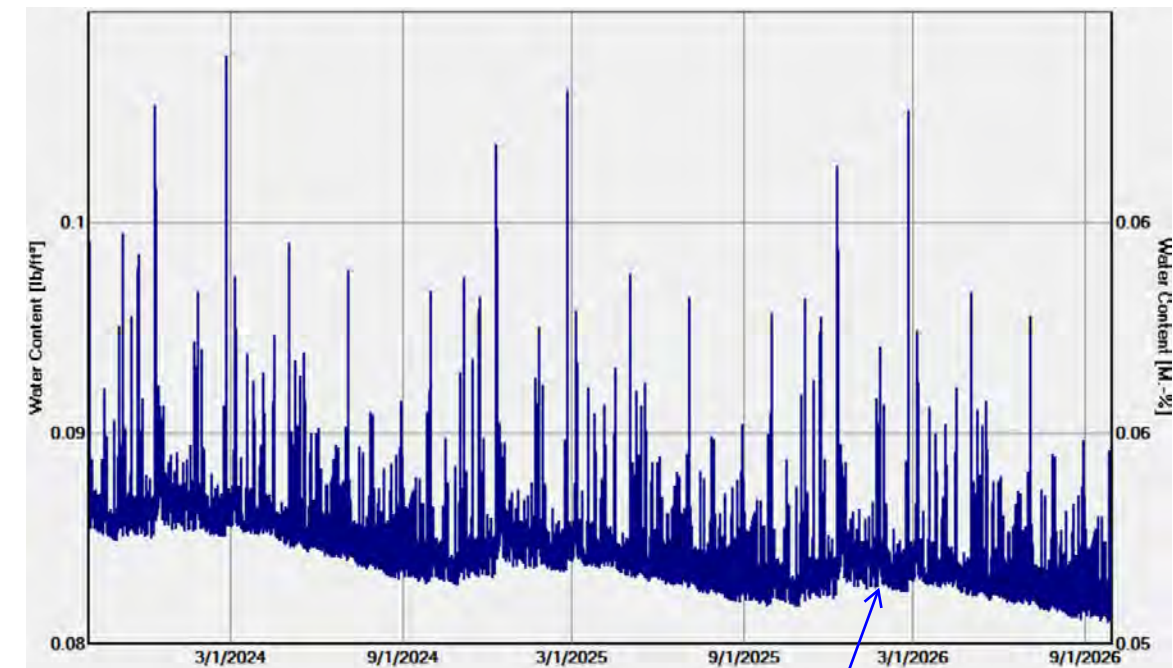
	- Limestone (Georgian Bay Limestone)	30.0 in
	- Lime Mortar, fine	3.0 in
	- Limestone (Georgian Bay Limestone)	37.0 in
	- Lime Mortar, fine	6.0 in
	- Limestone (Georgian Bay Limestone)	16.0 in

Total Water Content - Existing Masonry Wall



Total Water Content (for the entire wall assembly) increases during the 3-year period

Water Content - Limestone Layer 1



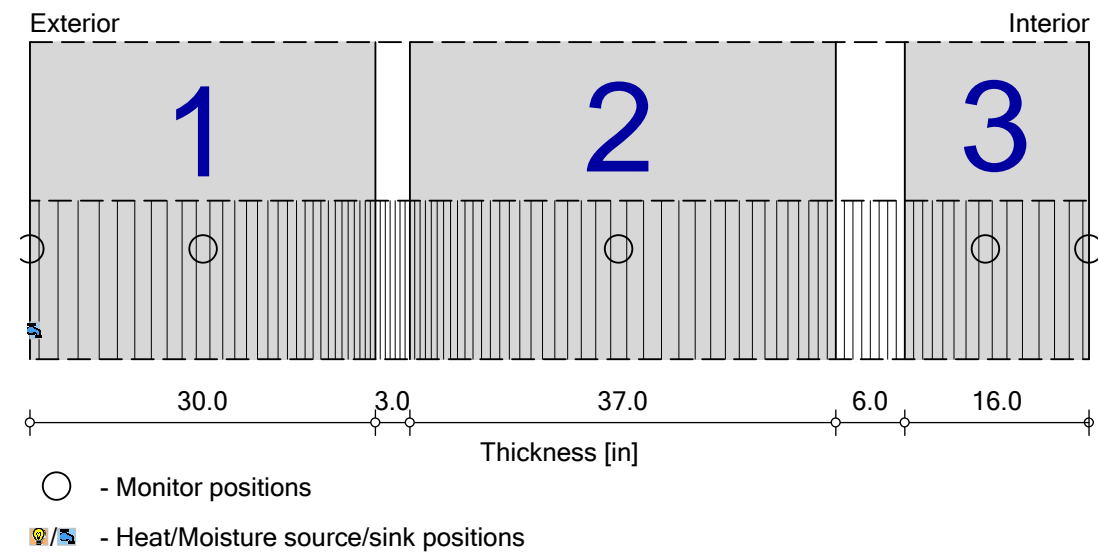
Water content at this exterior layer fluctuates with weather and precipitation events, with a modest downward seasonal trend

South Masonry Wall Analysis

Existing South Masonry Wall

Boundary Conditions

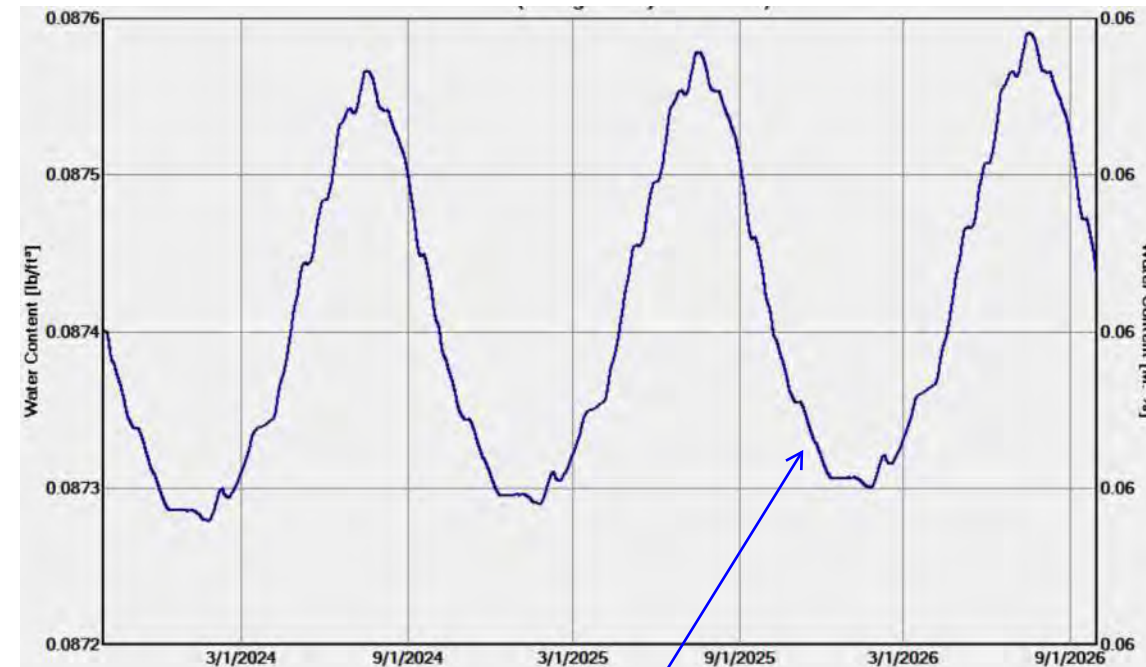
Exterior (left side) Albany, NY
 Interior (right side) 55° F with fluctuation of 25° F; and 72% RH with a 50% amplitude
 Moisture Source Exterior Limestone Layer - 1% (ANSI/ASHRAE standard 160)



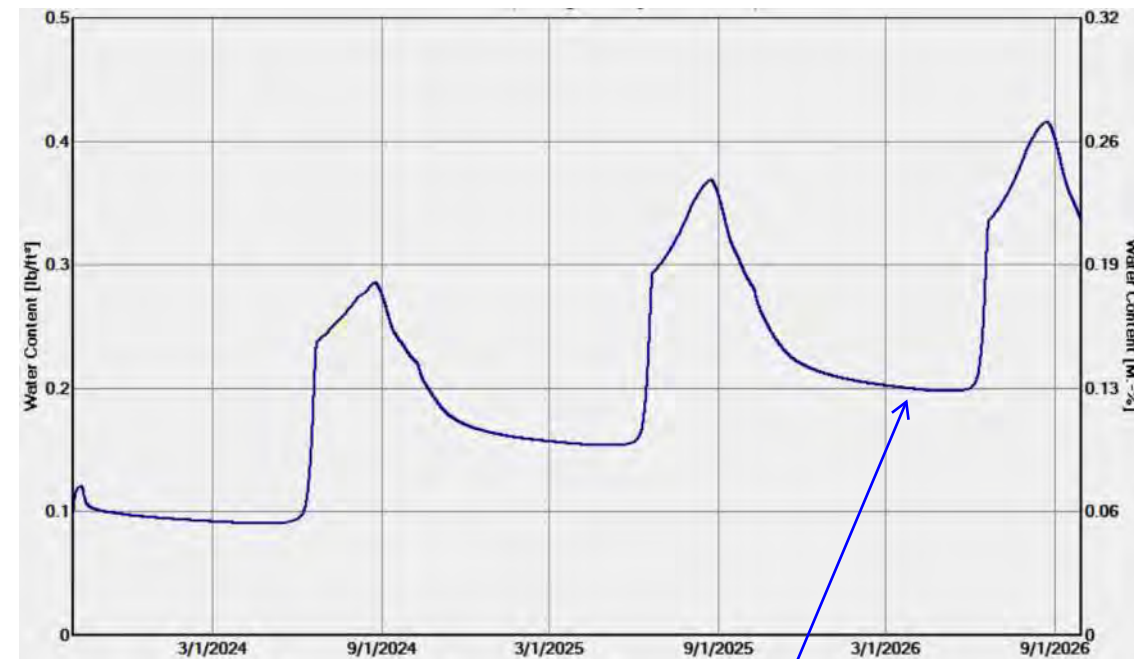
Materials:

	- Limestone (Georgian Bay Limestone)	30.0 in
	- Lime Mortar, fine	3.0 in
	- Limestone (Georgian Bay Limestone)	37.0 in
	- Lime Mortar, fine	6.0 in
	- Limestone (Georgian Bay Limestone)	16.0 in

Water Content - Limestone Layer 2



Water Content - Limestone Layer 3

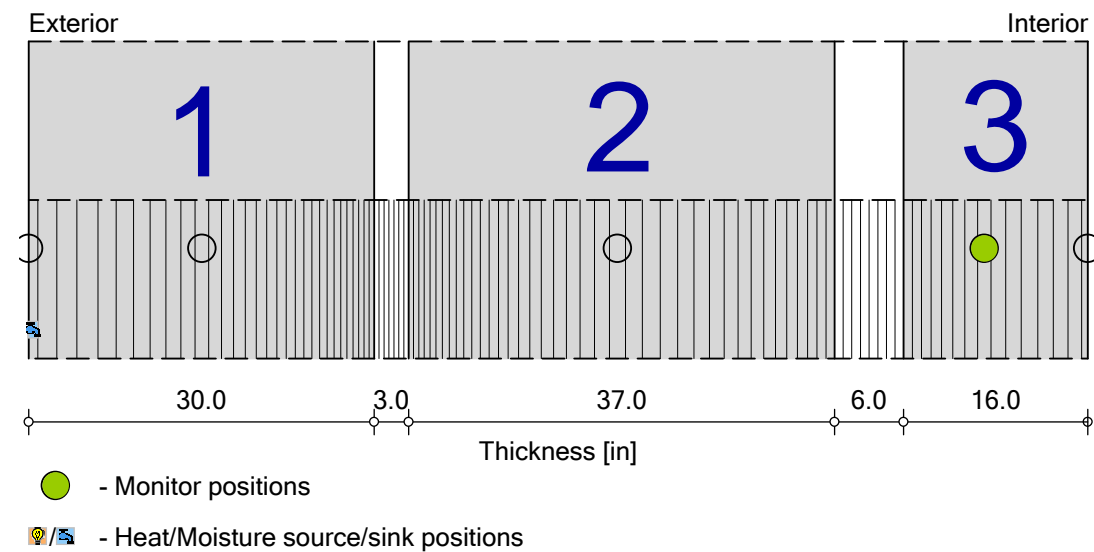


South Masonry Wall Analysis

Existing South Masonry Wall

Boundary Conditions

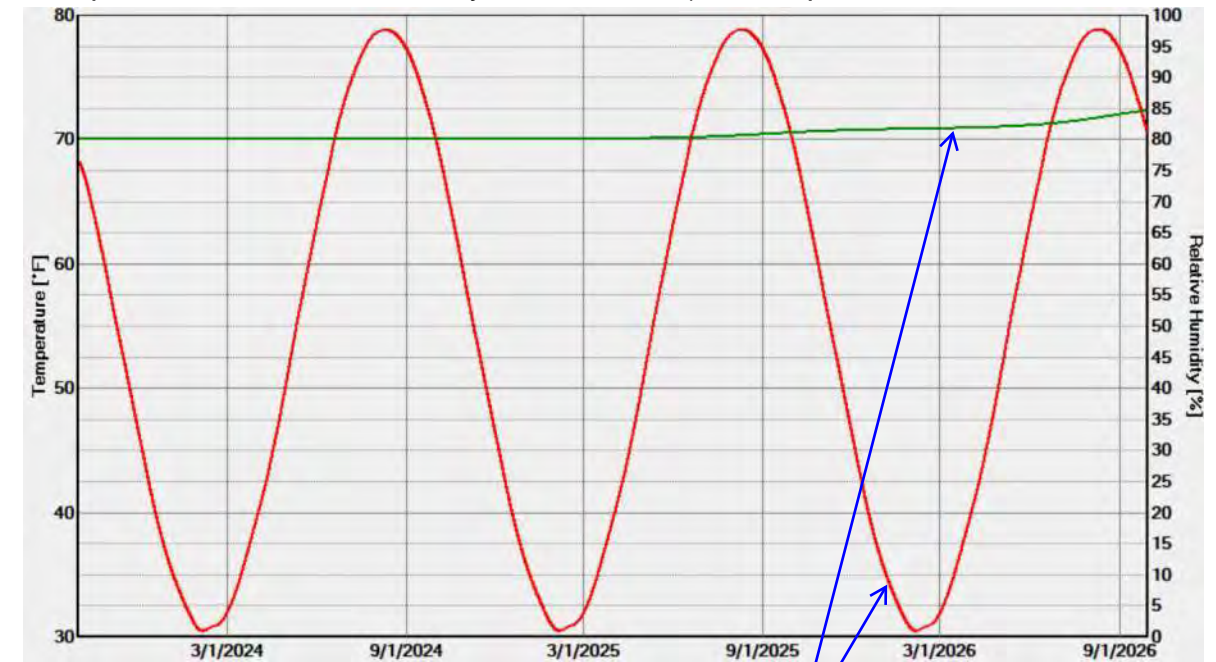
Exterior (left side) Albany, NY
 Interior (right side) 55° F with fluctuation of 25° F; and 72% RH with a 50% amplitude
 Moisture Source Exterior Limestone Layer - 1% (ANSI/ASHRAE standard 160)



Materials:

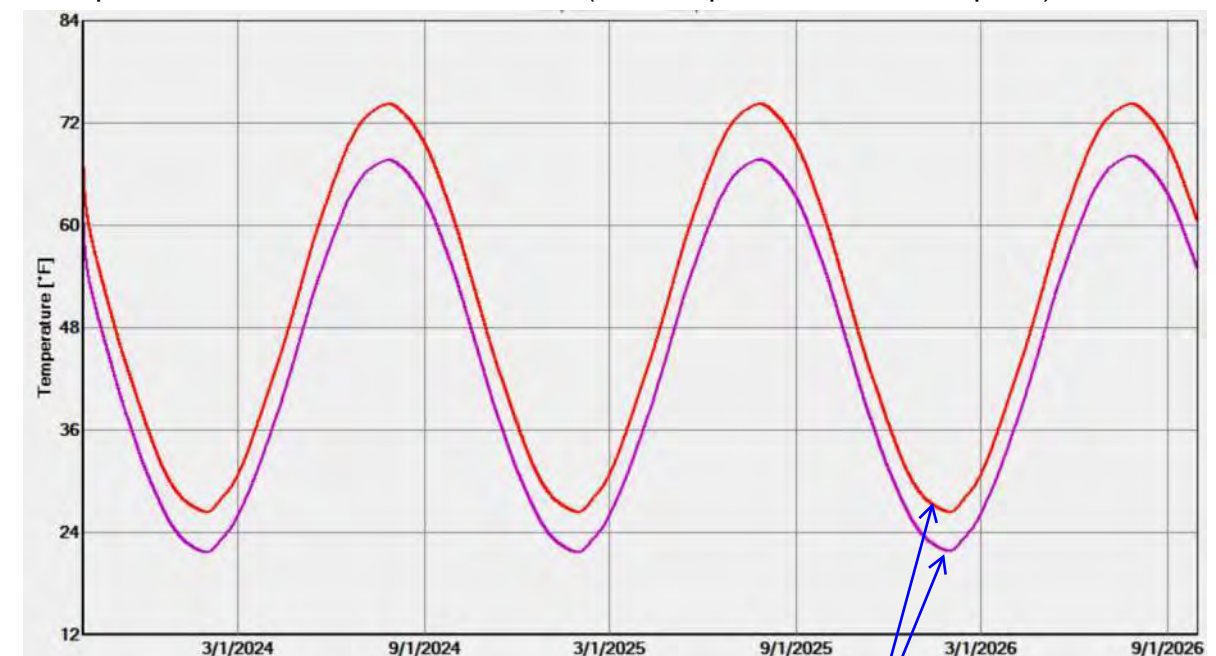
	- Limestone (Georgian Bay Limestone)	30.0 in
	- Lime Mortar, fine	3.0 in
	- Limestone (Georgian Bay Limestone)	37.0 in
	- Lime Mortar, fine	6.0 in
	- Limestone (Georgian Bay Limestone)	16.0 in

Temperature / Relative Humidity at **Monitor 3** (--- temperature / - - - relative humidity)



Temperature fluctuates seasonally; Relative Humidity (RH) trends upward during the 3-year period

Temperature / Dew Point at **Monitor 3** (--- temperature / - - - dew point)



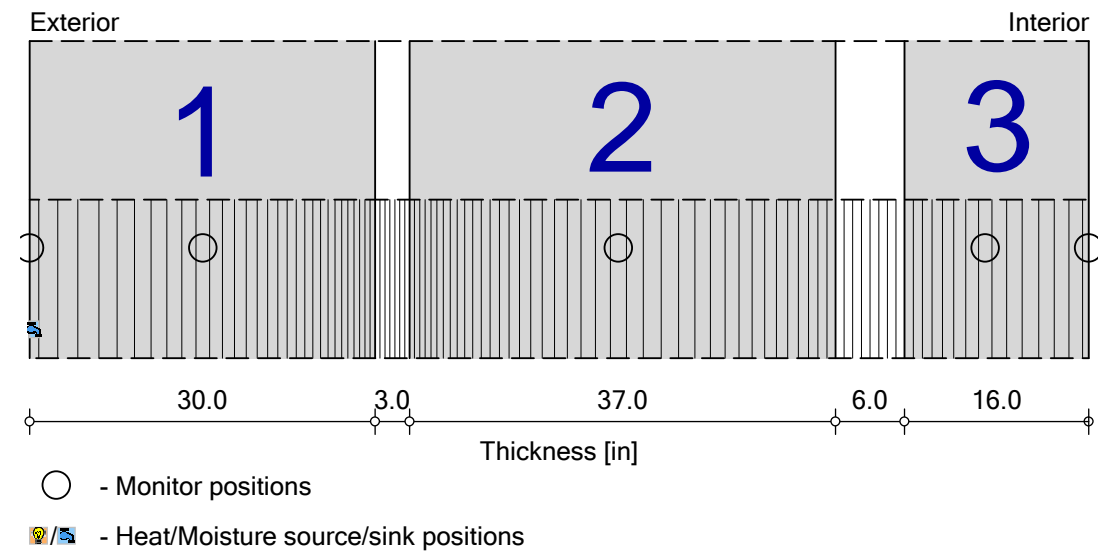
Temperature fluctuates seasonally; Temperature and Dew Point do not intersect (signifies low condensation risk)

South Masonry Wall Analysis

Existing South Masonry Wall (Ten Year Period)

Boundary Conditions

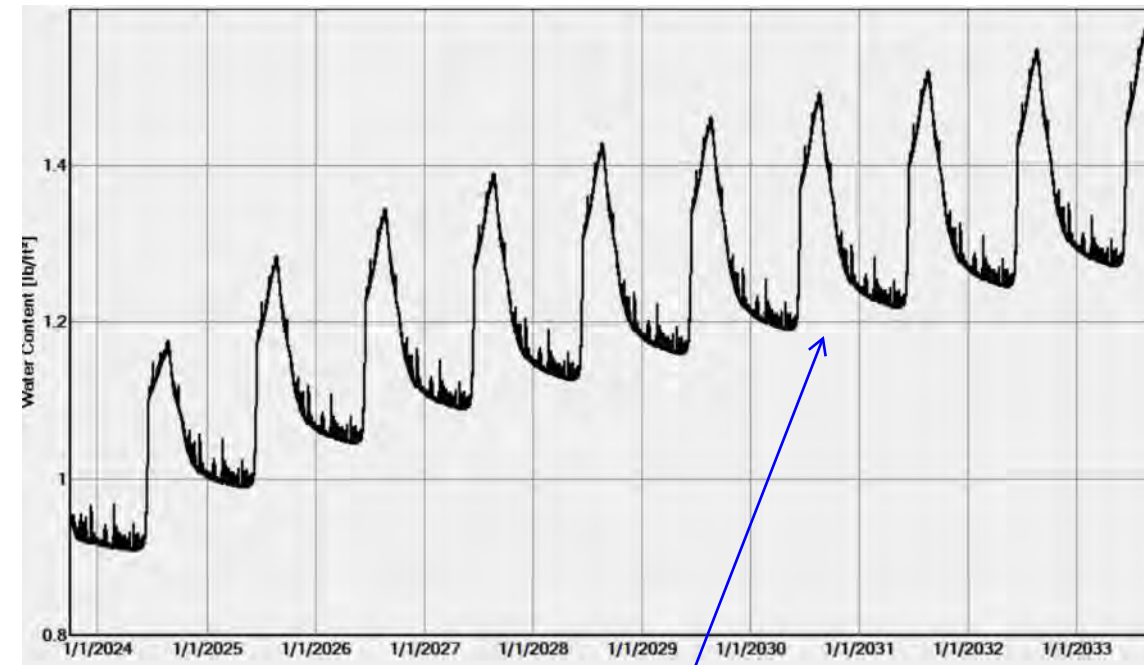
Exterior (left side) Albany, NY
 Interior (right side) 55° F with fluctuation of 25° F; and 72% RH with a 50% amplitude
 Moisture Source Exterior Limestone Layer - 1% (ANSI/ASHRAE standard 160)



Materials:

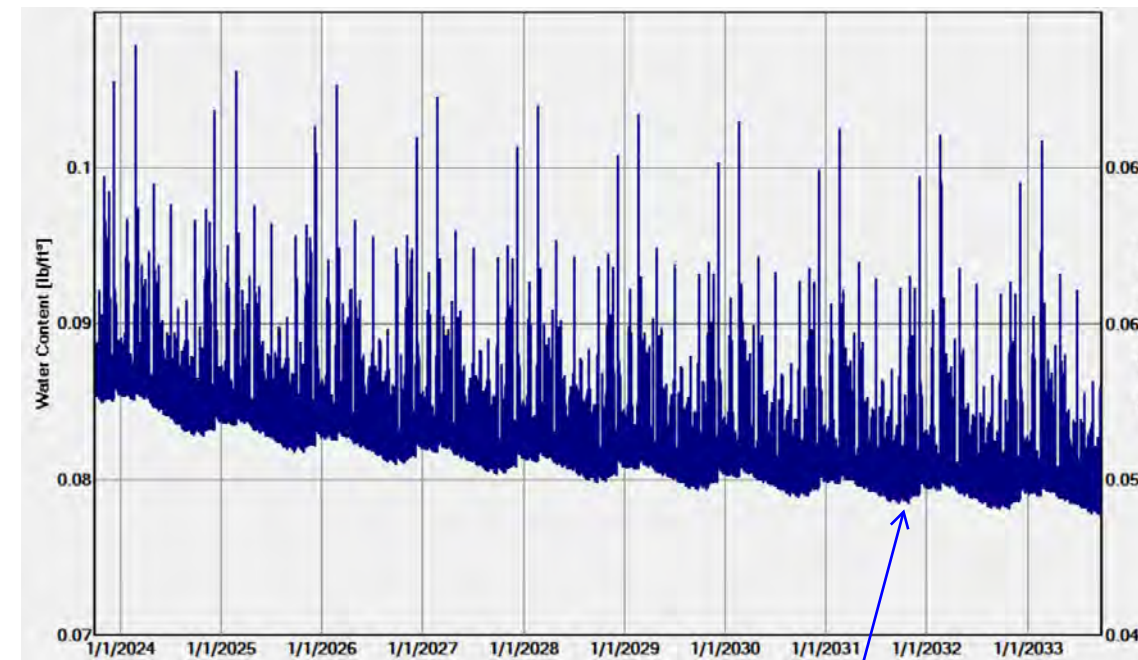
	- Limestone (Georgian Bay Limestone)	30.0 in
	- Lime Mortar, fine	3.0 in
	- Limestone (Georgian Bay Limestone)	37.0 in
	- Lime Mortar, fine	6.0 in
	- Limestone (Georgian Bay Limestone)	16.0 in

Total Water Content - Existing Masonry Wall



Total Water Content (for the entire wall assembly) increases during the 10-year period

Water Content - Limestone Layer 1



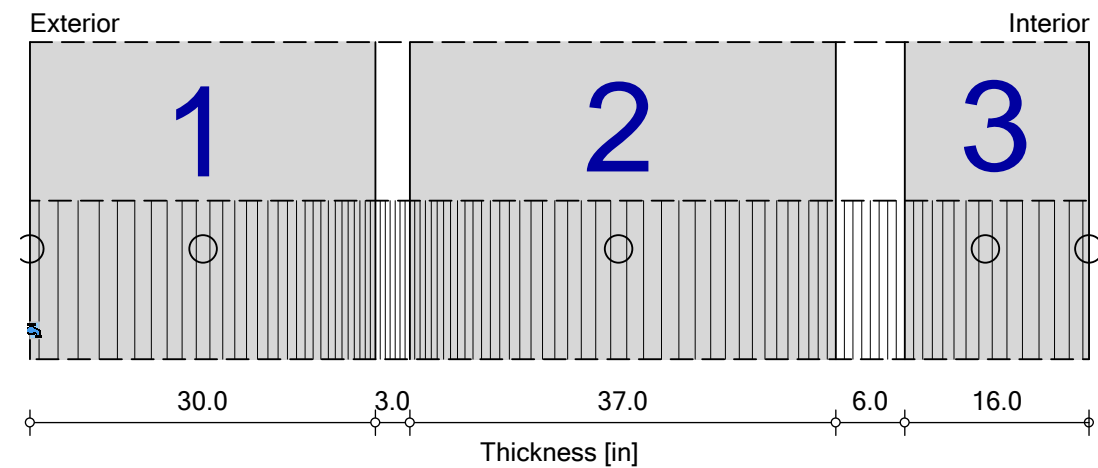
Water content at this exterior layer fluctuates with weather and precipitation events, with a modest, consistent downward trend

South Masonry Wall Analysis

Existing South Masonry Wall (Ten Year Period)

Boundary Conditions

Exterior (left side) Albany, NY
 Interior (right side) 55° F with fluctuation of 25° F; and 72% RH with a 50% amplitude
 Moisture Source Exterior Limestone Layer - 1% (ANSI/ASHRAE standard 160)

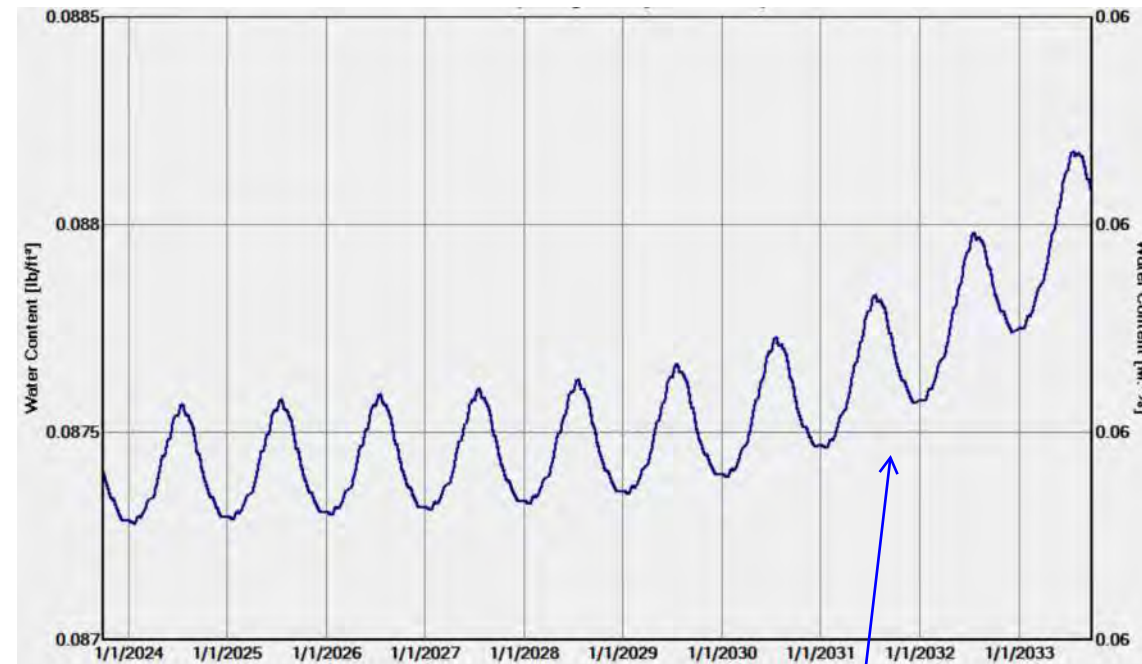


○ - Monitor positions
 - Heat/Moisture source/sink positions

Materials:

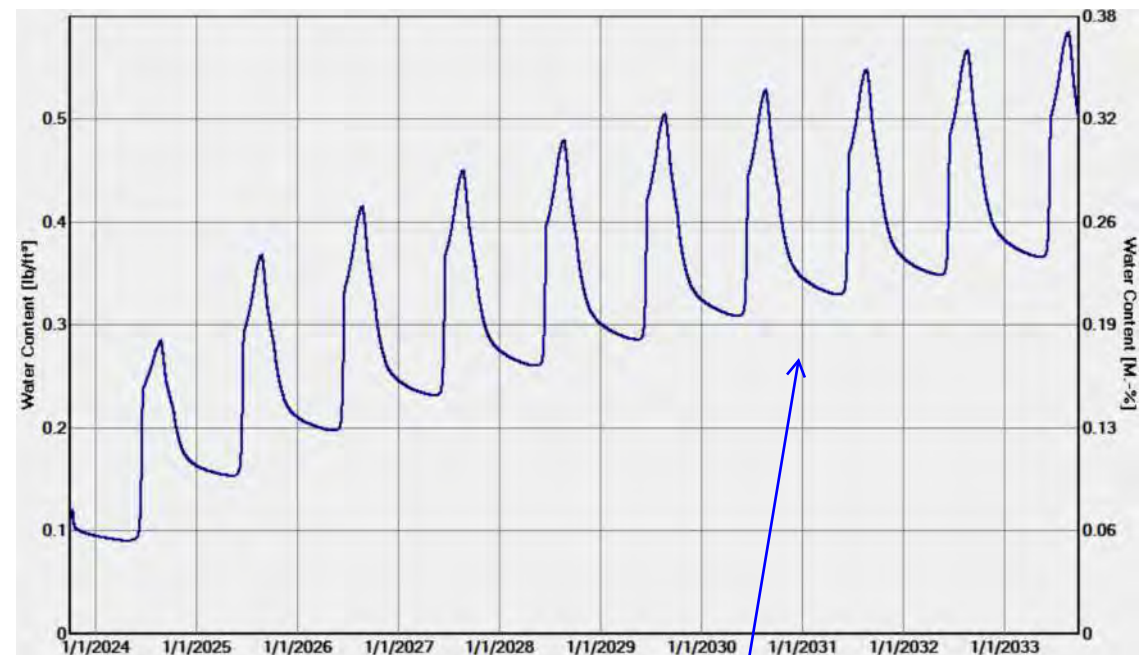
	- Limestone (Georgian Bay Limestone)	30.0 in
	- Lime Mortar, fine	3.0 in
	- Limestone (Georgian Bay Limestone)	37.0 in
	- Lime Mortar, fine	6.0 in
	- Limestone (Georgian Bay Limestone)	16.0 in

Water Content - Limestone Layer 2



Water content at the middle layer fluctuates seasonally, with modest upward trend that increase more rapidly after six years

Water Content - Limestone Layer 3



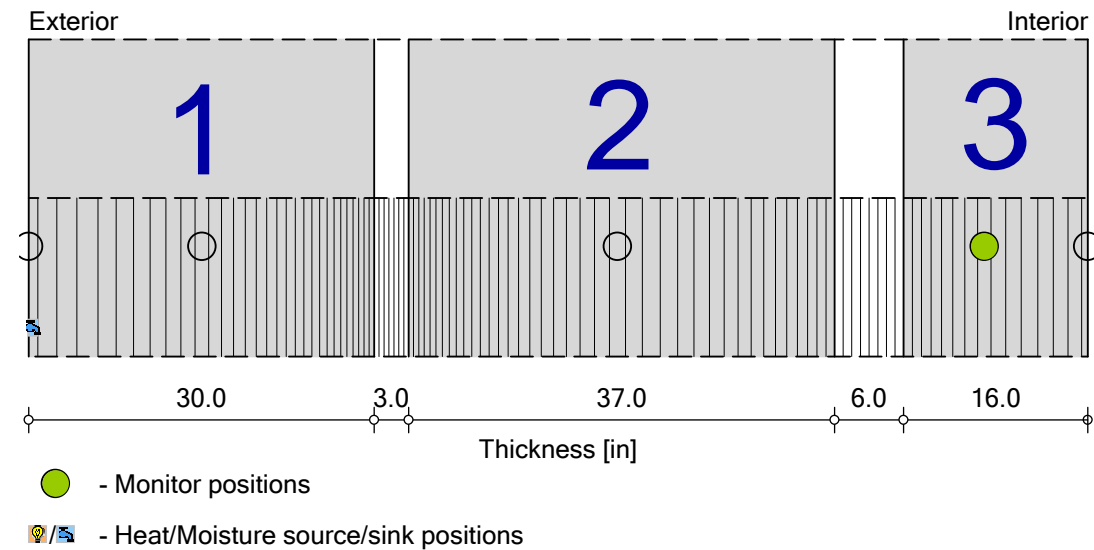
Water content at the interior layer fluctuates seasonally, with significant increase during the 10-year period

South Masonry Wall Analysis

Existing South Masonry Wall (Ten Year Period)

Boundary Conditions

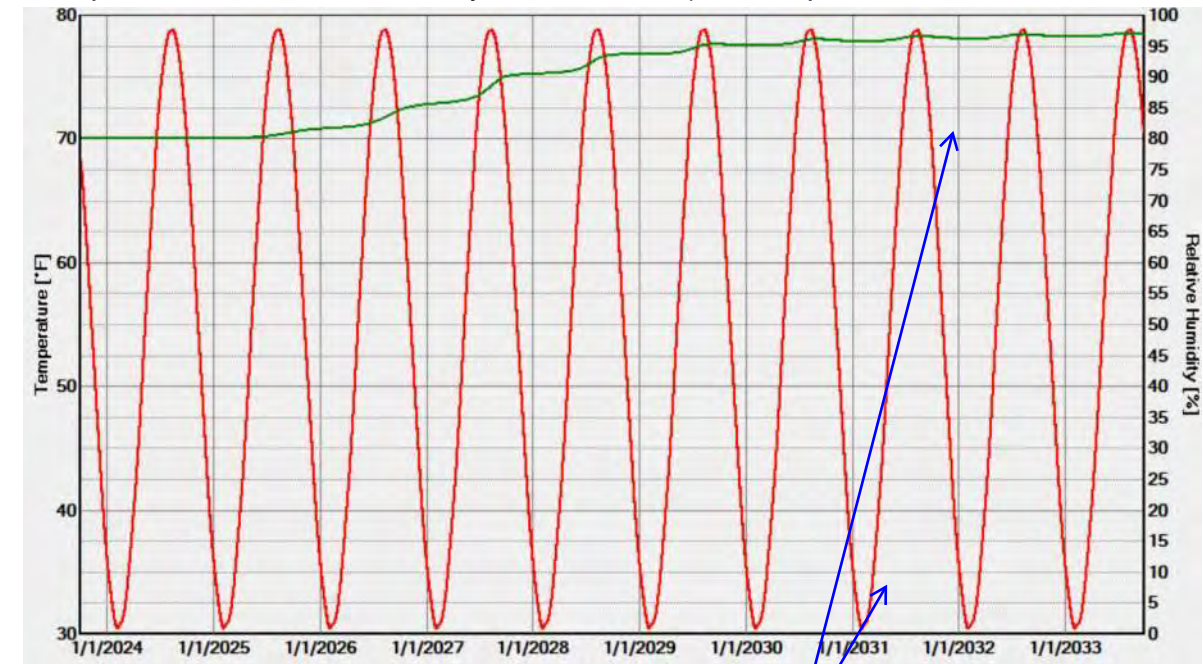
Exterior (left side) Albany, NY
 Interior (right side) 55° F with fluctuation of 25° F; and 72% RH with a 50% amplitude
 Moisture Source Exterior Limestone Layer - 1% (ANSI/ASHRAE standard 160)



Materials:

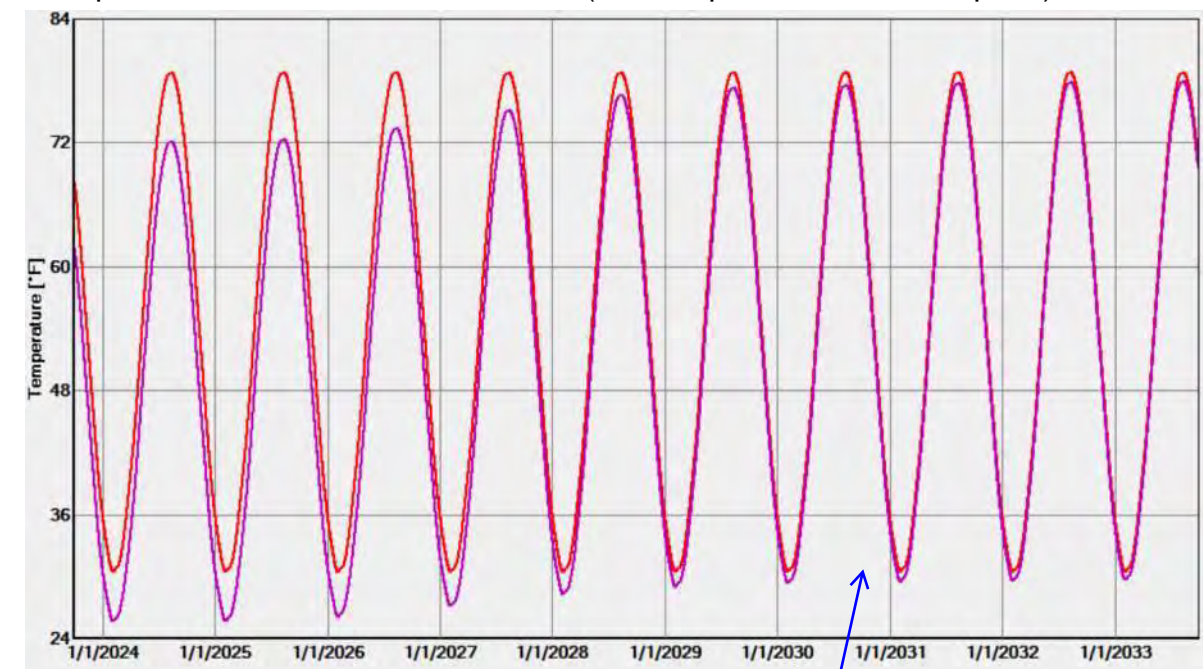
	- Limestone (Georgian Bay Limestone)	30.0 in
	- Lime Mortar, fine	3.0 in
	- Limestone (Georgian Bay Limestone)	37.0 in
	- Lime Mortar, fine	6.0 in
	- Limestone (Georgian Bay Limestone)	16.0 in

Temperature / Relative Humidity at **Monitor 3** (--- temperature / --- relative humidity)



Temperature fluctuates seasonally; Relative Humidity (RH) trends upward during the 10-year period

Temperature / Dew Point at **Monitor 3** (--- temperature / --- dew point)



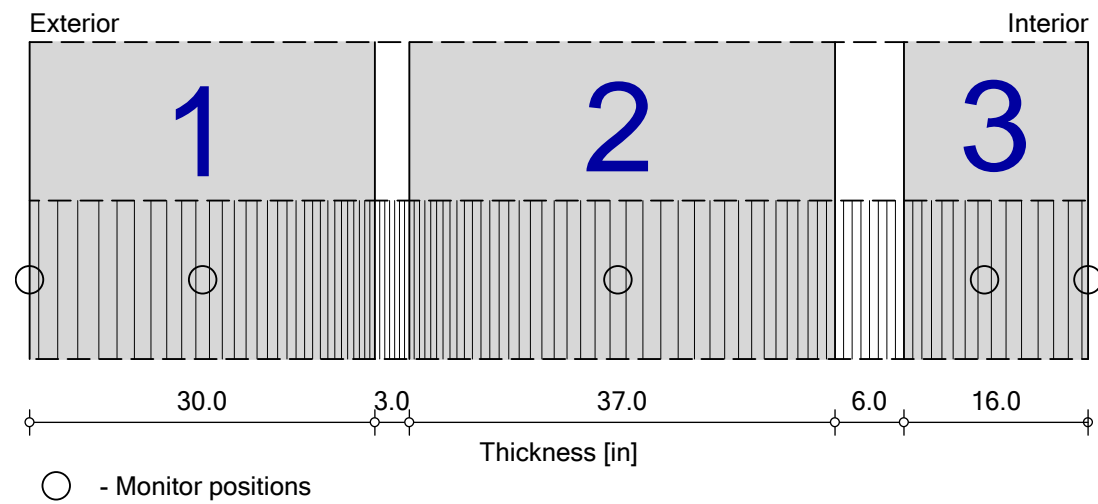
Temperature fluctuates seasonally; Temperature and Dew Point do not intersect, but graphs begin to intersect after six years (signifies condensation risk)

South Masonry Wall Analysis



South Masonry Wall - No Added Moisture + Reduced Interior RH

Boundary Conditions

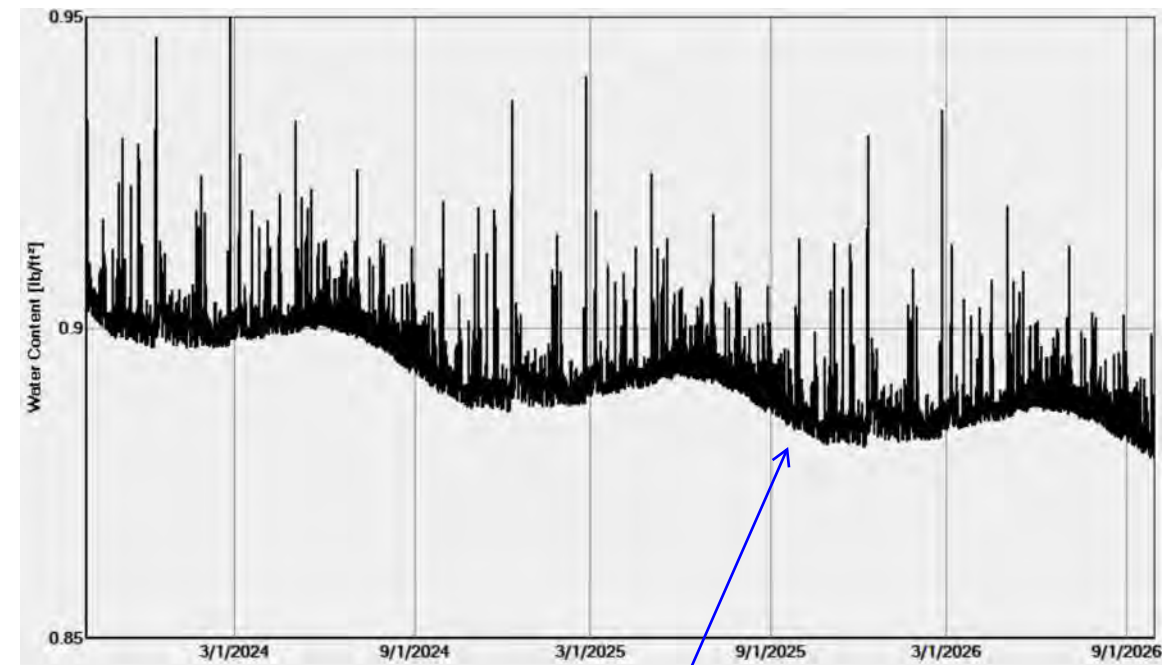
Exterior (left side) Albany, NY
 Interior (right side) 55° F with fluctuation of 25° F; and 60% RH with a 20% amplitude



Materials:

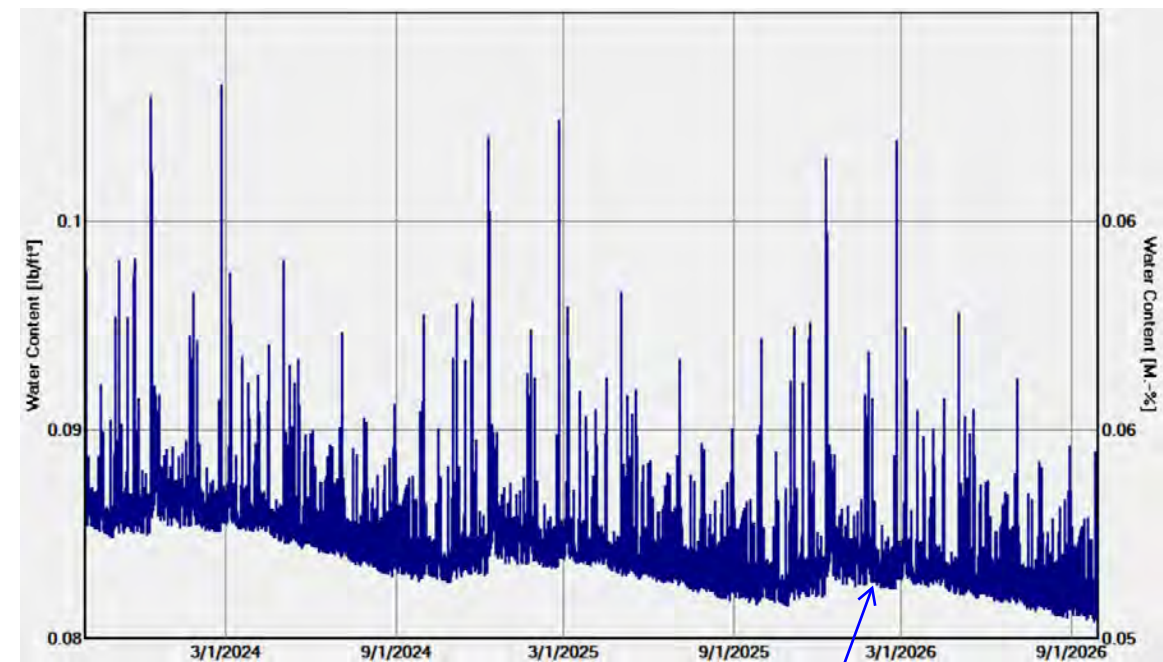
	- Limestone (Georgian Bay Limestone)	30.0 in
	- Lime Mortar, fine	3.0 in
	- Limestone (Georgian Bay Limestone)	37.0 in
	- Lime Mortar, fine	6.0 in
	- Limestone (Georgian Bay Limestone)	16.0 in

Total Water Content - Existing Masonry Wall



Total Water Content (for the entire wall assembly) trends downward during the 3-year period

Water Content - Limestone Layer 1



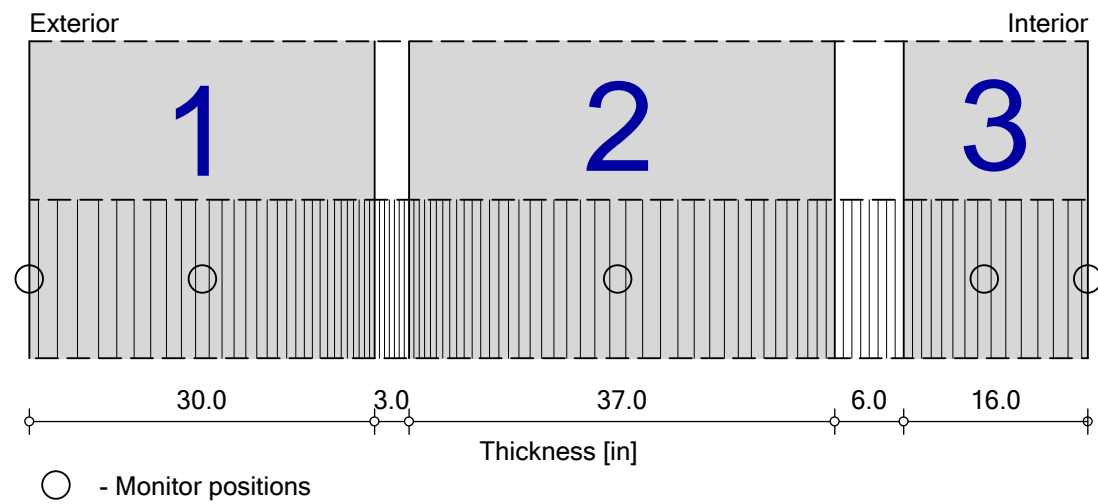
Water content at this exterior layer fluctuates with weather and precipitation events, with a modest downward seasonal trend

South Masonry Wall Analysis

South Masonry Wall - No Added Moisture + Reduced Interior RH

Boundary Conditions

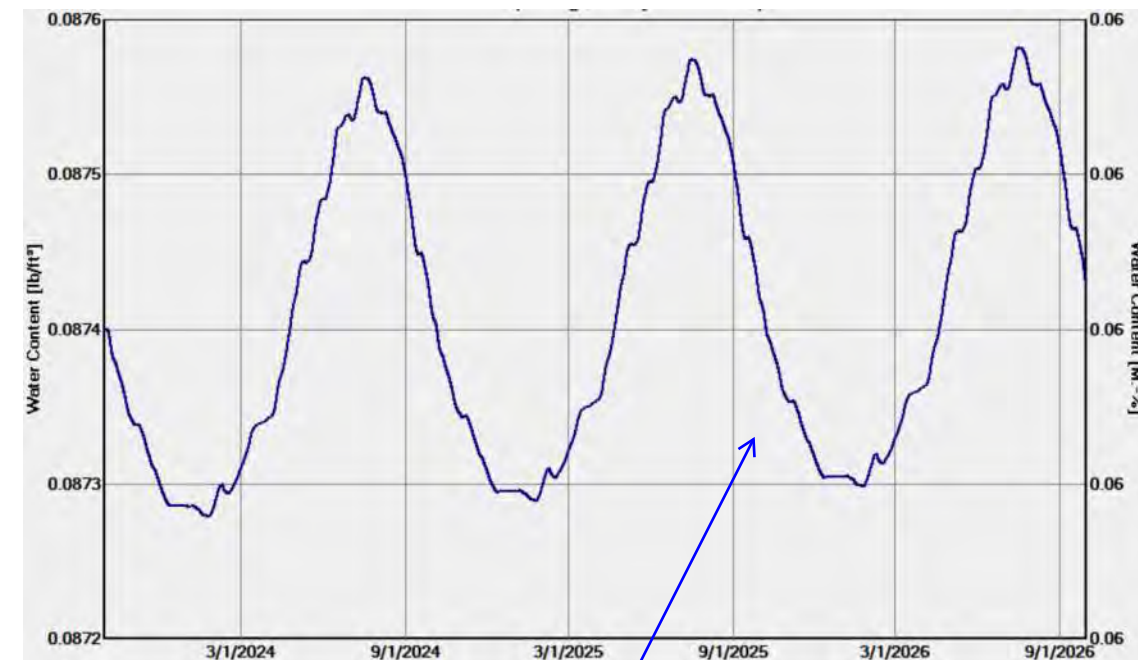
Exterior (left side) Albany, NY
 Interior (right side) 55° F with fluctuation of 25° F; and 60% RH with a 20% amplitude



Materials:

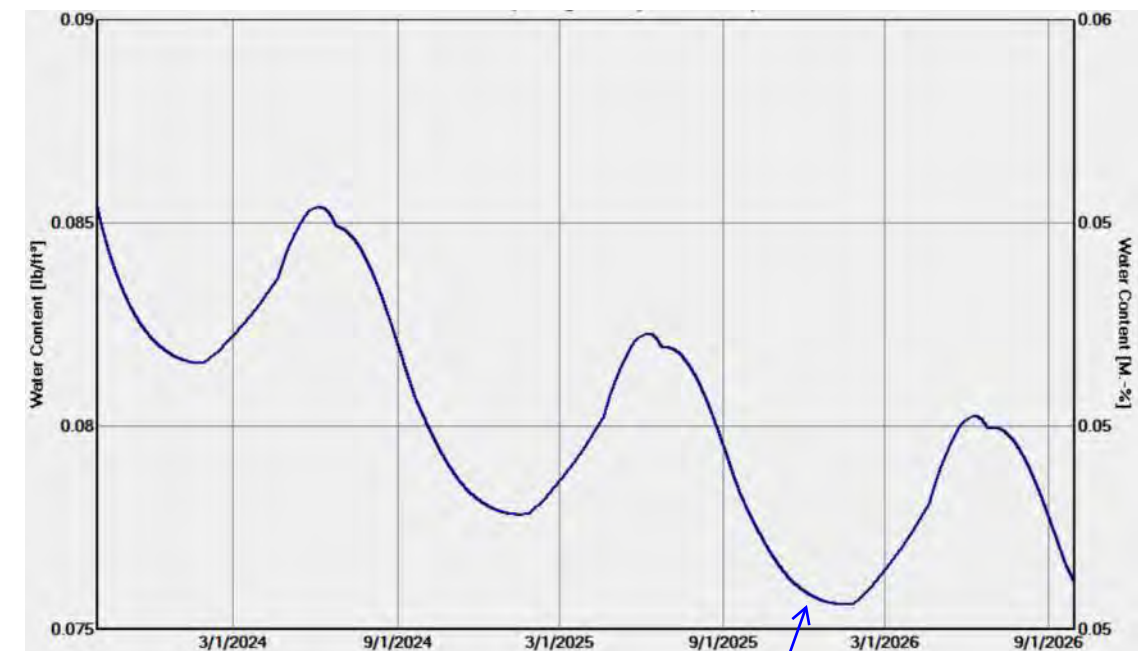
- Limestone (Georgian Bay Limestone) 30.0 in
- Lime Mortar, fine 3.0 in
- Limestone (Georgian Bay Limestone) 37.0 in
- Lime Mortar, fine 6.0 in
- Limestone (Georgian Bay Limestone) 16.0 in

Water Content - Limestone Layer 2



Water content at the middle layer fluctuates seasonally, with minimal upward trend

Water Content - Limestone Layer 3



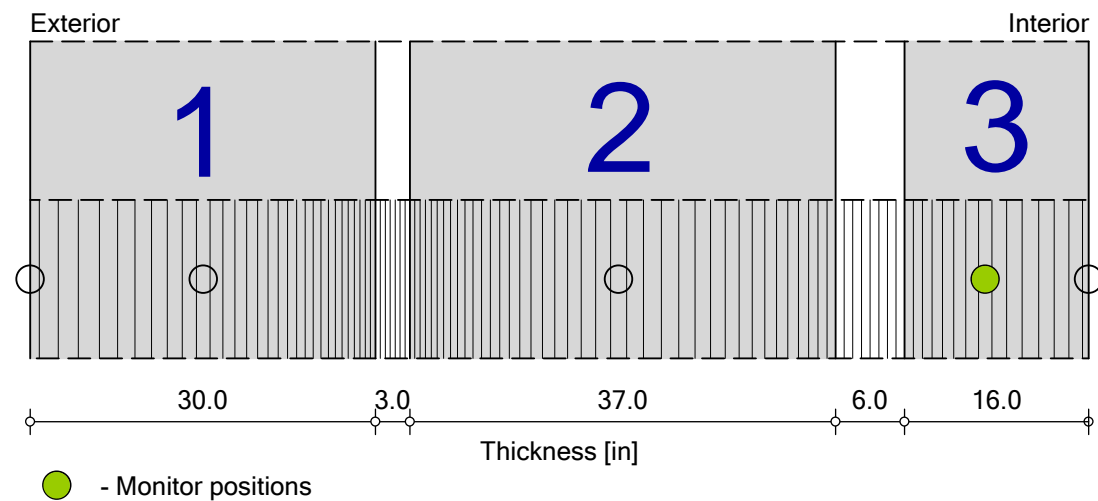
Water content at the interior layer fluctuates seasonally, with decreasing moisture during the 3-year period

South Masonry Wall Analysis

South Masonry Wall - No Added Moisture + Reduced Interior RH

Boundary Conditions

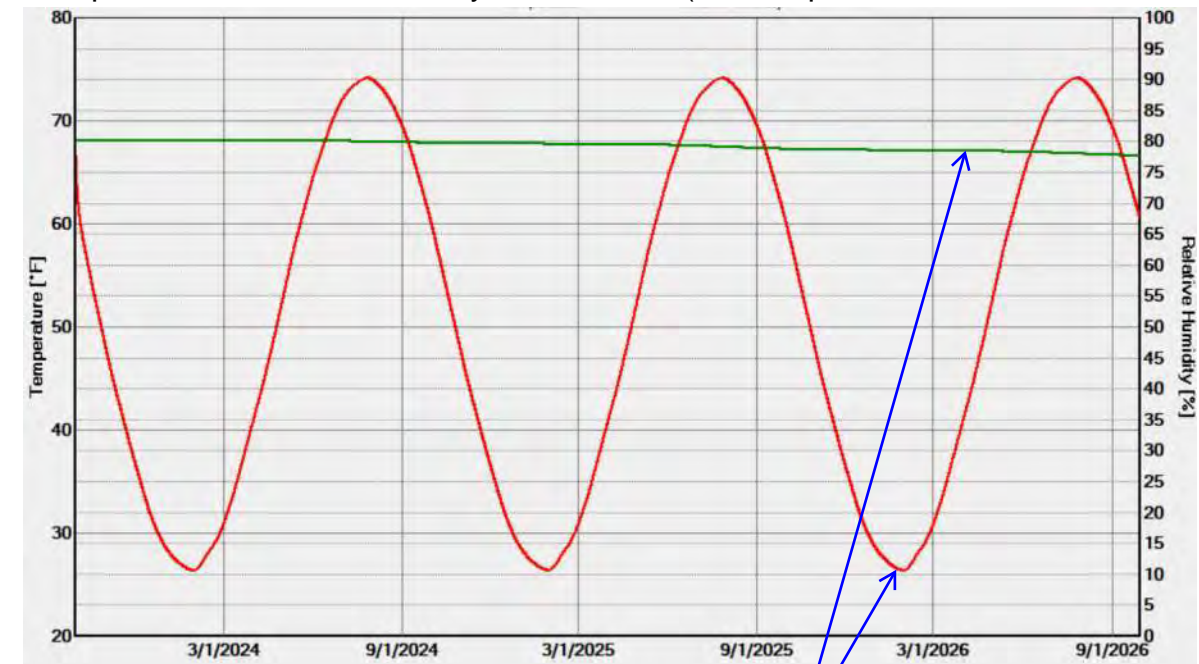
Exterior (left side) Albany, NY
 Interior (right side) 55° F with fluctuation of 25° F; and 60% RH with a 20% amplitude



Materials:

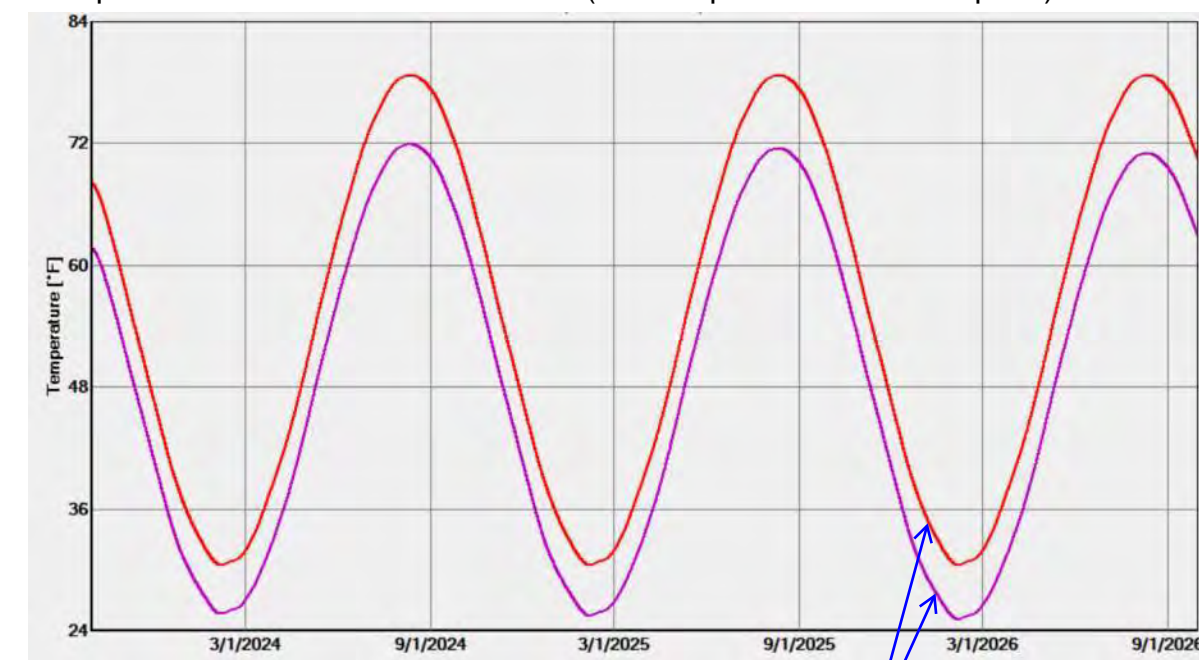
	- Limestone (Georgian Bay Limestone)	30.0 in
	- Lime Mortar, fine	3.0 in
	- Limestone (Georgian Bay Limestone)	37.0 in
	- Lime Mortar, fine	6.0 in
	- Limestone (Georgian Bay Limestone)	16.0 in

Temperature / Relative Humidity at **Monitor 3** (--- temperature / --- relative humidity)



Temperature fluctuates seasonally; Relative Humidity (RH) trends downward during the 3-year period

Temperature / Dew Point at **Monitor 3** (--- temperature / --- dew point)



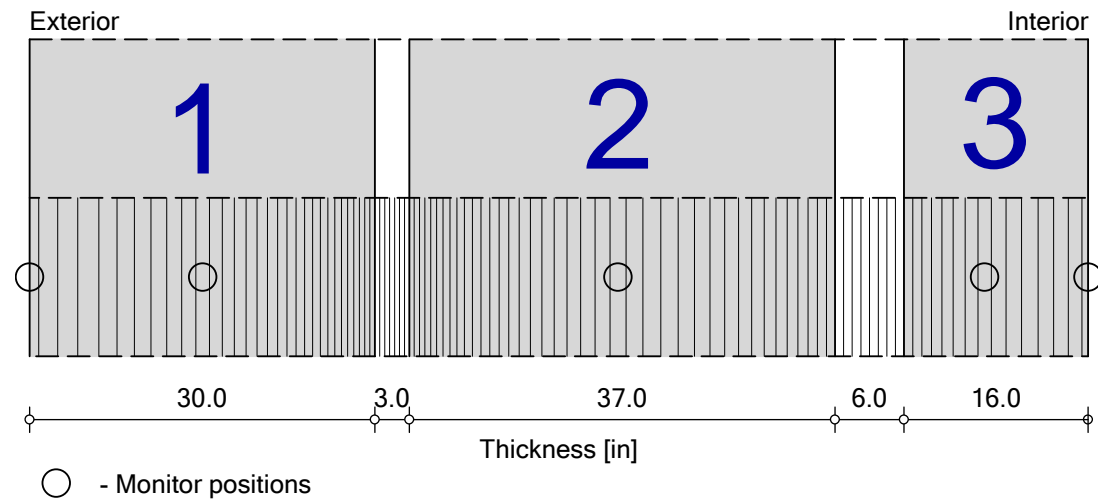
Temperature fluctuates seasonally; Temperature and Dew Point do not intersect (signifies low condensation risk)

South Masonry Wall Analysis

South Masonry Wall - No Added Moisture + Reduced Interior RH (Ten Year Period)

Boundary Conditions

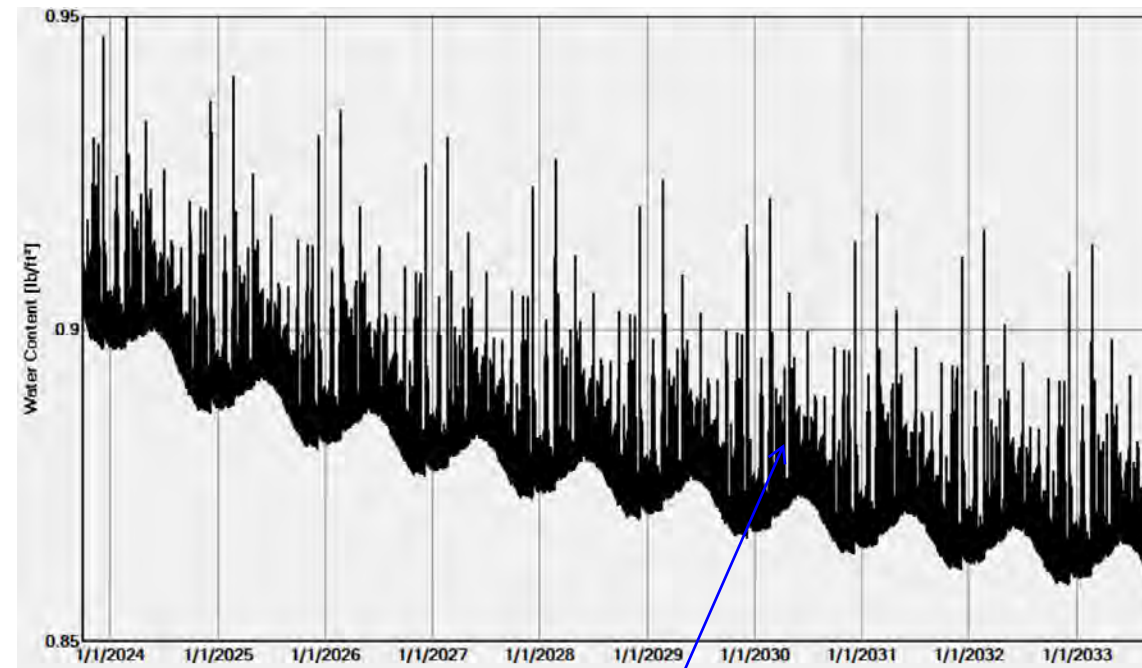
Exterior (left side) Albany, NY
 Interior (right side) 55° F with fluctuation of 25° F; and 60% RH with a 20% amplitude



Materials:

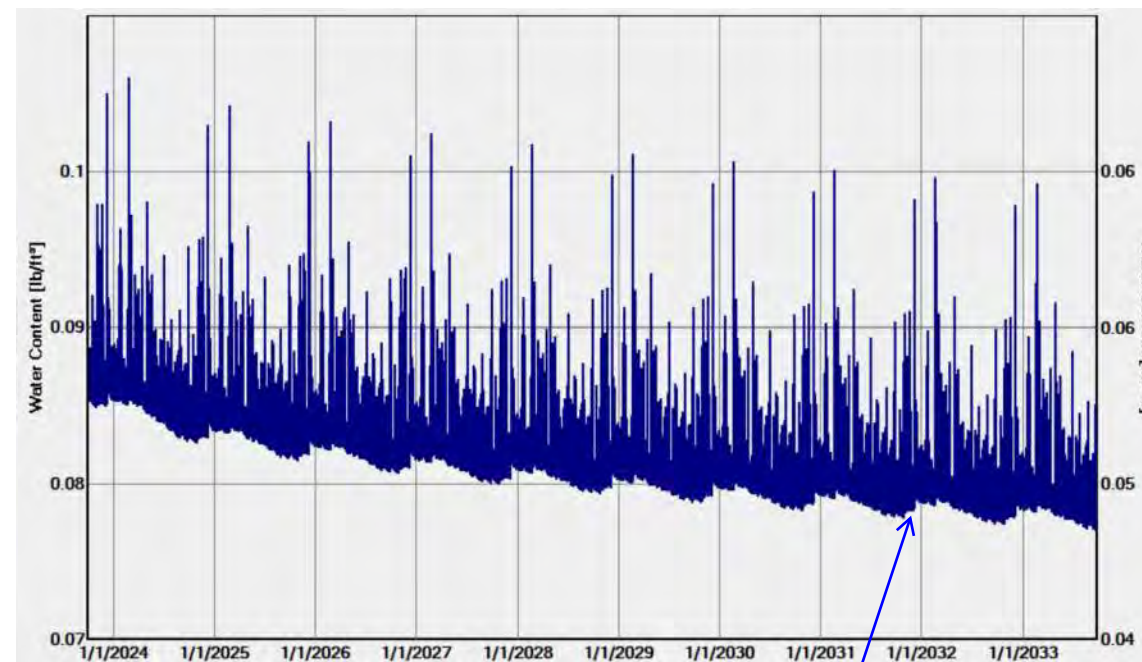
- Limestone (Georgian Bay Limestone) 30.0 in
- Lime Mortar, fine 3.0 in
- Limestone (Georgian Bay Limestone) 37.0 in
- Lime Mortar, fine 6.0 in
- Limestone (Georgian Bay Limestone) 16.0 in

Total Water Content - Existing Masonry Wall



Total Water Content (for the entire wall assembly) trends downward during the 10-year period

Water Content - Limestone Layer 1



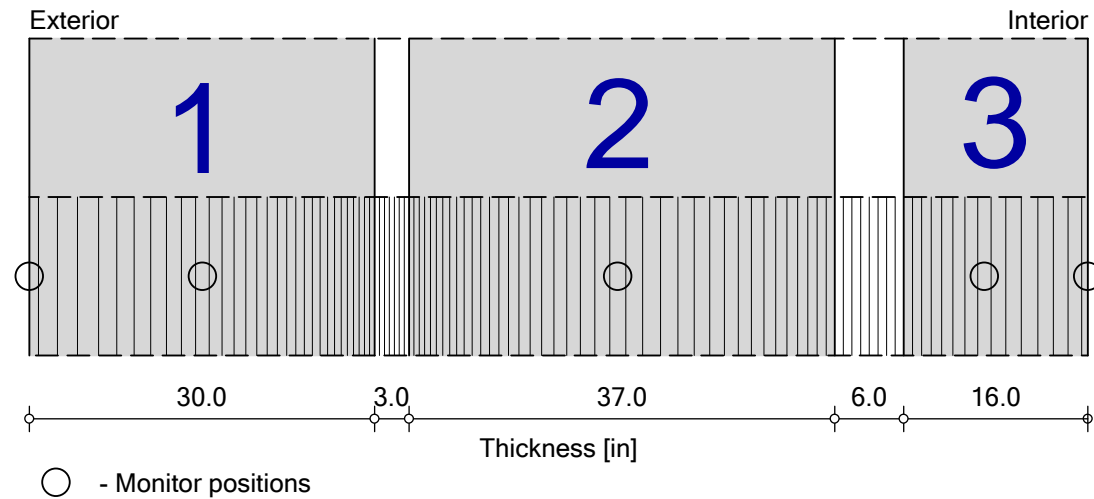
Water content at this exterior layer fluctuates with weather and precipitation events, with a consistent downward trend

South Masonry Wall Analysis

South Masonry Wall - No Added Moisture + Reduced Interior RH (Ten Year Period)

Boundary Conditions

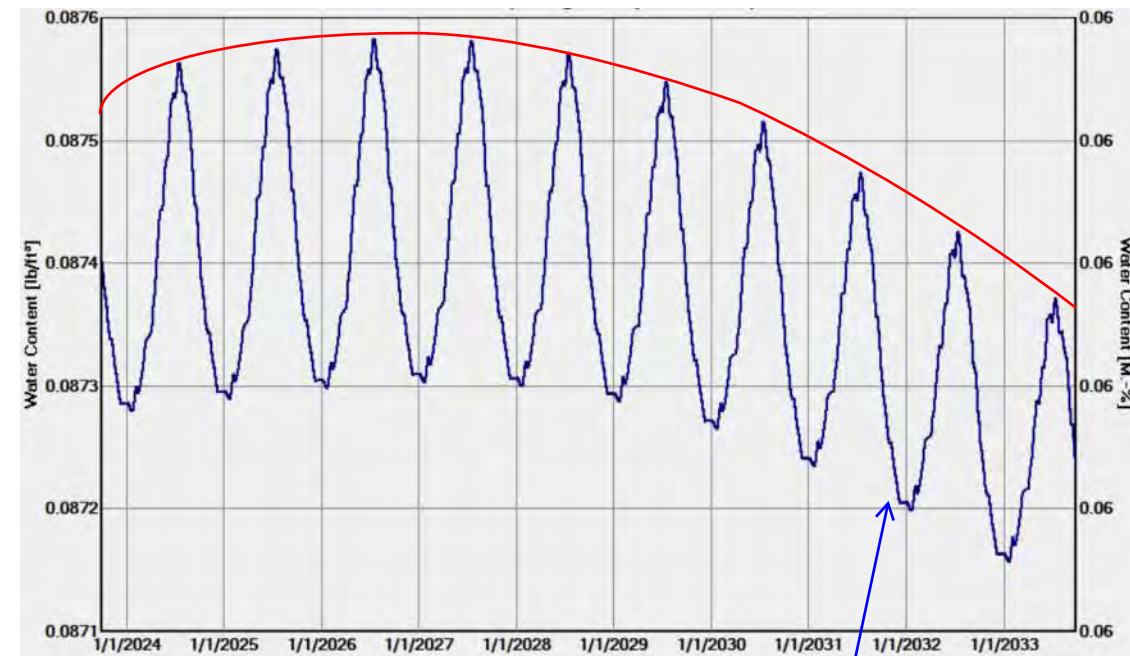
Exterior (left side) Albany, NY
 Interior (right side) 55° F with fluctuation of 25° F; and 60% RH with a 20% amplitude



Materials:

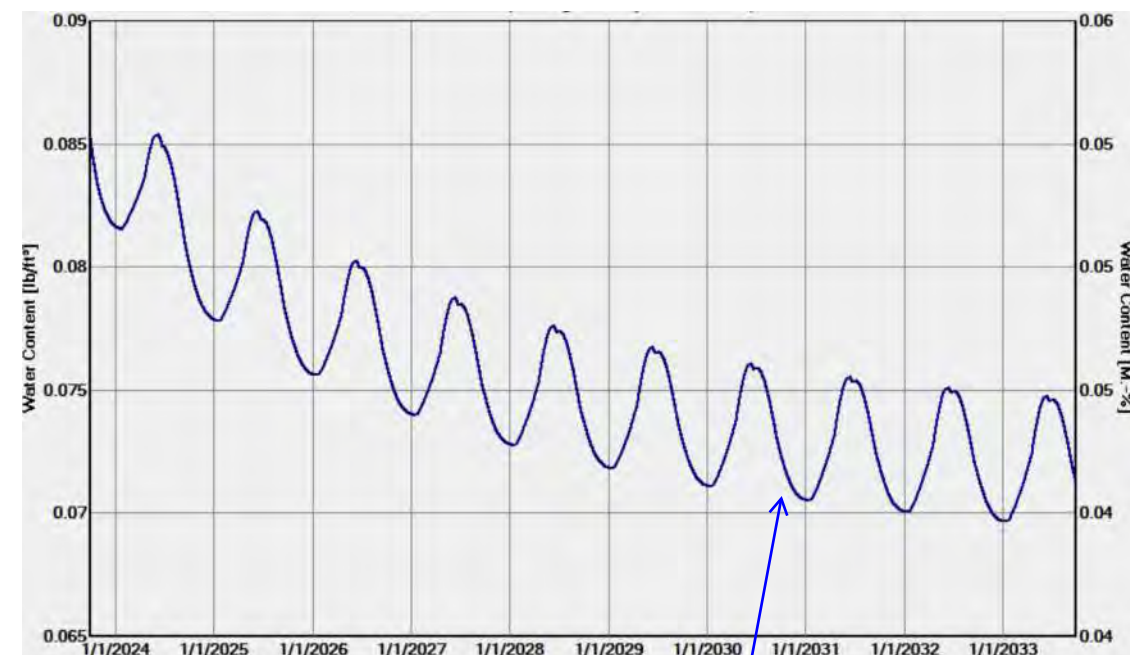
- Limestone (Georgian Bay Limestone) 30.0 in
- Lime Mortar, fine 3.0 in
- Limestone (Georgian Bay Limestone) 37.0 in
- Lime Mortar, fine 6.0 in
- Limestone (Georgian Bay Limestone) 16.0 in

Water Content - Limestone Layer 2



Water content at the middle layer fluctuates seasonally, initially with minimal upward trend that reverses after three years

Water Content - Limestone Layer 3



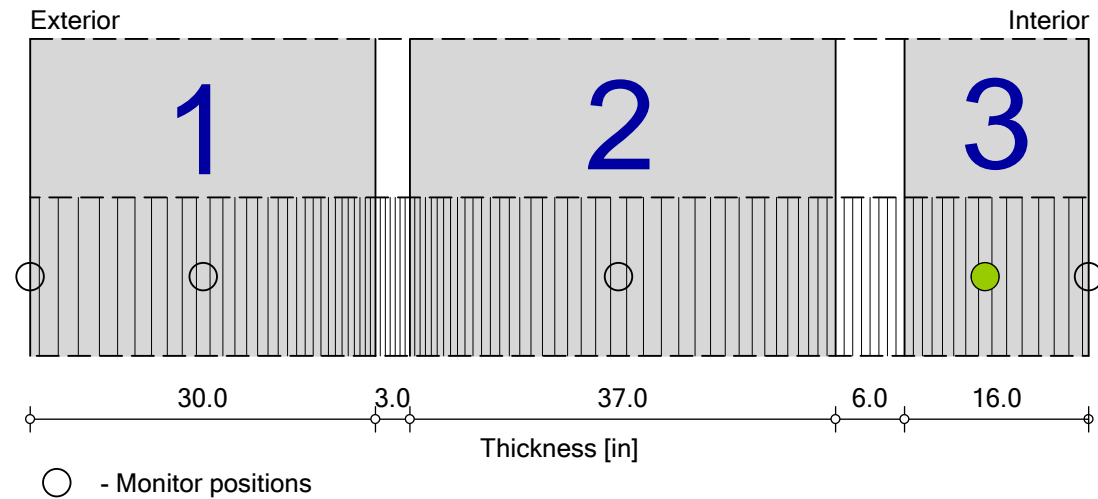
Water content at the interior layer fluctuates seasonally, with decreasing moisture during the 10-year period

South Masonry Wall Analysis

South Masonry Wall - No Added Moisture + Reduced Interior RH (Ten Year Period)

Boundary Conditions

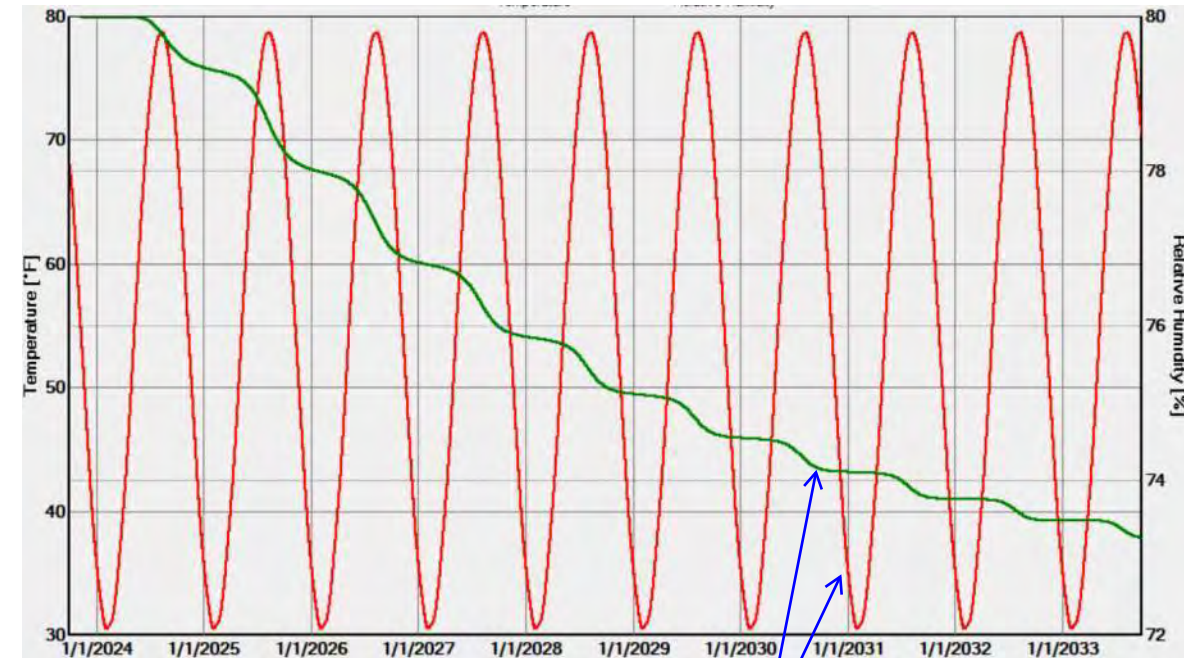
Exterior (left side) Albany, NY
 Interior (right side) 55° F with fluctuation of 25° F; and 60% RH with a 20% amplitude



Materials:

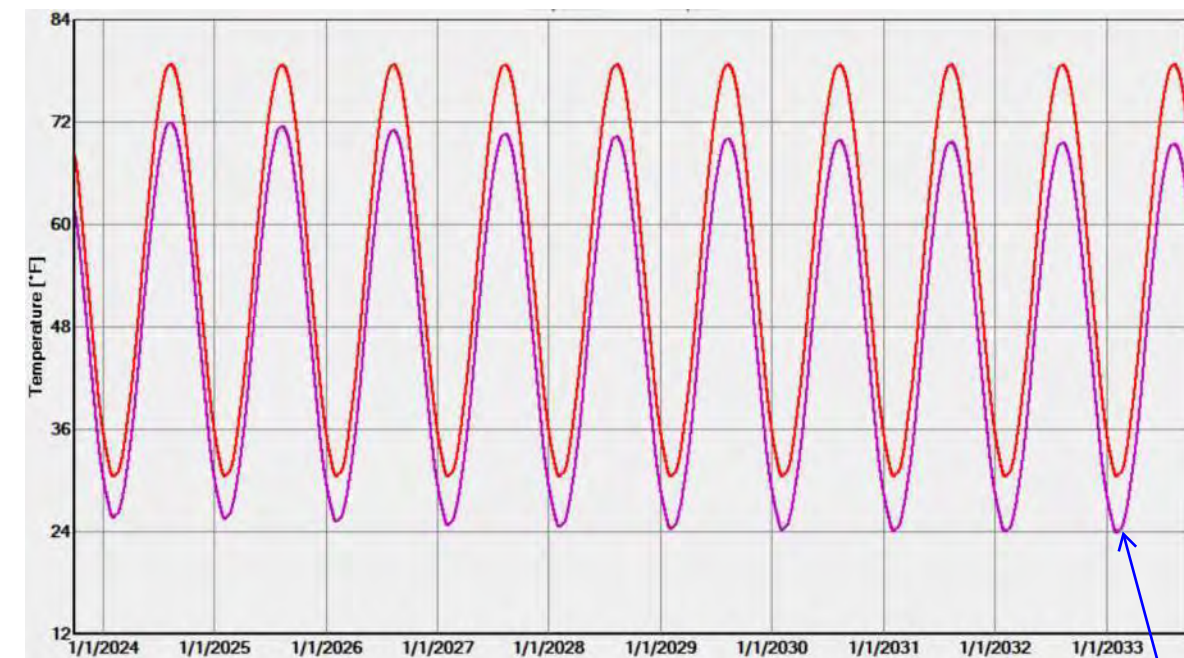
- Limestone (Georgian Bay Limestone) 30.0 in
- Lime Mortar, fine 3.0 in
- Limestone (Georgian Bay Limestone) 37.0 in
- Lime Mortar, fine 6.0 in
- Limestone (Georgian Bay Limestone) 16.0 in

Temperature / Relative Humidity at **Monitor 3** (--- temperature / --- relative humidity)



Temperature fluctuates seasonally; Relative Humidity (RH) trends downward during the 10-year period

Temperature / Dew Point at **Monitor 3** (--- temperature / --- dew point)



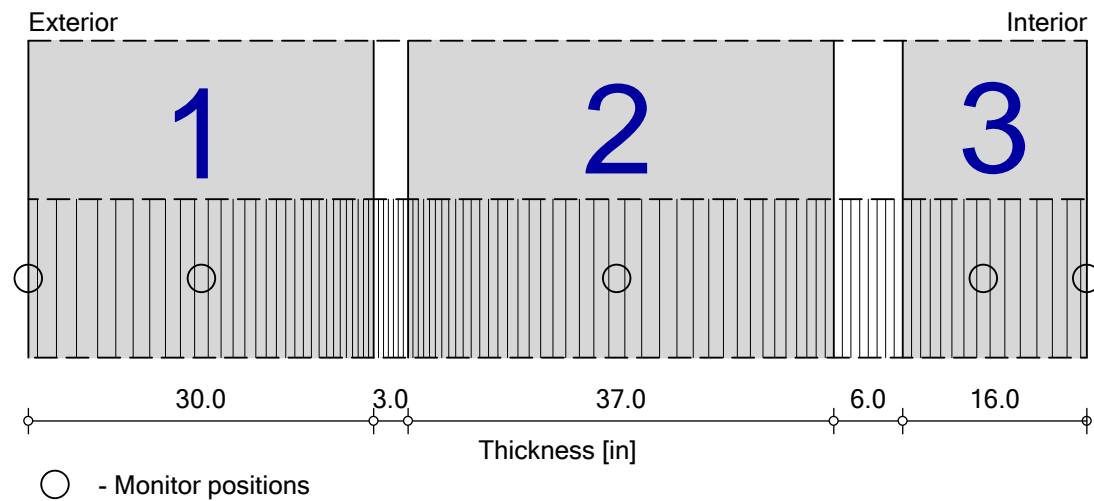
Temperature fluctuates seasonally; Temperature and Dew Point do not intersect; graphs grow further apart during the 10-year period (signifies reduced condensation risk)

South Masonry Wall Analysis

South Masonry Wall - Without Added Moisture

Boundary Conditions

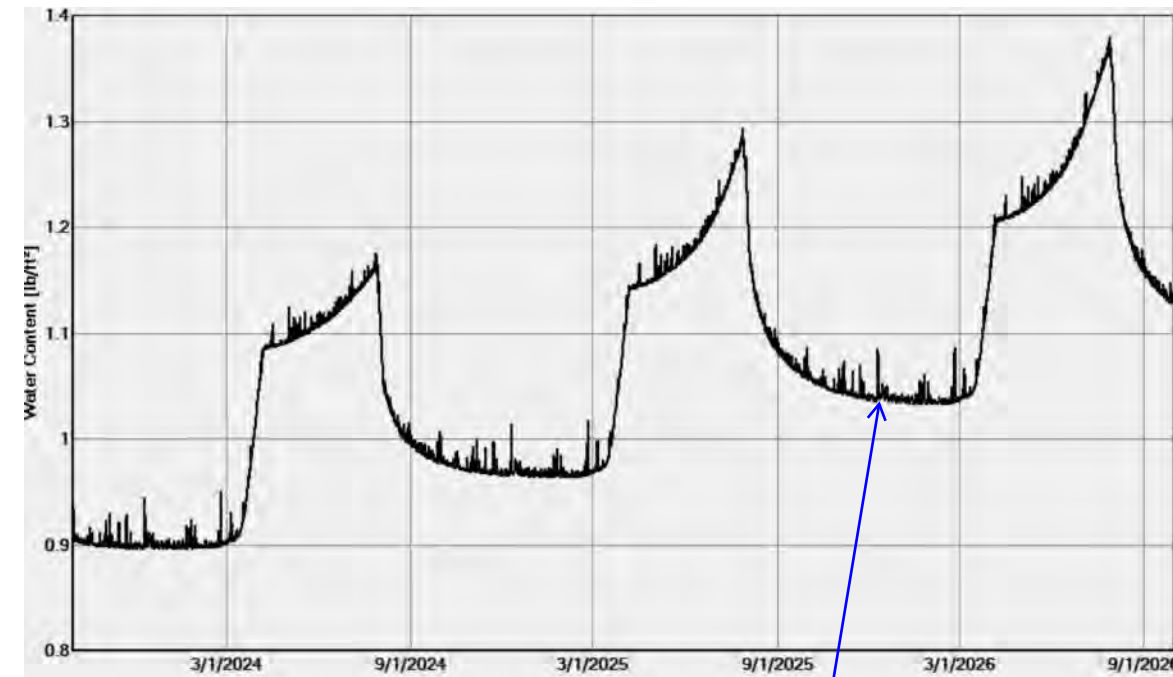
Exterior (left side) Albany, NY
 Interior (right side) 55° F with fluctuation of 25° F; and 72% RH with a 50% amplitude



Materials:

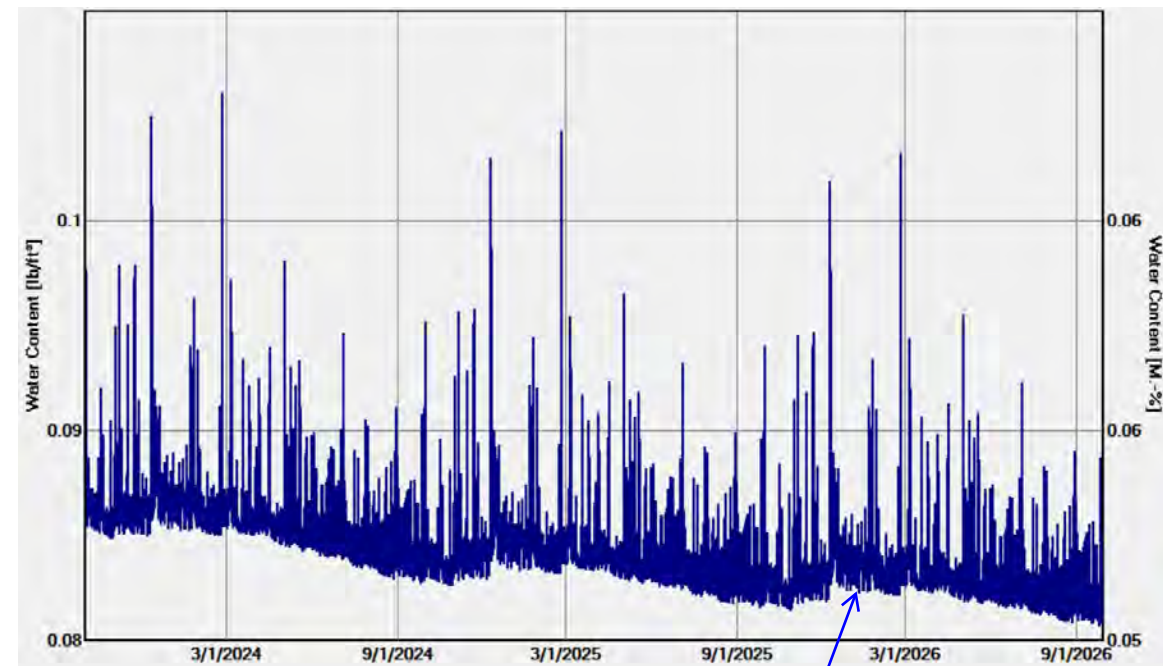
- Limestone (Georgian Bay Limestone) 30.0 in
- Lime Mortar, fine 3.0 in
- Limestone (Georgian Bay Limestone) 37.0 in
- Lime Mortar, fine 6.0 in
- Limestone (Georgian Bay Limestone) 16.0 in

Total Water Content - Existing Masonry Wall



Total Water Content (for the entire wall assembly) increases during the 3-year period (similar to Existing, Page 3)

Water Content - Limestone Layer 1



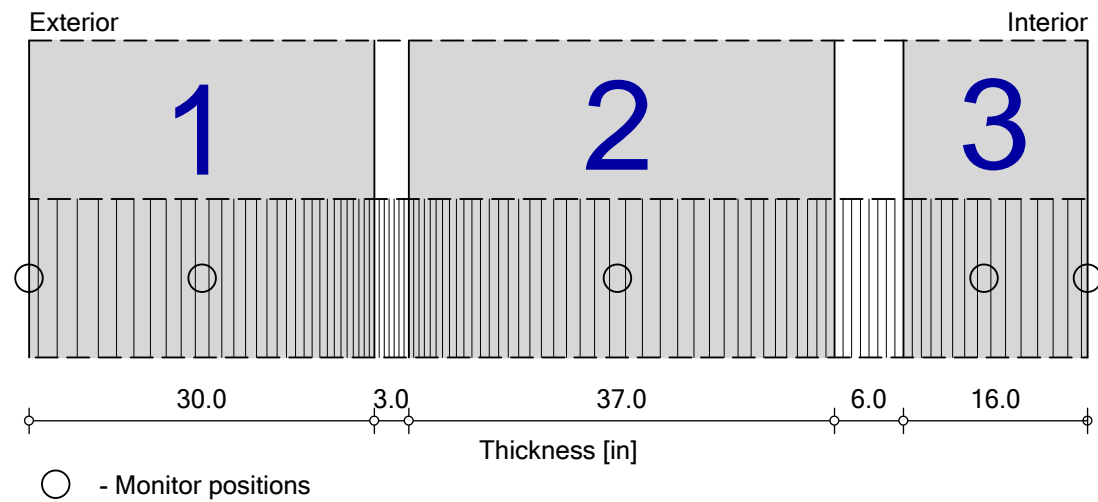
Water content at this exterior layer fluctuates with weather and precipitation events, with a modest downward seasonal trend

South Masonry Wall Analysis

South Masonry Wall - Without Added Moisture

Boundary Conditions

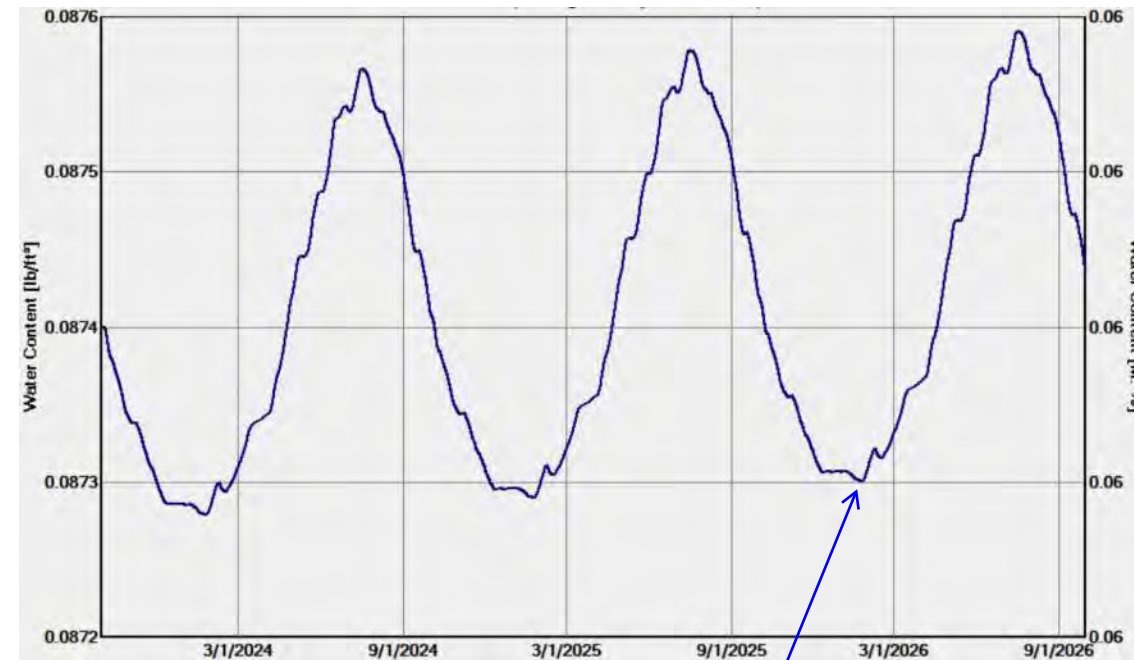
Exterior (left side) Albany, NY
 Interior (right side) 55° F with fluctuation of 25° F; and 72% RH with a 50% amplitude



Materials:

- Limestone (Georgian Bay Limestone) 30.0 in
- Lime Mortar, fine 3.0 in
- Limestone (Georgian Bay Limestone) 37.0 in
- Lime Mortar, fine 6.0 in
- Limestone (Georgian Bay Limestone) 16.0 in

Water Content - Limestone Layer 2



Water content at the middle layer fluctuates seasonally, with modest upward trend

Water Content - Limestone Layer 3



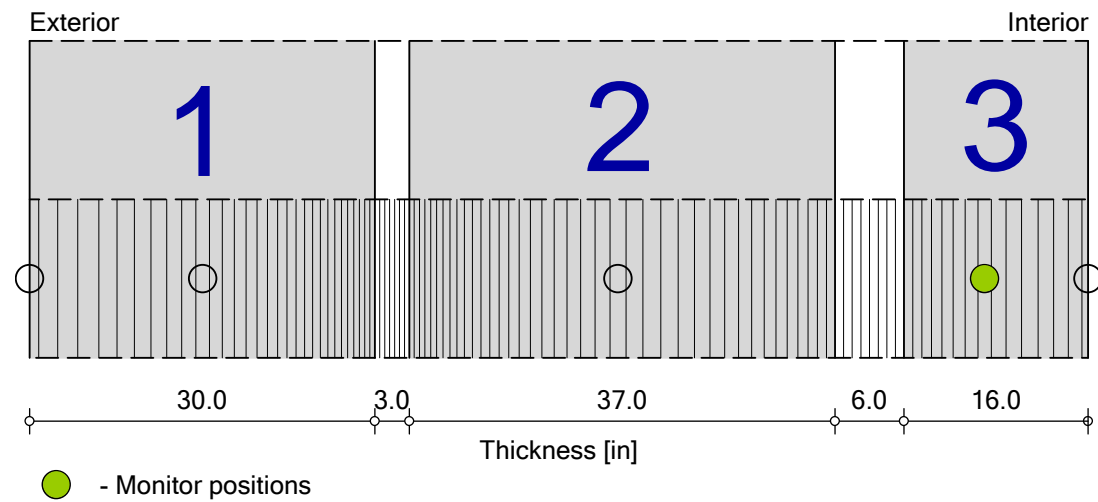
Water content at the interior layer fluctuates seasonally, with significant increase during the 3-year period

South Masonry Wall Analysis

South Masonry Wall - Without Added Moisture

Boundary Conditions

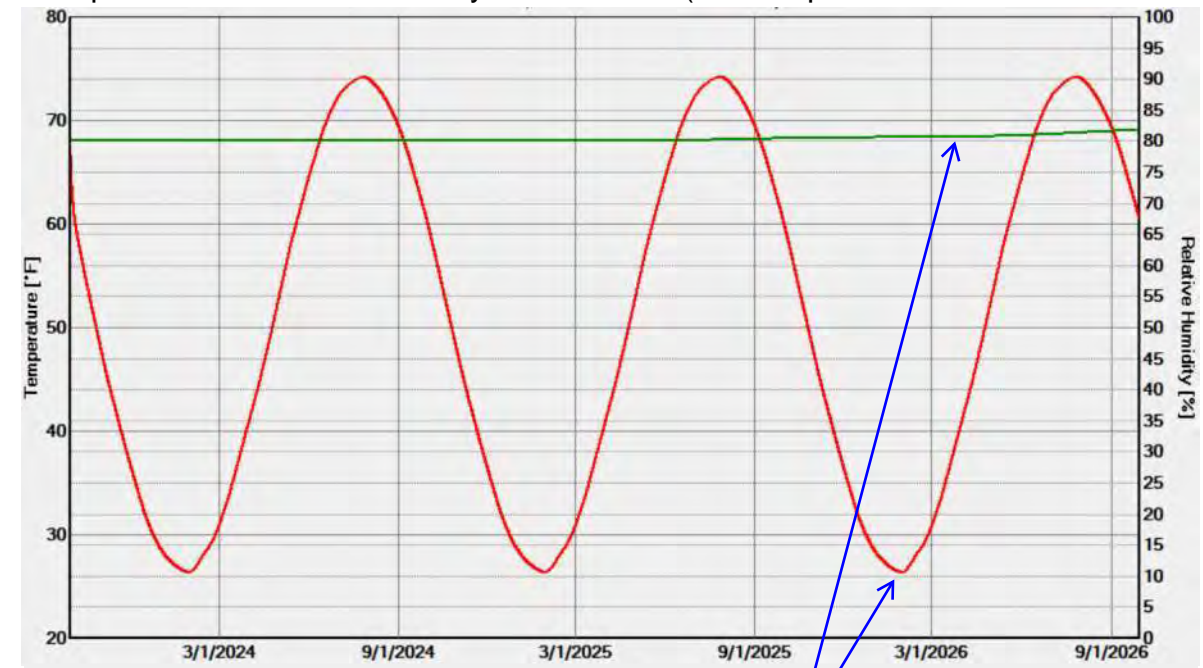
Exterior (left side) Albany, NY
 Interior (right side) 55° F with fluctuation of 25° F; and 72% RH with a 50% amplitude



Materials:

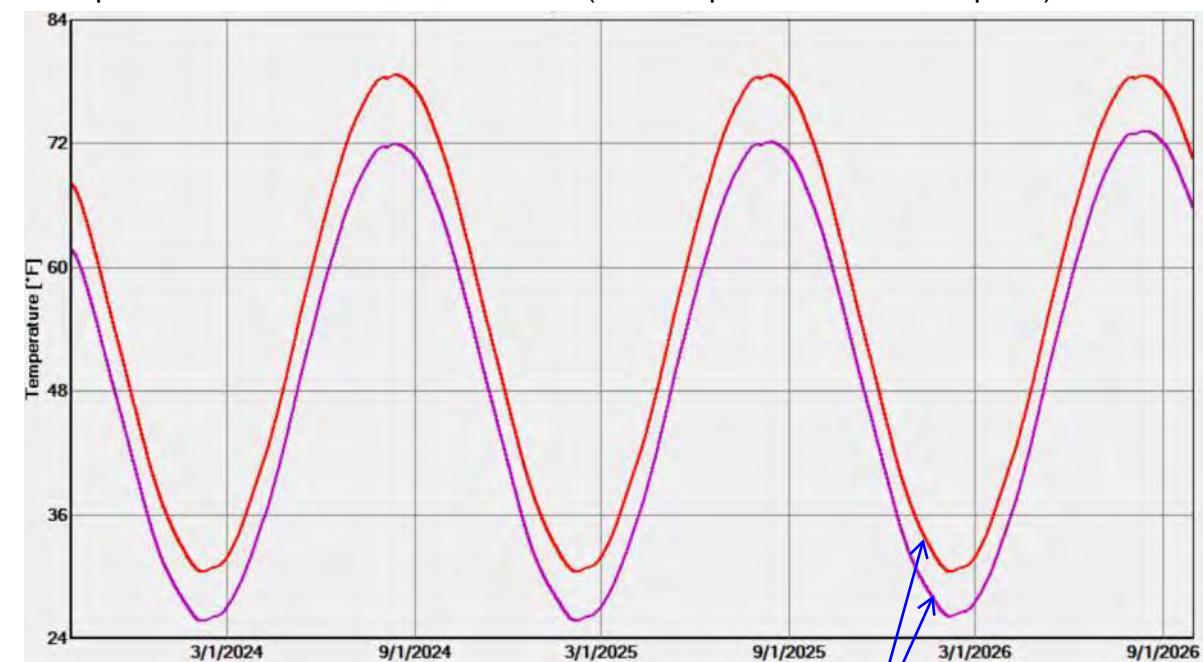
	- Limestone (Georgian Bay Limestone)	30.0 in
	- Lime Mortar, fine	3.0 in
	- Limestone (Georgian Bay Limestone)	37.0 in
	- Lime Mortar, fine	6.0 in
	- Limestone (Georgian Bay Limestone)	16.0 in

Temperature / Relative Humidity at **Monitor 3** (--- temperature / --- relative humidity)



Temperature fluctuates seasonally; Relative Humidity (RH) trends upward during the 3-year period

Temperature / Dew Point at **Monitor 3** (--- temperature / --- dew point)



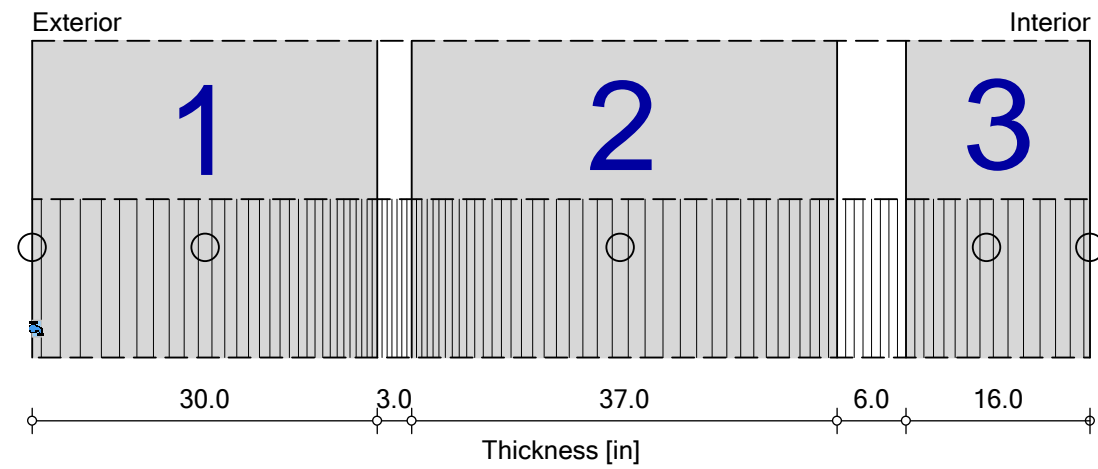
Temperature fluctuates seasonally; Temperature and Dew Point do not intersect (signifies low condensation risk)

South Masonry Wall Analysis

South Masonry Wall - With Increased Moisture

Boundary Conditions

Exterior (left side) Albany, NY
 Interior (right side) 55° F with fluctuation of 25° F; and 72% RH with a 50% amplitude
 Moisture Source **Exterior Limestone Layer - 3%**

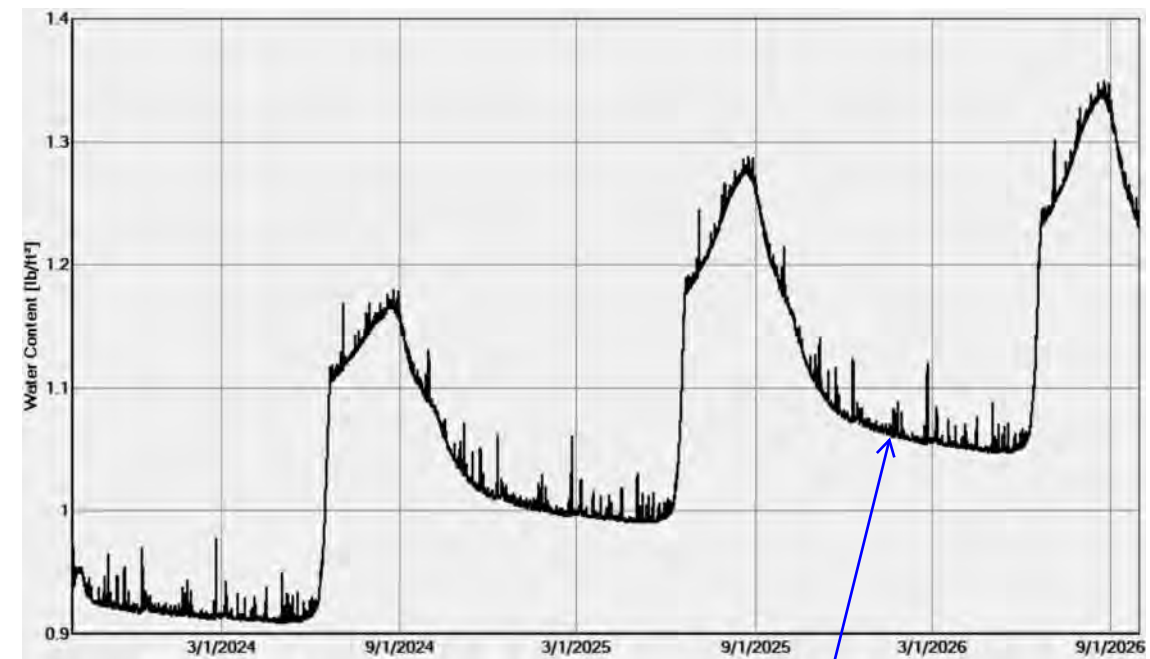


○ - Monitor positions
 - Heat/Moisture source/sink positions

Materials:

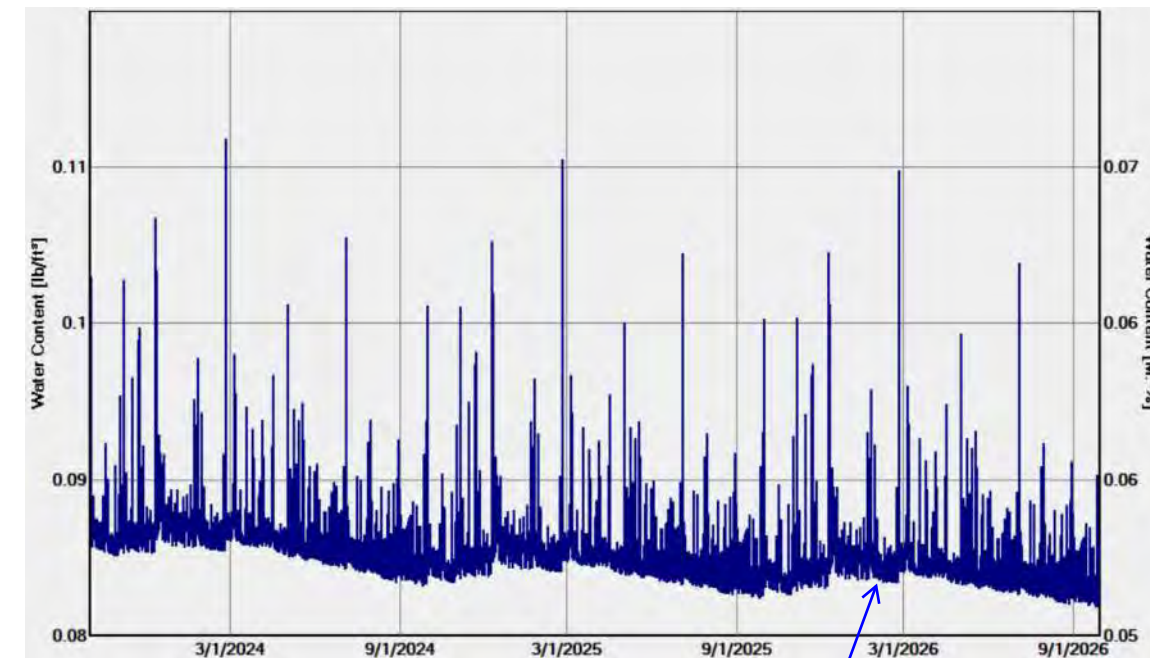
	- Limestone (Georgian Bay Limestone)	30.0 in
	- Lime Mortar, fine	3.0 in
	- Limestone (Georgian Bay Limestone)	37.0 in
	- Lime Mortar, fine	6.0 in
	- Limestone (Georgian Bay Limestone)	16.0 in

Total Water Content - Existing Masonry Wall



Total Water Content (for the entire wall assembly) increases during the 3-year period (similar to Existing, Page 3)

Water Content - Limestone Layer 1



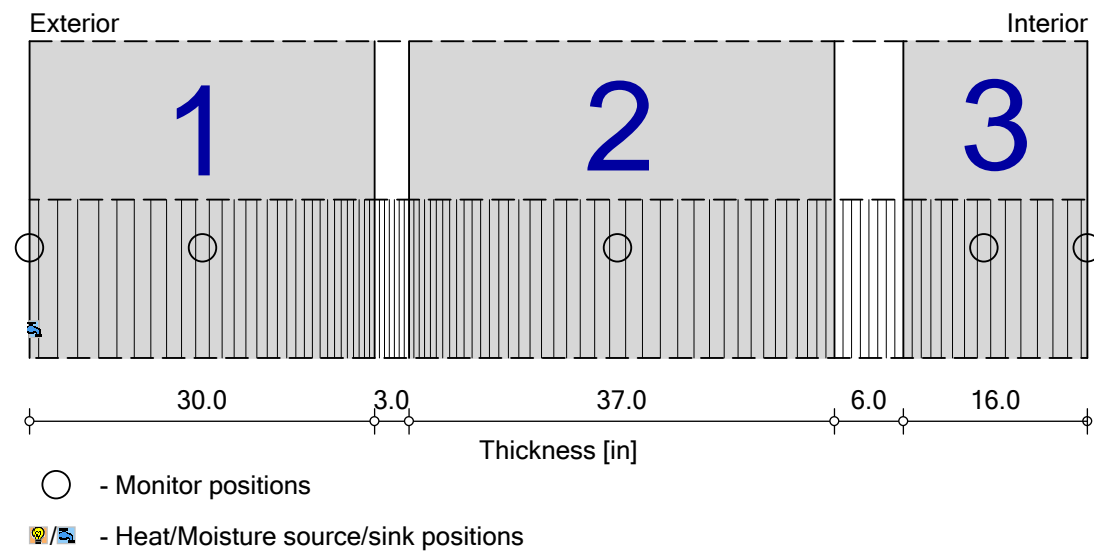
Water content at this exterior layer fluctuates with weather and precipitation events, with a modest downward seasonal trend

South Masonry Wall Analysis

South Masonry Wall - With Increased Moisture

Boundary Conditions

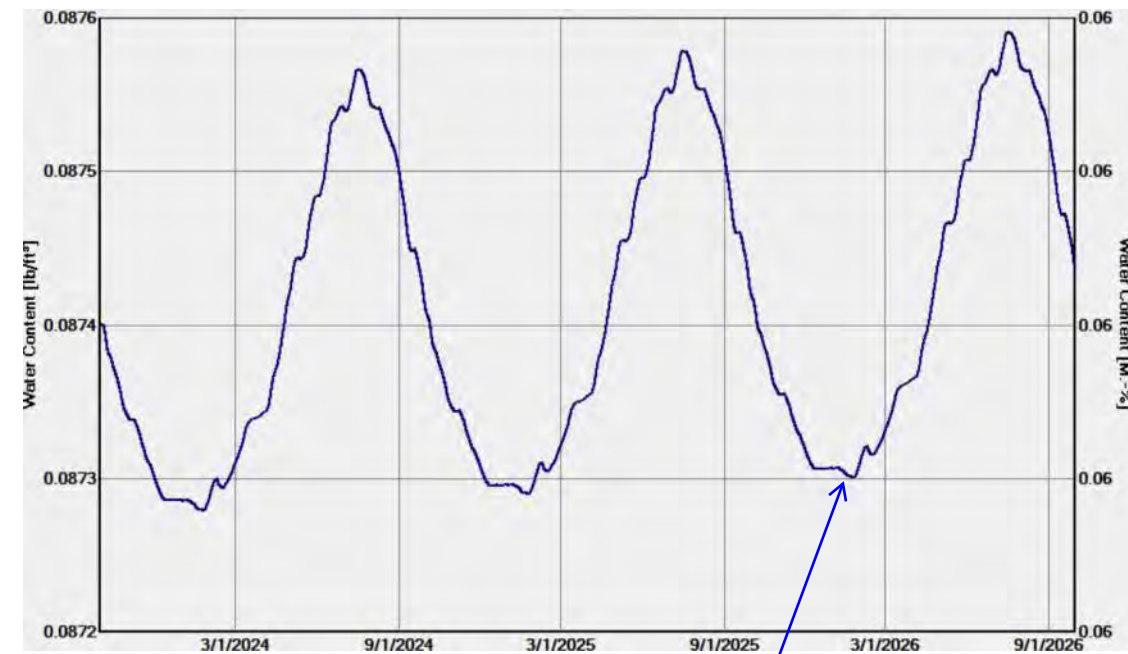
Exterior (left side) Albany, NY
 Interior (right side) 55° F with fluctuation of 25° F; and 72% RH with a 50% amplitude
 Moisture Source **Exterior Limestone Layer - 3%**



Materials:

	- Limestone (Georgian Bay Limestone)	30.0 in
	- Lime Mortar, fine	3.0 in
	- Limestone (Georgian Bay Limestone)	37.0 in
	- Lime Mortar, fine	6.0 in
	- Limestone (Georgian Bay Limestone)	16.0 in

Water Content - Limestone Layer 2



Water content at the middle layer fluctuates seasonally, with minimal upward trend (similar to Existing, Page 4)

Water Content - Limestone Layer 3



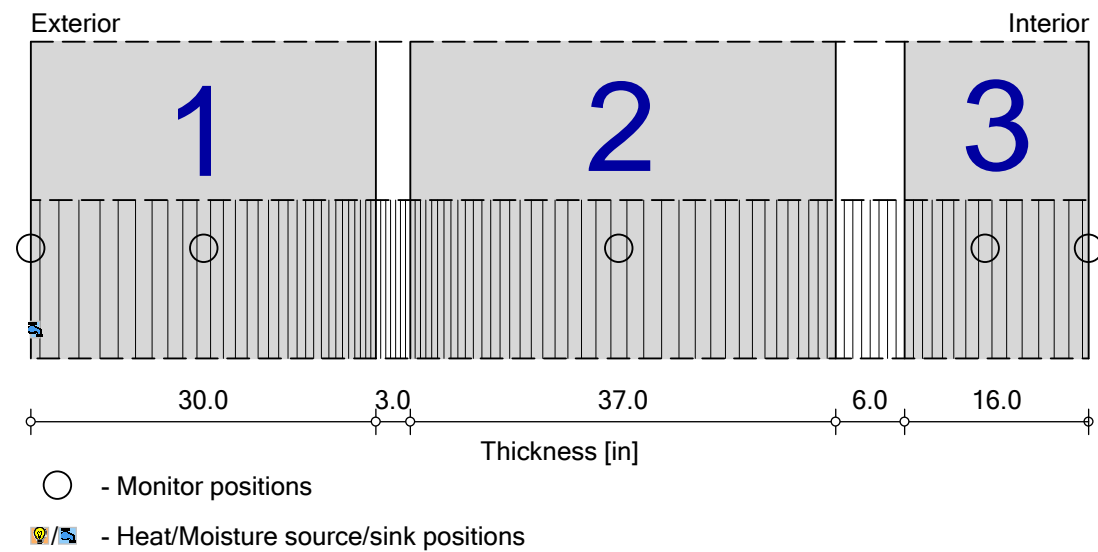
Water content at the interior layer fluctuates seasonally, with increasing moisture during the 3-year period (similar to Existing, Page 4)

South Masonry Wall Analysis




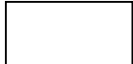

South Masonry Wall - With Increased Ambient Temperature

Boundary Conditions

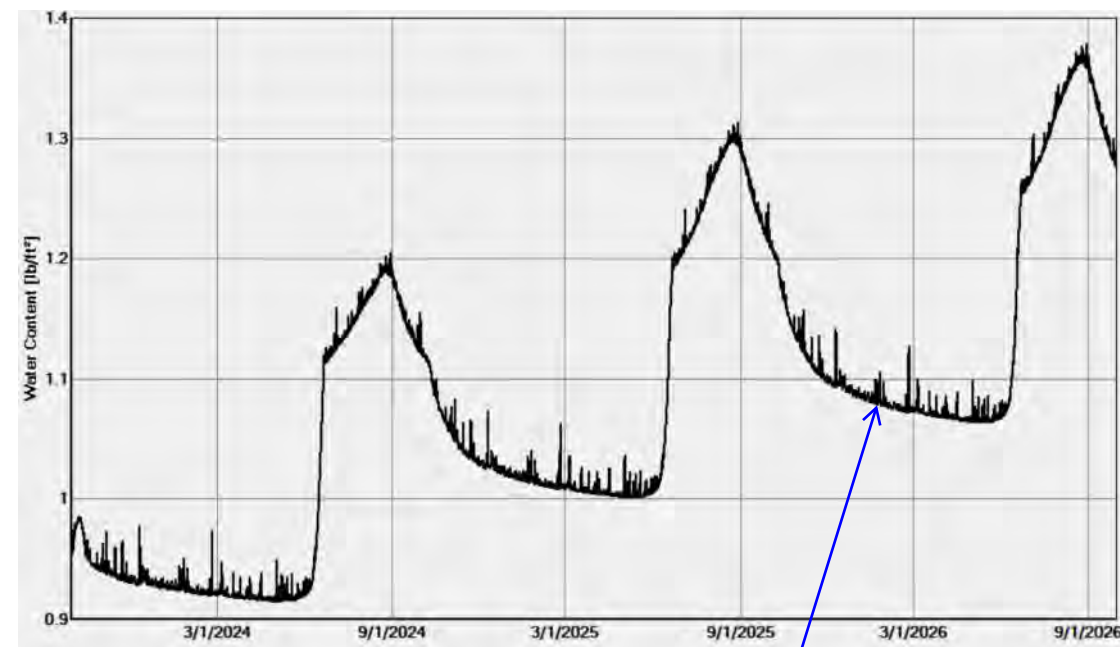
Exterior (left side) Albany, NY
 Interior (right side) **60° F with fluctuation of 20° F**; and 72% RH with a 50% amplitude
 Moisture Source Exterior Limestone Layer - 1% (ANSI/ASHRAE standard 160)



Materials:

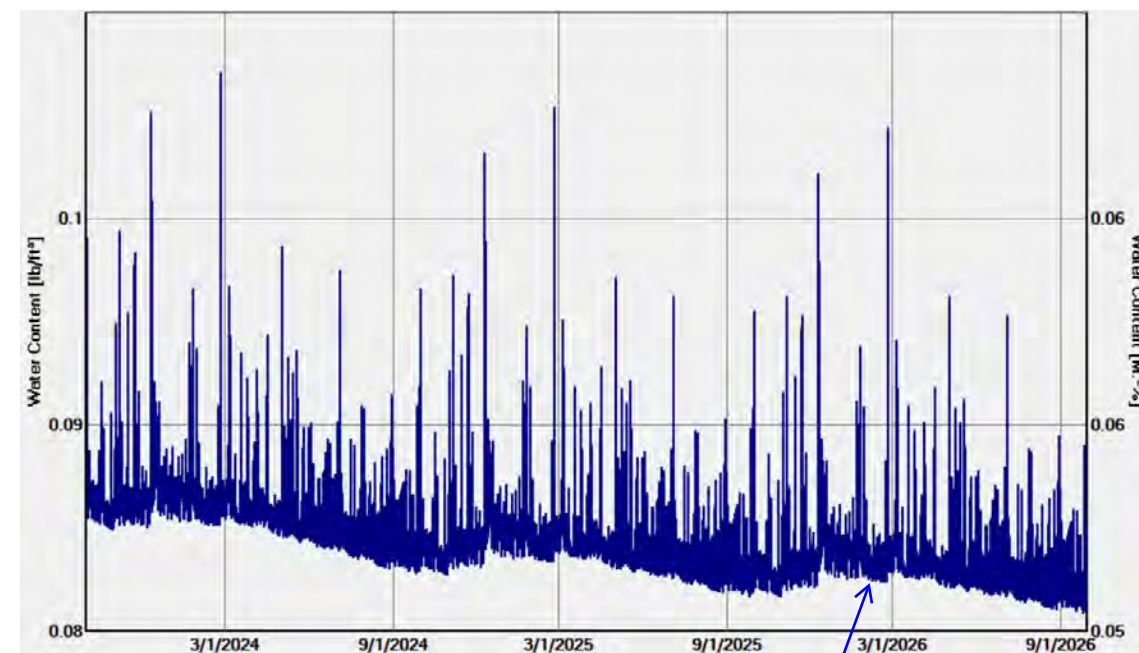
	- Limestone (Georgian Bay Limestone)	30.0 in
	- Lime Mortar, fine	3.0 in
	- Limestone (Georgian Bay Limestone)	37.0 in
	- Lime Mortar, fine	6.0 in
	- Limestone (Georgian Bay Limestone)	16.0 in

Total Water Content - Existing Masonry Wall



Total Water Content (for the entire wall assembly) increases during the 3-year period (similar to Existing, Page 3)

Water Content - Limestone Layer 1



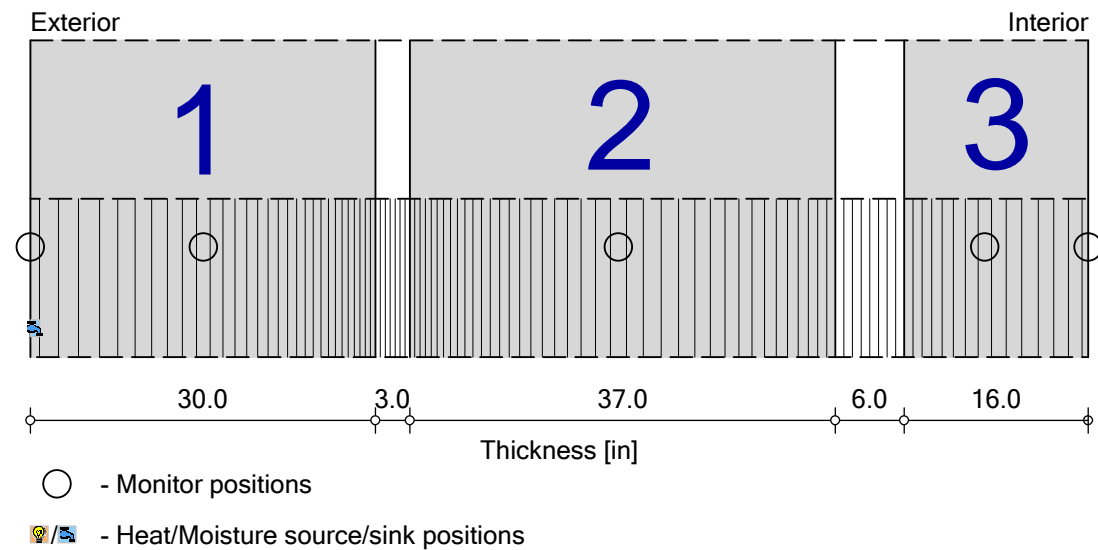
Water content at this exterior layer fluctuates with weather and precipitation events, with a modest downward seasonal trend

South Masonry Wall Analysis

South Masonry Wall - With Increased Ambient Temperature

Boundary Conditions

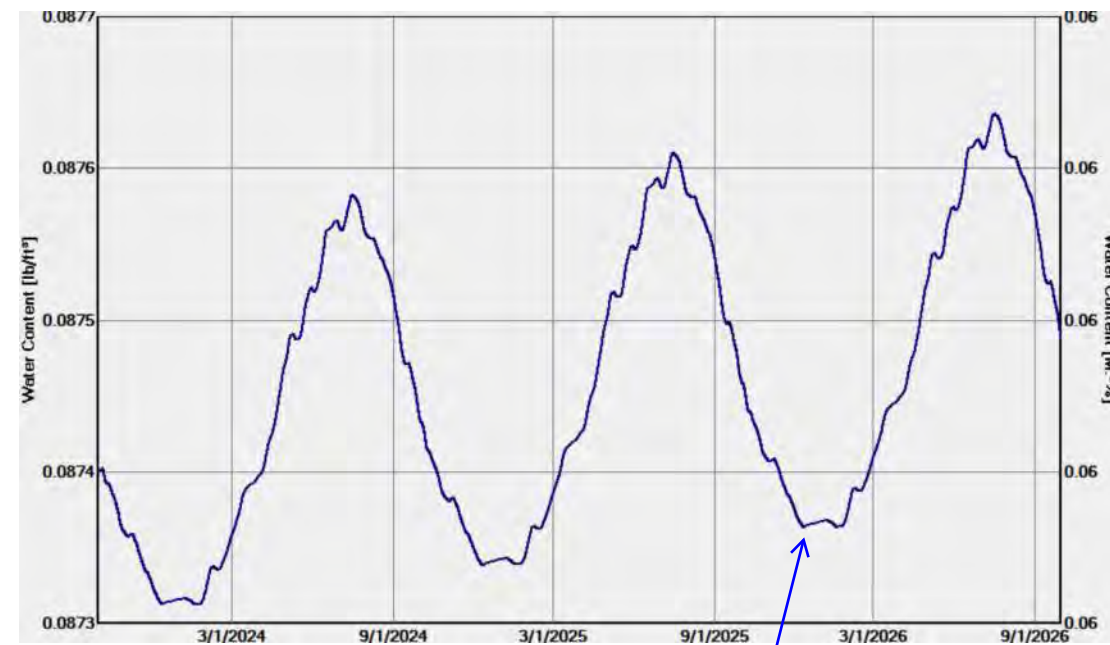
Exterior (left side) Albany, NY
 Interior (right side) **60° F with fluctuation of 20° F**; and 72% RH with a 50% amplitude
 Moisture Source Exterior Limestone Layer - 1% (ANSI/ASHRAE standard 160)



Materials:

	- Limestone (Georgian Bay Limestone)	30.0 in
	- Lime Mortar, fine	3.0 in
	- Limestone (Georgian Bay Limestone)	37.0 in
	- Lime Mortar, fine	6.0 in
	- Limestone (Georgian Bay Limestone)	16.0 in

Water Content - Limestone Layer 2



Water content at the middle layer fluctuates seasonally, with minimal upward trend (similar to Existing, Page 4)

Water Content - Limestone Layer 3



Water content at the interior layer fluctuates seasonally, with increasing moisture during the 3-year period (similar to Existing, Page 4)

South Masonry Wall Analysis

Introduction

Intent

The intent of the WUFI analysis is to first establish a model of the existing configuration and climatic condition (referred to as the 'existing model') and then manipulate the climatic conditions to study their impact upon drying the stone masonry walls.

Model Description

WUFI Pro Version 6.7 software, as described by its developer, "allows realistic calculation of the transient coupled one- and two-dimensional heat and moisture transport in walls and other multi-layer building components exposed to natural weather". The software was used to model the existing proposed skylight assemblies.

Existing Assembly

The exterior wall assembly used in the WUFI model is based upon the information obtained by one of the cores made by Atkinson-Noland & Associates, Inc. for their Goodman Jack tests from the core hole made at the south wall (Ground Floor South Interior core, Core ID = ANA-SOUTH-4).

Weather location for the model was Albany NY as being the closest available data for the climate for the Bennington VT location.

The existing model includes a 'moisture source' at the exterior material layer. This additional moisture source simulates water infiltration into the stone masonry wall due to naturally occurring precipitation, based upon ANSI/ASHRAE standard 160, which is a 1% fraction of the rain load was used in the existing model.

For interior climate, data for a full year of recorded interior relative humidity and temperature was reviewed and entered into the model as 55° F with fluctuation of 25° F; and 72% RH with a 50% amplitude

Hygrothermal Behavior Summary

For the Existing Assembly, the WUFI model indicates that generally, the total water content within the full thickness of the masonry wall trends upward for the three-year model period. The model indicates that moisture content at the inner wythe of stone increases at a higher rate than the middle wythe, while water content at the exterior wythe decreases (Existing South Masonry Wall model, Pages 3-8). The moisture content within the modeled material layers is consistent with the observable conditions of the masonry wall.

Of all the variables that were manipulated, reduction of interior climate relative humidity was most effective for reducing masonry total water content (South Masonry Wall - No Added Moisture + Reduced Interior RH models, Pages 9-14). This model used an interior climate with 60% RH with a 20% amplitude with 55° F with fluctuation of 25° F

One model simulated the wall with no additional moisture source and a second model simulated the wall with 3% fraction of rain load moisture source. Both models indicate some change in moisture content. The model with no additional moisture shows modest change in moisture content at outer, middle and interior wythes of masonry (Existing South Masonry Wall - Without Added Moisture, Pages 15-17). When additional moisture source is increased to 3%, there is some, but only a modest increase in water content across the material layers (Existing South Masonry Wall - With Increased Moisture, Pages 18-19).

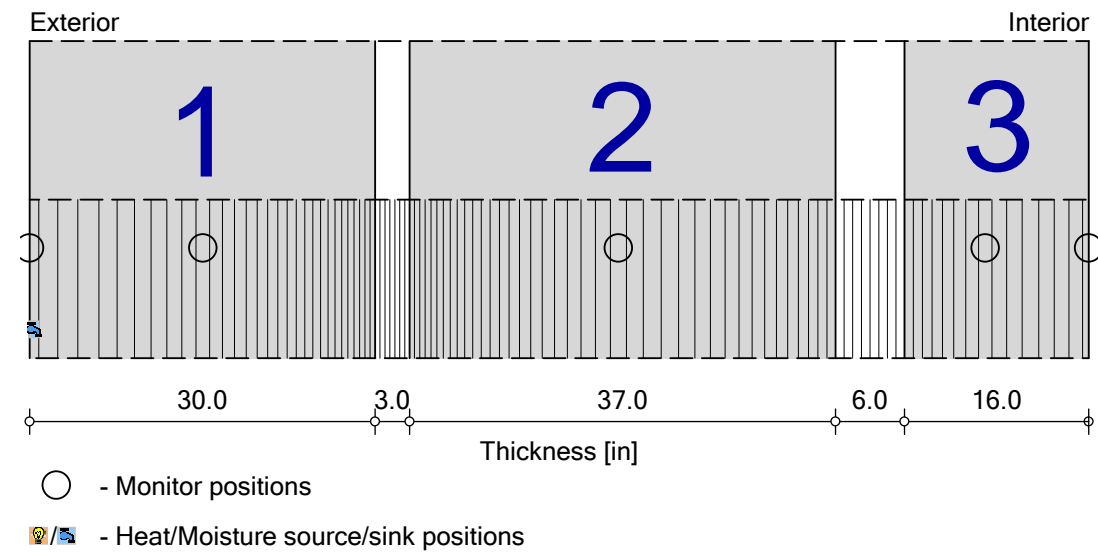
One model simulated interior climate with increased ambient air temperature with 60° F with fluctuation of 20° F; and 72% RH with a 50% amplitude instead of the 55° F with fluctuation of 25° F existing condition. The model with increased interior air temperature shows modest change in moisture content at outer, middle and interior wythes of masonry (Existing South Masonry Wall - With Increased Ambient Temperature, Pages 20-21).

South Masonry Wall Analysis

Existing South Masonry Wall

Boundary Conditions

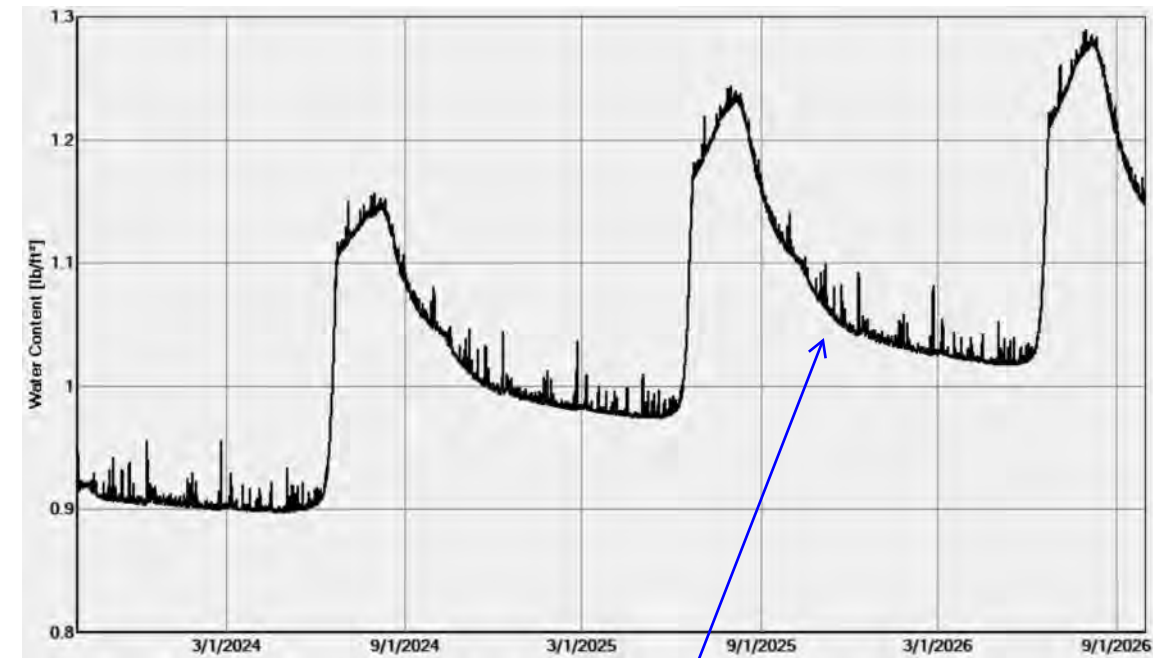
Exterior (left side) Albany, NY
 Interior (right side) 55° F with fluctuation of 25° F; and 72% RH with a 50% amplitude
 Moisture Source Exterior Limestone Layer - 1% (ANSI/ASHRAE standard 160)



Materials:

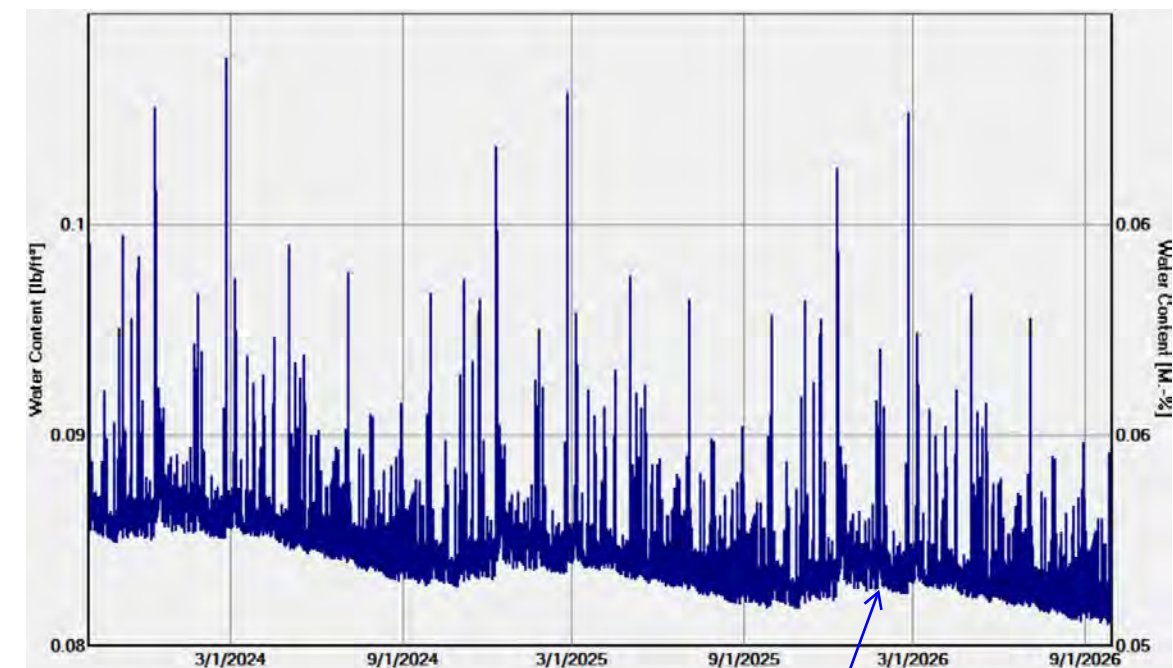
	- Limestone (Georgian Bay Limestone)	30.0 in
	- Lime Mortar, fine	3.0 in
	- Limestone (Georgian Bay Limestone)	37.0 in
	- Lime Mortar, fine	6.0 in
	- Limestone (Georgian Bay Limestone)	16.0 in

Total Water Content - Existing Masonry Wall



Total Water Content (for the entire wall assembly) increases during the 3-year period

Water Content - Limestone Layer 1



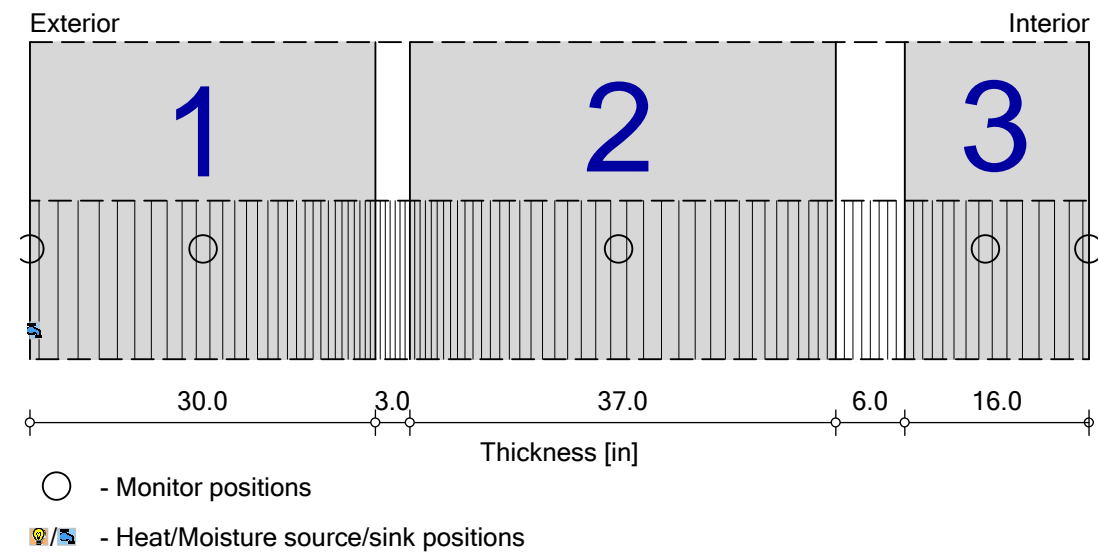
Water content at this exterior layer fluctuates with weather and precipitation events, with a modest downward seasonal trend

South Masonry Wall Analysis

Existing South Masonry Wall

Boundary Conditions

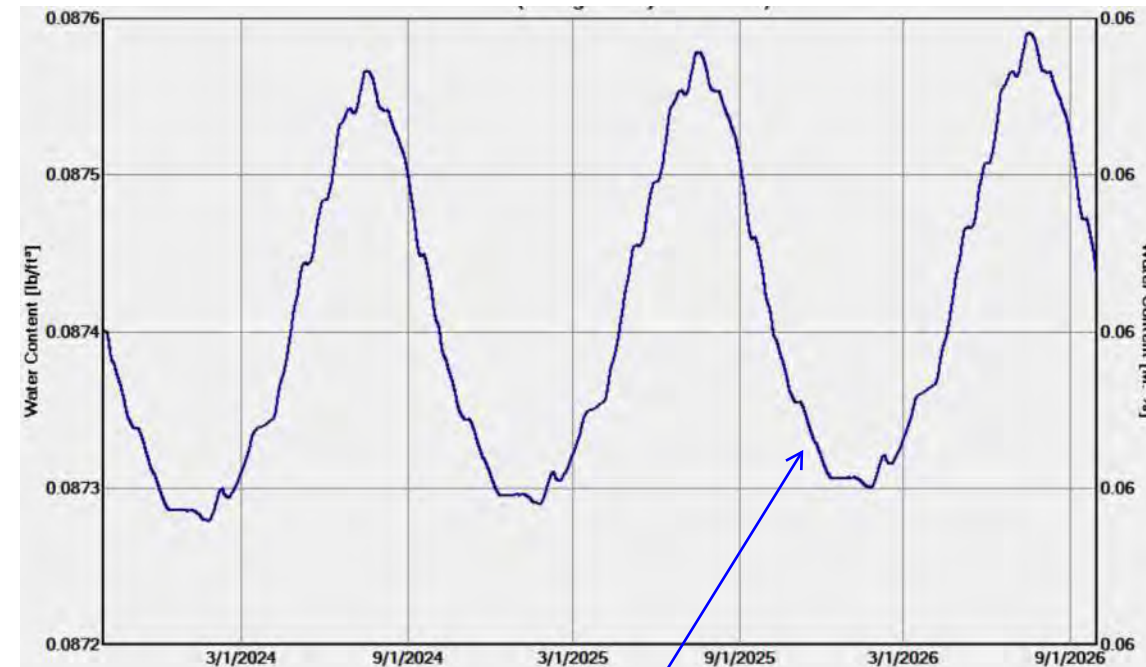
Exterior (left side) Albany, NY
 Interior (right side) 55° F with fluctuation of 25° F; and 72% RH with a 50% amplitude
 Moisture Source Exterior Limestone Layer - 1% (ANSI/ASHRAE standard 160)



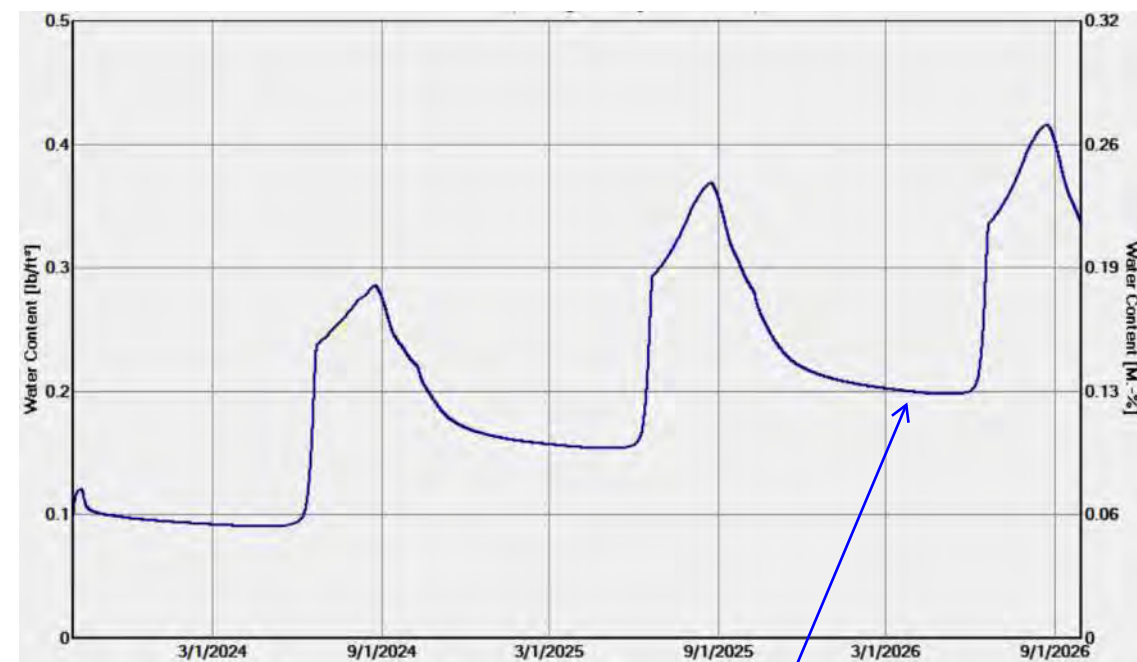
Materials:

	- Limestone (Georgian Bay Limestone)	30.0 in
	- Lime Mortar, fine	3.0 in
	- Limestone (Georgian Bay Limestone)	37.0 in
	- Lime Mortar, fine	6.0 in
	- Limestone (Georgian Bay Limestone)	16.0 in

Water Content - Limestone Layer 2



Water Content - Limestone Layer 3

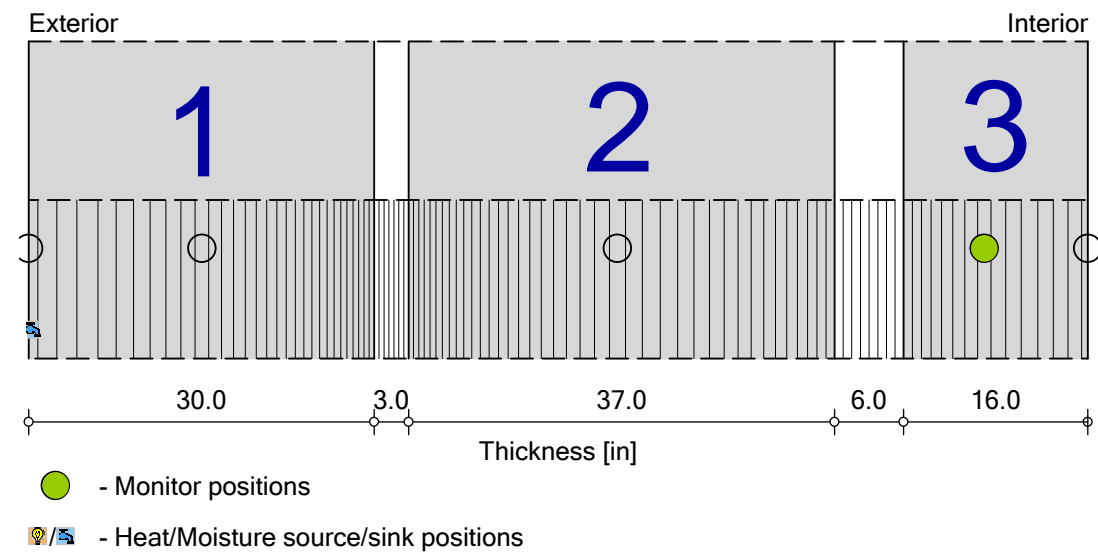


South Masonry Wall Analysis

Existing South Masonry Wall

Boundary Conditions

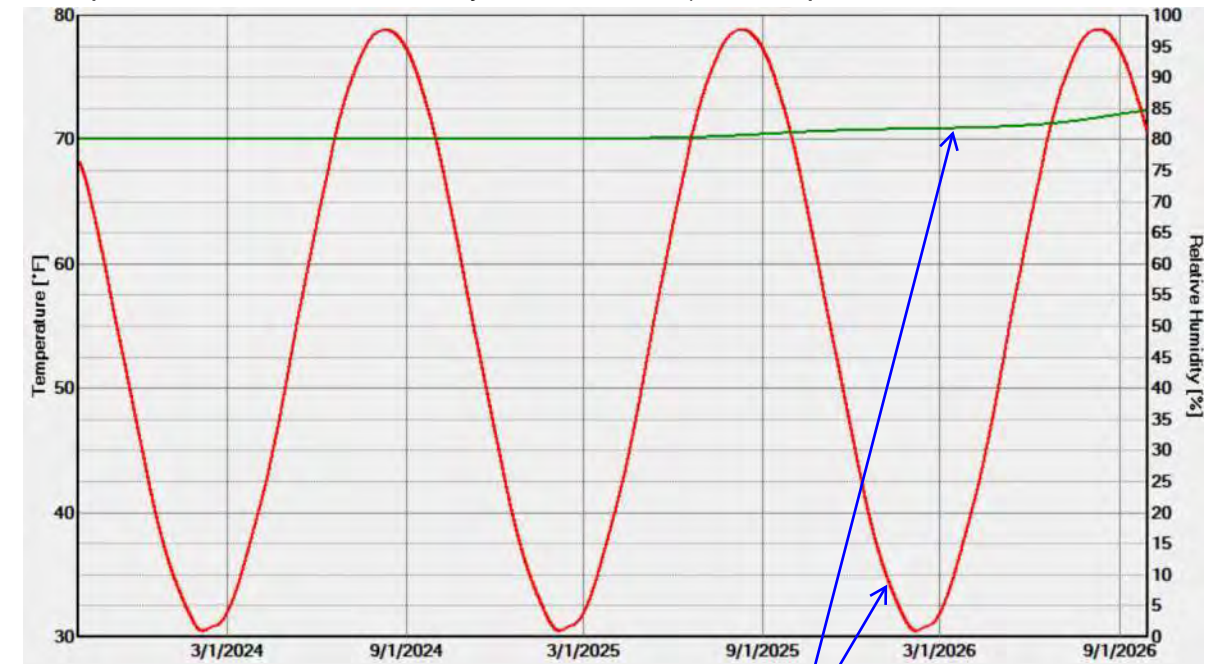
Exterior (left side) Albany, NY
 Interior (right side) 55° F with fluctuation of 25° F; and 72% RH with a 50% amplitude
 Moisture Source Exterior Limestone Layer - 1% (ANSI/ASHRAE standard 160)



Materials:

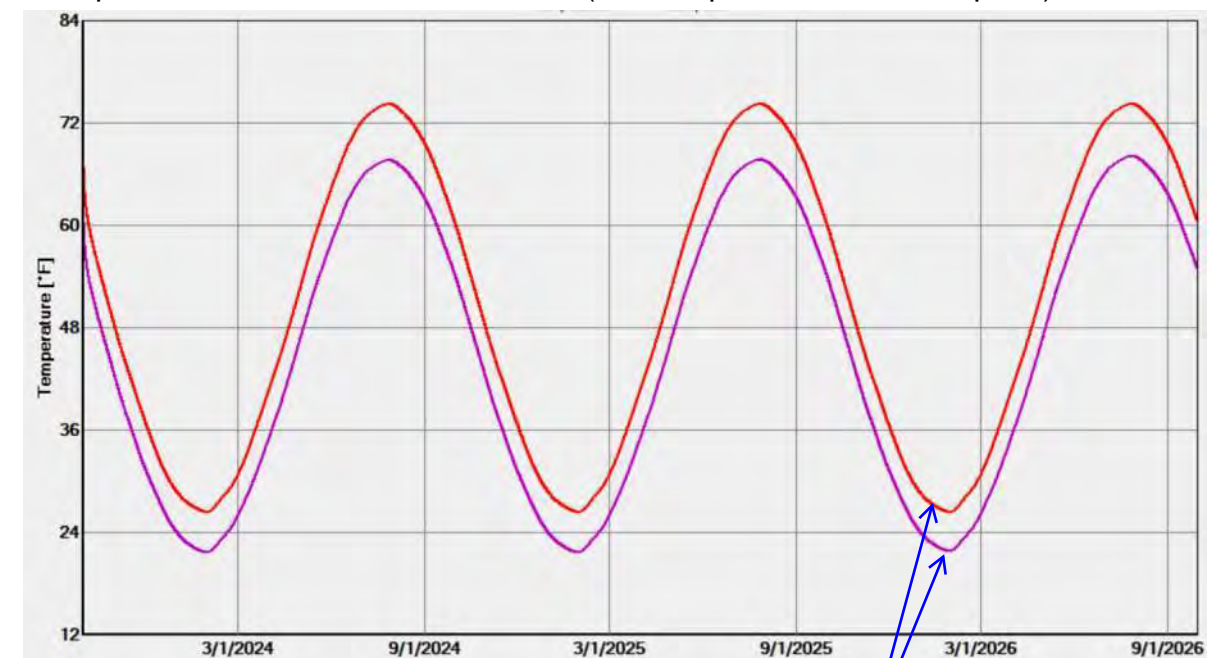
	- Limestone (Georgian Bay Limestone)	30.0 in
	- Lime Mortar, fine	3.0 in
	- Limestone (Georgian Bay Limestone)	37.0 in
	- Lime Mortar, fine	6.0 in
	- Limestone (Georgian Bay Limestone)	16.0 in

Temperature / Relative Humidity at **Monitor 3** (--- temperature / - - - relative humidity)



Temperature fluctuates seasonally; Relative Humidity (RH) trends upward during the 3-year period

Temperature / Dew Point at **Monitor 3** (--- temperature / - - - dew point)



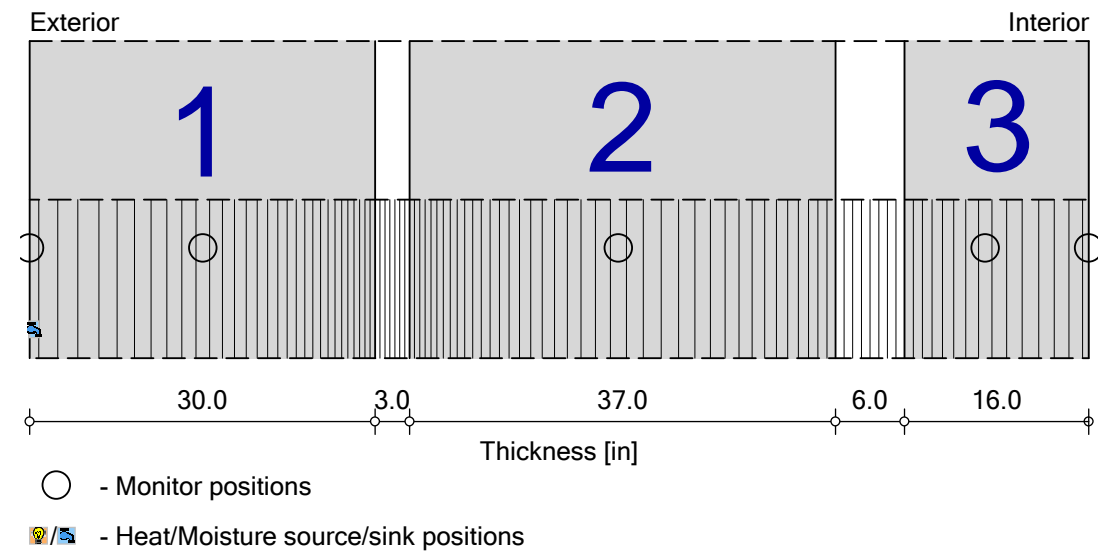
Temperature fluctuates seasonally; Temperature and Dew Point do not intersect (signifies low condensation risk)

South Masonry Wall Analysis




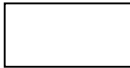

Existing South Masonry Wall (Ten Year Period)

Boundary Conditions

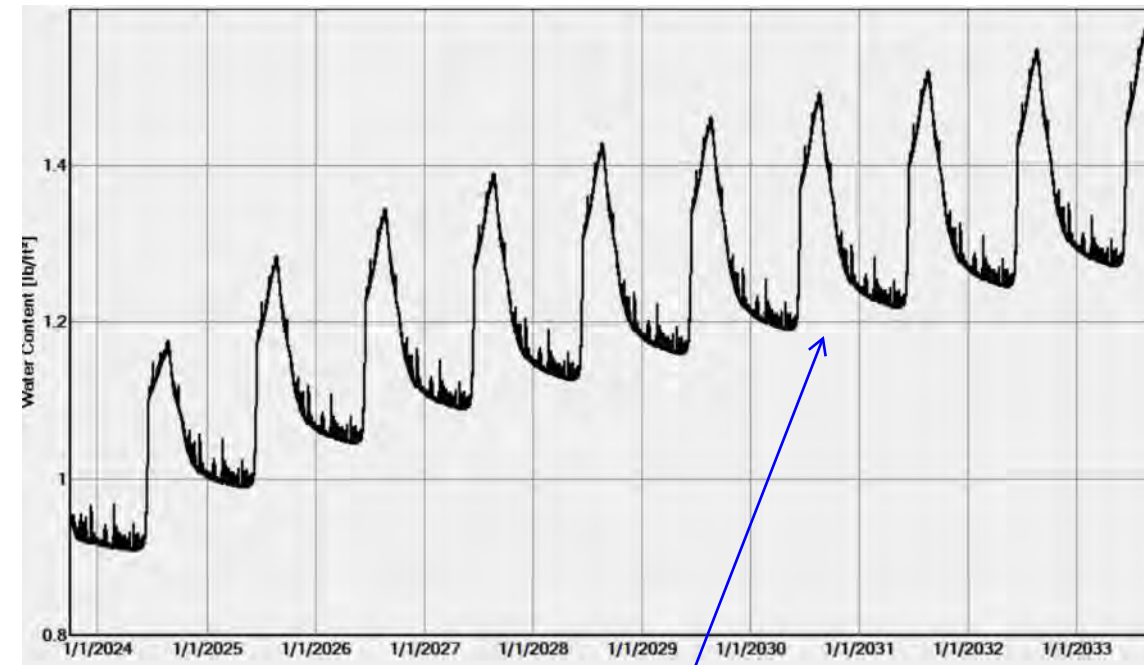
Exterior (left side) Albany, NY
 Interior (right side) 55° F with fluctuation of 25° F; and 72% RH with a 50% amplitude
 Moisture Source Exterior Limestone Layer - 1% (ANSI/ASHRAE standard 160)



Materials:

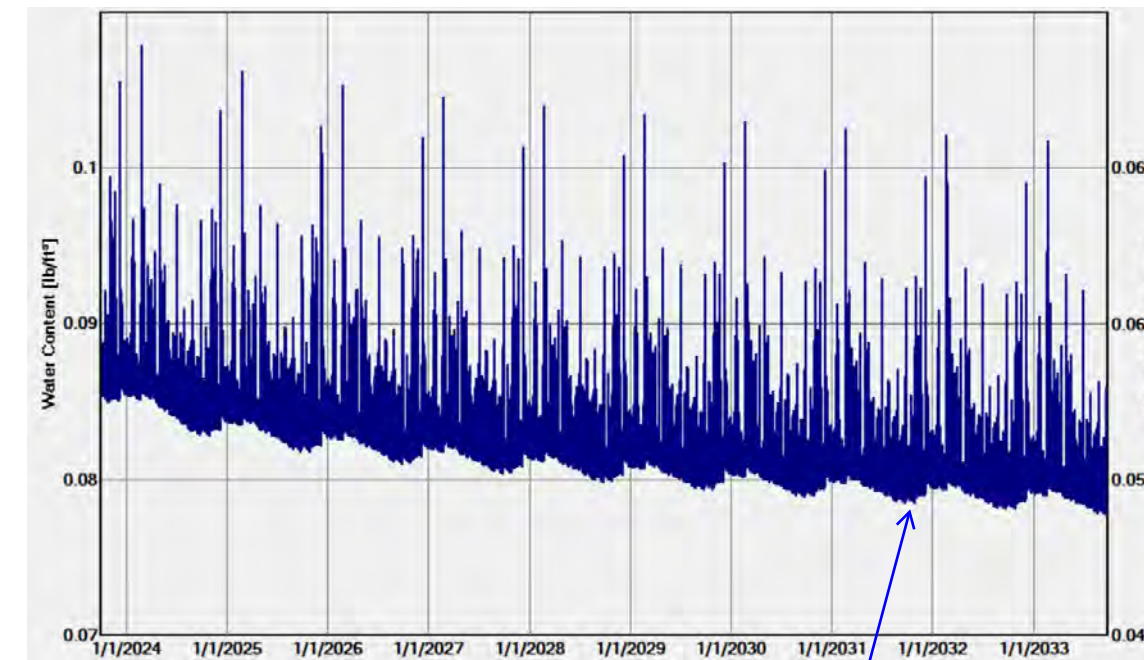
	- Limestone (Georgian Bay Limestone)	30.0 in
	- Lime Mortar, fine	3.0 in
	- Limestone (Georgian Bay Limestone)	37.0 in
	- Lime Mortar, fine	6.0 in
	- Limestone (Georgian Bay Limestone)	16.0 in

Total Water Content - Existing Masonry Wall



Total Water Content (for the entire wall assembly) increases during the 10-year period

Water Content - Limestone Layer 1



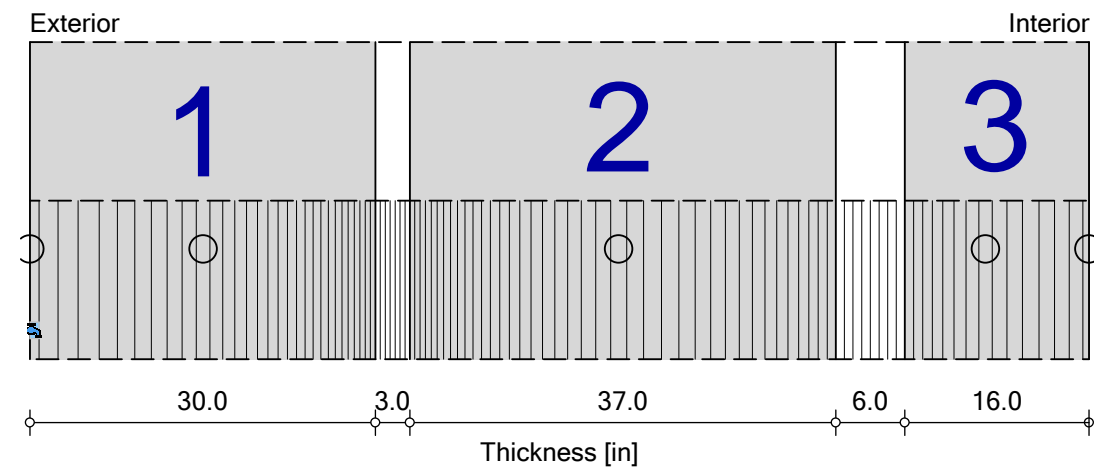
Water content at this exterior layer fluctuates with weather and precipitation events, with a modest, consistent downward trend

South Masonry Wall Analysis

Existing South Masonry Wall (Ten Year Period)

Boundary Conditions

Exterior (left side) Albany, NY
 Interior (right side) 55° F with fluctuation of 25° F; and 72% RH with a 50% amplitude
 Moisture Source Exterior Limestone Layer - 1% (ANSI/ASHRAE standard 160)

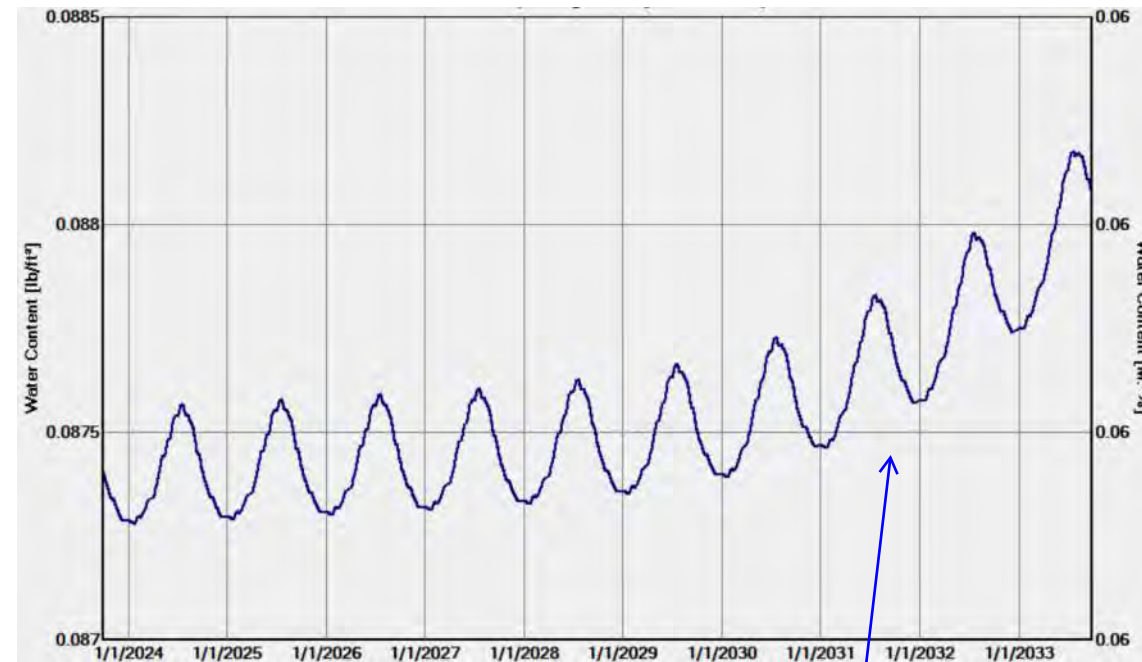


○ - Monitor positions
 - Heat/Moisture source/sink positions

Materials:

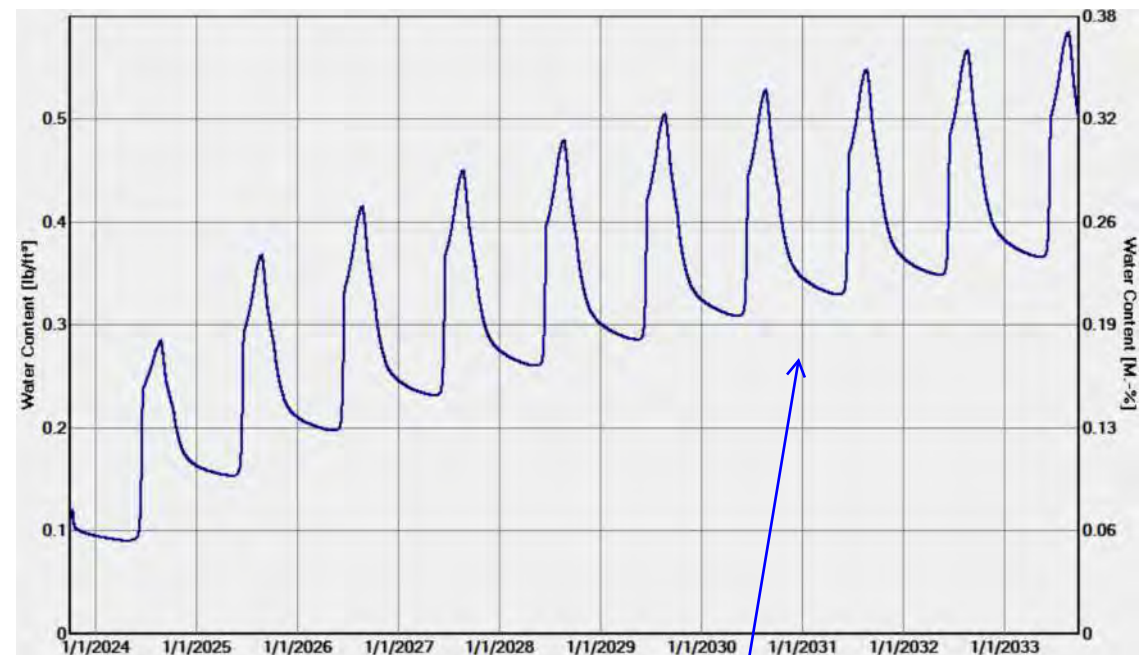
	- Limestone (Georgian Bay Limestone)	30.0 in
	- Lime Mortar, fine	3.0 in
	- Limestone (Georgian Bay Limestone)	37.0 in
	- Lime Mortar, fine	6.0 in
	- Limestone (Georgian Bay Limestone)	16.0 in

Water Content - Limestone Layer 2



Water content at the middle layer fluctuates seasonally, with modest upward trend that increase more rapidly after six years

Water Content - Limestone Layer 3



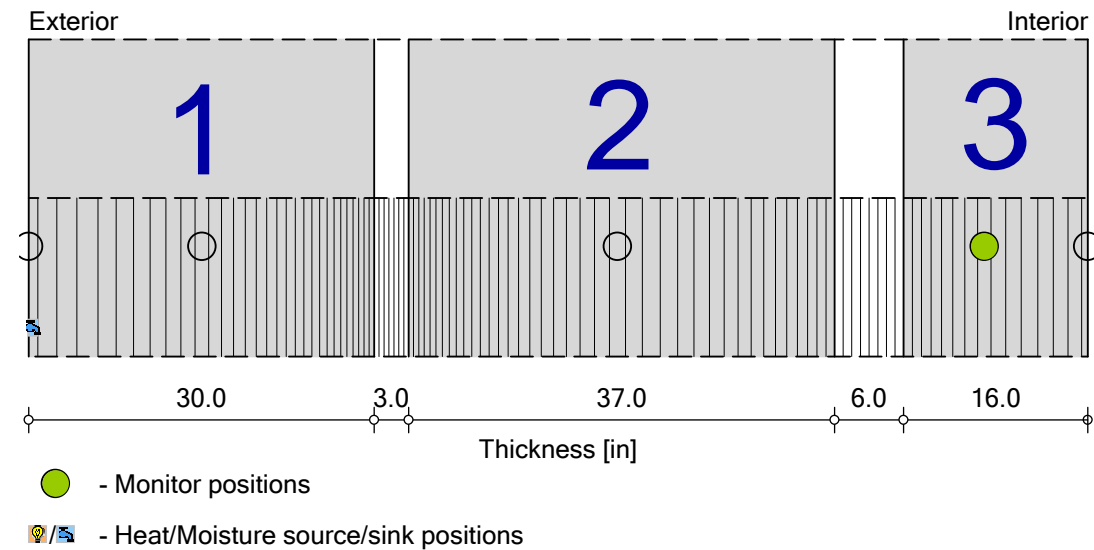
Water content at the interior layer fluctuates seasonally, with significant increase during the 10-year period

South Masonry Wall Analysis

Existing South Masonry Wall (Ten Year Period)

Boundary Conditions

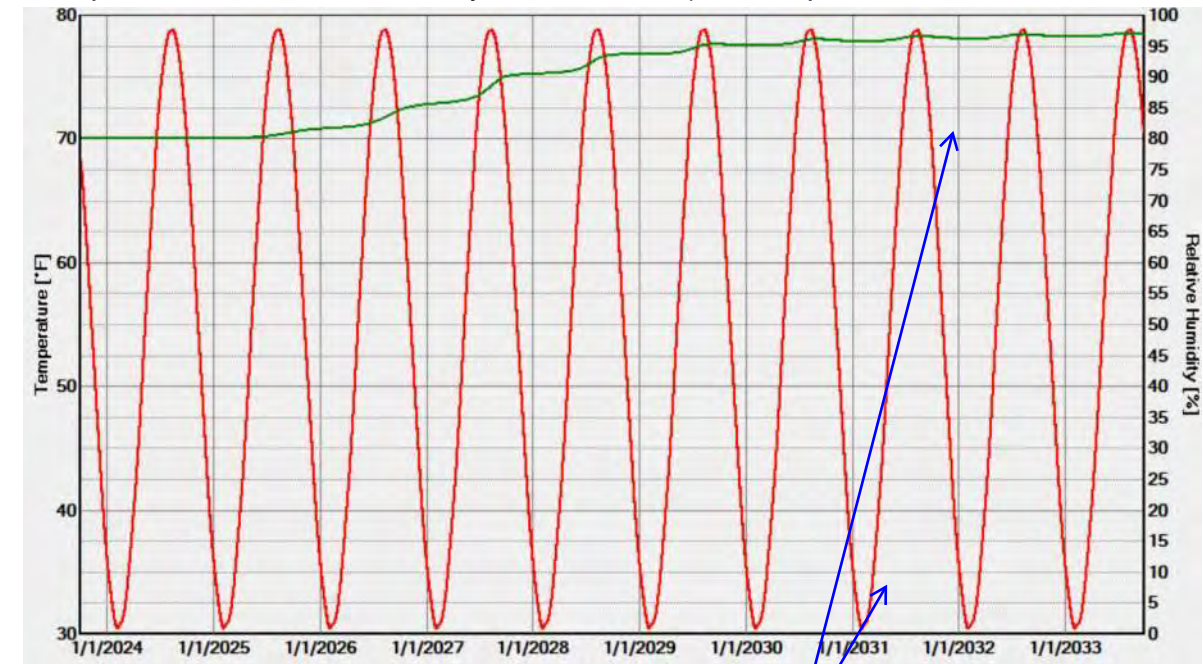
Exterior (left side) Albany, NY
 Interior (right side) 55° F with fluctuation of 25° F; and 72% RH with a 50% amplitude
 Moisture Source Exterior Limestone Layer - 1% (ANSI/ASHRAE standard 160)



Materials:

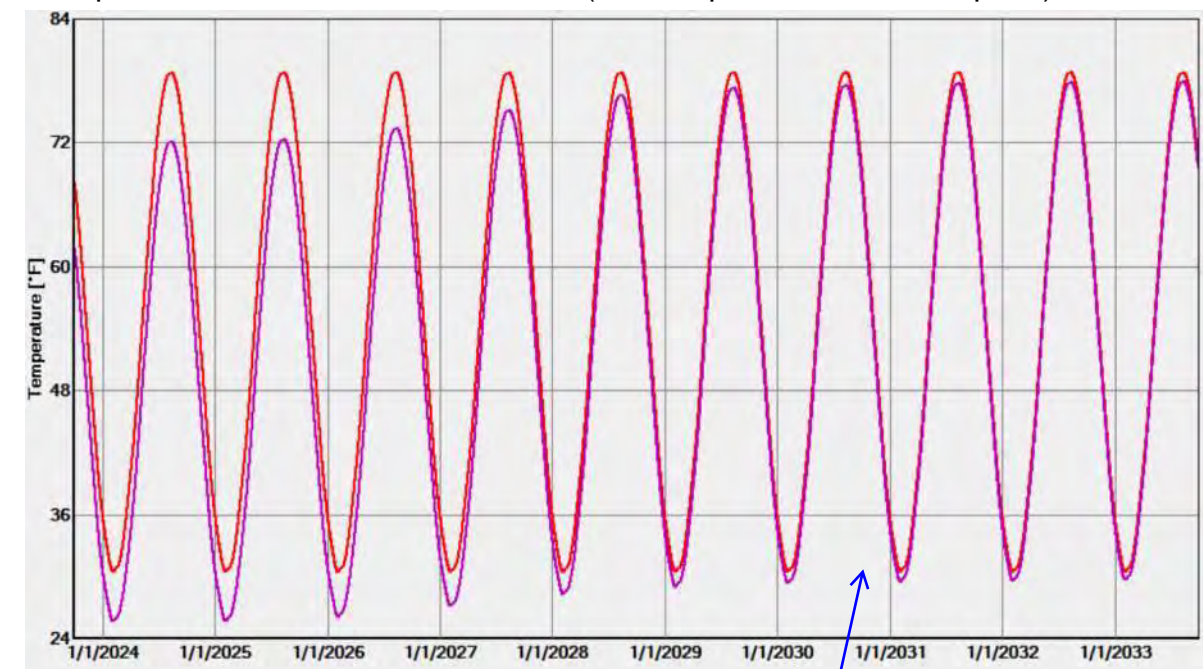
	- Limestone (Georgian Bay Limestone)	30.0 in
	- Lime Mortar, fine	3.0 in
	- Limestone (Georgian Bay Limestone)	37.0 in
	- Lime Mortar, fine	6.0 in
	- Limestone (Georgian Bay Limestone)	16.0 in

Temperature / Relative Humidity at **Monitor 3** (--- temperature / --- relative humidity)



Temperature fluctuates seasonally; Relative Humidity (RH) trends upward during the 10-year period

Temperature / Dew Point at **Monitor 3** (--- temperature / --- dew point)



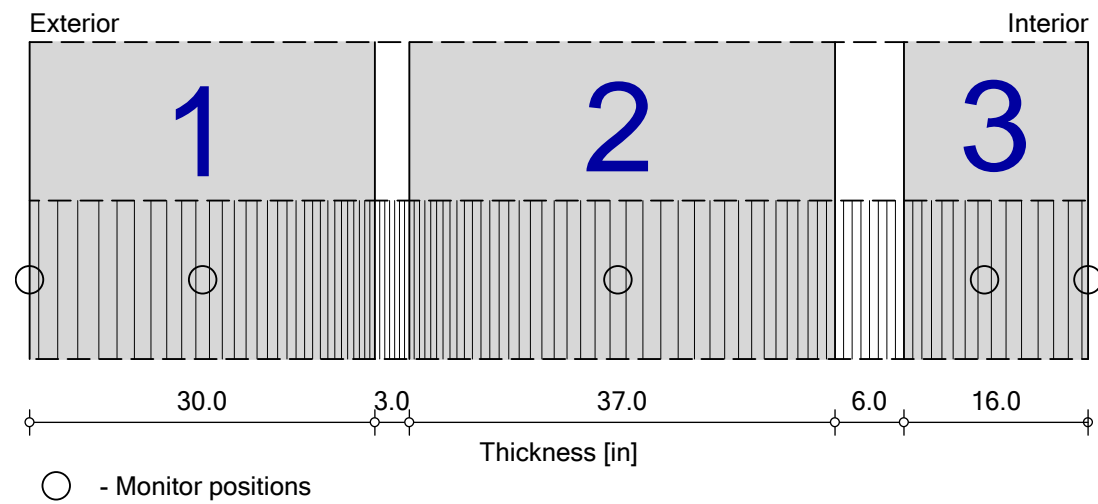
Temperature fluctuates seasonally; Temperature and Dew Point do not intersect, but graphs begin to intersect after six years (signifies condensation risk)

South Masonry Wall Analysis

South Masonry Wall - No Added Moisture + Reduced Interior RH

Boundary Conditions

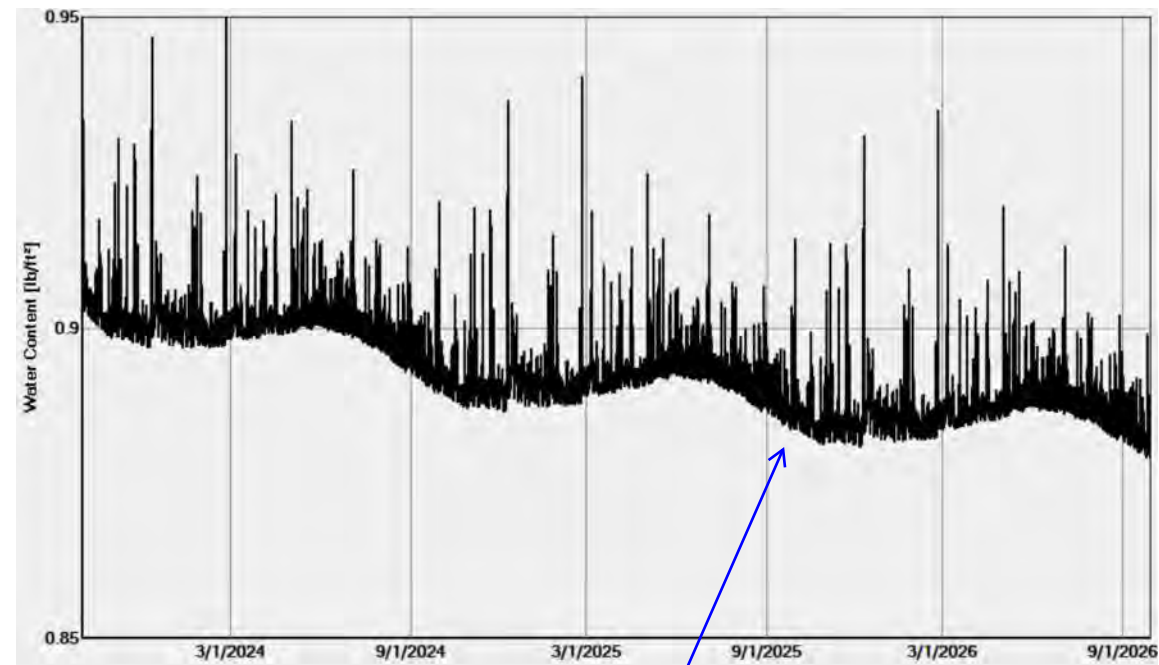
Exterior (left side) Albany, NY
 Interior (right side) 55° F with fluctuation of 25° F; and 60% RH with a 20% amplitude



Materials:

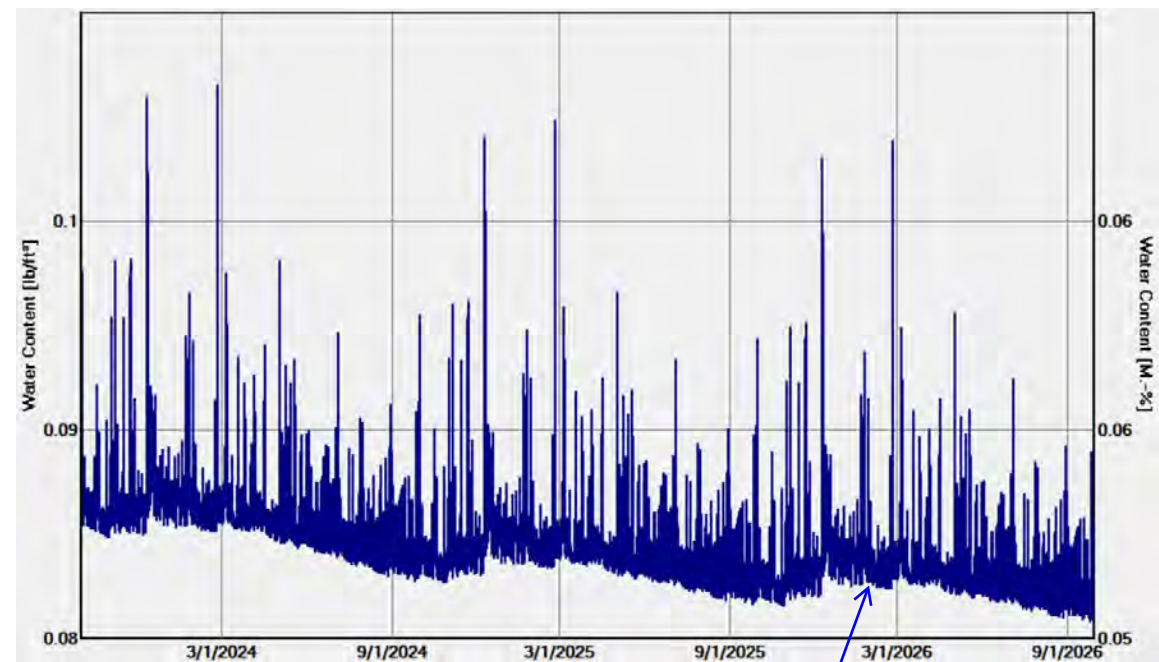
	- Limestone (Georgian Bay Limestone)	30.0 in
	- Lime Mortar, fine	3.0 in
	- Limestone (Georgian Bay Limestone)	37.0 in
	- Lime Mortar, fine	6.0 in
	- Limestone (Georgian Bay Limestone)	16.0 in

Total Water Content - Existing Masonry Wall



Total Water Content (for the entire wall assembly) trends downward during the 3-year period

Water Content - Limestone Layer 1



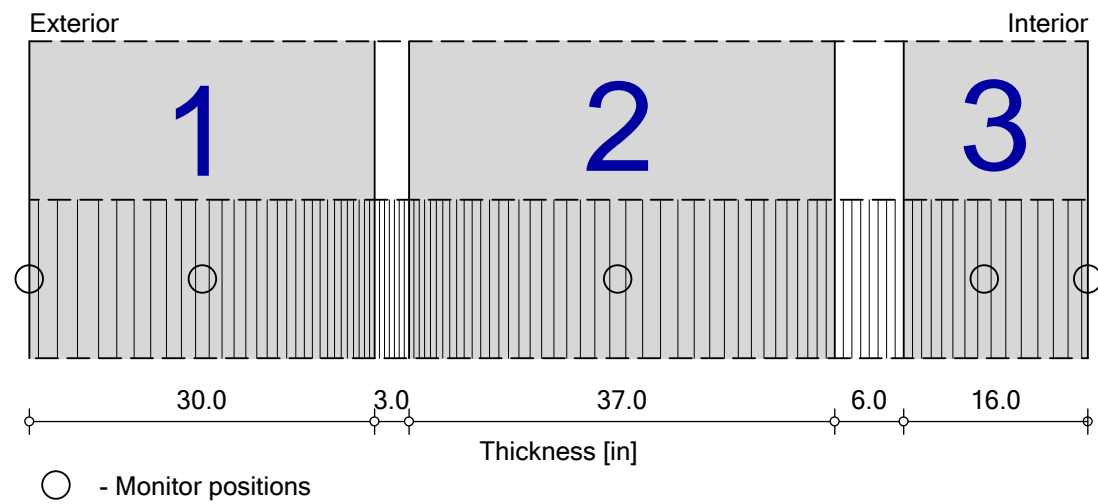
Water content at this exterior layer fluctuates with weather and precipitation events, with a modest downward seasonal trend

South Masonry Wall Analysis

South Masonry Wall - No Added Moisture + Reduced Interior RH

Boundary Conditions

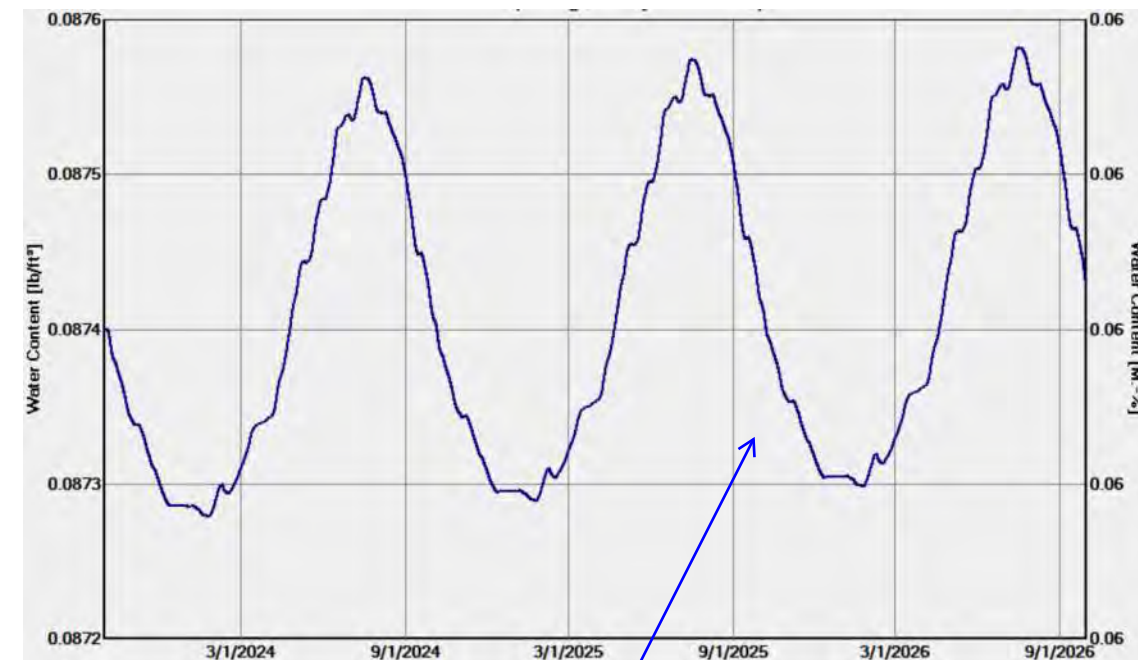
Exterior (left side) Albany, NY
 Interior (right side) 55° F with fluctuation of 25° F; and 60% RH with a 20% amplitude



Materials:

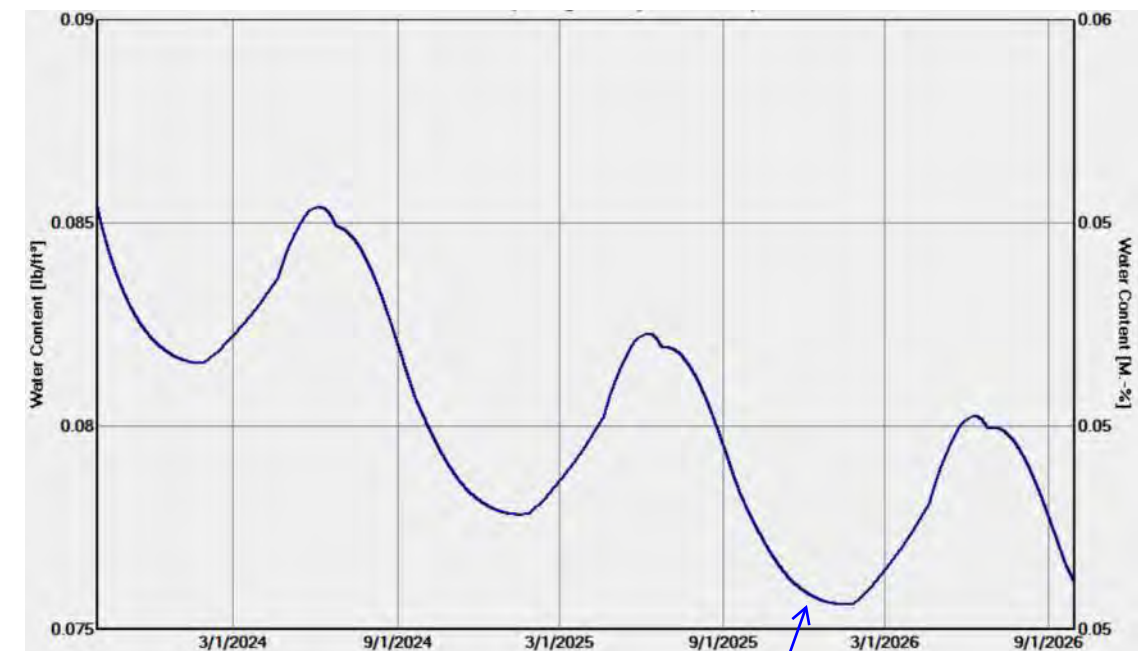
- Limestone (Georgian Bay Limestone) 30.0 in
- Lime Mortar, fine 3.0 in
- Limestone (Georgian Bay Limestone) 37.0 in
- Lime Mortar, fine 6.0 in
- Limestone (Georgian Bay Limestone) 16.0 in

Water Content - Limestone Layer 2



Water content at the middle layer fluctuates seasonally, with minimal upward trend

Water Content - Limestone Layer 3



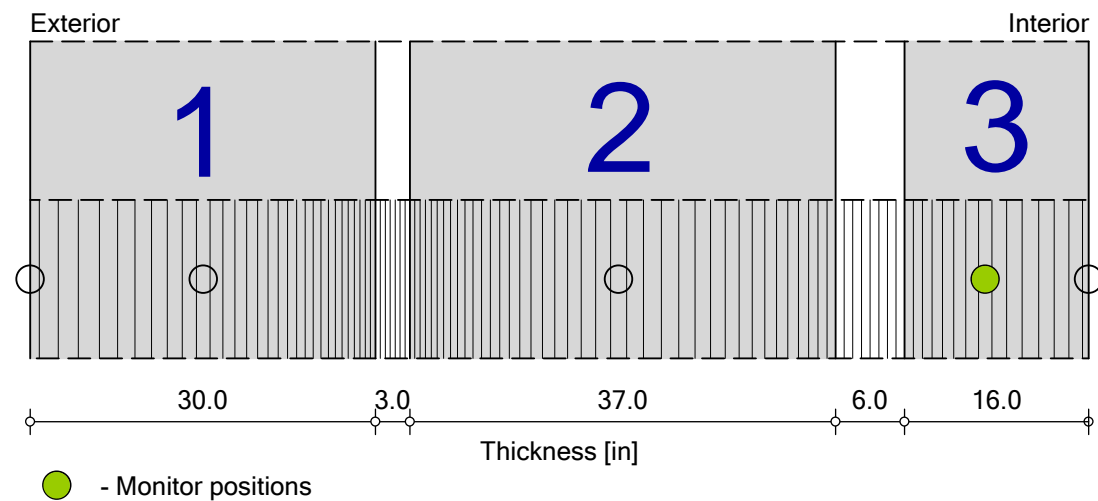
Water content at the interior layer fluctuates seasonally, with decreasing moisture during the 3-year period

South Masonry Wall Analysis

South Masonry Wall - No Added Moisture + Reduced Interior RH

Boundary Conditions

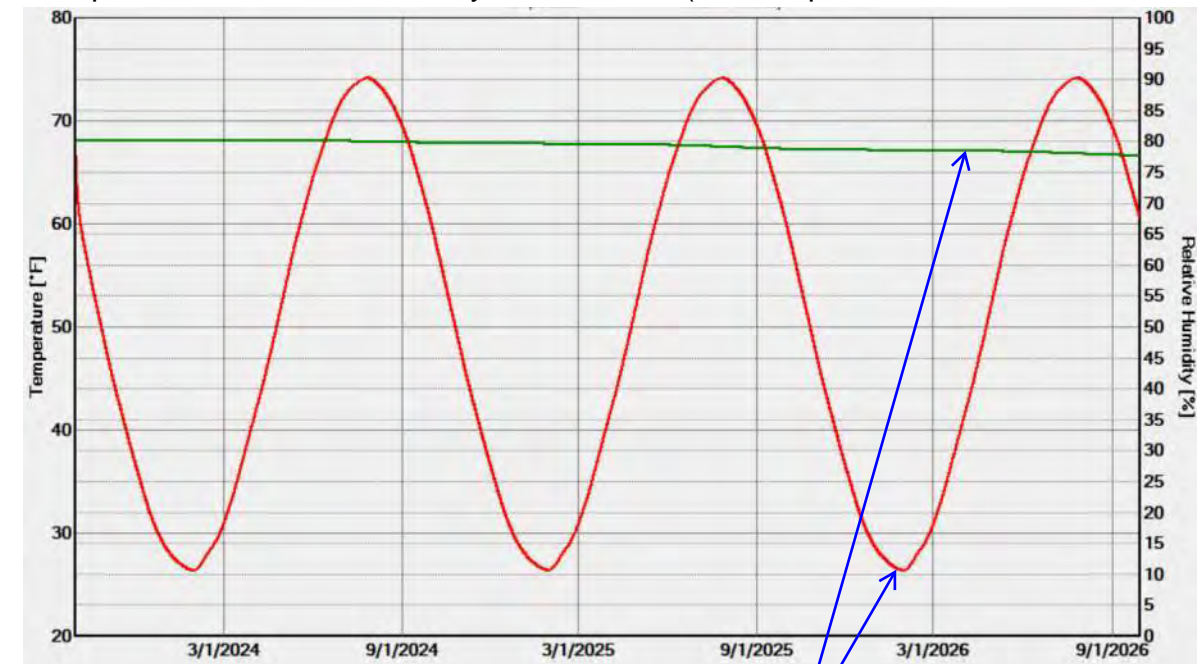
Exterior (left side) Albany, NY
 Interior (right side) 55° F with fluctuation of 25° F; and 60% RH with a 20% amplitude



Materials:

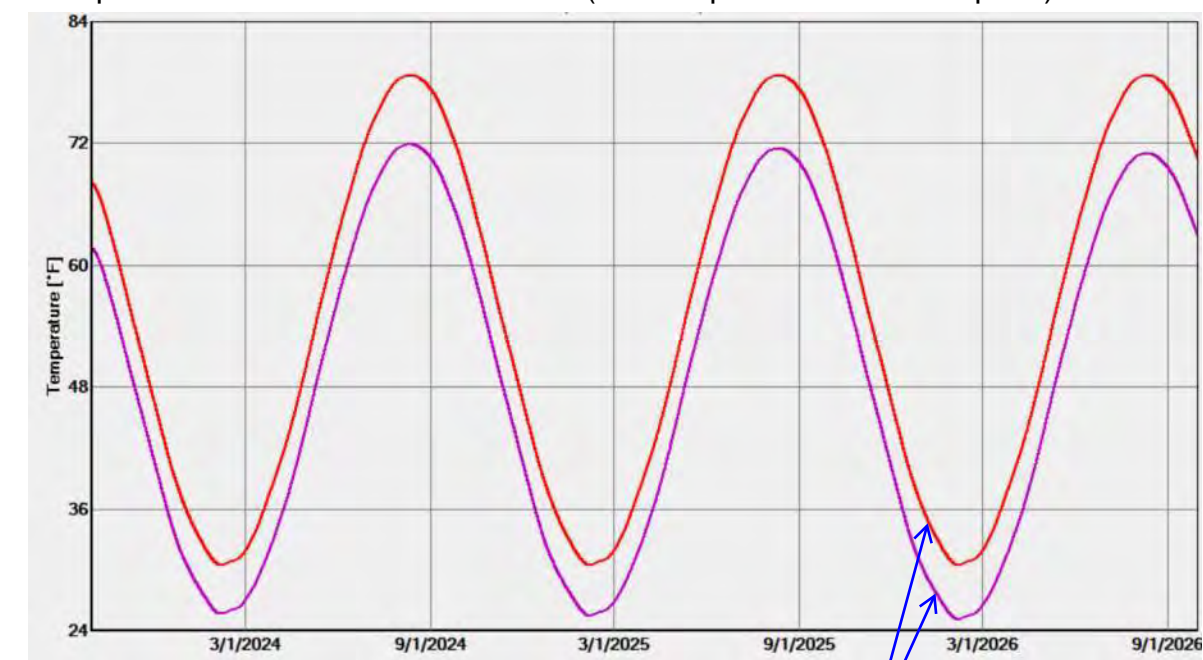
	- Limestone (Georgian Bay Limestone)	30.0 in
	- Lime Mortar, fine	3.0 in
	- Limestone (Georgian Bay Limestone)	37.0 in
	- Lime Mortar, fine	6.0 in
	- Limestone (Georgian Bay Limestone)	16.0 in

Temperature / Relative Humidity at **Monitor 3** (--- temperature / --- relative humidity)



Temperature fluctuates seasonally; Relative Humidity (RH) trends downward during the 3-year period

Temperature / Dew Point at **Monitor 3** (--- temperature / --- dew point)



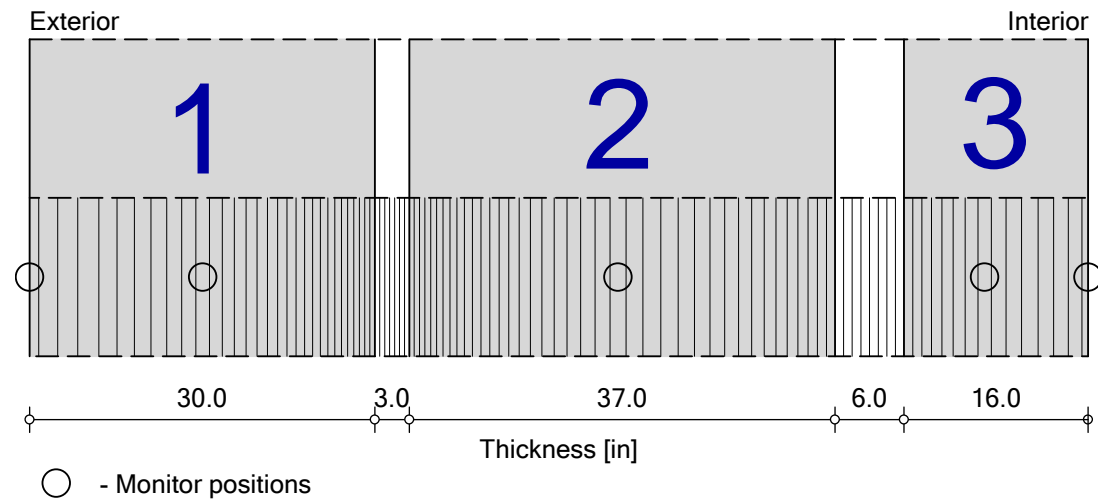
Temperature fluctuates seasonally; Temperature and Dew Point do not intersect (signifies low condensation risk)

South Masonry Wall Analysis

South Masonry Wall - No Added Moisture + Reduced Interior RH (Ten Year Period)

Boundary Conditions

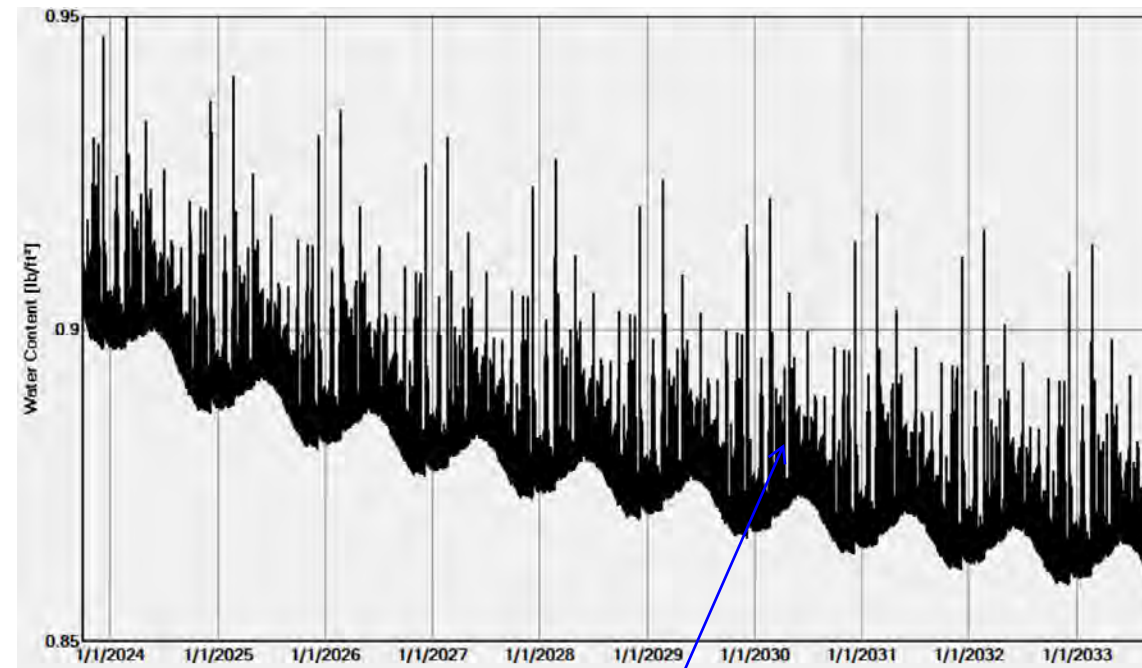
Exterior (left side) Albany, NY
 Interior (right side) 55° F with fluctuation of 25° F; and 60% RH with a 20% amplitude



Materials:

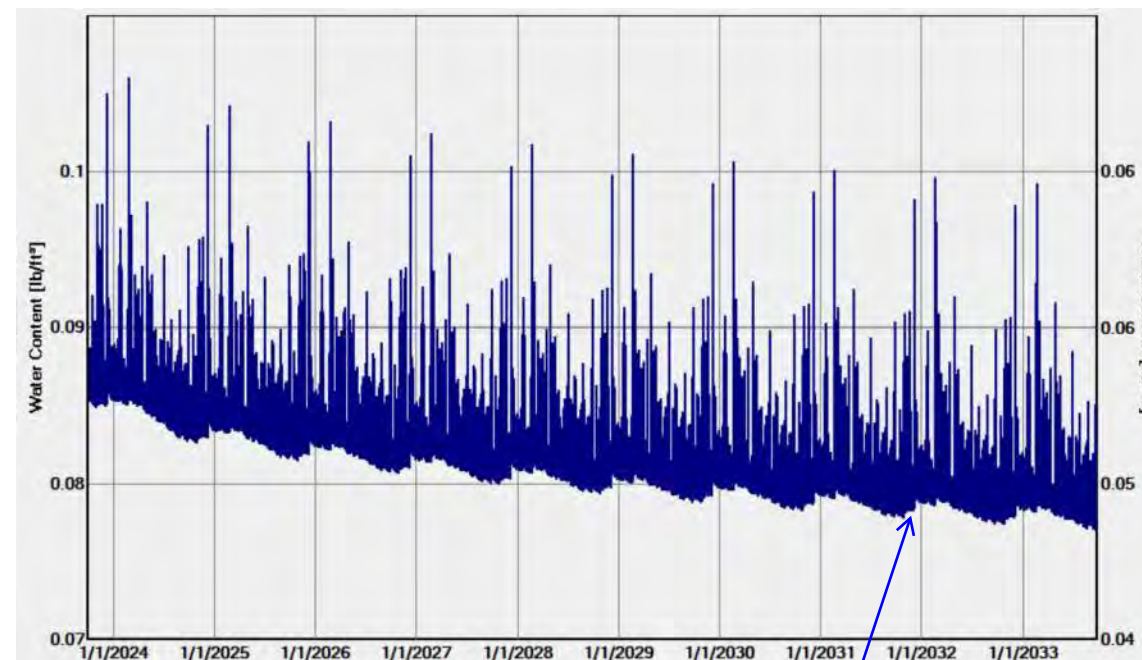
	- Limestone (Georgian Bay Limestone)	30.0 in
	- Lime Mortar, fine	3.0 in
	- Limestone (Georgian Bay Limestone)	37.0 in
	- Lime Mortar, fine	6.0 in
	- Limestone (Georgian Bay Limestone)	16.0 in

Total Water Content - Existing Masonry Wall



Total Water Content (for the entire wall assembly) trends downward during the 10-year period

Water Content - Limestone Layer 1



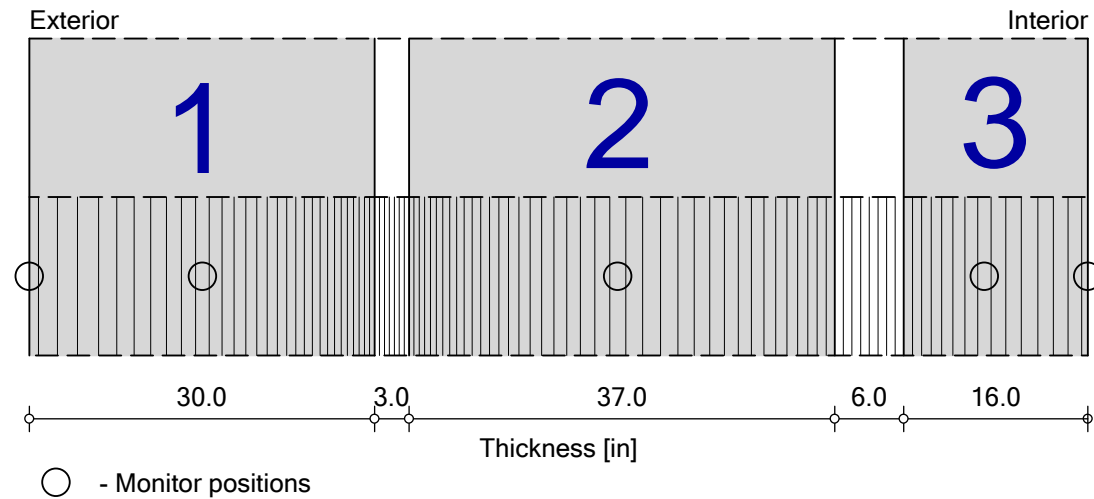
Water content at this exterior layer fluctuates with weather and precipitation events, with a consistent downward trend

South Masonry Wall Analysis

South Masonry Wall - No Added Moisture + Reduced Interior RH (Ten Year Period)

Boundary Conditions

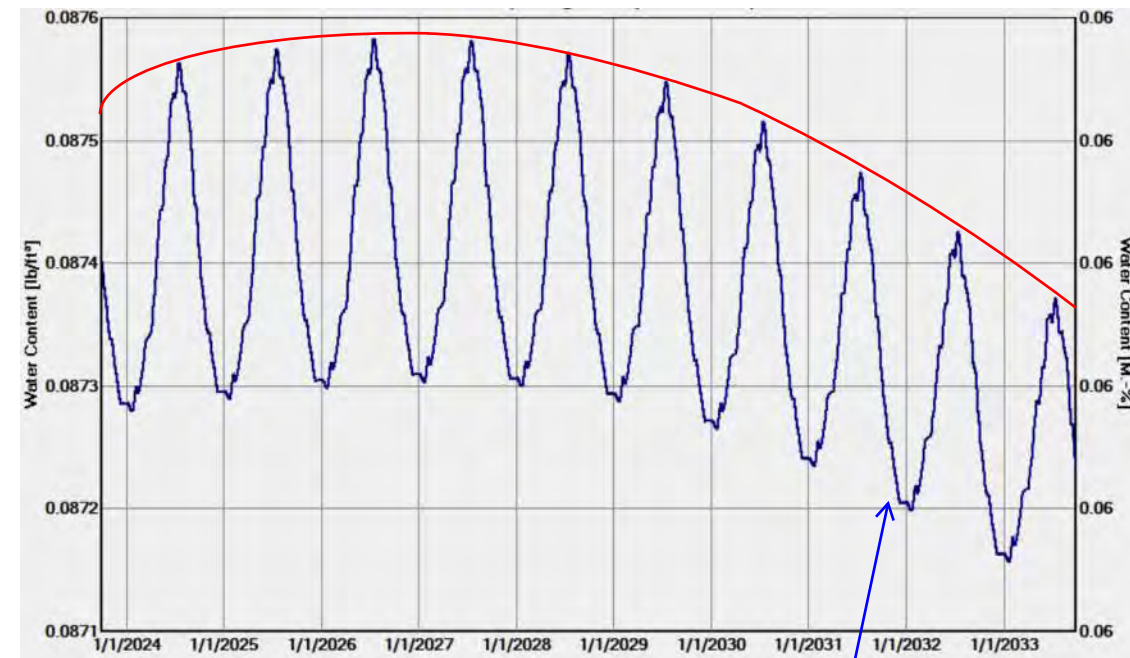
Exterior (left side) Albany, NY
 Interior (right side) 55° F with fluctuation of 25° F; and 60% RH with a 20% amplitude



Materials:

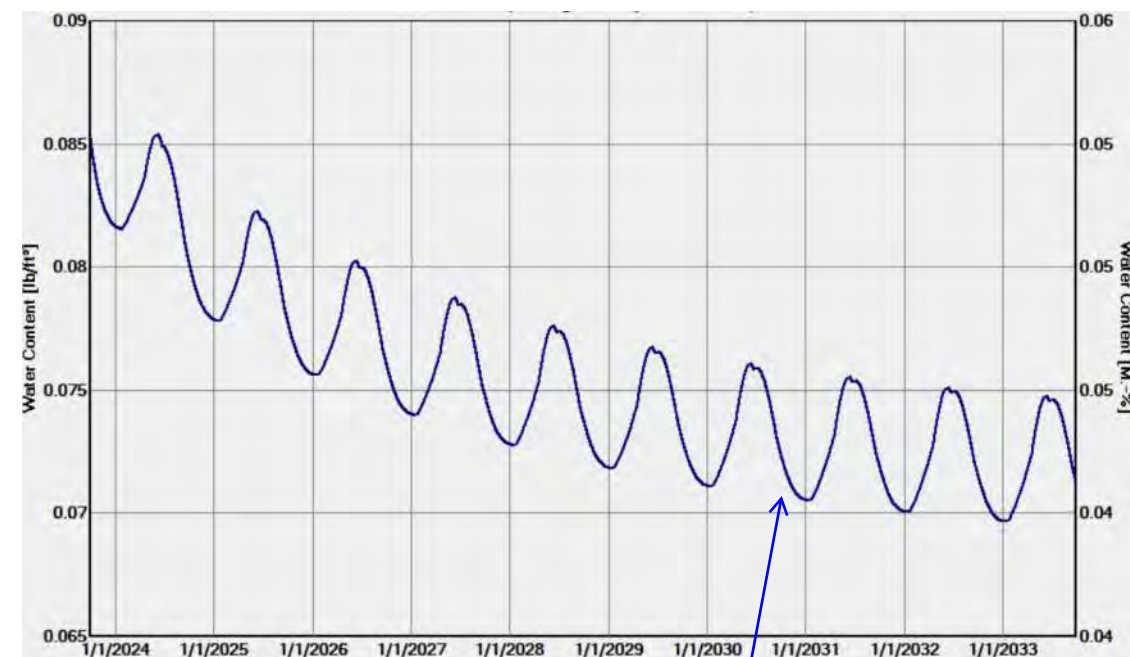
- Limestone (Georgian Bay Limestone) 30.0 in
- Lime Mortar, fine 3.0 in
- Limestone (Georgian Bay Limestone) 37.0 in
- Lime Mortar, fine 6.0 in
- Limestone (Georgian Bay Limestone) 16.0 in

Water Content - Limestone Layer 2



Water content at the middle layer fluctuates seasonally, initially with minimal upward trend that reverses after three years

Water Content - Limestone Layer 3



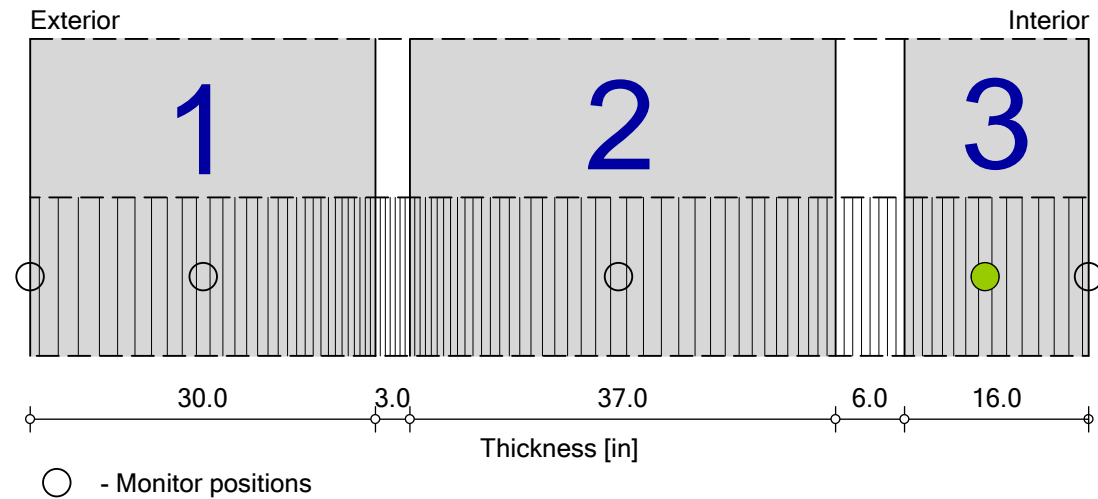
Water content at the interior layer fluctuates seasonally, with decreasing moisture during the 10-year period

South Masonry Wall Analysis

South Masonry Wall - No Added Moisture + Reduced Interior RH (Ten Year Period)

Boundary Conditions

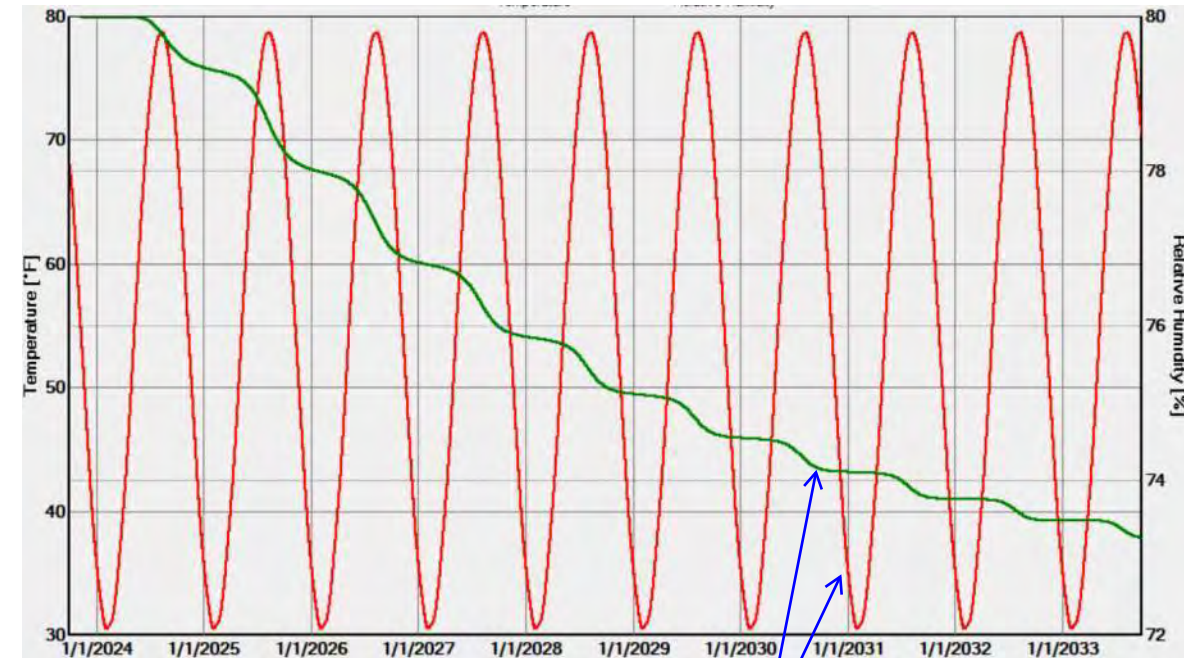
Exterior (left side) Albany, NY
 Interior (right side) 55° F with fluctuation of 25° F; and 60% RH with a 20% amplitude



Materials:

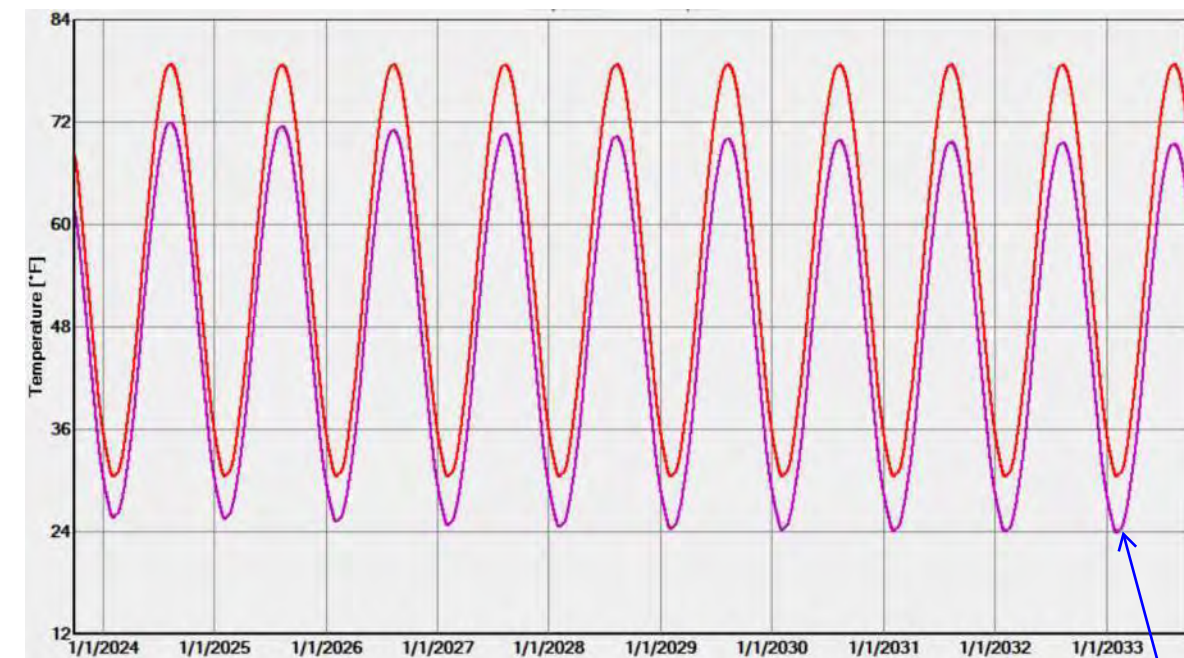
- Limestone (Georgian Bay Limestone) 30.0 in
- Lime Mortar, fine 3.0 in
- Limestone (Georgian Bay Limestone) 37.0 in
- Lime Mortar, fine 6.0 in
- Limestone (Georgian Bay Limestone) 16.0 in

Temperature / Relative Humidity at **Monitor 3** (--- temperature / --- relative humidity)



Temperature fluctuates seasonally; Relative Humidity (RH) trends downward during the 10-year period

Temperature / Dew Point at **Monitor 3** (--- temperature / --- dew point)



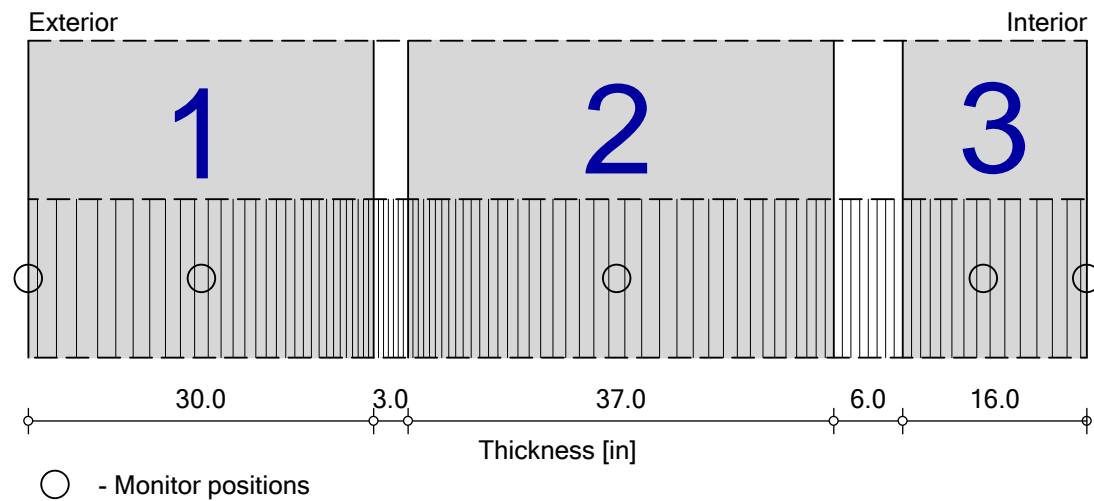
Temperature fluctuates seasonally; Temperature and Dew Point do not intersect; graphs grow further apart during the 10-year period (signifies reduced condensation risk)

South Masonry Wall Analysis

South Masonry Wall - Without Added Moisture

Boundary Conditions

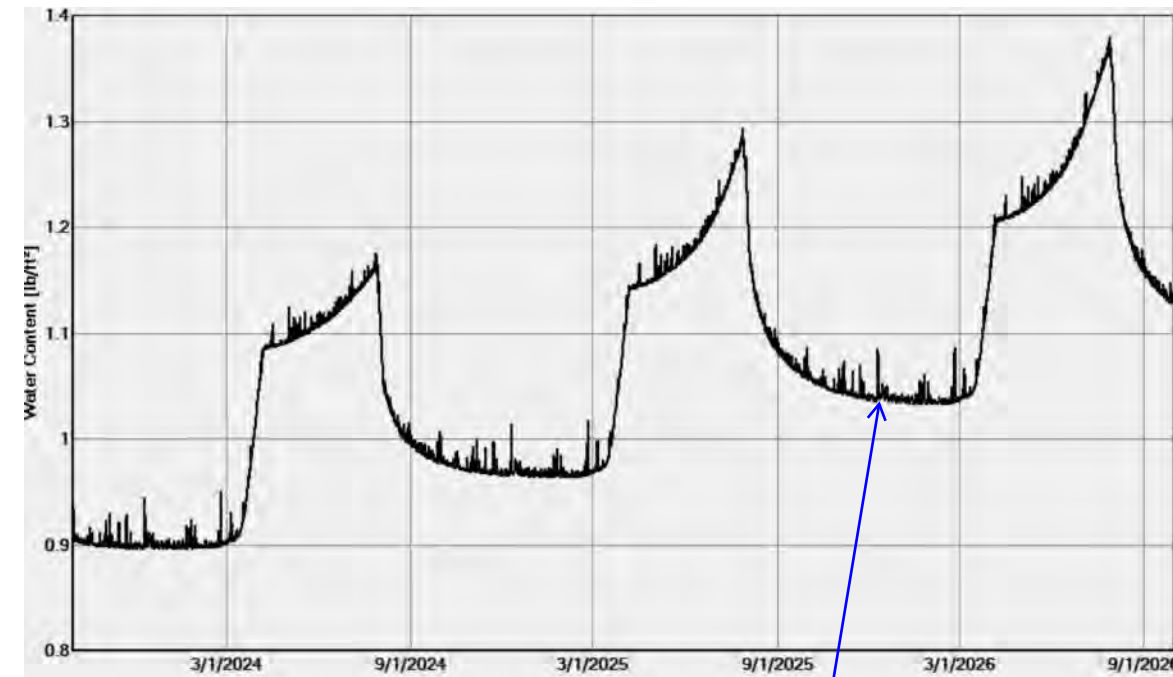
Exterior (left side) Albany, NY
 Interior (right side) 55° F with fluctuation of 25° F; and 72% RH with a 50% amplitude



Materials:

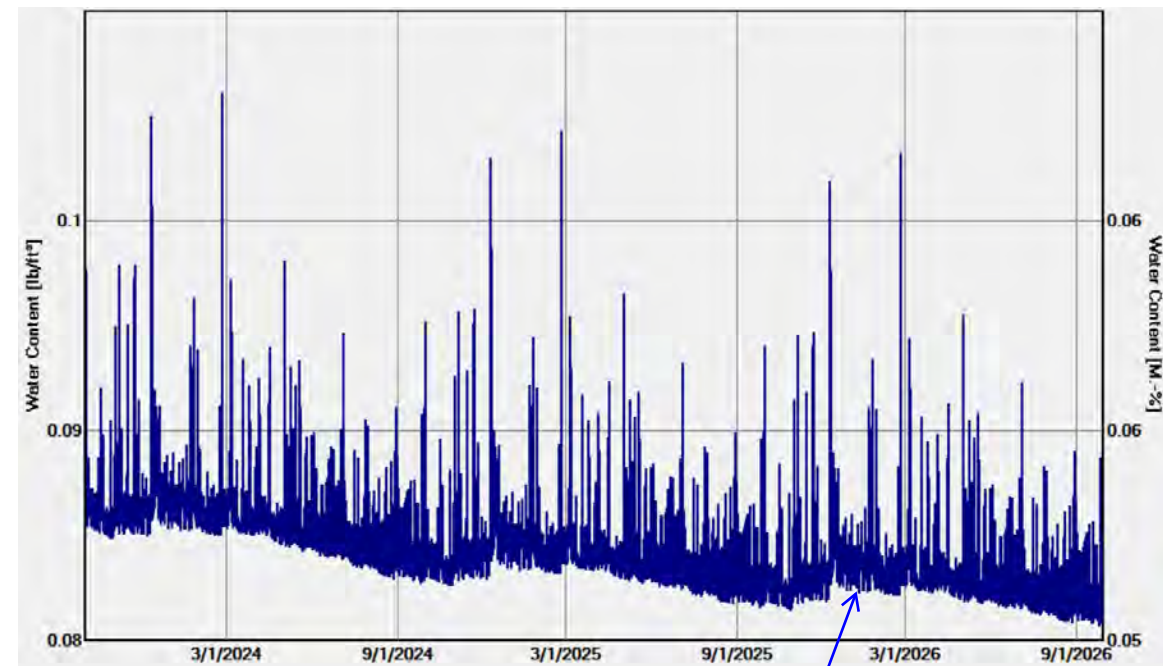
- Limestone (Georgian Bay Limestone) 30.0 in
- Lime Mortar, fine 3.0 in
- Limestone (Georgian Bay Limestone) 37.0 in
- Lime Mortar, fine 6.0 in
- Limestone (Georgian Bay Limestone) 16.0 in

Total Water Content - Existing Masonry Wall



Total Water Content (for the entire wall assembly) increases during the 3-year period (similar to Existing, Page 3)

Water Content - Limestone Layer 1



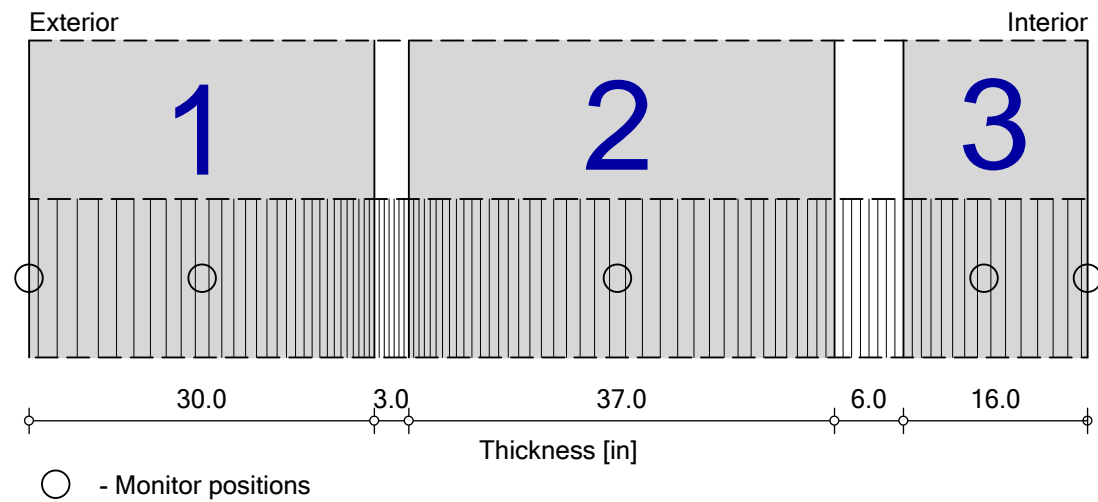
Water content at this exterior layer fluctuates with weather and precipitation events, with a modest downward seasonal trend

South Masonry Wall Analysis

South Masonry Wall - Without Added Moisture

Boundary Conditions

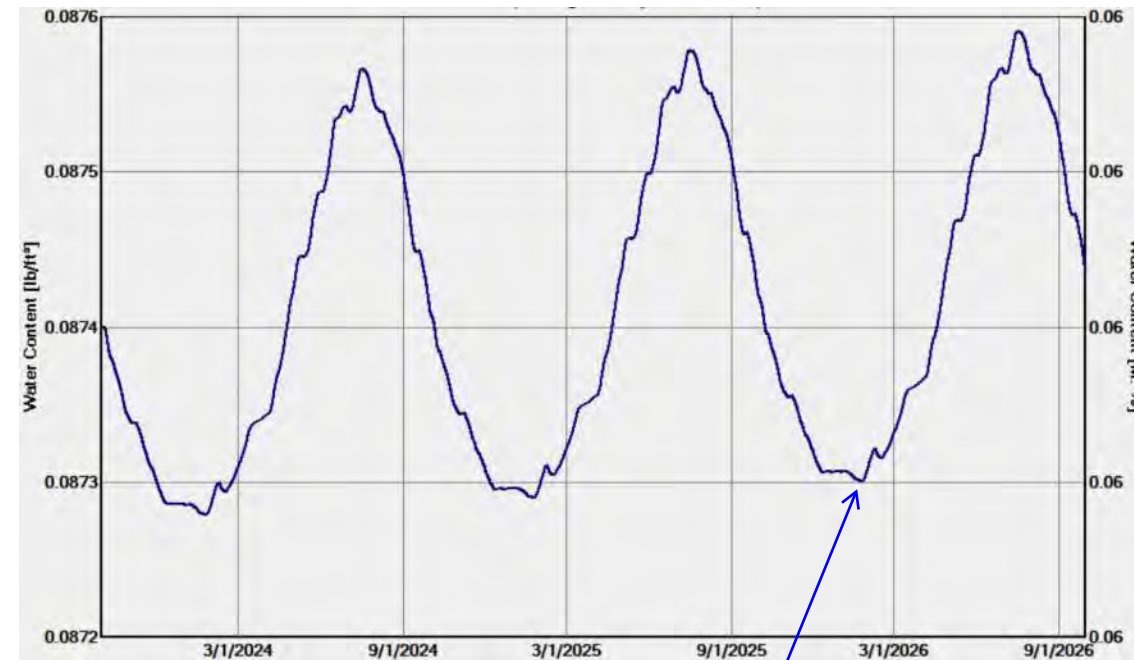
Exterior (left side) Albany, NY
 Interior (right side) 55° F with fluctuation of 25° F; and 72% RH with a 50% amplitude



Materials:

- Limestone (Georgian Bay Limestone) 30.0 in
- Lime Mortar, fine 3.0 in
- Limestone (Georgian Bay Limestone) 37.0 in
- Lime Mortar, fine 6.0 in
- Limestone (Georgian Bay Limestone) 16.0 in

Water Content - Limestone Layer 2



Water content at the middle layer fluctuates seasonally, with modest upward trend

Water Content - Limestone Layer 3



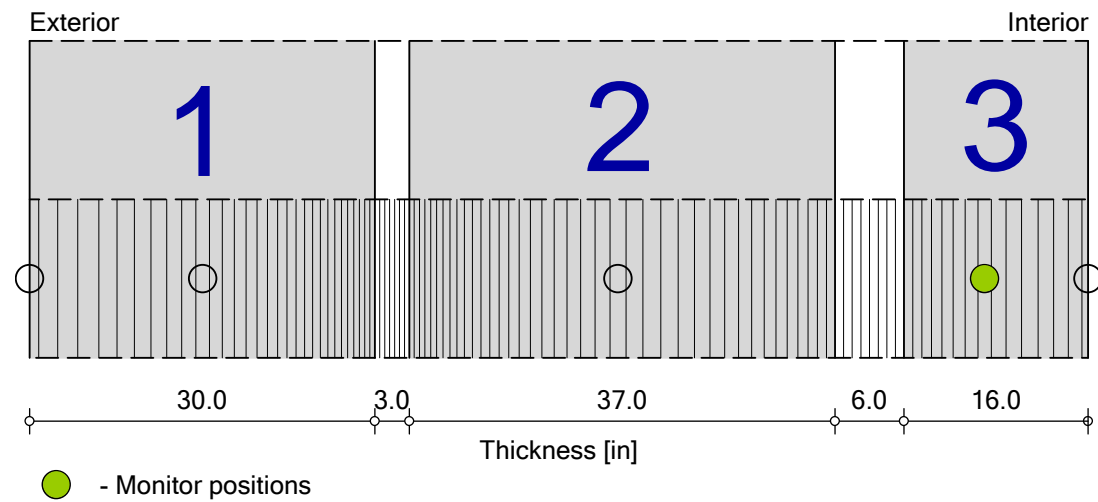
Water content at the interior layer fluctuates seasonally, with significant increase during the 3-year period

South Masonry Wall Analysis

South Masonry Wall - Without Added Moisture

Boundary Conditions

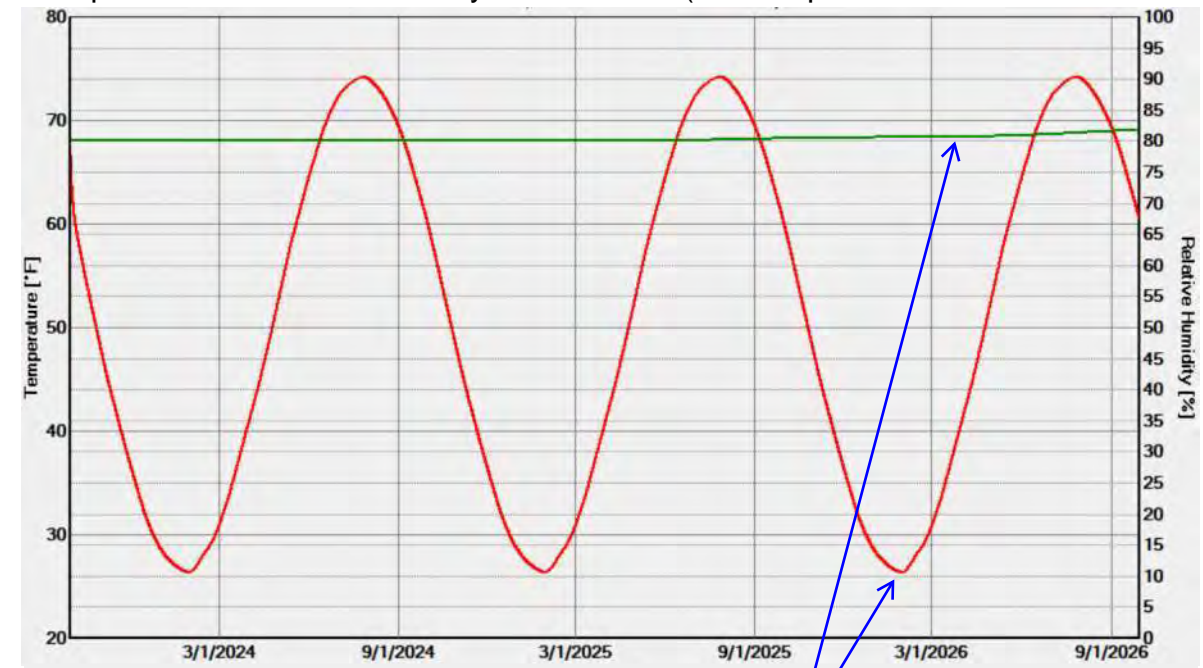
Exterior (left side) Albany, NY
 Interior (right side) 55° F with fluctuation of 25° F; and 72% RH with a 50% amplitude



Materials:

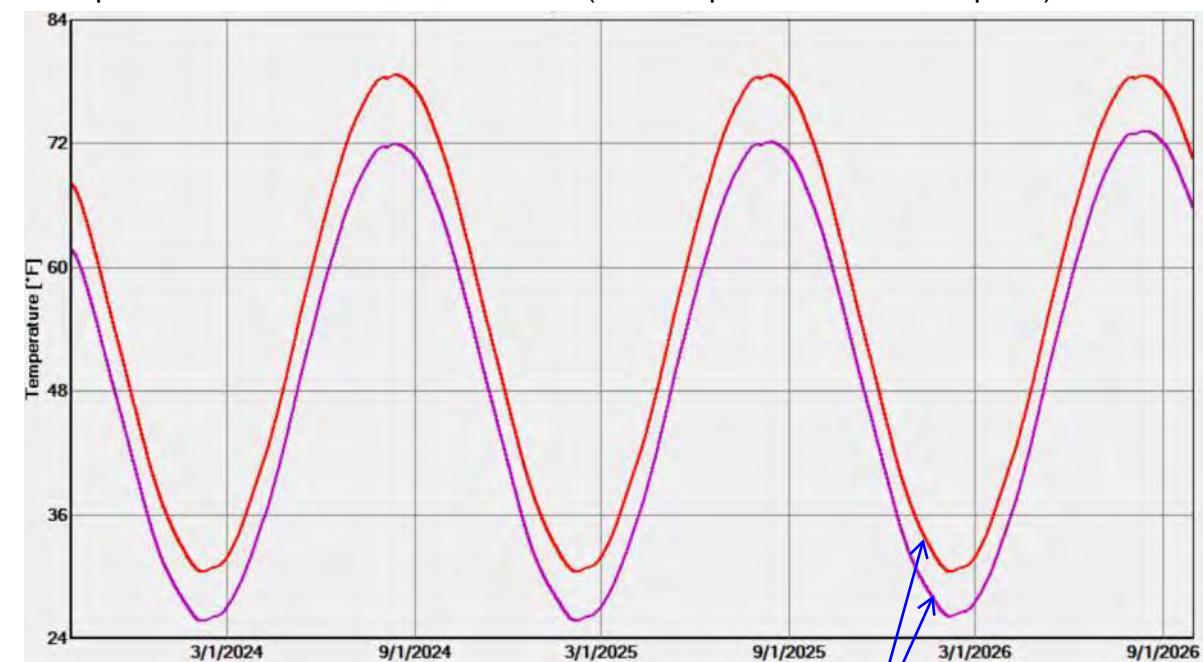
- Limestone (Georgian Bay Limestone) 30.0 in
- Lime Mortar, fine 3.0 in
- Limestone (Georgian Bay Limestone) 37.0 in
- Lime Mortar, fine 6.0 in
- Limestone (Georgian Bay Limestone) 16.0 in

Temperature / Relative Humidity at **Monitor 3** (--- temperature / --- relative humidity)



Temperature fluctuates seasonally; Relative Humidity (RH) trends upward during the 3-year period

Temperature / Dew Point at **Monitor 3** (--- temperature / --- dew point)



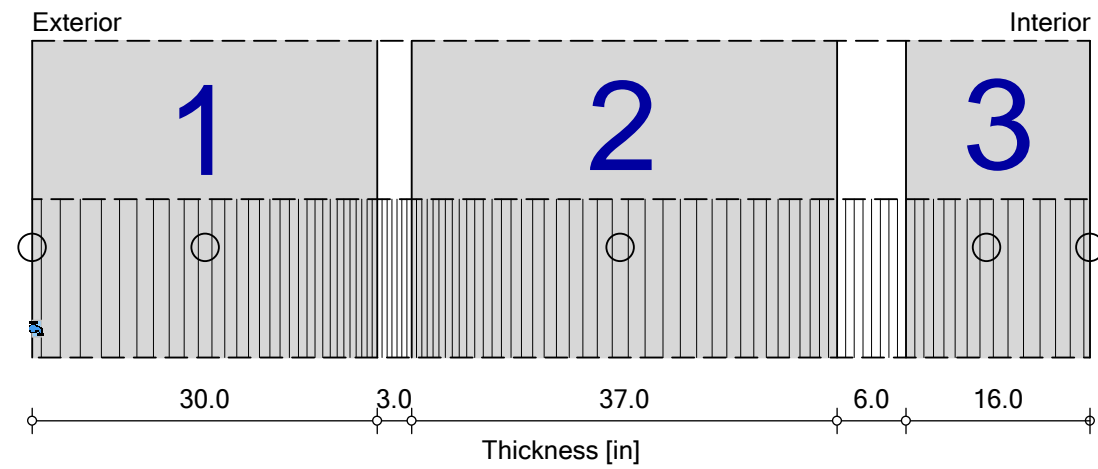
Temperature fluctuates seasonally; Temperature and Dew Point do not intersect (signifies low condensation risk)

South Masonry Wall Analysis

South Masonry Wall - With Increased Moisture

Boundary Conditions

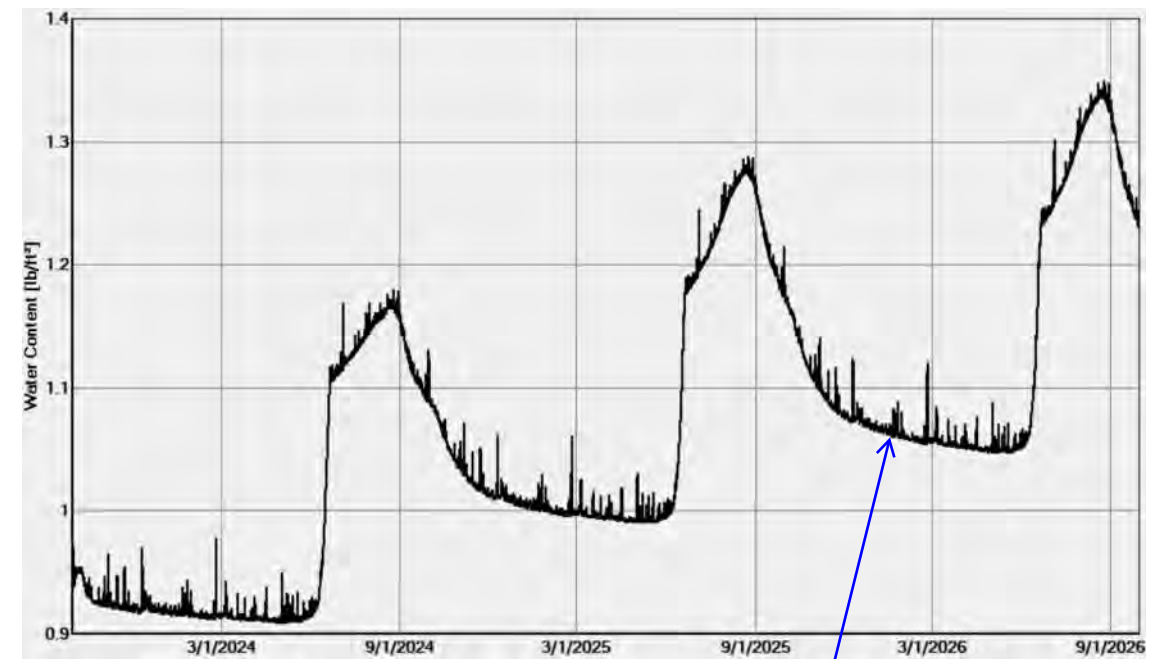
Exterior (left side) Albany, NY
 Interior (right side) 55° F with fluctuation of 25° F; and 72% RH with a 50% amplitude
 Moisture Source **Exterior Limestone Layer - 3%**



Materials:

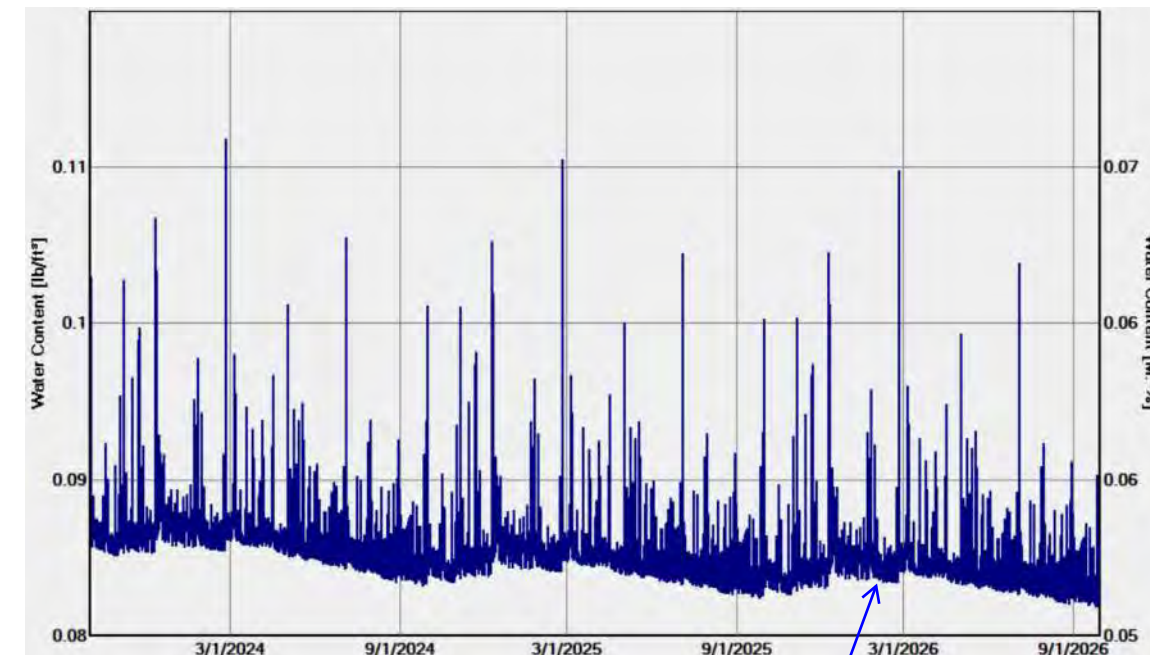
	- Limestone (Georgian Bay Limestone)	30.0 in
	- Lime Mortar, fine	3.0 in
	- Limestone (Georgian Bay Limestone)	37.0 in
	- Lime Mortar, fine	6.0 in
	- Limestone (Georgian Bay Limestone)	16.0 in

Total Water Content - Existing Masonry Wall



Total Water Content (for the entire wall assembly) increases during the 3-year period (similar to Existing, Page 3)

Water Content - Limestone Layer 1



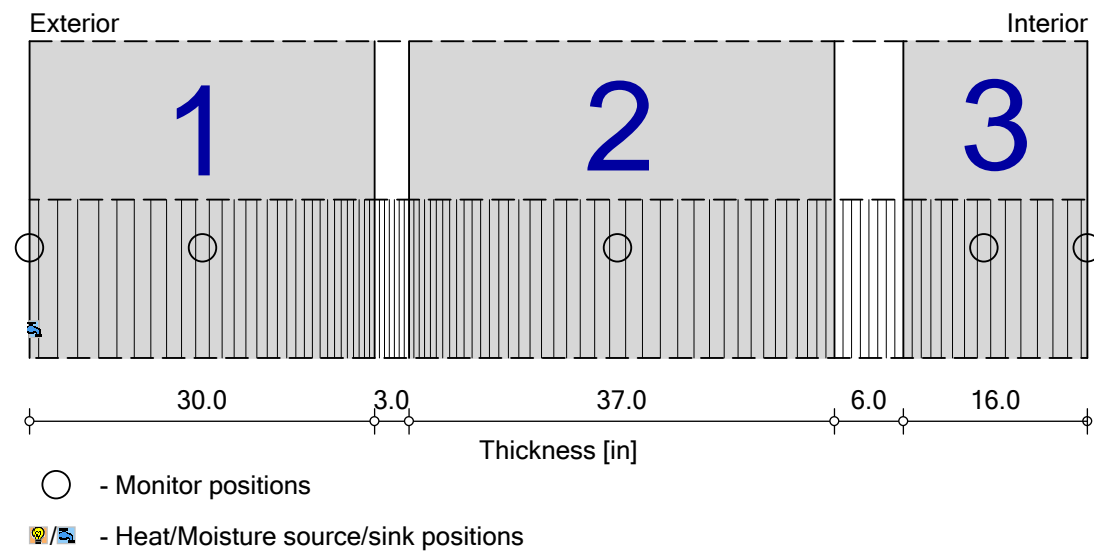
Water content at this exterior layer fluctuates with weather and precipitation events, with a modest downward seasonal trend

South Masonry Wall Analysis

South Masonry Wall - With Increased Moisture

Boundary Conditions

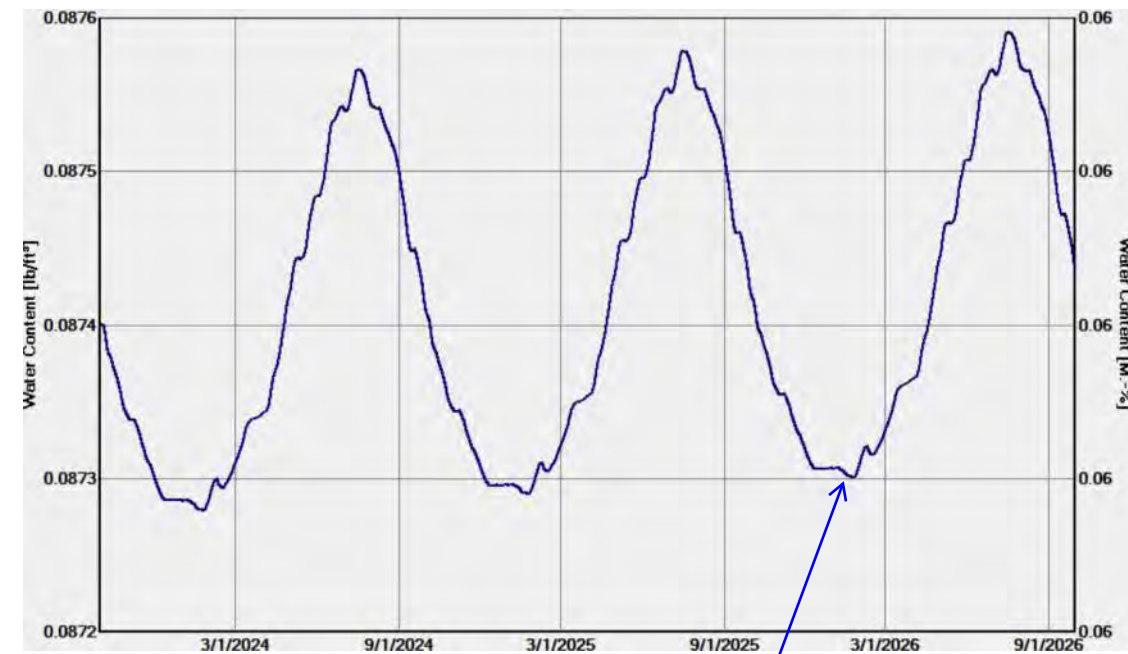
Exterior (left side) Albany, NY
 Interior (right side) 55° F with fluctuation of 25° F; and 72% RH with a 50% amplitude
 Moisture Source **Exterior Limestone Layer - 3%**



Materials:

	- Limestone (Georgian Bay Limestone)	30.0 in
	- Lime Mortar, fine	3.0 in
	- Limestone (Georgian Bay Limestone)	37.0 in
	- Lime Mortar, fine	6.0 in
	- Limestone (Georgian Bay Limestone)	16.0 in

Water Content - Limestone Layer 2



Water content at the middle layer fluctuates seasonally, with minimal upward trend (similar to Existing, Page 4)

Water Content - Limestone Layer 3



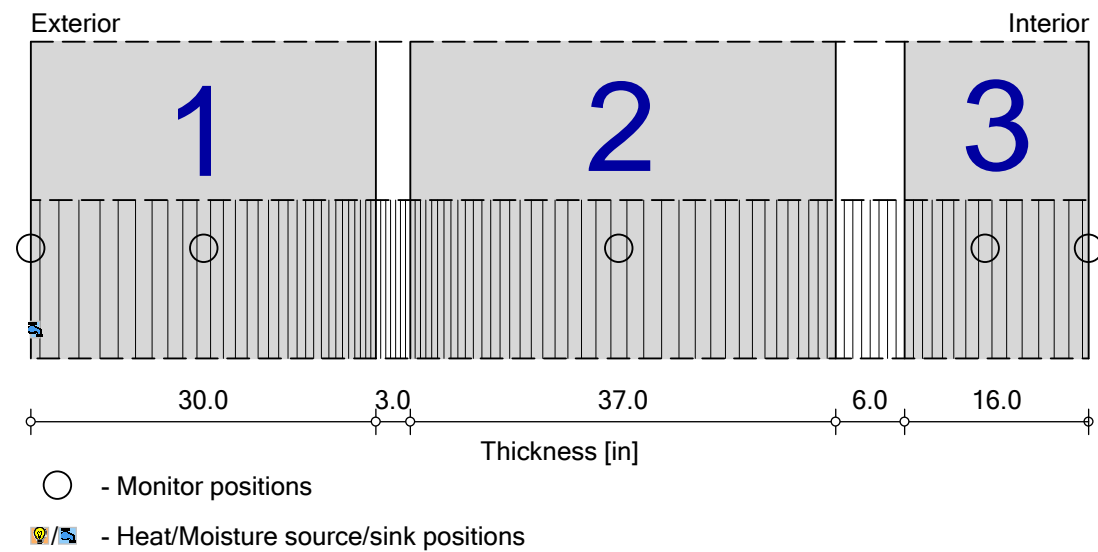
Water content at the interior layer fluctuates seasonally, with increasing moisture during the 3-year period (similar to Existing, Page 4)

South Masonry Wall Analysis

South Masonry Wall - With Increased Ambient Temperature

Boundary Conditions

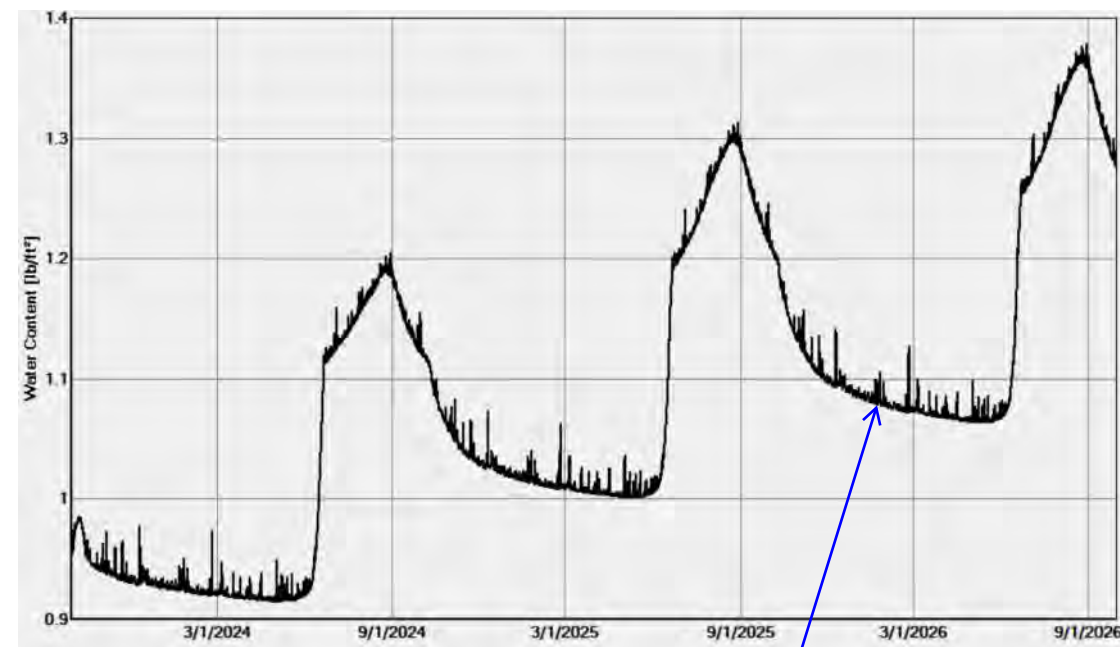
Exterior (left side) Albany, NY
 Interior (right side) **60° F with fluctuation of 20° F**; and 72% RH with a 50% amplitude
 Moisture Source Exterior Limestone Layer - 1% (ANSI/ASHRAE standard 160)



Materials:

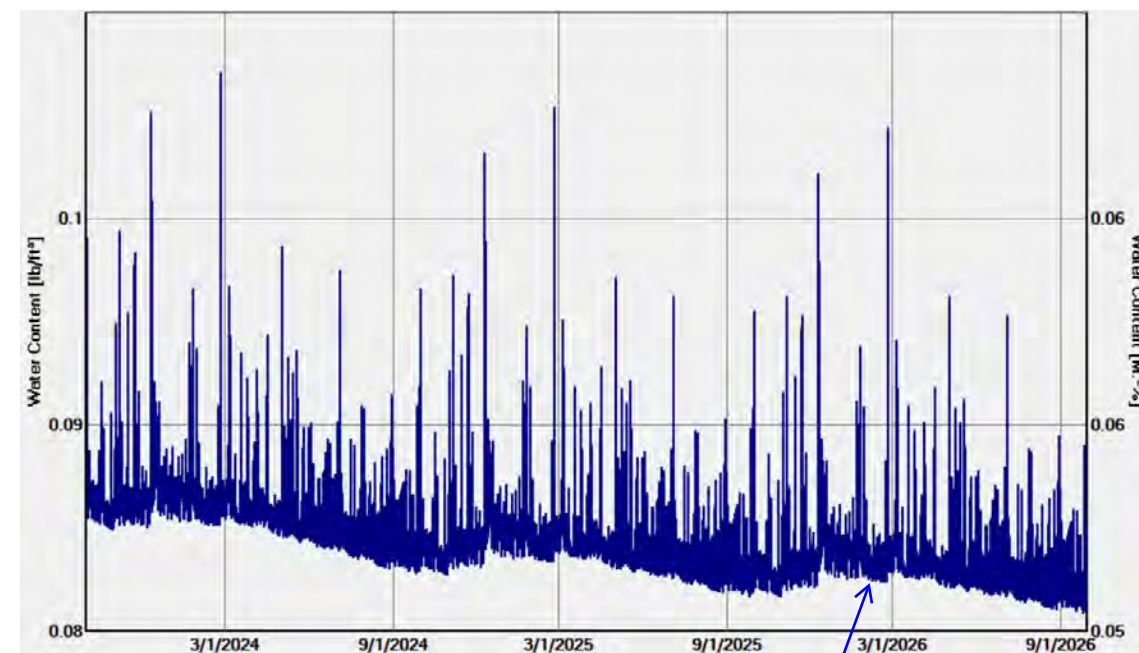
	- Limestone (Georgian Bay Limestone)	30.0 in
	- Lime Mortar, fine	3.0 in
	- Limestone (Georgian Bay Limestone)	37.0 in
	- Lime Mortar, fine	6.0 in
	- Limestone (Georgian Bay Limestone)	16.0 in

Total Water Content - Existing Masonry Wall



Total Water Content (for the entire wall assembly) increases during the 3-year period (similar to Existing, Page 3)

Water Content - Limestone Layer 1



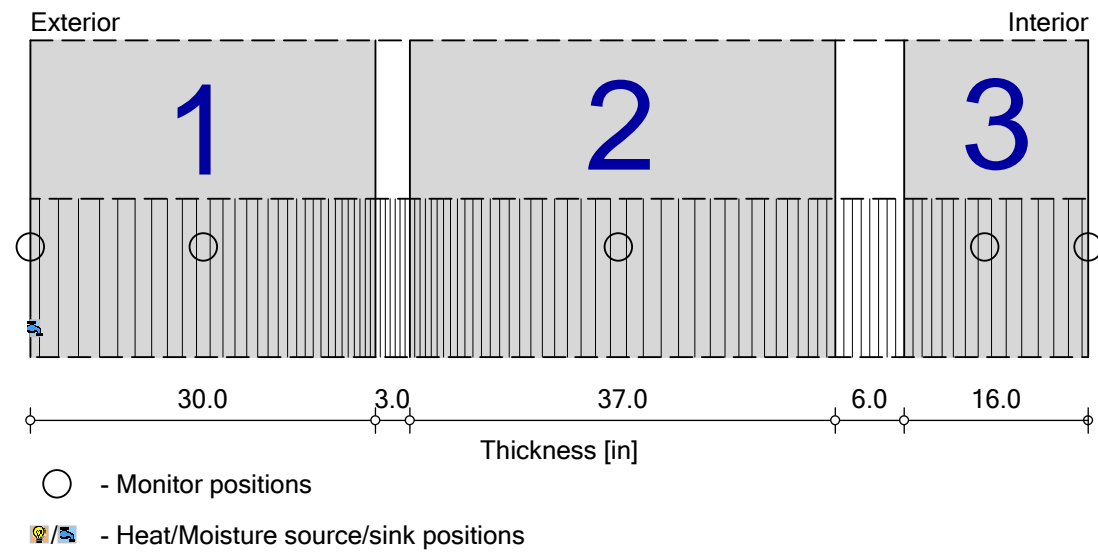
Water content at this exterior layer fluctuates with weather and precipitation events, with a modest downward seasonal trend

South Masonry Wall Analysis






South Masonry Wall - With Increased Ambient Temperature

Boundary Conditions

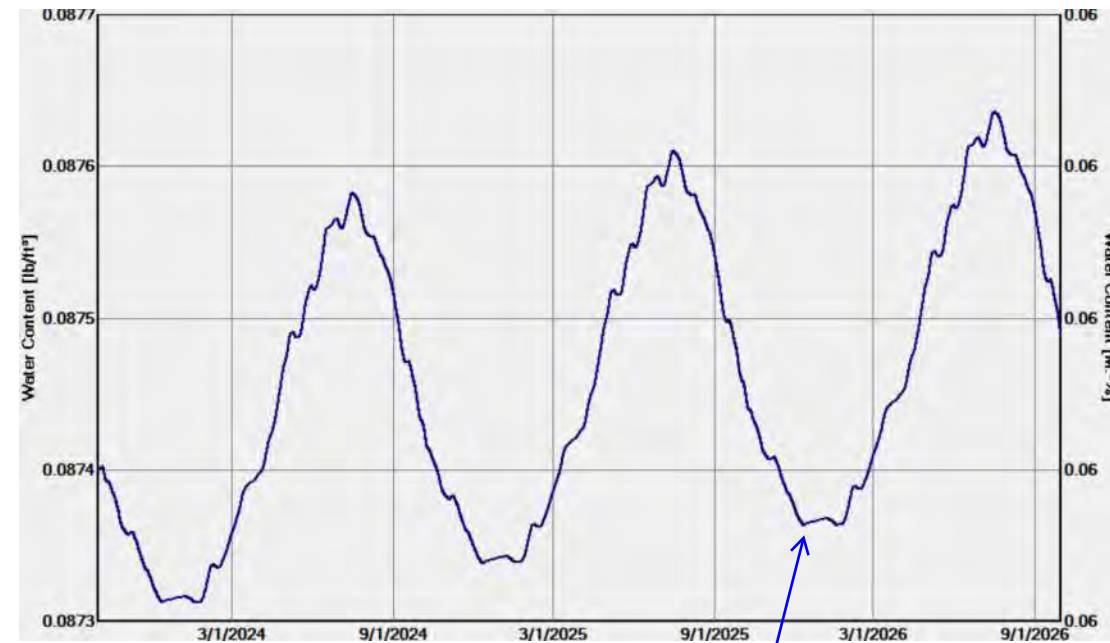
Exterior (left side) Albany, NY
 Interior (right side) **60° F with fluctuation of 20° F**; and 72% RH with a 50% amplitude
 Moisture Source Exterior Limestone Layer - 1% (ANSI/ASHRAE standard 160)



Materials:

	- Limestone (Georgian Bay Limestone)	30.0 in
	- Lime Mortar, fine	3.0 in
	- Limestone (Georgian Bay Limestone)	37.0 in
	- Lime Mortar, fine	6.0 in
	- Limestone (Georgian Bay Limestone)	16.0 in

Water Content - Limestone Layer 2



Water content at the middle layer fluctuates seasonally, with minimal upward trend (similar to Existing, Page 4)

Water Content - Limestone Layer 3



Water content at the interior layer fluctuates seasonally, with increasing moisture during the 3-year period (similar to Existing, Page 4)



SMOKESTACK LIGHTNING, INC.

Lightning Rods / Surge Protective Devices
37 Upper River Street -- Brookfield, MA 01506
Tel: (508) 867-9233 Fax: (508) 867-3586
williamsimpson@smokestackusa.com
www.SmokestackUSA.com

Friday, September 29, 2023
Stevens & Associates, P.C.
95 Main Street,
Brattleboro, VT 05301

Project: Bennington Battle Monument
Project Address: 15 Monument Circle
Bennington, VT 05201

Attn: Cory Frehsee

Regarding: Lightning protection visual inspection results

OVERVIEW

On Wednesday September 13th, 2023, a representative from Smokestack Lightning Inc. completed a visual inspection of the lightning protection system at the Bennington Battle Monument. The results of the inspection are based on compliance with NFPA 780, UL96a and LPI 175 standards for lightning protection system installations. The existing system consists of 1 class II copper air terminal/lightning rod and 2 class II copper conductors that extend through the interior of the monument and leave the structure below grade. The bulk of the system components that are installed are in place and in good condition, but there are deviations from the standard and issues of corrosion and deterioration that need to be rectified for full compliance. The largest issue is the design of the system with a single air terminal at the peak rather than the NFPA 780 required additional air terminals at lower levels.

LIGHTNING PROTECTION SYSTEM DETAILS BY MAJOR COMPONENT

Air Terminal: Please see images 1&2. There is one 1/2" diameter solid copper air terminal mounted to the finial at the top of this structure. It is currently held in place by copper strapping wrapped around the finial and bolted together. The rod itself appears to be in good condition, but this report would recommend a full-size bond between the finial and the rod itself to ensure full continuity. Also, due to the height of the structure the single air terminal does not meet current NFPA780 zone of protection requirements. To fully comply with current air terminal location requirements and achieve a Master Certification additional air terminals mounted below the peak of the spire will be required. To pursue the full NFPA780 complaint system there are several design options that will need to be evaluated in the design phase.

Conductor: Please see images 2-8. The conductors are in good condition from top to bottom of the structure. However, the fasteners are deteriorating in a progressively worse fashion from top to bottom of the monument. At the lower levels of the structure the fasteners are only barely held into place by what remains of the original fastener.

The main conductors on the corners of the tower are bonded together with a horizontally run conductor at several levels in the monument. This is required per NFPA and LPI standards for every 60 vertical feet for a structure of this height. Please see image 5 for an example. The visual inspection indicated that to fully comply with NFPA 780 standards 2-3 more horizontal connections between the

down conductors is required.

Grounding: Please see image 8. The conductors exit the building below grade. The condition of the grounding on the building exterior is unknown at the time of this report. The visual inspection confirmed that the two conductors appeared to exit the building in the basement space of the monument. This report recommends excavation around the perimeter of the monument to determine the actual condition of the ground grid/ground rods.

Common Bonding: The lightning protection system is bonded to the electrical ground wire in the basement level. The lightning protection is bonded to the steel platforms within the tower. The platforms bonds show some signs of corrosion, and this report recommends repair or replacement of these bonds to ensure full continuity. Please see image 5 for image of the platform bond. There is a bond to the ladder at the top of the tower through the ladder bolt into the tower, but this report recommends an additional bond to the ladder at the top of the ladder. Please see image 3 for a view of the ladder and conductor. There is no bond to the platform at the roof level. This report recommends bonding the platform below the ladder.

Surge Protection: There is no surge protection for the main electrical service panel in the monument. Surge protection is required on all electrical and communication services entering a structure per UL, NFPA and LPI standards.

BUDGET CONSIDERATIONS

There are several approaches ranging from minor repairs to updates and upgrades for a full UL, NFPA, LPI Master Certification. The cost estimate for repairing the existing system to its original condition is in the range of \$10,000 - \$20,000. The level of repairs and upgrades for a full Master Certification complying with NFPA 780 will cost \$50,000 - \$100,000. These budgets include all design work, materials, and installation, but do not include costs for access to the building exterior, which will be required for the full Master Certification level work.

Summary

Overall, the lightning protection system components are in good condition, but there are maintenance issues and deviations from UL, NFPA and LPI standard that need to be addressed for full compliance. The original design of a single air terminal does not comply with NFPA 780 requirements and could potentially allow for lightning strikes to the lower sections of the tower and result in severe damage. This report recommends further investigation of the condition of the grounding components of the lightning protection system and repairs and upgrades for full compliance with NFPA 780, UL 96 and LPI 175 standards.

Thank you,



William R. Simpson
LPI Master Installer/Designer #1415
UL Master Label System Installer/Designer



Image 1. ½” diameter class II copper air terminal mounted with bolted copper strapping to star finial. This report recommends a full-size bond between the finial and the air terminal. The strapping currently provides this bond but it is difficult to determine if there is adequate surface area for the connection.



Image 2. Bolted connection from air terminal to class II copper lightning conductor.



Image 3. The access ladder is directly over the main lightning conductor and is bonded to the lightning protection system at the base of the ladder through a thru bolt into the tower. This report recommends bonding the ladder at the top as well as at the bottom. Also, the platform below the ladder is not bonded into the lightning protection system. This report recommends that the platform be bonded into the system as well.



Image 4. Bolted connection to interior of finial mounting hardware. From this connection the conductors travel through the monument on the interior of the Northwest and Southeast corners.



Image 5. The patinaed copper wire runs horizontally and connects the 2 opposite conductors at 4 levels. This intermediate connection is required per NFPA, UL and LPI standards for structures of this height. The bond to the railing is showing some signs of corrosion.



Image 6. At the publicly accessible levels of the monument the conductors are protected by a copper conduit. To keep continuity between the conduit and the conductor a copper wedge is placed into the top of the conduit. This wedge is visible on some of the conduits but not the others. This report recommends confirming or bonding each copper conduit to the lightning protection conductor at the top and bottom of the conductor as required by the lightning protection standards.



Image 7. As the conductors travel through the monument the condition of the fasteners gets progressively worse. Towards the lower half of the tower many of the fasteners are mostly corroded and are only loosely holding to the inside wall of the tower. This report recommends addressing the moisture issues in the tower then replacing all, or at least the bottom half of the conductor fasteners in the tower.



Image 8. The two conductors that travel from the top of the tower to the base exit the structure below grade as in this picture. The condition of the grounding on the exterior is unknown at this point and this report recommends further investigation in the form of excavation around the exterior to determine the condition of the grounding. Also, this report recommends investigating and collecting any as built or plan drawings from the lightning protection system installation if they are available.



Image 9. There is no surge protection on the main electrical service panel in the monument. Surge protection is required for a complete lightning protection system on all incoming power and communication lines.

Langan Engineering, Environmental, Surveying, Landscape Architecture and Geology, D.P.C.
360 West 31st Street, 8th Floor New York, NY 10001 T: 212.479.5400 F: 212.479.5444

To: Cory Frehsee – Steven & Associates, P.C.

From: Prasoon Tiwari, P.E.; Arthur Alzamora Jr., P.E. (Langan)

Info: Andrew Ciancia – Langan
Sebastian Baculima Chicaiza – Langan
Rebecca Buntrock – Silman
Ben Harwood - Steven & Associates, P.C.

Date: March 13, 2024

Re: Geotechnical Engineering Memorandum
15 Monument Circle.
Bennington, Vermont
Langan Project No.: 170724002

This memorandum provides a summary of our geotechnical engineering investigation performed for the proposed scaffolding to support the planned maintenance work at the Bennington Battle Monument. The purpose of this study was to obtain information on subsurface conditions and provide geotechnical related recommendations for the proposed scaffolding system.

Monument information provided in this memo was compiled from our review of available site information, discussions with your office and our review of the specific project drawings (monument sections (S-01) and floor plans (V-01)), dated 12 May 2022.

Elevations referenced in this memorandum were taken from Elevation Plan (Drawing No. EL-01 to EL-04), dated 11 May 2022, that were prepared by Langan. All elevations contained herein are in feet and reference the North American Vertical Datum of 1988 (NAVD88). Elevations referenced in this memorandum were interpolated between points and should be considered approximate rather than precise.

PROJECT DESCRIPTION

The project site is located on 15 Monument Circle in Bennington, VT. The Bennington Battle Monument is a 307-foot-tall stone obelisk constructed circa 1891. The existing drawings indicate that there is one below grade level, with the slab about 10 feet below existing ground surface. A site location map is presented in Drawing No. 1.

Based on our discussions with your office and Silman, we understand that a scaffolding system is planned to be installed around the monument to access for repair and maintenance work on the monument. In addition to the scaffolding structure, we understand there has also been recent

discussions on the potential construction of a covered walkway at the site. The project site is generally level; however, we note that there is a slight downward slope in the grade as you move away from the monument in all directions.

SUBSURFACE EXPLORATION AND FINDINGS

In coordination with your office and Silman, our subsurface exploration program consisted of drilling three geotechnical borings identified as B-1 through B-3 and installing a groundwater observation well in completed boring B-3. The borings were located at about 30 feet away from the monument, as coordinated with the project team.

The borings were drilled by Cascade Remediation Services, LLC on 17 and 18 January 2024, under the full-time observation of a Langan engineer. A subsurface investigation plan is presented in Drawing No. 2.

Prior to drilling, borings were hand-cleared for the first 5 feet below grade for utility clearance. Borings were advanced using mud-rotary drilling techniques and a tri-cone roller bit. Drilling fluid and steel casing were used to provide support for the sidewalls of the borehole during drilling. Standard Penetration Tests (SPT)¹ N-values were measured, and soil samples were obtained continuously through the top 12-feet. Soil samples were retrieved using a 2-inch-diameter split-spoon sampler driven by a 140-pound automatic hammer in accordance with ASTM D1586. Recovered soil samples were visually examined and classified in the field by our engineer, in accordance with the Unified Soil Classification System (USCS).

Bedrock was cored using an HQ-size double-tube core barrel. The core barrel was equipped with a diamond-cutting bit in accordance with ASTM D-2113 (Rock Core Drilling). Rock type, percent recovery (REC) and Rock Quality Designation (RQD), were determined for each core run.

Soil/rock classification, standard penetration resistance, groundwater information, RQD and other field observations were recorded on the boring logs. Borings logs are included in Appendix A.

Observation Wells

A groundwater observation well was installed in completed boring B-3. The well consisted of 10 feet of 2-inch-diameter Schedule-40 PVC slotted-pipe (screen) and a solid riser PVC-pipe extending to ground surface. The annulus around the pipes were backfilled with filter sand to about 2 feet above

¹ The Standard Penetration Test is a measure of soil density and consistency. The SPT N-value is defined as the number of blows required to drive a 2-inch diameter split-barrel sampler 12-inches, after an initial penetration of 6 inches, using a 140 lb hammer falling freely from a height of 30 inches

the screen and sealed with a 2-foot-thick layer of bentonite pellets. A protective flush-mounted steel well cap was installed at the ground surface. The well-construction log is included in Appendix B.

SUBSURFACE CONDITIONS

The subsurface stratigraphy at the site consists of a layer of topsoil underlain by sandy clay, and then competent bedrock. A description of each stratum is given below in order of increasing depth. Representative subsurface profiles are provided in Drawing No. 3.

Topsoil

A layer of topsoil was encountered immediately below the ground surface. The topsoil generally consists of brown fine to medium sand, with varying amounts of silt, and gravel and extends up to about two feet below grade.

Sand and Sandy Clay

Below the layer of topsoil, a layer of brown, fine sand, with varying amounts of clay, silt and gravel was encountered in B-3(OW) and extended to a depth of about 5 feet, corresponding to about el. 862. The sand is classified generally as SC (clayey sand) in accordance with USCS.

In borings B-1 and B-2, a layer of brown to orangish brown, sandy clay, with varying amounts of gravel was encountered below the topsoil and extended to depths of about 7 to 12 feet below grade. N-values within the sandy clay layer ranged from about WOH (weight of hammer) to refusal. The sandy clay is classified generally as CL (clay) in accordance with USCS.

Bedrock

Bedrock was encountered beneath the sand/clay layer in all three borings and depth to bedrock was observed to be vary from about 7 to 12 feet below the existing ground surface.

Bedrock was classified as light grey dolostone. The bedrock was generally observed to be in a fresh to moderately weathered condition, fracture spacing was generally very close (0.75 inch to 2.5 inches) to moderate (8 inches to 2 feet). Rock-core recovery (REC) values varied from about 88 and 100 percent, with an average of 94 percent, and rock-quality designation (RQD) varied from about 37 to 68 percent with an average of 52 percent.

A bedrock geologic map of Vermont is also presented in Drawing No. 4.

Groundwater

Groundwater level was monitored in the observation well installed in boring B-3(OW). The ground water level was measured at the end of second day of our subsurface exploration. The measured static groundwater was about 10 feet below grade corresponding to about el 857. In general, the groundwater level was recorded within about two feet of the top of bedrock surface, indicative of a potential “perched” water conditions.

Laboratory Testing

Laboratory tests were performed on selected rock and soil samples to define physical and mechanical properties. The laboratory tests consisted of:

- Two Sieve Analyses (ASTM D 6913)
- Two Atterberg limit Tests (ASTM D 4318)
- Two Rock Unconfined Compressive Strength (ASTM D 7012)

The lab testing results are provided in Appendix C.

SEISMIC EVALUATION

This section provides the results of our seismic evaluation for the site in accordance with the general procedures outlined in the 2015 Vermont Building Code. We assume that the existing structure will be Structural Occupancy Risk Category II/III. Based on subsurface conditions encountered on site, we recommend the site be designated Site Class B – “Rock”. The architect and structural engineer must confirm the structure occupancy/risk category.

Table No. 1 below provides our recommended parameters for use in seismic design of the existing structure. The seismic design parameters may change and will need to be re-evaluated.

Table No. 1 – Building Code Seismic Design Parameters

Seismic Design Parameter	Recommended Value	2015 Vermont Building Code Reference
Mapped Spectral Acceleration for short periods (S_s)	0.184 g	Section 1613.3.1
Mapped Spectral Acceleration for 1-second period (S_1)	0.072 g	
Site Class	B	Section 1613.3.2
Site Coefficient for short periods (F_a)	1.00	Tables 1613.3.3(1) and 1613.3.3(2)

MEMO

Seismic Design Parameter	Recommended Value	2015 Vermont Building Code Reference
Site Coefficient for 1-second period (F_v)	1.00	
Design spectral response acceleration at short periods (S_{DS})	0.123 g	Section 1613.3.4
Design spectral response acceleration at 1-sec period (S_{D1})	0.048 g	
Seismic Design Category	A	Table 1613.3.5

Liquefaction Evaluation

Since the monument foundations are believed to be bearing directly on bedrock, liquefaction does not need to be considered for design.

GEOTECHNICAL DESIGN AND RECOMMENDATIONS

Existing Monument

In review of the Elevation Plan prepared by Langan (Drawing No. EL-01 to EL-04), dated 11 May 2022, we understand that the basement level is at about El. 860. The subsurface profile observed during the subsurface investigation encountered bedrock at varying elevations from El. 856 to El. 861. When comparing the elevation of the below grade level at the moment with the depth to rock within the borings, it is believed that the existing monument is bearing on bedrock. Based on the borings performed at the site and discussions with Silman, it is believed that the foundations of the monument were likely proportioned for an allowable bearing capacity of about 10 tons per square foot (tsf).

When structures are bearing on bedrock and load is applied, we do not see a traditional settlement of the structure, but more of a compression of the rock surface. We note that since the monument is believed to be bearing on bedrock, we anticipate that when the monument was constructed it likely exhibited compression of the rock surface on the order of ½ inch or less. If additional loading is planned to be applied to the existing monument structure or foundations, we recommend that a test pit excavation be performed to identify the size, character and bearing material of the existing foundation.

Foundation System

It should be noted that at the time of this memorandum, structural loads for the planned scaffolding system and other ancillary structures were not provided. The selection of the foundation type will be governed by the layout, loading and allowable movement of the scaffolding system.

As discussed herein, bedrock was encountered between about 7 to 12 feet below existing grade. Considering the likely height/size and layout of the proposed scaffolding structure, we believe that the scaffolding system should be supported on a shallow foundation system (e.g., individual footings, mat foundation) bearing on competent rock. Scaffolding foundation elements bearing on bedrock can be designed for an allowable bearing capacity of up to 10 tsf.

Although the scaffolding loading was not provided, for structural items supported by foundations bearing on bedrock, we anticipate settlement of the foundations will be the result of elastic compression of the rock mass, which typically would be on the order of about ½ inch or less.

Foundation Subgrade

The foundation subgrades should be level and clear of standing or frozen water, debris, or other deleterious materials. We recommend that foundation subgrade be verified for bearing capacity by engineer familiar with the project conditions and that the footing bottoms have been adequately cleaned.

Uplift Resistance

Silman has indicated that the proposed scaffolding could be fairly slender and may or may not be braced back to the monument structure. Although this still needs to be determined, the layout of the scaffolding may result in tension or uplift loads on the foundation elements. If required, for any tension loads on the proposed temporary scaffolding, uplift forces can be resisted by post-tensioned tie-down anchors socketed into the underlying bedrock. Since the scaffolding could be in place for a long duration, we would recommend double corrosion-protected threaded bars meeting ASTM A-22 requirements can be used for this application. If tie-down anchors are to be used, then we recommend, Grade 150 threaded bars for reinforcement steel. The free-stress (unbonded) length should be at least 10 feet long, but additional length may be required to increase rock stability. Global failure of the bedrock must be considered when designing the location and free length of the anchors. The following table presents estimated design capacities for different anchor diameter sizes of varying length of bonded lengths assuming a socket into competent rock.

Table No. 2 – Typical Tie-down Capacities in Rock

Anchor Diameter (inch)	Reinforcement^a	Structural Capacity^b (kips)	Bond Length Required^c (feet)
4	1 of 1 inch Bar	50	15
4	1 of 1-1/4 inch Bar	100	20
6	1 of 1-3/4 inch Bar	150	20

- a: Grade 150 steel assumed
- b: Calculated as $0.6 * [\text{yield strength of steel}] * [\text{cross-sectional area of steel}]$
- c: Assuming an allowable peripheral shear of 40 psi for tension obtained with a factor of safety of 2, and length required to achieve capacity

The design capacity of the anchors should be evaluated for group effects, once the anchor design loads and locations are finalized.

Ancillary Structures

For lightly loaded ancillary structure, such as proposed covered walkway area, we believe the structure can likely be supported on spread footings bearing on soil below the frost depth (about 5 feet below the finished grade). The foundation elements should be proportioned assuming an allowable bearing capacity of 1 tsf. Once the foundation loading is finalized, the anticipated settlement can be estimated against the recommended bearing capacity.

As with foundations bearing on bedrock, the foundation subgrades on soil should be level and clear of standing or frozen water, debris, or other deleterious materials. Proof rolling of the exposed subgrades should be performed, and any areas containing deleterious materials or exhibiting evidence of poor subgrade, such as rutting or weaving beneath the compactor, should be removed to competent material, and replaced with compacted structural fill in accordance with the "Fill Material, Placement and Compaction Criteria" section below. We recommend that foundation subgrade be verified for bearing capacity by engineer familiar with the project conditions and that the footing bottoms have been adequately cleaned. These activities should be performed during a period of dry weather along with good and positive drainage of surface water. In any case, all measures should be taken to collect and divert runoff water away from the construction area.

It should be noted that if ancillary structures are planned to be constructed about 20 feet or greater from the nearest boring locations, subsurface conditions may vary with distance. Therefore, additional investigation may be required to verify the subsurface conditions at the proposed locations of the ancillary structures.

Adjacent Construction

Considering the age and sensitive nature of the monument structure, we recommend careful consideration for any new structures that are planned near the existing monument. With existing foundation elements bearing on bedrock, the adjacency of any planned structure elements should be reviewed for impacts but are typically less likely to have an impact if they match the existing foundation bearing level of the monument, which is on rock.

For those new foundation elements bearing above rock and within the influence zone of the existing structure, the new foundation would provide increased loads on the below grade structures. Any additional loading would need to be kept out of this influence to avoid additional loads being imposed on the existing below grade walls. The potential for influence on existing structures from new foundation elements, should be reviewed on a case-by-case basis; however, a typical influence zone to consider is a 1 horizontal to 1 vertical (1H:1V) or flatter influence zone measured from the bottom of the existing foundation level to the bottom of the “shallower” adjacent new foundation. A typical influence zone for the existing monument below grade structure is shown in Drawing No. 3.

Soil Excavation and Disposal

During foundation excavations, excess soil will be encountered above the bedrock. The soil material can likely be used as fill under non-structural areas. Any buried debris is recommended to be removed from the site and not used as backfill material. We recommend discussing the re-use and disposal of the existing fill on site with the environmental consultant, to determine if there are any environmental regulations or concerns that need to be considered.

SERVICES DURING DESIGN, CONSTRUCTION DOCUMENTS AND CONSTRUCTION QUALITY ASSURANCE

During final design, Langan will be retained to consult with the design team as geotechnical questions arise. Technical specifications and design drawings should incorporate Langan’s recommendations. Langan can assist the design team in preparing specification sections related to geotechnical issues such as earthwork and shallow foundations. Langan should also, when authorized, review the project plans and contractor submittals relating to materials and construction procedures for geotechnical work, to confirm the designs incorporate the intent of our recommendations.

Langan has investigated and interpreted the site subsurface conditions, and is, therefore, best-suited to observe for quality assurance and testing of geotechnical-related work during construction.

Recognizing that construction observation is the final stage of geotechnical design, Langan’s observing quality assurance during construction is necessary to confirm the design assumptions and design elements, to maintain our continuity of responsibility on this project, and to allow us to make changes to our recommendations, as necessary. The foundation system and general geotechnical construction methods recommended here are predicated upon Langan assisting with the final design and providing construction observation services for the owner. If Langan is not retained for these services, we cannot assume the role of geotechnical engineer of record, and the entity providing the final design and construction observation services must serve as the engineer of record.

Monitoring

We recommend that a monitoring program be developed and incorporated into the Contract Documents. Monitoring should include means to measure both structural movement and vibrations from construction operations. The type and locations of specific monitoring equipment, threshold values, and durations should be developed by the structural engineer based on review of the anticipated construction means. The monitoring program would likely include optical surveying, seismographs (vibration monitoring), and crack gauges.

Fill Material, Placement, and Compaction Criteria

Any material used for backfilling around foundations should consist of sand, gravel, crushed stone, crushed gravel or a mixture of these and must be free of organic, frozen and other deleterious materials. The fill should have a maximum particle size not greater than 2 inches and have less than 10% by dry weight passing a No. 200 sieve. The structural fill should be compacted to at least 95% of the material's maximum dry density, as determined by the Modified Proctor Compaction Test (ASTM D1557). The existing fill may be used, as long as it meets the gradation requirements discussed above. The use of recycled concrete aggregate, or the byproduct of blasting/tunneling (commercially known as mole rock), is not recommended for backfill.

Fill should be placed in uniform 12-inch-thick loose lifts. In restricted areas where only hand-operated compactors can be used, the maximum lift thicknesses should be limited to 6 inches. The appropriate water content at the time of compaction should be plus or minus 2 percentage points of optimum water content as determined by the laboratory compaction tests of the proposed fill. No fill should be placed on areas where standing water is observed or on frozen subsoil areas.

OWNER AND CONTRACTOR RESPONSIBILITIES

The contractor is responsible for construction quality control, which includes satisfactorily constructing the foundation system and any associated temporary works to achieve the design intent while not adversely impacting or causing loss of support to neighboring property, structures, utilities, roadways, etc. Construction activities that can alter the existing ground conditions such as excavation, fill placement, foundation construction, and related work can also induce stresses, vibrations, and movements in nearby structures and utilities, and disturb occupants. Contractors are solely responsible for ensuring that their activities will not adversely affect the structures and utilities and will not disturb occupants. Contractors must also take all necessary measures to protect the existing structures, utilities, and similar features during construction. By using this memorandum, the owner agrees that Langan will not be held responsible for any damage to adjacent structures, utilities, etc.

MEMO

The preparation and use of this memorandum is based on the condition that the project construction contract between the owner and their contractors will include (1) Langan being added to the project wrap or contractor's general liability insurance as an additional insured, and (2) language specifically stating the foundation contractor will defend, indemnify, and hold harmless the owner and Langan against all claims related to disturbance or damage to adjacent structures, utilities, other similar features, or properties.

LIMITATIONS

The conclusions and recommendations provided in this memorandum result from our interpretation of the geotechnical conditions existing at the site inferred from a limited number of borings and other explorations. Actual subsurface conditions may vary. Recommendations provided are dependent upon one another and no recommendation should be followed independent of the others.

Any proposed changes in structures or their locations should be brought to Langan's attention as soon as possible so we can determine whether such changes affect our recommendations. Information on subsurface strata and groundwater levels shown on the logs represent conditions encountered only at the locations indicated and at the time of investigation. If different conditions are encountered during construction, they should immediately be brought to Langan's attention for evaluation because they may affect our recommendations.

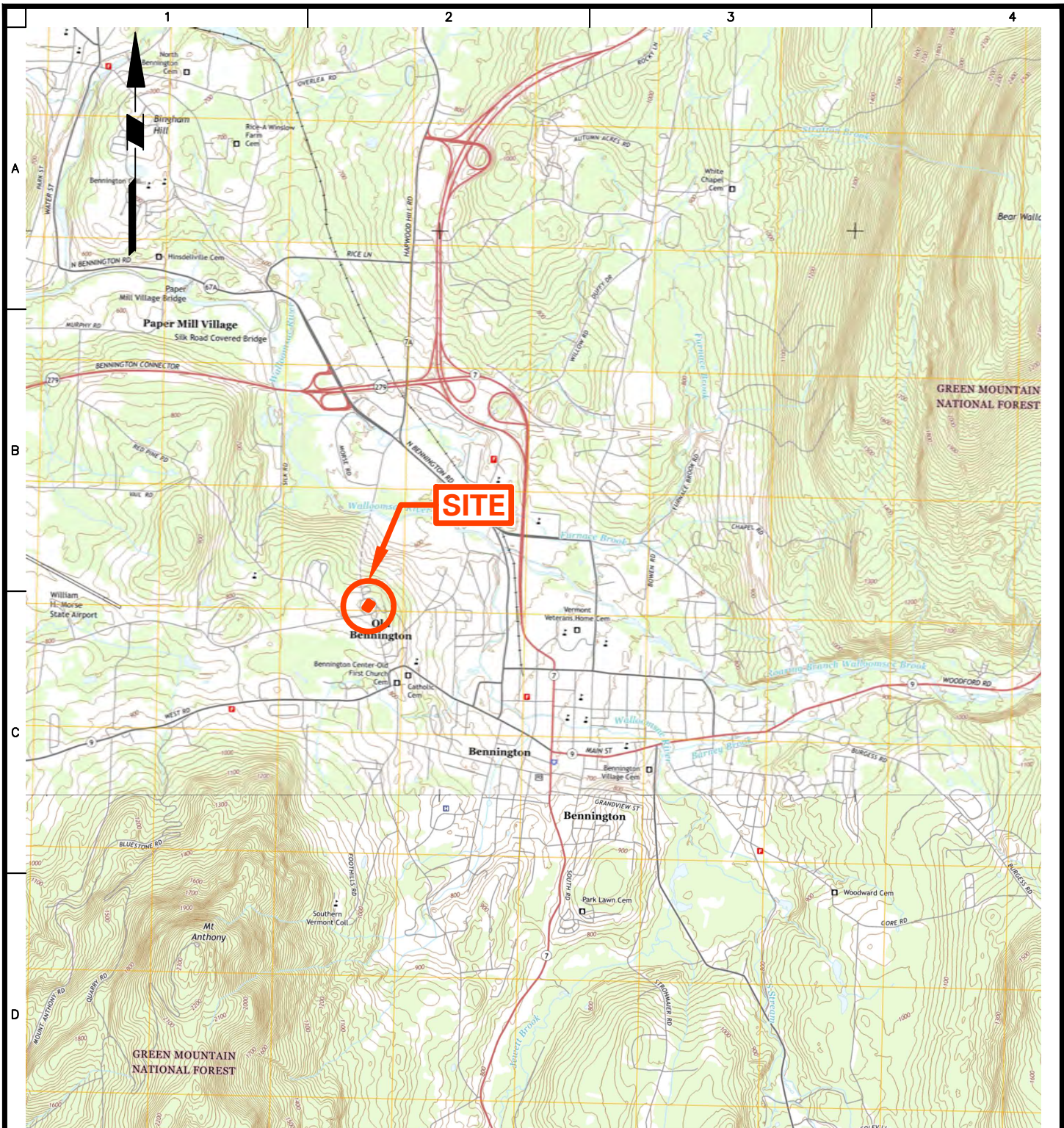
This memorandum has been prepared to assist the owner, architect, and structural engineer in the design process and is only applicable to the design of the specific project identified. The information in this memorandum cannot be used or depended on by engineers or contractors who are involved in evaluations or designs of facilities (including support of excavation, stabilization, etc.) on adjacent properties beyond the limits of that which is the specific subject of this memorandum.

Environmental issues (such as permitting or potentially contaminated soil and groundwater) are outside the scope of this study.

CLOSURE

We trust the information presented herein will be useful to Ownership, the design team and future contractors. Please feel free to contact us for further discussion or questions on material presented herein.

DRAWINGS



NOTE: ELEVATIONS ARE REFERENCED TO THE NORTH AMERICAN VERTICAL DATUM OF 1988 (NAVD 88).
SOURCE: "BENNINGTON, AND POWNAL QUADRANGLE MAP, VERMONT-BENNINGTON CO. 7.5-MINUTE SERIES", U.S. GEOLOGICAL SURVEY, 2011

WARNING: IT IS A VIOLATION OF THE NYS EDUCATION LAW ARTICLE 145 FOR ANY PERSON, UNLESS HE IS ACTING UNDER THE DIRECTION OF A LICENSED PROFESSIONAL ENGINEER, TO ALTER THIS ITEM IN ANY WAY.



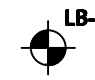
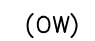
LANGAN Langan Engineering, Environmental, Surveying, Landscape Architecture and Geology, D.P.C. 21 Penn Plaza, 360 West 31st Street, 8th Floor New York, NY 10001 T: 212.479.5400 F: 212.479.5444 www.langan.com	Project	Drawing Title	Project No. 170724002	Drawing No.
	BENNINGTON BATTLE MONUMENT	SITE LOCATION MAP	Date 1/16/2024	1
	BENNINGTON	VERMONT	Drawn By JSB	
			Checked By PT	
			Sheet 1 of 4	



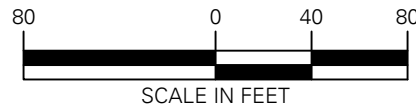
GENERAL NOTES:

1. BASE PLAN IS TAKEN FROM "BENNINGTON MONUMENT OVERALL SITE PLAN" BY VERMONT AGENCY OF NATURAL RESOURCES, DATED 27 APRIL 2023.
2. ALL BORING LOCATIONS SHOULD BE CONSIDERED APPROXIMATE.
3. ALL BORINGS WERE DRILLED BY CASCADE REMEDIATION SERVICES, BETWEEN 17 AND 18 JANUARY 2024, UNDER THE FULL-TIME INSPECTION OF A LANGAN ENGINEER.
4. ROCK CORING WAS PERFORMED USING TYPE HQ DOUBLE WALL CORE BARRELS.

LEGEND:

-  BORING LOCATION
-  OBSERVATION WELL

WARNING: IT IS A VIOLATION OF THE NYS EDUCATION LAW ARTICLE 145 FOR ANY PERSON, UNLESS HE IS ACTING UNDER THE DIRECTION OF A LICENSED PROFESSIONAL ENGINEER, LAND SURVEYOR OR GEOLOGIST, TO ALTER THIS ITEM IN ANY WAY.



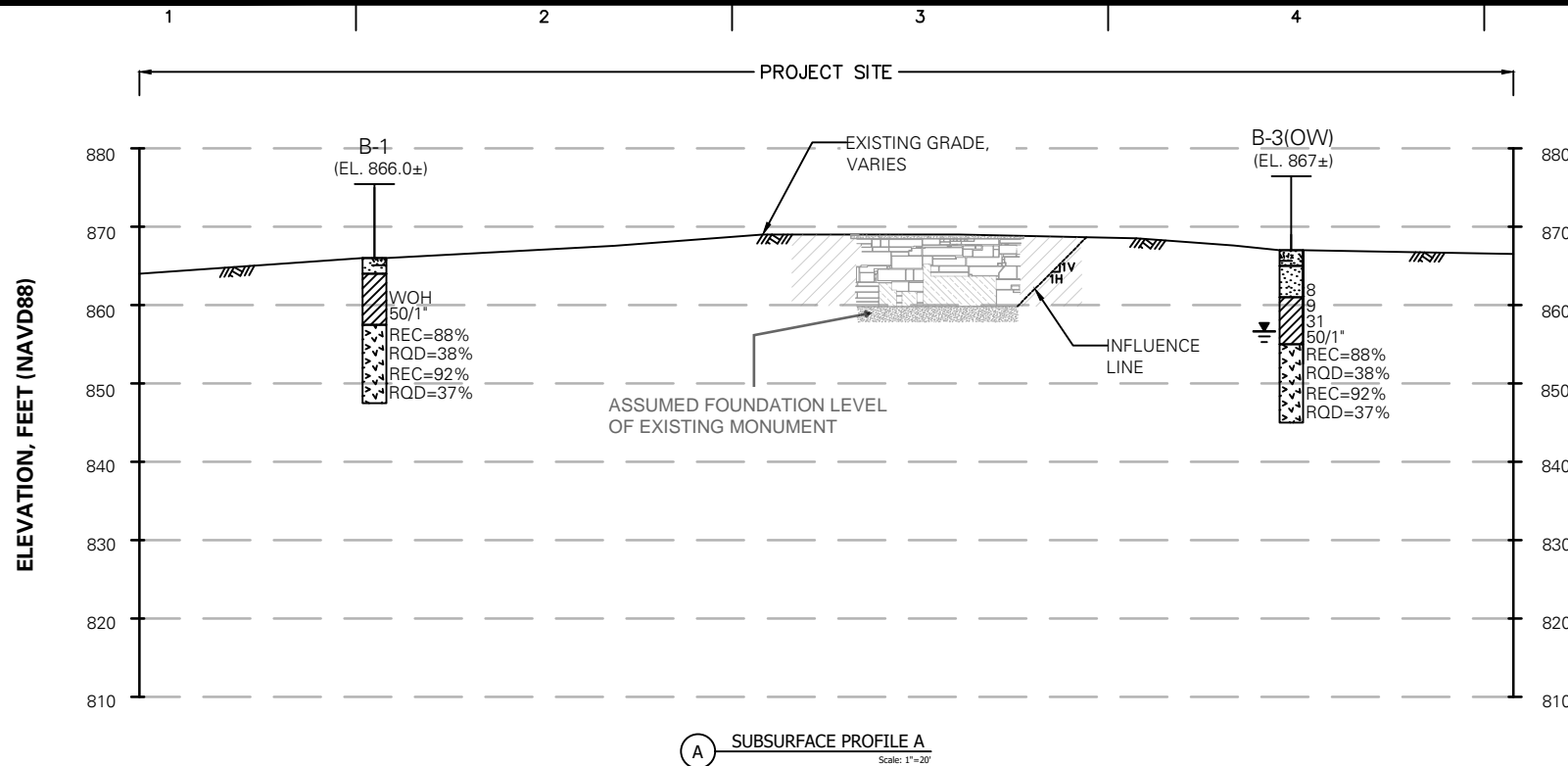
LANGAN
 Langan Engineering, Environmental, Surveying,
 Landscape Architecture and Geology, D.P.C.
 21 Penn Plaza, 360 West 31st Street, 8th Floor
 New York, NY 10001
 T: 212.479.5400 F: 212.479.5444 www.langan.com

Project
BENNINGTON BATTLE MONUMENT
 BENNINGTON VERMONT

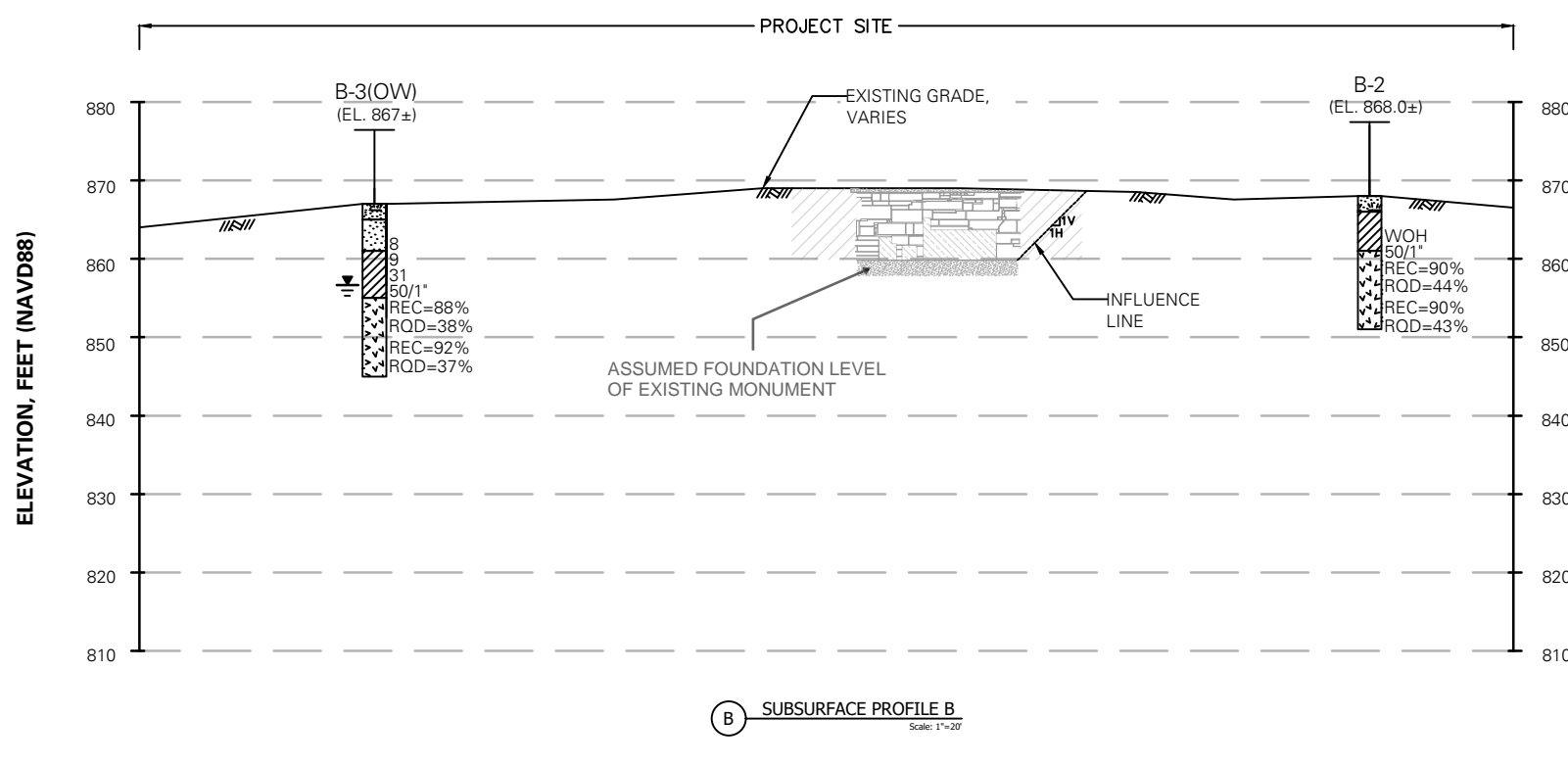
Drawing Title
SUBSURFACE INVESTIGATION PLAN

Project No.
 170724004
 Date
 1/19/2024
 Drawn By
 JSB
 Checked By
 PT

Drawing No.
2
 Sheet 2 of 4



(A) SUBSURFACE PROFILE A
Scale: 1"=20'

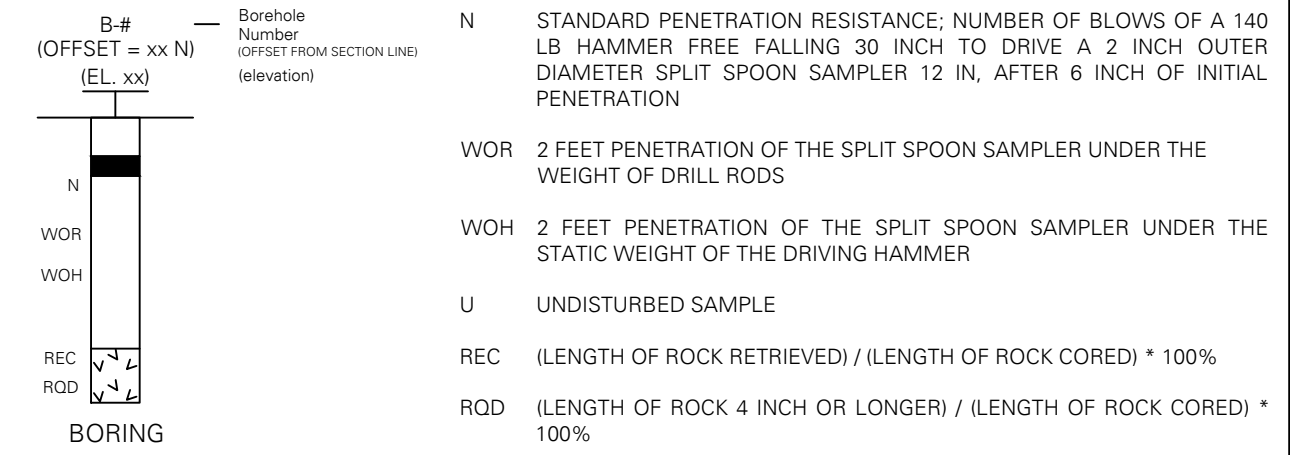


(B) SUBSURFACE PROFILE B
Scale: 1"=20'

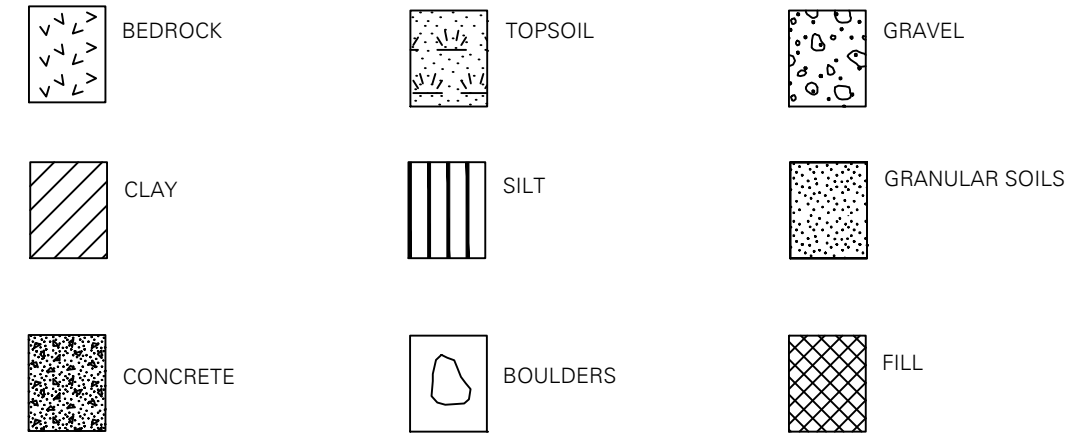
GENERAL NOTES:

1. ALL ELEVATIONS SHOWN HEREIN REFERENCE THE NORTH AMERICAN VERTICAL DATUM OF 1988 (NAVD88).
2. ALL BORING LOCATIONS WERE LAID OUT BY LANGAN REPRESENTATIVES BY MEASURING OFF OF EXISTING SITE FEATURES. ALL LOCATIONS SHOULD BE CONSIDERED APPROXIMATE.
3. REFER TO FIGURE 3 FOR LOCATION OF SECTION IN PLAN.
4. THE PROFILES SHOWN HEREIN REPRESENT GENERALIZED SUBSURFACE CONDITIONS INTERPRETED FROM WIDELY SPACED BORINGS. SOIL AND GROUNDWATER CONDITIONS MAY VARY BETWEEN POINTS OF EXPLORATION. VARIATIONS IN SUBSURFACE CONDITIONS SHOULD BE EXPECTED BETWEEN BORINGS.
5. THE SUBSURFACE LITHOLOGY IS AS INTERPRETED FROM RECOVERED SOIL SAMPLES. REFER TO BORING LOGS WITHIN APPENDIX A FOR ADDITIONAL INFORMATION.
6. ELEVATIONS FOR THE EXISTING MONUMENT WERE TAKEN FROM DRAWING TITLED "ELEVATION PLAN INTERIOR", PREPARED BY LANGAN, DATED 11 MAY 2022.

BORING FENCE KEY DIAGRAM AND LITHOLOGY NOTES:

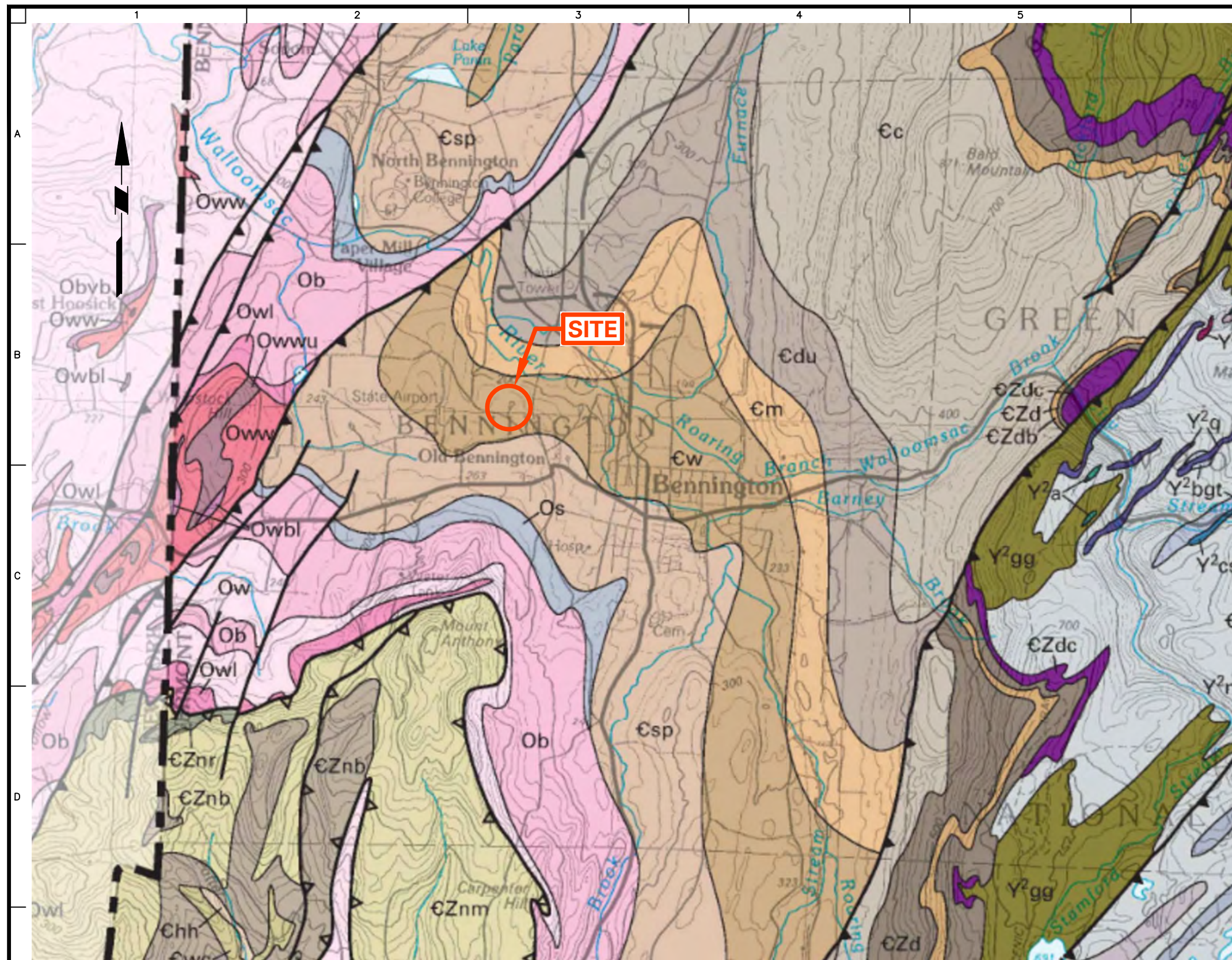


MATERIAL SYMBOLS:



WARNING: IT IS A VIOLATION OF THE NYS EDUCATION LAW ARTICLE 145 FOR ANY PERSON, UNLESS HE IS ACTING UNDER THE DIRECTION OF A LICENSED PROFESSIONAL ENGINEER, LAND SURVEYOR OR GEOLOGIST, TO ALTER THIS ITEM IN ANY WAY.

 Langan Engineering, Environmental, Surveying, Landscape Architecture and Geology, D.P.C. 21 Penn Plaza, 360 West 31st Street, 8th Floor New York, NY 10001 T: 212.479.5400 F: 212.479.5444 www.langan.com	Project	Drawing Title	Project No.	Drawing No.
	BENNINGTON BATTLE MONUMENT	SUBSURFACE PROFILES	170724004	3
			Date	
			3/13/2024	
		Drawn By		
		JSB		
		Checked By		
		PT		
				Sheet 3 of 4



- Ocu** Cutting Dolostone (Lower Ordovician)—Gray, thinly bedded dolomitic sandstone, grading upward into dolomitic limestone or mottled dolomitic marble. In southern Vermont east of the Taconic Range, unit is not recognized and may appear as sandy zones within rocks mapped as the Shelburne Marble
- Os** Shelburne Marble (Lower Ordovician)—Predominantly light-gray to white- and bluish-gray-streaked calcite marble and massive white- and green-streaked calcite marble. Locally contains intermediate dolostone and gray limestone beds
- Esp** Clarendon Springs Formation (Upper Cambrian)—Steel-gray-weathering, light-gray, massive calcitic dolostone grading upward into darker, more fissile calcitic dolostone containing white quartz knots near top; unit locally brecciated. Locally contains light-bluish-gray to whitish-gray calcite marble (Cspl) within dolostone and beneath the calcitic marbles of the overlying Shelburne Marble
- Cd** Danby Formation (Upper Cambrian)—Thin, light-gray beds of vitreous quartzite and crossbedded sandy dolostone. Unit discontinuous in southern Vermont
- Cw** Winooski Dolostone (Middle Cambrian)—Well-bedded dolostone weathering beige, cream, and buff, with green, red, or gray phyllite, siliceous partings, and thin beds of blue-quartz-pebble conglomerate and quartzite
- Cm** Monkton Quartzite (Middle Cambrian)—Reddish-brown, pebbly, thin- to thick-bedded sandstone, orangey-gray- and buff-weathering well-bedded dolostone, and reddish-brown-weathering dolomitic quartzite. Unit discontinuous in southern Vermont
- Cdu** Dunham Dolostone (Lower Cambrian)—Buff- and pink-mottled and massive, or light-gray, pinkish-gray-weathering, and massive to poorly bedded dolostone. Contains distinctive small pebbles and grains of well-rounded quartz; minor beds of dolostone-breccia and conglomerate occur near Rutland
- Ccb** Cheshire Quartzite (Lower Cambrian)—Light-gray- to tannish-gray-weathering, massive to poorly bedded vitreous quartzite, containing layers of dark-gray biotite-muscovite-quartz phyllite near top (Ccb); locally contains a mappable brown-weathering, gray to brown argillaceous quartzite member (Cca)
- Dalton Formation (Lower Cambrian and Neoproterozoic)**
(unit interingers to the north with rocks of the Tyson Formation and to the east with rocks of the Hoosac Formation)
 - EZc** Dalton Formation, undivided—Heterogeneous unit consisting of rusty- to tan-weathering flaggy feldspathic quartzite, tan-weathering quartz phyllite, and feldspathic quartzite
 - EZdq** Quartzite member—Tan to whitish-gray vitreous quartzite and minor blue-quartz-pebble quartzite
 - EZdb** Dark phyllite member—Dark-gray to gray, rusty-weathering, well-laminated tourmaline-biotite-muscovite-quartz phyllite containing thin beds of laminated quartzite. Resembles dark phyllite of the Moosalamoo Formation (EZmp), with which it is in part correlative
 - EZdfq** Feldspathic quartzite member—Light-tan to gray-weathering, massive to thin-bedded, flaggy, tourmaline-muscovite-feldspar quartzite and interbedded phyllitic quartzite
 - EZds** Lustrous quartz schist member—Dark-gray to silvery-gray, tourmaline-muscovite-biotite-quartz schist and feldspathic schist and quartzite. Occurs on eastern flank of the southern Green Mountain massif; similar in appearance to EZhs of the Hoosac Formation exposed to the east



REFERENCE: USGS, SCIENTIFIC INVESTIGATIONS MAP 3184, BEDROCK GEOLOGIC MAP OF VERMONT, SHEET 1 OF 3.

WARNING: IT IS A VIOLATION OF THE NYS EDUCATION LAW ARTICLE 145 FOR ANY PERSON, UNLESS HE IS ACTING UNDER THE DIRECTION OF A LICENSED PROFESSIONAL ENGINEER, LAND SURVEYOR OR GEOLOGIST, TO ALTER THIS ITEM IN ANY WAY.

LANGAN Langan Engineering, Environmental, Surveying, Landscape Architecture and Geology, D.P.C. 21 Penn Plaza, 360 West 31st Street, 8th Floor New York, NY 10001 T: 212.479.5400 F: 212.479.5444 www.langan.com	Project	Drawing Title	Project No.	Drawing No.
	BENNINGTON BATTLE MONUMENT	BEDROCK GEOLOGIC MAP	170724004	4
			Date	
			1/22/2024	
			Drawn By	
			JSB	
			Checked By	
			PT	
			Sheet	4 of 4

APPENDIX A

(GEOTECHNICAL BORING LOG)

Project Bennington Battle Monument			Project No. 170724002		
Location Bennington Battle Monument			Elevation and Datum Approx. el. 866.0 (NAVD 88)		
Drilling Company Cascade Remediation Services			Date Started 1/17/2024	Date Finished 1/18/2024	
Drilling Equipment Geoprobe Drill Rig			Completion Depth 18.5 ft	Rock Depth 8.5 ft	
Size and Type of Bit 3-7/8in Tricone Roller Bit			Number of Samples 4	Disturbed 0	Core 2
Casing Diameter (in) 4.00	Casing Depth (ft) 8.5		Water Level (ft.) First ∇ N/A	Completion ∇ N/A	24 HR. ∇ N/A
Casing Hammer Automatic	Weight (lbs) 140	Drop (in) 30	Drilling Foreman Erick Ramey		
Sampler 2in OD Split Spoon, HQ Corro Barrel			Field Engineer Sebastian Baculima		
Sampler Hammer Automatic	Weight (lbs) 140	Drop (in) 30			

Material Symbol	Elev. (ft)	Sample Description	Depth Scale	Sample Data					Remarks (Drilling Fluid, Casing Depth, Fluid Loss, Drilling Resistance, etc.)
				Number	Type	Recov. (in)	Penetr-resist BL/6in	N-Value (Blows/ft) 10 20 30 40	
	+866.0	Brown Silty fine to medium SAND, trace clay, some root, some glass (moist) [TOPSOIL]	0						Hand clear from 0ft to 5ft.; Took G-1 at 0 ft
	+864.0	Brown Clayey fine SAND, some silt, trace fine gravel (moist) [CL]	2	G-2	GRAB				Took G-2 at 2 ft
		Orangish brown CLAY, some fine sand, trace silt, rock fragments (moist) [CL]	5				2		Took S-1 at 5 ft
		Brown CLAY, some fine sand, trace silt, rock fragments (moist) [CL]	7	S-2	SS	18	3	50/1"	Took S-2 at 7 ft
	+857.5	Light gray DOLOSTONE; fine grained fresh to slightly weathered; close to very close fracture spacing; fractures shallow dipping to steeply vertical; rock quality poor; [BEDROCK]	8						Refusal encountered at 7.5ft. Drill to 8.5 ft. Hard drilling, moderate rig chatter, brown wash. Drive casing from 0 ft to 8.5 ft. Clean up the hole, brown wash. Stop drilling for the day (1/17/2024) at 8.5 ft; Start drilling for the day (1/18/2024) at 8.5 ft; Took C-1 at 8.5 ft.
		Light gray DOLOSTONE; fine to medium grained fresh to moderately weathered; close to moderate fracture spacing; fractures moderately vertical to steeply vertical; rock quality poor; [BEDROCK]	13	C-1	HQ		REC=53"/60"=88%	RQD=23"/60"=38%	Took C-1 at 13.5 ft.
			15	C-2	HQ		REC=55"/60"=92%	RQD=22"/60"=37%	Took C-2 at 15 ft.
	+847.5	End of Boring at 18.5ft.	18						Bottom of boring at 18.5 ft. Pull up casing. Backfill the hole with soil cuttings to match existing grade.

LANGAN

Log of Boring **B-2**

Sheet 1 of 1

Project Bennington Battle Monument			Project No. 170724002		
Location Bennington Battle Monument			Elevation and Datum Approx. el. 868.0 (NAVD88)		
Drilling Company Cascade Remediation Services			Date Started 1/18/2024	Date Finished 1/18/2024	
Drilling Equipment Geoprobe Drill Rig			Completion Depth 17.0 ft	Rock Depth 7.0 ft	
Size and Type of Bit 3-7/8in Tricone Roller Bit			Number of Samples	Disturbed 4	Undisturbed 0
Casing Diameter (in) 4.00			Casing Depth (ft) 6.5	Water Level (ft.) First ∇ N/A	Completion ∇ N/A
Casing Hammer Automatic	Weight (lbs) 140	Drop (in) 30	Drilling Foreman Erick Ramey		
Sampler 2in OD Split Spoon, HQ Corre Barrel			Field Engineer Sebastian Baculima		
Casing Hammer Automatic	Weight (lbs) 140	Drop (in) 30			

Material Symbol	Elev. (ft)	Sample Description	Depth Scale	Sample Data					Remarks (Drilling Fluid, Casing Depth, Fluid Loss, Drilling Resistance, etc.)
				Number	Type	Recov. (in)	Penetr-resist BL/6in	N-Value (Blows/ft) 10 20 30 40	
	+868.0	Brown CLAY, trace silt, trace fine sand, some glass, some root (moist) [TOPSOIL]	0						Hand clear from 0ft to 5ft ; Took G-1 at 0 ft
	+866.0	Brown CLAY, some fine to coarse sand, trace silt (moist) [CL]	2	G-1	GRAB				Took G-2 at 2 ft
		No Recovery	5	S-1	SS	0	10 WOH		Took S-1 at 5 ft
	+861.0	Brown to light brown CLAY, some fine to medium sand, trace silt, rock fragments (moist) [CL]	6	S-2	SS	5	10 50/1"		Took S-2 at 6 ft
		Light gray DOLOSTONE; fine grained fresh to slightly weathered; close to moderate fracture spacing; fractures near horizontal to shallow dipping; rock quality poor; [BEDROCK]	7						Attempted to drill from 6.5 ft to 8 ft. Hard drilling, heavy rig chatter, brown wash. Stop drilling at 7 ft. Drive casing from 0 ft to 7 ft. Clean up the hole, brown wash. Took C-1 at 7 ft.
		Light gray DOLOSTONE; fine grained fresh to slightly weathered; moderate to very close fracture spacing; fractures steeply vertical to shallow dipping; rock quality poor; [BEDROCK]	12	C-1	HQ				Took C-2 at 12 ft
	+851.0	End of Boring at 17ft.	17	C-2	HQ				Bottom of boring at 17ft below ground surface. Pull up casing and backfill the hole with soil cuttings to match existing grade.

Project Bennington Battle Monument			Project No. 170724002		
Location Bennington Battle Monument			Elevation and Datum Approx. el. 867.0 (NAVD88)		
Drilling Company Cascade Remediation Services			Date Started 1/17/2024		Date Finished 1/17/2024
Drilling Equipment Geoprobe Drill Rig			Completion Depth 22.0 ft		Rock Depth 12.0 ft
Size and Type of Bit 3-7/8in Tricone Roller Bit			Number of Samples Disturbed 6		Undisturbed 0 Core 2
Casing Diameter (in) 4.00		Casing Depth (ft) 12.0	Water Level (ft.) First ∇ N/A		Completion ∇ N/A 24 HR. ∇ 10.4
Casing Hammer Automatic	Weight (lbs) 140	Drop (in) 30	Drilling Foreman Erick Ramey		
Sampler 2in OD Split Spoon, HQ Corre Barrel			Field Engineer Sebastian Baculima		
Casing Hammer Automatic	Weight (lbs) 140	Drop (in) 30			

Material Symbol	Elev. (ft)	Sample Description	Depth Scale	Sample Data				Remarks (Drilling Fluid, Casing Depth, Fluid Loss, Drilling Resistance, etc.)
				Number	Type	Recov. (in)	Penetr-resist BL/6in	
	+867.0	Brown Silty fine to medium SAND, some root, some glass (moist) [TOPSOIL]	0					Hand clear from 0ft to 5ft.; Took U-1 at 0 ft
	+865.0	Brown Clayey fine SAND, trace fine gravel (moist) [SC]	2	G-1	GRAB			Took G-2 at 2 ft
	+862.0	Orangish brown Silty medium to fine SAND, trace clay, rock fragments (moist) [SM]	5	G-2	GRAB			Took G-1 at 5 ft
	+861.0	Orangish brown CLAY, trace fine sand, rock fragments (moist) [CL]	6	S-1	SS	6	11	Took S-2 at 6 ft
		Orangish brown CLAY, trace fine sand, rock fragments (moist) [CL]	7	S-2	SS	20	5	Took S-3 at 8 ft
		Orangish brown CLAY, trace fine sand, rock fragments, trace silt (moist) [CL]	10	S-3	SS	24	15	Took S-4 at 10 ft
			11	S-4	SS	15	19	
	+855.0	Light gray DOLOSTONE; fine to medium grained fresh weathered; close to moderate fracture spacing; fractures near horizontal to moderately vertical; rock quality fair; [BEDROCK]	12					Spoon bouncing at 11 ft. Drive casing from 0ft to 10ft. Drill from 11 ft to 12 ft. Hard drilling, heavy rig chatter, brown wash. Drive casing from 10ft to 12ft. Clean up the hole, brown wash; Took C-1 at 12 ft.
			13	C-1	HQ	REC=56"/60"=93%	RQD=40"/60"=68%	
			17					Took C-2 at 17 ft
		Light gray DOLOSTONE; fine to medium grained slightly weathered; close to very close fracture spacing; fractures steeply vertical to moderately vertical; rock quality poor; [BEDROCK]	18					
			19	C-2	HQ	REC=60"/60"=100%	RQD=22"/60"=37%	
	+845.0	End of Boring at 22ft.	22					Bottom of boring at 22 ft below ground surface. Install water observation well. Pull up casing.

APPENDIX B

(GROUNDWATER OBSERVATION WELL LOG)

PROJECT Bennington Battle Monument			PROJECT NO. 170724002			
LOCATION Bennington, VT			ELEVATION AND DATUM el. 867 ± (NAVD 88)			
DRILLING AGENCY Cascade Remediation Services			DATE STARTED 1/17/2024		DATE FINISHED 1/17/2024	
DRILLING EQUIPMENT Geoptobe Drill Rig			DRILLER George Zackman			
SIZE AND TYPE OF BIT 3-7/8in Tricone Roller Bit			LANGAN REP. Sebastian Baculima Chicaiza			
METHOD OF INSTALLATION The boring was advanced to 22 feet below the existing ground surface using mud rotary drilling techniques and HQ core barrel. After backfilling the hole with 2 feet of filter sand, the well was installed to 20 feet below the ground surface, and consisted of 10 feet slotted PVC pipe (screen) and 9.5 feet solid PVC pipe (riser) at top. A flush-mount well cap was installed to seal the well.						
METHOD OF WELL DEVELOPMENT The observation well was flushed clean and developed using a pump.						
TYPE OF RISER PVC		DIAMETER 2 inch	TYPE OF BACKFILL MATERIAL Soil Cuttings			
TYPE OF SCREEN Slotted PVC		DIAMETER 2 inch	TYPE OF SEAL MATERIAL Bentonite			
BOREHOLE DIAMETER 4 inch		TYPE OF FILTER MATERIAL Silica Sand				
TOP OF CASING	ELEVATION 867	DEPTH (ft) 0	WELL DETAILS		SUMMARY SOIL CLASSIFICATION	DEPTH (FT)
TOP OF SEAL	ELEVATION 861.5	DEPTH (ft) 5.5			Cover	
TOP OF FILTER	ELEVATION 859.5	DEPTH (ft) 7.5	2" PVC Riser		TOPSOIL	0.0
TOP OF SCREEN	ELEVATION 857.5	DEPTH (ft) 9.5			Soil Cuttings	
BOTTOM OF BORING	ELEVATION 845	DEPTH (ft) 22	2" PVC Screen		SAND	5.0
SCREEN LENGTH	LENGTH (ft) 10				Bentonite Seal	
SLOT SIZE	0.025 inch		Silica Filter Sand		CLAY	12.0
GROUNDWATER ELEVATIONS					BEDROCK	
ELEVATION	DATE	DEPTH TO WATER (ft)				
856.6	1/18/2024	10.4				
ELEVATION	DATE	DEPTH TO WATER (ft)				
ELEVATION	DATE	DEPTH TO WATER (ft)				
ELEVATION	DATE	DEPTH TO WATER (ft)				
ELEVATION	DATE	DEPTH TO WATER (ft)				
ELEVATION	DATE	DEPTH TO WATER (ft)				
ELEVATION	DATE	DEPTH TO WATER (ft)				
N.T.S.						
Langan Engineering, Environmental, Surveying, Landscape Architecture and Geology, D.P.C. 21 Penn Plaza, 360 West 31st Street, 8th Floor, New York, New York 10001						

APPENDIX C

(LABORATORY TEST RESULTS)



1017 Greeley Ave N
Union, NJ 07083
908-964-0786
www.RSAGEolab.com

Letter of Transmittal

Date: 1-25-24

Job No.: 869

Lab Log: 24-3169

Attention: Prasoan Tiwari
Langan Engineering & Environmental Services
360 West 31st Street, 8th Floor
New York, New York 10001

CC:

Re: BBM, Vermont
Langan#170724002

Sample(s) ID: **B-1 S-2, B-3 S-2, LB-1 C-1, B-3 C-1**

Dear Prasoan,

Please find attached results for the samples referenced above. The following lab testing was performed:

- ASTM D422 Sieve Analysis (2 tests)
- ASTM D4318 Atterberg Limits (2 tests)
- ASTM D7012 Unconfined Compressive Strength of Rock Cores (2 tests)

Regards,
RSA Geolab, LLC

Remarks: If you have any questions, please call 908-964-0786.

Signed: 

Dr. Raza S. Ahmed
President RSA Geolab, LLC

RSA's Geolab's Geotechnical Laboratory testing was performed and results reported in accordance with ASTM standards and accepted industry standards. No other representations or warranties either express or implied are given. RSA Geolab, LLC neither accepts responsibility for nor makes claim to the final use and purpose of the material tested. RSA Geolab, LLC owns all rights, title and interest of the work product. This report is intended for client's sole and exclusive use and not for the benefit of others and may not be used or relied upon by others. These documents must be considered proprietary information and should not be reproduced without the written approval of RSA Geolab, LLC.

Particle Size Distribution Report



% +3"	% Gravel		% Sand			% Fines	
	Coarse	Fine	Coarse	Medium	Fine	Silt	Clay
0.0	0.0	12.7	4.3	7.3	11.7	64.0	

SIEVE SIZE	PERCENT FINER	SPEC.* PERCENT	PASS? (X=NO)
.75	100.0		
.5	94.4		
.375	89.9		
#4	87.3		
#10	83.0		
#30	77.4		
#40	75.7		
#60	72.9		
#100	69.7		
#200	64.0		

Material Description

Light Olive Brown sandy lean clay

Atterberg Limits
 PL= 15 LL= 26 PI= 11

Coefficients
 D₈₅= 2.7768 D₆₀=
 D₅₀= D₃₀=
 D₁₀= C_u= C_c=

Classification
 USCS= CL AASHTO= A-6(4)

Remarks

* (no specification provided)

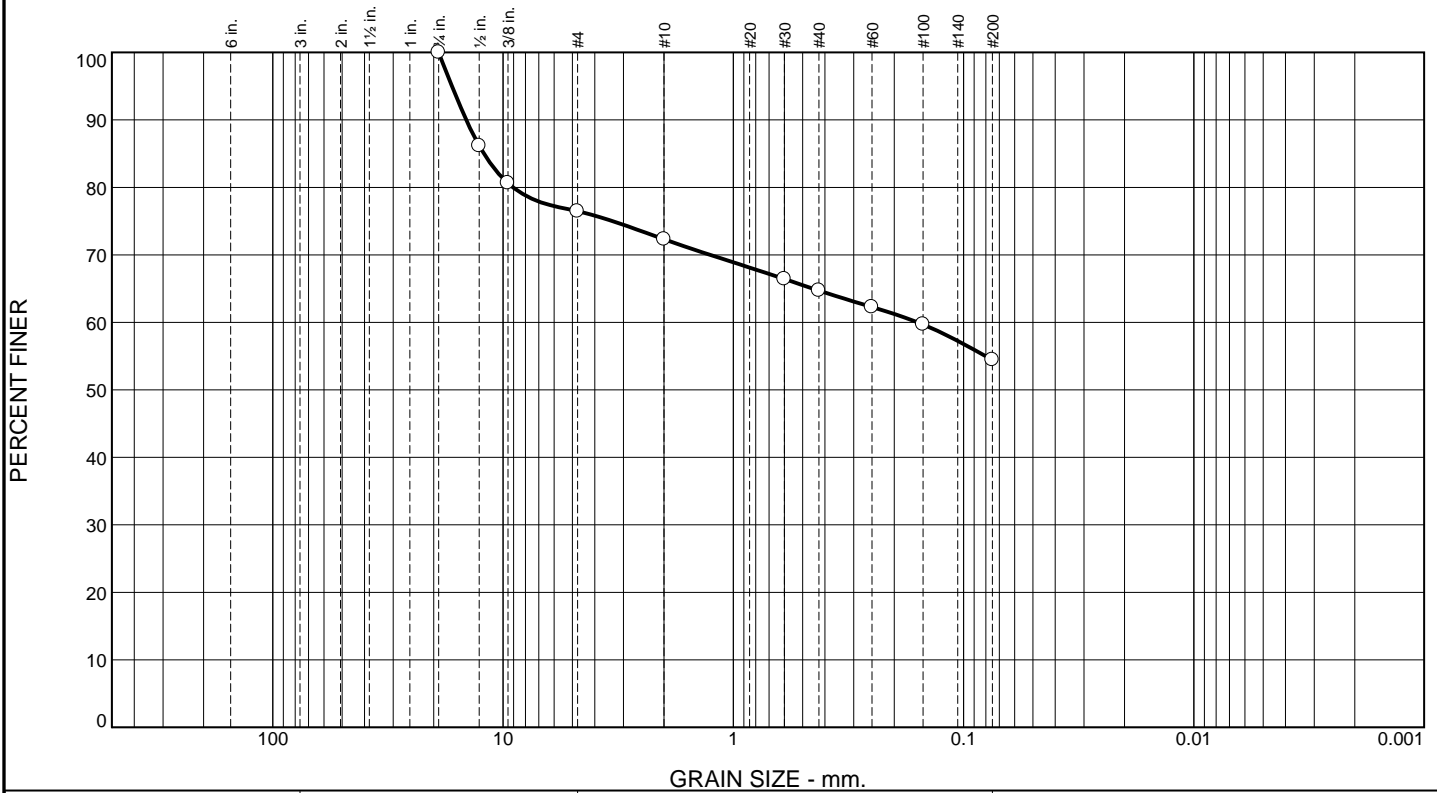
Sample Number: B-1 S-2 7-9'

Date: 1-25-24

RSA Geolab Union, New Jersey	Client: Langan Engineering Project: BBM, Vermont Proj.#170724002 Project No: 869
Figure	

Tested By: EE Checked By: KP

Particle Size Distribution Report



% +3"	% Gravel		% Sand			% Fines	
	Coarse	Fine	Coarse	Medium	Fine	Silt	Clay
0.0	0.0	23.5	4.2	7.6	10.3	54.4	

SIEVE SIZE	PERCENT FINER	SPEC.* PERCENT	PASS? (X=NO)
.75	100.0		
.5	86.2		
.375	80.6		
#4	76.5		
#10	72.3		
#30	66.4		
#40	64.7		
#60	62.3		
#100	59.7		
#200	54.4		

Material Description

Light Yellowish Brown gravelly lean clay with sand

Atterberg Limits

PL= 16 LL= 26 PI= 10

Coefficients

D₉₀= 14.4560 D₈₅= 12.1279 D₆₀= 0.1581
D₅₀= D₃₀= D₁₅=
D₁₀= C_u= C_c=

Classification

USCS= CL AASHTO= A-4(2)

Remarks

* (no specification provided)

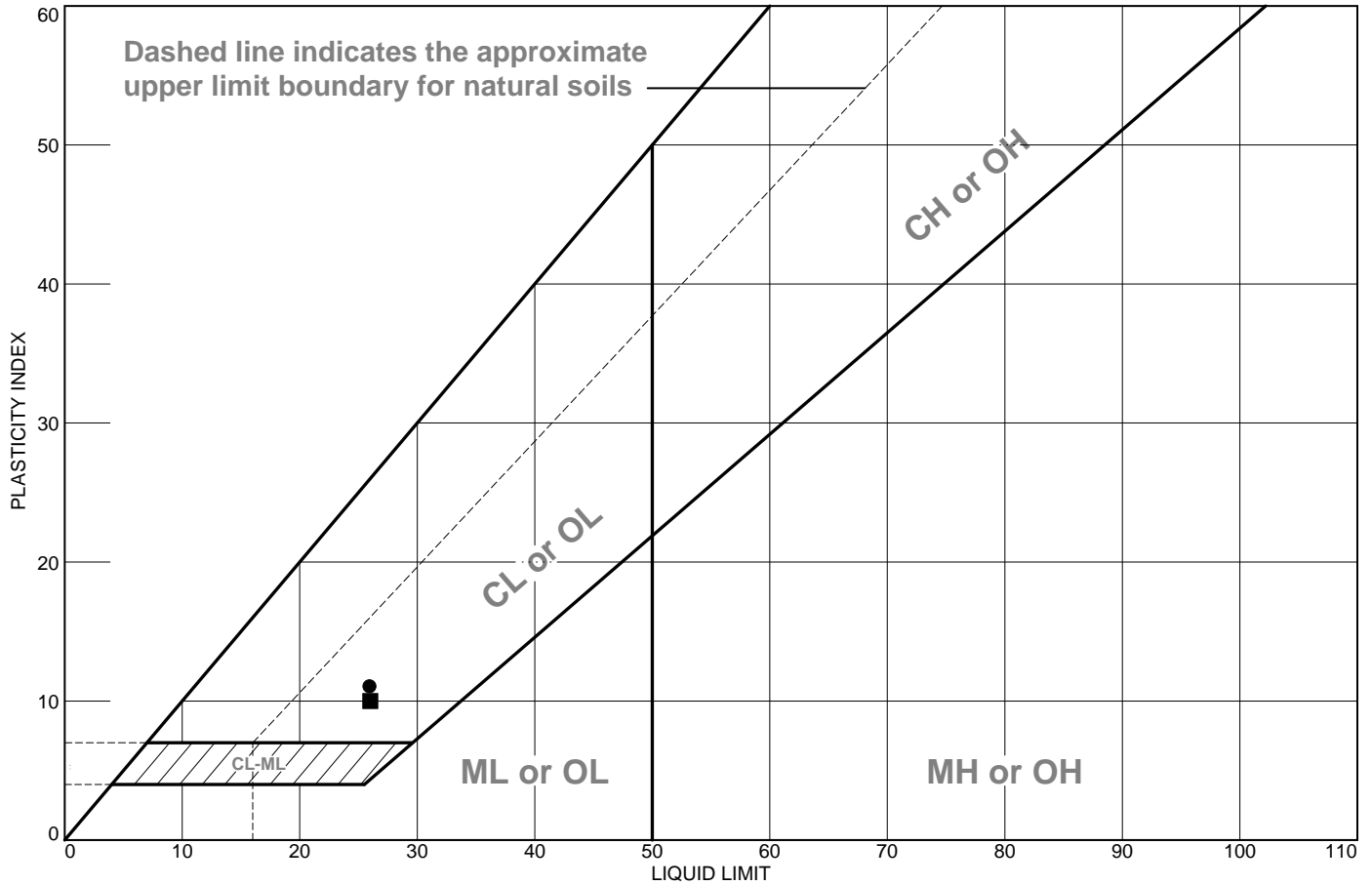
Sample Number: B-3 S-2 6-8'

Date: 1-25-24

<p>RSA Geolab</p> <p>Union, New Jersey</p>	<p>Client: Langan Engineering Project: BBM, Vermont Proj.#170724002 Project No: 869</p>
<p>Figure</p>	

Tested By: EE Checked By: KP

LIQUID AND PLASTIC LIMITS TEST REPORT



	MATERIAL DESCRIPTION	LL	PL	PI	%<#40	%<#200	USCS
●	Light Olive Brown sandy lean clay	26	15	11	75.7	64.0	CL
■	Light Yellowish Brown gravelly lean clay with sand	26	16	10	64.7	54.4	CL

Project No. 869 **Client:** Langan Engineering
Project: BBM, Vermont
 Proj.#170724002
 ● **Sample Number:** B-1 S-2 7-9'
 ■ **Sample Number:** B-3 S-2 6-8'

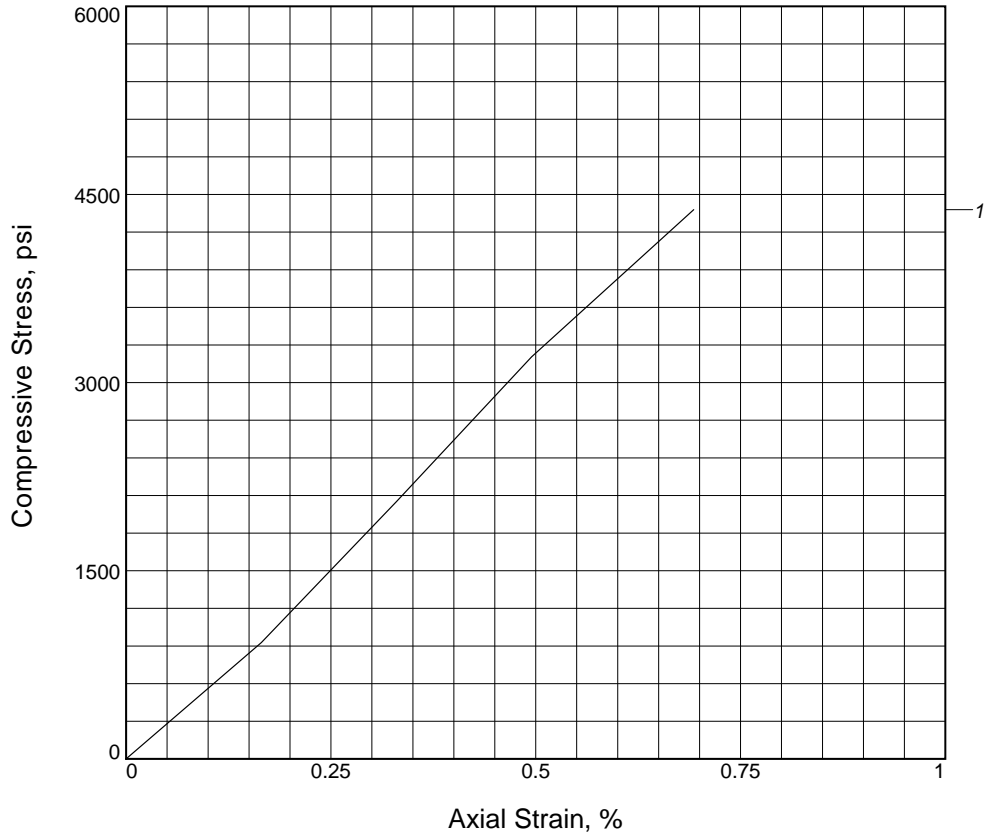
RSA Geolab
 Union, New Jersey

Remarks:
 ● 1-25-24

Figure

Tested By: EE Checked By: KP

UNCONFINED COMPRESSION TEST



Sample No.	1		
Unconfined strength, psi	4379.24		
Undrained shear strength, psi	2189.62		
Failure strain, %	0.7		
Strain rate, in./min.	0.050		
Water content, %	N/A		
Wet density, pcf	174.5		
Dry density, pcf	N/A		
Saturation, %	N/A		
Void ratio	N/A		
Specimen diameter, in.	2.50		
Specimen height, in.	6.06		
Height/diameter ratio	2.43		

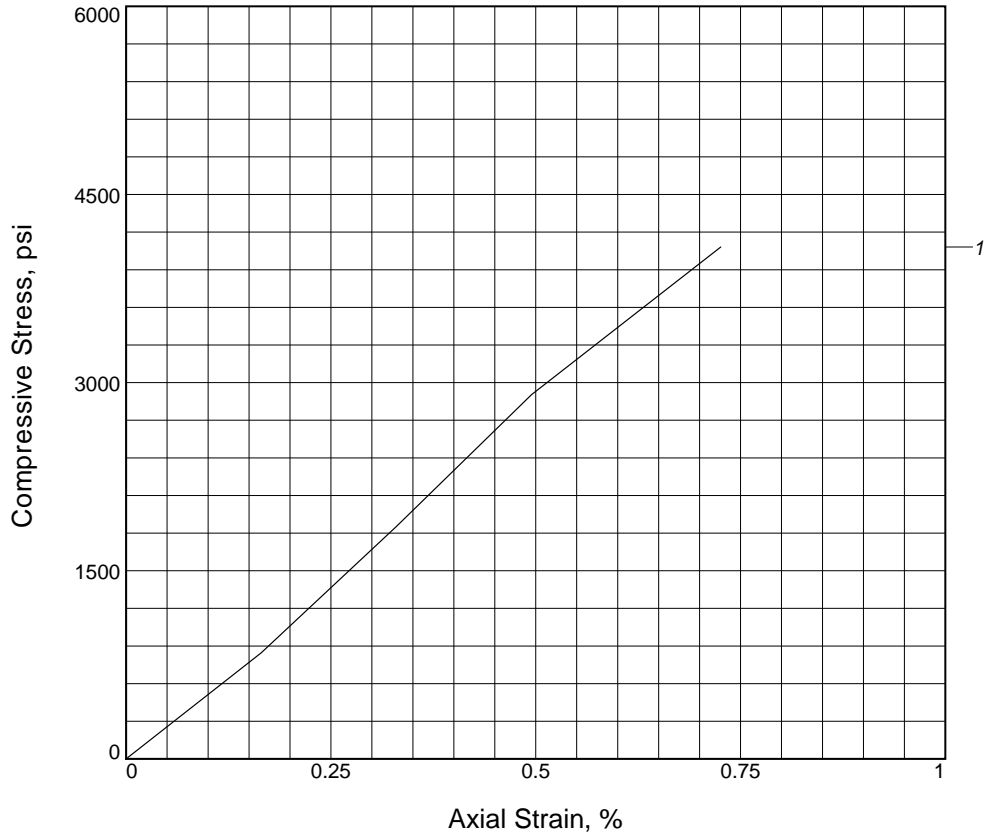
Description: Gray rock core

LL =	PL =	PI =	Assumed GS= 2.7	Type: ASTM D7012
-------------	-------------	-------------	------------------------	-------------------------

<p>Project No.: 869</p> <p>Date Sampled: 1-25-24</p> <p>Remarks: Sample strength exceeds maximum load cell capacity.</p> <p>Figure _____</p>	<p>Client: Langan Engineering</p> <p>Project: BBM, Vermont Proj.#170724002</p> <p>Sample Number: B-3 C-1 12-14'</p> <hr/> <p style="text-align: center;">UNCONFINED COMPRESSION TEST RSA Geolab Union, New Jersey</p>
--	--

Tested By: EE **Checked By:** KP

UNCONFINED COMPRESSION TEST



Sample No.	1		
Unconfined strength, psi	4081.33		
Undrained shear strength, psi	2040.66		
Failure strain, %	0.7		
Strain rate, in./min.	0.050		
Water content, %	N/A		
Wet density, pcf	174.5		
Dry density, pcf	N/A		
Saturation, %	N/A		
Void ratio	N/A		
Specimen diameter, in.	2.50		
Specimen height, in.	6.06		
Height/diameter ratio	2.43		

Description: Gray rock core

LL =	PL =	PI =	Assumed GS= 2.7	Type: ASTM D7012
-------------	-------------	-------------	------------------------	-------------------------

<p>Project No.: 869</p> <p>Date Sampled: 1-25-24</p> <p>Remarks: Sample strength exceeds maximum load cell capacity.</p> <p>Figure _____</p>	<p>Client: Langan Engineering</p> <p>Project: BBM, Vermont Proj.#170724002</p> <p>Sample Number: LB-1 C-1 8-10'</p> <hr/> <p style="text-align: center;">UNCONFINED COMPRESSION TEST RSA Geolab Union, New Jersey</p>
--	--

Tested By: EE **Checked By:** KP

B-3 C-1
L#24-3169



SA Geolab
Compression of Rock Cores
Loading Data ASTM D7012

Project: BBM -17072

Client: Langan

Sample Identification: B-3 C-1 12'-14'

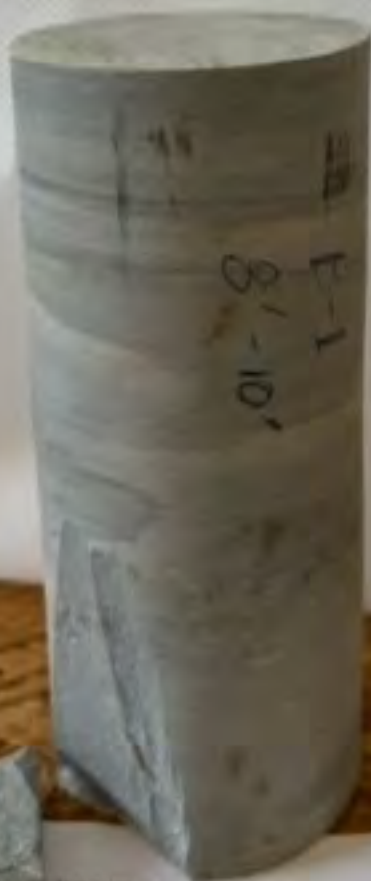
Strain Rate: 0.05 in/min

L#24-3169

Date: 1/22/24

Test #: 1 of 1

LB-1 C-1 L#24-3169



Project: BBM-17024002

Location: Langan

Core Identification: LB-1 C-1 8'-10'

Rate: 0.05 in/min

BSA Geolab
Division of Rock Cores
#1MD7012

L#24-3169

Date: 1/22/24

Test #: 1 of 1